THÈSE POUR OBTENIR LE GRADE DE DOCTEUR
DÉLIVRÉ PAR L'UNIVERSITÉ DE MONTPELLIER

En Science de la mer

Préparée au sein de l'École doctorale GAIA

Et de l'Unité de recherche UMR MARBEC

En partenariat international avec The University of Cape Town (Afrique du Sud)

Patterns among micronekton communities in relation to environmental conditions at two shallow seamounts in the south-western Indian Ocean

Présentée par **Pavanee ANNASAWMY**

Angelee

Le 24 Septembre 2019

Sous la direction de **Francis MARSAC** (Directeur de thèse)
et **Colin ATTWOOD** (co-Directeur de thèse)

Devant le jury composé de

[**Christophe MENKES**- Directeur de Recherche, IRD, Nouvelle Calédonie]	[Rapporteur]
[**Patrice BREHMER**- Chargé de Recherche, IRD, Brest]	[Rapporteur]
[**Catherine ALIAUME**- Professeur, Université de Montpellier]	[Présidente du jury]
[**Coleen MOLONEY**- Professeur, University of Cape Town]	[Examinatrice]
[**Christophe GUINET**- Directeur de Recherche, CEBC-CNRS, Chizé]	[Examinateur]
[**Francis MARSAC**- Directeur de recherche, IRD, Sète et University of Cape Town]	[Directeur de thèse]

Declaration

I hereby declare that except where specific reference is made to the work of others, the contents of this thesis dissertation are original and have not been submitted in whole or in part for consideration for any other degree or qualification in this, or any other University. This dissertation contains three authored accepted papers as main chapters, as requested for a "PhD by publication" by the University of Montpellier. This dissertation contains less than 80 000 words excluding appendices, bibliography, footnotes, tables and equations and has less than 150 figures.

Pavanee Annasawmy,

July 2019

I hereby confirm that I have been granted permission by the University of Cape Town's Doctoral Degrees Board to include the following publications in my PhD thesis. The co-authors have agreed to the inclusion of these publications:

Annasawmy, P., Ternon, J-F., Cotel, P., Cherel, Y, Romanov, E., Roudaut, G., Lebourges-Dhaussy, A., Ménard, F., Marsac, F., 2019. Micronekton distribution and assemblages at two shallow seamounts in the south-western Indian Ocean: Insights from acoustics and mesopelagic trawl data. Prog. Oceanogr. 178. https://doi.org/10.1016/j.pocean.2019.102161

Annasawmy, P., Ternon, J-F., Lebourges-Dhaussy, A., Roudaut, G., Herbette, S., Ménard, F., Cotel., P., Marsac, F., 2020a. Micronekton distribution as influenced by mesoscale eddies, Madagascar shelf and shallow seamounts in the south-western Indian Ocean: an acoustic approach. Deep-Sea Res. II.

Annasawmy, P., Cherel, Y., Romanov, E., Le Loch, F., Ménard, F., Ternon, J-F., Marsac, F., 2020b. Stable isotope patterns of micronekton at two shallow seamounts of the south-western Indian Ocean. Deep-Sea Res. II.

SIGNATURE: Signed by candidate

DATE: 15th of July 2019

NAME: Pavanee Annasawmy *STUDENT NUMBER: ANNPAV001*

Acknowledgements

Coming to the end of a long journey, I would like to, first and foremost, thank my thesis supervisor, Dr. Francis Marsac, for his continuous support, faith and optimism. Francis provided guidance and assistance throughout my Master's and PhD degree through the ICEMASA French-South African International Laboratory, which has given me the opportunity to work on interesting research questions in collaboration with various institutions. I aslo wish to thank my thesis co-supervisor Asso. Prof. Colin Attwood for providing support and assistance. Both Francis and Colin have encouraged the independent pursuit of my research interests and I am very grateful for this freedom. I am further grateful to have evolved by their side and to have learnt important skills necessary in conducting oceanographic research work at an international level.

Helpful comments and advice are thankfully acknowledged from members of my committee who have followed my work since the beginning. The committee members included Jean-François Ternon, Anne Lebourges-Dhaussy, Frédéric Ménard, Yves Cherel and Arnaud Bertrand. I admire their passion for scientific research. I am thankful for their valuable suggestions to improve this research work, and all the interesting and stimulating scientific discussions we have had.

I am grateful to the directors of UMR MARBEC (Sète, France) for their warm welcome and their words of encouragement during my stay in France. I wish to thank the University of Cape Town, especially Colin Attwood for providing all the necessary equipment for the organisation of a Taxonomic Workshop at UCT. I also wish to acknowledge Yves Cherel, Evgeny Romanov and Alexander Butch Hulley who took part in this workshop to confirm the identification of the mesopelagic fishes and squids caught during La Pérouse and MAD-Ridge cruises.

This work would not have been possible without all those people who have provided the necessary training and equipment such that I can complete all the steps required for the stable isotope analyses in due time:

Freeze-drying equipment: Sebastien Jaquemet (Laboratoire d'écologie marine, Université de La Réunion/ UMR Entropie); Bronwyn Arendze-Bailey (Molecular and Cell Biology Department, UCT, South Africa); Dawood Hattas (Department of Biological Sciences, UCT, South Africa).

Grinding and Lipid removal equipment: Luisa Metral (UMR MARBEC, Sète, France).

Carbonate removal and Encapsulation equipment: François Le Loc'h (UMR LEMAR, Plouzané, Brest).

Mass Spectrometry analyses were run by Jean-Marie Munaron and Clement Tanvet (UMR LEMAR, Plouzané, Brest), who have spent long hours in front of the mass spectrometer and computer to validate the stable isotopes data.

I would also like to acknowledge the captain and crew of the RV Antea for providing assistance during the data collection. I admire their professionalism and for providing efficient and quick solutions to unexpected problems encountered during our cruises, such that the scientific data collection and cruise plan were not affected.

Due to the nature of this co-badged PhD degree, administrative hurdles were varied and numerous and had to be overcome during these three years. I wish to thank the administrative staff at UCT, especially within the Department of Biological Sciences (Claire Khai), MA-RE (Sharon Bosma), the Faculty of Science Postgraduate office (Ayesha Shaik and Shahieda Samsodien), and IRD (Ghislaine Ferard Pouget), and acknowledge their patience and support in the face of unexpected and complicated situations.

This thesis, as well as conference attendance to present findings (10^{th} WIOMSA Symposium 2017; WGFAST 2018; ICEMASA Colloquium 2018; SANCOR meeting 2018) was made possible via funding provided by IRD (ARTS scholarship), ICEMASA bursaries and additional grants from UM and WIOMSA (travel grants). I am further grateful to ICEMASA for giving me the opportunity to travel to Brest on numerous occasions to work closely with Anne Lebourges-Dhaussy and Gildas Roudaut in the field of acoustics, and François Le Loc'h in the field of stable isotopes.

Last but not least, I wish to thank my family for their unconditional love, unwavering support and faith. This thesis is dedicated to my parents who have showed me the value of hard work and who have always encouraged me to aim higher.

Table of Contents

List of Figures

List of Tables

Thesis Abstract

Seamounts are ubiquitous topographic features across all ocean basins. They rise steeply through the water column from abyssal depths. Depending on their size, shape and summit depths, seamounts reportedly have an influence on the physical flow regimes which may promote the aggregation of zooplankton, micronekton, and top predators above or in the immediate vicinity of their summits. Micronekton form a key trophic link between zooplankton and top marine predators, and are divided into the broad categories: crustaceans, cephalopods and mesopelagic fishes. The vertical and horizontal distributions, assemblages and trophic relationships of micronekton were investigated at two shallow seamounts of the south-western Indian Ocean. La Pérouse is a steep bathymetric feature rising from a deep seabed located at 5000 m and with a summit depth at ~60 m below the sea level. This seamount is located at the north-western periphery of the oligotrophic Indian South Subtropical Gyre province. A seamount to the south of Madagascar, named "MAD-Ridge" in this study, has a summit depth at ~240 m below the sea level and rises from a base at ~1600 m. MAD-Ridge is located within an "eddy corridor" within the productive East African Coastal Province. The micronekton acoustic densities were greater at MAD-Ridge relative to La Pérouse, in accordance with the difference in productivity between the two sites. Physical processes within the cyclonic mesoscale eddy sampled during the MAD-Ridge cruise led to enhanced micronekton acoustic densities in the eddy relative to the MAD-Ridge seamount. While the shallow scattering layer (0-200 m) consisted of common oceanic micronekton species, the summits and flanks of La Pérouse and MAD-Ridge both showed presence of resident or seamount-associated fish species during day and night. Micronekton were also shown to exhibit a range of migration strategies such as diel vertical migration, mid-water migration and no diel migration. However, despite the differing productivity between both pinnacles, crustaceans, smaller-sized squids and mesopelagic fishes exhibited trophic levels ranging from 3 to 4 at both seamounts. This thesis highlights important knowledge gaps on seamount ecosystems and ecological patterns associated to shallow pinnacles. It also underlines the importance of studying seamount ecosystems of the south-western Indian Ocean in order to promote management and conservation measures for a sustainable use of such specific environments.

Synthèse des travaux en français

Les monts sous-marins sont des structures bathymétriques s'élevant de manière abrupte dans la colonne d'eau depuis une profondeur d'au moins 1000 m. Ils sont le plus souvent d'origine volcanique et sont répartis dans tous les bassins océaniques. En tant qu'obstacle topographique, les monts sous-marins peuvent être sources d'enrichissement biologique en influençant la circulation océanique qui impacte la disponibilité en sels nutritifs et les communautés marines le long de la chaine alimentaire (Pitcher et al., 2007). Les monts sous-marins peuvent également créer des perturbations locales qui favorisent l'agrégation des organismes marins, du phytoplancton aux prédateurs supérieurs. Le Pétrel de Barau, un oiseau marin qui s'alimente sur des zones productives en phytoplancton et en micronecton, comme la ride qui s'étend au sud de Madagascar, en est un exemple bien décrit (Pinet et al., 2012). Ainsi les monts sous-marins sont souvent considérés comme des points chauds de biodiversité (Morato et al., 2010), avec un certain degré d'endémisme répertorié dans la littérature, en particulier pour les espèces benthiques (Richer de Forges et al., 2000; Worm et al., 2003). Il a été constaté que 30-40% de la faune en poisson sur le sommet du Walters Shoal est endémique aux groupes d'îles connues comme les "West-Wind Islands" (Collette et Parin, 1991). Les monts sous-marins sont connus également pour agréger des espèces de poissons à forte valeur commerciale comme les thons et les poissons à rostre (Fonteneau, 1991; Holland et Grubbs, 2007, Marsac et al., 2014) et sont par conséquent soumis à une pression de pêche. Environ 15% des prises de thons à la palangre dans la zone de la Réunion provient de deux carrés statistiques adjacents au mont La Pérouse (Marsac et al., 2020).

Cependant, force est de constater que les monts sous-marins de l'océan Indien sont peu étudiés comparés aux monts Condor, Great Meteor, Vema et Kelvin de l'Atlantique ou les monts Bowie, Cross, Graveyard, Hancock, Hawaiian-Emperor, Jasper, Lord Howe, et Tasmanian du Pacifique, malgré un effort de pêche non négligeable sur ces structures. Cette thèse s'inscrit dans le cadre d'un projet du IIOE-2 (International Indian Ocean Expedition-2) qui a pour but de mieux comprendre l'écosystème pélagique autour de deux monts sous-marins du sud-ouest de l'Océan Indien. La Pérouse est un mont peu profond qui s'élève à environ 60 m sous la surface de la mer d'une base qui se situe à 5000 m de profondeur. Ce mont est situé au nord-ouest de l'île de la Réunion, au sein du gyre anticyclonique ISSG (Gyre subtropical du sud de

l'Inde). Sur la ride de Madagascar se situe un autre mont peu profond qui s'élève d'une base à 1600 m et qui culmine à environ 240 m sous la surface de la mer. Ce mont a été baptisé MAD-Ridge dans cette étude. Deux campagnes océanographiques ont été organisées en 2016 à bord du navire *Antea* de l'Institut de recherche pour le développement (IRD, France). Le but de la campagne La Pérouse était de charactériser l'environnement physique et biologique afin d'évaluer un possible impact du guyot sur la productivité océanique dans une zone généralement qualifiée d'oligotrophe, traversée par le courant sud-équatorial. Le thème général de la campagne MAD-Ridge était d'étudier l'influence des processus physiques liés aux interactions entre la circulation océanique et la topographie sur la production biologique autour du mont sous-marin.

Alors que les bas niveaux trophiques- le phytoplancton, zooplancton, l'ichthyoplancton ainsi que les prédateurs supérieurs ont été étudiés dans cette zone, peu d'études se sont intéressées au micronecton. Le micronecton est constitué principalement de crustacés, céphalopodes et poissons mésopélagiques qui mesurent de 2 à 20 cm en longueur. Bien que les gélatineux ne fassent pas officiellement partie de ce groupe, les salpes et pyrosomes, constituent une biomasse importante dans les chaluts mésopélagiques et jouent un rôle capital dans la pompe biologique de carbone. Certaines espèces de gélatineux sont les proies des poissons mésopélagiques et de prédateurs superieurs tels que le thon. Mes travaux de thèse ont donc pour but de contribuer à combler des lacunes sur le compartiment micronectonique associé aux écosystèmes des monts sous-marins. Les objectifs principaux étant (i) d'étudier la distribution horizontale et verticale du micronecton en fonction des tourbillons méso-échelles, du plateau continental de Madagascar et de reliefs sous-marins (**chapitre 3**), (ii) de décrire les communautés présentes et les différentes stratégies de migration de certaines espèces (**chapitre 4**), (iii) de déterminer les modes alimentaires et le niveau trophique du micronecton dans le réseau trophique pélagique (**chapitre 5**).

Dans le cadre de cette étude, les données satellites de chlorophylle de surface, d'anomalie de hauteur d'eau, de bathymétrie et de courant géostrophique ont été téléchargées des sites MODIS, COPERNICUS et de la NASA. Pendant les campagnes La Pérouse et MAD-Ridge, une CTD couplée à un profileur de courant- L-ADCP et d'un capteur de fluorescence, a été utilisée pour enregistrer des profils de courant, fluorescence, température, salinité et oxygène

dissous de la surface jusqu'à plus de 1000 m de profondeur. L'eau de mer a été prélevée en surface et à la profondeur du maximum de chlorophylle, puis filtrée à bord du bateau pour des analyses d'isotopes stables du carbone et de l'azote. Un échosondeur à quatre fréquences (38, 70, 120 et 200 kHz) a également été utilisé pour enregistrer la distribution spatiale et verticale du micronecton en continu pendant MAD-Ridge et de façon ponctuelle au cours de la campagne La Pérouse. Ces enregistrements ont été traités et analysés à terre avec le logiciel Matecho. Un chalut mésopélagique a été utilisé au cours des campagnes pour collecter le micronecton de jour comme de nuit et à différentes profondeurs. Les différentes communautés mésopélagiques ont été identifiées à bord du bateau et lors d'un atelier organisé à l'Université du Cap en Afrique du Sud avec des experts en taxonomie. A terre, les échantillons destinés aux analyses d'isotopes stables ont été lyophilisés, broyés, délipidés, décarbonatés (matière organique particulière-MOP- et zooplancton uniquement), encapsulés et analysés au spectromètre de masse au LEMAR à Brest. Les isotopes stables du carbone ($\delta^{13}C$) apportent des informations sur les sources de production primaire et le régime alimentaire alors que les isotopes stables de l'azote ($\delta^{15}N$) renseignent sur la position trophique de l'individu dans la chaine alimentaire.

Cette thèse se décline donc sur cinq chapitres principaux, suivis d'une discussion générale. Le **chapitre 1** fournit une description détaillée des interactions entre les processus physiques et les monts sous-marins pouvant conduire à une réponse biologique des niveaux trophiques faibles et supérieurs. Des exemples sont donnés de monts sous-marins ayant fait l'objet de nombreuses études dans l'Atlantique et le Pacifique. Certains monts peuvent atteindre la zone euphotique, d'autres la zone intermédiaire et d'autres encore sont plus profonds, le sommet n'atteignant pas 400 m sous la surface de la mer. Les monts sous-marins peuvent également être de forme circulaire, conique, elliptique ou allongée et peuvent faire partie d'une ride, d'un groupe de monts ou être isolé. De part leurs tailles, formes et structures, les monts sous-marins ont des impacts très differents sur la circulation océanique. Diverses pertubations de la circulation océanique ont été decrites dans la littérature (White et al., 2007). En tant qu'obstacles topographiques, les monts sous-marins peuvent bifurquer, piéger, fendre ou détruire les tourbillons méso-échelles (Schouten et al., 2000; Herbette et al., 2003; Adduce & Cenedese, 2004; Sutyrin, 2006; Lavelle & Mohn, 2010). Sous certaines conditions, un relevé topographique peut causer une élévation des isocèles (lignes de densité) (Owens & Hogg, 1980). Il a également été signalé que les monts sous-marins peuvent agir comme des puits

d'énergies pour l'énergie des ondes internes et provoquer des perturbations dans les profondeurs de l'océan (White & Mohn, 2004). Les processus liés à la topographie peuvent générer un mélange au-dessus du fond et comprennent la réflexion des ondes internes et la génération de marées internes (Eriksen, 1998; Kunze & Llewelllyn Smith, 2004). Sous certaines conditions, des colonnes de Taylor peuvent également être formées au-dessus d'un mont sous-marin. Ces colonnes de Taylor sont des tourbillons anticycloniques qui s'élèvent en colonnes au-dessus du mont et sont formées à partir des interactions entre les courants et le relevé topographique. Ils agissent comme des "pièges" pour les organismes planctoniques qui s'y agrègent en abondance. Si la productivité se trouve piégée sur le mont, cela peut attirer les consommateurs secondaires et tertiaires telles que les zooplanctons, les micronectons et éventuellement les prédateurs supérieurs.

Le **chapitre 2** dresse un aperçu des écosystèmes pélagiques du sud-ouest de l'océan Indien. Cette zone est délimitée à l'ouest par la côte africaine et l'île de Madagascar qui est positionnée en travers du courant sud-équatorial (South Equatorial Current), jouant ainsi un rôle crucial dans la circulation régionale en provoquant une bifurcation du courant en deux branches (nord et sud) sur sa côte orientale et la formation de tourbillons méso-échelles dans le canal du Mozambique et au sud de L'île. Le sud-ouest de l'océan Indien est également caracterisé par deux provinces biogéochimiques définies dans Longhurst (1998, 2007) comme étant l'ISSG et l'EAFR (Province côtière de l'Afrique de l'Est). La circulation anticyclonique à grande échelle qui prévaut dans l'ISSG entraîne un downwelling physique, qui limite l'apport de nutriments dans les couches de surface (Jena et al., 2013). D'autre part, les tourbillons méso-échelles qui dominent l'EAFR crés des conditions favorables à la prolifération de phytoplancton. Ces tourbillons méso-échelles sont d'une importance capitale pour les prédateurs supérieurs tels que les thons, espadons et oiseaux marins, qui utilisent ces structures comme zones d'alimentation. Les reliefs sous-marins du sud-ouest de l'océan Indien semblent aussi jouer un rôle important comme zones d'alimentation pour ces prédateurs supérieurs (Pinet et al., 2012). Les monts sous-marins du sud-ouest du l'océan Indien sont parmi les moins explorés au monde (Bhattacharya & Chaubey, 2001), avec seuls 15 monts de l'océan Indien ayant fait l'objet d'études biologiques (Sautya et al., 2011). Cette étude contribue donc à améliorer nos connaissances des processus physico-chimique entrainant une réponse biologique à deux monts sous-marins du sud-ouest de l'océan Indien.

Le **chapitre 3** de cette thèse se focalise sur l'influence des tourbillons méso-échelles, du plateau continental de Madagascar et des monts sous-marins peu profonds sur la distribution verticale et spatiale du micronecton avec une approche acoustique. Pendant la campagne MAD-Ridge, un dipôle (paire de tourbillons contra-rotatifs) était présent dans les environs de MAD-Ridge avec la composante anticyclonique stationnée sur le mont pendant toute la campagne et la composante cyclonique situé à l'ouest du mont. Le cyclone a causé une remontée de la thermocline et des eaux plus denses, ainsi qu'un enrichissement biologique caractérisé par des concentrations en chlorophylle plus élevées comparé à l'anticyclone. Les densités du micronecton étaient faibles dans l'anticylone et sur le sommet et les flancs du mont MAD-Ridge par rapport aux densités mesurées dans le tourbillon cyclonique et sur le plateau continental de Madagascar. Le micronecton a suivi le schéma habituel de migration nycthémérale, montant verticalement à la surface au crépuscule et descendant vers les couches plus profondes (moins de 400 m) à l'aube, sauf dans le tourbillon cyclonique pendant MAD-Ridge où des densités acoustiques plus importantes ont été enregistrées dans la couche de surface diurne. Ces densités acoustiques au sein du cyclone dans la couche de surface de jour, ont démontré une forte réponse au 38 kHz comparé au 70 et 120 kHz. Des études antérieures ont démontré que les poissons épi- et mésopélagiques ayant de petites vessies natatoires remplies de gaz et le plancton gélatineux ayant des inclusions de gaz, dominent la fréquence de 38 kHz (Porteiro & Sutton, 2007; Kloser et al., 2002; Kloser et al., 2009; Davison et al., 2015; Cascão et al., 2017; Proud et al., 2018). Les organismes se situant dans la couche de surface au sein du cyclone de jour étaient peut-être des poissons épi- et mésopélagiques remplis de gaz qui nageaient et se nourrissaient activement dans le cyclone, ou des organismes gélatineux avec des inclusions de gaz. Comme démontré dans ce chapitre, il y a peu de probabilité d'un enrichissement local causé par des interactions courants-topographie comme la formation de colonnes de Taylor ou la remontée des isocèles aux monts La Pérouse et MAD-Ridge. Les processus d'enrichissement rencontrés pendant la campagne MAD-Ridge, à savoir une forte productivité primaire et une densité élevée du micronecton, sont principalement liés aux upwellings au sud de Madagascar et à la dynamique des tourbillons méso-échelles, et probablement aussi à l'activité d'ondes internes.

Au cours de mon travail de thèse, j'ai donc mis en évidence que les tourbillons cycloniques peuvent concentrer une forte densité acoustique du micronecton dans la couche de surface (0-200 m) de jour, ce qui est contraire au comportement habituel de la majorité des espèces

micronectoniques qui occupent un habitat profond de jour. Généralement, les tourbillons cycloniques concentrent une forte densité de production primaire dans la couche euphotique, retenant ainsi le zooplancton et, à terme, les poissons mésopélagiques. Les densités acoustiques du micronecton étaient également plus élevées au mont MAD-Ridge comparé à La Pérouse. La dynamique des structures méso-échelles telles que les tourbillons cycloniques et anti-cycloniques au sud de Madagascar, augmente la production primaire et concentre une forte biomasse, abondance et densité acoustique du micronecton dans cette zone qui se démarque ainsi de la région oligotrophe du gyre ISSG au sein duquel se situe La Pérouse. Par mes travaux, j'ai mis en évidence que la distribution spatiale du micronecton dans le sud-ouest de l'océan Indien serait donc influencée par des processus physico-chimiques.

Le **chapitre 4** a pour but de déterminer la distribution verticale et les assemblages du micronecton aux monts La Pérouse et MAD-Ridge. La migration nycthémérale du micronecton est importante pour le transfert de nutriments et d'éléments essentiels de la surface vers les profondeurs. J'ai démontré que certaines espèces du micronecton sont capables d'effectuer de grandes migrations nycthémérales vers la surface (couche 0-200 m) au crépuscule et vers les profondeurs (>400 m) à l'aube. A l'aube, on observe plusieurs vagues de migration de la couche intermédiaire (200-400 m) vers les profondeurs (>400 m) et de la couche de surface vers les profondeurs. Il y a donc plusieurs stratégies de migration. Certaines espèces de la communauté mésopélagique migrent en-dessous de 800 m (probablement afin d'échapper aux prédateurs visuels) alors que d'autres espèces sont non-migrantes et se situent principalement dans la couche de surface (comme certains gélatineux) ou en profondeur telles que les *Cyclothone* sp., de jour comme de nuit.

Les données acoustiques analysées au cours de ma thèse ont également mis en évidence que la couche de surface (0-200 m) est constituée d'espèces de micronecton communes à divers bassins océaniques. Par contre, certaines espèces de poissons mésopélagiques, telle que les *Diaphus suborbitalis*, s'associent uniquement aux sommets et flancs des monts sous-marins La Pérouse et MAD-Ridge de jour comme de nuit. Il a déjà été constaté que de grandes populations de *D. suborbitalis* étaient associées au mont sous-marin de l'Équateur dans l'océan Indien (Parin & Prut'ko, 1985). Ces poissons se trouveraient sur les pentes à 500-600 m de profondeur

pendant la journée et remonteraient en bancs denses et compacts jusqu'à 80 à 150 m de profondeur la nuit pour se nourrir principalement de copépodes (Gorelova & Prut'ko, 1985), tout en étant la proie de plusieurs prédateurs supérieurs tels que les thons et espadons (Parin & Prut'ko, 1985). Ces espèces forment des bancs compacts sur les monts sous-marins afin de bénéficier probablement des avantages que confèrent ces espaces, tels que l'augmentation de proies, la diversité qu'offrent ces types d'habitats et des sites de repos. Cependant, force est de constater que des estimations plus faibles en abondance et biomasse du micronecton ont été enregistrées sur les sommets de La Pérouse et de MAD-Ridge comparé aux alentours immédiats de ces monts. L'obstruction physique créée par un mont sous-marin est supposée réduire la densité des animaux sur les flancs et les sommets, en particulier la nuit (eg. Genin et al., 1988; Diekmann et al., 2006; De Forest & Drazen, 2009).

Par le biais d'analyses d'isotopes stables du $\delta^{13}C$ et $\delta^{15}N$, le **chapitre 5** met en évidence les interactions trophiques du micronecton par rapport à la MOP et au zooplancton aux monts La Pérouse et MAD-Ridge. La MOP de surface a enregistré des valeurs en $\delta^{13}C$ supérieures à MAD-Ridge comparé à La Pérouse. La MOP se constitue généralement de phytoplancton, bactéries, matières fécales et détritus (Riley, 1971; Saino & Hattori, 1987; Fabiano et al., 1993; Dong et al., 2010; Liénart et al., 2017). Les concentrations en chlorophylle de surface étaient plus élevées à MAD-Ridge comparé à La Pérouse (Annasawmy et al., 2019). Les apports nutritifs à MAD-Ridge sont plus élevés qu'à La Pérouse de part l'action des remontées d'eau sur le plateau continental Malgache, entrainant ainsi un enrichissement en phytoplancton (Ramanantsoa et al., 2018), par l'advection au large de cette productivité côtière et/ou du plateau continental par le transport transversal (Noyon et al., 2018), et par un enrichissement au sein des tourbillons méso-échelles qui se déplacent sur le mont MAD-Ridge (De Ruijter et al., 2004; Vianello et al., 2020). La Pérouse, se situant loin des influences marquées par les remontées d'eau et loin des tourbillons à forte puissance, bénéficie moins des apports nutritifs, provoquant ainsi des valeurs en $\delta^{13}C$ moins élevées de la MOP.

Le **chapitre 5** décrit egalement que la MOP et le zooplancton ont des valeurs isotopiques inférieures aux crustacés, céphalopodes et poissons mésopélagiques à La Pérouse et à MAD-Ridge. Le niveau trophique des espèces de micronecton est influencé par le mode alimentaire de l'individu et la taille. Les omnivores (crustacés qui se nourrissent principalement de

zooplancton et de matières végétales) et carnivores (poissons mésopélagiques et céphalopodes qui se nourrissent essentiellement de copépodes, d'amphipodes, d'euphausiacés et d'ostracodes) sont fortement enrichis en $\delta^{15}N$ comparé aux filtreurs (salpes et pyrosomes) et détritivores (larves leptocéphales). Les filtreurs et détritivores ont généralement un niveau trophique de 2. Les crustacés, poissons mésopélagiques et petits céphalopodes se situe généralement à un niveau trophique entre 3 et 4, au-dessus du zooplancton et en-dessous des prédateurs supérieurs tels que les thons et les espadons. La taille d'un individu a généralement une influence sur ces valeurs de $\delta^{15}N$ en raison de la relation taille-proie (un individu plus grand ingérera une proportion plus importante de proies de grande taille ayant un $\delta^{15}N$ plus élevé que des proies de taille inférieure). Cette relation a été observée pour plusieurs espèces de micronecton. Cependant, il a été observé que les poissons mésopélagiques et benthopélagiques associés de façon quasi-permanente sur les sommets et les flancs de La Pérouse et de MAD-Ridge, ont le même niveau trophique quelles que soient leurs tailles. Ceci peut s'expliquer par le fait que ces espèces se nourrissent de proies similaires, ou bien de proies différentes mais ayant le même niveau trophique.

Le micronecton est donc un maillon important dans la chaine alimentaire de par la prédation qu'il exerce sur le zooplancton et comme source d'alimentation pour les prédateurs supérieurs tels que les thons et les espadons. Les différents processus contrôlant la distribution spatiale et verticale du micronecton méritent d'être détaillés car les prédateurs supérieurs marins dépendent de ce groupe, et indirectement les populations humaines par la pêche et ses autres activités économiques associées. Il est donc important de mieux comprendre le fonctionnement des écosystèmes marins associés aux monts sous-marins notamment le rôle des processus physiques qui influencent les différents maillons trophiques, afin de proposer des mesures adaptées à la conservation de ces espaces et à une exploitation raisonnée et durable de leurs ressources marines.

Cette étude a démontré le fonctionnement de l'écosystème de deux relevés topographiques peu étudiés du sud-ouest de l'océan Indien. Lorsqu'on replace les monts La Pérouse et MAD-Ridge dans un contexte régional, les densités acoustiques totales du micronecton au mont La Pérouse sont typiques de celles de la province de l'ISSG, tandis que les réponses acoustiques au mont MAD-Ridge sont typiques de celles de la province de l'EAFR. Les densités acoustiques en

micronectons étaient plus élevées dans l'EAFR et au mont sous-marin MAD-Ridge comparé à la province de l'ISSG et le mont sous-marin La Pérouse, probablement en raison de l'effet des tourbillons méso-échelle et de la productivité accrue dans l'EAFR. Aucune augmentation nette du micronecton n'a été observée aux monts sous-marins par rapport à l'océan environnant dans les provinces biogéochimiques. Cependant, des agréggations denses ont été observées collées aux sommets des deux monts pendant la journée, probablement en raison de la présence de poissons s'agrégeant de façon quasi-permanente sur les sommets et les flancs de ces monts.

Bien que les relevés topographiques soient omniprésents dans les océans du monde, les monts sous-marins et leurs écosystèmes sont encore mal connus. Seuls 0,4 à 4 % de la population mondiale des monts sous-marins ont été directement échantillonnés pour la recherche scientifique (Kvile et al., 2014). Le partage et l'accessibilité des données constituent autant d'obstacles importants à la recherche sur les monts sous-marins. La présente étude vient donc enrichir les connaissances actuelles sur le fonctionnement de l'écosystème des monts sous-marins. Un résultat important de cette étude est la présence d'agréggations denses sur les sommets et les flancs de La Pérouse et de MAD-Ridge de jour comme de nuit. Ce résultat est similaire à celui d'autres études précédentes, dans lesquelles des poissons ont été trouvés en association étroite avec des monts sous-marins dans plus de 150 cas (Kvile et al., 2014). Malgré leurs topographies complexes et leurs processus physiques locaux, il a été démontré que les monts sous-marins confèrent des avantages sélectifs au regroupement des poissons qui utilisent ces caractéristiques pour s'alimenter, se reproduire ou se reposer (Porteiro & Sutton, 2007). L'intégration des observations de cette étude dans des bases de données mondiales telles que le SEEF (Seamount Ecosystem Evaluation Framework) (Kvile et al., 2014) peut aider à identifier les lacunes dans nos connaissances, à caractériser les particularités de chaque mont sous-marin et à tester davantage les effets potentiels des monts sous-marins afin de comprendre quels sont les facteurs qui déterminent la dynamique des différents types de monts. Il est important de mieux comprendre les ecosystèmes associés à différents monts sous-marins afin de pouvoir proposer des mesures de gestion appropriées quant aux ressources associées.

Glossary of principal abbreviations

Regions, provinces and zones

AAIW	Antarctic Intermediate Water
ADT	Absolute Dynamic Topography
BPA	Benthic Protected Area
CTD	Conductivity Temperature Depth (rosette system)
DCM	Deep Chlorophyll Maximum
DSL	Deep scattering layer
DVM	Diel Vertical Migration
EAFR	East African Coastal Province
EBSA	Ecologically and Biologically Significant Area
EEZ	Exclusive Economic Zone
EMC	East Madagascar Current
Fmax depth	Depth of the maximum Fluorescence
IOTC	Indian Ocean Tuna Commission
ISSG	Indian South Subtropical Gyre
IYGPT	International Young Gadoid Pelagic Trawl
L-ADCP	Lowered Acoustic Doppler Current Profiler
MPA	Marine Protected Area
MSLA	Mean Sea Level Anomalies
NADW	North Atlantic Deep Water
NEMC	North East Madagascar Current
Nmi	Nautical mile
POC	Particulate Organic Carbon
POM	Particulate Organic Matter
RFMO	Regional Fisheries Management Organization
RGB	Red Green Blue (composite images generated from acoustic data)
s_a	Area scattering coefficient

s_A, NASC	Nautical Area Scattering Coefficient
SEC	South Equatorial Current
SEMC	South East Madagascar Current
SIODFA	Southern Indian Ocean Deepsea Fishers Association
SIOFA	Southern Indian Ocean Fisheries Agreement
SSC	Sea surface chlorophyll
SSL	Shallow scattering layer
s_v	Volume backscattering coefficient
Sv	Volume backscattering strength
SWIO	South West Indian Ocean
SWIOFC	Southwest Indian Ocean Fisheries Commission
SWIR	Southwest Indian Ridge
TL	Trophic Level
TSG	Thermosalinograph
uCDW	upper Circumpolar Deep Water
WIO	Western Indian Ocean

Chapter 1: General Introduction

1.1 Background

1.1.1 Seamount geology and characteristics

Seamounts are ubiquitous features of the world's oceans. Depending on their definition, there are an estimated 200 000 seamounts (Kitchingman & Lai, 2004; Wessel, 2007; Clark et al., 2010b) (Fig. 1.1). Seamounts have an elevation >1000 m (IHO, 2008) whereas knolls have an elevation that ranges between 500-1000m. Approximately 30 000-60 000 seamounts and 138 000 knolls have been identified (Hillier & Watts, 2007; Costello et al., 2010; Yesson et al., 2011). An estimated 24 000 to 100 000 large seamounts remain uncharted (Hillier & Watts, 2007; Wessel et al., 2010). Seamounts may also occur as chains perpendicular to a ridge, as isolated topographic features or in clusters (Kitchingman & Lai, 2004; Etnoyer et al., 2010). Most seamounts are the result of intense oceanic volcanism (Craig & Sandwell, 1988; Wessel, 2001; Yesson et al., 2011) and are associated with intraplate hotspots, mid-ocean ridges or island arcs (Wessel, 2007; Yesson et al., 2011).

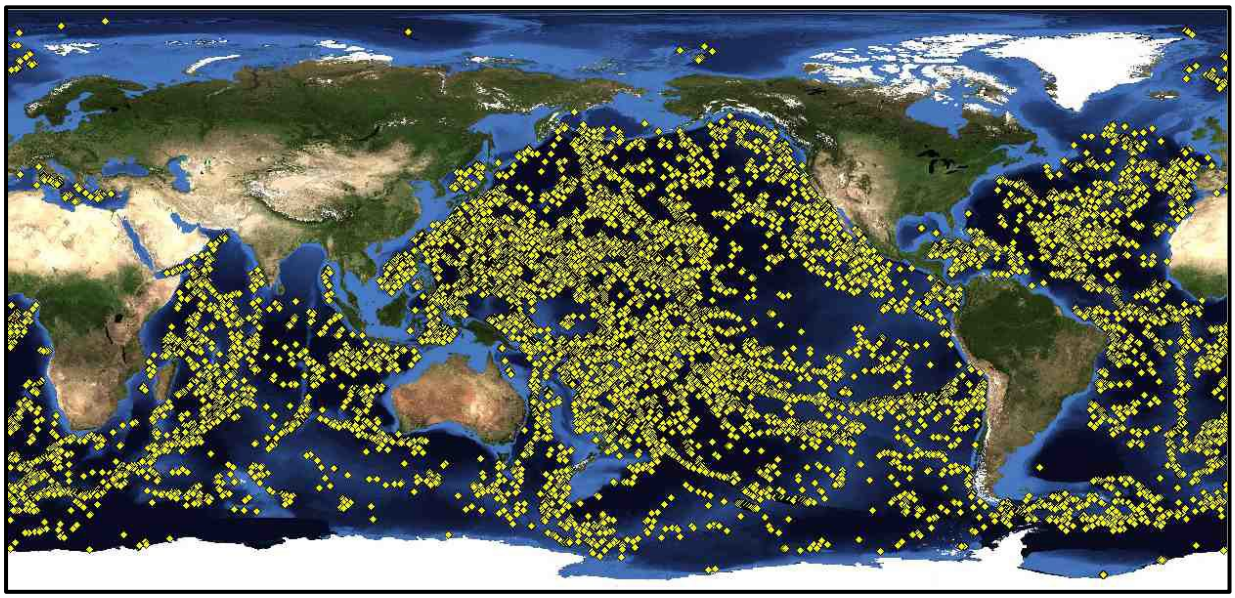

Figure 1.1 Estimated global distribution of large seamounts with an elevation >1500 m (yellow diamond symbols) based on data described in Kitchingman & Lai, 2004 (Source: Clark, 2009).

The majority of seamounts are composed of basalt (Wessel, 2007). Approximately 50 million tons of basalt per year are estimated to be required to produce seamounts (Iyer et al., 2012), alongside several other factors deemed necessary to control the birth and development of such features (Craig & Sandwell, 1988). An adequate supply of magma with sufficient hydraulic head and latent heat is deemed essential to penetrate the oceanic lithosphere without freezing during ascent. For a volcano to develop, the lithosphere must remain over the heat source or

magma pool for a sufficient amount of time (Craig & Sandwell, 1988). In the early stages of formation, seamounts on the deep seafloor may exhibit strong axial symmetry. The seamount may ultimately grow if additional magma is available and if the seafloor is mechanically strong (Wessel, 2007). Seamounts can be observed using satellite altimetry (Wessel, 2001; Kitchingman & Lai, 2004).

1.1.2 Physical processes resulting from current-topography interactions

As topographic obstacles rising from abyssal depths, interactions are expected with the local physical flow regime causing increased hydrodynamic activities in the vicinity of the seamount, relative to the flat abyssal ocean (White et al., 2007; Mohn et al., 2009). These pinnacles may also disrupt large scale oceanic flow (Royer, 1978). Seamounts may be circular, elongated, conical or elliptical in shape and may be shallow, intermediate (summit below the euphotic zone but within the upper 400 m) and deep (summit below 400 m) (White & Mohn, 2004). There is also an ecological definition associated to seamounts with shallow seamounts penetrating the euphotic zone (Yesson et al., 2011), middle-depth seamounts reaching the base of the euphotic zone from 1500 m depth while deeper seamounts are found below the zone of influence of the deep-scattering layer (Pitcher et al., 2007). The particular combination of seamounts' shapes, sizes and summit depths ultimately determines the physical flow processes. A variety of flow disturbances have been described (White et al., 2007; Fig. 1.2) and a number of flow-topography interactions have been observed at pinnacles of the Atlantic and Pacific Oceans (Appendix: Table A).

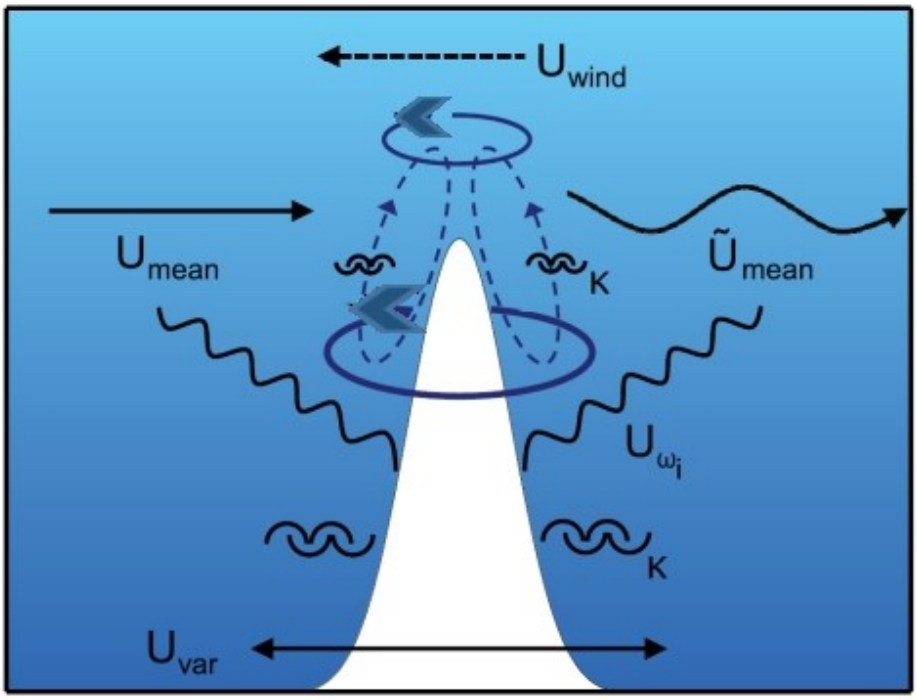

Figure 1.2 Characteristic features of motion at an isolated southern hemisphere seamount. These features, including a vertical circulation cell, isopycnal doming and anticyclonic-horizontal circulation, are shown near the summit depth, superimposed on oscillatory currents and oscillatory temperature and salinity distributions. The occurrence, properties and variability of these features depend on local turbulence K, internal waves $U_{\omega i}$ (propagating horizontally and vertically), and on incident mean current U_{mean}, eddies $\tilde{U}_{mean}$, tidal and other oscillations U_{var}, and possibly wind-driven currents U_{wind} (Source: adapted from Lavelle & Mohn, 2010).

1.1.2.1 Eddy-topography interactions

Mesoscale eddies, that range in diameter from 10 to 300 km, are typically produced as a result of wind stress circulation patterns (Falkowski et al., 1991; Mann & Lazier, 2006). These eddies are circulating water masses and are either cyclonic (clockwise rotation in the southern hemisphere) or anticyclonic (anticlockwise rotation in the southern hemisphere) (Bakun, 1996). The cyclonic rotation may lead to a doming and localized upwelling of cold, deep, nutrient-rich waters into the euphotic zone (Falkowski et al., 1991) whereas anticyclonic rotation may lead to a depression of isotherms and downwelling of nutrient-rich waters.

As topographic obstacles, seamounts may either bifurcate, trap, split or destroy eddies (Schouten et al., 2000; Herbette et al., 2003; Adduce & Cenedese, 2004; Sutyrin, 2006; Lavelle & Mohn, 2010). Outcomes of eddy-seamount interactions largely depend on the seamount's dimensions (width, height and orientation) (van Geffen & Davies, 1999) and current speeds. Eddies with diameters up to ~37 km have been reported to be formed from the North Pacific

current and seamount interactions north of Hawaii (Royer, 1978). Some seamounts such as the Emperor Seamount Chain in the Pacific Ocean may act as generators of quasi-stationary mesoscale eddies (Bograd et al., 1997). Haida eddies from the northeast Pacific have been shown to be associated with Bowie seamount, with the Haida-2000a eddy being trapped on the seamount for a period of 3 months (Dower et al., 2004). Numerical models have also shown that an eddy may cross a ridge or be rebounded by the topography, preventing the eddy from crossing the ridge on its first encounter (van Geffen & Davies, 2000b).

The propagation of Meddies (Mediterranean Water eddies), formed from the Mediterranean outflow near the continental slope of Portugal, may also have weak, moderate or strong interactions with seamounts of the Atlantic Ocean (Bashmachnikov et al., 2009). Weak interactions can lead to deflection of Meddies after the latter have rotated some distance around large seamounts (van Geffen & Davies, 2000a). The deflection of a Meddy was observed by the Gorringe Bank aka. Gorringe Ridge (Bower et al., 1995) in the Atlantic. At Seine seamount in the subtropical northeast Atlantic, portion of a Meddy was seen to escape the seamount after having performed several rotations around the summit (Baschmachnikov et al., 2009). Strong interactions of Meddies with seamounts can lead to vortex trapping or splitting (Baschmachnikov et al., 2009). Meddies were partially split after collision with Hyères and Irving seamounts (Shapiro et al., 1995) and destroyed by Sedlo (Bashmachnikov et al., 2009), Hyères (Richardson et al., 1989; 2000), Josephine (Schultz Tokos et al., 1994; Richardson et al., 2000), Lion seamounts and pinnacles in the Horseshoe chain in the Atlantic Ocean (Richardson et al., 2000). A Meddy was further cleaved into two approximate equally sized smaller Meddies by Cruiser and Irving seamounts (Richardson et al., 2000).

1.1.2.2 Local processes at seamounts- Isopycnal doming

Localised processes are also observed at seamounts, such as isopycnal doming (Owens & Hogg, 1980), formation of enclosed circulation cells (Freeland, 1994), amplification and rectification of tidal motions (Brink, 1995), and increased vertical mixing (Kunze & Sanford, 1996; Eriksen, 1998). Isopycnal doming, i.e. upwelling on the upstream side of a topographic feature and doming of density surfaces, is due to ocean currents impinging on a seamount (Martin & Christiansen, 2009) or due to the rectification by trapped waves for sub-inertial frequencies (Mohn & Beckmann, 2002). The doming of isotherms is generated when the fluid is forced to rise over the pinnacle due to the associated geostropically induced anticyclonic tendency of the flow field (Brainard, 1986). Topographic obstacles may cause a dome-like

structure in the temperature, salinity and density fields (Torres et al., 2004) and can result from Taylor cone formations (White et al., 2007).

1.1.2.3 Local processes at seamounts- Taylor columns

Trapped, enclosed circulations over topographic obstacles are known as Taylor columns (or cones) and have been reported to occur over some seamounts of the Atlantic and Pacific oceans (Appendix: Table A). The Taylor-Proudman Theorem showed that when a steady and homogeneous flow encounters a seamount, an anticyclonic circulation following the isobaths is generated with any fluid being trapped in a stagnant area above the topographic obstacle, thus creating a Taylor column (Huppert, 1975; Huppert & Bryan, 1976; White & Mohn 2004; Fig. 1.3). Flow transitioning to equilibrium will cause two counter rotating vortices to form over idealized Gaussian-shaped seamounts, with stronger impinging flows causing the cyclonic vortex to be shed downstream (White et al., 2007) while the anticyclonic vortex remains over the seamount (Huppert & Brian, 1976; Lavelle & Mohn, 2010).

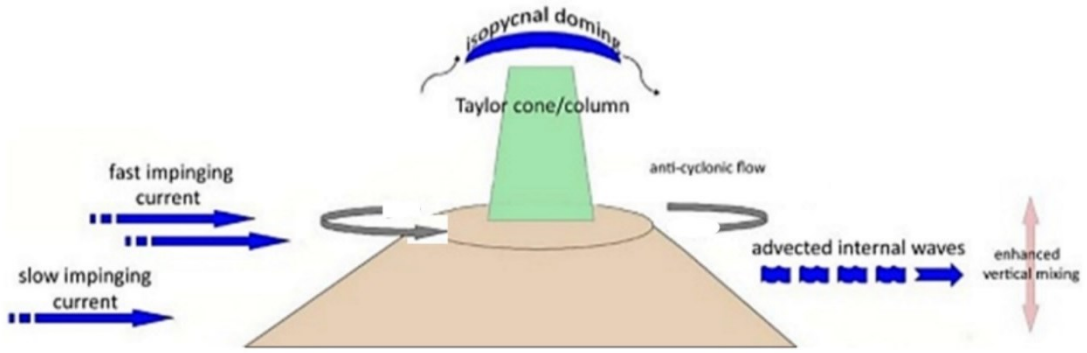

Figure 1.3 Characteristic features of motion at an isolated seamount, including flow patterns, and features such as Taylor columns, isopycnal doming and processes such as enhanced vertical mixing [Source: adapted from Henry et al., 2012].

Factors such as seamount's shape, size, depth (of the summit), turbulence, stratification, current speed and direction, may influence the development of a Taylor Column. In those instances where the water column is stratified, the Taylor column does not extend to the sea surface and is hence known as a "Taylor cap" (González-Pola et al., 2012). If the current velocity is too high, a Taylor cap will not persist over the seamount (Lavelle & Mohn, 2010). A set of non-dimensional parameters such as the Rossby number (Ro: a measure for the relative importance of advective and rotational effects), the Burger number (a measure for the strength of stratification) and the fractional height of the seamount (α), may be used as criteria for the formation of localised induced circulation around a seamount (Turnewitsch et al., 2004; White

et al., 2007; Fig. 1.4). Taylor caps may form over idealized Gaussian-shaped seamounts for specific combinations of Ro and α (Chapman & Haidvogel, 1992) and as such, Taylor columns will only form transiently.

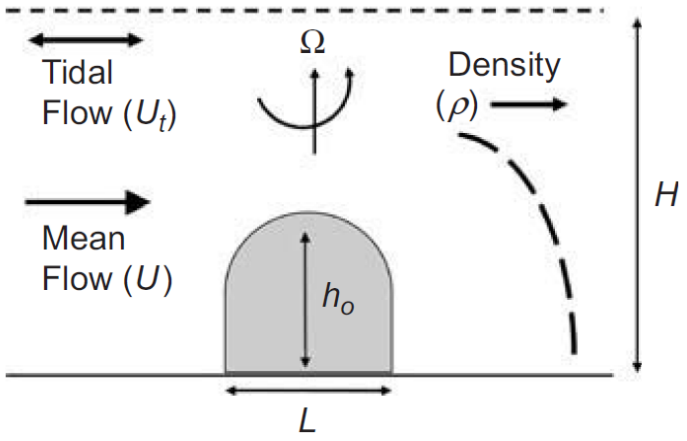

The Rossby number	$Ro = U/f \times L$
The relative height of the seamount to water depth	$\alpha = h_0/H$
The Burger number	$B = N \times H/f \times L$

Figure 1.4 Diagram of the main factors controlling the localised dynamic processes at isolated topographic features, with U_t representing the tidal flow; U, the mean flow; ρ the water density with depth; L the seamount width in m; h_0 is the height of the seamount relative to the water depth H; N, the vertical stratification, Ω, the Earth's angular velocity, and f, the Coriolis parameter [White et al., 2007].

1.1.2.4 Local processes at seamounts- Tidal amplification and rectification

Closed anticyclonic circulation cells around seamounts may also arise through tidal rectification, i.e. the generation of residual mean currents over the seamount by tidal flow (Mohn, 2002; White et al., 2007). A variety of processes such as seamount-trapped waves, tidal rectification and amplification, generation of internal tides and locally enhanced turbulent mixing, may arise through the interaction of tides with isolated seamounts (Mohn & White, 2010). Tidal amplification over seamounts is due to the squeezing of flow as it passes over the topographic feature and formation of wave motions which are trapped at the bottom of the seamount (Brink, 1989) and rotate in an anticyclonic direction about the seamount (Beckmann et al., 2001). Periodic tidal forcing is a dominant phenomenon at the Great Meteor seamount in the North Atlantic, leading to closed circulation cells, generation of internal waves, flow

rectification and trapped waves (Mohn & Beckmann, 2002). Tidal rectification was shown to play an important role in generating anticyclonic circulations above the summit of Porcupine Bank along the shelf-edge west of Ireland and result in dome-like deformations in the temperature and density fields (Mohn, 2002).

1.1.2.5 Local processes at seamounts- Internal waves and vertical mixing

Seamounts have also been reported to act as energy sinks for internal wave energy which cause perturbations in the deep ocean (White & Mohn 2004). Topographically related processes that can generate mixing above the bottom include internal wave reflection and generation of internal tides (Eriksen, 1998; Kunze & Llewellyn Smith, 2004). When internal waves reflect from the bottom, the energy density and vertical current shear produced by the internal wave changes, leading to wave overturn and/or turbulent mixing (White & Mohn, 2004). Studies have shown a 100 to 10 000-fold increase in turbulent mixing at shallow topographic features relative to the far field (Lueck & Mudge, 1997). Enhanced turbulent mixing at seamounts may aid additional nutrient fluxes to the euphotic zone (Clark et al., 2010b).

1.1.3 Biological responses at seamounts

1.1.3.1 Seamount productivity

The dynamic conditions at seamounts are suggested to favour enhanced productivity (White & Mohn, 2004). The uplifting of isotherms through Taylor cap formation or internal wave deflection, may bring deeper nutrient rich water over the seamount where, under favourable light conditions, may enhance local productivity in the surface waters above the seamount (Dower et al., 1992; Genin, 2004; White & Mohn 2004). In order to have a significant effect on higher trophic levels, phytoplankton entrapment of the order of weeks or months is necessary (Boehlert & Genin, 1987; Rogers, 1994), with anticyclonic vortices generated by topography-current and topography-internal/tidal wave interactions acting as retention mechanisms for this organic matter generated locally or advected from the far field (Vilas et al., 2009).

1.1.3.2 Zooplankton dynamics at seamounts

In theory, enhanced primary production at seamounts caused by local dynamic current-topography interactions, offer higher food concentrations to zooplankton communities relative to the surrounding open ocean (Hirch et al., 2009). Interactions of zooplankton communities with topographic features have been suggested to result in gap formation (areas devoid of vertically migrating zooplankton) (Fig. 1.5), enhanced patchiness within the gaps and downstream of the seamount (Isaacs & Schwartzlose, 1965) and increased numbers of

crustacean carcasses over the seamount (Haury et al., 2000), with the three processes reported to be tightly linked (Haury et al., 2000; White & Mohn, 2004).

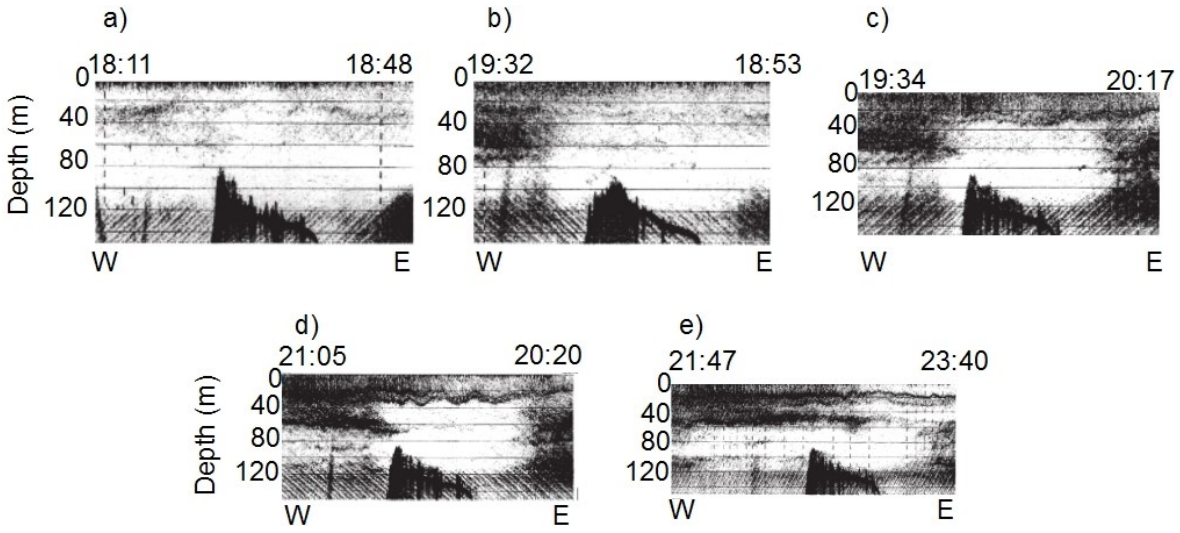

Figure 1.5(a-e) Sequential acoustic transects of the 120 kHz frequency across Sixtymile Bank (west of California, USA), showing a gap formation in zooplankton distributions over the summit. By the last transect (e), the gap had advected ~3 km eastward and was beginning to fill with intrusions of zooplankton carried by the currents (Source: Haury et al., 2000).

An increase in zooplankton densities has been observed in the waters above Minami-kasuga seamount both within and above a dome of cold dense water (Genin & Boehlert, 1985). However, no significant increase in zooplankton biomass has been observed above Seine, Sedlo (Hirch et al., 2009), Senghor, Ampère (Denda & Christiansen, 2014; Denda et al., 2017a), Cobb (Dower & Mackas, 1996), Dom João de Castro (Sobrinho-Gonçalves & Cardigos, 2006), Volcano 7 (Saltzman & Wishner, 1997) and Condor (Carmo et al., 2013) seamounts. Gaps devoid of vertically migrating zooplankton have also been observed above the summit of Sixtymile bank (Genin et al., 1994; Haury et al., 2000; Fig. 1.5).

The reduction of zooplankton biomass has been attributed to either predation by resident seamount-associated fishes, displacement of migrating and deep-water zooplankton taxa during the day and active avoidance of the seamounts (Martin & Christiansen, 2009; Denda & Christiansen, 2014). The physical displacement of migrating zooplankton and predation pressure have been suggested to lead to gap formation in zooplankton distribution (Haury et al., 2000), with average abundances being higher away from the summit rather than within the gaps (Genin et al., 1994). Increased predation pressure has further been hypothesized to result in increased carcasses at Dowd seamount, Fieberling Guyot, Sixtymile bank (Haury et al.,

2000) and above the summit of Jasper seamount (Haury et al., 1995). This predation pressure is believed to be influenced by the topography itself which blocks zooplankton communities in their pre-dawn descent, exposing them to visual predators in daylight (Genin, 2004; Clark et al., 2010b).

In the upper layers of the open ocean, zooplankton represents a key link between primary production and higher trophic levels, such as micronekton and ultimately top predators (Potier et al., 2007). Some argue, however, against the bottom-up transfer of energy from locally enhanced primary production through upwelling at abrupt features (Genin & Dower, 2007; Morato et al., 2009). Indeed, as mentioned previously, phytoplankton entrapment of the order of weeks or months would be necessary to have an influence on secondary and tertiary consumers (Genin & Dower, 2007). Other mechanisms which have been suggested to promote aggregations of zooplankton over abrupt topographies (Genin, 2004; Genin & Dower, 2007):

1) Topographic blockage of daily migrating organisms

Also known as the "sound-scattering layer interception hypothesis", the "topographic blockage" hypothesis suggests that migrating organisms are blocked by the seamount topography and become trapped above the seamount at dawn before being consumed by predators (Genin, 2004) (Fig. 1.6).

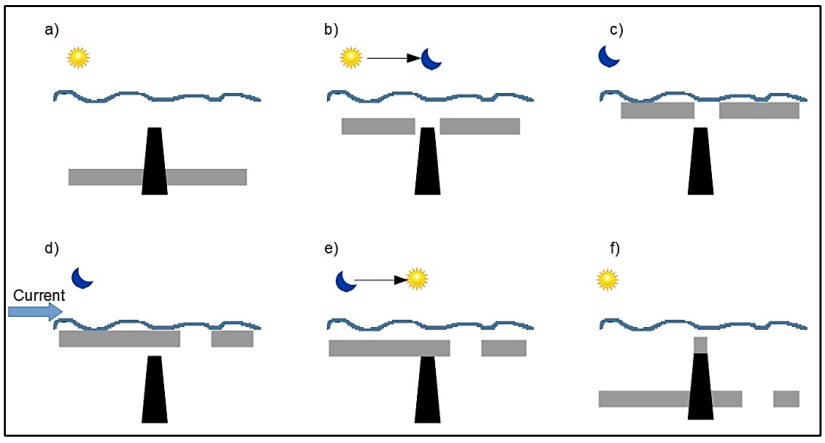

Figure 1.6 Schematic showing the bottom trapping of vertically migrating zooplankton (horizontal grey bar) over a seamount (black polygon) where the summit is deeper than the photic layer but shallower that the daytime depth of migrating zooplankters. Sun and moon symbols indicate day and night. The current is considered to flow from left to right throughout the water column for simplicity (Source: adapted from Genin & Dower, 2007).

The schematic diagram shows the migrating zooplankton to be found on the seamount slopes during the day (Fig. 1.6a). At sunset, the organisms ascend to the photic layer, forming a gap

the width of which equals to that of the seamount at the depth where the migrating zooplankton were found during the day (Fig. 1.6b). The zooplankton drift with the surface current, gradually displacing the gap in zooplankton distribution away from the seamount. Other organisms are advected horizontally from the upstream region to above the seamount summit (Fig. 1.6c, d). At sunrise, the zooplankton start their descent. A layer of zooplankton is found above the entire shallow summit (Fig. 1.6e) and is blocked by the topography, unable to complete their descent to deeper layers (Fig. 1.6f).

2) Accumulation of animals maintaining their depth by swimming against upwelling

Some organisms are able to actively swim against vertical currents in order to maintain their position at specific depths in the water column (Genin, 2005). Counter-upwelling depth retention is believed to occur to avoid more illuminated waters during daytime (Genin, 2004). Organisms would hence remain in deeper layers. Another explanation for depth retention is the preferential association of organisms with layers of high food concentrations.

3) Accumulation by depth retention of animals swimming against downwelling

Zooplankton may also exhibit depth retention by swimming upward against downwelling currents. These counter-downwelling accumulations of organisms have been reported to occur mostly in the photic layer and the exact mechanisms explaining this behaviour are unclear (Genin, 2004).

4) Amplification of currents above abrupt features leading to enhanced fluxes of suspended food.

The above mentioned mechanisms that might cause biomass to accumulate at seamounts generate "trophic focusing", whereby prey from large volumes of flowing water is accumulated in a relatively small area above the seamount, subsidizing higher trophic levels such as pelagic fishes and marine mammals that aggregate over their concentrated prey (Genin, 2004; Carmo et al., 2013). The magnitude of this subsidy depends on the flow speed, the concentration of plankton and detritus and the ability of the resident communities to trap drifting food particles (Genin & Dower, 2007). Unlike corals and sponges that remain stationary and wait for currents to bring food, mobile organisms can swim and enhance their encounter rate with their prey (Genin & Dower, 2007).

1.1.3.3 Seamount associated fish species

Seamounts allow fish to rest in the quiescent shelters offered by the topography during non-feeding intervals, while they continuously sense the abundance of prey in the flowing water. Fish will feed in the flow when the prey flux is high. In the open ocean, fish have to swim

constantly to find rich patches of prey (Genin, 2004). This is the basis of the "feed-rest" hypothesis (Genin & Dower, 2007; Porteiro & Sutton, 2007) believed to be supported by the horizontal flux of allochthonous prey that pass seamounts and sustain rich communities living on seamounts (Morato et al., 2009; Clark et al., 2010b). Several studies have shown that a number of species can be defined as being "seamount-associated", i.e. they occur almost exclusively or in higher abundance over a seamount as opposed to adjacent waters (De Forest & Drazen, 2009). A list of common seamount-associated fish species is given in the Appendix section (Table B).

Population maintenance of seamount-associated species in the face of increased current speeds may depend on a range of behavioural and physical mechanisms (Wilson & Boehlert, 2004). It has been observed that populations of *Maurolicus muelleri* and *Gnathophausia longispina* are able to adjust their depths throughout the night through exposure to differential current directions. *Maurolicus muelleri* and *G. longispina* that had been advected from the summit would descend to bottom layers at the seamount flank, then orient in an upflank direction such that they can migrate vertically up the slope to shallower layers by nightfall (Wilson & Boehlert, 2004). To prevent advective loss from the seamount, seamount-associated species orient themselves and reduce nearest-neighbour distances, thus allowing individuals to be in the direction that densities of scatterers are the greatest, i.e. toward the summit (Wilson & Firing, 1992). The association of these species with seamounts may hence confer some selective advantages such as "habitat diversification" in which seamounts provide a range of favourable habitats (both pelagic and benthic) (Denda et al., 2017c; Letessier et al., 2017), enhanced feeding success (Haury et al., 1995; Wilson & Boehlert, 2004), decreased energy loss through the "feed-rest" hypothesis (Genin & Dower, 2007) and enhanced encounter rate with other con-specifics for reproduction (De Forest & Drazen, 2009).

1.1.3.4 Mesopelagic organisms at seamounts

The mesopelagic fish species *M. muelleri* and *C. maderensis* and the crustacean *G. longispina* are few examples of a widespread and common group of organisms collectively called micronekton. They form a substantial biomass with an estimated number of >10 000 million tons of mesopelagic fishes in oceanic waters worldwide and 380 million tons of Antarctic Krill recorded in the Southern Ocean (Atkinson et al., 2009; Irigoien et al., 2014). Micronekton are a diverse assemblage of crustaceans (including large euphausiids, pelagic decapods, and mysids), cephalopods (small species and juvenile stages of large oceanic species) and fishes (mainly mesopelagic species and juveniles of pelagic nekton) (Brodeur & Yamamura, 2005;

De Forest & Drazen, 2009; Drazen et al., 2011; Ménard et al., 2014; Annasawmy et al., 2018). They range in size from 2-20 cm. Micronekton organisms are important in the energy transfer to higher trophic levels since several species are preyed upon by apex predators such as tuna, swordfish and seabird (Guinet et al., 1996; Bertrand et al., 2002; Potier et al., 2007; Cherel et al., 2010; Danckwerts et al., 2014; Jaquemet et al., 2014). They also play a key role in energy transfer to the deep ocean via respiration, excretion and natural mortality (Hidaka et al., 2001; Catul et al., 2011; Bianchi et al., 2013). Several species of micronekton undergo diel vertical migrations (DVM) of several hundred metres to the surface waters at dusk and to deeper waters at dawn (Lebourges-Dhaussy et al., 2000; Béhagle et al., 2014; Annasawmy et al., 2018).

Gelatinous salps and pyrosomes are also commonly caught in mesopelagic trawl surveys. Salps and pyrosomes are pelagic tunicates that feed in surface waters (Zeldis et al., 1995; Perissinotto & Pakhomov, 1998; Décima et al., 2018). They exhibit non-selective feeding (Nishikawa et al., 1995; Kremer, 2002) and are important in the carbon and nitrogen export to the deep ocean through the sinking of their large and rapidly sinking fecal pellets (Bruland & Silver, 1981; Morris et al., 1988; Caron et al., 1989; Phillips et al., 2009; Henschke et al., 2016; Iversen et al., 2017). They are further important in the rapid sedimentation of microflagellates and coccoliths that are too small to be consumed by other herbivores (Iseki, 1981). Salps' fecal pellets thus play an important role in contributing to the energy requirements of bathypelagic organisms (Wiebe et al., 1979; Iseki, 1981; Kremer, 2002). Some species of salps and pyrosomes are known to undertake DVM over several hundred metres to the surface layer at night (Wiebe et al., 1979; Andersen & Sardou, 1994; Madin et al., 2006; Décima et al., 2018) and even to perform reverse migrations by streaming up the water column during the day (Madin et al., 1996). Some salps are prey to other micronekton such as *Cubiceps pauciradiatus* (Potier et al., 2008). Gelatinous plankton are also preyed upon by several apex predators including lancetfish *Alepisaurus ferox* (albeit in small proportions; Potier et al., 2007), yellowfin tuna *Thunnus albacares* (Grubbs et al., 2001), bluefin tuna *Thunnus thynnus*, little tunny *Euthynnus alletteratus*, spearfish *Tetrapturus belone*, swordfish *Xiphias gladius* and loggerhead sea turtles *Caretta caretta* (Cardona et al., 2012).

Several studies have found higher biomasses of micronekton scattering layers at seamounts' flanks and summits relative to the surrounding ocean, e.g. the Emperor seamount in the Pacific (265m, Boehlert, 1988); Cross in the Pacific (330 m, Johnston et al., 2008); Condor (182-214 m) and Gigante (161 m) in the Azores (Cascão et al., 2017). By contrast, other studies based on net surveys have found reduced micronekton abundance over Cross pinnacle (De Forest &

Drazen 2009; Drazen et al., 2011) and reduced mesopelagic fish densities, species numbers and diversity above the flanks of Atlantis (250-400 m) and Great Meteor (330 m) seamounts in the NE Atlantic (Pusch et al., 2004), and Sixtymile Bank (97 m) in the North Pacific (Haury et al., 2000).

Several hypotheses have been developed to explain the high abundance and biomass estimates of micronekton typically observed at seamounts: (1) enhanced primary and secondary production due to local physico-chemical processes (Dower et al., 1992; Mouriño et al., 2001), (2) advection and retention of organisms from the surrounding ocean (Isaacs & Schwartzlose, 1965; Genin, 2004; Wilson & Boehlert, 2004), (3) the "feed-rest" hypothesis (Genin & Boehlert, 1985; Porteiro & Sutton, 2007; Cascão et al., 2017), (4) lunar-related light illumination in the form of the lunar cycle with increased abundance during the new moon phase (Drazen et al., 2011), and (5) population maintenance at the summit through a combination of physical and behavioural mechanisms such as directed swimming behaviours to prevent advection to the far field (Wilson & Boehlert, 2004). The hypotheses formulated to explain low biomasses at seamounts are equally numerous and include: (1) predation, (2) advection of organisms from the summit due to physical processes, (3) active avoidance of the summit (Martin & Christiansen, 2009; Pusch et al., 2004) because of the presence of a hard substrate or increased predator abundance (Drazen et al., 2011), or because organisms have daytime depths that are deeper than the depth of the summit (De Forest & Drazen 2009), and (4) moon phase with a reduction in abundance during full moon (Drazen et al., 2011).

According to Porteiro & Sutton (2007), interactions of midwater fishes with seamounts can be divided into four groups:

1) Mesopelagic fauna that undergo their daily vertical migration process by migrating to the epipelagic layer (above 200 m) at night and interacting with seamounts during their migration process (Fig. 1.7). These organisms may be advected over seamounts by surface currents at night and remained trapped at the summit of shallow seamounts at dawn before being predated upon, resulting in a "gap formation" above seamounts.

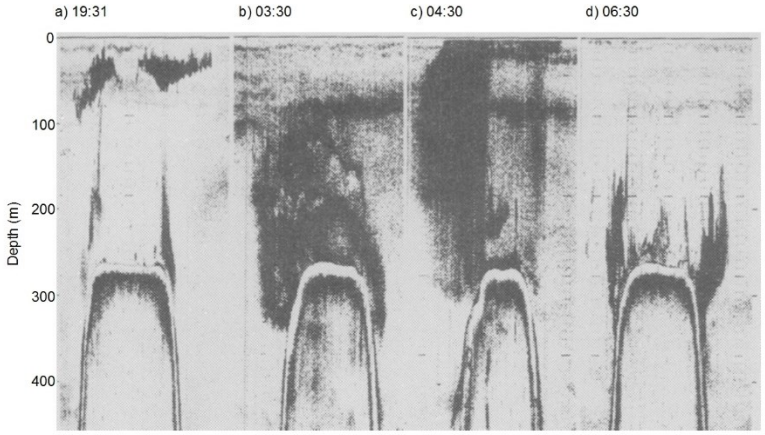

Figure 1.7 Time-series from 19:31 pm to 06:30 am of acoustic transects of the 38 kHz frequency over Southeast Hancock seamount on 17-18 July 1984. (a) At dusk, the scattering layers (consisting mainly of the fish M. muelleri), migrated vertically up the water column to ~50 m. (b) The scattering layer developed around the seamount at night. (c) The scattering layer remained stationary in the surface waters throughout the night and as light intensity increased, some scatterers moved downward. (d) Some scatterers remained above the seamount flanks late in the morning at depths as shallow as ~170 m (Source: Boehlert, 1988).

2) Weakly migrant or non-migrant midwater fishes that enter the benthopelagic zone around seamounts. These species may not be able to counter strong currents and are hence advected over seamounts and are found in equally great abundances at seamount and non-seamount stations.

3) Adults of meso- and bathypelagic species that dwell in the benthopelagic realm probably to increase feeding efficiency through the "feed-rest" hypothesis (Fig. 1.8)

4) "Pseudoceanic" or "neritopelagic" species that occur near seamounts and are absent or less abundant in oceanic waters and that resist advection off the seamounts.

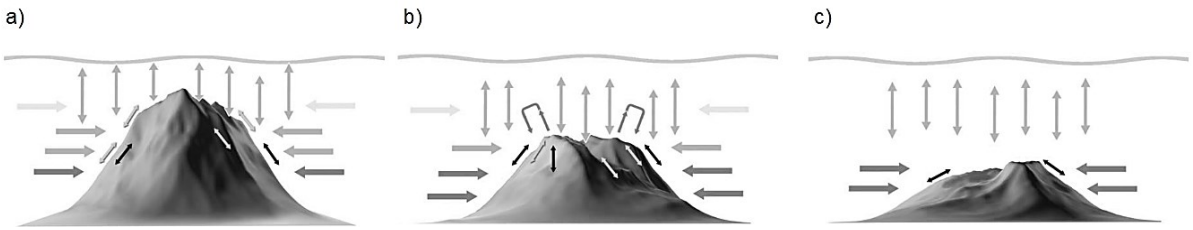

Figure 1.8 Interactions between the different groups of deep-pelagic fishes and seamounts of various heights with the summit entering (a) epipelagic layers, (b) mesopelagic layers, and (c) bathypelagic layers. Horizontal arrows: non-migrant and weakly migrant meso- and bathypelagic fishes that are laterally advected to the benthopelagic zone around seamounts. Vertical arrows: Vertically migrating fishes interacting with the seamounts during their DVM.

Black arrows near seamount: adults of meso- and bathypelagic micronekton species dwelling in the benthopelagic zones. Grey arrows near seamount: non-migrant micronekton fish species associating with the benthopelagic layers of seamounts. U-shaped arrows: migrant micronekton fish species associated with the benthopelagic layers of seamounts and performing DVM (Source: Porteiro & Sutton, 2007).

Mechanisms advecting or trapping micronekton at seamounts are equally important since it has been reported that several seamount-dwelling predators rely heavily on migrating micronekton (Sutton et al., 2010). At the Southeast Hancock seamount, pelagic armorheads, *Pseudopentaceros wheeleri*, were shown to rely heavily on migrating micronekton (pelagic tunicates, crustaceans and mesopelagic fishes) that were advected and trapped over the summit during their morning descent (Seki & Somerton, 1994). Epibenthic *Sebastes* spp. have been shown to feed on the crustaceans *Euphausia pacifica*, advected above Nidever bank by strong currents (Genin et al., 1988). At Sedlo seamount, the seamount-associated benthopelagic fishes, orange roughy (*Hoplostethus atlanticus*), were demonstrated to rely on non-migrant deeper meso- and bathypelagic prey items such as large lanternfishes and dragonfishes (Barcelos, 2005). Several studies, however, have shown the vulnerability of seamount-aggregating fishes to exploitation by commercial fisheries (Ingole & Koslow, 2005; Morato et al., 2006; Watson et al., 2007).

1.1.4 Large-scale fisheries at seamounts

A large number of seamounts from around the world are subjected to fishing pressures (Clark et al., 2007) (Fig. 1.9) both for primary (that occur exclusively on seamounts) and secondary seamount species (not occurring exclusively on seamounts) (Fig. 1.10a, b). After 10 years of commercial exploitation by Soviet and Japanese vessels and over 800 000 tons of cumulative catch, pelagic armorheads (*Pseudopentaceros richardsoni*) were reportedly fished to commercial extinction on the Hawaiian and Emperor seamount chains in the 1960s (Koslow, 2007). Strong decreases in orange roughy catch rates over time were observed over New Zealand seamounts due to extensive bottom trawling (Clark, 1999; 2001). A pattern of serial depletion of seamount demersal and benthic fish populations has been observed, whereby the fishery drives the target species to near depletion before moving onto new seamounts as catches decline (Clark, 1999).

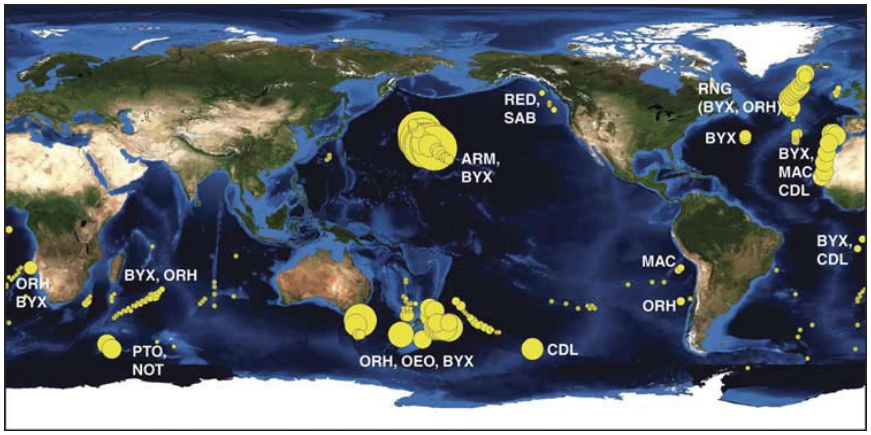

Figure 1.9 Relative size of historical (1960-1980) seamount fisheries for Alfonsino (BYX), Orange roughy (ORH), Oreos (OEO), Cardinalfish (CDL), Redfish (RED), Pelagic armorhead (ARM), Mackerel (MAC), Roundnouse grenadier (RNG), Sablefish (SAB), Notothenid cods (NOT) and Toothfish (PTO). Data are gridded by 1° squares. Circle size is proportional to total catch for that grid square, maximum is 85 000 tons (Source: Clark et al., 2007).

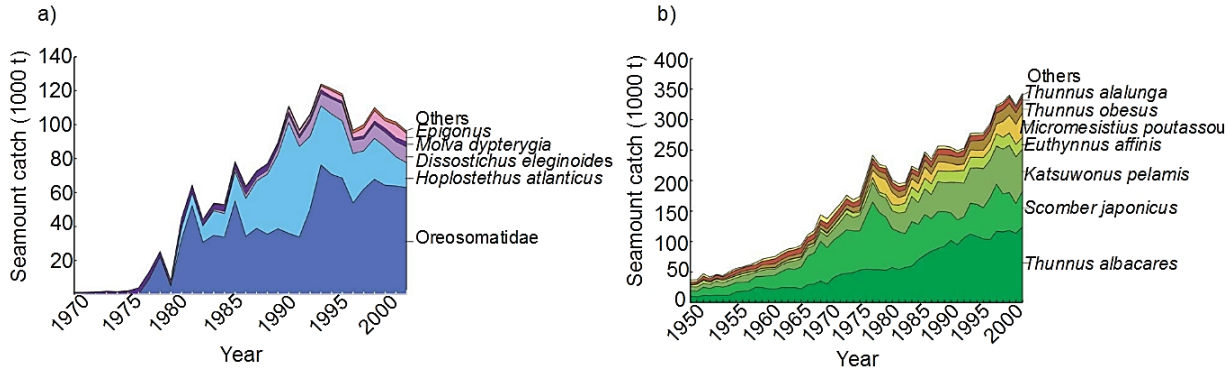

Figure 1.10 Global catch of (a) primary seamount species (caught primarily/ exclusively on seamounts), (b) secondary seamount species (not found exclusively/ primarily from seamount habitats), based on data described in Watson et al., 2004 (Source: Watson et al., 2007).

1.1.5 Regular seamount visitors

A number of other fisheries also regularly take place over seamounts such as those for the pelagic top predators, yellowfin, bigeye (*Thunnus obesus*), albacore (*Thunnus alalunga*), skipjack (*Katsuwonus pelamis*) and northern bluefin tunas (Fonteneau, 1991; Watson et al., 2007; Morato et al., 2010b; Dubroca et al., 2013; Marsac et al., 2014) (Fig. 1.10b). These species are not restricted to seamounts but are widely dispersed in oceanic environments and only occasionally converge to seamounts. The residence times of yellowfin tunas ranged from ~15 days at Espiritu Santo seamount in the Gulf of California (Klimley et al., 2003) and 18 days at Cross seamount (Holland & Grubbs, 2007). Bigeye tuna had residence times of ~32-98 ± 19 days (Holland et al., 1999; Sibert et al., 2000; Holland & Grubbs, 2007) or 25 ± 12 days

at Cross (Musyl et al., 2003). Some seamounts have been documented to be attractive, not only for benthopelagic organisms and tunas, but also billfishes (Morato et al., 2010a), sharks (Klimley & Nelson, 1984; Klimley et al., 1988; Hazin et al., 1998; Litvinov, 2007; Junior et al., 2009; Meyer et al., 2010; Morato et al., 2010a; Barnett et al., 2012), sea turtles (Santos et al., 2007; Fiori et al., 2016; Vassallo et al., 2018), seabirds (Haney et al., 1995; Thompson et al., 2007, Morato et al., 2008; Amorim et al., 2008; Paiva et al., 2010; Newton & DeVogelaere, 2013; Villani et al., 2014), and marine mammals such as whales (Worm et al., 2003; Johnston et al., 2008; Newton & DeVogelaere, 2013; Wong & Whitehead, 2014; McDonald et al., 2009; Dulau et al., 2017) and dolphins (Kaschner, 2007; Morato et al., 2008; Giorli et al., 2015). The main hypotheses explaining why large-scale migratory pelagic species might be attracted to seamounts include:

i) Seamounts may provide navigational waypoints to fish movements (Holland et al., 1999; Fréon & Dagorn, 2000; Holland & Grubbs, 2007; Litvinov, 2007).

Seamounts reportedly have distinct geo-magnetic signatures that tunas and sharks might be able to detect and orient to (Walker, 1984; Meyer et al., 2005) in their large pan-oceanic migrations, also known as “magnetic topotaxis” (Klimley, 1993). Seamounts may host these species transiently wherein the fishes briefly leave the seamount to forage for food and orient to the latter after foraging (Holland & Grubbs, 2007).

ii) Seamounts may provide enhanced foraging opportunities to top predators (Holland et al., 2003; Klimley et al., 2003; Kaschner, 2007; Santos et al., 2007; Morato et al., 2008; Johnston et al., 2008; Giorli et al., 2015).

Foraging opportunities for apex predators may be enhanced at seamounts through the processes mentioned above, including enhanced upwelling events, development and retention of primary and secondary production of the order of weeks or months, the topographic blockage hypothesis and the “feed-rest” hypothesis (Genin, 2004; Genin & Dower, 2007; Porteiro & Sutton, 2007; Morato et al., 2009). It has been suggested that humpback whales use seamounts as supplementary feeding areas during their migrations (Garrigue et al., 2015) and that killer whales and beaked whales may use seamounts as barriers to herd prey into denser groups (Heimlich-Boran, 1988; Johnston et al., 2008).

iii) Seamounts may represent favourable breeding habitats

Seamounts may be attractive as breeding habitats (Garrigue et al., 2015), as suggested for male humpback whales (*Megaptera novaeangliae*) visiting La Pérouse seamount in the Indian Ocean for residence times of ~1-17.5 days during the peak of the breeding season, from July to September (Dulau et al., 2017; Fig. 1.11). The New Caledonian humpback whale population have also been reported to aggregate at Antigonia pinnacle for an average of ~9.4 ± 5.8 days during their breeding period (Garrigue et al., 2015).

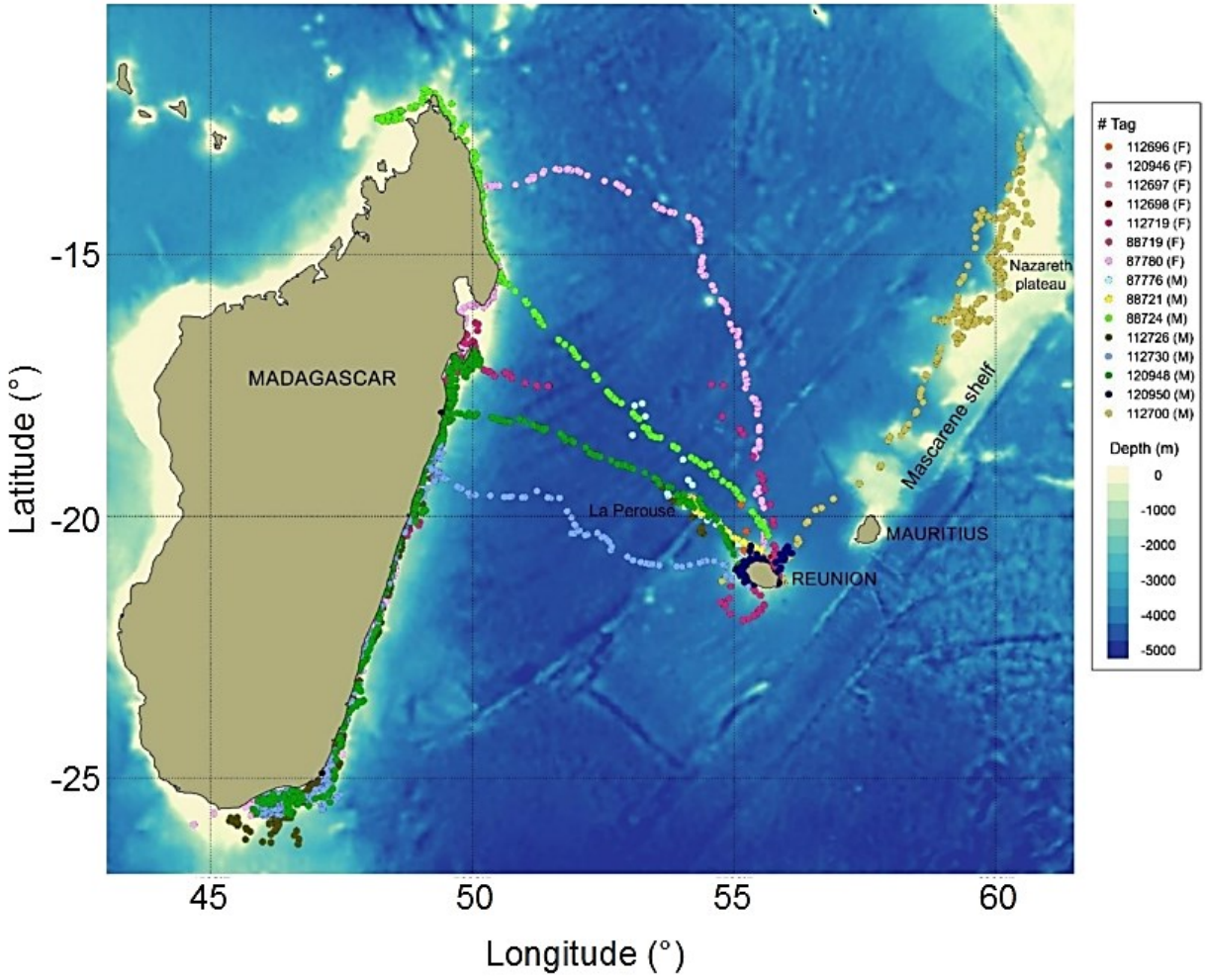

Figure 1.11 Received Argos locations from humpback whales tagged in Réunion in 2013 (F: Female, M: Male). Male humpback whales engaged in localized behaviour in Réunion Island, La Pérouse seamount, St Brandon Shoal and Madagascar, while females engaged in localized behaviour at Réunion Island and Ile Sainte-Marie (Source: Dulau et al., 2017).

iv) Seamounts may function as "cleaning stations" for oceanic sharks and rays (O'Shea et al., 2010; Oliver et al., 2011).

Pelagic thresher sharks (*Alopias pelagicus*) reportedly frequently visit Monad Shoal seamount in the Philippines to interact with the blue streaked cleaner wrasse (*Labroides dimidiatus*) that

remove ectoparasites (Oliver et al., 2011). Cleanerfish at Osprey reef seamount in Australia were also observed removing ectoparasites from the mobulid ray (*Manta birostris*) and sharks belonging to the Carcharhinidae and Sphyrnidae families which would transit to the seamount (O'Shea et al., 2010).

Oceanic fronts have been reported to enhance aggregation of pelagic visitors at seamounts by generating increased allochthonous productivity and hence creating more foraging opportunities (Morato et al., 2016). It has been hypothesized that tunas may force their prey to the surface where they are further concentrated by common dolphins, thus attracting seabirds to the seamount (Morato et al., 2008). Seamounts may thus be hotspots of pelagic biodiversity, with higher species richness of pelagic predatory fishes associated with the seamount relative to coastal and oceanic regions (Morato et al., 2010a; Worm et al., 2003).

1.1.6 Seamount endemism

Seamounts have further been hypothesized to support high levels of endemism, which is one of the most contradicted paradigms in seamount ecology (McClain, 2007; Rowden et al., 2010a, 2010b). Endemic species are those that are restricted to a single or chain of seamounts only (Stocks & Hart, 2007). Seamount habitats have been speculated to be isolated and hence to promote local speciation leading to seamount species having limited, compressed geographic ranges thereby increasing levels of endemism (Hubbs, 1959). Some authors have reported levels of endemism of 15.4% among invertebrates and 11.6% among fishes from over 100 seamounts worldwide, although 72% of that dataset comes from only five seamounts (Wilson & Kaufmann, 1987). Other authors have found levels of endemism of 29-34% over seamounts in the Tasman Sea and southeast Coral Sea (De Forges et al., 2000), endemism of <3% in antipatharian, scleractinian and gorgonian corals at seamounts in the northeast Atlantic (Hall-Spencer et al., 2007), and endemism in the Pacific octocoral genus *Chrysogorgia* at New England and Corner seamounts (Pante et al., 2015). No endemic species of invertebrates and benthopelagic fish were recorded on the summit plateau of Seine (Christiansen et al., 2009), Ampère (Christiansen et al., 2015) and the Norfolk ridge (Samadi et al., 2006) seamounts.

Much of the debate around endemicity arise from our inability to sample seamount ecosystems and non-seamount pools successfully (Rogers, 1994; McClain, 2007; Hart & Pearson, 2011). In the analysis of endemicity, the degree of connectivity of seamounts to neighbouring island and landmasses and recruitment mechanisms are important variables to consider (Hart & Pearson, 2011). Contrary to the "seamount endemicity" hypothesis, seamounts have also been

postulated to serve as "sources" and/or "sinks" of propagules from nearby habitats, with populations of invertebrates on seamounts being the source of propagules for adjacent slope sinks (Rowden et al., 2010a). This forms the basis of the "stepping stone" hypothesis, whereby seamounts aid species dispersal within the region, possibly powered by large-scale currents and eddies (Wilson & Kaufman, 1987; Boehlert et al., 1994; Christiansen et al., 2015; Packmor et al., 2015).

1.1.7 Larval dispersal and seamount connectivity

Marine ecological connectivity between distant ecosystems is mediated through two types of connections: passive circulation connectivity aided by ocean currents and/or active migratory connectivity achieved by actively swimming marine species (Cowen, 2006; Popova et al., 2019). Larval type (long-lived vs. short-lived) and/or larval behaviour (larvae moving vertically in the water column or post-larvae attaching to floating materials) may also significantly influence the dispersal of a population (Bradbury & Snelgrove, 2001; Cowen, 2006; Stocks & Hart, 2007) and hence its endemicity/ connectivity. Larvae released by populations at Fieberling Guyot, Cobb seamount and Porcupine bank were either settled into the benthos (if the larvae were benthic), were swept off the seamounts or were retained in Taylor caps (Parker & Tunnicliffe, 1994; Kloppmann et al., 2001; Mohn, 2002) and related features by forming patches of larvae with anomalously high abundances that originate near the summit but are later advected to the far-field and shed from the seamount by shifting impinging currents (Mullineau & Mills, 1997). An increase in larval abundance in the seamount waters at Senghor relative to the open ocean has been recorded, suggesting retention of larvae by mechanisms such as enhanced vertical mixing generated by the displacement of isotherms and isohalines (Denda et al., 2017a). Flow patterns reportedly contribute to seamount connectivity by aiding the transport of *M. muelleri* from the southern Emperor seamount to the region of Southeast Hancock seamount (Boehlert et al., 1994). Larval dispersal and exchange may result in significant genetic exchange and mixing between species on seamounts and the surrounding environment (Mullineau & Mills, 1997; Stocks & Hart, 2007), leading to species being genetically connected (Samadi et al., 2006).

1.1.8 Seamount conservation and management strategies

Seamount ecosystems may be significantly altered by human activities including deep-sea bottom trawling through the removal of coral habitats, the overexploitation of stocks and seabed mining for cobalt, ferro-manganese nodules and polymetallic sulphides (Clark & Koslow, 2007; Probert et al., 2007; Pitcher et al., 2010; Clark & Dunn, 2012). These impacts

highlight a pressing need to address the question of conservation and ecosystem-based management of seamounts. Seamounts are good candidates for the set-up of Marine Protected Area (MPA) networks promoted by the OSPAR Convention (OSPAR Commission, 2004) and the Natura 2000 network of protected areas established by member states of the European Commission (Santos et al., 2009). Management actions require a balance between exploitation and conservation, both of fisheries and habitats (Probert et al., 2007). No single management model is applicable to all seamounts (Probert et al., 2007; Clark et al., 2010b).

Management tools are likely to include two complementary categories: site-specific (long-term) and activity-related (short-term) (Probert et al., 2007; Clark et al., 2010b; Clark et al., 2012). Site-specific regulations may include the implementation of single MPA or a network of MPAs and/or no-take zones (Probert et al., 2007; Barnett et al., 2012), identification and conservation of specific pelagic diversity hotspots (Worm et al., 2003), implementation of catch limits and/or small MPAs for individual features at specific times of the year to protect the target species nursery grounds and spawning aggregations thereby preventing local and serial depletion of stocks (Clark & Dunn, 2012; Fontes et al., 2014) and marine reserves to protect seabirds' resting and foraging grounds during their breeding seasons (Amorim et al., 2008). Activity-related management measures may comprise effort control through the prohibition of all fishing or specific gear types, set-up of line retrieval times, depth limits, establishment of catch quotas and bycatch quotas and licences or technical modifications to existing fishing gears so they have a lesser impact on seamount ecosystems (Clark & Koslow, 2007; Santos et al, 2007; Probert et al., 2007; Clark, 2009; Clark & Dunn, 2012).

Since most seamounts are located in areas beyond national jurisdiction, conservation measures and actions can only be implemented and enforced in cooperation with member states at a regional and international level (such as the Regional Fisheries Management Organisations), based on scientific information and consistent with international law (Probert et al., 2007), and based on open dialogue and free exchange of information between all the stakeholders and seamount users (Gubbay, 2005; Clark et al., 2010b). Several frameworks and criteria are now available for classifying individual seamounts as ecologically and biologically significant areas (EBSA) (Taranto et al., 2012), for the economic valuation of seamount ecosystems (Ressurreição & Giacomello, 2013), or for delineating Large Marine Ecosystems (LMEs) (Probert, 1999) to reduce threats and develop comprehensive and sustainable management strategies. Conservation actions can further be prioritized by grouping seamounts according to their general characteristics (Probert et al., 2007).

An essential input to all conservation and management actions is the accurate information about the geographic distribution of habitats and their associated biological resources (Clark et al., 2012). Unfortunately, data with respect to benthic habitats are available only for a small percentage of seamounts globally. Significant knowledge gaps exists on seamount ecosystems of the Indian Ocean (Clark et al., 2010b), although ~40 years of fishing mark the history of the South West Indian Ocean seamounts (Zucchi et al., 2018). Regarding non-living resources, permits have been awarded to the Chinese contractor COMRA (China Ocean Mineral Resources Research and Development Association) for exploration of seabed minerals of the South West Indian Ridge (Guduff et al., 2018). The ocean governance framework in the Western Indian Ocean (WIO) is complex with various legal and institutional frameworks and regional powers including the Nairobi Convention and the Regional Fisheries Bodies- the IOTC (Indian Ocean Tuna Commission), SIOFA (South Indian Ocean Fisheries Agreement) and SWIOFC (Southwest Indian Ocean Fisheries Commission).

Limited management measures have been implemented by the SIOFA. One such conservation measure is the delineation of 13 benthic protected areas (BPAs) where bottom or midwater trawling are banned. However, these measures do not regulate mining or oil/drilling activities. Other measures include limits on bottom fishing effort and catch and exclusion of gears (traps and lines). No MPAs have been set-up along the South West Indian Ridge (Guduff et al., 2018). The significant knowledge gaps identified during the 2016 and 2017 SIOFA meetings have been the cause of the rejection of a proposal to convert the SIODFA's BPAs into formal VME (Vulnerable Marine Ecosystem) closures. Future research should thus strategically target these understudied regions, types of seamounts and critical ecological processes. Research should also aim at employing novel sampling and analysis technologies, using predictive modelling tools to predict habitat suitability for benthic species in poorly studied regions (Tittensor et al., 2009; Guduff et al., 2018) and standardizing data collection and sharing (Clark et al., 2010b).

1.2 Conclusion

Some seamounts from the Atlantic and Pacific basins were reported to significantly enhance biomass of primary, secondary and tertiary consumers if physical processes are developed and maintained for a sufficient amount of time to allow a biological response to occur. While processes conducive for biological enhancement has been thoroughly studied at some seamounts of the Atlantic and Pacific oceans (Appendix: Tables A & B), our knowledge pool is limited, especially in the south-western Indian Ocean. Chapter 2 will hence aim at shedding new light on the general pelagic ecosystem within the South West Indian Ocean (SWIO). The

prevailing physical processes and topographic features of the SWIO, likely influencing the distribution, abundance and behaviour of lower through to higher trophic levels, will be described.

1.3 Thesis Aims and Objectives

This research project was inspired by the recognition that the La Pérouse and MAD-Ridge seamounts may host ecologically and biologically important organisms, that they are being exploited by fisheries and that the significant knowledge gaps have led to a lack of conservative measures to protect the associated ecosystems. This work is the first to investigate the dynamics of mesopelagic communities at La Pérouse and MAD-Ridge.

Chapter 2 is dedicated to a detailed overview of the pelagic ecosystem of the south-western Indian Ocean. The relevance of physical oceanographic processes, seamounts and ridges of the south-western Indian Ocean for top predator species is also presented, along with fisheries impact and governance aspects. The La Pérouse and MAD-Ridge seamounts are introduced as case studies whereby the bathymetry, chemical oceanography, plankton, ichthyoplankton and mesozooplankton communities were investigated during two recent cruises.

Chapter 3 examines the influence of mesoscale eddies, continental shelf and the shallow seamounts, La Pérouse and MAD-Ridge, on the vertical and horizontal distributions of micronekton. The conditions for the formation of Taylor columns are presented. The influence of environmental variables and productivity on micronekton communities at La Pérouse and MAD-Ridge are investigated. Micronekton's diel vertical migration patterns are also revisited in light of the acoustic and environmental data collected.

Chapter 4 investigates the prevailing environmental conditions at the La Pérouse and MAD-Ridge seamounts using satellite data. The distributions and assemblages of micronekton communities are presented, using a combination of mesopelagic trawl data and a multi-frequency acoustic visualisation technique. This acoustic visualisation technique has allowed the investigation of the relative contribution of each frequency to the overall backscatter and identification of dense aggregations of scatterers associated with the seamounts' summits and flanks. Micronekton's vertical and horizontal distributions and the different migration strategies of various species are analysed in more detail.

Chapter 5 interrogates the stable isotope patterns at the La Pérouse and MAD-Ridge seamounts using stable carbon ($\delta^{13}C$) and nitrogen ($\delta^{15}N$) isotopic values of soft tissues of

selected micronekton taxa. The trophic interactions between particulate organic matter (POM), zooplankton, gelatinous organisms and micronekton are studied in more detail, along with the factors likely influencing stable isotope compositions. A seamount effect is further investigated by comparing the stable isotope values of omnivorous/ carnivorous fishes sampled at the seamounts' flanks, vicinities and summits relative to the southern Mozambique Channel. The stable isotope values of the seamount-associated fish species identified in Chapter 5 are analysed.

Chapter 6 highlights key findings from Chapters 3-5 and expands on their implications to science, fishers and management. Chapter 6 further discusses the overall micronekton acoustic densities at the La Pérouse and MAD-Ridge seamounts relative to the wider geographic area within the ISSG and EAFR provinces. Knowledge gaps and fruitful avenues of future research are key elements outlined in a forward-looking perspective.

Chapter 2: Pelagic ecosystem and seamounts of the south-western Indian Ocean

L'Homme et la Mer

Homme libre, toujours tu chériras la mer !
La mer est ton miroir ; tu contemples ton âme
Dans le déroulement infini de sa lame,
Et ton esprit n'est pas un gouffre moins amer.

Tu te plais à plonger au sein de ton image;
Tu l'embrasses des yeux et des bras, et ton coeur
Se distrait quelquefois de sa propre rumeur
Au bruit de cette plainte indomptable et sauvage.

Vous êtes tous les deux ténébreux et discrets:
Homme, nul n'a sondé le fond de tes abîmes;
Ô mer, nul ne connaît tes richesses intimes,
Tant vous êtes jaloux de garder vos secrets!

Et cependant voilà des siècles innombrables
Que vous vous combattez sans pitié ni remord,
Tellement vous aimez le carnage et la mort,
Ô lutteurs éternels, ô frères implacables!

Charles Baudelaire, 1861

2.1 The South West Indian Ocean: General Overview

2.1.1 Geomorphology and sedimentation

The latitudinal range of the South West Indian Ocean (SWIO) extends from 0 to 30-35°S while the longitudinal range encompasses the area between eastern Africa to 60°E. While the Indian Ocean is the third largest ocean in the world (Ingole & Koslow, 2005), it remains relatively less well explored scientifically relative to the Atlantic and Pacific Oceans. The geomorphological characteristics of the Indian Ocean comprise islands, mid-ocean ridges, abyssal plains, deep-sea trenches, submarine plateaus and seamounts, with the latter being poorly studied habitats (Demopoulos et al., 2003; Ingole & Koslow, 2005). The distribution of seamounts varies across ocean basins. The Pacific basin accounts for ~8950 potential seamounts relative to the Atlantic, Indian and Southern Oceans (2760, 1650 and 880, respectively) (Hillier & Watts, 2007; Kitchingman et al., 2007; Wessel, 2007; Etnoyer et al., 2010). The low abundance of seamounts in the Indian Ocean has been associated with the smaller magmatic activity and cooler mantle temperatures in the region (Mendel & Sauter, 1997). Most seamounts present in the Indian Ocean are associated with its ridge systems (Ingole & Koslow, 2005; Fig. 2.1).

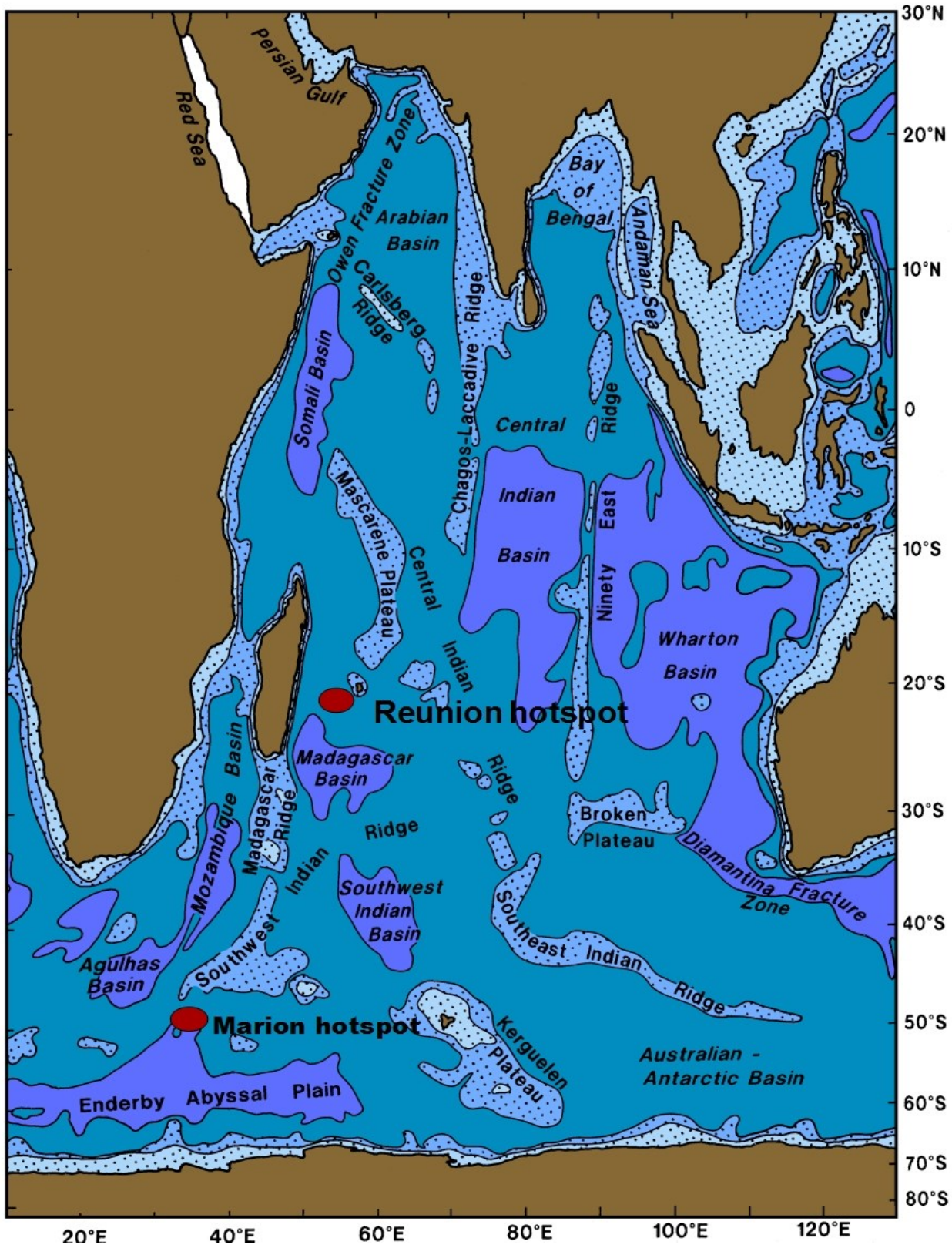

Figure 2.1 Major ridge system, basins and two hotspots of the Indian Ocean bounded by the African, Asian, Australian and Antarctic continents [Source: adapted from Tomczak & Godfrey, 2002].

The Madagascar Ridge is an elongated plateau that has originated from volcanism of the Marion hotspot (Sinha et al., 1981; Zhang et al., 2011; Fig. 2.1). It stretches 400 km across and ~1300 km southwards from the Madagascar landmass and connects at 42°S with the Southwest Indian Ridge (SWIR) (Sinha et al., 1981; Zucchi et al., 2018). The Madagascar ridge system can be separated into two domains north and south of 31°S that differ in sea-floor topography, acoustical basement relief and sediment cover (Goslin et al., 1980). In the northern portion of the ridge, sediments are confined in narrow pockets between the numerous basaltic highs on a relatively old crust. In the southern portion of the ridge, the sediment cover is thicker and regularly layered on a younger oceanic crust (Goslin et al., 1980). The Mascarene Basin, on the other hand, extends between Madagascar and the Mascarene Plateau (Schlich, 1974). The Mascarene Plateau was formed from the Réunion hotspot (Bonneville et al., 1997). The shallow part of the Mascarene Plateau is 20-100 m deep along the banks that have steep descending slopes to ~3000-5000 m (New et al., 2005). The curvature of the Mascarene ridge is typical of the curvature of an island arc extending ~2000 km from Seychelles to Mauritius (Kamen-Kaye & Meyerhoff, 1980; Gallienne et al., 2004). The southern Mascarene Ridge consists of dark, fine-grained, grey basalt and younger volcanic rocks (Schlich, 1974), while the northern portion of the ridge exhibits older rocks (Kamen-Kaye & Meyerhoff, 1980).

The ocean floor in the Indian Ocean is dominated by sediments containing a high proportion of calcium carbonate (Berger, 1974; Kolla et al., 1980; Demopoulos et al., 2003). Pelagic red clay and turbidites are present in the deepest parts of the Mascarene Basin (McCave et al., 2005). Hard substrata in the Indian Ocean consist of ferromanganese concretions (Demopoulos et al., 2003) and manganese nodules at ~4000 m depth (Ingole & Koslow, 2005). The rubble and coral frameworks at Middle of What seamount along the SWIR were reported to be coated with manganese deposits (Narayanaswamy et al., 2017). Benthic-biological activity and strong bottom currents are deemed responsible for the presence of these nodules at the sediment-water interface (Demopoulos et al., 2003).

2.1.2 Water masses and circulation patterns

The Indian Ocean exhibits a complex system of water masses (Fig. 2.2). Warm and salty Tropical Surface Water occupies the upper layers (within the top 250 m) (Fig. 2.2). Some of the deeper parts to the north-west of Réunion Island consists of Red Sea Intermediate Water (Gordon et al., 1987) and the upper Circumpolar Deep Water (New et al., 2007). Both to the north-west of Réunion Island and south of Madagascar, other intermediate water masses are present- the South Indian Central Water/ the Sub-Antarctic Mode Water and the Antarctic

Intermediate Water (New et al., 2005; Vianello et al., 2020; Fig. 2.2). The Red Sea Intermediate Water is mostly observed near the Mascarene Plateau where it may meet with the Antarctic Intermediate Water (New et al., 2005). Bottom and deep waters of the Indian Ocean are mostly derived from the Atlantic and they are constrained to spread through deep fracture zones such as the Atlantis II fracture zone along the SWIR at longitude 57°E and latitude 33°S (Muller et al., 2000; Demopoulos et al., 2003; MacKinnon et al., 2008) where strong mixing of these deep- and bottom-waters occurs (MacKinnon et al., 2008). Once across the SWIR, depths below 3800 m are occupied by cold Antarctic Bottom Water that leaves the circumpolar current (Tomczak & Godfrey, 2001; Demopoulos et al., 2003). The Indian Deep Water formed from the North Atlantic Deep Water (Le Pichon, 1960) and carried into the Indian Ocean with the Upper Circumpolar Current, occupies depths between 1500 and 3800 m (Ingole & Koslow, 2005). Part of the Atlantic water flowing inside the Indian Ocean, particularly the North Atlantic Deep Water, is balanced in the surface layer by flow from the Agulhas Current (Agulhas leakage; Beal et al., 2011). The Agulhas Current is fed from the South Equatorial Current (SEC) which is in turn fed from waters coming from the Pacific ocean as the "Indonesian Through-Flow" (Tomczak & Godfrey, 2001; McCave et al., 2005).

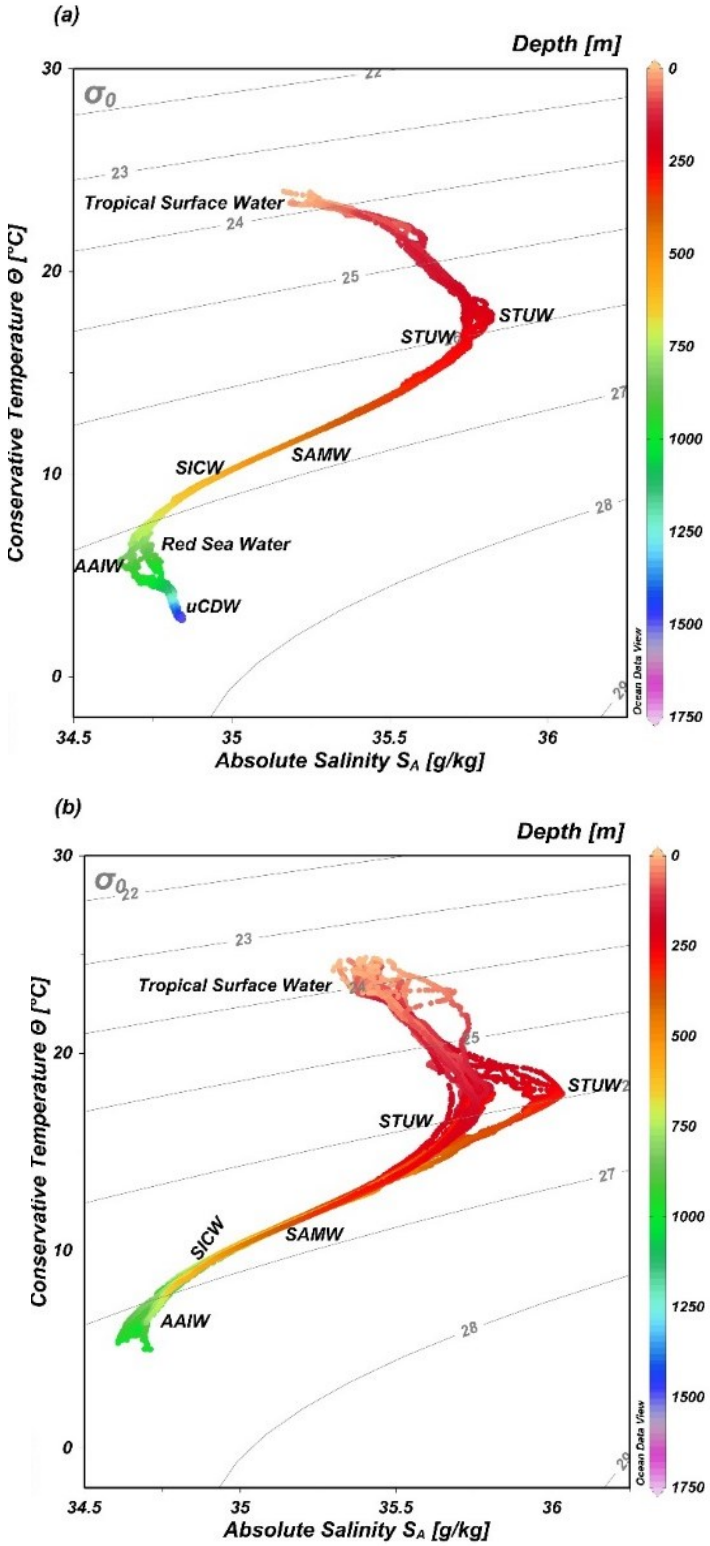

Figure 2.2 Temperature-Salinity diagrams indicating the water masses in the SWIO. Conservative Temperature (°C) vs. Absolute Salinity (g kg^{-1}) (as in Vianello et al., 2020) profiles (a) to the North West of Réunion Island, and (b) south of Madagascar, showing the AAIW (Antarctic Intermediate Water), SICW (South Indian Central Water), SAMW (Sub-Antarctic Mode Water), STUW (Subtropical Under Water) and Tropical surface Waters. The Red Sea Water and uCDW (upper Circumpolar Deep Water) were observed to the north-west of Réunion Island.

The shallow water circulation (upper 500 m), at ~15°S, consists of the westward-flowing and warm SEC that carries waters from the "Indonesian through-flow" across the Indian Ocean through gaps between the Saya de Malha and Nazareth banks at 12-13°S (New et al., 2005). The SEC forms a sharp boundary between nutrient-rich waters of the north-western Indian Ocean near Seychelles from the nutrient-poor water masses of the SWIO around the Mascarene Islands (New et al., 2005; Obura, 2012). On reaching the Madagascar landmass, the SEC bifurcates to form the northward and southward branches of the East Madagascar Current (NEMC and SEMC respectively) (Fig. 2.3) (Quartly & Srokosz, 2004; McCave et al., 2005; Quartly et al., 2005; Hall et al., 2017; Zucchi et al., 2018). The northward branch (NEMC) flows around the northern tip of Madagascar before branching again when reaching the east African coast, to form the East African coastal current (EACC) flowing equatorwards. The resulting southern branch flow southwards through the Mozambique Channel, with mesoscale eddies being formed at the narrower part of the channel at 17°S (De Ruijter et al., 2002; Quartly & Srokosz, 2004; Lutjeharms et al., 2012). Four to seven mesoscale eddies per year transit through the Mozambique Channel, from north to south (Schouten et al., 2003; Tew-Kai & Marsac, 2009, 2010).

The narrow and nutrient-poor SEMC (Quartly & Srokosz, 2004) retroflects on reaching the southernmost tip of the Madagascar continental shelf, a process during which various mesoscale eddies and current fragments may become detached (Lutjeharms et al., 1981; De Ruijter et al., 2004). The development of mesoscale dipoles (pair of contra-rotating eddies) has been regularly observed to the south of Madagascar where the SEMC separates from the shelf (De Ruijter et al., 2004). These eddies generally propagate in a west- and south-westward direction, with some reaching the Agulhas Current to the south of Africa (De Ruijter et al., 2004). Periods of enhanced dipole formation have been found to coincide with El Niño cycles and the negative phases of the Indian Ocean Dipole (De Ruijter et al., 2004). Upwelling cells also occur on the continental shelf south of Madagascar (Machu et al., 2002). These are most likely due to the dynamic effects of upwelling favourable wind stress and frictional interaction between the Madagascar continental shelf slope and the southward flowing EMC (De Ruijter et al., 2004; Machu et al., 2002; Ho et al., 2004; Ramanantsoa et al., 2018).

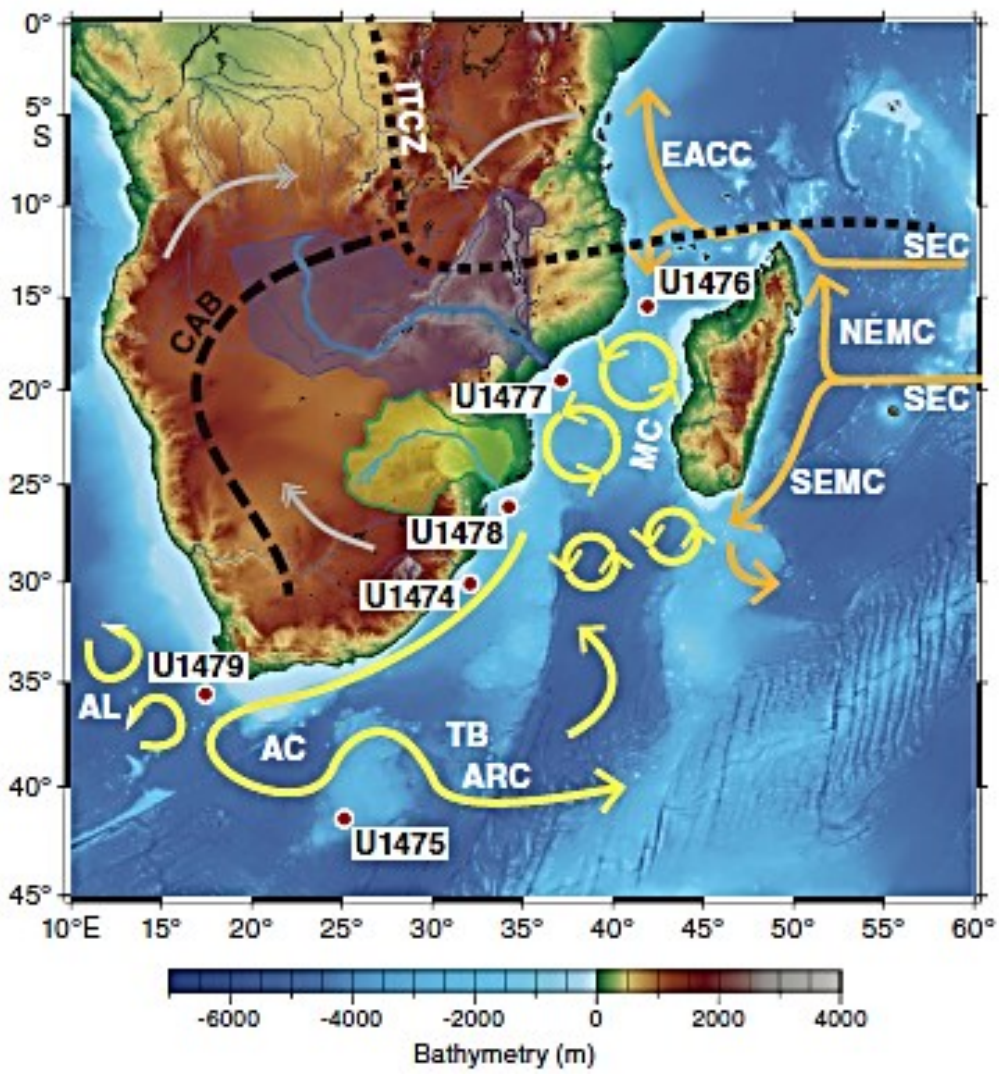

Figure 2.3 Schematic diagram of major surface currents (yellow and orange arrows) in the SWIO, labelled AC (Agulhas Current), SEC (South Equatorial Current), SEMC (South East Madagascar Current), NEMC (North East Madagascar Current), EACC (East Africa Coastal Current), ARC (Agulhas Return Current), AL (Agulhas Leakage). Atmospheric circulation over Southern Africa is also shown (grey lines). The Mozambique Channel (MC) and Transkei Basin (TB) are labelled. The Intertropical Convergence Zone (ITCZ) and the Congo Air Boundary (CAB) (dashed lines) are labelled. U1476, U1477, U1478, U1474, U1479 and U1475 represent drill sites during the International Ocean Discovery Program, IODP, JOIDES Resolution, Expedition 361. The colour bar indicates bathymetry (m) [Source: Hall et al., 2017].

2.1.3 Biogeochemical provinces of the SWIO

The East African Coastal Province (EAFR) and Indian South Subtropical Gyre (ISSG) are two major provinces of the SWIO (Fig. 2.4). The ISSG province is bounded by the SEC to the north (Longhurst, 1998). The prevailing large-scale anticyclonic circulation pattern of the ISSG leads to a physical downwelling, that limits the supply of nutrients to the surface layers (Jena et al., 2013). The ISSG province is characterised by low nutrients and chlorophyll *a* concentrations

(Jena et al., 2013) relative to the EAFR which shows higher sea surface primary production and elevated chlorophyll *a* concentrations all year round (Annasawmy et al., 2018). Based on *in situ* CTD (Conductivity Temperature Depth) data, the mean surface fluorescence concentrations were six times less in the ISSG, with deeper Deep Chlorophyll Maximum (DCM), relative to the Mozambique Channel in the EAFR (Annasawmy et al., 2018). The observed pattern could be ascribed to riverine outflow and presence of mesoscale eddies which advected productivity into the Mozambique Channel (Pous et al., 2014; Hood et al., 2017; Annasawmy et al., 2018). Elevated concentrations of nutrients and chlorophyll *a* were also observed in the upwelling region south of Madagascar (Machu et al., 2002). During austral summer, these nutrient-rich waters within the intensified upwelling cells along the south coast of Madagascar are transported offshore by mesoscale eddies (Raj et al., 2010).

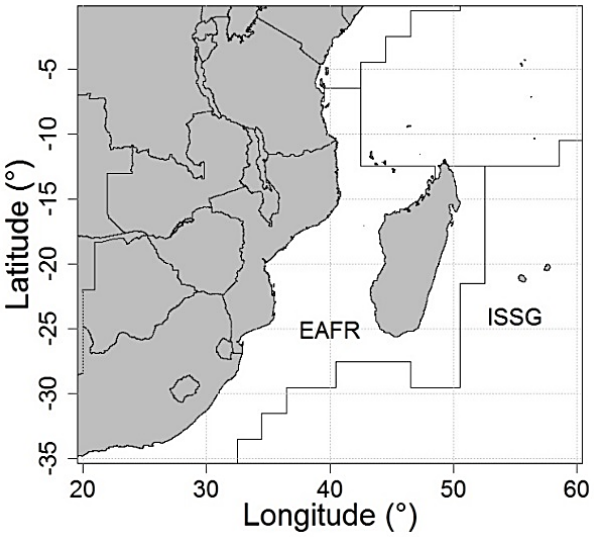

Figure 2.4 Longhurst's (1998) biogeochemical provinces EAFR (East African Coastal Province) and ISSG (Indian South Subtropical Gyre) of the SWIO.

Significant enrichments of nutrients and chlorophyll may occur within mesoscale eddies, with the potential for nutrients to be transported centrally to the euphotic zone by rotary motion within cyclonic eddies (Falkowski et al., 1991) and peripherally within anticyclonic ones (Martin et al., 2001; Raj et al., 2010). "Eddy pumping" processes may increase phytoplankton growth in an otherwise oligotrophic ocean (Falkowski et al., 1991; Oschlies & Garcon, 1998) due to the doming of water masses which bring nutrients closer to the surface where irradiance conditions are favourable for phytoplankton growth (Longhurst, 2007). Eddies may influence plankton communities by horizontal advection (either by stirring of surface currents around the eddy boundaries or trapping of specific water parcels having unique biological and physical

properties), by the vertical transport of nutrients into the photic zone, and by water column stratitication (whereby cells are maintained and concentrated in the photic layer by the eddy) (Gaube et al., 2014). During the forced phase, anticyclonic eddies may be characterised by accumulation of warm, chlorophyll-depleted water in the centre and nutrient-enriched water at the outer edge (Falkowski et al., 1991; Lévy et al., 2001; Tew Kai & Marsac, 2010). Phytoplankton blooms may aggregate secondary and tertiary consumers including zooplankton, micronekton and larger nekton (Piontkovski & Williams, 1995) that further attract top predators. This transfer of energy from primary producers to top predators is believed to be rapid in the tropical Indian Ocean (Longhurst, 1998), indicating that prey for top predators becomes readily available shortly after the onset of these blooms (Pinet et al., 2012).

2.1.4 Biological compartments of the ISSG and EAFR provinces

2.1.4.1 Phytoplankton pigments

In oligotrophic environments, light and nutrient (including nitrate, silicate and iron) concentrations limit phytoplankton growth (Thomalla et al., 2011). Autotrophic organisms in these areas depend on nutrient recycling or on vertical flux of nutrients from deeper waters into the euphotic zone (Altabet & Francois, 1994). In such systems, mesoscale eddies may play a significant role in making nutrients available to phytoplankton in the photic layer (Falkowski et al., 1991; McGillicuddy et al., 1998). Previous studies have found enhanced surface total chlorophyll *a* concentrations (which are general indicators of phytoplankton biomass, Ewart et al., 2008) within cyclones relative to anticyclones of the Mozambique Channel (Barlow et al., 2014). Furthermore, studies have found low concentrations of small phytoplankton cells to characterise subtropical waters in the south-west indian subtropical gyre (Thomalla et al., 2011). This indicates that productivity was based almost entirely on recycled ammonium and urea instead of nitrate (Thomalla et al., 2011).

Previous studies conducted in the ISSG province to the south of Mauritius Island (MICROTON cruise- DOI: 10.17600/10110010) and in the EAFR province within the Mozambique Channel (MESOP 2010 cruise- DOI: 10.17600/10110020/30) have shown a pre-dominance of prokaryotes at the sea surface, while flagellates were dominant at the DCM (Fig. 2.5). This is consistent with observations that prokaryotes are present in warm surface waters (>22°C) in the SWIO (Barlow et al., 2008; 2014) and flagellates dominate the DCM in the Mozambique Channel (Barlow et al., 2014). Prokaryotes have a high proportion of the photo-pigment PPC (photoprotective carotenoids) (Barlow et al., 2014) in their cells and hence they proliferate at high irradiance, low nutrient surface oligotrophic environments (Cavicchioli et al., 2003).

Flagellates, on the other hand, have higher concentrations of total chlorophyll *a* (whose major role is to absorb light) and PSC (photosynthetic carotenoids) in their cells (Barlow et al., 2008). These flagellates are hence better adapted to survive the low-light and nutrient-replete conditions of the DCM. Diatoms were more abundant within the oligotrophic ISSG province relative to the more productive EAFR province. Studies have also found dominance of diatoms in anticyclonic eddies and were related to high rates of vertical mixing (Thompson et al., 2007; Ewart et al., 2008).

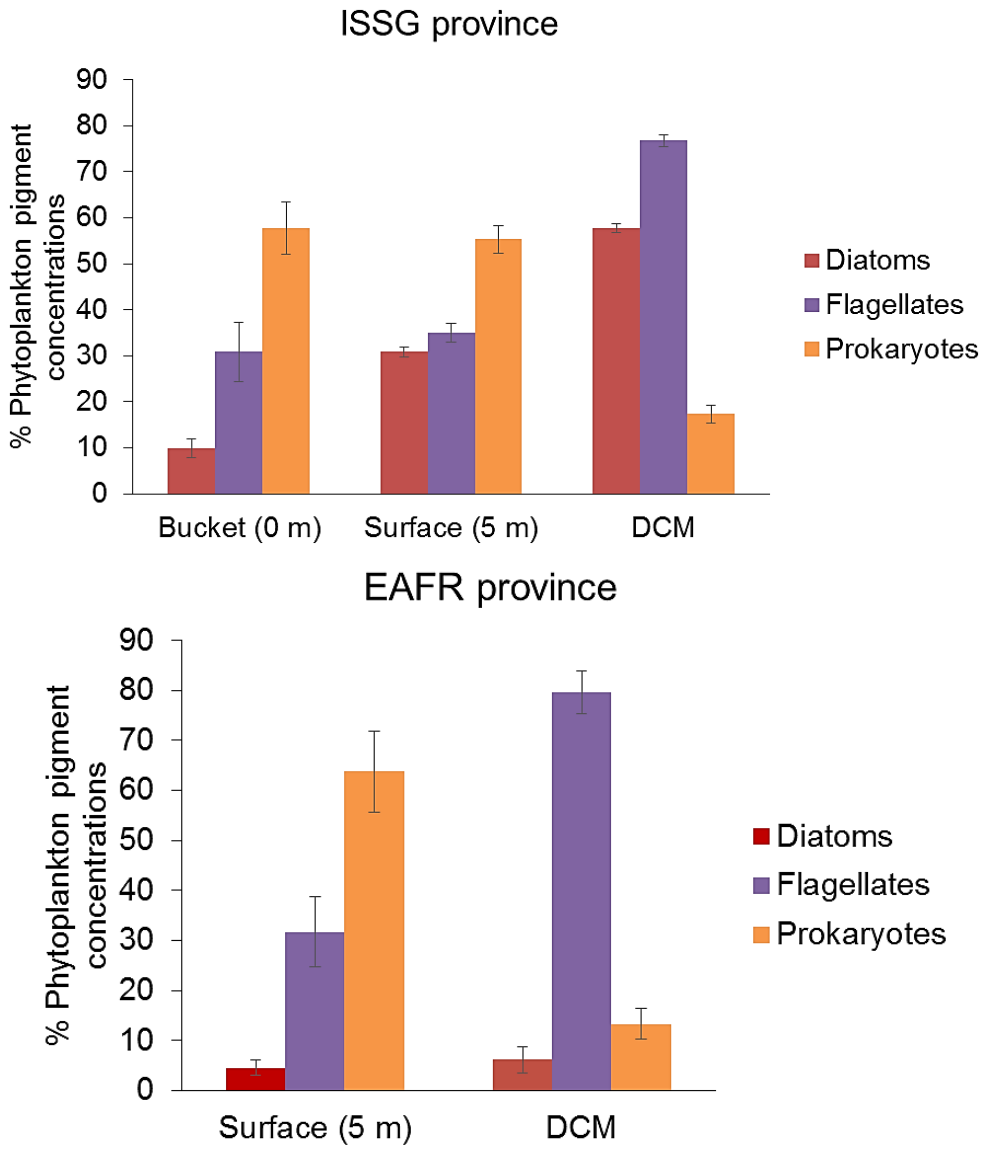

Figure 2.5 Relative contributions of diatoms, flagellates and prokaryotes within the ISSG and EAFR provinces.

2.1.4.2 Mesozooplankton

Zooplankton biomass may also be linked to the surrounding productivity and increased food availability. Higher zooplankton biomasses, associated with higher concentrations of nutrients,

were recorded in the northern and equatorial Indian Ocean. Comparatively, the ISSG province recorded the lowest nutrient concentrations and zooplankton biomasses (Bailey, 1968; Rao, 1973; Madhupratap, 1983). Copepods are generally the numerically dominant zooplankton taxa recorded in the Indian Ocean (Gallienne et al., 2004; Conway, 2005), followed by chaetognaths, ostracods, tunicates and siphonophores (Madhupratap, 1983). Previous studies conducted in the Mozambique Channel recorded enhanced zooplankton biovolume over the African shelf, at divergence and cyclonic eddy stations relative to anticyclonic and frontal stations (Huggett, 2014). The mesozooplankton community in the Mozambique Channel was found to be strongly dominated by small copepods (Dupuy et al., 2016), appendicularians, ostracods and chaetognaths (Huggett, 2014). Copepods can obtain food from different sources of organic matter in dissolved or particulate form, in the form of detritus or living prey (Poulet, 1983), likely explaining their high recorded abundances from surveys in the Mozambique Channel (Huggett, 2014; Dupuy et al., 2016).

Studies from different regions of the Indian Ocean have found copepods to constitute ~40-90% by number of the diet of lanternfishes, with minor contributions from amphipods, euphausiids, ostracods, chaetognaths, larvaceans, molluscs and polychaetes (Dalpadado & Gjøsæter, 1988). Larger lanternfishes were observed to feed on larger prey such as chaetognaths, fish larvae and polychaetes, without completely excluding smaller prey items from their diet (Dalpadado & Gjøsæter, 1988). Furthermore, zooplankton fractions remaining in the first 170 m of the water column by day are important prey items of the fishes that surface tuna feed upon (Roger, 1994).

2.1.4.3 Micronekton

Micronekton were sampled during previous IRD cruises in the ISSG and EAFR provinces (Potier et al., 2014; Annasawmy et al., 2018). With the sampling seawater volume accounted for, a greater biomass of mesopelagic organisms (crustaceans, squids, mesopelagic fishes and gelatinous plankton), were recorded in the southern and central Mozambique Channel (MESOP 2009 and 2010 cruises) relative to the ISSG (MICROTON cruise) to the south of Mauritius Island (Potier et al., 2014; Annasawmy et al., 2018). The combined action of riverine input and entrainment of productivity and chlorophyll *a* from the African landmass to the Mozambique Channel by mesoscale eddies may favour the aggregation of zooplankton (Huggett, 2014) and micronekton in the EAFR (Annasawmy et al., 2018). Productivity and resulting secondary and tertiary consumer abundances were lower in the ISSG relative to the eutrophic Mozambique Channel.

Among the mesopelagic broad categories, gelatinous organisms and fishes dominated the total biomass estimates across the cruises in the SWIO. Gelatinous organisms were poorly identified during MESOP 2009, 2010 and MICROTON cruises because species broke apart in the nets making identification impossible, hence the low representation of these organisms in total net counts. Mesopelagic fishes and crustaceans dominated the abundance estimates during MICROTON and MESOP 2009. Squids were the most poorly represented in terms of abundance and biomass estimates across all cruises most probably due to net avoidance behaviours of species.

Studies have shown the distribution of micronekton biomass to be seasonal, with highest values recorded south of 20°S in summer and north of 12°S in winter along longitude 110°E (Legand, 1967). However, no seasonal pattern in micronekton acoustic backscatter were observed in a latitudinal gradient between 20-50°S (Béhagle et al., 2016). The authors also noted low backscatter intensities within the surface layer in winter relative to summer in the Polar Frontal Zone (Béhagle et al., 2016). Micronekton biomasses may be seasonal in the SWIO and tightly linked to the productivity in the region although further studies are required to test this hypothesis.

The mean volume backscatter intensities were also strongly correlated with the position of fronts and water masses (Boersch-Supan et al., 2017). Mesoscale features such as cyclones recorded greater micronekton acoustic densities relative to anticyclones in the Mozambique Channel (Béhagle et al., 2014). The periphery of eddies exhibited large micronekton aggregations relative to the core (Sabarros et al., 2009). Other studies found higher species richness of micronekton in divergences and fronts that were characterised by low and high geostrophic velocities but small sea surface height anomalies (Lamont et al., 2014), relative to the core of cyclonic and anticyclonic eddies (Potier et al., 2014). Processes enhancing the biomass of micronekton in nutrient poor environments are key in controlling the abundance and distribution of higher trophic level organisms that have high energetic demands (Roger, 1994). Bouts of productivity (either seasonal or caused by physical processes) are important to sustain top predator species, especially in the south-western tropical Indian Ocean where background oceanic productivity is low and micronektonic prey are patchily distributed (Weimerskirch, 2007).

2.1.4.4 Predator species

Assemblages of seabirds, sea turtles, marine mammals, pelagic fishes and elasmobranches in the SWIO were shown to reflect the broad ecoregions- EAFR, ISSG, and Indian Monsoon Gyre (Longhurst, 1998) and habitat types- shelf, slope and oceanic (Weimerskirch, 2007; Laran et al., 2017). Below is a non-exhaustive list of some of the most prominent predators and marine mammals and their preferred dwelling (migrating and foraging) grounds and favourite prey, with respect to the circulation patterns and topographic features of the SWIO.

Seabirds

The tropical WIO is a hotspot for seabird colonies that are concentrated at three major breeding sites- Seychelles, the Mozambique Channel, and the Mascarene Archipelago (Tree, 2005; Catry et al., 2009; Le Corre et al., 2012; Laran et al., 2017). Studies suggest that marine birds depart from their respective colonies and commute to predictable productive mesoscale features such as frontal zones, eddies, shelf edges, upwelling zones (Weimerskirch, 2007) and seamounts (Le Corre et al., 2012). Elevated seabird densities have been reported to the south of Madagascar including the Madagascar continental shelf, MAD-Ridge and Walters Shoal seamounts (Le Corre et al., 2012; Mannocci et al., 2014).

Breeding Barau's petrels forage mainly on large nektonic squids such as *Sthenoteuthis oualaniensis* (Kojadinovic et al., 2007) and epi-, meso- pelagic fishes to the south of Madagascar, including MAD-Ridge and Walters Shoal seamounts, during their long trips between October and March (Stahl & Bartle, 1991; Le Corre et al., 2012; Pinet et al., 2012). Breeding red-tailed tropicbirds of Europa Island and Nosy Vé (southwest Madagascar) also forage around Walters Shoal during austral summer from November to April (Le Corre et al., 2012). Breeding shearwaters avoid the shallow waters of the Mascarene region (Catry et al., 2009) whereas chick-rearing Barau's petrels forage locally around Réunion Island during their short trips (Le Corre et al., 2012). Site fidelity to distant foraging grounds at specific periods is likely supported by the high probability for these birds of finding productive sites with relevant prey items (Weimerskirch, 2007). After the breeding period, most of these birds migrate to the central Indian Ocean or eastwards (Stahl & Bartle, 1991; Le Corre et al., 2012).

Marine birds show annual and seasonal (either summer or winter) or non-seasonal breeding, with the breeding pattern being driven by physical oceanographic patterns which influence the productivity and hence the prey availability (Le Corre, 2001; Jaquemet et al., 2007; Monticelli et al., 2007; Pinet et al., 2012). Foraging seabirds including sooty terns (*Sterna fuscata*), red-

footed boobies (*Sula sula*) and Audubon's shearwaters (*Puffinus Iherminieri*) that breed during austral winter (June-October) rely on the presence of subsurface predators such as tunas and dolphins which make prey readily available in the upper layer of the water column (Le Corre, 2001; Jaquemet et al., 2007; Monticelli et al., 2007). Seabirds also aggregate in areas with higher oceanic productivity (Monticelli et al., 2007) during austral winter when sea surface temperatures are the lowest and when thermal fronts occur (Le Corre, 2001). Seabirds including frigatebirds, sooty terns *Sterna fuscata* and red-footed boobies *Sula sula* perform long foraging trips of ~1000 km during the breeding season to feed on flying fish and squids (Cherel et al., 2008). The foraging grounds of the Great Frigatebirds *Fregata minor* were more frequently associated with higher surface chlorophyll concentrations and cyclonic vortices (Weimerskirch et al., 2010).

Marine turtles

The WIO is believed to host five species of marine turtles including the green turtle *Chelonia mydas*, the hawksbill *Eretmochelys imbricata*, loggerheads *Caretta caretta*, leatherbacks *Dermochelys coriacea* and the olive ridley *Lepidochelys olivacea* (Bourjea et al., 2008). These turtles nest on beaches of countries neighbouring the WIO (Bourjea et al., 2008) and forage in their national waters (Taquet et al., 2006; Bourjea et al., 2008; Jean et al., 2010; Mencacci et al., 2010; Ballorain et al., 2013). Loggerhead turtles were reported to consume crustaceans and molluscs in coastal habitats and jellyfish during their pelagic journeys, while leatherbacks were reported to feed exclusively on gelatinous zooplankton (Du Preez et al., 2018). The foraging patterns of leatherback turtles is also reportedly linked to mesoscale eddies, convergence or upwelling areas that concentrate prey. Leatherback turtles in the Mozambique Channel may remain associated with mesoscale eddies for prolonged periods (Lambardi et al., 2008).

Cetaceans

The WIO also reportedly hosts 33 cetacean species including seven species of baleen whales, ten toothed whales and sixteen delphinids (Kiszka et al., 2007; van der Elst & Everett, 2015). Due to their coastal or inshore habitats along southern Africa and island states in the region (Braulik et al., 2015; Viricel et al., 2016; Bouveroux et al., 2018), the delphinid species are less likely associated with seamounts along the Madagascar, South West Indian and Mascarene Ridges. Risso's dolphins, however, which prefer steep-sloped bottoms near the outer edge of continental shelves, occur off eastern and southern Madagascar (Jefferson et al., 2014).

Delphinids from the region have been reported to feed on mesopelagic prey including fishes, cephalopods and crustaceans (Braulik et al., 2015). In the SWIO, Delphininae and Globicephalinae were reported to optimise their foraging success by feeding at shallow depths in regions of accessible and high prey densities (Lambert et al., 2014). *Stenella* spp. and *Tursiops* spp. were reported to forage mostly at night in the epipelagic zone (0-200 m), following the vertical migration of mesopelagic communities at dusk (Lambert et al., 2014). These species are occasionally able to perform deep dives down to 400 m (Benoit-Bird & Au, 2003; Lambert et al., 2014). Sperm and beaked whales were shown to dive deeper and exploit prey resources in the bathypelagic zone (Lambert et al., 2014; Fig. 2.6). Cetaceans respond directly to the density, horizontal and vertical distributions of the deep scattering layer and with respect to their diving abilities (Lambert et al., 2014; Hazen & Johnston, 2010). The distribution of pilot whales was associated with high acoustic densities of prey in the mid- and deep layers. Stenella dolphins and false killer whales were correlated with a shallower backscattering layer (Lambert et al., 2014; Hazen & Johnston, 2010; Fig. 2.6).

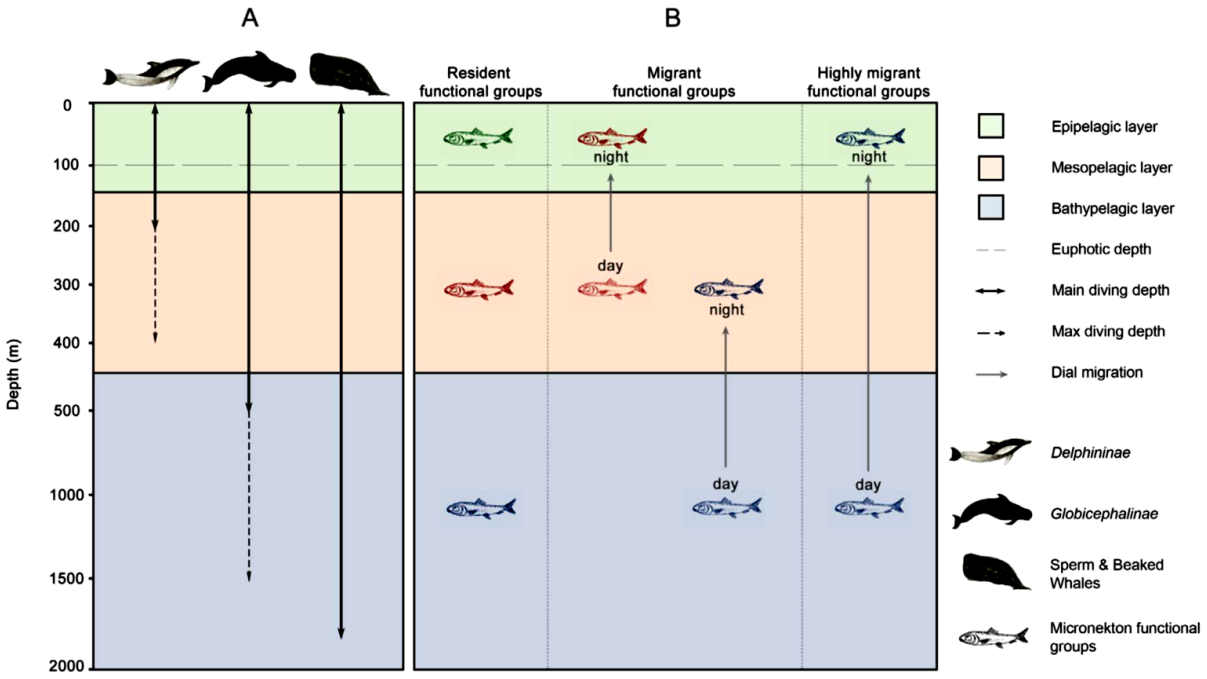

Figure 2.6 Modelled vertical distribution of (A) cetaceans and (B) scattering layers (prey items for top predators) in the water column [Source: Lambert et al., 2014].

Compared to the southeast Indian Ocean, the SWIO exhibits low humpback whale (*Megaptera novaeangliae*) aggregations (Best et al., 1998; Trudelle et al., 2019; Fig. 2.7). Four breeding sub-stocks of humpback whales have been identified in the SWIO by the International Whaling Commission (Fig. 2.7). The occasional blooms southeast of Madagascar and north of the

Crozet Plateau reportedly attract humpback whales and the whale sharks *Rhincodon typus* to the region (Brunnschweiler et al., 2009; Fossette et al., 2014). The Mozambique Channel is also reportedly an important habitat for whale sharks probably due to suitable sea surface temperatures and chlorophyll *a* concentrations (Sequeira et al., 2012). Réunion Island, Madagascar, La Pérouse and Walters Shoal seamounts are important breeding sites for humpback whales during austral winter (Best et al., 1998; Dulau-Drouot et al., 2012; Cerchio et al., 2013; Dulau et al., 2017). The occasional high humpback whale density at Walters Shoal has been reported to be due to the presence of large numbers of the crustacean *Systellapsis* sp. and the fish *Trachurus* at the seamount (Best et al., 1998; Shotton, 2006). A high proportion of blue whales were caught along the Madagascar Ridge by Soviet vessels from 1958 to 1973, while these cetaceans reportedly avoided oligotrophic central gyres such as the ISSG (Branch et al., 2007). Within the SWIO, Delphininae and Globicephalinae had low predicted densities in the ISSG province around the Mascarene Islands relative to the more productive Mozambique Channel where predicted densities were the highest (Mannocci et al., 2014; Laran et al., 2017). A high level of connectivity in terms of whale movements was also observed between the Mascarene and Madagascar regions (Dulau et al., 2017).

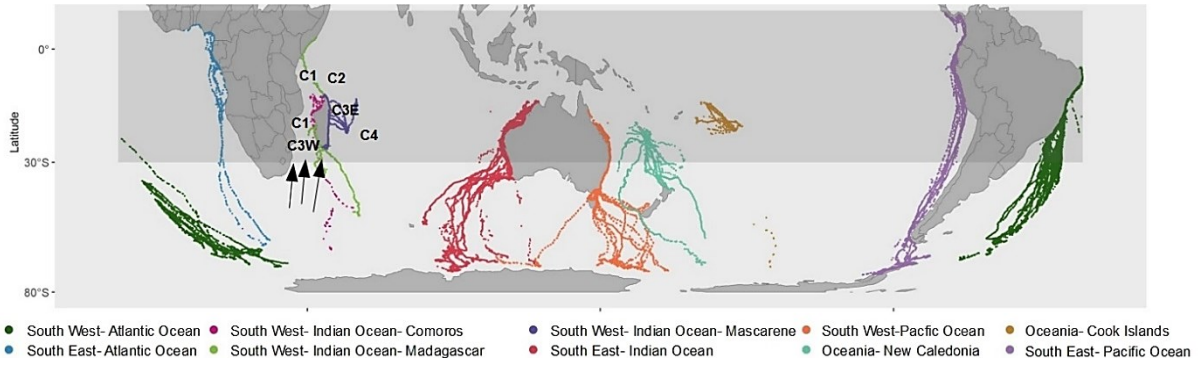

Figure 2.7 Trajectories of humpback whale stocks and sub-stocks (coloured) recognised by the International Whaling Commission. Arrows represent the postulated migration routes of humpback whales in the SWIO from the sub-Antarctic region [Source: Ersts et al., 2011 and Trudelle et al., 2019].

Billfishes and tunas

The hotspots of the swordfish, *Xiphias gladius*, in the Indian Ocean were associated with areas of high chlorophyll *a* concentrations and mesoscale activities to the southeast coast of Madagascar (Sabarros et al., 2014). Swordfish were shown to undertake large vertical migrations and forage at great depths, to a maximum of 600 m (Stillwell & Kohler, 1985). In the Mozambique Channel, smaller-sized swordfish foraged mostly on mesopelagic fishes (Nomeidae and Diretmidae), while larger individuals preyed on cephalopods Ommastrephidae

and Onychoteuthidae (Potier et al., 2007, 2008; Ménard et al., 2007, 2013). However, the foraging pattern of swordfish may not only depend on prey availability, but also on a certain degree of prey selection. Swordfish in the EAFR province that foraged close to Madagascar Island, consumed a greater proportion and diversity of lower trophic level micronekton species relative to similar-sized individuals that consumed a greater proportion of larger-sized squids in the ISSG province (Annasawmy et al., 2018).

Physical oceanographic processes such as the edge of anticyclonic eddies stimulate phytoplankton growth in surface layers, leading to phytoplankton blooms and high prey densities for adult yellowfin tunas in the Indian Ocean (Fonteneau et al., 2008). The spatial distributions of large tunas were reported to strongly overlap with Longhust's (2007) biogeochemical provinces (Reygondeau et al., 2012). Few studies have investigated the relationship between catch rate of tuna species and presence of seamounts from the SWIO. Marsac et al. (2014) have shown that the Coco de Mer seamount at the equator in the Indian Ocean sustains large catches of skipjack, yellowfin and smaller proportions of bigeye tunas. The author has suggested that local enrichment processes may lead to an increase in foraging opportunities for these top predators. However, the presence of an anchored ship acting like Fishing Aggregating Devices, along with the geo-magnetic properties of the seamount may jointly contribute to attract predators near the summit (Marsac et al., 2014).

Yellowfin tunas are known to be non-selective feeders, with their foraging patterns depending on prey availability rather than selectivity (Roger, 1994). Yellowfin tunas from the Indian Ocean have been reported to spend most of their time in the surface layer of the water column (Potier et al., 2004; 2007) in areas in which the mixed layer depth is shallow and the stratification is strong (Miller, 2007; Fig. 2.8). Surface swimming yellowfin tunas from the Seychelles region fed exclusively on stomatopods, whereas the deep-dwelling individuals foraged on crustaceans, crab larvae, fish (including myctophids and small scombridae) and cephalopods (Potier et al., 2004; 2007; Zudaire et al., 2015). Potier et al. (2004) have suggested that the food chain leading to these tunas is relatively short in the WIO since crustaceans and smaller-sized individuals are dominant in the diet. Spawning yellowfin tunas, on the other hand, were reported to feed intensively on cigarfish *Cubiceps pauciradiatus* due to the specific energy content of this species (Zudaire et al., 2015). Hence, the diets of these top predators may also depend on their specific energetic needs during their life cycle.

Surface swimming bigeye tunas further preyed extensively on stomatopods and cephalopods (including *Stenoteuthis oualaniensis* and *Ornithoteuthis volatilis*) and deeper-dwelling individuals fed on cephalopods and fish (Potier et al., 2004; Fig. 2.8). The myctophid-dominant diet of bigeye tunas is consistent with norturnal and/or twilight feeding, reflecting the DVM of their prey items (Sardenne et al., 2016). Free swimming schools of skipjack tunas from the WIO were reported to occur within 25 km of favourable feeding habitats (Druon et al., 2017) and to have a lower consumption of myctophids but a higher consumption of crustaceans in their diet (Sardenne et al., 2016). Albacore tuna caught from the southern coast of South Africa, on the other hand, were shown to preferentially predate on two species of fish (*L. hectoris* and *M. muelleri*) and one cephalopod *L. lorigera* (Munschy et al., 2016). In subtropical oceanic waters, yellowfin, bigeye and albacore tunas were further reported to forage at different times of the day (Olson et al., 2016; Fig. 2.8).

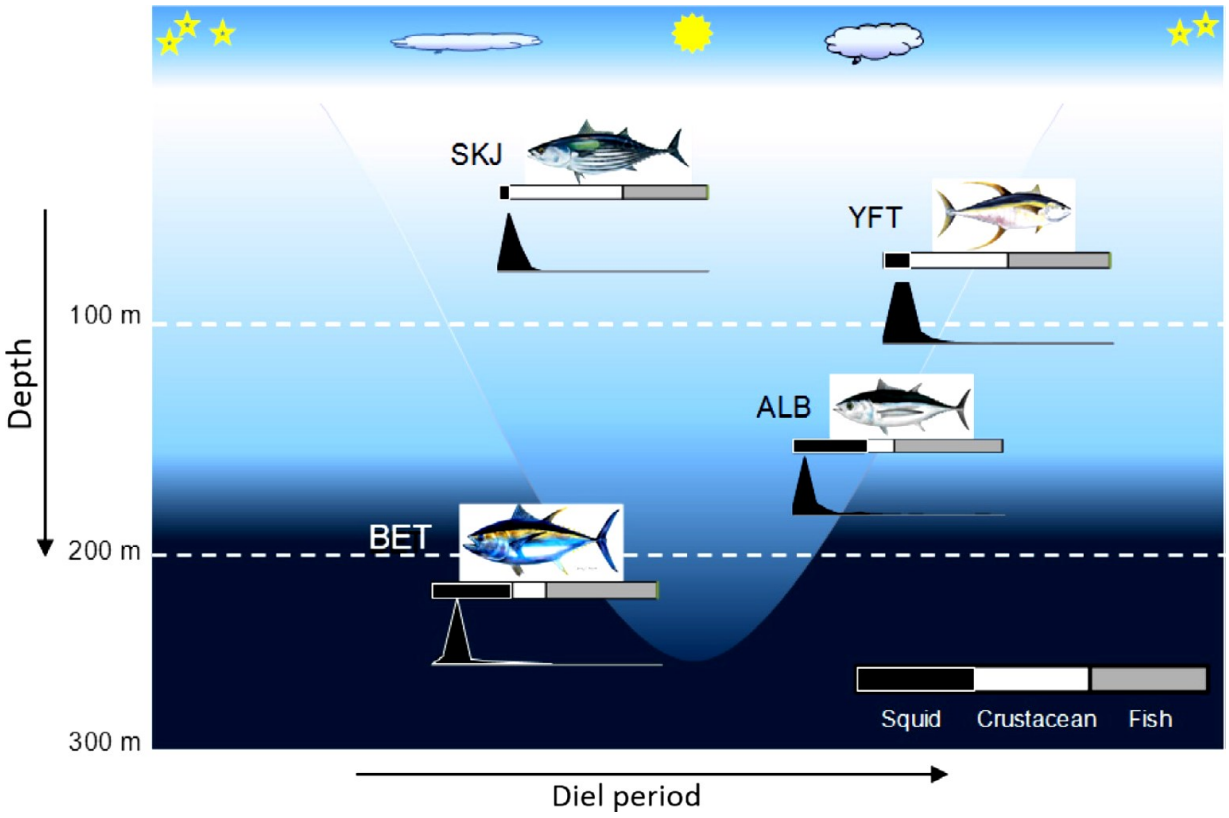

Figure 2.8 Schematic illustration of the niche partitioning of ALB (Albacore tuna), BET (Bigeye tuna), SKJ (Skipjack tuna) and YFT (Yellowfin tuna) in the western Indian Ocean. The bars represent the importance of the main prey categories (squid: black; crustacean: white; fish: grey) in the diet of each predator. The histograms represent the size distribution of the prey for each predator with the maximum prey size being 500 mm [Source: Olson et al., 2016].

Sharks

Little is known about the shark species from the SWIO apart from their high bycatch rates in tuna and swordfish pelagic longline and purse seine fisheries (García-Cortés & Mejuto, 2002; Amandè et al., 2008; Rabehagasoa et al., 2012). The stomach contents of several shark species, including the sandbar, *Carcharhinus plumbeus* (Cliff et al., 1988), dusky shark, *Carcharhinus obscurus* (Dudley et al., 2005), shortfin mako, *Isurus oxyrinchus* (Groeneveld et al., 2014), blacktip, *Carcharhinus limbatus* (Dudley & Cliff, 1993); tiger, *Galeocerdo cuvier*, smooth hammerhead, *Sphyrna zygaena*, scalloped hammerhead, *S. lewini,* and great hammerhead, *S. mokarran*, are dominated by cephalopods and teleosts to a large extent, and elasmobranchs and crustaceans to a lesser extent (Smale & Cliff, 1998; De Bruyn et al., 2005). The dominance of continental-shelf dwelling and deep-water cephalopods in the KwaZulu-Natal area off the coast of southern Africa, is believed to support common dolphins and sharks (Smale & Cliff, 1998). The link between shark distribution and seamount presence is poorly established in the SWIO except along the SWIR where male and females of a new catshark species, *Bythaelurus naylori* sp. n. have been discovered in relatively large numbers (Ebert & Clerkin, 2015). Males and females of a new species of the catshark, *B. bachi*, have been discovered at Walters Shoal seamount (Weigmann et al., 2016). Error seamount (Mount Error Guyot) in the north-western Indian Ocean host the catshark *B. stewarti* that was reported to feed mostly on cephalopods and teleosts (Weigmann et al., 2018).

2.2 Industrical fisheries in the SWIO

In 2015, the SWIO countries (Southern, Eastern Africa and island states) reportedly produced ~13% of the WIO (FAO Area 51) total fish landings, which itself produced ~40% of the Indian Ocean landings (FAO, 2016). The WIO contributes barely 6% of the global fish catches. However, several small island countries of the WIO, including Maldives, Mauritius and Seychelles, are heavily reliant on marine fisheries for food security and for the national economies as source of foreign exchange (Kimani et al., 2009). Demersal and industrial fisheries occur in the SWIO and target a range of species as shown below.

2.2.1 Demersal fisheries

Demersal species can be classified into either benthic (those species being negatively buoyant and living off the bottom) or benthopelagic (species that have buoyancy mechanisms to maintain themselves in the water column to feed) (Koslow, 1996). Demersal fishes are generally closely associated with reefs and the benthic environment (van der Elst et al., 2009)

along shelves, continental slopes (Everett et al., 2015) and seamounts. Demersal species, that are closely associated with seamounts, generally have robust bodies with well-developed caudal organs and strong locomotory abilities to avoid advection by strong currents (Koslow, 1996). These organisms may hence benefit from shelter regions offered by the topography and from the locally generated and/or advected foraging opportunities (Isaacs & Schwartzlose, 1965; Genin et al., 1988, 1994; Seki & Somerton, 1994; Koslow, 1996). Some of these deep-sea fishes also depend on local physical processes for basin-scale larval dispersal. Populations of adult orange roughy, for example, have been reported to depend on water masses such as AAIW (Antarctic Intermediate Water) and NADW (North Atlantic Deep Water) that provide optimal salinity conditions for larval dispersal (Clark et al., 2010a).

Aggregations of several demersal fish species on seamounts have led to the boom of specific fisheries. Seamounts of the Indian Ocean have been targeted by commercial fishing vessels for primary seamount species including alfonsino (*Beryx splendens*) and orange roughy (*Hoplostethus atlanticus*) (Ingole & Koslow, 2005; Bensch et al., 2009). Spawning orange roughy were targeted on the Madagascar Ridge, peaking in 1999 and 2000 at around 7000 t, before declining in subsequent years (Ingole & Koslow, 2005; FAO, 2016) (Fig. 2.9). This fishery has experienced a boom-and-bust phase following US market demands, with the orange roughy population being reduced to more than 85%, partly due to its slow growth rate, low fecundity and delayed reproduction (Lack et al., 2003). Other bycatch species caught in the orange roughy fishery include black, spiky and smooth oreo (*Allocyttus niger*, *Neocyttus rhomboidalis* and *Pseudocyttus maculatus* respectively) and deep-sea sharks, along with small quantities of black corals (*Antipatheria* spp.) taken in bottom trawl fishing operations (Bensch et al., 2009; Lack et al., 2013).

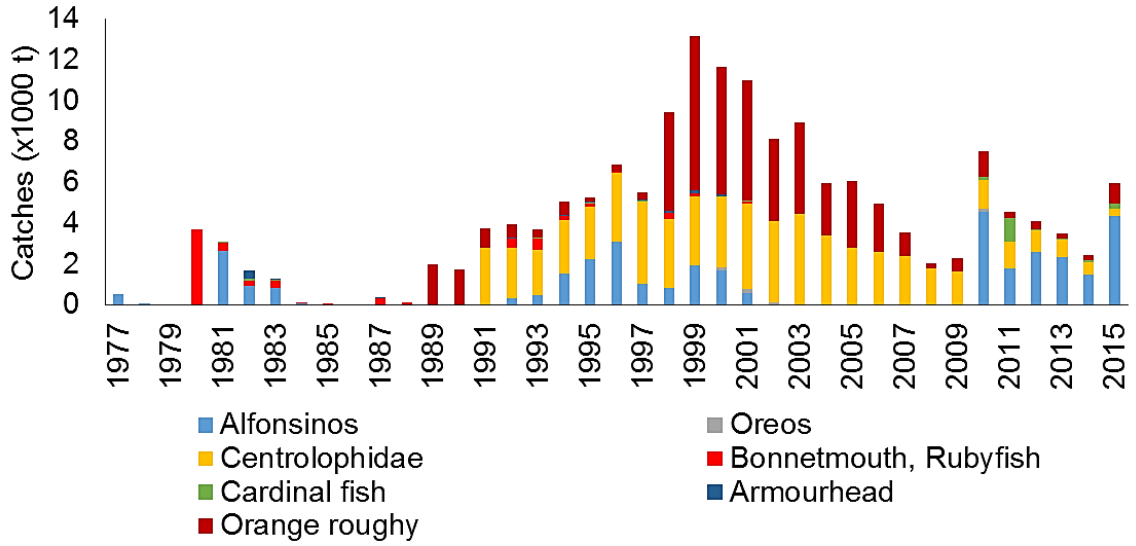

Figure 2.9 Catches (in 1000 tons) from 1977-2015 for the most commonly caught deep-sea fishes from the Southern Indian Ocean (Source: FAO, 2016).

2.2.2 Pelagic fisheries

Small pelagic resources including scads, sardines, anchovies and horse mackerels are also exploited by inshore fishers from the WIO. However, the tonnage contribution of these resources is considerably less than that for large pelagic resources (van der Elst et al., 2009). Large pelagic fish resources comprising yellowfin, bigeye, albacore and skipjack tunas, billfishes (swordfish, marlins, sailfish), sharks, seerfishes (wahoos) and dolphinfish, are widely distributed throughout the WIO (Stéquert & Marsac, 1989). While the purse seine fishery operates mostly north of 12°S and in the Mozambique Channel, the longline fishery operates more widely throughout the whole Indian Ocean, to the South of Madagascar, around the Seychelles Plateau and the Mascarene region. Purse seiners catch schools associated with Fish Aggregating Devices and those being unassociated, i.e. swimming freely. The former are caught throughout the WIO, however with a greater intensity in the Somali Basin and in the Mozambique Channel (Fonteneau et al., 2000; Fonteneau, 2010). The free schools are mostly exploited in the Equatorial Counter Current, from 0-10°S (Fonteneau, 2010).

Yellowfin tunas from the Indian Ocean (409 000 t in 2017) are exploited industrially by purse seine and longline fisheries, and artisanally by handline, gillnet, pole and line fisheries (IOTC, 2018). Bigeye tunas (90 000 t in 2017) are primarity exploited by longliners that catch adult fish whereas purse seiners catch juvenile fish between 10°N and 15°S. However, a secondary fishing zone is found between latitudes 25°S-40°S. The centre of the ISSG province has very low bigeye catches (Fonteneau, 2010). Albacore is mostly caught by longline south of 10°S.

The SWIO region has shown a large increase in catches since the 1990s, with some activity in the vicinity of seamounts such as La Pérouse (Fonteneau, 2010). From 2001 to 2017, albacore tuna and swordfish were caught in higher proportions and yellowfin and bigeye tunas in lower numbers by longline fisheries in the vicinity of Réunion Island, as shown with high resolution data (1° square) provided by three fleets of the region (Fig. 2.10).

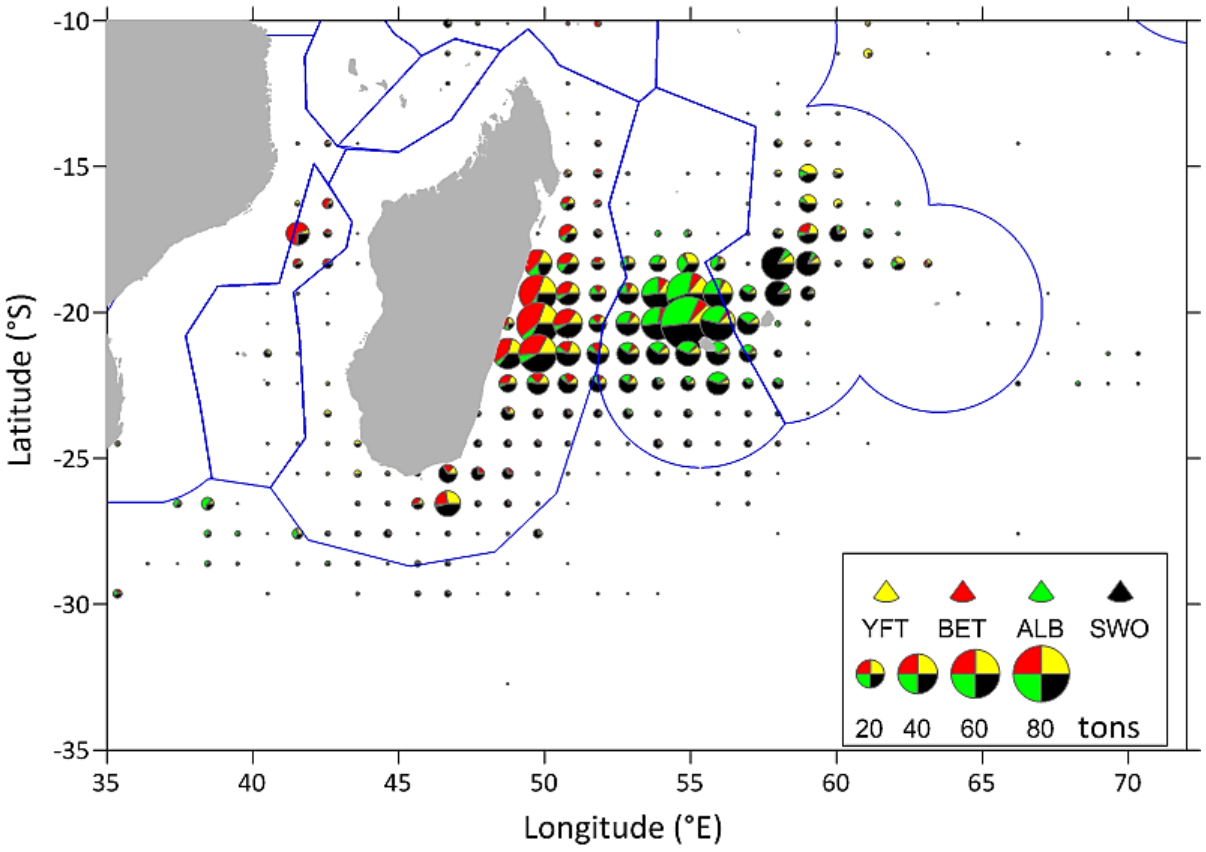

Figure 2.10 Longline catches (by 1° square) of yellowfin (YFT), bigeye (BET), albacore (ALB) tunas and swordfish (SWO) in tons from France (Réunion Island), Mauritius and Seychelles fleets in the SWIO from 2001-2017. Neighbouring countries' Exclusive Economic Zones are shown by blue lines [Data Souce: IOTC C/E database, 2018].

Longline catches along the continental slope to the south of Madagascar were mostly dominated by swordfish, with yellowfin and bigeye tunas being caught in lower numbers. The map using the lower resolution data (5° square) provided by all fleets in the region, show that both species diversity and volume of the catches increased from east to west. The relative proportion of swordfish increased along the Madagascar Ridge compared to the ISSG province (Fig. 2.11). Swordfish is known to be associated to oceanographic features such as seamounts

and frontal eddies (Sedberry & Loefer, 2001) which is a characteristic of the Madagascar Ridge.

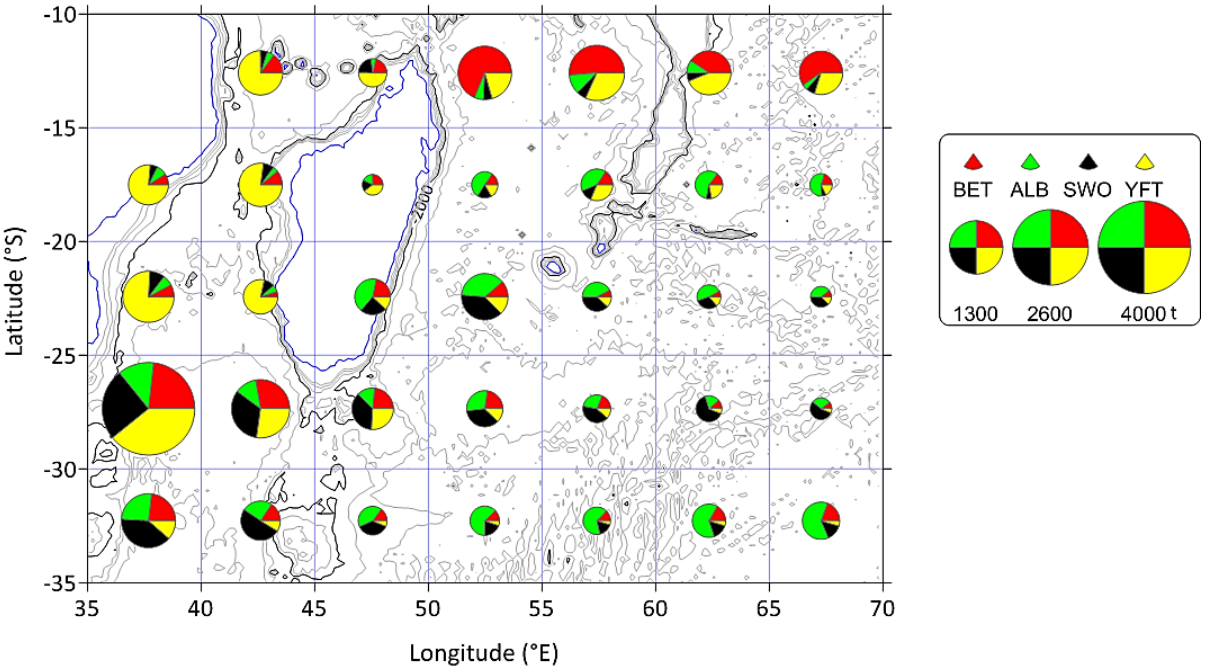

Figure 2.11 Longline catches (by 5° square) of yellowfin (YFT), bigeye (BET), albacore (ALB) tunas and swordfish (SWO) in tons from 1995 to 2015, combining all longline fleets operating in the Indian Ocean. Isobaths are represented in the background (1000 m depth interval). The 2000 m isobaths is represented by a black line [Data sources: IOTC C/E database, (2018) and ETOPO1 database].

Other pelagic fisheries also occur in the SWIO, such as those for crustaceans, prawns and lobsters (Ivanov & Krylov, 1980; Pollock et al., 2000). Fisheries from the WIO yielded 350 000 tons of crustaceans, dominated by shrimps and crabs in 2003 (van der Elst et al., 2009). French trawlers and a Spanish vessel reportedly caught deep-sea lobster *Palinurus barbarae* at Walters Shoal seamount (Collette & Parin, 1991; Bensch et al., 2009). Few crustacean fisheries from the Western Indian Ocean are managed on a national level and none is managed collectively at the regional level (van der Elst et al., 2009). High mortality rates of silky sharks *Carcharhinus falciformis* caught in purse seine fisheries were recorded in the Indian Ocean (Poisson et al., 2014). Bycatch rates from trawl fisheries in the WIO are also non-negligible (Fennessy, 1994; Fennessy & Groeneveld, 1997; van der Elst et al., 2009).

2.3 Marine governance in the SWIO

The SWIO supports several industrial, semi-industrial, recreational and artisanal fisheries for both pelagic and demersal resources, many of which are still unregulated or poorly regulated

due to a lack of scientific, technical, financial, human-resource and management capacities (Kimani et al., 2009; van der Elst et al., 2009). The marine biological resources of the SWIO are threatened by overfishing, bycatch and mortality of discarded organisms, fishery-induced impacts, illegal fishing practices, plastic and agricultural pollution, habitat degradation and deep-sea mining (Kimani et al., 2009). Twelve marine organisms in the SWIO are either listed as near threatened (such as the Indo Pacific humpback dolphins), as vulnerable (including sperm whales, Dugongs, Herald petrels, olive Ridley turtles), and as endangered or critically endangered (for e.g. Barau's petrels, Mascarene petrels, the green, hawksbill, loggerhead and leatherback sea turtles, and hammer sharks) (Laran et al., 2017). Marine mammals, sea turtles and elasmobranchs are at risk of decline since they are incidentally caught by fisheries.

There are still significant knowledge gaps on the biological characteristics, fishing pressure, fish stocks and effects of anthropogenic activities on marine resources of the SWIO (van der Erst et al., 2009). The fact that pelagic resources such as tunas and billfishes are highly migratory across ocean basins and nations' Exclusive Economic Zones (EEZ), further calls for integrative and cooperative science management plans from the different nations in the region (Pentz et al., 2018). This difficult task is implemented by Regional Fisheries Management Organisations (RFMO). For several stocks (mostly coastal small pelagic and demersal fishes, as well as seamount-associated fishes), the status is uncertain with underreported catches when there are no observers on board, leading to uncertainties in fish stock assessments (Kimani et al., 2009). As usual, fisheries managers are tied between the need to devise policies that maximise social and economic benefits, while balancing the sustainable economic yield of the fishery and ensure viability of the resource (Kimani et al., 2009).

According to the FAO, 75% of fisheries from the WIO are being exploited at their maximum biological productivity (i.e. the MSY- Maximum Sustainable Yield), while the remainder are currently overexploited (Kimani et al., 2009). Due to the remoteness of certain areas, monitoring, controlling and surveillance of fishing activities are difficult, especially for illegal, unreported and unregulated (IUU) fishing (Kimani et al., 2009). The RFMOs established under the UN Convention on the Law of the Sea (UNCLOS), are responsible for ensuring the proper management of fish stocks (optimal use and conservation) in the respective regions. RFMOs are the formal institutions enabling cooperation between nations outside of their EEZs. However, contracting parties whose interests will be negatively impacted can block the reforms proposed by RFMOs or adopt moderate quota reductions instead of approaches such as MPA

networks, thus reducing the management capacity of the organisation (Gjerde et al., 2013; Pentz & Klenk, 2017).

Seventeen RFMOs currently cover the different high-sea regions in the world ocean. In the Indian Ocean, the IOTC (Indian Ocean Tuna Commission) is mandated to manage tuna and tuna-like species in the Indian Ocean EEZs and on the high seas (Pentz et al., 2018). The rules and decisions adopted by the IOTC apply to countries that are members of the organisation (31 in 2017). These countries are strongly encouraged by international law (Article 17 of the UNFSA) to cooperate and abide by the rules and regulations set by the regional managing body, although IUU fishing may still occur (Gjerde et al., 2013). Another RFMO is the South West Indian Ocean Fisheries Commission (SWIOFC), composed of 12 countries. The SWIOFC aims at ensuring sustainable use of living resources (other than tunas and billfishes) in the SWIO region, and promoting the Large Marine Ecosystems (LMEs) approach initiated during the South West Indian Ocean Fisheries Project (SWIOFP) and the Agulhas-Somali Current Large Marine Ecosystem (ASCLME) projects (Vousden et al., 2008).

There are increasing incentives for the set-up of MPAs in the region, including on the high seas (Laran et al., 2017). MPAs set-up in several jurisdictions via a high seas treaty targeting Biodiversity Beyond National Jurisdictions (BBNJ) may be of critical importance in protecting high seas ecosystems (Pentz et al., 2018) in the long run. However for a significant positive impact to be observed, the MPAs will need to have four or five of the following features: older (>10 years), larger (>100 km^2), isolated by deep water or sand, non-extractive and effectively enforced (Edgar et al., 2014). Several other conventions such as UNESCO Biosphere Reserves, the UNEP's Convention on Biological Diversity and Regional Seas Programme, Ramsar convention sites and the International Maritime Organization has been developed to better conserve and manage vulnerable sites to fishing and pollution (Attwood et al., 1997). A complete closure of certain areas of the high seas to fishing pressure may yield longer benefits via spill over effects into domestic EEZs. A system of MPA networks may also be beneficial via spillover effects and protection of adjacent areas (Roberts et al., 2018). Having mobile closures with different areas closed to fishing at different periods may prove more successful than spatial closures or seasonal closures due to high mobility of some species (Grantham et al., 2008). The downside is the difficulty to perform efficient monitoring, control and surveillance of such entities at reasonable costs, especially on the high seas.

Several areas of the SWIO, including the Mozambique Channel and south of Madagascar are recognised as being biodiversity hotspots and ecologically and biologically significant areas (EBSAs), with significant polymetallic nodules (Fig. 2.12). Nations including China, Germany, India and Korea have exploration permits for deep-sea mining along the SWIR (Guduff et al., 2018). Some management efforts have been initiated in the SWIO such as promotion of responsible fishing practices by the Southern Indian Ocean Deepsea Fishers Association (SIODFA) and implementation of benthic protected areas (BPA) on the high seas within the Southern Indian Ocean Fisheries Agreement (SIOFA) boundary. However, significant knowledge gaps identified during the 2016-2017 SIOFA meetings have led to the rejection of a proposal to convert SIODFA's BPAs into formal VME (Vulnerable Marine Ecosystem) closures (Guduff et al., 2018). More recently, five new protected areas on the high seas have been declared by SIOFA at its MoP5 (5th Meeting of the Parties in 2018) encompassing Atlantis Bank, Coral seamount, Fool's Flat, Middle of What seamount and Walters Shoal seamount (IUCN, 2018). However, these closures apply only to bottom trawling and do not cover other fishing gears. Very few areas are regularly or completely closed on the high seas of the SWIO, with few exceptions to the south-eastern coast of South Africa and further south towards the Southern Ocean (Guduff et al., 2018).

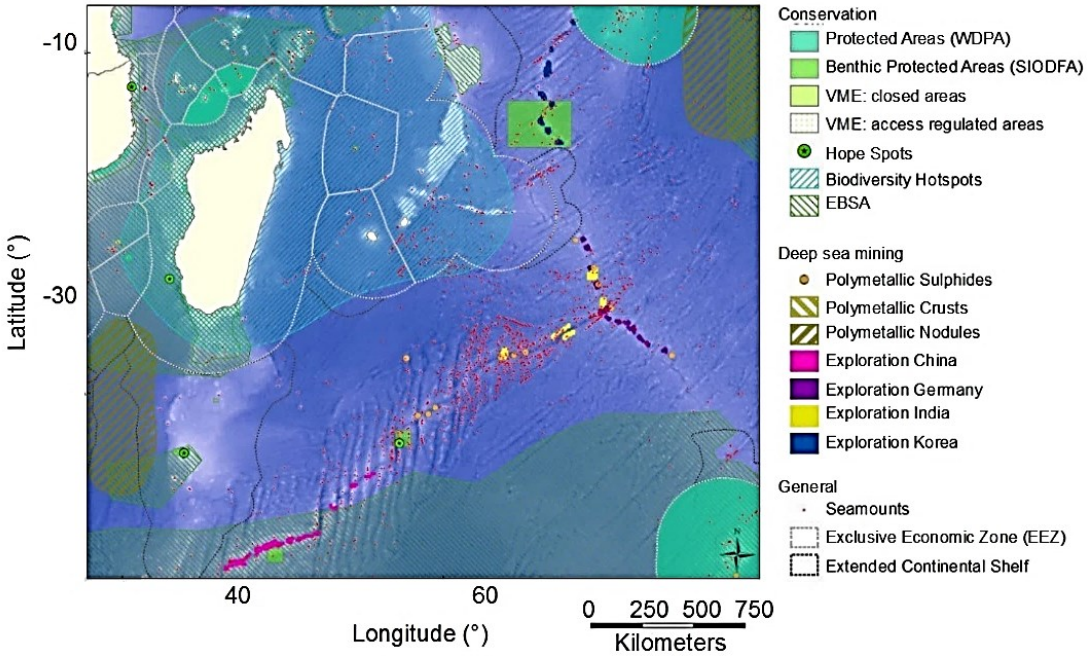

Figure 2.12 *Map of the SWIO showing the distribution of seamounts having elevations >1000 m and protected, closed and access regulated areas. The EEZ and extended continental shelf of states in the region are denoted, along with areas with conservation incentives. Deep sea mining exploration for polymetallic sulphides, crusts and nodules by China, Germany, India and Korea are shown (Source: Guduff et al., 2018).*

2.4 Seamounts of the SWIO

Seamounts of the SWIO may add further complexity to the local flow patterns and productivity. Only 15 seamounts have reportedly been explored biologically from the Indian Ocean (Sautya et al., 2011). Seamounts of the SWIO are thus among the least explored systems globally (Bhattacharya & Chaubey, 2001). A series of dedicated cruises have started shedding new light on the ecosystems associated to seamounts (Fig. 2.13). Some of these cruises include earlier expeditions forming part of the IIOE (International Indian Ocean Expedition) on the RV *Anton Brunn* at Walters Shoal seamount in 1964, devoted mainly to benthic biology. Soviet expeditions on the RV *Akademik Kurchatov* (6th cruise) and RV *Rift* (2nd cruise) in 1983, RV *Vityaz II* (17th cruise) in 1988, the RV *Akademik Mstislav Keldysh* (7th cruise) in 1984-1985, were conducted at seamount ecosystems of the SWIO. However, some of the resulting publications from these Soviet expeditions are either inaccessible or written in Russian. More recent seamount cruises in the SWIO include expeditions at Walters Shoal as part of the ACEP-III (African Coelacanth Ecosystem Programme) programme on the RV *Algoa* in 2014. Atlantis, Sapmer, Middle of What, Melville and Coral seamounts of the SWIR (Fig. 2.13) were investigated during recent cruises on the RV Dr *Fridjtof Nansen* in 2009 and on the RV *James Cook* in 2011. La Pérouse and MAD-Ridge seamounts were explored in 2016 on the RV *Antea* and Walters Shoal in 2017 on the RV *Marion Dufresne*.

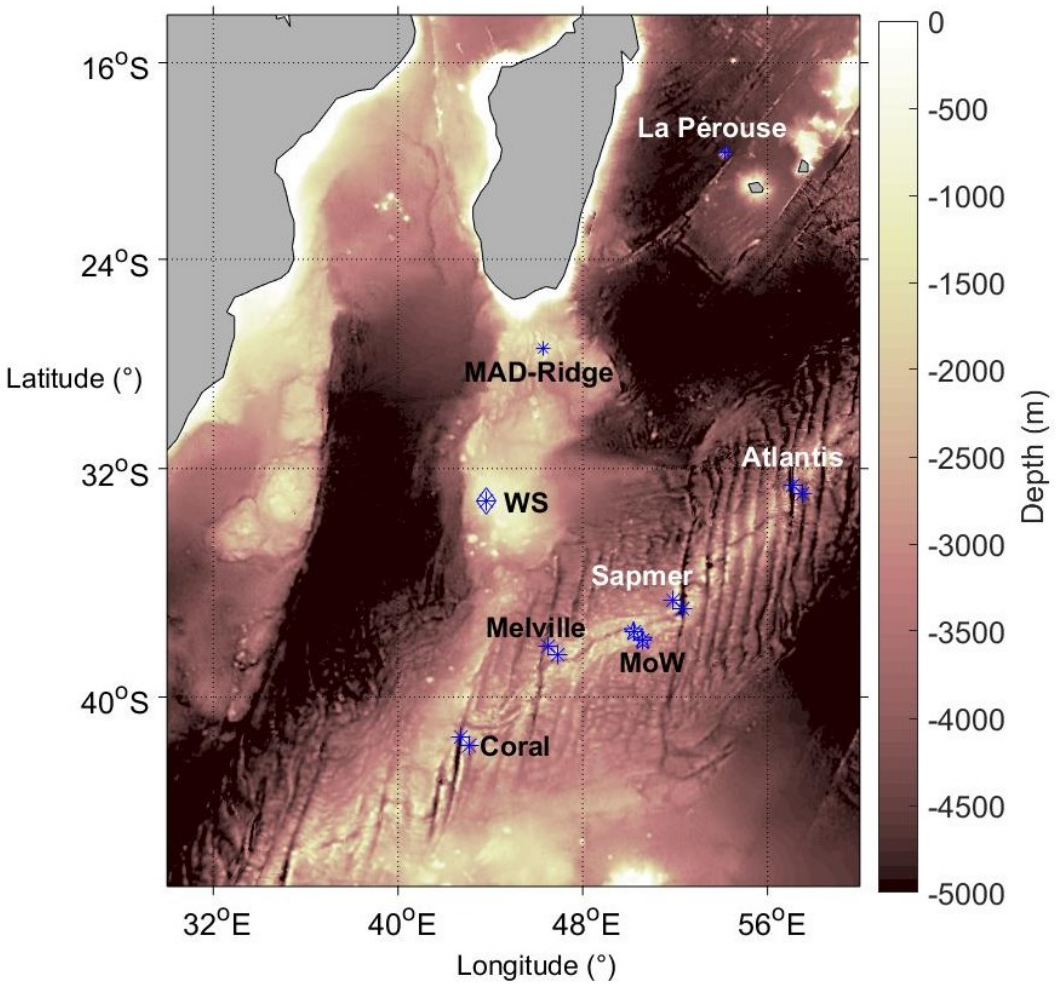

Figure 2.13 Seamounts being the focus of dedicated research cruises from 1964 to 2017: La Pérouse- in the Mascarene Basin; MAD-Ridge- along the Madagascar Ridge; WS- Walters Shoal at the southern tip of the Madagascar Ridge; Atlantis, Sapmer, MoW-Middle of What, Melville and Coral along the SWIR. The colour bar represents depth (m) below the sea surface.

2.4.1 Seamount Endemism

During an earlier cruise at Walters Shoal seamount (summit depth ~18 m), an endemic alpheid shrimp species, *Alpheus waltervadi* (Kensley, 1981), an endemic isopod, *Jaeropsis waltervadi* (Kensley, 1975), and recently, a new species of rock lobster, *Palinurus barbarae* (Groeneveld et al., 2006) were identified. During a more recent expedition (2011), new species of hippolytid shrimps, *Lebbeus ketophilos* sp. nov., and *Eualus oreios* sp. nov. were reported at Coral seamount (summit depth at ~200 m) (Nye, 2013). According to O'Loughlin et al. (2013), this expedition also sampled three new sea cucumber species, *Amphigymnas staplesi*, *Pannychia taylorae* and *Psolus atlantis*, on Atlantis Bank (summit depth at ~700 m) and Coral seamount. Following this expedition, seamounts of the SWIR have been reported to host new species of carnivorous sponges (Hestetun et al., 2017). Sponge diversity and taxonomic composition was

further investigated during the 2014 ACEP-III programme on the RV *Algoa* at Walters Shoal (Payne, 2015), with nine sponge specimens reported as new to science (Payne, 2015). Following these records, endemism seems to occur at SWIO seamounts. However, such observations have to be cautiously interpreted since levels of endemism may be much lower than previously suspected due to the low sampling effort in the region. It is believed that the fauna at seamounts generally reflects the regional species pool (Rogers & Taylor, 2011). Limited and inconsistent sampling coverage does not allow an accurate testing of the seamount endemism hypothesis (Hestetun et al., 2017).

2.4.2 Deep-sea fauna at SWIR seamounts

Reefs are other important components of the SWIO, providing shelter and acting as fish nurseries (Salm, 1983; Ahamada et al., 2004; Turner & Klaus, 2005). Studies modelling global habitat suitability for Scleratinian corals and Octocorals have shown the SWIO between 20°S and 60°S to be one of the most favourable habitats for stony corals from the surface to ~2500 m depth (Tittensor et al., 2009, 2010). Stony corals are also likely to be present along seamount peaks of the Madagascar Ridge (Tittensor et al., 2009; Davies & Guinotte, 2011) and in the Southern Indian Ocean (UNEP, 2006).

Deep-sea polychaetes were sampled at Coral, Melville, Middle of What and Atlantis seamounts across the SWIR. The most common benthic organisms along the SWIR were hard corals, octocorals and sponges (Rogers & Taylor, 2011). Atlantis Bank was also shown to host large populations of sea fans, siphonophores, lobsters and crabs. Across the SWIR, at Coral, Melville, Middle of What and Atlantis seamounts, a total of 122 solitary and 27 colonial scleractinian corals were collected at depths between 172 and 1395 m, corresponding to specific water masses including the subtropical waters, AAIW and uCDW (upper Circumpolar Deep Water) (Pratt et al., 2019). Coral seamount recorded a greater abundance and species diversity in subfossil Scleractinia relative to the other seamounts, most likely due to the high microbial community, surface chlorophyll concentrations and suitable thermal conditions over a wider depth range (Pratt et al., 2019). The Madagascar Ridge and SWIR were also predicted to be favourable habitats for soft corals Calcaxonia (Yesson et al., 2012).

2.4.3 Pelagic ecosystem at SWIR seamounts

The Dr *Fridtjof Nansen* cruise investigated the pelagic ecosystem at five seamounts in the SWIR, including Atlantis, Sapmer (summit depth ~332 m), Middle of What (~1078 m), Coral, and Melville (~120 m) (Groeneveld & Koranteng, 2017). There were little evidence for Taylor

column formation at these seamounts due to the relative instability in the flow patterns and strong currents associated with mesoscale eddies and the Agulhas Return Current (Read & Pollard, 2017). However, the generation of internal tides was observed at Coral, Sapmer and Melville banks due to the interactions of barotropic tides with the pinnacles (Read & Pollard, 2017). Factors such as latitude, internal tides, vertical displacement of isopycnals and strong vertical mixing were found to favour the delivery of nutrients to the euphotic zone and to enhance phytoplankton biomass at Coral and Melville (Read & Pollard, 2017).

A seamount effect on phytoplankton was observed on shallow seamounts Coral and Melville due to increased upwelling of organic matter (Sonnekus et al., 2017). The authors reported higher species richness and abundance of crustaceans including several lophogastrids collected at seamount stations relative to abyssal plains and ridge slopes (Letessier et al., 2017). However, an effect of the SWIR on the backscattering strength could not be detected, although increased backscatter were observed at the Subtropical and Subantarctic Fronts in the vicinity of Coral seamount (Boersch-Supan et al., 2017). The SWIO has been reported to be a hotspot of cephalopod diversity (Laptikhovsky et al., 2017). The increase in habitat availability offered by seamounts is believed to be the likely cause for the observed increase in richness of crustaceans and cephalopod communities (Vereshchaka, 1995).

2.4.4 Pollution impact on SWIR seamounts

Seamounts of the SWIO, although being remote and isolated features, are not free from pollution. Marine litter from the SWIR were dominated by fishing gear, with some seamounts- Sapmer seamount and Melville Bank- having a higher abundance of litter items than Atlantis, Middle of What or Coral seamounts (Woodall et al., 2015; Fig. 2.14). The fishing gear litter at seamounts of the SWIR were found to be heavily encrusted with corals and hydroids. Fish, crinoids, anemones, sea urchins and brittle stars, on the other hand, used the litter as habitat or as substrata for hiding or egg laying. However, entanglement were also observed and may constitute a negative impact on marine organisms. Plastic items, metal components, and other types of litter further contributed to the pollution of this ridge. The authors estimated that over 38 million litter items are present along seamounts of the SWIO (Woodall et al., 2015) partly due to lack of appropriate policies and conservation measures.

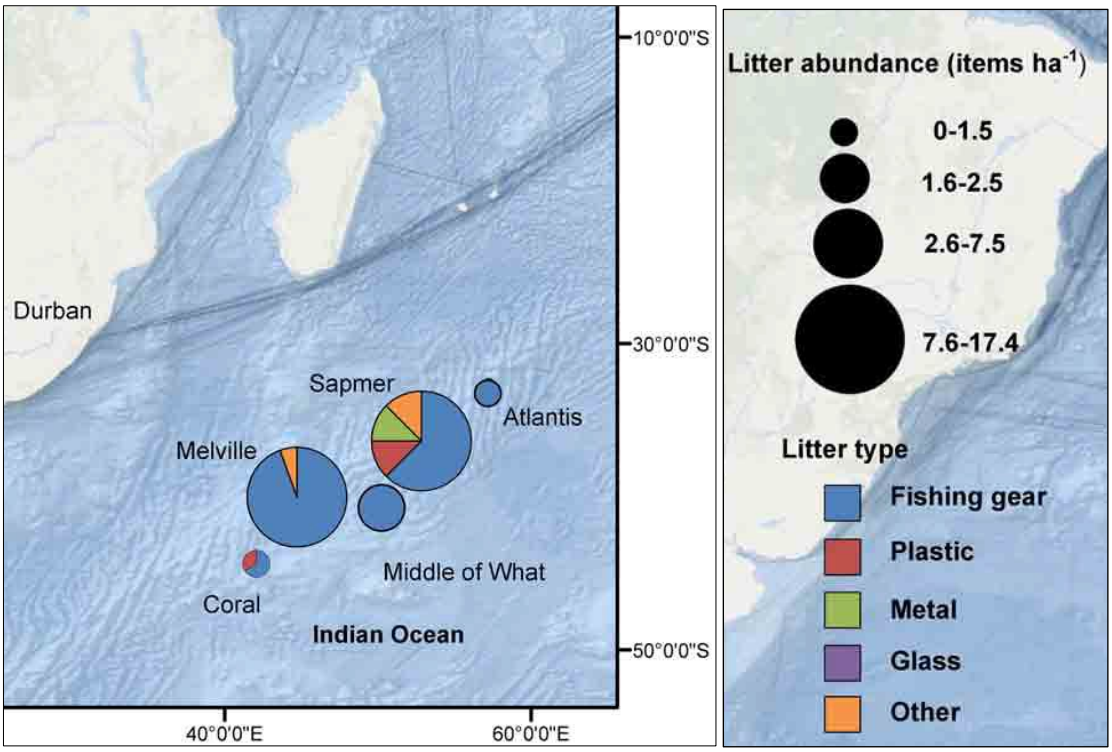

Figure 2.14 Benthic litter densities (items ha^{-1}) and composition, observed by remotely operated vehicle video systems, for seamounts of the SWIR [Source: adapted from Woodall et al., 2015].

2.5 Case Study: La Pérouse and MAD-Ridge seamounts

As part of the Second International Indian Ocean Expedition (IIOE-2) science plan, surveys were conducted at two seamounts in the SWIO. These include La Pérouse seamount and an un-named pinnacle along the Madagascar Ridge in 2016 on board the RV *Antea*. La Pérouse is located at 19°43'S and 54°10'E, i.e. ~160 km to the north west of Réunion Island. At 27°29'S and 46°16'E, is located an unnamed seamount lying ~240 km to the south of Madagascar on the northern part of the Madagascar Ridge. This feature has been termed "MAD-Ridge".

2.5.1 Bathymetry

While the water column rises from a depth of 5000 m in the vicinity of La Pérouse seamount (Fig. 2.15a), it extends from the surface to a maximum depth of 2000 to 3000 m (Sinha et al., 1981) over most of the Madagascar Ridge (Fig. 2.15b). The Madagascar continental slope rises from 1500 m depths to the continental shelf that is ~50 km wide south of Madagascar (Goslin et al., 1980).

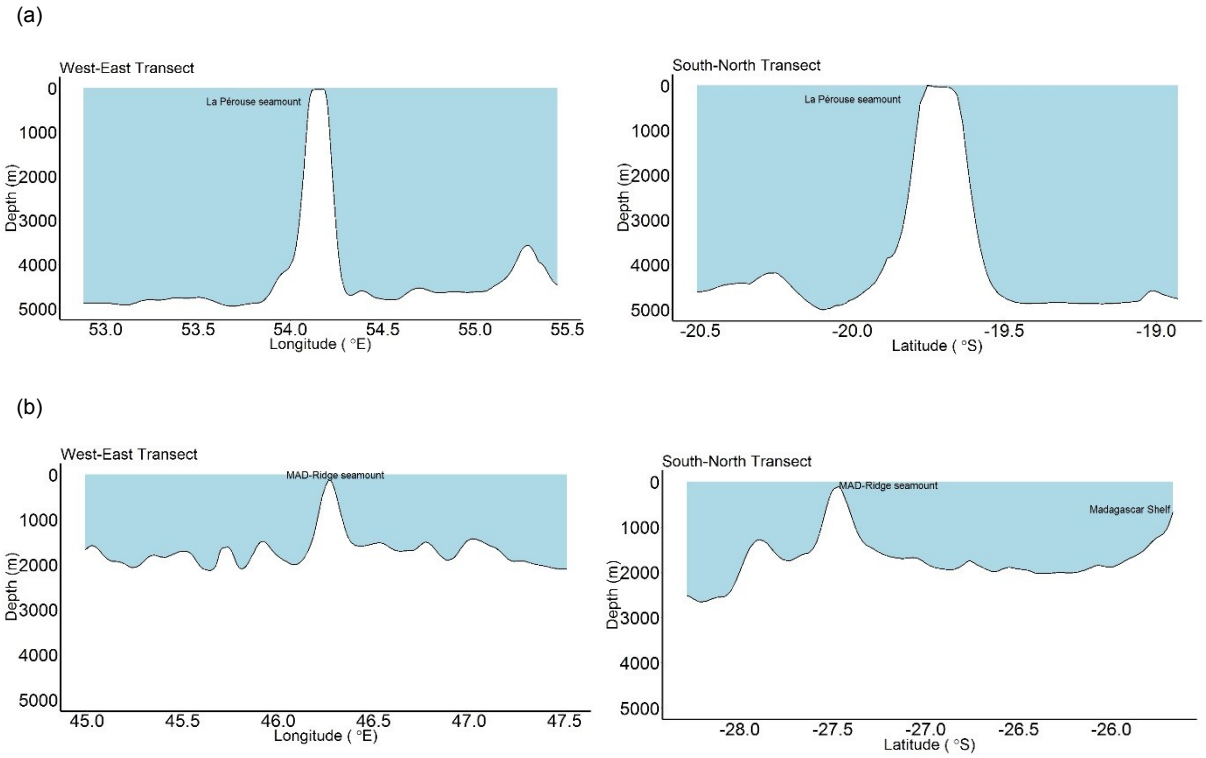

Figure 2.15 Bathymetry along the West-East and South-North transects at (a) La Pérouse and (b) MAD-Ridge seamounts.The colour bar represents the depth (m) below the sea surface.

La Pérouse therefore, unlike MAD-Ridge, is not part of a ridge system. The summit of La Pérouse reaches ~60 m below the sea surface and is 10 km long (Fig. 2.16). MAD-Ridge seamount rises from 1600 m from the ocean floor to a summit depth of ~240 m below the sea surface and is 33 km long (north to south) and 22 km wide (east to west). MAD-Ridge is bounded by four other topographic features with summit depths at 600 m, 800 m, 900 m and 1200 m between latitudes 27-28°S and longitudes 46-46°45'E.

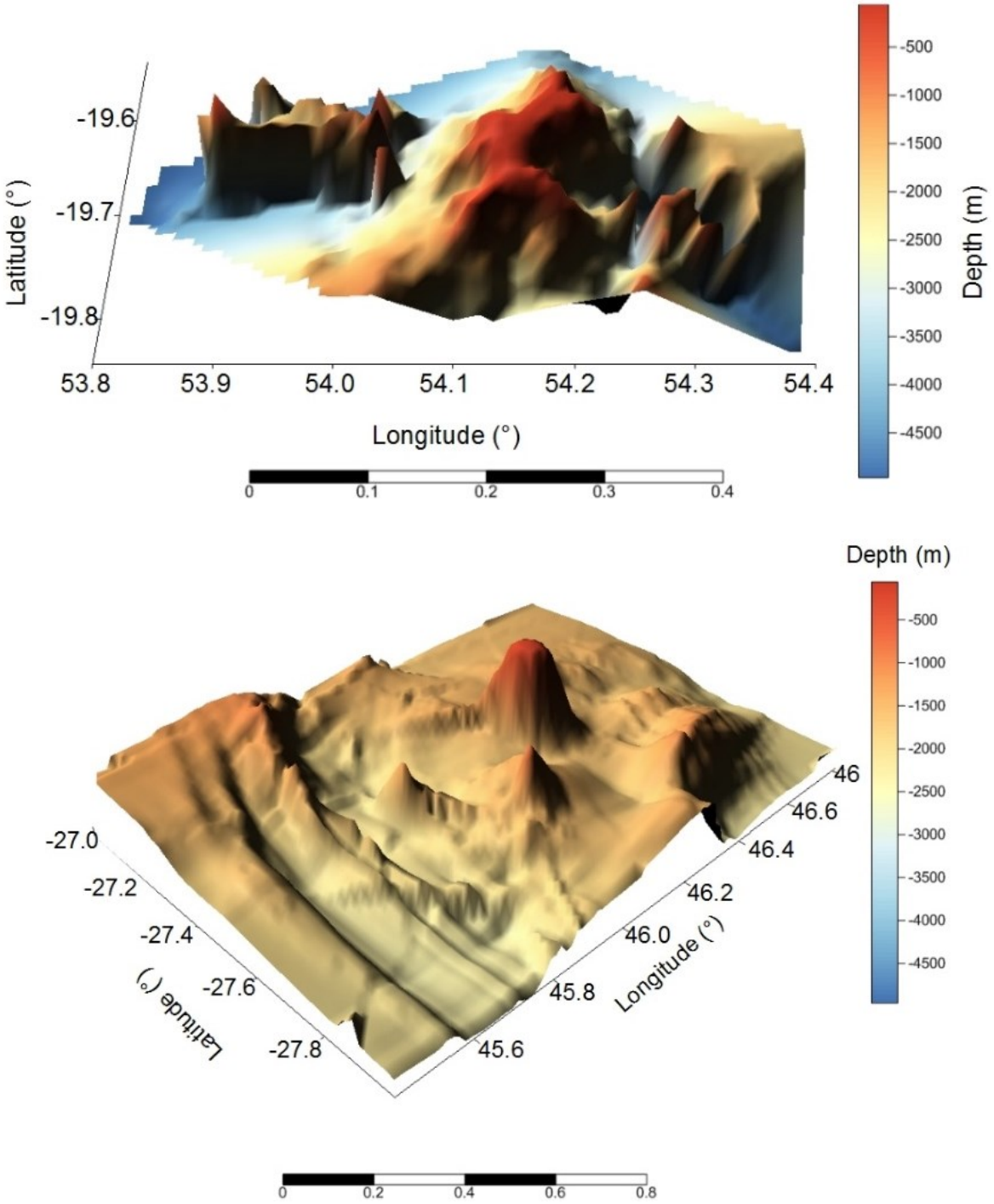

Figure 2.16 A 3D-bathymetry of La Pérouse and MAD-Ridge seamounts. The colour bar represents the depth (m) below the sea surface.

2.5.2 Nutrient concentrations

While La Pérouse seamount is located within the oligotrophic ISSG province (Longhurst, 1998) with low mesoscale activity, MAD-Ridge is located in the EAFR province, within an eddy corridor with significant mesoscale dynamics all year round (Vianello et al., 2020).

Mesoscale cyclonic and anticyclonic eddies spin off the SEMC and are advected to MAD-Ridge seamount. The dipole occurrence within the vicinity of MAD-Ridge pinnacle was estimated at 38.5% from 1993 to 2016. During MAD-Ridge cruise, an eddy dipole was present in the vicinity of the pinnacle, with the anticyclonic eddy being stationed on the seamount. The resulting mesoscale activity during MAD-Ridge cruise led to the shoaling of nutrients (nitrate, nitrite, phosphate and silicate) in the euphotic zone within the cyclonic eddy and over the shelf, and deepening of nutrients within the anticyclone (Fig. 2.17).

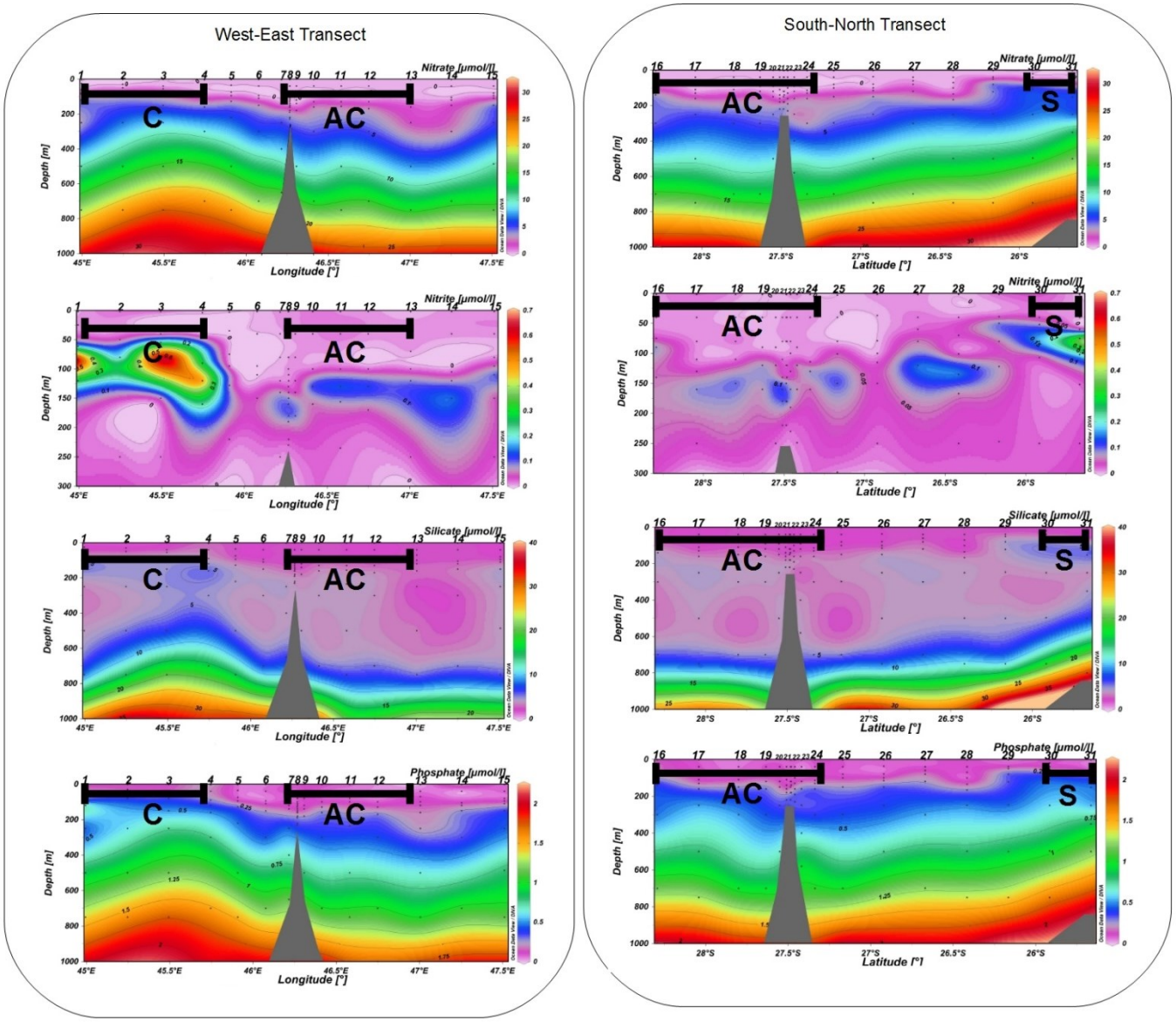

Figure 2.17 Concentrations of nitrate, nitrite, silicate and phosphate (µmol l^{-1}) along cyclonic (labelled C) and anticyclonic (labelled AC) stations across the West-East and the anticyclonic (AC) stations and shelf (labelled S) stations across the South-North transects during MAD-Ridge cruise.

The vertical nutrient profiles at La Pérouse were homogeneous relative to MAD-Ridge, with nitrate concentrations below the detection limit and lower phosphate and silicate concentrations in the top 100 m of the water column and a gradual increase in deeper waters (Fig. 2.18). A peak in nitrate, nitrite, silicate and phosphate concentrations were observed in the euphotic zone between 100-200 m with maximum concentrations of 5.7, 0.26, 6.0 and 0.52 µmol l^{-1} respectively.

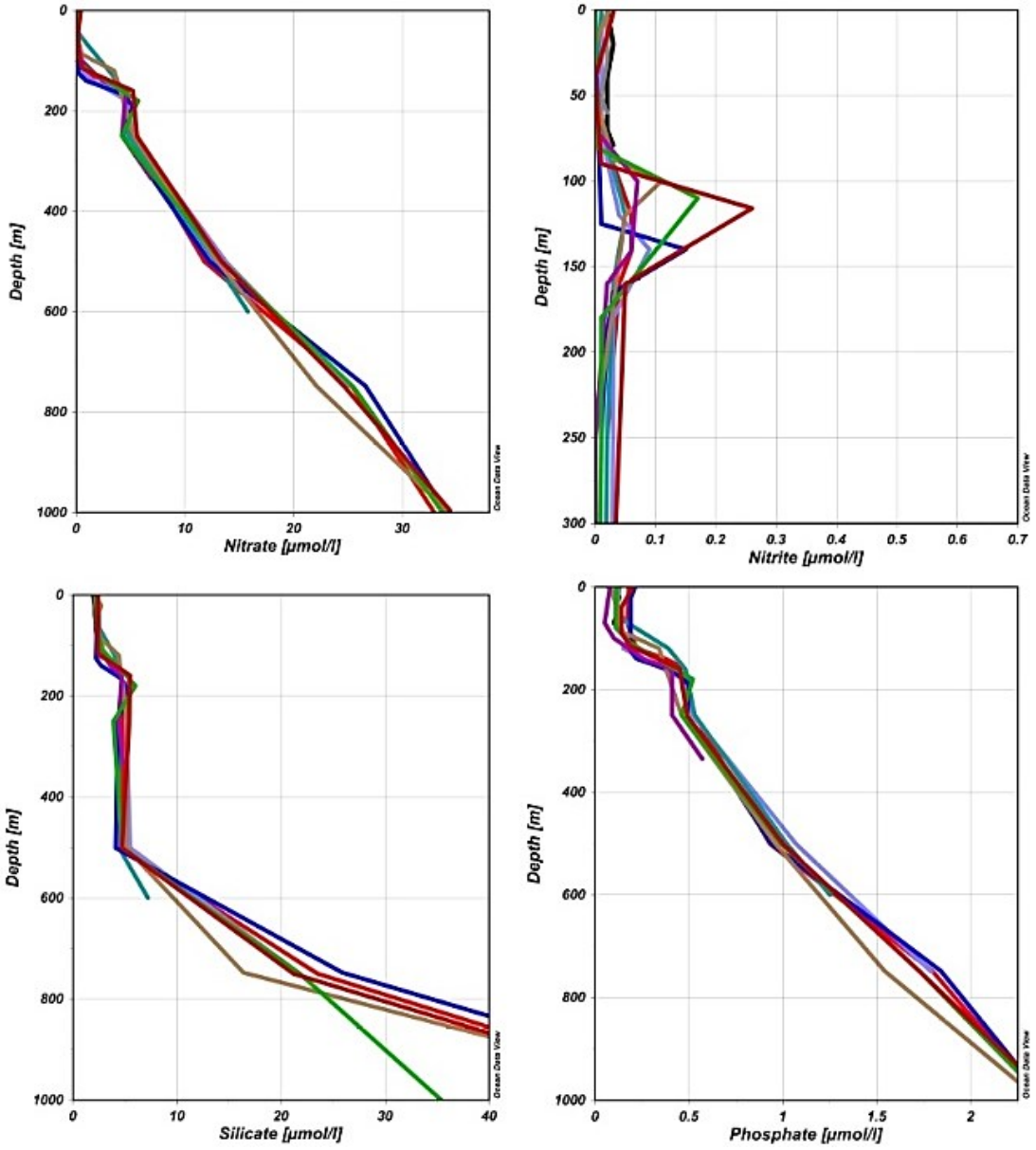

Figure 2.18 Vertical profiles of nitrate, nitrite, silicate and phosphate in µmol l^{-1} at La Pérouse seamount.

2.5.3 Phytoplankton communities at MAD-Ridge seamount

The authors Rocke et al. (2020) investigated the pico- and nanoplankton composition in the upper 250 m of the water column at MAD-Ridge seamount and the main findings of the research are presented below. The MAD-Ridge cruise recorded enriched picoplankton and nanoplankton carbon biomass within the cyclonic eddy (probably partially due to the higher nitrite concentrations), and at the edges of the anticyclonic eddy. In the anticyclone sampled during the cruise, picoeukaryotes and *Prochlorococcus* dominated carbon biomass over *Synechococcus*. Picoeukaryotes dominated the bulk of the carbon biomass within the size fraction (0.2-2 μm) along the West-East and North-South transects, likely resulting from suitable conditions brought about by fresh nutrients and organic matter being entrained from the Madagascar shelf to the euphotic zone at MAD-Ridge. Overall, low picoplankton biomass were recovered over the MAD-Ridge pinnacle itself due to possible current disturbance and competition between different phytoplankton types for regenerated nutrients. However, the authors reported a peak in picoplankton biomass near the slope of the seamount at station 19 (Fig. 2.19) between 40-100 m depth. They attributed this peak to a response due to enhanced turbidity on the slopes (Vianello et al., 2020) along with nutrient enrichment from the anticyclone which likely contributed to the resuspension of organic matter into the water column (Rocke et al., 2020). Jasmine et al. (2009) have shown pico- and nanoplankton to contribute ~90% of total chlorophyll *a* present in oligotrophic areas. Picoplankton are believed to be dominant under nitrate-depleted conditions due to their high surface area to volume ratio and sustain secondary production (mostly zooplankton) through the microbial foodweb (Jasmine et al., 2009).

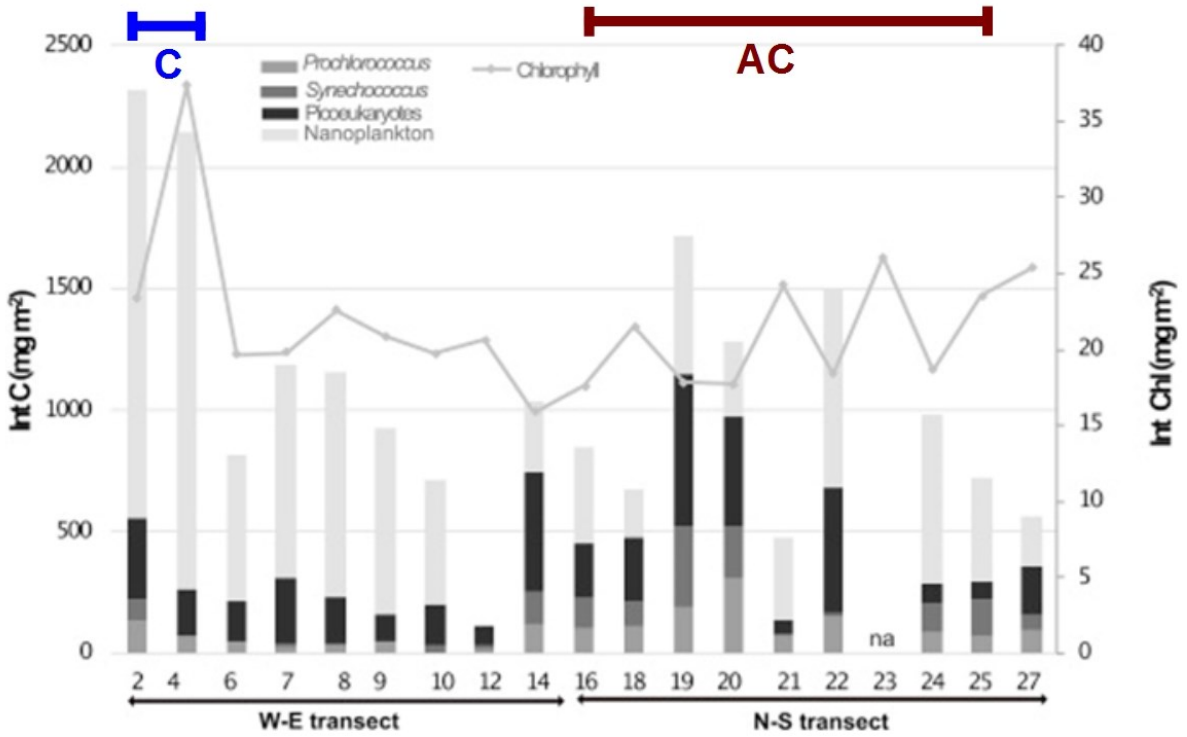

Figure 2.19 Integrated Prochlorococcus, Synechococcus and Picoeukaryotes carbon biomass (in µgC m^{-2}) and chlorophyll concentrations (in mg m^{-2}) for all stations within the cyclone (labelled C) along the West-East and within the anticyclone (labelled AC) along the North-South transects during the MAD-Ridge cruise [Source: Rocke et al., 2020].

2.5.4 Mesozooplankton at La Pérouse and MAD-Ridge vs. Walters Shoal

The mesozooplankton communities at La Pérouse, MAD-Ridge and Walters Shoal seamounts were investigated by Noyon et al. (2020) and the main findings of their research work are presented below. No clear seamount effect in terms of either enhancement or depletion of mesozooplankton communities were recorded at La Pérouse, MAD-Ridge and Walters Shoal seamounts relative to off-seamount locations. Walters Shoal showed lower abundance of mesozooplankton than the other two seamounts most likely due to seasonality and the mesozooplantkon population dynamics. At La Pérouse, MAD-Ridge and Walters Shoal, the mesozooplankton abundance was strongly dominated by calanoid copepods (70% of the total abundance). The biomass was dominated by copepods and carnivorous chaetognaths at La Pérouse and MAD-Ridge, and copepods and euphausiids at Walters Shoal.

The eddy dipole likely had an influence on mesozooplankton communities. High abundance and biovolume of zooplankton and over a deeper area were observed in the cyclonic eddy at MAD-Ridge than within the anticyclone where lower zooplankton concentrations in the upper 25 m were observed. The authors note a possible link between the food availability and

zooplankton at the cyclonic stations. The edge of the anticyclone was shown to exhibit higher zooplankton abundance than the core of the eddy, matching previous observations that peripheries of eddies are richer (Sabarros et al., 2009). The authors, however, reported a peak in zooplankton abundance and biovolume at station 18 close to the seamount slope. They attributed this effect to sampling at dusk and DVM of organisms but noted the presence of small organisms that do not perform strong DVM and concluded to a natural patchiness of these organisms at this station and across a greater depth range. The authors reported a system dominated by small mesozooplankton communities at MAD-Ridge, enabling a high biomass of predators to be supported (Noyon et al., 2020). At La Pérouse, higher zooplankton abundances were recorded downstream relative to upstream, possibly linked to the varied current profile from the north to the south of the pinnacle.

2.5.5 Ichthyoplankton assemblages at La Pérouse and MAD-Ridge vs. Walters Shoal

The ichthyoplankton faunal assemblages were investigated at La Pérouse, MAD-Ridge and Walters Shoal by Harris et al. (2020) are the main findings of these studies are summarized below. MAD-Ridge recorded a greater number of species, species diversity and density of fish larvae than La Pérouse and Walters Shoal (Fig. 2.20). MAD-Ridge further recorded a greater number of neritic fish larvae relative to La Pérouse and Walters Shoal (Fig. 2.20). The authors attributed these observations to the transport of larvae from the nearby coastal waters and from the Madagascar continental slope by mesoscale eddies.

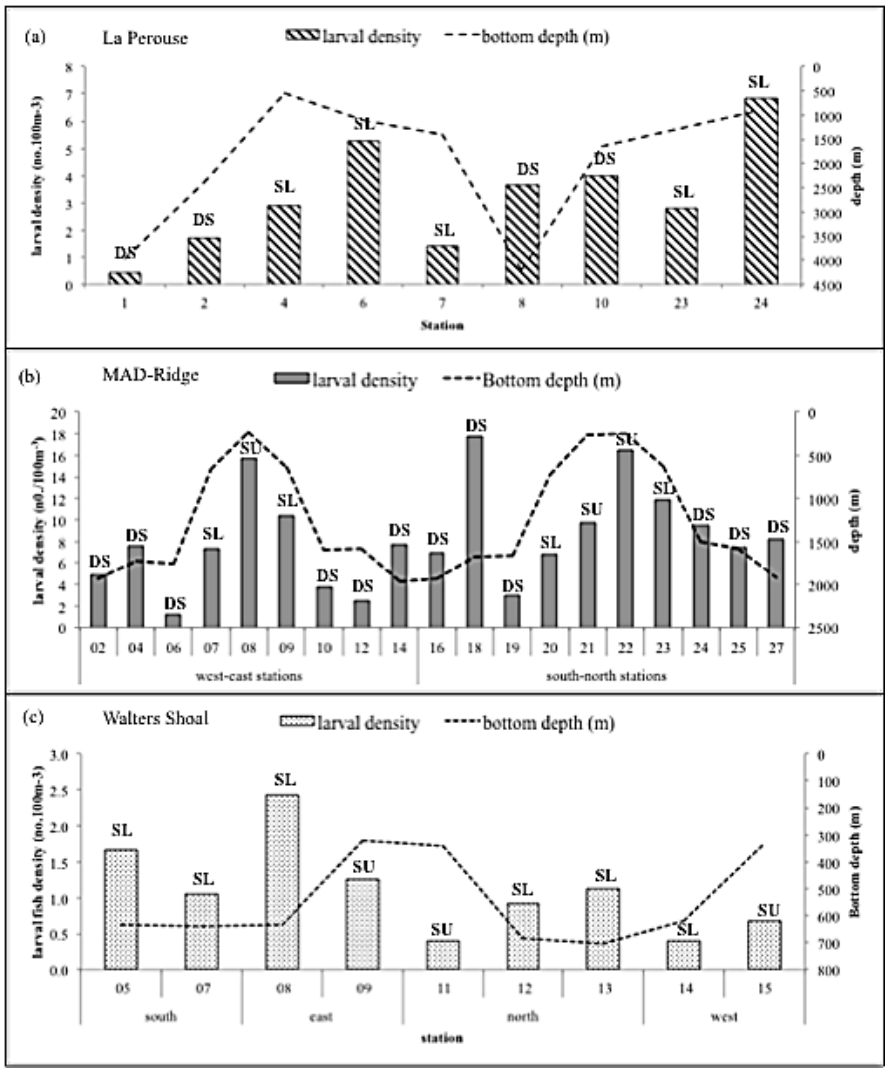

Figure 2.20 Larval fish densities (no. 100 m^{-3}) and bottom depth (m) at each station for (a) La Pérouse, (b) MAD-Ridge and (c) Walters Shoal. DS represents stations found in the deep-sea, SL represent slope stations, SU- summit stations [Source: Harris et al., 2020].

The fish larvae at all three seamounts were numerically dominated by the Myctophidae and Gonostomatidae families (Harris et al., 2020). The most abundant myctophid and gonostomatid larval species were *Diaphus* spp. and *Cyclothone* sp. at both La Pérouse and MAD-Ridge. Larval fish of the Molidae family (*Ranzania laevis*) were also abundantly caught at MAD-Ridge than at La Pérouse and Walters Shoal. The authors reported presence of all larval developmental stages present at each seamount which they attributed to local spawning of some species near the pinnacles. Larval densities were higher over the summit of both La Pérouse and MAD-Ridge than at off-summit locations, with the exception of station 18 of the MAD-Ridge cruise, which recorded the highest larval density relative to all other stations. The authors suggested DVM of larval taxa might be responsible for the peak observed at station 18. On the

summit of La Pérouse and MAD-Ridge, postflexion and preflexion larval developmental stages were most abundantly caught relative to other developmental stages. The eddy dipole interface (between the cyclone and anticyclone) recorded the lowest larval fish density.

2.6 Conclusion

The SWIO is an atypical region since it is bounded by the African landmass to the West and with a large island, Madagascar, centrally positioned in the pathway of the SEC leading to the shedding of mesoscale eddies in the Mozambique Channel and to the south of Madagascar. The deep water masses also have to navigate through fracture zones, banks and ridges to flow through the SWIO. Those ridges constitute important habitats for a wide variety of coral species and sponges. They represent an elevation of the seafloor and allow efficient cold-water coral growth that prefer the high-nutrient water mass uCDW, which is constrained to flow through the numerous basement highs and crests within the ridge. These coral communities may represent important habitats for various benthic organisms, some of which are preferentially associated with seamounts to benefit from shelter regions and enhanced foraging opportunities.

The lower trophic levels of the SWIO include *Prochlorococcus*, *Synechococcus*, *Picoeukaryotes*, diatoms and flagellates. These plankton communities support a wide range of mesozooplankton including copepods, amphipods, euphausiids, ostracods and chaetognaths, which in turn support gelatinous organisms, crustaceans, squids and mesopelagic fishes. Various predators including seabirds, swordfish and tunas reportedly use the highly dynamic mesoscale eddies and elevated topographic features during their migration patterns or/and as foraging grounds. Swordfish, tunas, breeding seabirds reportedly depend on prey availability and hence tend to aggregate in areas of high prey biomasses. These top predators and demersal organisms are being subjected to fishing pressures in the SWIO and there is an apparent lack of conservation measures to better protect marine resources from anthropogenic disturbances including pollution, fishing and deep-sea mining.

Several cruises and research works have already investigated the benthic assemblages, deep-sea fauna, physical oceanography and biological oceanography (phytoplankton, zooplankton and ichthyoplankton) at SWIO seamounts. One compartment of the SWIO that has received little attention to date are the micronekton which, as seen in Chapter 1, constitute a key element in the carbon biological pump and in the trophic link between zooplankton and top predators. Although some species are able to actively swim, they may be influenced by the complex topography and hydrodynamic patterns of the SWIO and in turn influence the distribution of top predator species. Chapter 3, hence, aims at understanding the distribution of micronekton as influenced by mesoscale eddies, two shallow seamounts and the Madagascar continental shelf in the SWIO.

Chapter 3: Influence of mesoscale eddies, shallow seamounts and continental shelf on micronekton's distribution

Extrait du *Petit poème des poissons de la mer*

Je me suis penché sur la mer
Pour communiquer mon message
Aux poissons:
«Voilà ce que je cherche et que je veux savoir»

Les petits poissons argentés
Du fond des mers sont remontés
Répondre à ce que je voulais…

Antonin Artaud, 1926

Micronekton distribution as influenced by mesoscale eddies, Madagascar shelf and shallow seamounts in the south-western Indian Ocean: an acoustic approach

Pavanee Annasawmy[1, 2*], Jean-François Ternon[1], Anne Lebourges-Dhaussy[3], Gildas Roudaut[3], Steven Herbette[4], Frédéric Ménard[5], Pascal Cotel[1], Francis Marsac[1, 2]

[1] *MARBEC, Univ. Montpellier, CNRS, Ifremer, IRD, Sète, France*

[2] *Department of Biological Sciences and Marine Research Institute/ICEMASA, University of Cape Town, Cape Town, South Africa*

[3] *LEMAR, IRD, UBO, CNRS, Ifremer, Plouzané, France*

[4] *Laboratoire d'Océanographie Physique et Spatiale (LOPS), IUEM, Univ. Brest, CNRS, Ifremer, IRD, Brest, France*

[5] *Aix Marseille Univ., Université de Toulon, CNRS, IRD, MIO, Marseille, France*

* Corresponding author: angelee-pavanee.annasawmy@ird.fr

Abstract

An investigation of the vertical and horizontal distributions of micronekton, as influenced by mesoscale eddies, the Madagascar shelf and shallow seamounts, was undertaken using acoustic data collected during two research cruises at an unnamed pinnacle (summit depth ~240 m), thereafter named "MAD-Ridge", and at La Pérouse seamount (~60 m) in the south-western Indian Ocean. MAD-Ridge is located to the south of Madagascar, in an "eddy corridor", known both for its high mesoscale activity and high primary productivity. In contrast, La Pérouse is located on the outskirts of the Indian South Subtropical Gyre (ISSG) province, characterised by low mesoscale activity and low primary productivity. During the MAD-Ridge cruise, a dipole was located in the vicinity of the seamount, with the anticylclone being almost stationary on the pinnacle. Total micronekton acoustic densities were greater at MAD-Ridge than at La Pérouse. Micronekton acoustic densities of the total water column were lower within the anticyclone than within the cyclone during MAD-Ridge. Micronekton followed the usual diel vertical migration (DVM) pattern, except within the cyclone during MAD-Ridge where greater acoustic densities were recorded in the daytime surface layer. The backscatter intensities were stronger at the 38 kHz than at the 70 and 120 kHz frequencies in the daytime surface layer at MAD-Ridge cyclonic stations. These backscatter intensities may correspond to gas-filled swimbladders of epi- and mesopelagic fishes actively swimming and feeding within the cyclone or gelatinous organisms with gas inclusions. Findings in this study evidenced that the distributions of micronekton and DVM patterns are complex and are influenced significantly by physical processes within mesoscale eddies. The mesoscale eddies' effects were dominant over any potential seamount effects at the highly dynamic environment prevailing at MAD-Ridge during the cruise. No significant increase in total micronekton acoustic densities was observed over either seamount, but dense aggregations of biological scatterers were observed on their summits during both day and night.

Keywords: micronekton, diel vertical migration, mesoscale eddies, Madagascar shelf, seamount, south-western Indian Ocean

3.1. Introduction

Features such as mesoscale cyclonic and anticyclonic eddies, upwelling events, tidal fronts, shelves, seamounts and river runoff play a significant role in regional ecosystems (Bakun, 2006; Mann & Lazier, 2006; Benitez-Nelson & McGillicuddy, 2008). Mesoscale cyclonic and anticyclonic eddies are ubiquitous in the world's oceans (Chelton et al., 2011). They have time-scales of approximately 10-30 days and horizontal scales between 10 and 100 km (Mann & Lazier, 2006; Chelton et al., 2011). In oligotrophic systems, eddies are important features because they provide mechanisms whereby the physical energy of the ocean is converted to trophic energy to support biological processes (Bakun, 2006; Godø et al., 2012). Cyclonic eddies, through upwelling of nutrients in their centres from deeper layers to the euphotic zone, are usually known to enhance local productivity (Owen, 1980, 1981; McGillicuddy & Robinson, 1997; McGillicuddy et al., 1998; Klein & Lapeyre, 2009; Huggett, 2014; Singh et al., 2015). Anticyclonic eddies may promote the development of frontal structures (Bakun, 2006). In anticyclones, highly productive waters may be entrained laterally from nearby regions to the eddy periphery or upwelling of nutrients may occur along the eddy boundary (McGillicuddy, 2016). At the frontier between eddies, smaller-scale or submesoscale features (elongated filaments with a 10-km width) have been reported to enhance nutrient supply and primary productivity in oligotrophic conditions (Lévy et al., 2001, 2018; Klein & Lapeyre, 2009). Biological responses to eddies, however, are complex and depend on a range of factors including seasonal modulation of the mixed layer depth (Dufois et al., 2014), timing, magnitude and duration of nutrient input and also on eddy properties such as the formation, intensity, age and eddy-induced Ekman pumping (Benitez-Nelson & McGillicuddy, 2008).

Continental shelves and seamounts are also features that may lead to enhanced productivity when certain conditions are met. Upwelling regions south of Madagascar have been observed to be biological hotspots with increased productivity (Raj et al., 2010; Ramanantsoa et al., 2018) and increased acoustic biomass estimates of pelagic fish and whale sightings (Pripp et al., 2014). Phytoplankton types may also differ between continental shelves and ocean basins, with shelf areas exhibiting larger phytoplankton cells because of the processes leading to high nutrient concentrations in the euphotic zone and cells rapidly take up nutrients (Nishino et al., 2011). Seamounts are ubiquitous features of the world's oceans and have been reported to influence the prevailing ocean currents (Royer, 1978; White et al., 2007), creating various local dynamic responses such as formation of a Taylor column, isopycnal doming (Mohn & Beckmann, 2002), enclosed circulation cell (White et al., 2007), upwelling, vertical mixing of nutrient-rich waters and enhanced productivity (Boehlert & Genin, 1987; Genin, 2004). In a nutrient-limited environment like the south-western Indian Ocean, processes injecting nutrients into the euphotic zone (such as mesoscale features,seamounts, coastal upwelling events and river runoff) are likely to modulate

the chlorophyll *a* signature by increasing phytoplankton growth, attracting a range of secondary and tertiary consumers such as zooplankton and micronekton.

Mesopelagic micronekton are actively swimming organisms that typically range in size from 2-20 cm. They include diverse taxonomic groups (De Forest & Drazen 2009) such as crustaceans (adult euphausiids, pelagic decapods and mysids), squids (small species and juvenile stages of large oceanic species) and fishes (mainly mesopelagic species and juveniles of other fish) (Brodeur et al., 2005; Brodeur & Yamamura 2005; Ménard et al., 2014). Gelatinous organisms are under-represented components of the mesopelagic community (Lehodey et al., 2010; Kloser et al., 2016). Micronekton are important in the energy transfer to higher trophic levels because they are preyed upon by various top marine predators (Guinet et al., 1996; Bertrand et al., 2002; Potier et al., 2007; Cherel et al., 2010; Danckwerts et al., 2014; Jaquemet et al., 2014). They also transport energy to deeper regions of the ocean via respiration, excretion and natural mortality (Hidaka et al., 2001; Catul et al., 2011; Bianchi et al., 2013). This energy transport is made possible by the extensive DVM patterns of some micronekton species, with the organisms migrating to the upper 200 m of the water column at dusk and below 400 m at dawn (Lebourges-Dhaussy et al., 2000; Béhagle et al., 2014; Annasawmy et al., 2018). Diel vertical migration is believed to result from a compromise between the need to feed and to avoid predation (Heywood, 1996), with light being the main controlling factor in initiating ascent and descent (Heywood, 1996; Andersen et al., 1998; Brierley, 2014). The distribution of micronekton communities across ocean basins is not uniform (Judkins & Haedrich, 2018). Some studies have reported higher biomasses of micronekton scattering layers at seamount flanks and summits relative to the surrounding ocean, e.g. the Emperor (265m, Boehlert, 1988) and Cross seamounts in the Pacific (330 m, Johnston et al., 2008); Condor (182-214 m) and Gigante (161 m) seamounts in the Azores (Cascão et al., 2017).

At the ocean-basin scale, the western side of the oligotrophic ISSG biogeochemical province (Longhurst, 1998; 2007) holds reduced micronekton abundances and acoustic densities relative to the dynamic and more productive EAFR province (Annasawmy et al., 2018). Within the ISSG and EAFR provinces, features such as eddies, coastal upwelling at the Madagascar shelf and seamounts may further impact the local productivity, resulting in significant variability in micronekton distributions via bottom-up processes. This work investigates the influence of mesoscale eddies, the south Madagascar shelf and two shallow seamounts, La Pérouse and an unnamed pinnacle on the Madagascar Ridge, hereafter called "MAD-Ridge", in shaping micronekton vertical and horizontal distributions by combining data from ship-based platforms (acoustics, current profiler and CTD) and satellite altimetry.

3.2 Material and Methods

3.2.1 Cruises

Two research surveys were carried out on board the RV *Antea* at La Pérouse (19°43'S and 54°10'E) and MAD-Ridge seamounts (27°29'S and 46°16'E). La Pérouse (summit depth ~60 m) is located along the north-western boundary of the ISSG province and MAD-Ridge (summit depth ~240 m) is located on the southern boundary of the EAFR (Fig. 3.1a). The La Pérouse cruise (DOI: 10.17600/16004500) investigated the area within 10-18 km around the seamount from the 15 to 30 September 2016 (Fig. 3.1b). The MAD-Ridge Leg 1 cruise (DOI: 10.17600/16004800) was divided into a West-East transect (248 km long from hydrographic station 1 to 15) and a South-North transect (292 km long from hydrographic station 16 to 31) and took place from the 8 to 24 November 2016 (Fig. 3.1a and 3.2a).

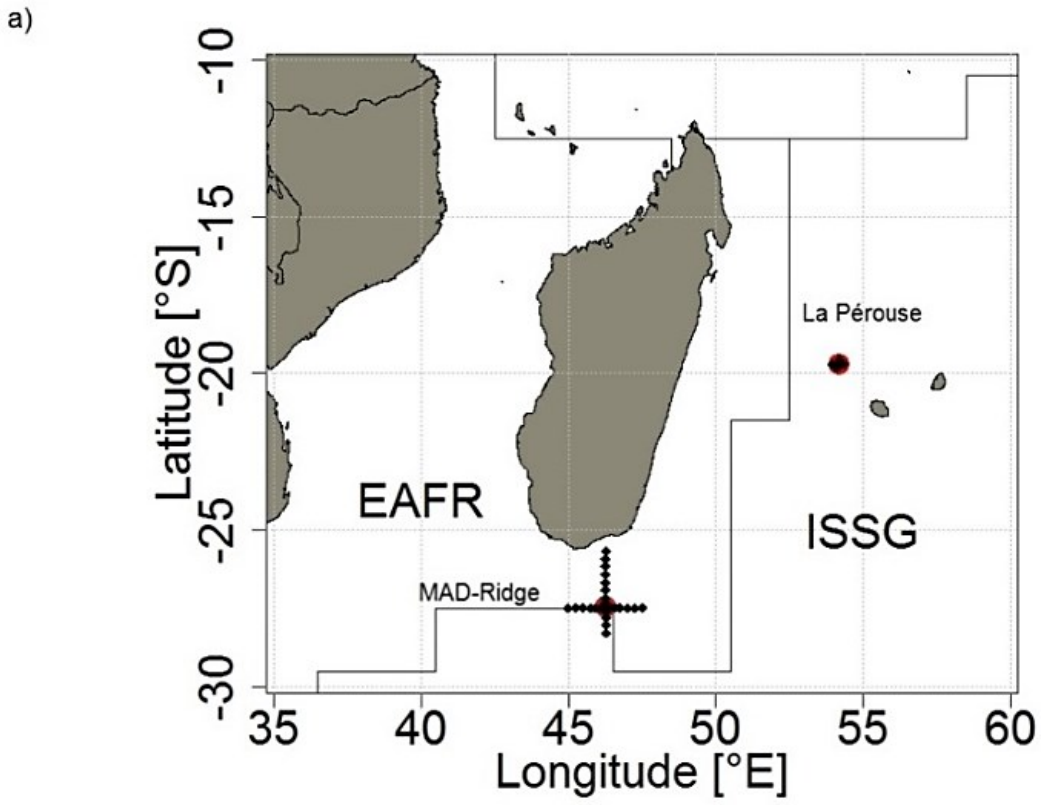

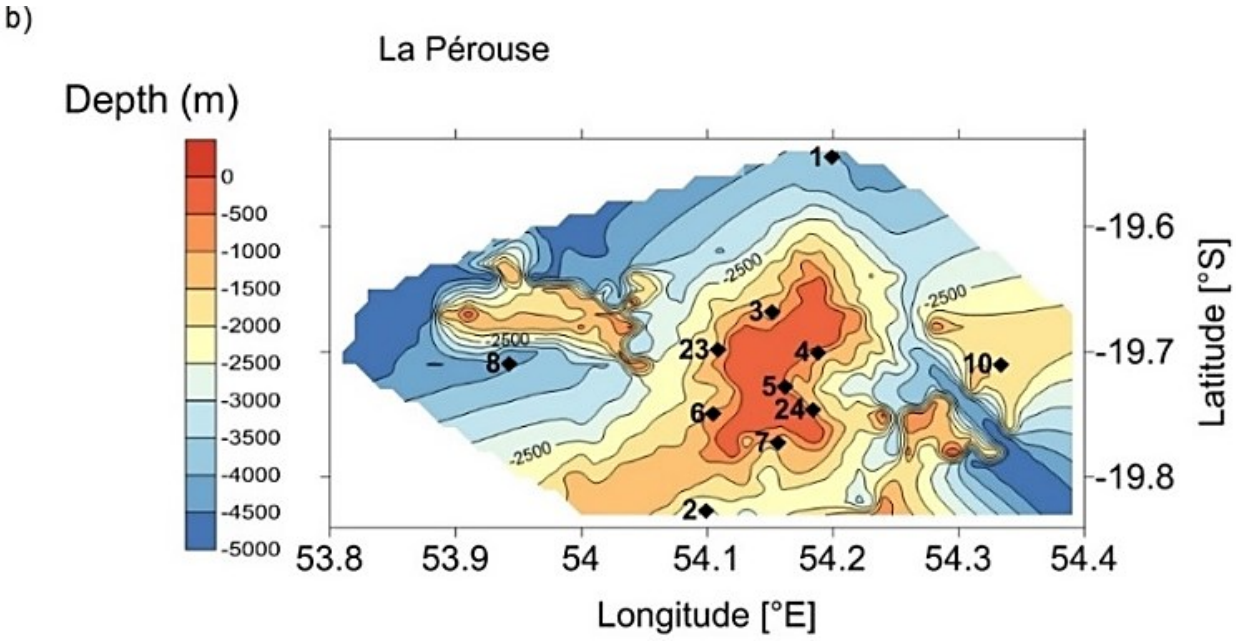

Figure 3.1(a) Map of MAD-Ridge and La Pérouse CTD stations (diamond symbols) conducted in the East African Coastal (EAFR) and Indian South Subtropical Gyre (ISSG) provinces respectively. Longhurst's (1998) biogeochemical provinces are delimited by black solid lines. Landmasses are shown in grey and seamount summits in red. (b) The La Pérouse CTD stations are plotted on the bathymetry (m). The colour bar represents the depth below the sea surface.

3.2.2 Satellite data

The mesoscale eddy field during both the La Pérouse and MAD-Ridge cruises were described using daily delayed-time Absolute Dynamic Topography (ADT) with 1/4° (~25 km) spatial resolution. Delayed-time ADT was produced and distributed by the Copernicus Marine Environment Monitoring Service project (CMEMS) and available at http://marine.copernicus.eu/, from which absolute geostrophic currents have been calculated and used to derive dynamic parameters (see next section). Delayed-time Mean Sea Level Anomalies (MSLA) data, with 1/4° (~25 km) spatial resolution in the vicinity of MAD-Ridge seamount were also downloaded from http://marine.copernicus.eu/, and used for direct eddy field representation.

3.2.3 Field Sampling

3.2.3.1 In situ bathymetry

The 12 kHz frequency of a Simrad EA500 echosounder was used to acquire a detailed bathymetry of the seamounts. The bathymetry data were interpolated on a regular grid using the Golden Surfer © software (version 10.3.705).

3.2.3.2 Hydrographic stations

A Sea-Bird 911+ CTD rosette system equipped with a Wetlabs ECO FL fluorometer was used to profile temperature, fluorescence and dissolved oxygen from the surface to a depth of ~1000 m during the La Pérouse and MAD-Ridge cruises. Discrete samples of chlorophyll *a* measured by high pressure liquid chromatography was used to calibrate the fluorescence sensor of the CTD during both cruises and to determine the depth range where the maximum chlorophyll *a* values (Fmax) were found. The integrated chlorophyll *a* concentrations between 2 and 200 m (mg m^{-3}) was calculated by taking the sum of chlorophyll *a* values in that depth range. The average depths of the thermocline were assessed from the CTD profiles using the 20°C isotherm depth as a proxy.

Two 300 kHz RDI (upward and downward-looking) L-ADCP current profilers attached to the CTD frame were used to investigate the vertical structure of the current field during both cruises. The S-ADCP data were collected with a 75 kHz RDI Ocean Surveyor II. As L-ADCP data were missing at MAD-Ridge stations 2 and 3, S-ADCP data were used instead. Both datasets showed strong correlations which allowed the use of the L- with the S-ADCP (Vianello et al., 2020). For each hydrographic station, the average current speed (in cm s^{-1}) over the depth range 104-304 m, was calculated from the west-east zonal (u) and south-north meridional (v) velocity components measured by the S-ADCP or L-ADCP.

A classification of MAD-Ridge hydrographic stations (numbered 1-31, Fig. 3.2) was performed based on their location relative to the mesoscale eddies (cyclonic, anticyclonic, interface between the dipole), to the seamount (summit or flank, both within the anticyclonic eddy) and to the Madagascar shelf. This classification was based on the hydrology (temperature-salinity profiles) of each station and a standard dynamic parameter, the Okubo-Weiss parameter, W (Okubo, 1970; Weiss, 1991; Isern-Fontanet et al., 2004). The latter is calculated from equation 1 below, where S_n is the normal strain, S_S the shear strain, ω the relative vorticity, and u and v (Eq. 2 below) are the surface geostrophic velocity components derived from the absolute dynamic topography (altimetry). The Okubo-Weiss parameter allows the separation of the flow into a vorticity-dominated region ($W<-W_0$) and a strain-dominated region ($W>W_0$), with $W_0= 0.2\sigma_W$, (σ_W being the standard deviation in the whole domain) (Isern-Fontanet et al., 2004). It has been used widely in the south-western Indian Ocean by Halo et al. (2014) to distinguish the core of eddies ($W>-W_0$) from the periphery of eddies ($W<-W_0$) and is given by:

$$W=S_n^2 + S_s^2 - \omega^2 \qquad \text{Eq. 1,}$$

where:

$$Sn = \frac{\partial u}{\partial x} - \frac{\partial v}{\partial y},\ S_S = \frac{\partial v}{\partial x} + \frac{\partial u}{\partial y},\ \omega = \frac{\partial v}{\partial x} - \frac{\partial u}{\partial y}$$

However, *W* values have to be used cautiously against *in situ* data because the spatial resolution of the altimetry is low (~25km) relative to each station. Therefore, for each station, the altimetry data were complemented by the available *in situ* data such as sea surface temperature and salinity obtained from a ship-mounted thermosalinograph and dissolved oxygen obtained from the CTD. This combined set of information allowed us to segregate the stations into different categories (see example for stations 3, 5 and 13 in the Appendix: Fig. A, and Table 3.1).

Table 3.1 List of MAD-Ridge Leg 1 classified hydrographic stations: UN for unresolved; C for Cyclonic; D.I for Dipole Interface; AC for Anticyclonic; S for summit; F for flank; Sf for Shelf.

Station Number	Day/ Sunset	ADT (m)	MSLA (m)	Vorticity (s^{-1})	Okubo-Weiss (s^{-2})	Temper-ature (°S) TSG	Salinity (PSU) TSG	Sea floor Depth (m)	Classifi-cations
1	Day	0.89	-0.19	-1.21E-05	1.63E-11	23.68	35.36	1573	UN
2	Day	0.82	-0.27	-1.97E-05	5.00E-11	23.92	35.36	1930	C
3	Sunset	0.84	-0.25	-2.94E-05	-5.32E-10	23.89	35.38	1630	C
4	Day	0.96	-0.15	-1.50E-05	-4.97E-10	23.72	35.30	1730	C
5	Day	1.08	-0.03	-5.80E-07	1.02E-10	24.37	35.14	1460	D.I
6	Day	1.21	0.10	1.49E-05	6.14E-11	24.71	35.18	1760	UN
7	Day	1.30	0.20	2.86E-05	-3.34E-10	24.40	35.21	670	F/AC
8	Day	1.33	0.23	3.15E-05	-4.92E-10	24.39	35.22	240	S/AC
9	Day	1.36	0.25	3.14E-05	-5.33E-10	24.33	35.22	645	F/AC
10	Day	1.42	0.32	3.01E-05	-5.85E-10	24.31	35.28	1600	AC
11	Day	1.46	0.36	2.86E-05	-6.71E-10	24.49	35.28	1733	AC
12	Day	1.45	0.37	2.54E-05	-5.62E-10	24.55	35.29	1585	AC
13	Day	1.41	0.35	2.55E-05	-6.09E-10	24.42	35.28	1505	AC
14	Day	1.31	0.27	1.81E-05	-3.23E-10	24.40	35.23	1964	UN
15	Day	1.18	0.16	6.75E-07	7.35E-11	24.79	35.28	2110	UN
16	Day	1.25	0.22	1.94E-05	-2.80E-10	24.25	35.21	1927	AC
17	Day	1.34	0.28	1.95E-05	-2.20E-10	24.57	35.29	2380	AC
18	Sunset	1.41	0.32	2.44E-05	-3.40E-10	24.58	35.28	1674	AC
19	Day	1.43	0.33	2.69E-05	-4.79E-10	24.38	35.22	1668	AC
20	Day	1.41	0.31	2.76E-05	-4.98E-10	24.65	35.23	720	F/AC
21	Day	1.4	0.30	2.77E-05	-5.06E-10	24.84	35.24	257	S/AC
22	Day	1.41	0.30	2.63E-05	-4.58E-10	24.40	35.24	255	S/AC
23	Day	1.41	0.30	2.58E-05	-4.32E-10	24.77	35.24	621	F/AC
24	Day	1.4	0.28	2.42E-05	-3.50E-10	24.77	35.24	1502	AC

25	Day	1.38	0.27	2.22E-05	-2.12E-10	24.77	35.24	1585	AC
26	Day	1.32	0.22	1.50E-05	1.14E-11	24.46	35.14	1747	UN
27	Day	1.25	0.20	8.21E-06	1.09E-12	24.46	35.14	1916	UN
28	Day	1.21	0.23	9.75E-06	-9.40E-11	24.47	35.14	2125	UN
29	Day	1.11	0.23	2.25E-06	3.08E-11	24.73	35.15	1875	UN
30	Day	1.00	0.21	-7.82E-06	7.21E-11	24.77	35.21	1436	Sf
31	Sunset	0.95	0.19	-7.39E-06	1.82E-10	24.68	35.30	840	Sf

3.2.3.3 Zooplankton sampling

Daytime zooplankton samples were collected with a 200-µm-mesh oblique Bongo net towed at a speed of 1-2 knots to a maximum depth of 200 m during the La Pérouse cruise (0.28 m^2 mouth area). A 200-µm-mesh oblique Multinet was towed to a maximum of 200 m during the MAD-Ridge cruise (0.25 m^2 mouth area) (Noyon et al., 2020). Samples from both cruises were emptied into a 200 µm sieve, poured into sampling jars with filtered seawater and stored in 4% buffered formaldehyde at room temperature on board before being analysed using a Hydroptic Zooscan following the protocols in Gorsky et al. (2010). Detailed zooplankton sampling and analyses were investigated in Noyon et al. 2020.

3.2.3.4 Acoustic sampling

A Simrad EK60 echosounder operating at four frequencies was used during both the La Pérouse and Leg 1 of the MAD-Ridge cruises: 38 kHz at 1000 W transmitted power, 70 kHz (acquired range of 500 m) at 750 W, 120 kHz (250 m) at 200 W and 200 kHz (150 m) at 90 W. The water column was correctly sampled to a depth of 735 m during data acquisition for the 38 kHz frequency of the La Pérouse cruise, with data being of poor quality below that depth. For comparison with the La Pérouse cruise, echo-integrated acoustic data for the 38 kHz frequency of the MAD-Ridge cruise has also been selected down to 735 m in this chapter. The pulse duration was set at 0.512 ms. The transducers were calibrated prior to both cruises following the procedures recommended in Foote et al. (1987). MAD-Ridge acoustic data were collected along the West-East and South-North transects (Fig. 3.2a) at a vessel speed of 8-9 knots. Additional transects were also conducted during day and night in close proximity to the MAD-Ridge summit and flanks at vessel speed of 8-9 knots (see Fig. 3.7 a, b)

The Matecho software (an open source IRD tool computed with MATLAB 7.11.0.184, Release 2010b- and based on the IFREMER's Movies3D software; Trenkel et al., 2009; Perrot et al., 2018) was used to process acoustic data from both cruises. Background, transient and impulsive noises along with attenuated signals (Perrot et al., 2018) were removed using the algorithms designed in De Robertis & Higginbottom (2007) and Ryan et al. (2015). An offset of 10 m below the sea surface was applied to

account for the acoustic detection of the surface turbulence. During both cruises, echo-integration of the acoustic data was performed on 1-m layers at an elementary sampling distance unit of 0.1 nmi (nautical mile) and at a threshold of -80 dB to exclude scatterers not representative of the micronekton community (Béhagle et al., 2017). The micronekton acoustic density was determined by the nautical area scattering coefficient NASC (s_A, m^2 nmi^{-2}), related to the backscattered energy (MacLennan et al., 2002). NASC can be used as a proxy of the relative biomass of micronekton provided assumptions that the composition of scattering layers and the resulting scattering properties of micronekton are relatively homogeneous (Béhagle et al., 2014). The volume backscattering strength (Sv, dB re 1 m^{-1}; MacLennan et al., 2002) was also calculated for each frequency (38 kHz, 70 kHz and 120 kHz) to obtain the relative acoustic density of scatterers per unit volume and was used to generate Red Green Blue (RGB) composite images (see next section). The water column at the 38 kHz frequency was separated into the following depth categories, based on epipelagic and mesopelagic layers: surface (10-200 m), intermediate (200-400 m), deep (400-735 m) and total water column (10-735 m). Diurnal and nocturnal periods were assessed using Matecho software through visual analysis of the echograms.

3.2.4 Data visualisation

Vertical distributions of the environmental descriptors (current speed, temperature, and chlorophyll *a*) were mapped from the surface to ~1000 m (except for chlorophyll) along the West-East and South-North transects of MAD-Ridge Leg 1 (Fig. 3.2b, c) using the Section mode of the software Ocean Data View (ODV, version 4.5.7; Schlitzer, 2013). The chlorophyll *a* data were only mapped from the surface to 300 m because values were below the minimum level of detection deeper than that (Fig. 3.2d). Data interpolation between sampling stations was carried out using the DIVA (Data-Interpolating Variational Analysis) gridding option in ODV that spatially interpolates observations on a regular grid in an optimal way by taking into account coastlines and bathymetric features to structure and divide the domain on which estimations are performed.

Acoustic data were represented using RGB colour coding. RGB composite images were generated in MATLAB (version 2016) based on the 38 kHz, 70 kHz and 120 kHz echo-integrated acoustic data of selected transects during the MAD-Ridge and La Pérouse cruises. The 38, 70 and 120 kHz echo-integrated acoustic data were given in red, green and blue colour codes respectively on each RGB plot, with the dynamic of the Sv values in dB for each frequency being converted in 256 levels (0-255) of each colour. A linear transformation of the backscatter was applied to each frequency (fr):

$$\text{Colour index (fr)} = [255/ (\text{High scale threshold} - \text{Low scale threshold})] \times [\text{Sv (fr)} - \text{Low scale threshold}], \quad \text{Eq. 3}$$

where the high and low scale thresholds are the maximum and minimum backscatter for hue visualisations, respectively. Sv (fr) is the backscatter value at each frequency. This acoustic visualisation technique is useful in determining the relative contribution of each frequency to the overall backscatter (red means that Sv 38 is dominant, and similarly for green and blue, Sv 70 and Sv 120 are respectively dominant) and to identify dense aggregations of scatterers (Sv 38, Sv 70 and Sv 120 all dominant and seen as "white patches"). On a RGB composite image based on the 38, 70 and 120 kHz frequencies, a dark red colour indicates a dominant but low 38 kHz backscatter, whereas a light red colour indicates a dominant but high 38 kHz backscatter. The same rule applies to the green (70 kHz) and blue (120 kHz) hues. Kloser et al. (2002) used a similar approach, but the composite image was produced by assigning a separate colour palette to each frequency (12, 38 and 120 kHz) and dynamically optimising the frequencies to highlight the amplitude differences in the echogram.

3.2.5 Statistical analyses

Kruskal Wallis tests and pairwise Wilcoxon rank sum tests were performed to assess the differences in integrated chlorophyll *a* concentrations between classified hydrographic stations. In order to cover the largest depth range, day and night acoustic transects at 38 kHz frequency were further selected to investigate the micronekton acoustic densities in close proximity to the summits and flanks of the pinnacles (see Fig. 3.7a, b). As the 38 kHz frequency data did not follow a normal distribution, non-parametric Wilcoxon rank sum tests were performed to investigate the overall acoustic densities in each of the depth categories (surface: 10-200 m, intermediate 200-400 m and deep: 400-735 m) between La Pérouse and MAD-Ridge seamounts, and between day and night. Daytime acoustic density estimates representing the vertical distribution of micronekton across the depth categories (surface, intermediate, deep and total water column: 10-735 m) and averaged over 0.4 nmi on each side of the classified stations during MAD-Ridge cruise were investigated using non-parametric Kruskal-Wallis (KW) tests and pairwise Wilcoxon rank sum tests. All statistical tests were performed with version 3.3.1 of the R package.

3.2.6 Taylor column theoretical calculation

The following non-dimensional factors were used to determine the likelihood of a Taylor column formation over La Pérouse and MAD-Ridge summits (White et al., 2007), depending on the mean water stratification, the mean flow field, the latitude (earth's rotation effect) and the shape of the seamount:

(1) The Rossby number, Ro, with $\mathrm{Ro} = \frac{U}{f*L}$,

where U is the typical flow speed (0.3 m s^{-1} at La Pérouse and 0.5 m s^{-1} at MAD-Ridge); $f = 2 * \Omega * \sin(latitude)$, where Ω is Earth's angular velocity at 0.0000729 rads s^{-1}; the $\sin(latitude)$ is sin(19.72) at La Pérouse and sin(27.48) at MAD-Ridge; and L is the average width of the seamounts (10 000 m for La Pérouse and 27 500 m for MAD-Ridge). Ro estimates were calculated at 0.27 at La Pérouse and 0.17 at MAD-Ridge.

(2) The relative height of the seamount (h_0) to water depth (H), with $\alpha = \frac{h0}{H}$,

where α was calculated at 0.99 at La Pérouse and 0.85 at MAD-Ridge.

(3) A combination of Ro and α gives the blocking parameter *Bl* (where $Bl = \frac{\alpha}{Ro}$),

which controls the formation of a Taylor column (White et al., 2007). A *Bl* value of 3.66 was calculated at La Pérouse and 4.88 at MAD-Ridge. According to Chapman & Haidvogel (1992), for seamounts taller than α ≈ 0.4, true Taylor caps will form if Ro <0.15 and *Bl* > ~2 for Gaussian-shaped seamounts with moderate stratification. According to the authors, Taylor cones will not form if the Rossby number exceeds the upper bound of 0.15-0.2.

3.3 Results

3.3.1 Synoptic ocean circulation during the MAD-Ridge cruise

A cyclonic/anticyclonic eddy dipole was encountered along the West-East transect (hydrographic stations 1-15) of Leg 1 of the MAD-Ridge cruise, whereas the South-North transect (hydrographic stations 16-31) was mostly located inside the anticyclonic eddy and reached the Madagascar shelf (Fig. 3.2a). Along the West-East transect, at hydrographic station 5, a sharp front can be observed in the sea surface temperature and salinity data collected from the ship-mounted thermosalinograph, indicating the transition between cyclonic and anticyclonic circulations (Appendix: Fig. A). This transition area coincided with the largest current velocity recorded at the surface (158 cm s^{-1}) and in the depth layer 104 and 304 m (99 cm s^{-1}) relative to all other stations along the West-East and South-North transects (Fig. 3.2b).

MAD-Ridge hydrographic stations were divided into six categories, according to whether they belonged to the cyclonic eddy (C: stations 2, 3, 4), anticyclonic eddy (AC: stations 10-13, 16-19, 24, 25), dipole interface (Dipole I.: station 5), seamount summit and anticyclonic eddy (Summit/AC: stations 8, 21, 22), seamount flank and anticyclonic eddy (Flank/AC: stations 7, 9, 20, 23) and shelf (Shelf: stations 30, 31). The other hydrographic stations 1, 6, 14, 15, 26-29 could not be accurately resolved using the criteria mentioned in Section 3.2.3.2 and in the Appendix (Fig. A) and were not assigned to any of the listed categories.

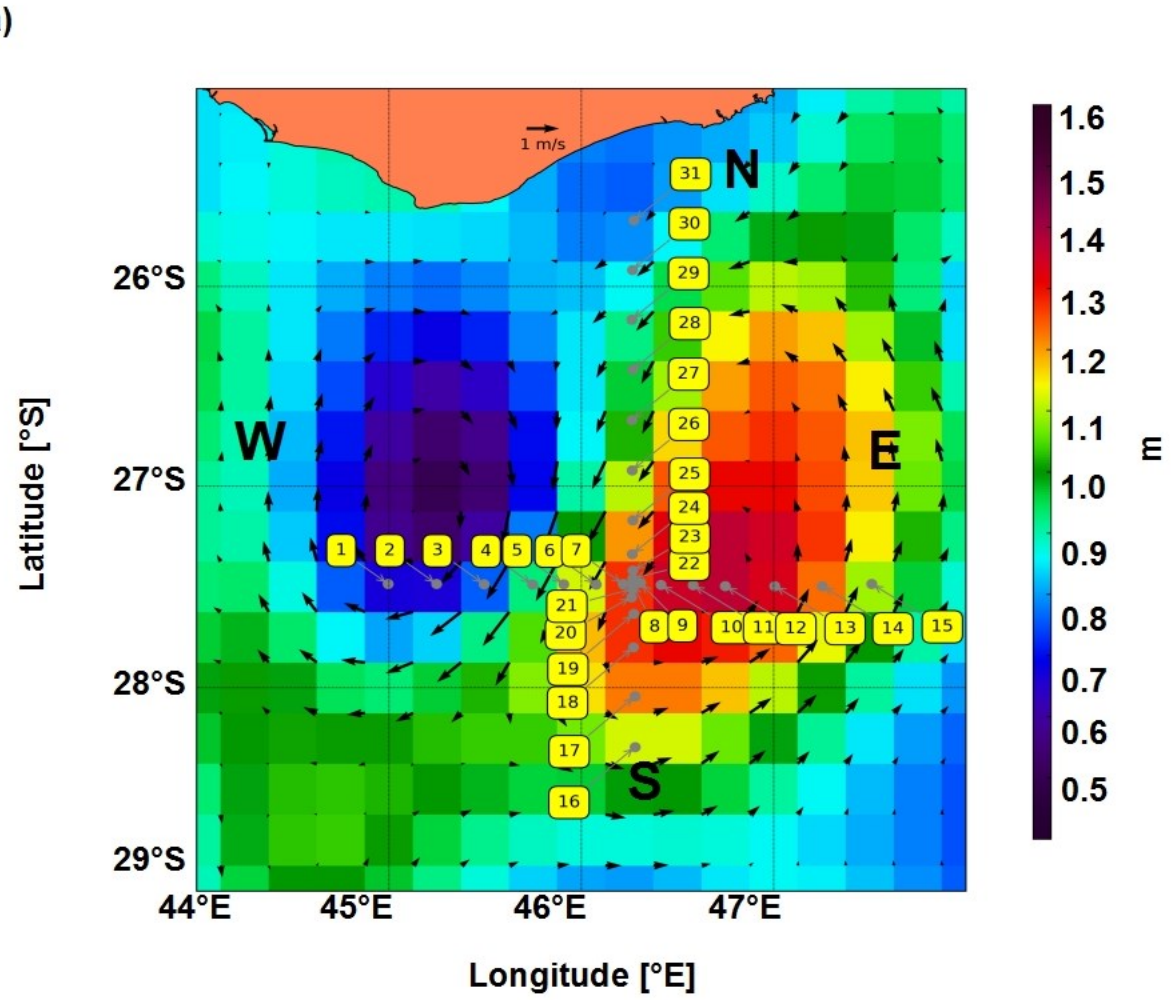

Figure 3.2(a) Satellite surface absolute dynamic height (m) on 19 November 2016 during MAD-Ridge cruise. Geostrophic velocity vectors (m s^{-1}) (black arrows) and the position of CTD stations numbered 1 to 31 (grey dots) are superimposed along the West-East (W-E) and South-North (S-N) transects. The Madagascan landmass is shown in orange.

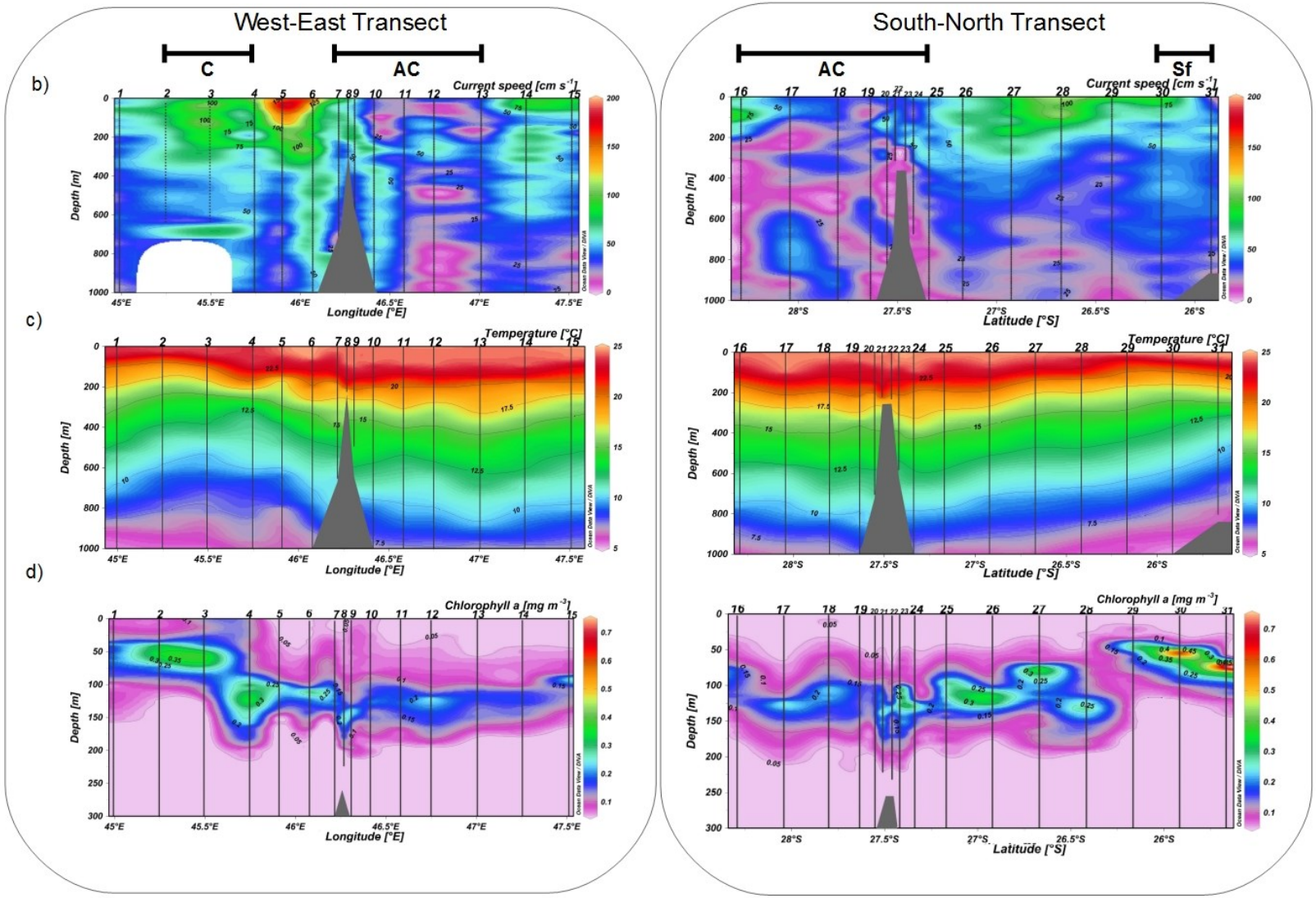

Figure 3.2 Vertical distributions of (b) current speed (cm s^{-1}), (c) temperature (°C), and (d) chlorophyll a (mg m^{-3}) for MAD-Ridge Leg 1 West-East transect (CTD stations labelled 1-15, left panels) across the cyclonic (C) and anticyclonic (AC) eddies, and South-North transect (CTD stations labelled 16-31, right panels) across the anticyclonic eddy and on the Shelf (Sf). Thhe MAD-Ridge seamount and the Madagascan shelf are shown in grey.

3.3.2 Hydrography and chlorophyll concentration during the MAD-Ridge cruise

Surface temperatures among the station categories varied between 23.7°C (cyclonic station 4) and 24.9°C (Summit/AC station 21). The cyclonic and shelf stations were characterised by shallower thermocline (79-165 m and 97-117 m, respectively) than the anticyclonic stations. The anticyclonic, Summit/AC and Flank/AC stations were characterised by a relatively deeper thermocline (159-219 m, 206-209 m and 181-212 m, respectively) (Fig. 3.2c). Fmax values of 0.35-0.38 mg m^{-3} and 0.62-0.74 mg m^{-3} were recorded at the cyclonic and shelf stations respectively, at depths of 54-122 m and 56-73 m, respectively (Fig. 3.2d). The anticyclonic, Summit/AC and Flank/AC stations had deeper Fmax depths (82-129 m, 131-153 m and 101-144 m) relative to the cyclonic and shelf stations, with Fmax values of 0.16-0.30 mg m^{-3}, 0.25-0.31 mg m^{-3} and 0.17-0.33 mg m^{-3}, respectively. Integrated chlorophyll *a* concentrations were statistically different between the classified hydrographic stations (KW, $H=7.59$, $p < 0.05$), especially between the cyclonic and anticyclonic stations (pairwise comparisons, $p < 0.05$). The mean ± S.D integrated chlorophyll *a* concentrations between 2 and 200 m were estimated at 29.1 ± 7.3 mg m^{-3} and 19.3 ± 2.1 mg m^{-3} within the cyclonic and anticyclonic eddies respectively.

3.3.3 Micronekton acoustic densities at the MAD-Ridge seamount

West-East Transect

The daytime total micronekton acoustic densities of the 38 kHz echosounder frequency exhibited a decreasing trend along the West-East transect, with the greatest responses recorded across stations 1-2 within the cyclonic eddy during Day_I (1705 m^2 nmi^{-2}) (Fig. 3.3a). The lowest acoustic responses were recorded across the Summit/AC station 8 during Day_III (755 m^2 nmi^{-2}) and stations 13-15 at the eastern periphery of the anticyclonic circulation during Day_V (702 m^2 nmi^{-2}). The night-time total micronekton acoustic densities were greater than the daytime acoustic responses and also exhibited a decreasing trend along the West-East transect. The greatest acoustic densities were recorded during Night_I (3241 m^2 nmi^{-2}) between cyclonic stations 3 and 4 and the lowest densities were recorded during Night_IV (1417 m^2 nmi^{-2}) between stations 12 and 13 at the anticyclonic periphery (Fig. 3.3a). Differences of 1536 m^2 nmi^{-2}, 1297 m^2 nmi^{-2}, 1058 m^2 $nmi^{-2}$and 595 m^2 nmi^{-2} in the micronekton acoustic responses were recorded between Night_I-Day_I, Night_II-Day_II, Night_III-Day_III and Night_IV-Day_IV, respectively.

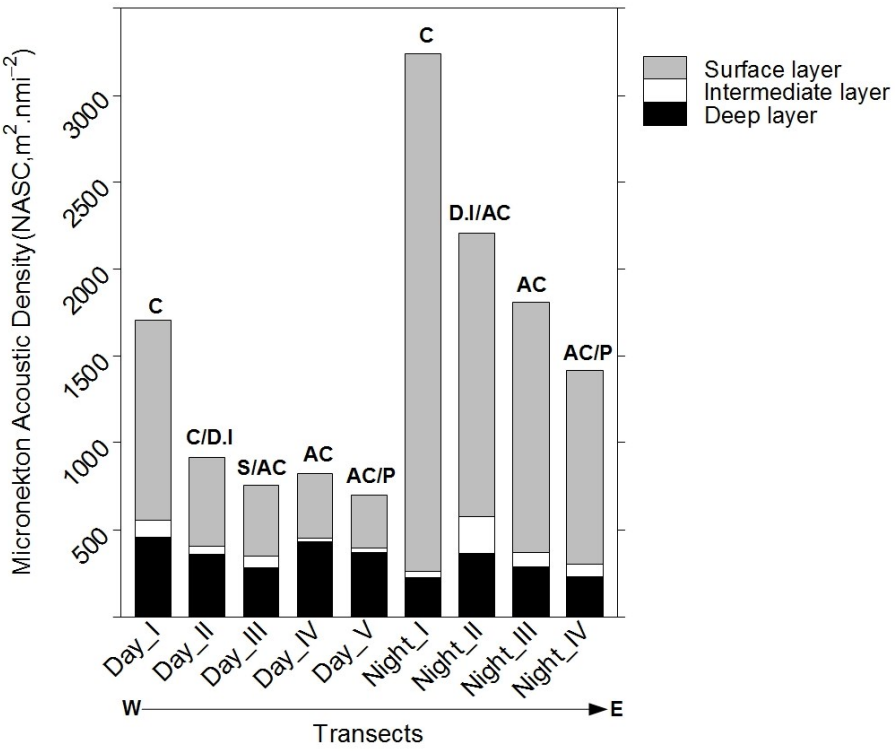

Figure 3.3(a) West-East (W-E) transect of MAD-Ridge: Mean micronekton acoustic density (s_A, m^2 nmi^{-2}) from Day_I to Day_V and Night_I to Night_IV: grey for surface layer (10-200 m), white for intermediate layer (200-400 m) and black for deep layer (400-735 m). Stacked bars are labelled: C (Cyclonic), C/D.I (Cyclonic/Dipole Interface), S/AC (Summit/ Anticyclonic), AC (Anticyclonic), AC/P (Antycyclonic/Eddy periphery) and D.I (Dipole Interface).

Interestingly, the surface layer gathered higher percentage acoustic densities than the deep layer during Day_I (stations 1-2), Day_II (Stations 4-6) and Day_III (stations 7-9), whereas the deep layer showed greater percentage acoustic densities than the surface layer during Day_IV and Day_V (Fig. 3.3a). The surface layer at night displayed 92%, 74%, 79% and 79% acoustic densities from Night_I to Night_IV, whereas the deep layer gathered 7% across Night_I and 16% across Night_II to Night_IV (Fig. 3.3a). The intermediate layer displayed the lowest percentage acoustic responses (1-10%) during day and night.

The echogram of the 38 kHz frequency showed organisms aggregating on the summits of deep topographic features labelled X and Y between 300 and 500 m and on the MAD-Ridge summit (Fig. 3.3b). These organisms contributed to the higher acoustic densities within the intermediate layer across Night_II relative to the intermediate layer across other transects. This echogram also provided evidence of organisms migrating to deeper layers (below 400 m) at sunrise and forming a dense aggregation between 400 and 600 m between the deep topographic feature Y and MAD-Ridge seamount (Fig. 3.3b).

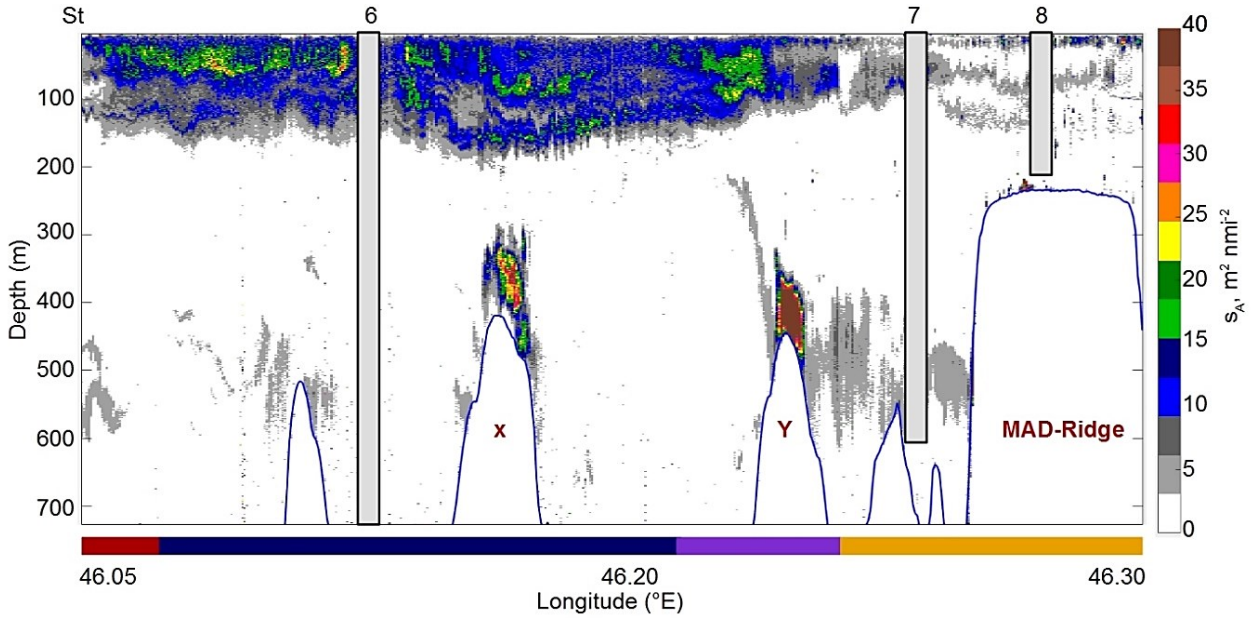

Figure 3.3(b) Echogram of the 38 kHz frequency across CTD stations 6-8 (denoted by striped bars). Deep topographic features X and Y and MAD-Ridge seamount are labelled in red. The colour bar indicates s_A in m^2 nmi^{-2}. Periods corresponding to sunset, night, sunrise and day are denoted by red, blue, violet and gold horizontal rectangles, respectively.

RGB composite images showed a dominant and strong 38 kHz backscatter (red dominating the RGB plot) between ~20 and 70 m across cyclonic stations 2 and 3 during daytime and between ~20 and 120 m across cyclonic stations 3 and 4 during the night and at sunrise (Fig. 3.3c). Between anticyclonic stations 10-12 and across stations 13 and 15, the backscatter of the 38 kHz frequency was dominant but lower between ~20 and 80 m relative to the cyclonic stations. At these anticyclonic stations, the dominant and stronger 120 kHz backscatter between ~80 and 140 m during daylight matches the Fmax depth of 82 and 129 m.

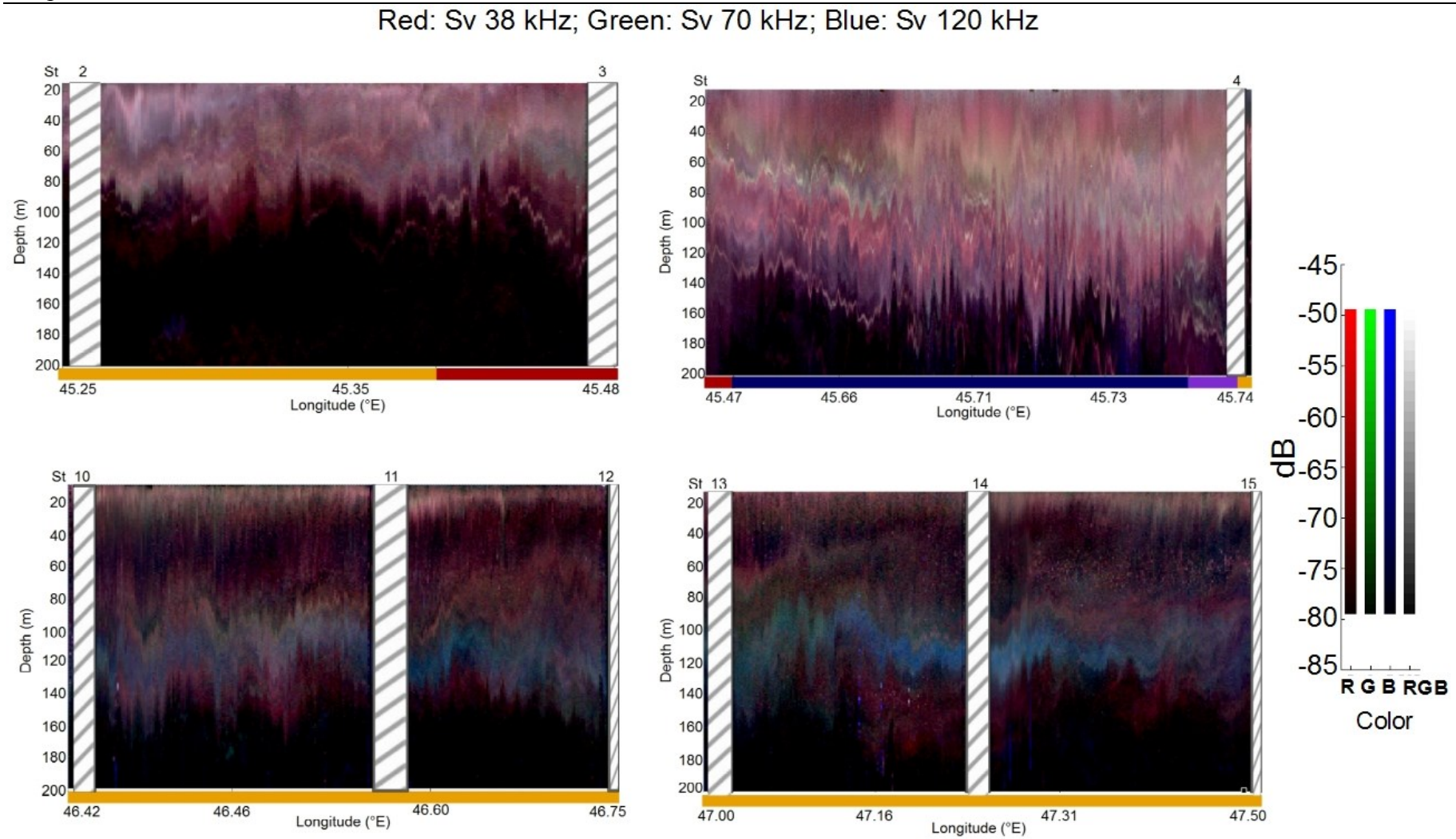

Figure 3.3(c) RGB composite images of Sv values (dB re 1 m^{-}1) across cyclonic CTD stations 2-3 and 4 and anticyclonic stations 10-12 and stations 13-15 (denoted by striped bars). The 38, 70 and 120 kHz frequencies were given red, green and blue colour codes, respectively, as explained in the methods. Periods corresponding to sunset, night, sunrise and day are denoted by red, blue, violet and gold horizontal rectangles, respectively.

South-North transect

The total daytime acoustic densities of the 38 kHz echosounder frequency across the South-North transect were greater during Day_VI (1050 m^2 nmi^{-2}) at the southern boundary of the anticyclonic circulation, decreased during Day_VII (805 m^2 nmi^{-2}) and Day_VIII (647 m^2 nmi^{-2}) along the summit/flanks and within the anticyclonic circulation, before increasing at the northern periphery of the same circulation during Day_IX (1014 m^2 nmi^{-2}) and at shelf station 30 during Day_X (1022 m^2 nmi^{-2}) (Fig. 3.4a). The night-time acoustic responses followed the same pattern as the daytime acoustic densities along the South-North transect, with the greatest responses across Night_VI (2609 m^2 nmi^{-2}) at the southern periphery of the anticyclonic circulation and Night_IX (2733 m^2 nmi^{-2}) at its northern boundary. The lowest responses along the South-North transect were recorded across Night_VII (1938 m^2 nmi^{-2}) and Night_VIII (1717 m^2 nmi^{-2}) over the summit and within the anticyclonic circulation. Differences of 1559 m^2 nmi^{-2}, 1132 m^2 nmi^{-2}, 1071 m^2 $nmi^{-2}$and 1719 m^2 nmi^{-2} in the micronekton acoustic densities were recorded between Night_VI-Day_VI, Night_VII-Day_VII, Night_VIII-Day_VIII and Night_IX-Day_IX, respectively.

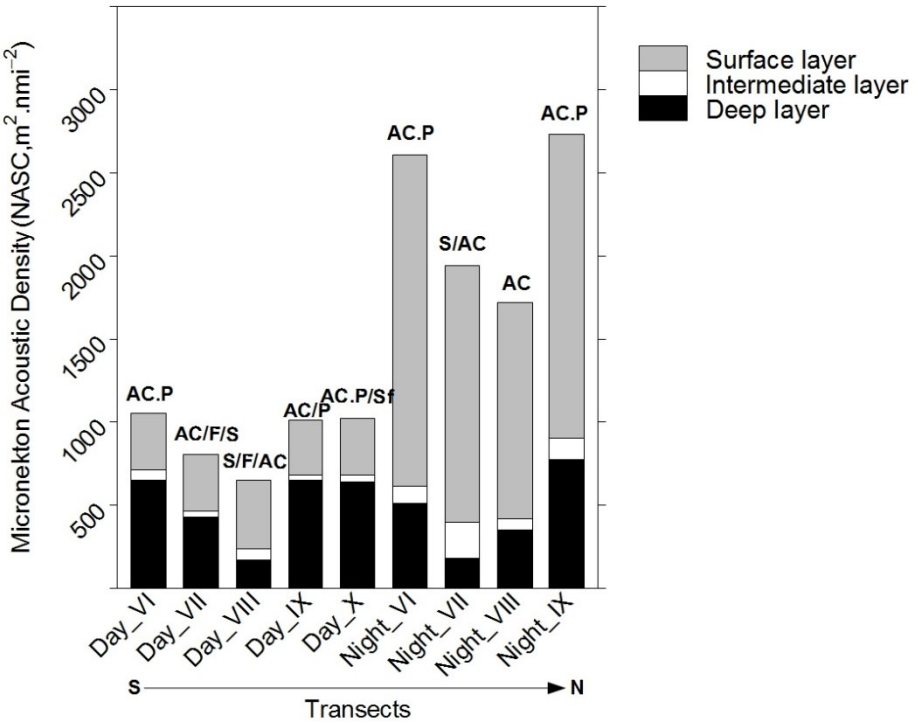

Figure 3.4(a) South-North (S-N) transect of MAD-Ridge: Mean micronekton acoustic density (s_A, m^2 nmi^{-2}) from Day_VI to Day_X and Night_VI to Night_IX: grey for surface layer (10-200 m), white for intermediate layer (200-400 m) and black for deep layer (400-735 m). Stacked bars are labelled: AC (Anticyclonic), AC/F/S (Anticyclonic/Flank/Summit), S/F/AC (Summit/Flank/Anticyclonic), AC/P (Anticyclonic/Eddy periphery) and AC.P/S (Anticyclonic eddy periphery and shelf), S/AC (Summit/Anticyclonic) and AC.P (Anticyclonic eddy periphery).

In contrast with Day_I, Day_II and Day_III along the West-East transect, the percentage micronekton acoustic responses at the 38 kHz echosounder frequency in the surface layer during the day was lower than that in the deep layer across all stations of the South-North transect, except at the summit station during Day_VIII (Fig. 3.4a). Across Night_VI to Night_IX, the surface layer displayed 76%, 80%, 76% and 67% of micronekton acoustic responses, whereas the deep layer recorded 20%, 9%, 20%, and 28%. Similar to the West-East transect, the intermediate layer along the South-North transect displayed the lowest percentage micronekton acoustic responses (4-11%) during day and night.

RGB composite images showed a dominant and relatively high 38 kHz backscatter between ~20-100 m across stations 21, 22, 23 (on the summit and flank, within the anticyclonic circulation) and shelf stations 30 and 31 (Fig. 3.4b). The 120 kHz backscatter was dominant between ~100 and 140 m, corresponding with Fmax depths ranging from 116 to 138 m at these stations. Across the shelf, the 120 backscatter was dominant between 60 and 80 m, corresponding to Fmax depths of 56-73 m at these stations. Regions of high Sv can be observed on the MAD-Ridge seamount (seen as “white patches” at 150-250 m on the RGB composite image between CTD stations 21 and 22), corresponding to aggregations of scatterers on the seamount summit (Fig. 3.4b).

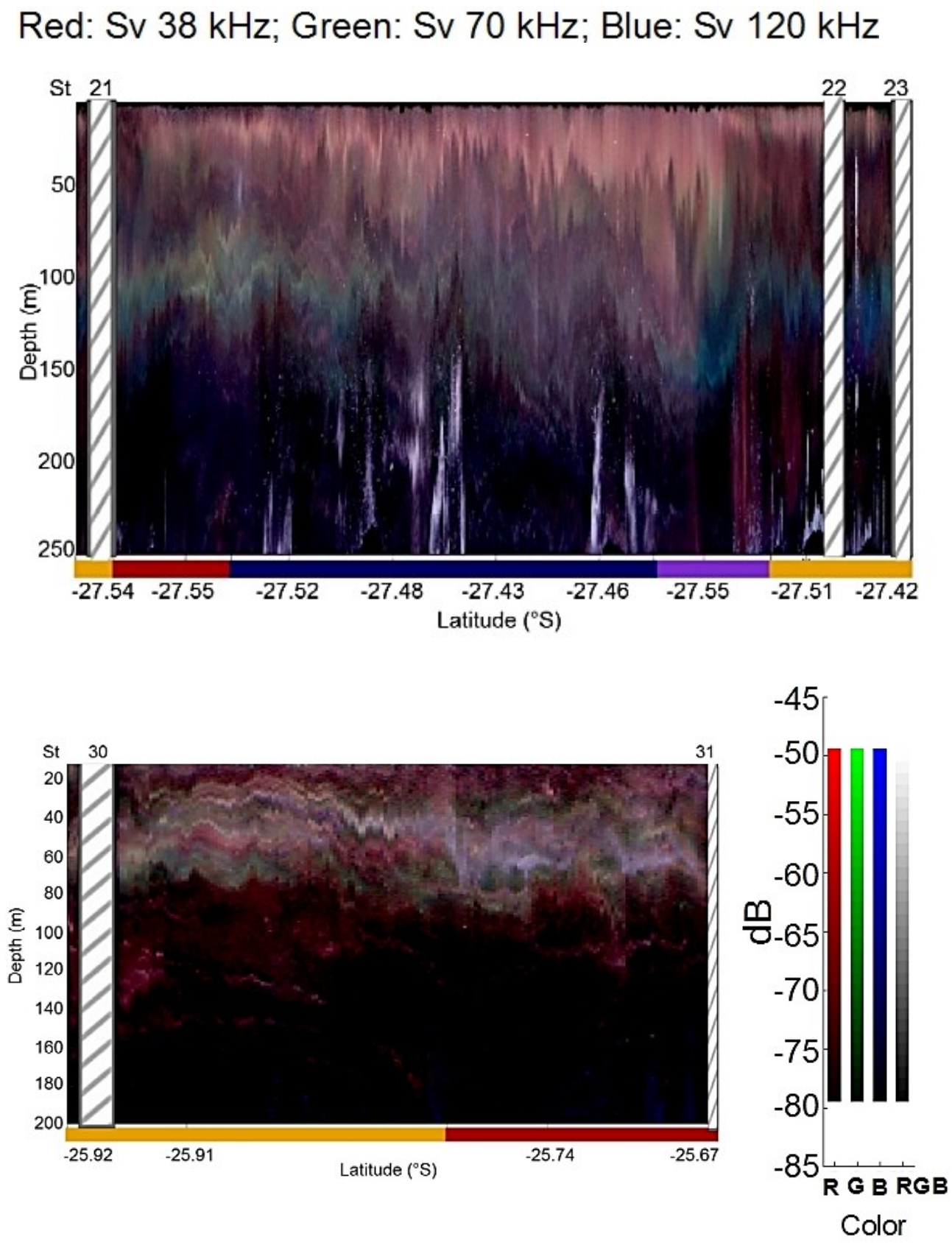

Figure 3.4(b) RGB composite images of Sv values (dB re 1 m^{-1}) at anticyclonic CTD stations 21-23 and shelf stations 30-31 (labelled by striped bars). The 38 kHz, 70 kHz and 120 kHz frequencies were given red, green and blue colour codes, respectively. Periods corresponding to sunset, night, sunrise and day are denoted by red, blue, violet and gold horizontal rectangles, respectively on the plots.

3.3.4 Environmental factors influencing micronekton distribution during the MAD-Ridge cruise

Median micronekton acoustic densities in the total water column and in the surface layer were the highest within the cyclonic eddy than in any other station category ($p < 0.05$) (Fig. 3.5a). The Flank/AC stations showed higher median micronekton acoustic densities of the total water column relative to the Summit/AC stations (Fig. 3.5a). The Summit/AC stations exhibited higher median micronekton acoustic densities in the surface layer than in the AC and Dipole I. stations ($p < 0.05$) (Fig. 3.5a). Micronekton acoustic densities in the deep layer had the same overlapping ranges across all station categories except over the Summit/AC stations ($p < 0.05$). Station 18, which was conducted at sunset, within the anticyclonic eddy showed high micronekton acoustic densities in the total water column (1461 ± 531 m^2 nmi^{-2}), with the acoustic backscatter being distributed almost equally in the surface and deep layers (506 ± 345 and 559 ± 298 m^2 nmi^{-2} respectively) and in lower concentrations in the intermediate layer (397 ± 154 m^2 nmi^{-2}). This station can be considered as being anomalous relative to the other anticyclonic stations. However, when this station was removed from the above KW and pairwise analyses, the outcome remained unchanged.

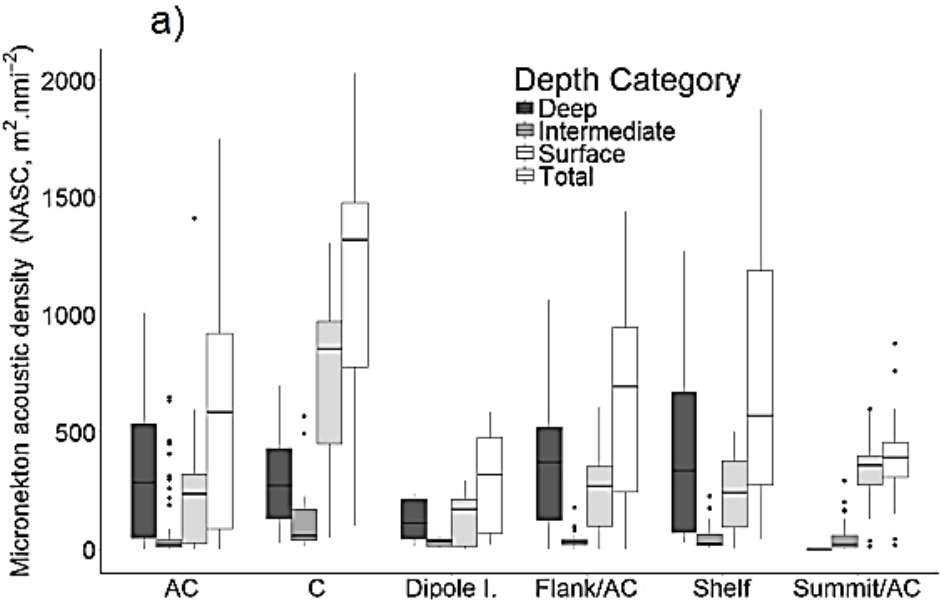

Figure 3.5(a) Boxplots of the total micronekton acoustic densities (s_A, m^2 nmi^{-2}) of the 38 kHz frequency in the deep (400-735 m), intermediate (200-400 m), surface layers (10-200 m) and total water column (10-735 m) for the transects at CTD stations: 10-13, 16-19, 24, 25 (AC: anticyclonic); 2, 3, 4 (C: cyclonic); 5 (Dipole Interface); 7, 9, 20, 23 (Flank/AC); 30, 31 (Shelf); and 8, 21, 22 (Summit/AC) of the MAD-Ridge cruise.

To summarise, the cyclonic eddy stations recorded the greatest micronekton acoustic densities of the total water column and were characterised by negative SLA relative to the other station

categories (Fig. 3.5a). The cyclonic eddy and shelf stations were characterised by the coldest temperature at 100 m, shallower Fmax, the highest integrated chlorophyll *a* concentrations between 2 and 200 m and the greatest mean zooplankton biovolumes (Fig. 3.5c-f). The anticyclonic circulation recorded lower micronekton acoustic densities in the total water column than the cyclonic circulation (Fig. 3.5a). These stations were characterised by positive SLA, warmer temperatures at 100 m, deeper Fmax, lower integrated chlorophyll *a* between 2 and 200 m and higher variability of zooplankton biovolumes than the cyclonic stations (Fig. 3.5b-f). The seamount summit stations did not exhibit remarkable micronekton acoustic densities, nor integrated chlorophyll *a* and mean zooplankton biovolumes among station categories (Fig. 3.5a, e, f). The station at the dipole interface recorded the lowest micronekton acoustic densities, although values were not significant ($p < 0.05$) compared with the other station categories, and were characterised by slightly negative SLA (Fig. 3.5a, b) and the highest mean current speed between of 99.1 m s^{-1} relative to all other stations (mean ± S.D. of 40.6 ± 19.2 m s^{-1}).

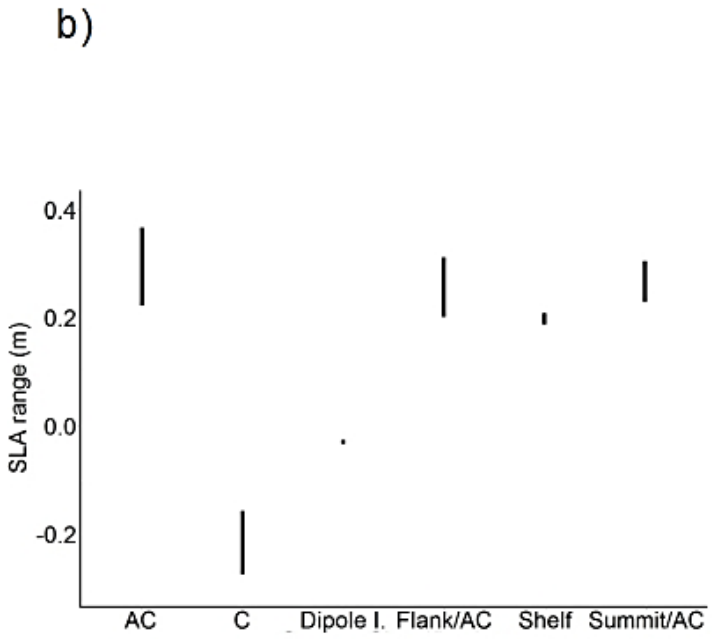

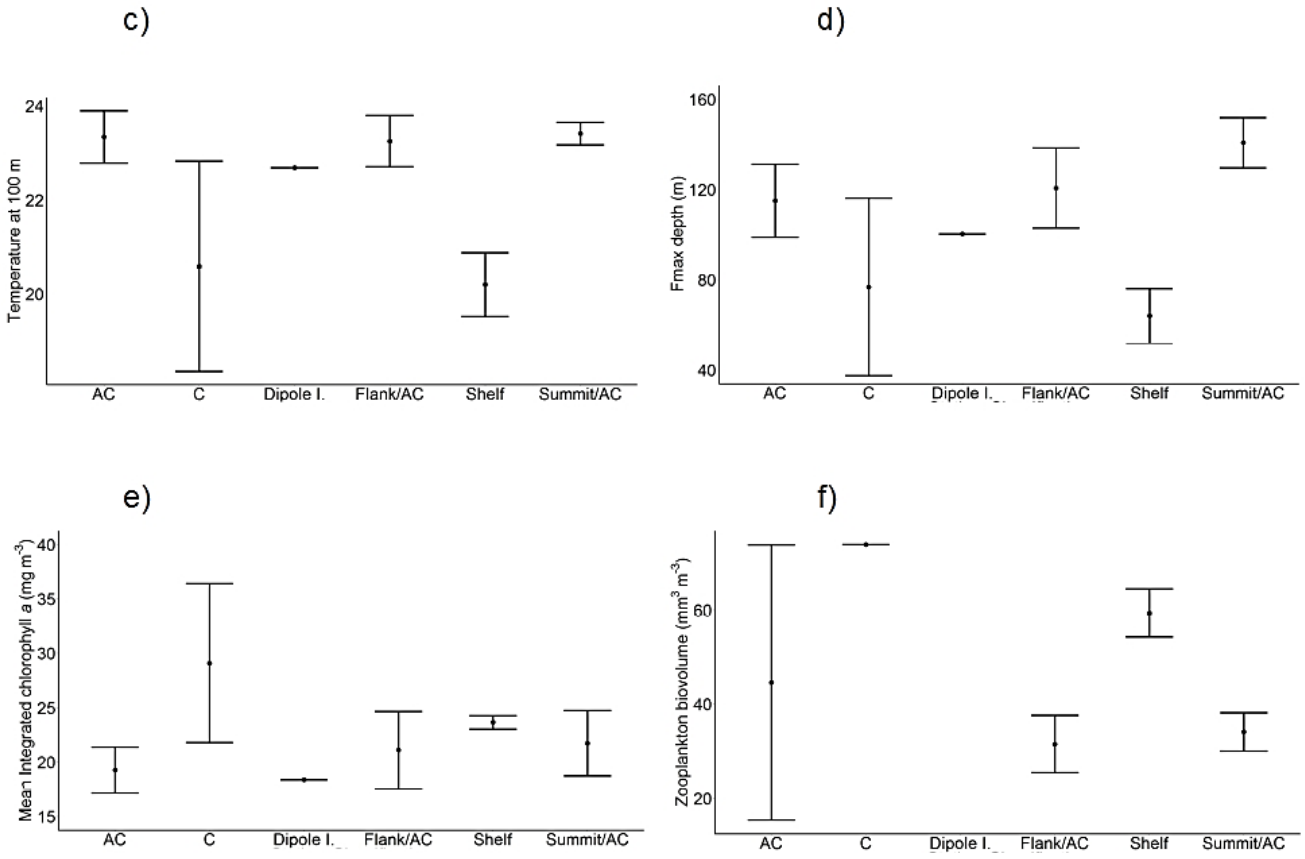

Figure 3.5 Mean and standard deviations of the variables (b) SLA (m), (c) Temperature at 100 m, (d) Fmax depth (m), (e) integrated chlorophyll a between 2-200 m (mg m^{-3}), and (f) zooplankton biovolume (mm^3 m^{-3}) plotted for the AC, C, Dipole I., Flank/AC, Shelf and Summit/AC stations.

3.3.5 Physical and biological oceanography at La Pérouse seamount

During the La Pérouse cruise, the seamount was under the influence of a weak cyclonic eddy with geostrophic speeds of <1 m s^{-1} and satellite surface absolute dynamic topography heights of ~1.1 m (Fig. 3.6). ADCP measurements recorded a current velocity of ~10-40 cm s^{-1} in the vicinity of the La Pérouse seamount, in the upper 200 m (Marsac et al., 2020). Surface temperatures ranged between 23 and 24°C, with a deeper thermocline (152-181 m) at La Pérouse (flanks and offshore stations combined) than at MAD-Ridge cyclonic stations. Maximum chlorophyll *a* values of 0.18 - 0.44 mg m^{-3} at Fmax depth between 65 and 140 m were recorded at all stations.

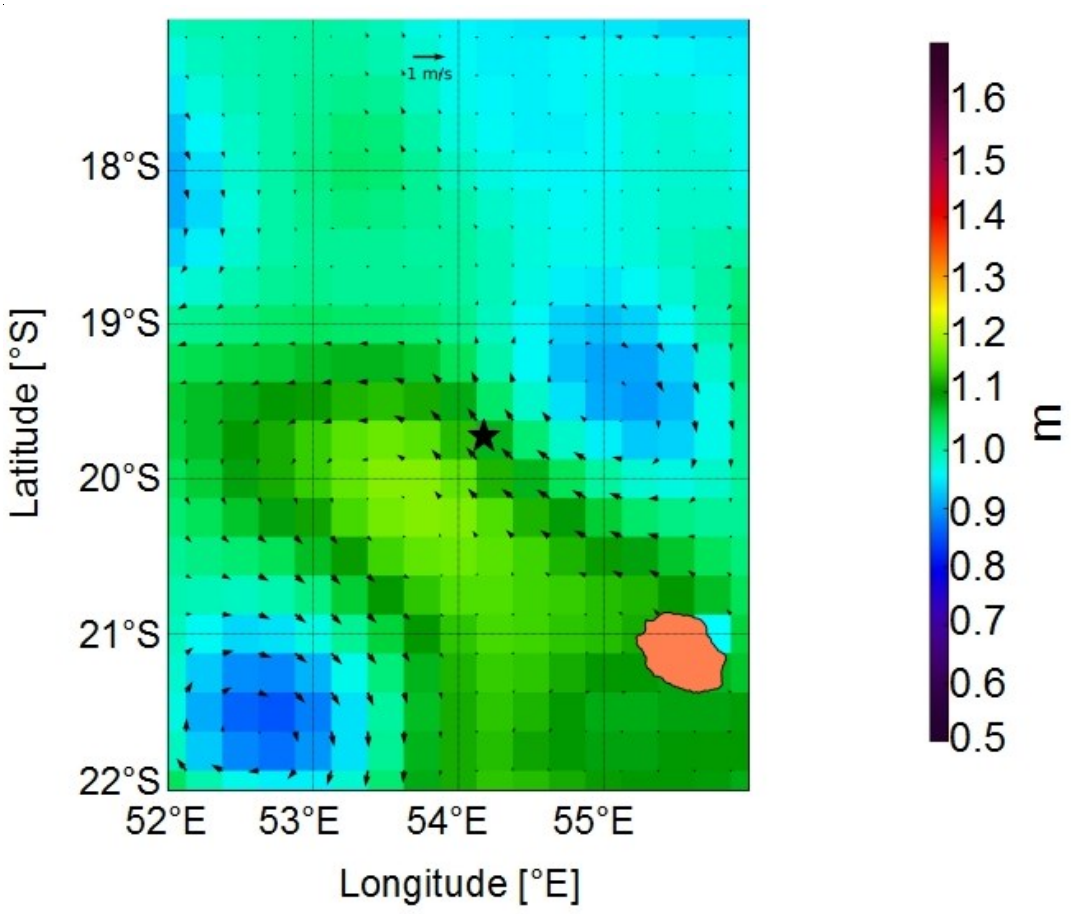

Figure 3.6 Satellite surface absolute dynamic height (m) on 16 September 2016 during the La Pérouse cruise showing La Pérouse seamount (black star). Geostrophic velocity vectors (m s^{-1}) (black arrows) are superimposed. Réunion landmass is shown in orange.

3.3.6 Comparison of micronekton acoustic densities at both seamounts

Wilcoxon tests performed on the 38 kHz frequency showed the overall acoustic densities of the depth categories (surface, intermediate and deep) differed significantly between La Pérouse and MAD-Ridge and between day and night ($p < 0.05$) along the transects mapped in Fig. 3.7. The mean acoustic densities for the 38 kHz frequency of the total water column (10-735 m) were lower over La Pérouse summit and flanks (Fig. 3.7a) during day (653 ± 689 m^2 nmi^{-2}) and night (903 ± 600 m^2 nmi^{-2}) relative to MAD-Ridge (Day: 1448 ± 1268 m^2 nmi^{-2}; Night: 2261 ± 1035 m^2 nmi^{-2}) summit and flanks (Fig. 3.7b). During the day and the night, the surface layer displayed a greater percentage of acoustic responses relative to the deep layer both at La Pérouse (Day - Surface: 87.5%, Day - Deep: 7.2%; Night - Surface: 94.2%, Night - Deep: 0.6%) and MAD-Ridge (Day - Surface: 57.2%, Day - Deep: 34.6%; Night - Surface: 74.3%, Night - Deep: 17.0%). The intermediate layer displayed percentage acoustic densities of 5-9% during day and night and at both seamounts.

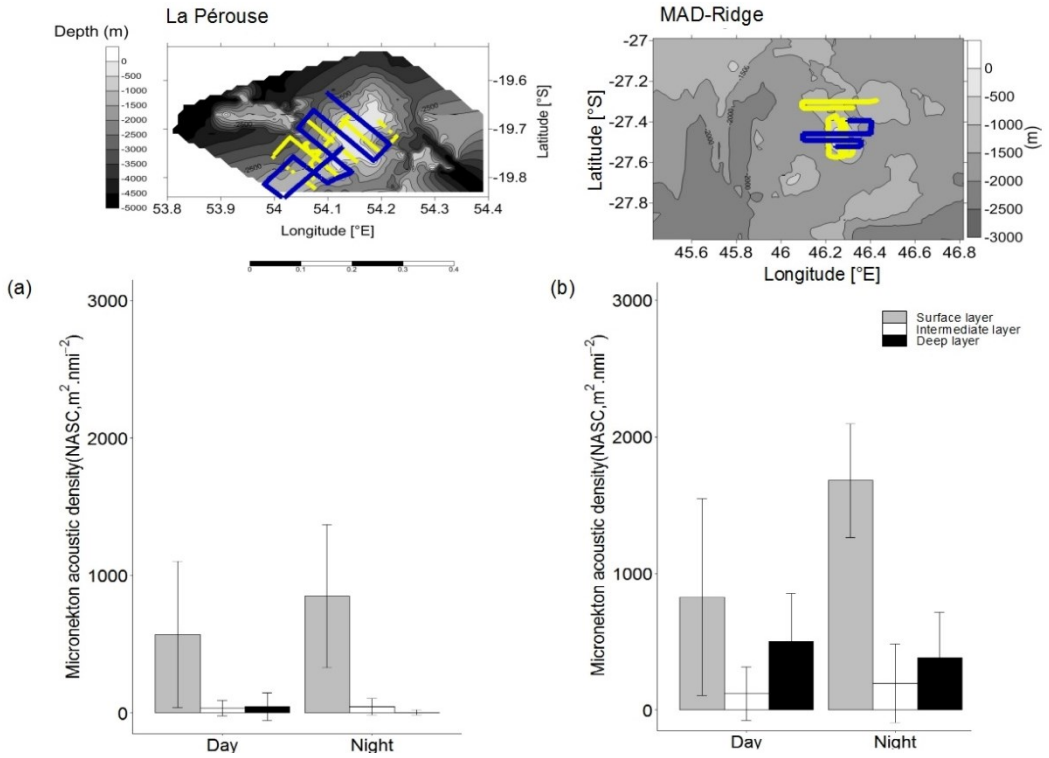

Figure 3.7 Map of La Pérouse and MAD-Ridge, daytime (yellow lines) and night-time (blue lines) acoustic transects plotted on the bathymetry. The colour bar indicates bathymetry (m) and the scale bar is given. Bar charts of mean micronekton acoustic densities (s_A, m^2 nmi^{-2}) ± standard deviations during day and night: grey for surface layer (10-200 m), white for intermediate layer (200-400 m) and black for deep layer (400-735 m) at (a) La Pérouse and (b) MAD-Ridge.

RGB composite images showed relatively low but dominant 38 kHz backscatter between depths of ~20 and 60 m both at La Pérouse (Fig. 3.7c) and MAD-Ridge (Fig. 3.7d) during the day. A stronger response to the 120 kHz frequency relative to the 38 kHz frequency was observed between ~100 and 180 m at La Pérouse and between ~100 and 125 m at MAD-Ridge during the day. At night, the 38 kHz backscatter was overall stronger and more dominant relative to the 70 kHz backscatter between depths of ~20 and 180 m both at La Pérouse and MAD-Ridge (Fig. 3.7e and 3.7f). Regions of high acoustic densities (seen as "white patches" on RGB composite images) were observed at the La Pérouse and MAD-Ridge summits during day and night (Fig. 3.7c, d, e and f).

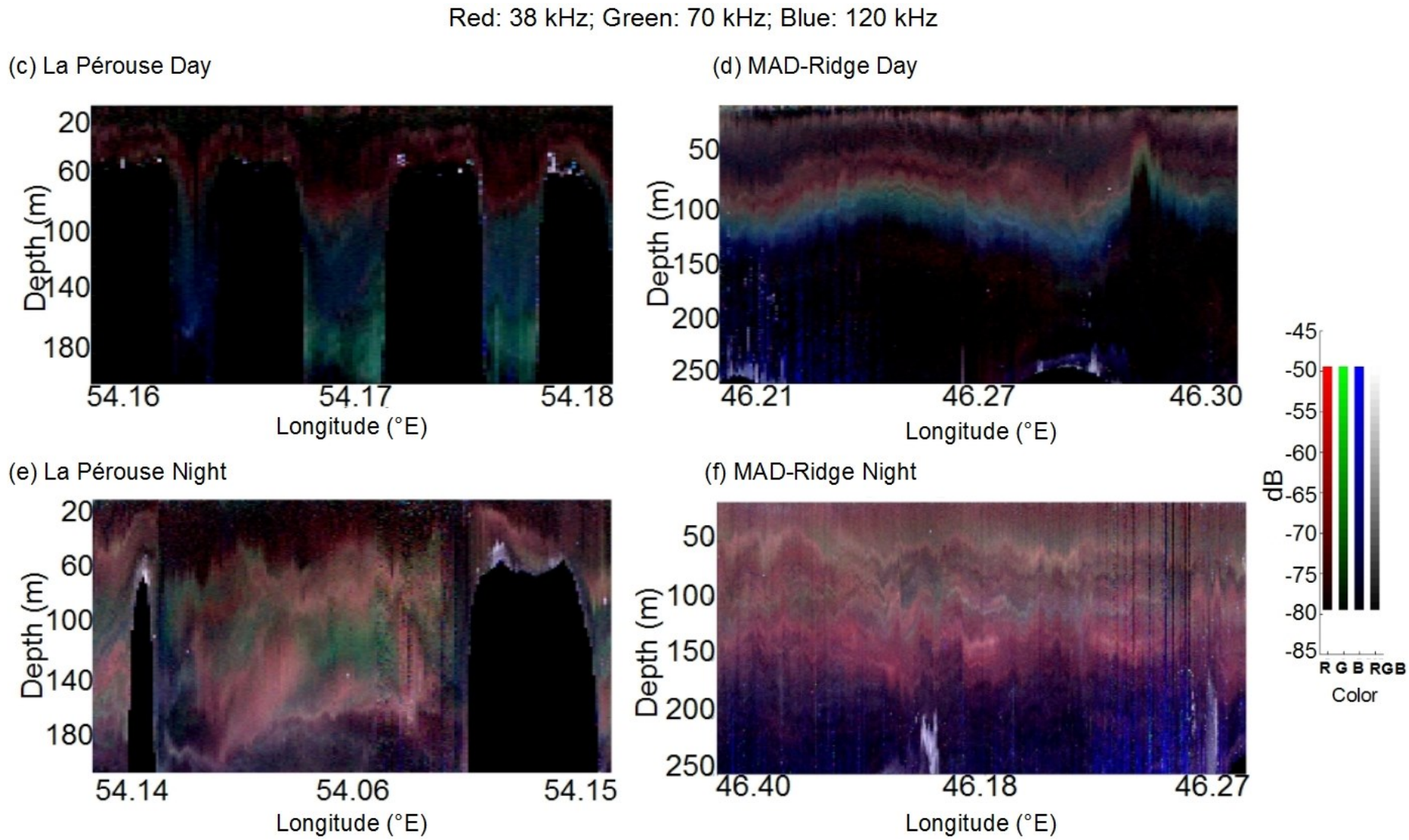

Figure 3.7 RGB composite images of S_V values (dB re 1 m^{-1}) of (c) La Pérouse day, (d) MAD-Ridge day, (e) La Pérouse night and (f) MAD-Ridge night. The MAD-Ridge and La Pérouse summits are shown in black. The 38, 70 and 120 kHz frequencies were given red, green and blue colour codes respectively. Regions of high SV are denoted by "white patches" on the RGB composites.

3.4 Discussion

3.4.1 Oceanographic conditions during the MAD-Ridge and La Pérouse cruises

This thesis demonstrated the strong influence of mesoscale cyclonic and anticyclonic eddies on the physical and biological properties at MAD-Ridge seamount. The doming of isotherms and shallowing of the Fmax depth was observed within the cyclonic eddy during the MAD-Ridge cruise. Such processes are associated with eddy-induced pumping and upwelling of cool, nutrient-rich waters, triggering an increase in primary production in the photic layer (McGillicuddy & Robinson, 1997; McGillicuddy et al., 1998; Klein & Lapeyre, 2009; Huggett, 2014; Singh et al., 2015). Phytoplankton within mesoscale cyclonic eddies can also grow in response to advection and subsequent retention of surrounding nutrient-rich waters within eddies (José et al., 2014; Lamont et al,. 2014). The anticyclonic eddy in this study was characterised by a deeper thermocline and Fmax, with a decrease in productivity in the photic layer than in the cyclonic eddy.

The Madagascar shelf also had a significant effect on the physical and biological processes during the MAD-Ridge cruise. The thermocline and Fmax depth were shallower on the shelf than at the other stations within the anticyclonic eddy. Previous studies have shown that the coastal regions south of Madagascar are more productive than surrounding waters (Raj et al., 2010; Pripp et al., 2014; Ramanantsoa et al., 2018) owing to coastal upwelling events driven by interactions between the East Madagascar Current and the continental shelf and by upwelling favourable winds (Ramanantsoa et al., 2018). This productivity can be entrained by mesoscale features that spin off the East Madagascar Current, farther south, potentially towards MAD-Ridge (Noyon et al., 2018; Ockhuis et al., 2017).

La Pérouse seamount, on the other hand, is located on the edge of the ISSG and was under the influence of a weak mesoscale eddy field during the cruise there, reflecting average conditions observed throughout the year in this region, as shown by Pous et al. (2014) using the OSCAR product (https://podaac.jpl.nasa.gov/dataset/OSCAR_L4_OC_third-deg). Apart from disturbances caused by the seamount to circulation, phytoplankton and zooplankton at a small scale along the flanks (Marsac et al., 2020), the average conditions in the La Pérouse area with relatively deep thermocline and Fmax depth, were typical of the oligotrophic ISSG province. Overall, during the time of the cruises, sea surface chlorophyll concentrations were twice as low within the region of the La Pérouse seamount as at the MAD-Ridge seamount (Annasawmy et al., 2019).

3.4.2 Diel vertical migration of micronekton

Micronekton is a diverse group of organisms capable of demonstrating various swimming behaviours (active swimming or passive drifting) and vertical migration strategies (diel migrants, semi-migrants or non-migrants) (Brodeur & Yamamura 2005). In this study, the different DVM patterns of micronekton were observed. Vertically migrating organisms ascended to the surface (above 200 m) at sunset and descended below 400 m at sunrise in the vicinity of both MAD-Ridge and La Pérouse, whereas only a small proportion of non-migrant or semi-migrant micronekton remained in the deep layer by day at both seamounts. On average, a difference of 595 m^2 nmi^{-2} to 1719 m^2 nmi^{-2} was recorded between day and night periods at MAD-Ridge (West-East and South-North transects) and a difference of 790 m^2 nmi^{-2} between day and night at La Pérouse. These differences between alternate day and night periods are likely caused either by the vertical migration of micronekton towards the surface at night for feeding purposes, sometimes from layers deeper than 735 m (i.e. beyond the range set for the 38 kHz transducer in this chapter), and/or the lateral advection of organisms.

Micronekton acoustic densities were greater in the surface layer than in the deep layer during the day at cyclonic eddy stations. This particular finding contradicts the general paradigm that micronekton are located in deeper layers by day (eg. Baliño & Aksnes, 1993; Andersen et al., 1998; Bertrand et al., 1999; Lebourges-Dhaussy et al., 2000; Benoit-Bird & Au, 2004; Domokos et al., 2010; Godø et al., 2009, 2012; Drazen et al., 2011; Béhagle et al., 2014; Menkes et al., 2015; Béhagle et al., 2016; Bianchi & Mislan, 2016; Annasawmy et al., 2018). Micronekton do not only undertake direct swimming in vertical and horizontal planes, but may also drift passively. Previous studies have reported passive drifting of the mesopelagic myctophid *Benthosema glaciale* with swimming speeds of 0-0.02 m s^{-1} along weak tidal currents and short bouts of active swimming in a vertical direction with swimming speeds of 0.05 m s^{-1}, possibly during feeding (Torgersen & Kaartvedt, 2001; Kaartvedt et al., 2009). This species has also been reported to undertake reverse DVM, ascending to approximately 200 m by day to forage on midwater plankton (Kaartvedt et al., 2009). The reverse DVM pattern is not common, with only some species of zooplankton (Ohman et al., 1983; Lampert, 1989) and mesopelagic fishes having been reported to ascend to the surface layer during the day to optimise feeding opportunities (Lebourges-Dhaussy et al., 2000; Kaartvedt et al., 2009).

Some micronekton taxa may also preferentially stay in the surface layer during the day to reduce competition during feeding. The micronekton species *Myctophum asperum*, *Myctophum nitidulum, Symbolophorus evermanni*, and *Chromis brevirostis* showed delayed

vertical migration at night in the Kuroshio region of the western North Pacific, with specific peak feeding hours and specialisation on different food organisms in order to reduce competition (Watanabe et al., 2002). Daylight surface observations are rare but were made for the mesopelagic fish *Benthosema pterotum* in the Gulf of Oman (Gjøsæter, 1978, 1984), the myctophid *Benthosema pterota* off the coast of Central America (Alverson, 1961) and the myctophid *Vinciguerria nimbaria* in the eastern Tropical Atlantic (Marchal & Lebourges-Dhaussy, 1996; Lebourges-Dhaussy et al., 2000). The reasons for the daylight surface occurrence of *V. nimbaria* has been linked to the presence of potential preys such as zooplankton at the Fmax depth (Lebourges-Dhaussy et al., 2000). Previous studies also have found the deep-dwelling cod *Micromesistius poutassou* which usually resides at a depth of 300-500 m, migrating to the surface of anticyclonic eddies probably to enhance feeding opportunities (Godø et al., 2012). Micronekton organisms within the cyclonic eddy during MAD-Ridge might have adopted a combination of these strategies and this possibility is discussed in more detail below.

3.4.3 Influence of mesoscale features on micronekton vertical and horizontal distribution

As shown earlier, the vertical and horizontal distributions of micronekton at MAD-Ridge were significantly influenced by mesoscale processes linked to the presence of cyclonic and anticyclonic eddies. The daytime s_A values within the eddy dipole interface were the lowest relative to the other hydrographic station categories used in this analysis. Harris et al. (2020) also recorded lower larval fish densities at the eddy dipole interface than at cyclonic and anticyclonic circulation stations. This can be attributed to the strong currents measured at this location that have led to the dispersion of micronekton communities. Alternatively, micronekton may have migrated below the depth range scanned by the 38 kHz transducer at that station due to a combination of strong currents and daytime light intensities.

Overall, acoustic densities of the total water column recorded within the cyclonic eddy were approximately twice as great as those recorded within the anticyclonic circulation during both day and night. The integrated chlorophyll *a* and zooplankton biovolume maxima found in the cyclonic eddy, matched the micronekton maxima, during day and night. Micronekton biomass is reported to be dependent on the availability of planktonic prey (Menkes et al., 2015), and hence on the oceanographic drivers of plankton production, as observed in this study. In the anticyclonic eddy, the downwelling mechanism of nutrient-depleted surface waters may have led to a reduction of chlorophyll *a* concentrations in the euphotic zone, and a subsequent

reduction in mesozooplankton abundance and micronekton acoustic densities during both day and night. Previous studies conducted in the Mozambique Channel have also reported lesser micronekton acoustic densities in anticyclonic relative to cyclonic eddies (Béhagle et al., 2014). However, the same authors pointed out some variability in eddy-induced biological responses, with one case of higher micronekton density in an anticyclonic eddy that was attributed to larger and more mobile organisms that are less influenced by mesoscale features than smaller organisms.

The RGB composite images have revealed the presence of a strong and dominant 38 kHz backscatter in the surface layer during the day across the cyclonic eddy (Fig. 3.3c). Previous studies have demonstrated that epi- and mesopelagic fishes with small gas-filled swimbladders and gelatinous plankton with gas inclusions dominate the 38 kHz frequency (Porteiro & Sutton, 2007; Kloser et al., 2002; Kloser et al., 2009; Davison et al., 2015; Cascão et al., 2017; Proud et al., 2018). The occurrence of these organisms at the surface (10-200 m) by day may be considered a response to the cyclonic eddy exhibiting relatively high integrated chlorophyll *a* concentrations and zooplankton biovolumes. The question arises, though, whether these micronekton species showed reverse migration strategies and actively remained in the shallow layer by day or whether they were passively entrained with the current within the cyclonic circulation. This shallow scattering layer may also have consisted of gelatinous organisms, which as other zooplankton, responded to the localised cyclonic productivity. The mesoscale cyclonic eddy may also have provided physical mechanisms that led to zooplankton retention and concentration, thereby increasing the encounter rate between micronekton and their prey. The micronekton organisms, likely epi- and mesopelagic fishes, would then preferentially stay in the surface layer by day to increase their feeding opportunities.

3.4.4 Influence of seamounts on micronekton vertical and horizontal distributions

Dense aggregations of scatterers were observed over deep topographic features labelled X and Y peaking at 430 m and 460 m, during night-time and sunrise, respectively (Figure 3.3b). These dense aggregations may have been migrating during the time of the cruise, upwards over feature X at night or downwards at feature Y at sunrise. Alternatively, they may be non-migrating organisms that remained preferentially associated with these topographic features during day and night. Studies have suggested that the bottom-trapping mechanism as well as the horizontal flux of non-migrating zooplankton maintain the densities of zooplanktivorous fishes at seamounts of intermediate depth (Genin & Dower, 2007). A range of other factors

such as the quiescent shelters offered by these topographies and the absence of shallow diving predators (Porteiro & Sutton, 2007) may also account for the presence of these dense aggregations at the features labelled X and Y.

Micronekton acoustic densities over the summit and flanks of MAD-Ridge were lower than the acoustic densities recorded within the cyclonic eddy and over the Madagascar shelf. However, the acoustic densities surrounding MAD-Ridge's summit and flanks were greater than those recorded in the vicinity of the summit and flanks of La Pérouse. Although there were clear mechanisms leading to enhanced productivity within the cyclonic eddy and over the Madagascar shelf, the local physical and biological dynamics over La Pérouse and MAD-Ridge seamounts were less straightforward. No clear enhancement in micronekton acoustic densities was observed over MAD-Ridge compared with the surrounding vicinity (within 14 nmi of the summit) at the time of the cruises (Annasawmy et al., 2019).

In the literature, Taylor columns that form over seamounts are often seen as physical processes that are capable of enhancing productivity and isolating the seamount waters from the large-scale environment (Genin & Boehlert, 1985; Dower et al., 1992; Genin, 2004). The α, Ro and Bl values were above the threshold set in literature (Chapman & Haidvogel,1992; White et al., 2007), at both La Pérouse and MAD-Ridge during the cruises. The mesoscale eddy activity in the MAD-Ridge area may have dominated any potential seamount effect. The summit of MAD-Ridge during most of the cruise was under the influence of the anticyclonic eddy and current speeds exceeded 0.5 m s^{-1}, thus making the formation of a Taylor column very unlikely. The MAD-Ridge's seamount shape may also not be favourable to the formation of such features because the threshold set for α values in theoretical calculations was exceeded. Additionally, because of the presence of the anticyclonic eddy feature over MAD-Ridge's summit, there was a downward deflection of isotherms between the surface and ~200 m, instead of an uplifting as seen across other studies (Genin & Boehlert 1985; Boehlert & Genin, 1987; Dower & Mackas, 1996). MAD-Ridge is located in an "eddy corridor" to the south of Madagascar. Previous studies have found evidence of a westward drift of eddies at an estimated speed of 7.3 ± 1.7 cm s^{-1} in the vicinity of the pinnacle, along 27°S and 45°E (Pollard & Read., 2017). Phytoplankton entrapment during several weeks would be needed to allow growth of zooplankton and to attract micronekton species (Genin & Boehlert 1985; Boehlert & Genin, 1987; Dower et al., 1992). In such a dynamic system, strong currents may continuously sweep away phytoplankton cells from the summit. Phytoplankton retention mechanisms may not be sufficiently long to have a significant impact on higher trophic levels such as zooplankton and

micronekton, potentially explaining the lower micronekton acoustic densities recorded directly above MAD-Ridge's summit during the cruise relative to the cyclonic eddy and shelf stations.

La Pérouse's pinnacle is believed to cause disruptions in the current velocities because flank stations (within 3 km of the summit) exhibited a larger diversity of current velocities and directions than control stations (10-21 km away) (Marsac et al., 2020). Over La Pérouse seamount, the formation of a Taylor column was very unlikely to have occurred because current speeds of 0.3 m s^{-1} and greater were recorded. The complex crescent shape of the seamount may not be favourable for the development of a steady anticyclonic circulation characteristic of Taylor columns. The La Pérouse wider region is under the influence of the anticyclonic circulation pattern of the ISSG province characterised by a deep thermocline, a halocline and a DCM at 100-150 m, with chlorophyll *a* concentrations <0.3 mg m^{-3} between the surface and 200 m as observed in our study and in Jena et al. (2012, 2013). Overall mean acoustic densities of micronekton at the La Pérouse seamount were thus typical of those of the ISSG province both during day and night (Annasawmy et al., 2018).

Common to both La Pérouse and MAD-Ridge seamounts is the presence of dense aggregations of scatterers (seen as "white patches" on RGB composite images, Fig. 3.4b and 3.7c-d) directly above the summits during day and night. A combination of trawls and acoustic data revealed these dense aggregations to consist of the myctophids *Diaphus suborbitalis* (both La Pérouse and MAD-Ridge), *Benthosema fibulatum*, *Hygophum hygomii* and the benthopelagic fish *Cookeolus japonicus* on MAD-Ridge's summit and flanks (Annasawmy et al., 2019). Populations of *D. suborbitalis* have also been reported to be located between 500 and 600 m during the day along the flanks of the Equator seamount in the Indian Ocean, and to ascend to the summit of the seamount at dusk to feed on copepods (Gorelova & Prut'ko, 1985; Parin & Prut'ko, 1985; Porteiro & Sutton, 2007), while *B. fibulatum* has been found associated with the Hawaiian Cross seamount in the Pacific (De Forest & Drazen, 2009). Dense aggregations of scatterers were also observed above a ridge off the coast of Baja California and was thought to consist of the fish *Sebastodes*, anchovy and juvenile hake that prey on migrating zooplankton (Isaacs & Schwartzlose, 1965). Similar aggregations of scatterers were observed on the Southeast Hancock seamount in the central North Pacific, consisting of resident populations of the fish *Maurolicus muelleri* and the mysid *Gnathophausia longispina* (Boehlert et al., 1994). Time-series of acoustic transects showed these organisms to be concentrated on the seamount flanks at 400 m, before rising to the surface at dusk and streaming vertically downwards at dawn, with some scatterers remaining above the flanks at 170 m even during daylight. The

association of these fishes with seamounts may confer some selective advantages such as increased feeding opportunities (Wilson & Boehlert, 2004), increased habitat diversity (Wilson & Boehlert, 2004; Porteiro & Sutton, 2007), shelter areas for spawning, or decreased energy loss by using the seamount as a shelter during non-feeding intervals (Cascão et al., 2017).

The maintenance of a population at a seamount also depends on local recruitment or advection of eggs and larvae from the shelf or neighbouring islands and seamounts (Boehlert et al., 1994; Diekmann et al., 2006). According to Harris et al. (2020), higher larval densities mostly of the families Myctophidae, Bregmacerotidae, Gonostomatidae and Molidae were recorded at MAD-Ridge's summit. According to those authors, this observation points to some local spawning processes at the pinnacle. The MAD-Ridge seamount is close to shallow and deep topographic features and to the Madagascar shelf, features from which larvae might have been advected (Crochelet et al., 2020). The presence of a greater proportion of neritic species over the summit of MAD-Ridge seamount relative to La Pérouse seems to favour this hypothesis (Harris et al., 2020). The mesoscale activity on the Madagascar shelf and at MAD-Ridge may allow the periodic replenishment of advected larvae over the pinnacle (Harris et al., 2020; Crochelet et al., 2020), corresponding with enhanced micronekton acoustic densities compared to La Pérouse.

3.5 Concluding Remarks

This work has suggested a link between the physical processes leading to enhanced productivity and the biological response of micronekton. Two main processes were identified to have a positive effect on the observed productivity: 1) the influence of the cyclonic eddy through the enrichment of surface waters, 2) the advection of shelf waters with high chlorophyll *a* concentrations. La Pérouse and MAD-Ridge seamounts did not show any enhanced biomass of micronekton, as reported to be the case for other seamounts. However, despite the differing productivity levels at both seamounts, dense aggregations of scatterers were observed on the summits during day and night. This study has therefore suggested that seamount-associated species were the only seamount effect detected and that in a highly dynamic environment like south of Madagascar, mesoscale features have a stronger influence than seamounts on micronekton acoustic densities.

Acknowledgements

The authors acknowledge the work carried out by the non-scientific and scientific staff on board the RV *Antea* in taking part in the data acquisition and data processing. The study was mainly supported by the Flotte Océanographique Française (French Oceanographic Fleet) and IRD in relation to the logistics of the RV *Antea*. Additional funding was also received from Région Réunion (Réunion Regional Council) for the La Pérouse cruise, and from the Fonds Français pour l'Environnement Mondial (FFEM) as part of the FFEM-SWIO project on Areas Beyond National Jurisdiction (ABNJ) of the South West Indian Ocean for the MAD-Ridge cruise. Pavanee Annasawmy was the beneficiary of a doctoral bursary granted by the Institut de Recherche pour le Développement (IRD, France) and the ICEMASA French-South African International Laboratory.

Inter-chapter I

As seen in Chapter 2, seabirds breed at island states in the SWIO and regularly use seamounts or regions of enhanced productivity such as upwelling at continental shelves and within mesoscale eddies during their foraging trips. Tunas and swordfish may benefit from seamounts in the region for foraging, during their migrations and/or as navigational waypoints. These species also take advantage of mesoscale eddies for enhanced foraging opportunities. Humpback whales were further reported to use La Pérouse seamount during their breeding season. Different micronekton communities thus support a wide range of top predators in the SWIO. The spatial distribution of micronekton is not uniform across this region, which likely influences the foraging patterns of these predators. It is now well accepted that the spatial distribution of top predators is often associated with prey availability.

Chapter 3 aimed at investigating which feature between two shallow seamounts, the Madagascar continental shelf and mesoscale eddies, would exhibit a greater density of available prey for top predators. Local dynamic processes caused by current-topography interactions such as Taylor columns and isopycnal domings could have contributed to the retention of plankton and aggregation of zooplankton and micronekton over the summits of La Pérouse and MAD-Ridge. However, these anticyclonic circulation cells are unlikely to occur at the seamounts. Both pinnacles recorded lower acoustic densities of micronekton relative to the cyclonic eddy observed during MAD-Ridge. The La Pérouse seamount is located on the outskirts of the ISSG province and is characterised by weaker mesoscale dynamics, deeper thermocline and lower maximum fluorescence, which are typical of oligotrophic marine systems. The MAD-Ridge seamount, on the other hand, is located along the Madagascar ridge in a region with high mesoscale activities. Productivity at the Madagascar shelf were associated with high micronekton acoustic densities. This productivity and micronekton larvae may further be entrained from the shelf to the MAD-Ridge pinnacle by the action of mesoscale eddies. These physical processes may be responsible for the higher acoustic densities recorded at MAD-Ridge relative to La Pérouse.

The micronekton acoustic densities were also not uniform within mesoscale features, with the cyclonic eddy showing greater acoustic estimates relative to the anticyclone encountered during the MAD-Ridge cruise. The shallower depth of the maximum fluorescence, lower temperature values, higher chlorophyll *a* concentrations in the euphotic zone (as seen in

Chapter 3), enriched picoplankton and nanoplankton carbon biomass and greater zooplankton biovolumes (as seen in Chapter 2), may have contributed to this increase in micronekton backscatter intensities within the cyclone. The different micronekton communities may hence be able to respond to physical environmental cues and aggregate in areas with greater productivity and zooplankton prey availability. While the La Pérouse and MAD-Ridge seamounts did not show enhanced acoustic densities of micronekton on their summits and flanks relative to their surroundings, dense aggregations were recorded over their summits. Some organisms may hence preferentially associate with the summits of these pinnacles during day and night.

Acoustics is a powerful tool that can be used to estimate the biomass of mesopelagic organisms throughout whole cruise transects. However, the species composition cannot be accurately determined based solely on acoustic techniques. Chapter 4 will hence investigate the composition of the micronekton communities using a combination of trawl data and a multi-frequency acoustic visualisation technique. The composition of the dense aggregations of scatterers observed over the summit of the pinnacles in Chapter 3 will be determined. Chapter 3 has also shown that some micronekton communities swim vertically to the surface at dusk and to deeper layers at dawn. However, the different species within the micronekton may exhibit different migration strategies than just DVM. The seamounts may further influence organisms in their migration patterns and this will be investigated in Chapter 4.

Chapter 4: Micronekton distributions and assemblages at two shallow seamounts of the south-western Indian Ocean

From left to right: Argyropelecus aculeatus (MAD-Ridge cruise) and Acanthuridae (La Pérouse cruise), identified during the 2017 Taxonomy Workshop organised at the Department of Biological Sciences, UCT.

Photo Credit: ***Ukarapo T. Mungunda*** *(Honours in Marine Biology, UCT)*

Photo title: The Beauty and the Beast

Digital Imaging Techniques: Nikon Stereoscopic Zoom Microscope SMZ1500 with a ring light and fibre optic arms, at 0.75 X Magnification. The Nikon DS Camera Control Unit DS-U2 & DS-5M Camera head and NIS-Elements imaging program was used.

Micronekton distributions and assemblages at two shallow seamounts of the south-western Indian Ocean: Insights from acoustics and mesopelagic trawl data

Pavanee Annasawmy[1, 2*], Jean-François Ternon[1], Pascal Cotel[1], Yves Cherel[3], Evgeny V. Romanov[4], Gildas Roudaut[5], Anne Lebourges-Dhaussy[5], Fréderic Ménard[6], Francis Marsac[1, 2]

[1] *MARBEC, Univ Montpellier, CNRS, Ifremer, IRD, Avenue Jean Monnet, CS 30171, 34203 Sète cedex, France*

[2] *Department of Biological Sciences and Marine Research Institute, University of Cape Town, Private Bag X3, Rondebosch 7701, Cape Town, South Africa*

[3] *Centre d'Etudes Biologiques de Chizé (CEBC), UMR7372 du CNRS-Université de la Rochelle, 79360 Villiers-en-bois, France*

[4] *Centre technique d'appui à la pêche réunionnaise (CAP RUN)-NEXA, 97420 Le Port, Île de la Réunion, France*

[5] *Institut de Recherche pour le Développement (IRD), UMR LEMAR 195 (UBO/CNRS/IRD), Campus Ifremer, BP 70, 29280 Plouzané, France*

[6] *Aix Marseille Univ, Université de Toulon, CNRS, IRD, MIO, Marseille, France*

* Corresponding author: angelee-pavanee.annasawmy@ird.fr

Abstract

Micronekton distributions and assemblages were investigated at two shallow seamounts of the south-western Indian Ocean (SWIO) using a combination of trawl data and a multi-frequency acoustic visualisation technique. La Pérouse seamount (summit depth ~60 m) is located on the outskirts of the oligotrophic Indian South Subtropical Gyre (ISSG) province with weak mesoscale activities and low primary productivity all year round. The "MAD-Ridge" seamount (thus termed in this study; ~240 m) is located in the productive East African Coastal (EAFR) province with high mesoscale activities to the south of Madagascar. Higher micronekton species richness was recorded at MAD-Ridge compared to La Pérouse. Resulting productivity at MAD-Ridge seamount was likely due to the action of mesoscale eddies advecting productivity and larvae from the Madagascar shelf rather than local dynamic processes such as Taylor column formation. Mean micronekton abundance/biomass, as estimated from mesopelagic trawl catches, were lower over the summit compared to the vicinity of the seamounts, due to net selectivity and catchability and depth gradient on micronekton assemblages. Mean acoustic densities in the night shallow scattering layer (SSL: 10-200 m) over the summit were not significantly different compared to the vicinity (within 14 nautical miles) of MAD-Ridge. At La Pérouse and MAD-Ridge, the night and day SSL were dominated by common diel vertically migrant and non-migrant micronekton species respectively. While seamount-associated mesopelagic fishes such as *Diaphus suborbitalis* (La Pérouse and MAD-Ridge) and *Benthosema fibulatum* performed diel vertical migrations (DVM) along the seamounts' flanks, seamount-resident benthopelagic fishes, including *Cookeolus japonicus* (MAD-Ridge), were aggregated over MAD-Ridge summit. Before sunrise, mid-water migrants initiated their vertical migration from the intermediate to the deep scattering layer (DSL, La Pérouse: 500-650 m; MAD-Ridge: 400-700 m) or deeper. During sunrise, the other taxa contributing to the night SSL exhibited a series of vertical migration events from the surface to the DSL or deeper until all migrants have reached the DSL before daytime. Possible mechanisms leading to the observed patterns in micronekton vertical and horizontal distributions are discussed. This thesis contributes to a better understanding of how seamounts influence the DVM, horizontal distribution and community composition of micronekton and seamount-associated/resident species at two poorly studied shallow topographic features in the south-western Indian Ocean.

Keywords: micronekton, seamount, south-western Indian Ocean, acoustics, seamount-associated fauna

4.1 Introduction

Seamounts are ubiquitous underwater topographic features, usually of volcanic origin, which rise steeply through the water column from abyssal depths. They exhibit various shapes (conical, circular, elliptical or elongated) with the summit reaching various depths below the sea surface. Shallow seamounts are those reaching into the euphotic zone. As topographic obstacles, seamounts may influence prevailing ocean currents by disrupting the oceanic flow and causing spatial and temporal variability in the current field (Royer, 1978; White et al., 2007). The combined interaction of various seamount characteristics, stratification and oceanic flow conditions may provide local dynamic responses at seamounts such as formation of a Taylor Column or Cone, isopycnal doming (Mohn & Beckmann, 2002), enclosed circulation cells and enhanced vertical mixing (White et al., 2007). The aforementioned physical processes may cause various responses over seamounts, notably, upwelling and vertical mixing of nutrient-rich waters from deeper to shallower layers and enhanced productivity (Boehlert & Genin, 1987; Genin, 2004). The enclosed, semi-enclosed circulation pattern around seamounts may also be important retention mechanisms for drifting organisms produced over, or advected from the far field into the vicinity of the pinnacle (White et al., 2007).

Seamounts are important for fisheries around the world since they aggregate large pelagic organisms of commercial value such as tunas (Fonteneau, 1991; Holland & Grubbs, 2007; Dubroca et al., 2013), alfonsinos and orange roughy (Ingole & Koslow, 2005; Bensch et al., 2009). In the SWIO, seamount-associated fisheries gradually developed since the early 1970s, targeting various species, including alfonsinos (*Beryx* sp.), rubyfish (*Plagiogeneion rubiginosus*), cardinalfish (*Epigonus* sp.), pelagic armourhead (*Pentaceros richardsoni*), rudderfish (*Centrolophus niger*), bluenose (*Hyperoglyphe antarctica*), and later expanded to orange roughy (*Hoplostethus atlanticus*) and oreos (Oreosomatidae) throughout ridge systems of the southern Indian Ocean including Walters Shoal and deeper areas such as Madagascar and Mozambique ridges (Collette & Parin, 1991; Romanov, 2003; Clark et al., 2007; Parin et al., 2008; Rogers et al., 2017). Tunas are subjected to fishing pressures at the Travin Bank, also known as the “Coco de Mer” (Indian Ocean), since its discovery in the late 1970s (Marsac et al., 2014). Several hypotheses have been proposed to explain the high densities of marine megafauna associated with seamounts. La Pérouse seamount may present favourable breeding habitats for humpback whales (Dulau et al., 2017). Seamounts may provide navigation aids in fish movements and tunas may gather around these features to enhance the encounter rate with other con-specifics (Fréon & Dagorn, 2000) or they may be attracted by aggregations of prey

(Holland & Grubbs, 2007; Morato et al., 2008). Organisms inhabiting the mesopelagic zone, the micronekton, represent an important forage fauna for top predators (Guinet et al., 1996; Cherel et al., 2010; Danckwerts et al., 2014; Jaquemet et al., 2014; Potier et al., 2004, 2007, 2014).

Micronekton can be divided into the broad taxonomic groups- crustaceans, cephalopods and mesopelagic fishes (Brodeur & Yamamura, 2005; De Forest & Drazen, 2009). They typically range in size from 2 to 20 cm. Gelatinous organisms are under-represented components of the mesopelagic community, with only few authors (Lehodey et al., 2010; Kloser et al., 2016) including these organisms in the micronekton group. Micronekton form dense sound-scattering layers since some of them reflect sound in the water, due to their swimbladders, hard shells and gas inclusions (Simmonds & MacLennan, 2005; Kloser et al., 2009). Different scatterers are expected to have different relative frequency responses (Benoit-Bird & Lawson, 2016). While organisms with gas-filled structures such as epi-mesopelagic fishes with gas-filled swimbladders and gelatinous organisms with pneumatophores dominate the 38 kHz frequency (Porteiro & Sutton, 2007; Kloser et al., 2002, 2009; 2016; Davison et al., 2015; Cascão et al., 2017; Proud et al., 2018), large crustaceans, small copepods, squids and non-gas bearing fishes are relatively weak scatterers at this frequency (Cascão et al., 2017; Proud et al., 2018). Euphausiid shrimps are better targets at 70 kHz (Furusawa et al., 1994; Simmonds & MacLennan, 2005). Smaller plankton are stronger targets at 120 kHz compared to the 38 kHz and is a commonly used feature for separating plankton and fish marks on echograms (Simmonds & MacLennan, 2005).

Some micronekton taxa undergo diel vertical migration (DVM) from deep to shallower layers (upper 200 m) at dusk and from shallow to deeper layers (below 400 m) at dawn (Lebourges-Dhaussy et al., 2000; Béhagle et al., 2014; Annasawmy et al., 2018). Other taxa were shown to exhibit delayed migration (Watanabe et al., 2002), reverse migration (Alverson, 1961; Gjosaeter, 1978, 1984; Marchal & Lebourges-Dhaussy, 1996; Lebourges-Dhaussy, 2000), mid-water migration or non-migration (Annasawmy et al., 2018). It is thought that the spatial/horizontal distribution of micronekton communities is also not uniform across the Atlantic (Judkins & Haedrich, 2018) and SWIO (Annasawmy et al., 2018). Various physical processes such as mesoscale eddies, proximity to continental shelves and landmasses, and seamounts may influence the distribution of micronekton. Seamounts, by introducing irregularities into the pelagic environment, such as a hard substrate, disrupted current flows, increased primary productivity, entrapment of plankton, and presence of benthic predators, are

thought to influence the abundance, biomass, diversity and taxonomic composition of micronekton (Genin 2004; Wilson & Boehlert, 2004; De Forest & Drazen, 2009).

Although seamounts in other ocean basins are hypothesized to have a general influence on mesopelagic communities (De Forest & Drazen, 2009; Tracey et al., 2012), little is known about the micronekton dynamics at La Pérouse and MAD-Ridge seamounts, two shallow topographic features of the SWIO. La Pérouse is located 90 nautical miles (nmi) to the North West of Réunion Island (Fig. 4.1a), on the outskirts of the oligotrophic ISSG province (Longhurst, 2007). The summit depth is ~60 m below the sea surface and is 10 km long with narrow and steep flanks. MAD-Ridge seamount (thus termed in this study) is located along the Madagascar Ridge, 130 nmi to the south of Madagascar (Fig. 4.1b). The summit depth is ~240 m below the surface and is 33 km long (north to south) and 22 km wide (east to west). MAD-Ridge is located within an "eddy-corridor" along the Fort Dauphin upwelling area and is frequently crossed by mesoscale eddies spinning off the South East Madagascar Current (Pollard & Read, 2015; Vianello et al., 2020). These eddies may become trapped over the seamount and have an influence on the assemblages and DVM patterns of micronekton communities.

The main objectives of this study are to investigate (1) the prevailing environmental conditions at La Pérouse and MAD-Ridge seamounts using satellite data, (2) the vertical and horizontal distributions of the scattering layers at MAD-Ridge using acoustic data, (3) the micronekton assemblages at La Pérouse and MAD-Ridge using trawl data, and (4) whether La Pérouse and MAD-Ridge summits aggregate higher biomasses/densities of micronekton compared to the immediate vicinity of the seamounts, using acoustic and trawl data.

4.2 Methods

4.2.1 Study area and scientific cruises

La Pérouse cruise (DOI: 10.17600/16004500) was carried at latitude 19°43'S and longitude 54°10'E on board the RV *Antea* from the 15th to the 30th of September 2016, departing from/returning to Réunion Island (Fig. 4.1a). MAD-Ridge cruise (DOI: 10.17600/16004800 and 10.17600/16004900) was divided into two legs: Leg 1 from Réunion Island to Fort Dauphin (Madagascar) from 8 to 24 November 2016, and Leg 2 from Fort Dauphin (Madagascar) to Durban (South Africa) from 26 November to 14 December 2016. MAD-Ridge

seamount (latitude 27°28.38'S and longitude 46°15.67'E), was sampled for acoustics and trawling during Leg 2 of this cruise on board the RV *Antea* (Fig. 4.1b).

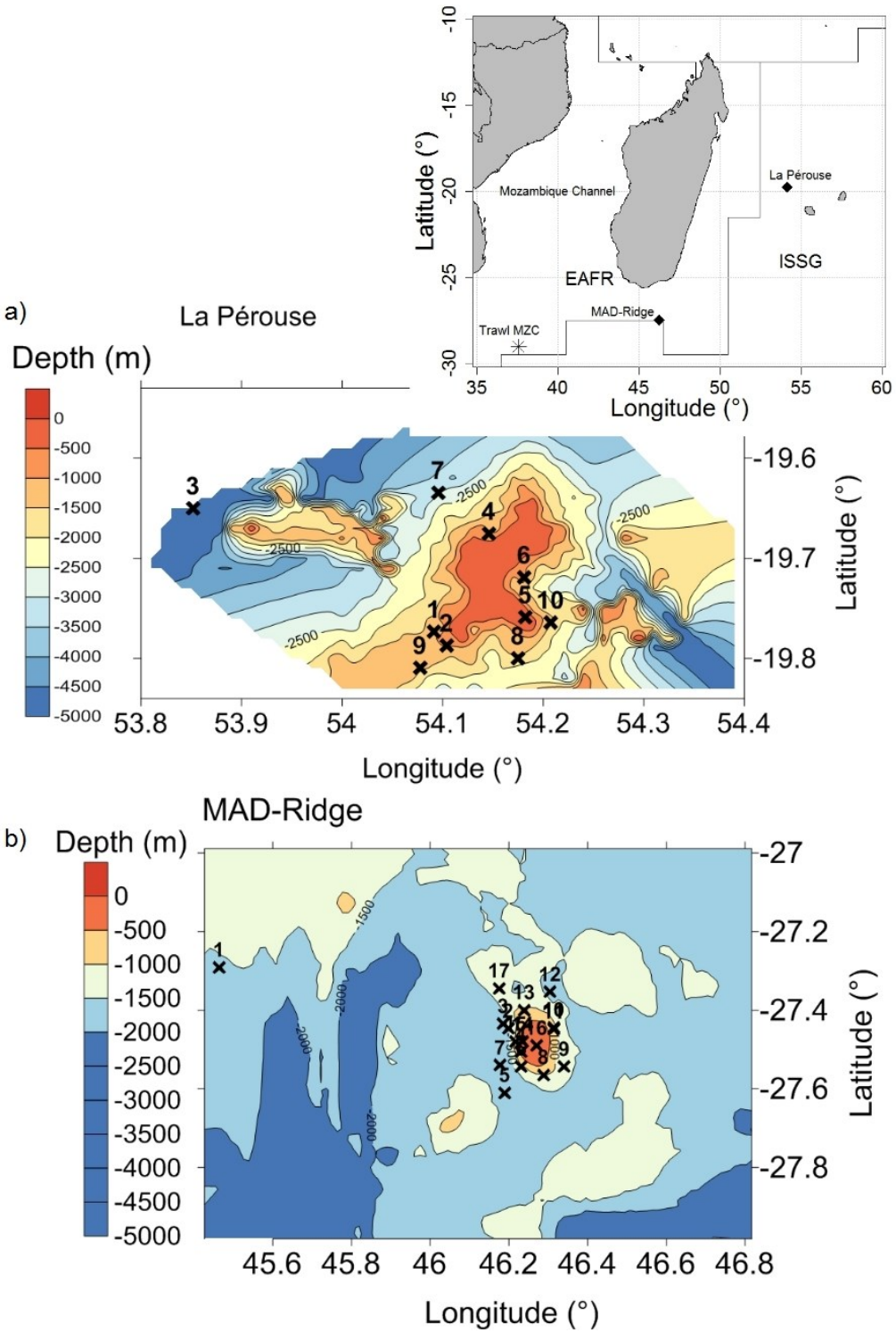

Figure 4.1 Map of the (a) La Pérouse trawl stations numbered 1 to 10, (b) MAD-Ridge trawl stations numbered 1 to 17 plotted on the bathymetry (m). The colour bar indicates depth below the sea surface (m). ISSG and EAFR refer to Longhurst's (1998) biogeochemical provinces. "Trawl MZC" refers to Trawl #21 carried in the Mozambique Channel.

4.2.2 Satellite monitoring of La Pérouse and MAD-Ridge seamounts

Delayed-time mean sea level anomalies (MSLAs) at a daily and 1/4° resolution, produced and distributed by the Copernicus Marine Environment Monitoring Service project (CMEMS) and available at http://marine.copernicus.eu/, were used to describe the mesoscale eddy field at the time of La Pérouse and MAD-Ridge cruises. Sea surface chlorophyll (SSC) data, with a daily and 4.5 km resolution was downloaded from the MODIS sensor (http://oceancolor.gsfc.nasa.gov) and was used to calculate 5-day averages to obtain a proxy of surface oceanic primary production. Monthly mean chlorophyll *a* concentrations for the defined regions (La Pérouse: 18.5°-20°S/53°-55°E; MAD-Ridge: 27°-28°S/44°-48°E; Fig. 4.2c) were averaged from January to December 2016 to investigate the annual variability in chlorophyll *a* concentration/productivity.

4.2.3 Acoustic surveys

Acoustic surveys were carried out with a Simrad EK60 echosounder operating at four frequencies during both cruises: 38 kHz (750 m of acquired range), 70 kHz (500 m), 120 kHz (250 m) and 200 kHz (150 m). The transducers were calibrated prior to the cruises following the procedures recommended in Foote et al. (1987). The pulse duration was set at 0.512 ms and the transmitted power at 1000 W (38 kHz), 750 W (70 kHz), 200 W (120 kHz) and 90 W (200 kHz) during data acquisition periods. The water column was correctly sampled to a depth of 750 m during data acquisition for the 38 kHz frequency. La Pérouse acoustic data were intermittently recorded during transits and few mesopelagic trawl stations. The acoustic transects during MAD-Ridge transit periods were petal-shaped (Petals I-VII, see Fig. 4.3a), starting from the seamount summit either at sunset between 3:48 pm and 4:10 pm Universal Time (Petals I-II) or at night between 6:13 pm and 7:20 pm (Petals III-VII) until the next morning between 05:38 am and 06:29 am (see Fig. 4.3b-h).

Acoustic data were processed with the Matecho software (an open source IRD tool computed with MATLAB 7.11.0.184, Release 2010b- and based on the Ifremer's Movies3D software; Trenkel et al., 2009; Perrot et al., 2018). Acoustic data sampled during transit (~8-9 knots) and trawl stations (~2-3 knots) were processed and echo-integrated separately, with different parameters to account for the differing ship speed. Transient (multiple pings) and background noises, bottom echoes and attenuated signals were removed using the algorithms designed by De Robertis & Higginbottom (2007) and Ryan et al. (2015). The first 10 m below the sea surface was removed to account for the presence and over amplification of the signal due to surface bubbles. Echo-integrations of acoustic data were performed on 1-m layers at a threshold

of -80 dB to exclude scatterers not representative of the micronekton community (Béhagle et al., 2017). The echo-integration cell size was fixed at 0.1 nmi during transit periods and at 10 pings during trawl stations. The volume backscattering strength (Sv, dB re 1 m^{-1}, MacLennan et al., 2002) was calculated to obtain the relative acoustic densities of scatterers per unit volume. The water column was separated into three depth categories, based on epi-mesopelagic layers: surface/shallow (10-200 m), intermediate (200-400 m) and deep (400-750 m).

Red Green Blue (RGB) composite images were generated in MATLAB (version 2016), based on the 38, 70 and 120 kHz MAD-Ridge echo-integrated acoustic data. This acoustic visualisation technique is useful in determining the relative contribution of each frequency to the overall backscatter, in identifying the different scattering layers and dense micronekton aggregations. It is used to enhance and colour-code sample volumes with similar acoustic features. The 38, 70 and 120 kHz echo-integrated acoustic data were given in red, green and blue colour codes respectively on each RGB plot, with the dynamic of the Sv values for each frequency being converted in 256 levels of each colour. A linear transformation of the backscatter was applied for each frequency:

Colour index (fr) [0 to 255] = [255/ (High scale threshold – Low scale threshold)] x [Sv (fr) – Low scale threshold], whereby the high scale threshold is the maximum backscatter for hue visualisation, the low scale threshold is the minimum backscatter for hue visualisation and Sv (fr) is the backscatter value at frequency (fr) which can be the 38 kHz/70 kHz/120 kHz frequency.

In the resulting RGB composite, the “hue” gives the frequency with the highest backscatter. On an RGB composite image based on the 38, 70 and 120 kHz echo-integrated acoustic data and given in red, green and blue colour codes respectively, a dark red colour indicates a dominant but low 38 kHz backscatter, whereas a light red colour indicates a dominant and high 38 kHz backscatter. The same rule applies to the blue (120 kHz) and green (70 kHz) hues. A black dominating hue on the RGB plot indicates that all backscatter values are under the low scale threshold of -80 dB.

4.2.4 Net sampling

Ten epi-mesopelagic tows were performed at La Pérouse and 17 tows at MAD-Ridge (Fig. 4.1a and 5.1b). Trawl MZC (#21) was carried in the Mozambique Channel (Fig. 4.1) and will be used as reference for open-water trawls compared to trawls 1-17 carried at MAD-Ridge seamount. A 40m long International Young Gadoid Pelagic Trawl (IYGPT) was used, having

an 80 mm knotless nylon delta mesh netting at the front tapering and 5 mm at the codend and a mouth opening of ~96 m^2. The trawl was towed at a ship speed of 2-3 knots at the targeted depth for 60 min during La Pérouse cruise and 30 min during MAD-Ridge cruise. During both cruises, the sampling depth was that of the sound scattering layer in that ship position and at that time of day, with no rigid plan of sampling preselected depths. Trawl depth was monitored with a Scanmar depth sensor during both cruises. The total volume of water filtered by the net tows was calculated by multiplying the distance travelled during the tows by the area of the trawl mouth opening to account for the differing sampling durations during the cruises. The total volume of water filtered during La Pérouse ranged from 379 408 m^3 to 871 181 m^3, and from 154 086 m^3 to 312 321 m^3 during MAD-Ridge. Trawl stations were further classified into the categories- summit, flank and vicinity, according to whether they occurred on the summit plateaus of the seamounts, on the slopes (carried out within 2 km from the baseline), or within the vicinity of the seamounts (i.e. any trawl not carried out on the summit and flanks) (as in Marsac et al., 2020).

The mesopelagic organisms collected during both cruises were sorted on board, divided into four broad categories: gelatinous organisms, crustaceans, cephalopods and fishes. The wet mass (WM) in grams was recorded for each category. Total length of selected gelatinous organisms, abdomen and carapace length of selected crustaceans, dorsal mantle length of selected cephalopods and standard length of selected fishes were measured. The micronekton components were counted and identified to the lowest possible taxon on board and also onshore from frozen samples preserved at -20°C. The total micronekton abundance estimates were calculated by dividing the total number of individuals per trawl by the volume of water filtered and multiplying by the average thickness of the day/night backscattering layer (100 m) and expressed as abundance within the backscattering layer (ind. m^{-2}) (as in Kwong et al., 2018). Similarly, the total biomass of organisms collected per trawl (g WM m^{-2}) was calculated by dividing the total wet mass (WM g) of micronekton broad categories per trawl by the volume of water filtered and multiplying by the average thickness of the day/night backscattering layer (100 m). The habitat ranges of available micronekton taxa were obtained from literature (Clarke & Lu, 1975; Pearcy et al., 1977; Smith & Heemstra, 1986; van der Spoel & Bleeker, 1991; Brodeur & Yamamura, 2005; Davison et al., 2015; Romero-Romero et al., 2019). Organisms were classified as being epipelagic (<200 m), mesopelagic (from 200 to 1000 m), bathypelagic (below 1000 m to ~100 m from the seafloor) and benthopelagic (living near the bottom) according to definitions of the vertical zonation of the pelagic ocean from Del Giorgio

& Duarte (2002) and Sutton (2013). Detailed fish species size distributions and compositions from both La Pérouse and MAD-Ridge cruises are described in Cherel et al. (2020).

4.2.5 Data visualisation and statistical analyses

La Pérouse and MAD-Ridge seamount bathymetry data were acquired with the 12 kHz frequency of a Simrad EA 500 echosounder. The bathymetry data were interpolated on a regular grid using the software Surfer version 10.3.705. Wilcoxon rank sum tests were performed to investigate the differences in mesopelagic trawl abundance and biomass estimates between La Pérouse and MAD-Ridge, and the mean acoustic densities over the summit and vicinity of MAD-Ridge.

Micronekton species richness was calculated using R (3.3.1) vegan package (version 2.5-1, Oksanen et al., 2018). The PRIMER v6 software was used to perform multivariate analyses according to Clarke & Warwick (2001) on La Pérouse and MAD-Ridge micronekton abundance datasets to test for the effects of depth (shallow, deep or intermediate), trawl location (vicinity, flank or summit) and time of day (day or night) on micronekton abundance and to identify the shallow-dwelling/deep-dwelling and seamount-associated/resident fauna. The fourth root transformation was used on species abundance data to down-weight strongly abundant species, thus allowing rare species to exert some influence on the similarity calculation (Clarke & Warwick, 2001). Resemblance matrices were created from the Bray-Curtis measure of similarity and were used to run the SIMPROF (similarity profile) permutation testing to identify statistically significant cluster of samples. Non-metric dimensional scaling (MDS) were used to produce 2-dimensional ordination of samples according to the selected grouping variables Depth category, Trawl location and Time of day. Bubble plots were overlaid on the MDS ordination diagrams to represent the relative abundance of the selected species per trawl station (plotted at the bubble centres). The larger the bubble, the greater the mean number of individuals were captured at that site. One-way ANOSIM (analysis of similarities) was calculated to test for significant differences in the micronekton community composition according to the factors Depth, Trawl location and Time of Day. The SIMPER (similarity percentages) analysis was carried out to identify the taxa contributing most to the similarities/dissimilarities within each resultant cluster group.

4.3 Results

4.3.1 Prevailing environmental conditions at La Pérouse and MAD-Ridge seamounts

During La Pérouse cruise in September 2016, the seamount was under the influence of a weak cyclonic eddy with a MSLA of ~-10 cm (Fig. 4.2a). The SLA ranged from -26 to 10 cm throughout the cruise. MAD-Ridge was under the influence of an eddy dipole with the anticyclonic feature being trapped on the seamount during the cruise in November 2016 (Fig. 4.2b). The MSLA during MAD-Ridge Leg 1 was ~10 cm at the eddy periphery and ~40 cm within the core of the anticyclone. The annual primary productivity, derived from satellite observations, followed the same pattern in both regions of La Pérouse and MAD-Ridge seamounts, with maximum values reached in July, as a result of an intense mixing caused by the austral winter trade winds, and minimum values observed during austral summer (January-March and November-December) (Fig. 4.2c). Both La Pérouse and MAD-Ridge cruises took place during a decreasing trend of oceanic productivity. Although, the annual mean chlorophyll *a* concentration depicted the same cycle at both seamounts, chlorophyll *a* concentrations at MAD-Ridge were twice higher than at La Pérouse all year round.

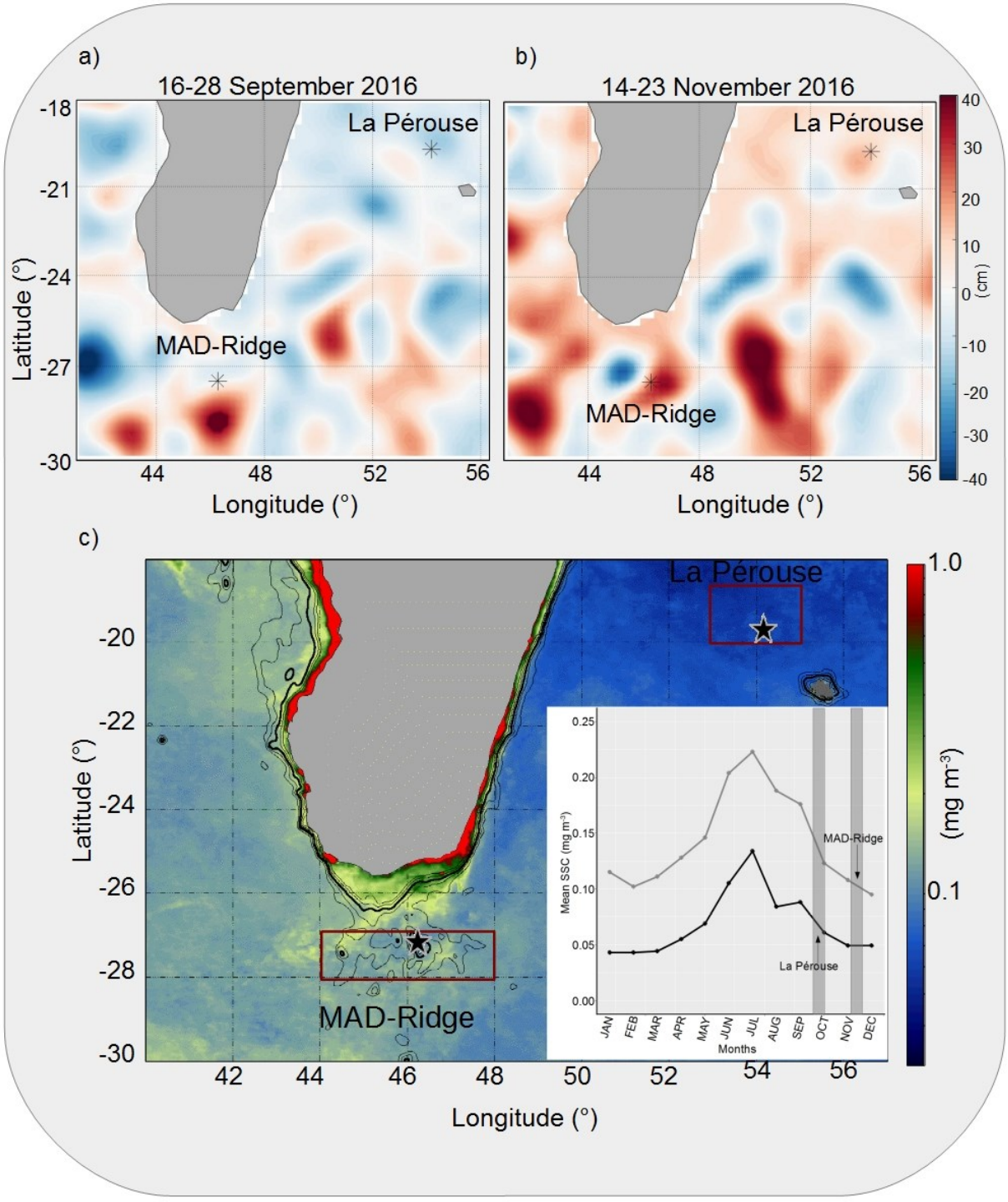

Figure 4.2 Averaged sea level anomaly (MSLA) map, with La Pérouse and MAD-Ridge seamounts shown as black star symbols, and dated (a) 16-28 September 2016, (b) 14-23 November 2016. The colour bar indicates the SLA in cm, with positive SLA (red) and negative SLA (blue). (c) Averaged satellite image of surface chlorophyll a distribution from 18/09/2016 to 07/12/2016. Monthly mean surface chlorophyll a values for the region defined by the red squares are depicted from January to December 2016. The dates of La Pérouse and MAD-Ridge cruises are marked by grey bars on the monthly mean plot. The colour bar indicates the surface chlorophyll a concentration in mg m^{-3}.

4.3.2 Vertical and horizontal distributions of biological scatterers at MAD-Ridge

The highest mean acoustic densities (Sv) of the 38 kHz frequency were observed at night in the surface layer (10-200 m) across all petals (I-VII) at MAD-Ridge (Fig. 4.3a-h). The mean acoustic densities in the surface layer showed a decreasing trend at sunrise and during daytime (Petals I to VII, Fig. 4.3b-h) while gradually increasing in the deep layer across petals II to VI (Fig. 4.3c-g). The intermediate layer showed the lowest acoustic densities compared to the surface and deep layers, although a peak can be observed during sunrise when organisms vertically migrated towards deeper layers. A peak in daytime acoustic densities in the deep layer can be observed across petals II and IV (Fig. 4.3c and 4.3e), that can be attributed to an intensification of the backscatter over the seamount flanks (Fig. 4.4a, b and c).

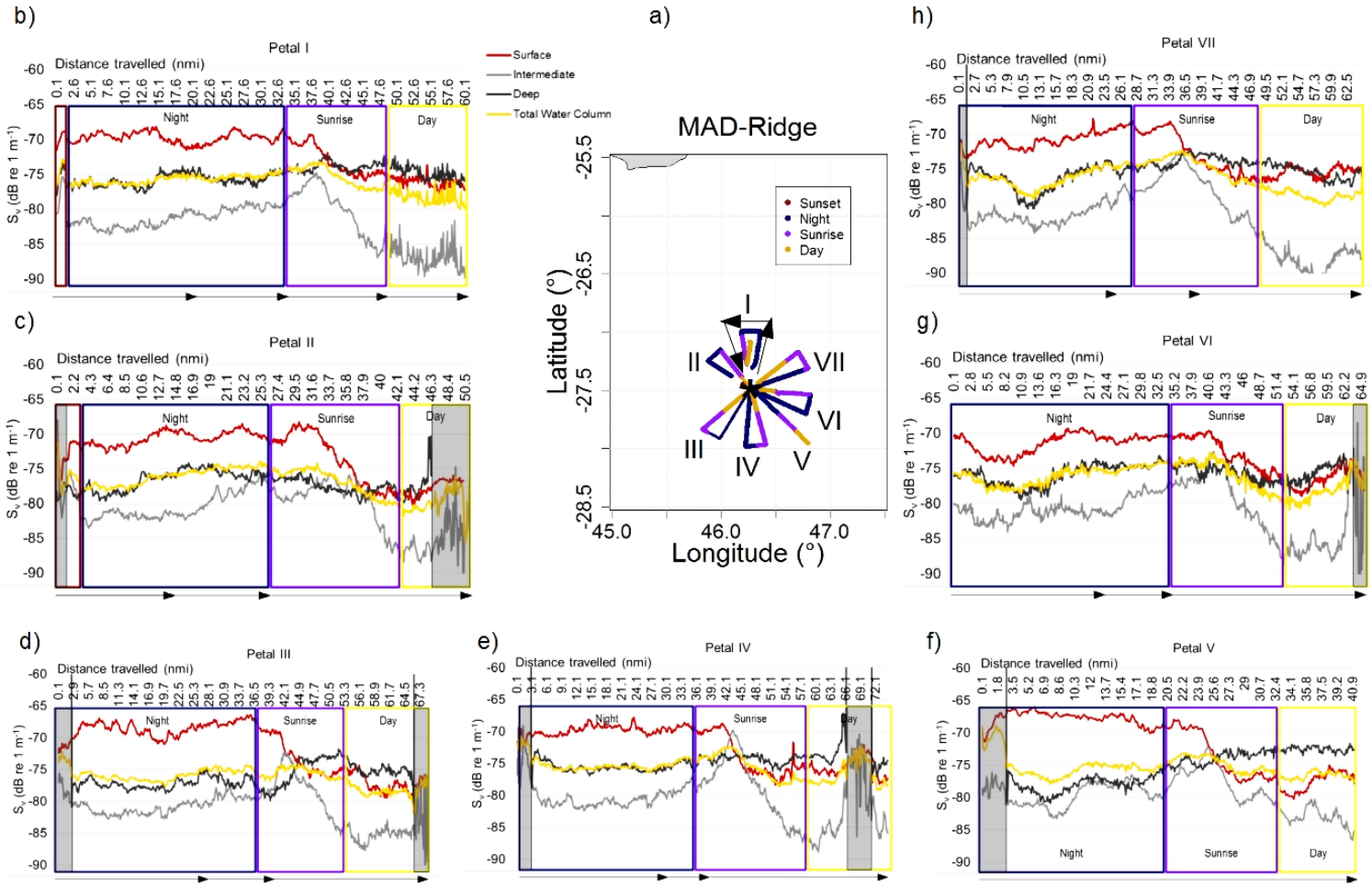

Figure 4.3(a) Petal-shaped acoustic transects I to VII carried at MAD-Ridge, starting at sunset/night (red/blue) at the summit (star symbol) and ending during the day (yellow) at the summit. Arrows give an example of change in ship direction. The Madagascar land mass is shown in grey. (b-h) Biomass density (Sv, dB re 1 m^{-1}) estimates for the 38 kHz frequency in the surface (10-200 m, red), intermediate (200-400 m, grey), deep layers (400-750 m, black), and total water column (yellow) for Petals I-VII. The time of day is denoted by coloured rectangles and black arrowheads denote the change in ship direction. The position of MAD-Ridge seamount is denoted by grey rectangles on plots c-h.

Echograms of the 38 kHz frequency showed organisms migrating from below 400 m (deep) to above 200 m (surface) at dusk across Petal II (Fig. 4.4a). Biological scatterers were also shown to perform a series of DVM events from the intermediate/surface layers to deeper layers before sunrise and during sunrise, reaching the DSL before daytime (Fig. 4.4a, b and c). Across petals IV, an increase in the mean acoustic densities in the daytime DSL can be observed (Fig. 4.3e), indicating a likely downward migratory trend of the biological scatterers to deeper layers and preferential association of some micronekton taxa with the flanks of MAD-Ridge seamount (Fig. 4.4c). A dense SSL between ~10-200 m and a DSL between ~400-700 m were observed throughout the night during MAD-Ridge cruise (Fig. 4.4a, b and c). After vertical migration of scatterers to deeper depths at dawn, the day SSL became less dense (compared to the night SSL) and persisted in the top 100 m of the water column. Biological scatterers were associated with MAD-Ridge seamount summit and flanks both during night-time and daytime.

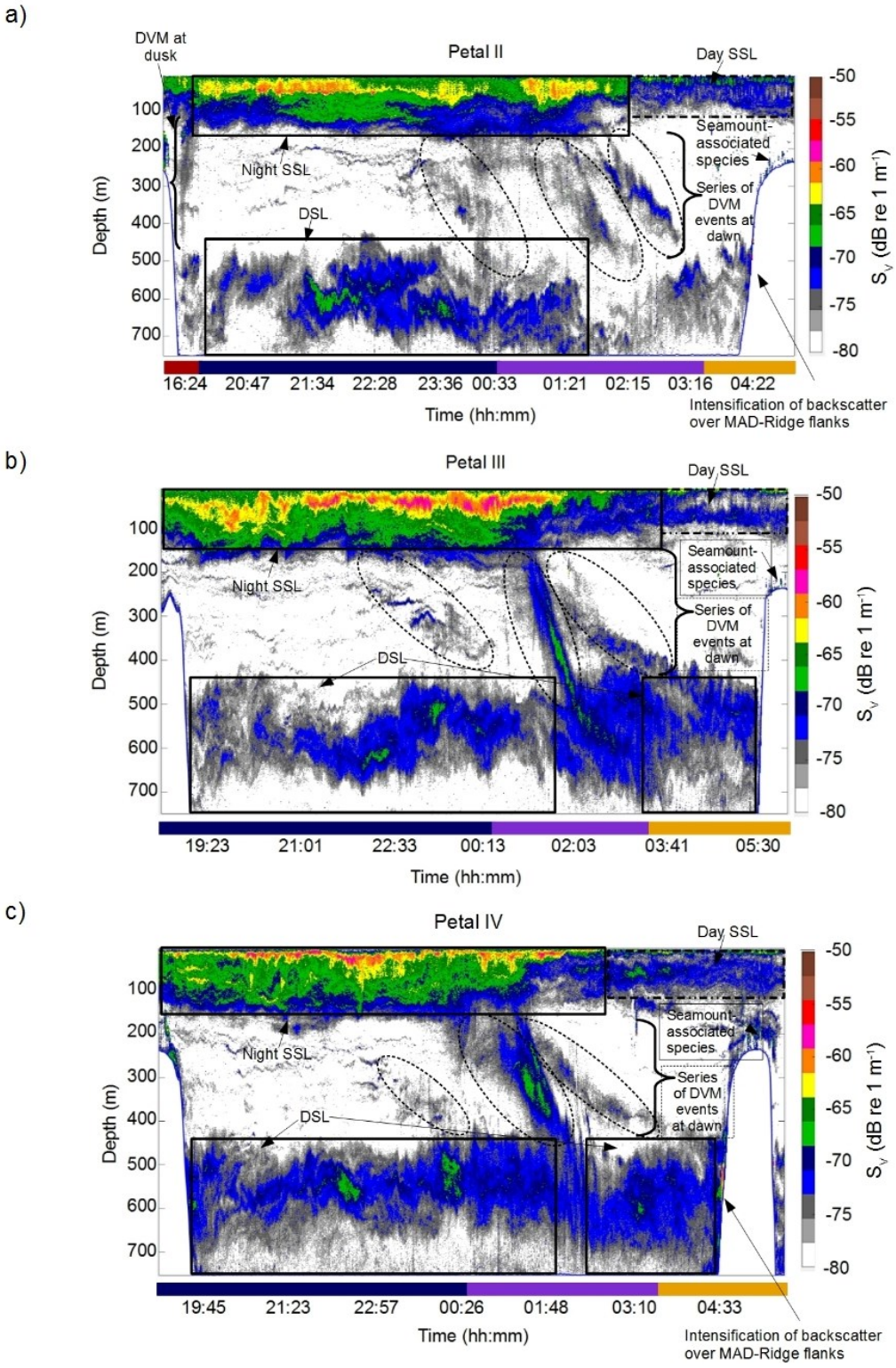

Figure 4.4 Echograms of the 38 kHz frequency during (a) Petal II at sunset, night, sunrise and daytime denoted by red, blue, violet and gold coloured rectangles respectively, (b) Petal III, and (c) Petal IV. Diel vertical migraton (DVM) at dusk is denoted for Petal II. Circular dotted lines denote the series of DVM events from the intermediate layer and from the SSL. The night SSL and day SSL are denoted by solid and dotted rectangles respectively. The DSL is denoted by solid rectangles. Backscatter from seamount-associated species are also noted. The colour bar indicates Sv in dB re 1 m^{-1}.

To investigate the influence of MAD-Ridge summit, the mean night-time acoustic densities of the 38 kHz frequency between 10 and 250 m over the summit and at the seamount vicinity (within 14 nmi from the summit) were investigated along petals III-VII (Fig. 4.5a, b and c). Petals I and II were discarded since these transects were incomplete, not being carried from the summit. The mean acoustic densities in the top 250 m between the summit and vicinity of MAD-Ridge pinnacle were not statistically different ($W=43610$, $p > 0.05$). The highest acoustic responses to the 38 kHz frequency in the surface layer (10-250 m) at night can be observed across Petals IV and V, while Petal VI exhibited the lowest acoustic responses (Fig. 4.5b). RGB composites of the 38, 70 and 120 kHz frequencies across petals III-VII showed distinct scattering layers in the top 150 m of the water column, with some scatterers being strong targets at the 38 kHz frequency and others at the 70 and 120 kHz frequencies (Fig. 4.5c). The peak in acoustic densities over the summit across petal IV (Fig. 4.5b) may be attributed to the relatively high Sv between ~150 and 250 m (i.e. below the night SSL). Patches of relatively high Sv (seen as "white patches") can be observed on the seamount summit across petals IV, V and VII (Fig. 4.5c).

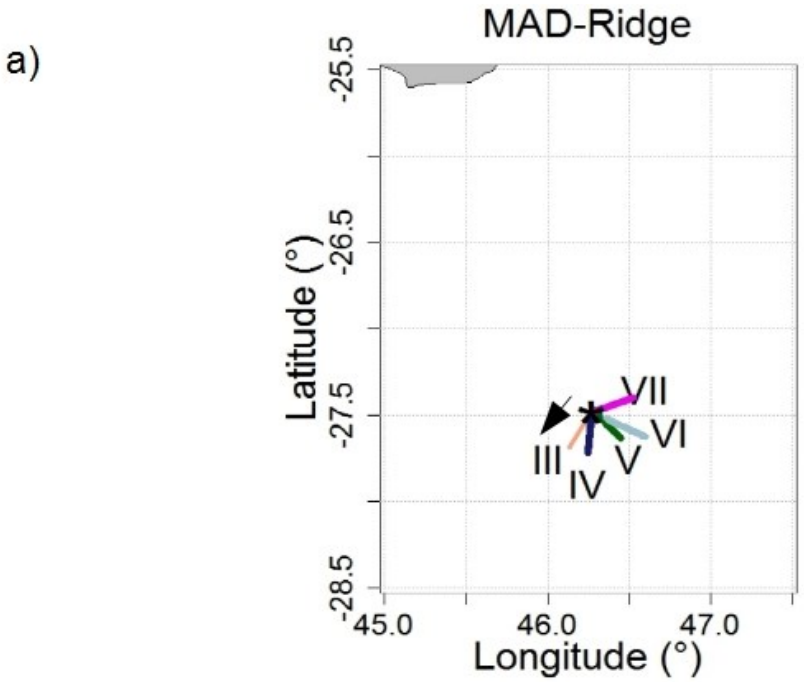

Figure 4.5(a) Night-time acoustic transects III to VII from the MAD-Ridge seamount summit (star symbol) to 14 nmi from the summit. The Madagascar land mass is shown in grey. Arrow indicates ship direction.

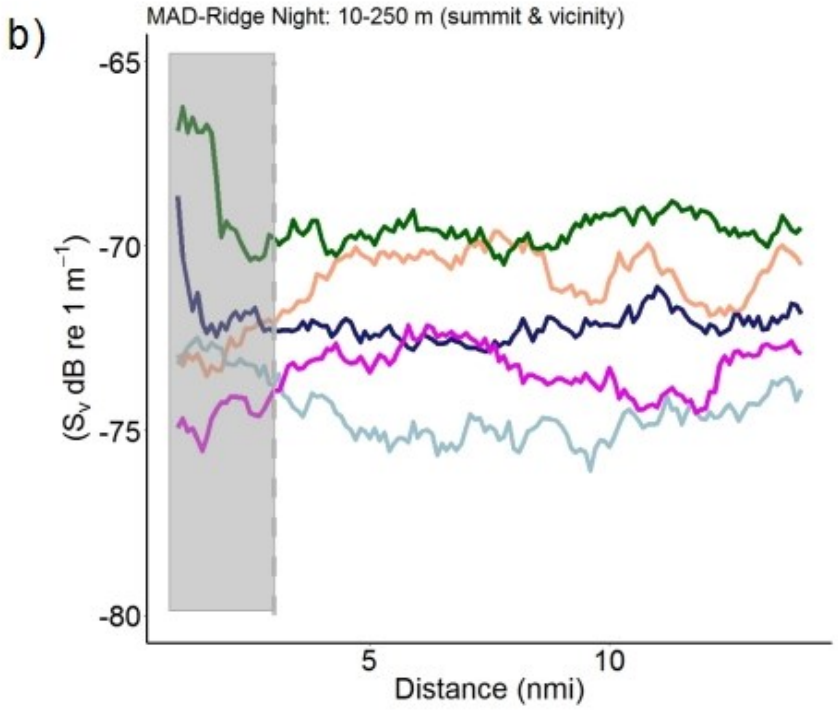

Figure 4.5(b) Acoustic density (Sv, dB re 1 m^{-1}) estimates for the 38 kHz frequency in the surface layer (10-250 m) at night, from the summit (grey bar) to 14 nmi away from the seamount (vicinity), for Petals III to VII.

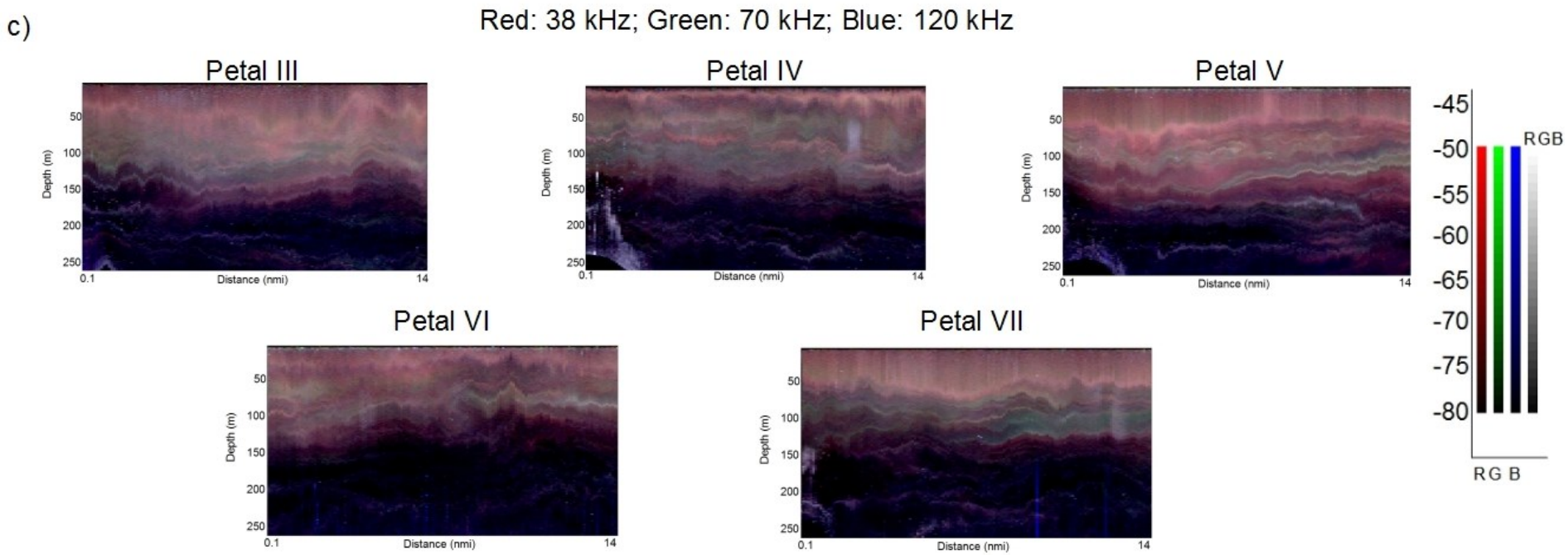

Figure 4.5(c) RGB composites of Sv values (dB re 1 m^{-1}) from 10-250 m for the selected acoustic transects III to VII, with the 38, 70 and 120 kHz frequencies given red, green and blue colour codes respectively.

4.3.3 Taxonomic composition of trawl catches

At La Pérouse seamount, 144 taxa from 10 trawls representing 7, 13, 17 and 107 taxonomic groups of gelatinous organisms, crustaceans, cephalopods and epi-mesopelagic fishes, respectively, were collected. At MAD-Ridge, 146 taxa from 17 trawls, representing 5, 10, 17 and 114 taxonomic groups of gelatinous organisms, crustaceans, cephalopods and epi-mesopelagic fishes, respectively, were collected. Six individuals of the benthopelagic fish species, *Cookeolus japonicus*, were further collected at MAD-Ridge seamount summit (Fig. 4.8d, 4.9b and 4.10c). MAD-Ridge and La Pérouse trawls caught 3, 9, 14 and 66 identical taxa of gelatinous organisms (jellyfish, salps and pyrosomes), crustaceans, cephalopods and epi-mesopelagic fishes respectively.

Micronekton abundance and biomass estimates were greater at MAD-Ridge compared to La Pérouse (Fig. 4.6a), however, values were not significantly different (Abundance:, W= 144.5, $p > 0.05$; Biomass: W=115, $p > 0.05$). Mean micronekton abundance and biomass estimates were lower over La Pérouse summit (0.004 ind m^{-2} and 0.006 g WM m^{-2}) compared to the vicinity (0.12 ± 0.10 ind m^{-2} and 0.24 ± 0.20 g WM m^{-2}). At MAD-Ridge, the summit also recorded lower abundance and biomass estimates (0.03 ind m^{-2} and 0.11 g WM m^{-2}) compared to the vicinity (0.33 ± 0.43 ind m^{-2} and 0.46 ± 0.22 g WM m^{-2}). The species richness was higher at MAD-Ridge (maximum species richness of 155) compared to La Pérouse (138), with the probability of encountering new or rare species with increasing fishing effort being higher at MAD-Ridge (Fig. 4.6b). The length distributions of organisms captured during both La Pérouse and MAD-Ridge were heavily skewed towards smaller sizes. Most of the mesopelagic organisms captured were less than 100 mm (Fig. 4.6c), except for a few larger nektonic squid such as Cranchiidae (339 mm- mantle length) and fish Nemichthyidae (614mm- standard length) during La Pérouse, and one salp (207 mm- total length), squid *Ommastrephes bartramii* (490 mm- mantle length) and fish Nemichthyidae (446 mm) during MAD-Ridge.

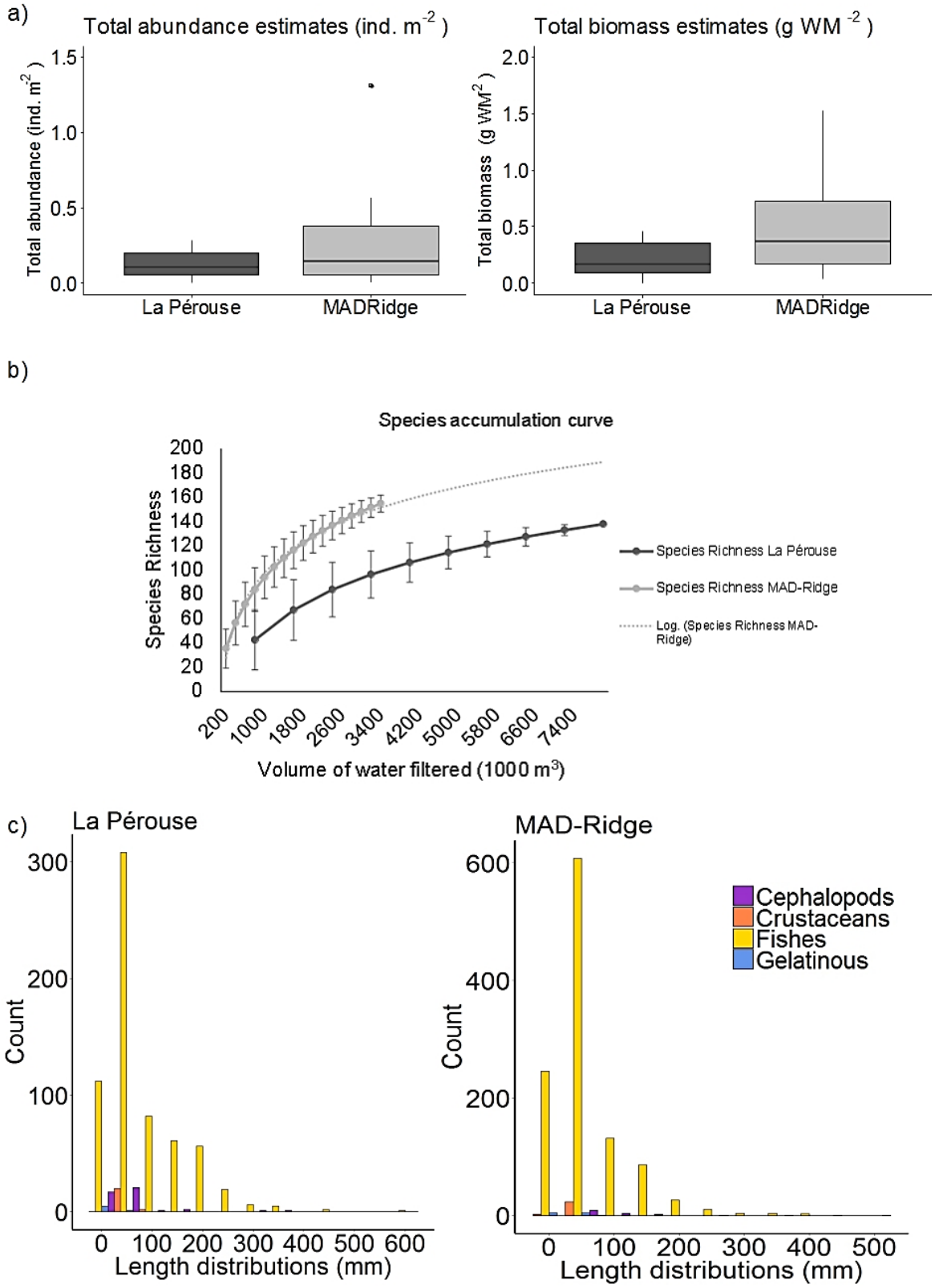

Figure 4.6 At La Pérouse and MAD-Ridge seamounts, (a) boxplot of total abundance and biomass estimates (in ind m^{-2} and g WM^{-2} respectively), (b) species richness with increasing sampling effort (volume of water filtered in 1000 m^3), (c) length distributions of selected gelatinous plankton, crustaceans, cephalopods and epi-mesopelagic fishes sampled.

Multivariate analysis of the taxa collected at La Pérouse seamount indicated that the sampling depth and trawl location were significant factors influencing micronekton community composition (ANOSIM, sampling depth: R= 0.38, $p < 0.05$; trawl location: R= 0.28, $p < 0.05$). However, there were no significant effect of the time of day probably due to the low daytime fishing effort (ANOSIM, R= 0.846, $p > 0.05$). The assemblages from the deep (400-600 m) and shallow (0-110m) depth categories were the most dissimilar (SIMPER, average dissimilarity= 68.9%), while those from the intermediate and deep categories were the least dissimilar (SIMPER, average dissimilarity= 58.1%). The assemblages from the vicinity and summit (SIMPER, average dissimilarity= 79.8%) and the flank and summit (SIMPER, average dissimilarity= 78.0%) were the most dissimilar, whereas those from the vicinity and flank were the least dissimilar (SIMPER, average dissimilarity= 59.3%). A main cluster at 42% similarity helped differentiate the night shallow, intermediate and deep tows carried at the flank and vicinity from the day trawl performed at the summit of La Pérouse (Fig. 4.7a).

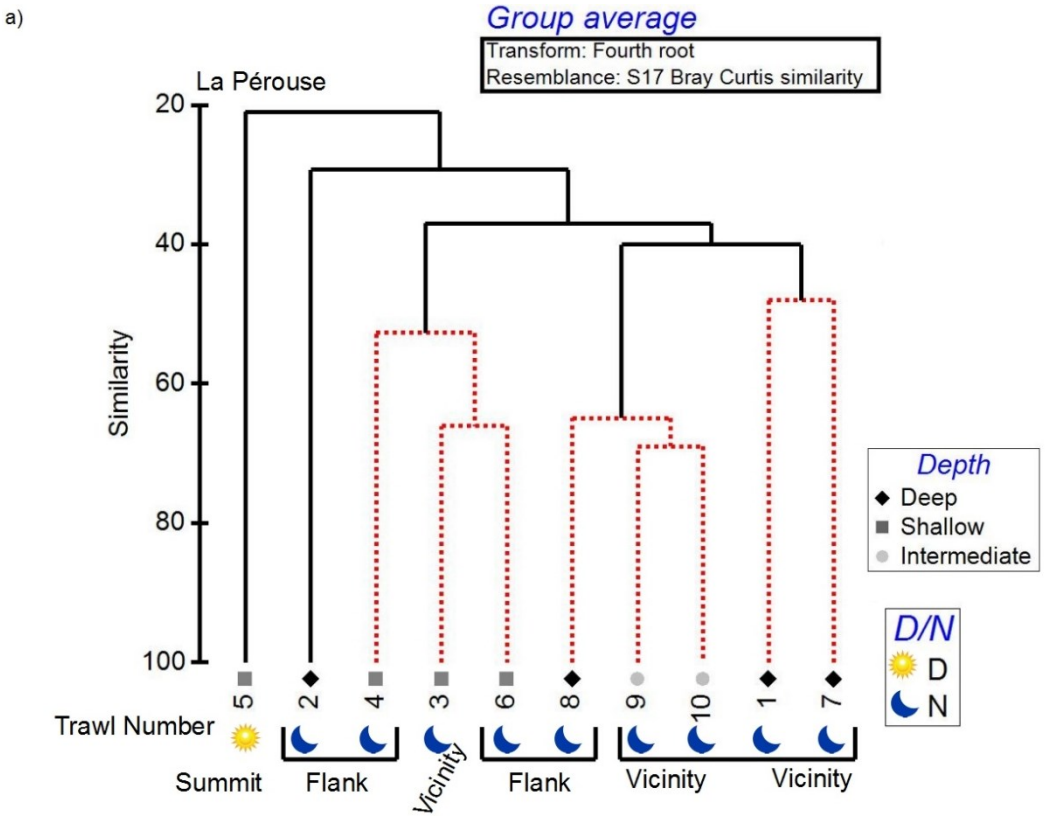

Figure 4.7(a) Similarity cluster dendrogram of species abundance at La Pérouse trawl stations 1 to 10. Brackets represent cluster groups at 42% (Day shallow summit, Night deep flank, night shallow vicinity and flank; night intermediate vicinity and Night deep vicinity).

The day shallow trawl over La Pérouse summit sampled a greater percentage abundance and biomass of gelatinous organisms, crustaceans and fishes (Fig. 4.7b). Fishes and gelatinous organisms were abundantly caught and in greater biomass compared to the other broad categories over the seamount's flanks in the deep layer at night. Gelatinous organisms were abundantly caught at all depth categories over the seamount summit, flanks and vicinity. Cephalopods were caught most abundantly and in greater biomass during the night shallow trawls compared to the night deep, intermediate and day shallow trawls (Fig. 4.7b and 4.9a).

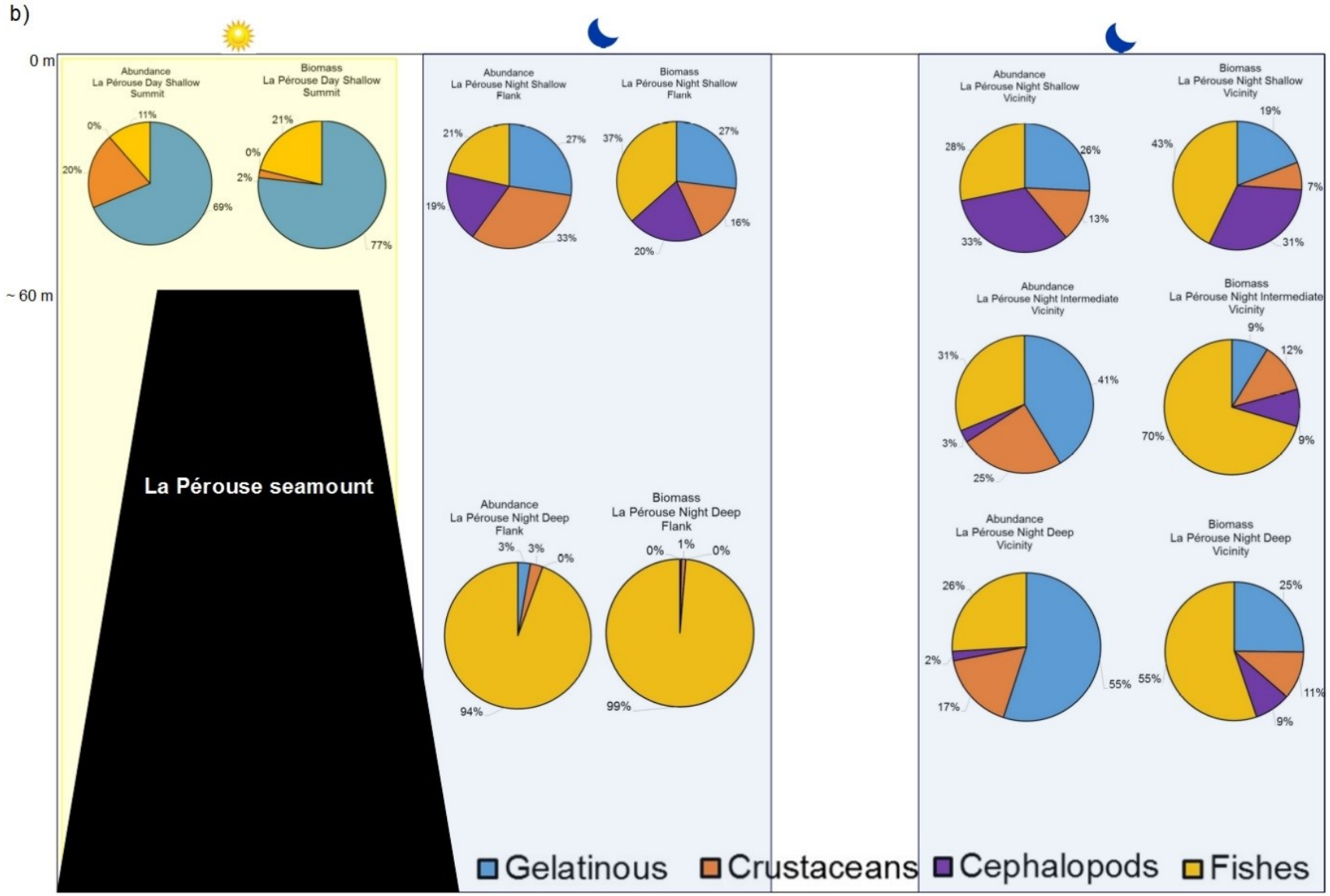

Figure 4.7(b) Schematic diagram of La Pérouse seamount. Pie charts represent the abundance and biomass of gelatinous organisms in blue, crustaceans in orange, cephalopods in violet and fishes in yellow, within the cluster groups.

Crustaceans were caught in all trawls at La Pérouse seamount (Fig. 4.7b) except the meso-bathypelagic crustacean *Pasiphaea* spp. and *Neognathophausia* that were caught in night deep and intermediate trawls only within the vicinity of the seamount as shown by bubble plot overlays of the MDS ordination (Fig. 4.7c). The sternoptychid *Argyropelecus aculeatus* and *Argyropelecus hemigymnus* were absent from the shallow trawls and were caught either in the intermediate and/or deep trawls at La Pérouse flanks and vicinity (Fig. 4.7c and 4.9a). The myctophid fish *Diaphus suborbitalis* was caught in high numbers, both in shallow and deep layers, on the flanks of La Pérouse seamount at night and were absent from tows conducted within the vicinity of the pinnacle (Fig. 4.7d). La Pérouse flanks also hosted four individuals of the sternoptychid *Argyripnus hulleyi* in the deep layer at night (Fig. 4.7d and 4.9a), which is the second record in literature of this species in the region (Cherel et al., 2020).

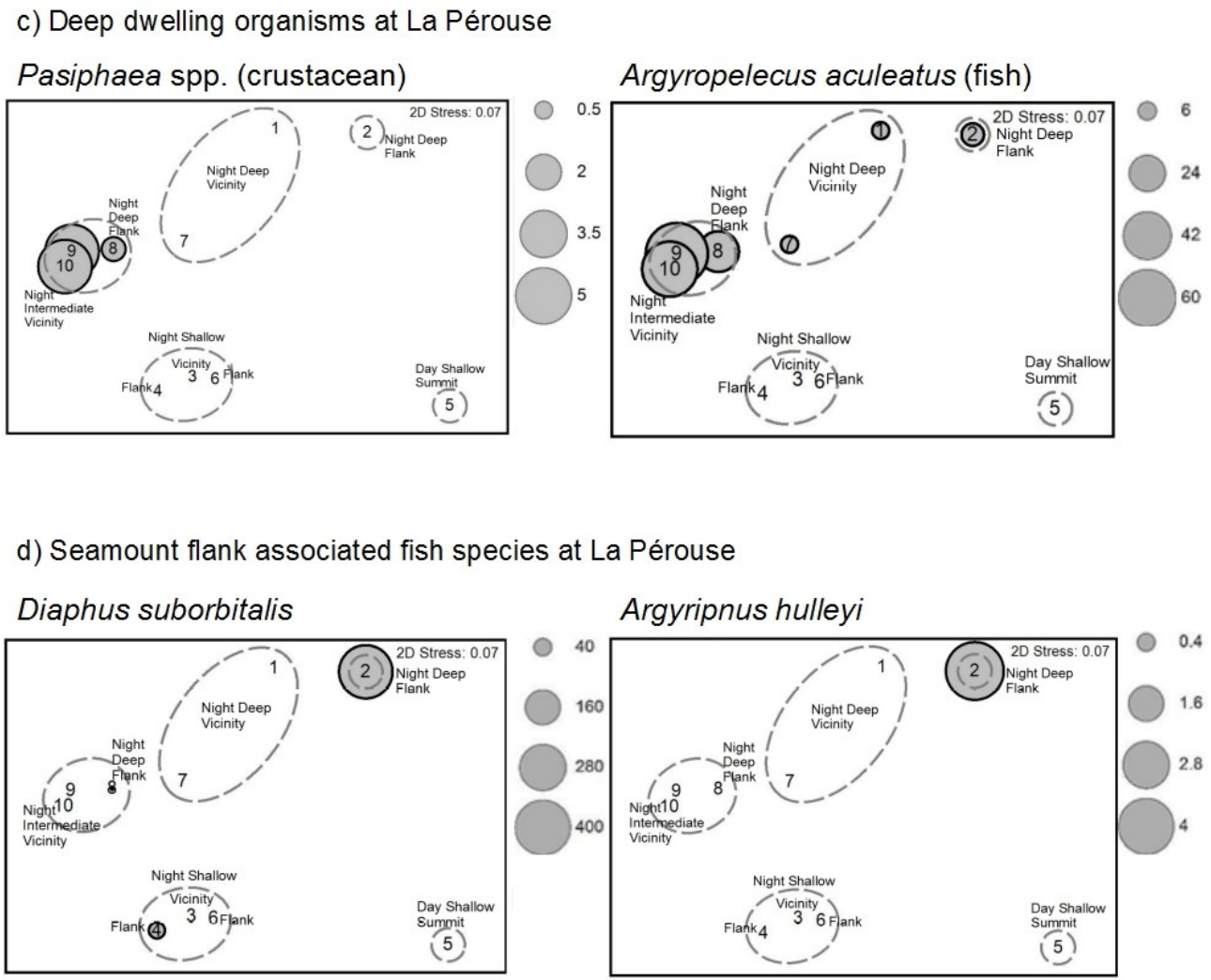

Figure 4.7 Bubble plot overlays of the MDS ordination representing the relative abundance of common (c) deep dwelling, (d) and seamount flank associated species. Trawl stations are numbered 1 to 10 on the bubble plots and dotted lines denote the 42% similarity clusters. The larger the bubble, the greater the number of individuals captured at that trawl station.

At MAD-Ridge, sampling depth, time of day and trawl location were significant factors influencing the micronekton community composition as shown by multivariate analyses of the micronekton taxa and species abundance data (Effect of sampling depth: ANOSIM, R= 0.35, $p < 0.05$; Effect of time of day: ANOSIM, R=0.37, $p < 0.05$; Effect of trawl location: ANOSIM, R=0.21, $p < 0.05$). A main cluster at 35% similarity confirmed a depth gradient in community composition in shallow and deep layers (Fig. 4.8a). Clusters at 30% similarity helped differentiate samples collected during night shallow tows at the seamount summit and flanks from all other tows carried out during the cruise. The assemblages from the deep (440-550 m) and shallow (0-210 m) depth categories were the most dissimilar (SIMPER, average dissimilarity= 69.9%; ANOSIM, R= 0.48, $p < 0.05$), whereas those from the intermediate and deep categories were the least dissimilar (SIMPER, average dissimilarity= 50.8%; ANOSIM, R=-0.33, R = -0.33, $p > 0.05$).

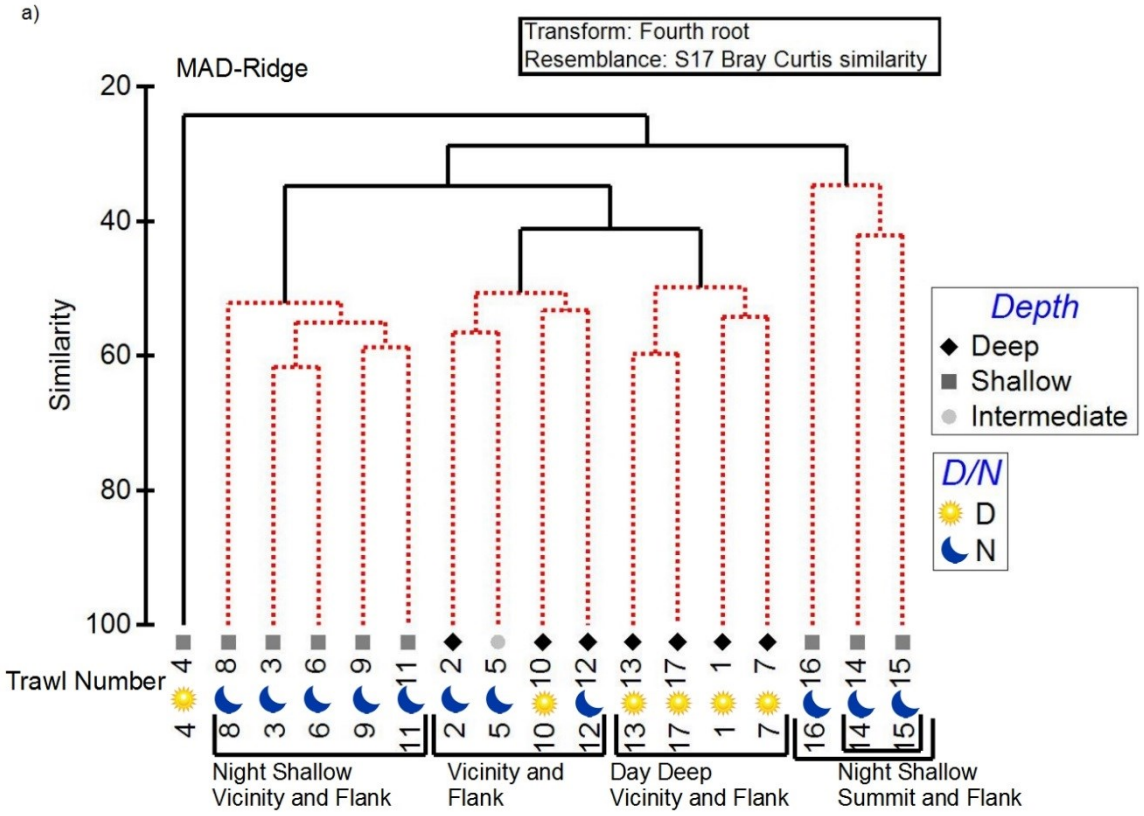

Figure 4.8(a) Similarity cluster dendrogram of species abundance at MAD-Ridge trawl stations 1 to 17. Brackets represent cluster groups at 35% (Night shallow, vicinity and flank; Day deep, vicinity and flank); and 30% similarities (Night shallow, summit and flank).

The majority of crustacean species were caught across all trawls (Fig. 4.8b), except *Pasiphaea* spp. caught in night deep trawls only (Fig. 4.9b). Cephalopods were caught most abundantly

and in greater biomasses in the shallow trawls compared to the intermediate and deep trawls (Fig. 4.8b and 4.9b). Gelatinous organisms and fishes were abundantly caught across all trawls in the shallow, intermediate and deep layers and at MAD-Ridge seamount summit, flanks and vicinity (Fig. 4.8b). Juveniles of the reef-associated epipelagic fish Acanthuridae was abundantly caught in night shallow trawls in the vicinity of MAD-Ridge seamount and not in the deep trawls (Fig. 4.8c and 4.9b). The vertical migrant *Ceratoscopelus warmingii* (Myctophidae) was abundantly caught in the shallow, intermediate and deep layers at the flanks and seamount vicinity (Fig. 4.8c and 4.9b). The fish *Cyclothone* sp. (Gonostomatidae) and *A. aculeatus* (Sternoptychidae) were absent from the shallow trawls during MAD-Ridge cruise (Fig. 4.8d and 4.9b). MAD-Ridge seamount attracted the mesopelagic fishes *D. suborbitalis*, *Neoscopelus macrolepidotus*, *Benthosema fibulatum* and *Diaphus knappi* (Fig. 4.8e). The summit also consisted of the apparently settled population of the benthopelagic *C. japonicus* as shown by bubble plot overlays of the MDS ordination (Fig. 4.8e).

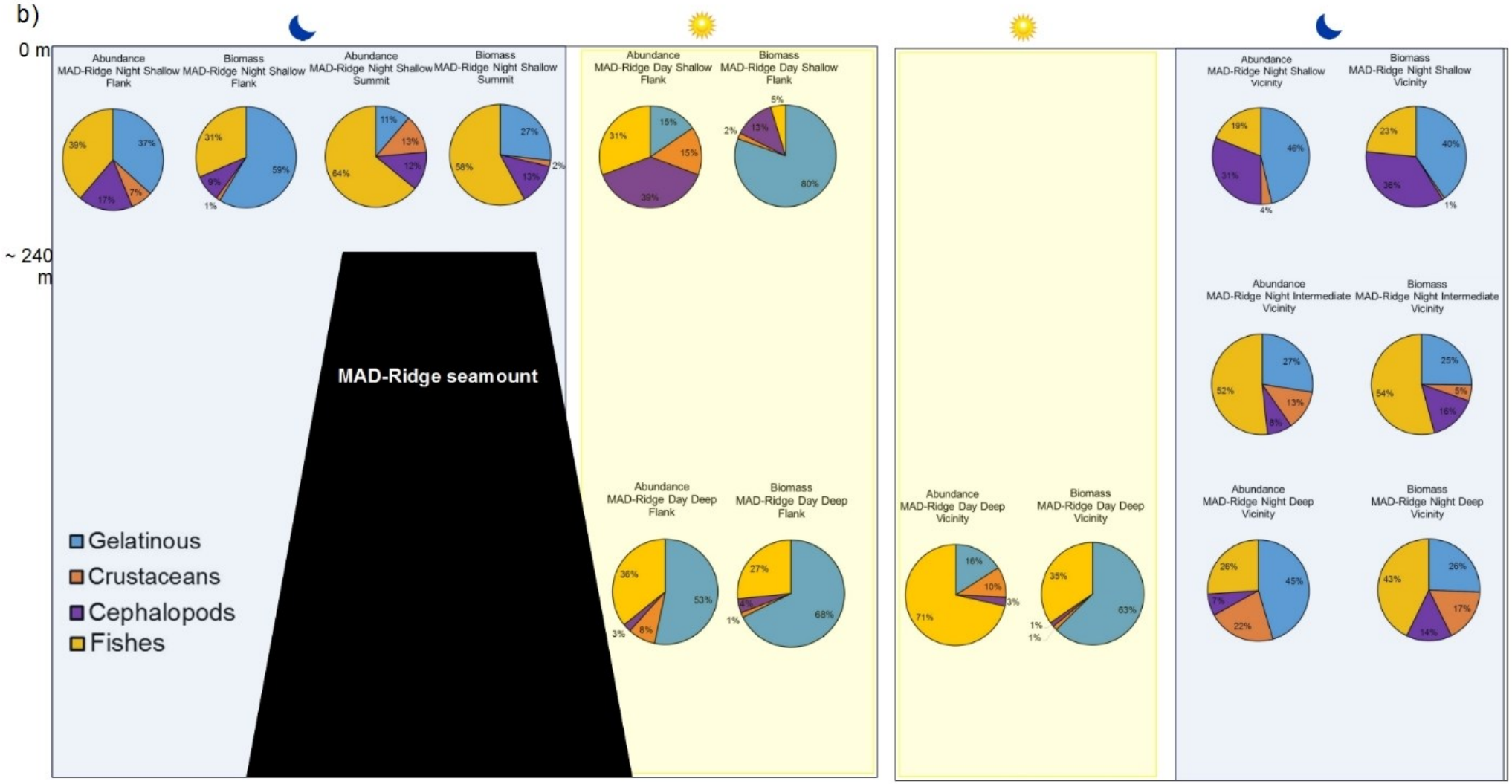

Figure 4.8(b) Schematic diagram of MAD-Ridge seamount. Pie charts represent the abundance and biomass of gelatinous organisms in blue, crustaceans in orange, cephalopods in violet and fishes in yellow, within the cluster groups.

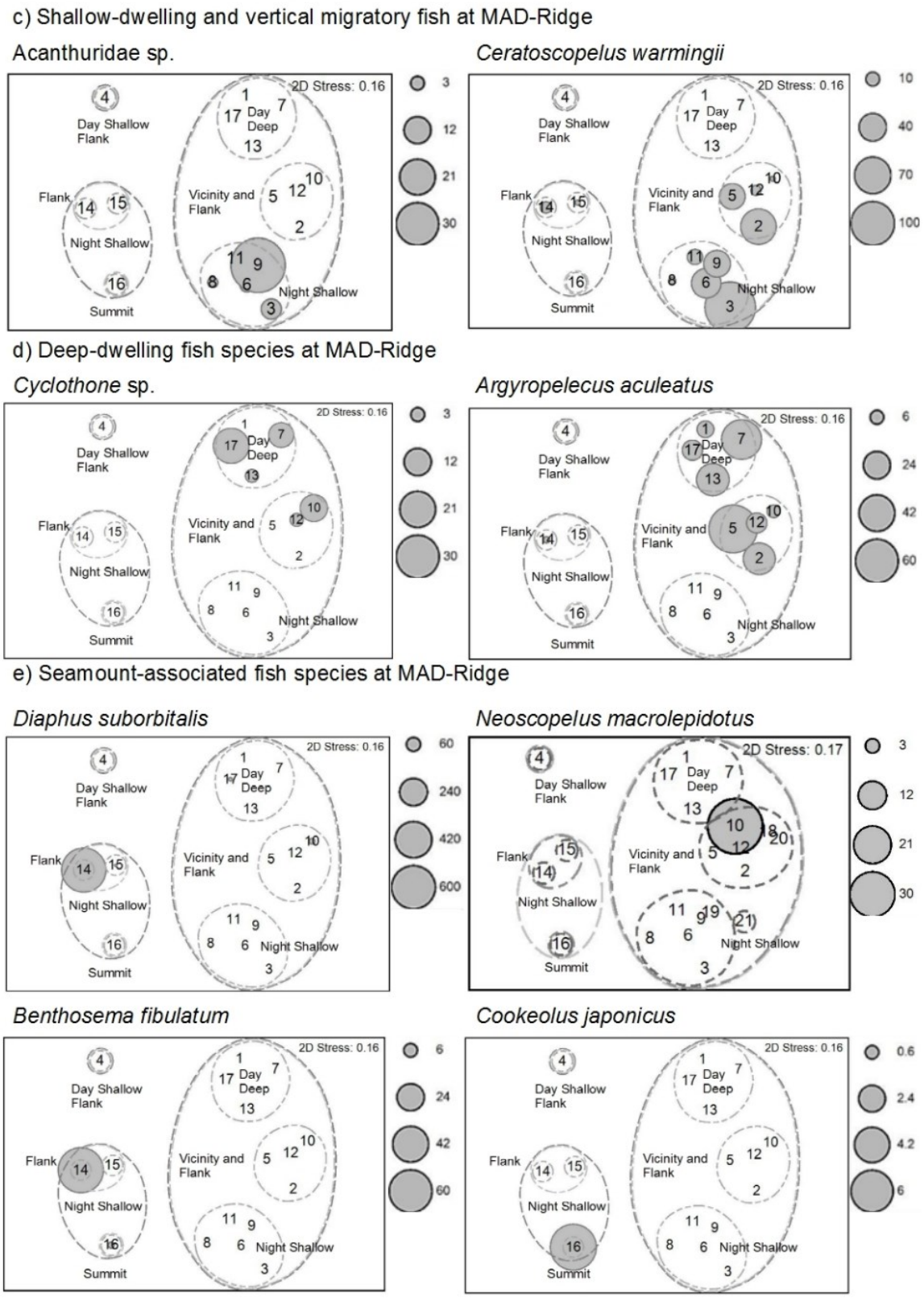

Figure 4.8 Bubble plot overlays of the MDS ordination representing the relative abundance of common (c) shallow-dwelling and vertical migratory fish species, (d) deep-dwelling, (e) and seamount summit and flank associated fish species. Trawl stations are numbered 1 to 17 on the bubble plots and dotted lines denote the 35% and 30% similarity clusters. The larger the bubble, the greater the number of individuals captured at that trawl station.

4.3.4 Micronekton community compositions and acoustic backscatter intensities

At La Pérouse seamount, the gelatinous organisms- salps and pyrosomes, unidentified shrimps, phyllosoma larvae, the squid *Abraliopsis* sp., leptocephali and the fish *C. warmingii* were caught across almost all trawls in the night SSL and DSL over the flanks and vicinity of the pinnacle (Fig. 4.9a). At MAD-Ridge, pyrosomes, salps, phyllosoma larvae, *Abraliopsis* sp. and the squid Enoploteuthidae were caught across almost all trawls in the day and night SSL, DSL and intermediate layer over the summit, flanks and vicinity of the seamount (Fig. 4.9b). The myctophid fish *Hygophum hygomii* was abundantly caught over the summit, flanks and in the vicinity of MAD-Ridge (Fig. 4.9b). Since the IYGPT net had no closing device, shallow water species might have contributed to the catch in deeper trawls as the net was lowered and retrieved.

The backscatter intensity within the day SSL between 10 and 100 m over La Pérouse summit was lower compared to MAD-Ridge summit (Fig. 4.9a and b). Over La Pérouse summit, the day SSL consisted of a greater percentage abundance and biomass of gelatinous organisms including various types of jellyfishes, salps, and the siphonophore Diphyidae along with three leptocephali and one juvenile *Chaetodon* (Fig. 4.9a). The night SSL during La Pérouse cruise extended from the surface to 200 m. Over La Pérouse flanks, the night SSL consisted of high numbers of the unidentified crustaceans and the meso-bathypelagic squid *Abraliopsis* sp. and lower numbers of the cephalopods Cranchiidae, Oegopsida, *Abralia* sp., and Octopoda, and epi-, meso- and bathypelagic fishes of the Gonostomatidae, Malacosteidae, Myctophidae, Paralepididae and Synodontidae families. The night SSL in the vicinity of La Pérouse included similar specimens as those sampled over the flanks, such as pyrosomes, jellyfishes, salps, unidentified shrimps, phyllosoma larvae, *Abraliopsis* sp., Cranchiidae, and Octopoda, and various types of fishes of the Myctophidae family.

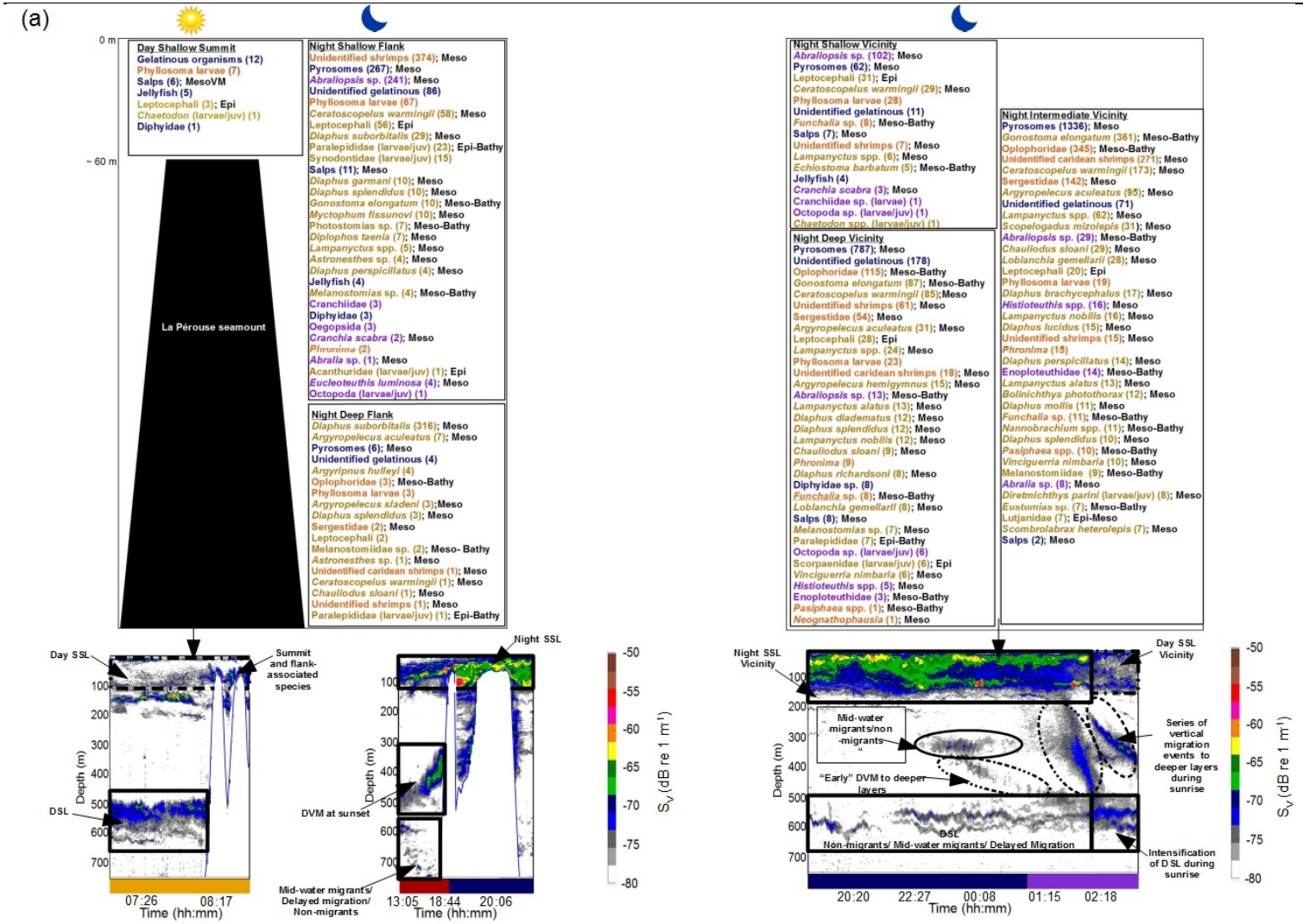

Figure 4.9(a) Schematics of La Pérouse seamount, listing the most dominant taxa (gelatinous organisms in blue, crustaceans in orange, cephalopods in violet and fishes in yellow), within the cluster groups. The numbers in brackets indicate the number of individuals caught. Organisms are classified as being epi (epipelagic), meso (mesopelagic), bathy (bathypelagic) and bentho (benthopelagic). Echograms of the 38 kHz frequency at sunset, night, sunrise and daytime are denoted by red, blue, violet and gold coloured rectangles respectively. The series of DVM events from the intermediate layer and from the SSL are denoted by circular dotted lines. The night SSL and day SSL are denoted by solid and dotted rectangles respectively. The DSL is denoted by solid rectangles. Backscatter from seamount-associated species are also noted. The colour bar indicates Sv in dB re 1 m^{-1}.

The DSL over the flanks and vicinity of La Pérouse was less dense at night-time compared to daytime and was located between 500 and 650 m compared to MAD-Ridge (400-700 m) (Fig. 4.9a). The night deep trawls over La Pérouse flanks consisted of pyrosomes and the seamount-associated fish *D. suborbitalis* in high numbers, the deep-dwelling *A. aculeatus*, the fish *A. hulleyi* (Cherel et al., 2020), and a variety of crustaceans and squids in lower numbers (Fig. 4.9a). *D. suborbitalis* were caught within the night SSL over the flanks of La Pérouse but not in the vicinity of the seamount. The night deep tows in the vicinity of La Pérouse consisted of the crustaceans Oplophoridae, unidentified shrimps, Sergestidae, *Phronima*, *Funchalia* sp., *Pasiphaea* spp., and *Neognathophausia*, the cephalopods *Abraliopsis* sp. and Octopoda, the weakly migrating/ non-migrating fishes *A. aculeatus* and *A. hemigymnus* and diel vertically migrating and mid-water migrating fishes of the Gonostomatidae, Melanostomiidae, Myctophidae, Stomiidae, Paralepididae, Scorpaenidae and Phosichthyidae families. Mid-water migrants showed earlier vertical migration from the intermediate to deeper layers at the end of the night, as shown by the echogram of the 38 kHz frequency. The majority of micronekton organisms however, migrated from the SSL to the DSL or deeper during sunrise in a series of migration events and contributed to the intensification of the backscatter within the DSL during daytime.

The night SSL over MAD-Ridge summit consisted of the gelatinous plankton salps and pyrosomes, crustaceans Oplophoridae, and unidentified shrimps, squids Enoploteuthidae, *Ornithoteuthis volatilis*, *Abraliopsis* sp., and Onychoteuthidae, and a range of diel vertically migrating fishes of the Myctophidae, Nomeidae and Melanostomiidae families (Fig. 4.9b). Few individuals of the slope-associated benthopelagic fish *C. japonicus* and juveniles of the reef-associated fish *Chaetodon* were collected within the night SSL over MAD-Ridge summit. The night SSL over the flanks of MAD-Ridge consisted of the crustaceans Oplophoridae, Sergestidae, *Funchalia* sp., *Euphausiacea* and *Phronima*, squids including Ommastrephidae, mesopelagic fishes and high numbers of gelatinous plankton. *D. suborbitalis* were sampled in higher numbers within the night SSL over the flanks and in lower numbers within the day deep tow over the flanks and within the vicinity of the seamount.

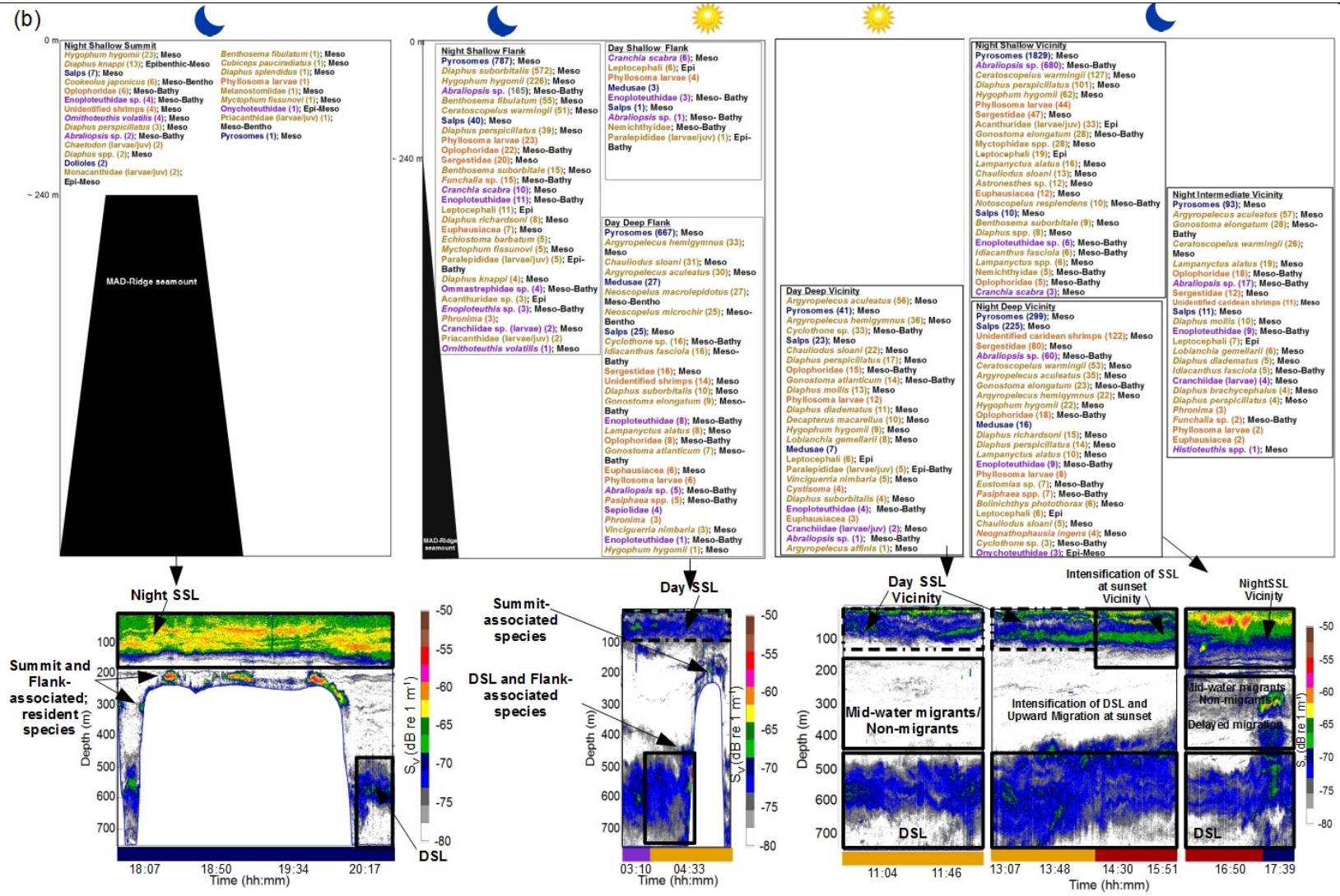

Figure 4.9(b) Schematics of MAD-Ridge seamount, listing the most dominant taxa (gelatinous organisms in blue, crustaceans in orange, cephalopods in violet and fishes in yellow), within the cluster groups. The numbers in brackets indicate the number of individuals caught. Organisms are classified as being epi (epipelagic), meso (mesopelagic), bathy (bathypelagic) and bentho (benthopelagic). Echograms of the 38 kHz frequency at sunset, night, sunrise and daytime are denoted by red, blue, violet and gold coloured rectangles respectively. The series of DVM events from the intermediate layer and from the SSL are denoted by circular dotted lines. The night SSL and day SSL are denoted by solid and dotted rectangles respectively. The DSL is denoted by solid rectangles. Backscatter from seamount-associated species are also noted. The colour bar indicates Sv in dB re 1 m^{-1}.

The day SSL over MAD-Ridge flanks comprised squids such as *Cranchia scabra*, *Abraliopsis* sp., Enoploteuthidae, and fishes such as Nemichthyidae, Paralepididae and leptocephali. The day deep tows over the flanks and in the vicinity of MAD-Ridge consisted of a range of crustaceans and migrating fish species of the Gonostomatidae, Myctophidae, Chauliodonthidae and Photichthyidae families commonly found in deeper layers during daytime. Day and night deep tows over the flanks and seamount vicinity consisted of the non-migrating fishes *A. aculeatus*, *A. hemigymnus*, *Cyclothone* sp. Echograms of the 38 kHz frequency showed high backscatter intensities over the summit and flanks of MAD-Ridge during night-time and daytime due to the presence of seamount summit and flank-associated/resident species. Before sunset at MAD-Ridge vicinity, the DSL was intensified and scatterers began streaming vertically upwards. A dense night SSL was formed within the first 200 m of the water column. Some micronekton species started their vertical migration from the DSL or deeper towards the SSL before sunset, other species during sunset and at night-time.

RGB composite images were analysed in conjunction with data of trawls #14, 15 and 16 to determine the acoustic responses of the micronekton captured and to make inferences about micronekton behaviour at the seamount summit as opposed to the southern Mozambique Channel (trawl #21) (Fig. 4.10). Trawls on the seamount summit predominantly sampled dense aggregations of organisms (seen as "white patches" on RGB composites), being strong targets at the 38, 70 and 120 kHz frequencies, and having a relatively flat response to all three frequencies (Fig. 4.10a and c). These trawls predominantly sampled the swimbladdered myctophid fishes *D. suborbitalis* and *B. fibulatum* over MAD-Ridge flanks (Fig. 4.10a), the mesopelagic fishes *H. hygomii* and *N. macrolepidotus*, and the benthopelagic fish *C. japonicus* over the summit (Fig. 4.10c). Trawl #15 sampled a greater number of pyrosomes which are strong targets at the 38 kHz frequency within the night SSL (Fig. 4.10b). Trawl #21 predominantly sampled organisms being strong targets at the 38 kHz frequency, with the fish *H. hygomii*, squid Enoploteuthidae, gelatinous pyrosomes and crustaceans Oplophoridae being the most abundantly caught (Fig. 4.10d). No dense aggregations ("white patches") were observed on RGB composite of trawl #21, as opposed to trawls over the seamount summit and flanks of MAD-Ridge. Organisms were more likely dispersed in the water column in the Mozambique Channel as opposed to the seamount summit and flanks where they formed dense aggregations.

RGB Composites of MAD-Ridge seamount

Red: 38 kHz; Green: 70 kHz; Blue: 120 kHz

a) Trawl #14

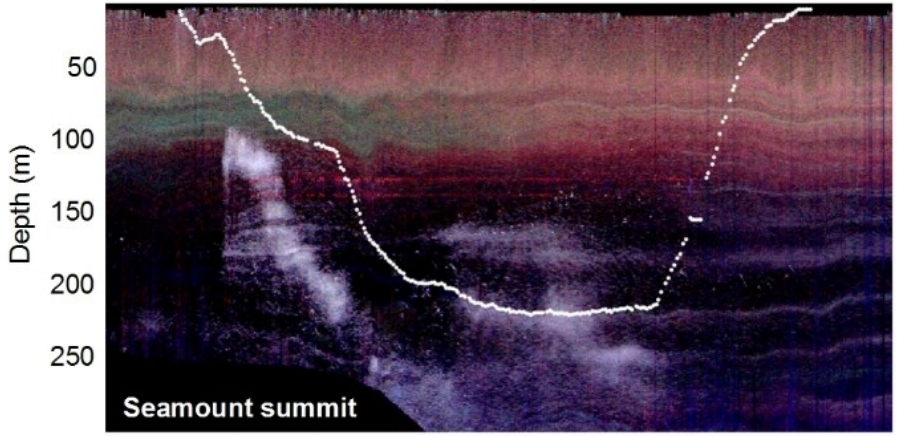

b) Trawl #15

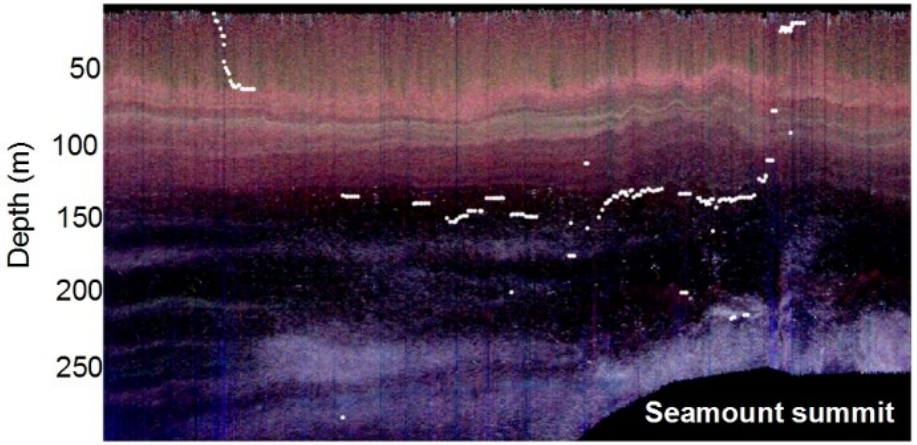

Frequency Diagrams and Frequency Responses

Trawl #14

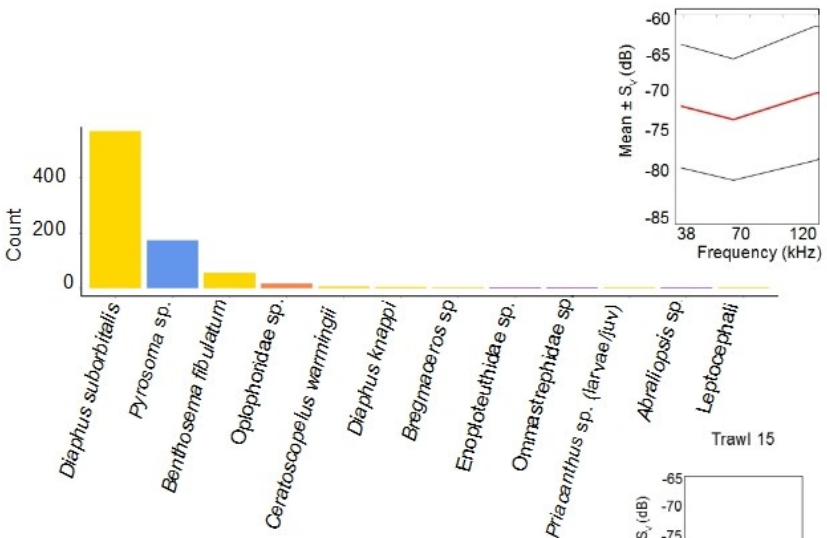

Trawl #15

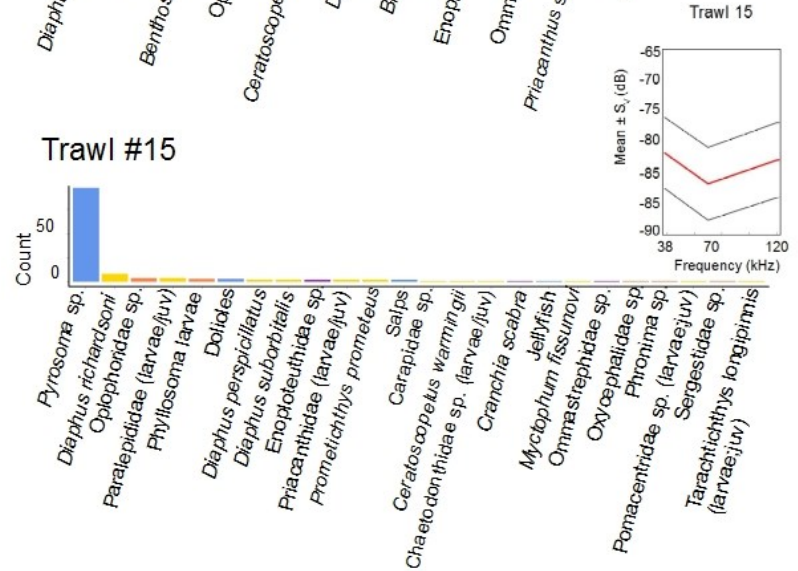

RGB Composites of MAD-Ridge seamount

Red: 38 kHz; Green: 70 kHz; Blue: 120 kHz

c) Trawl #16

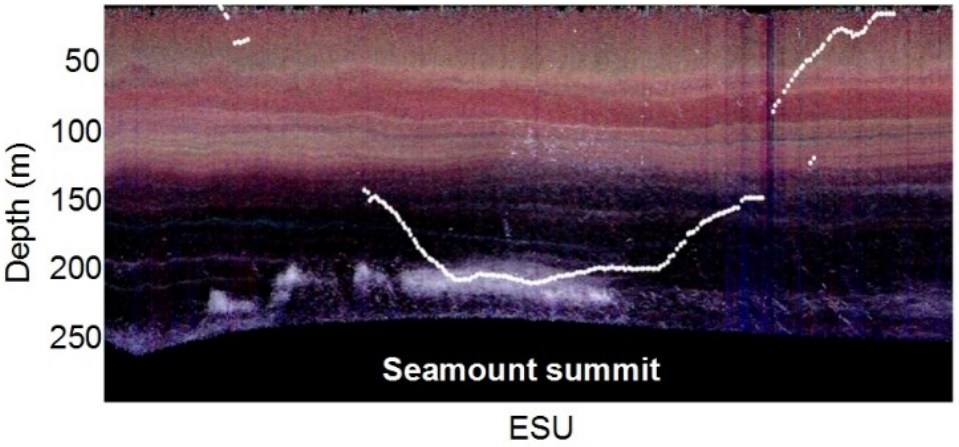

Frequency Diagrams and Frequency Responses

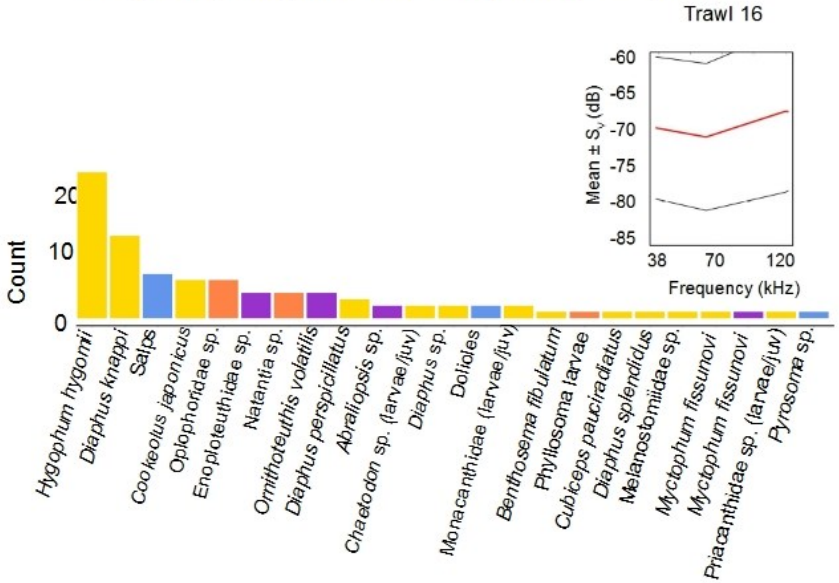

d) Trawl #21

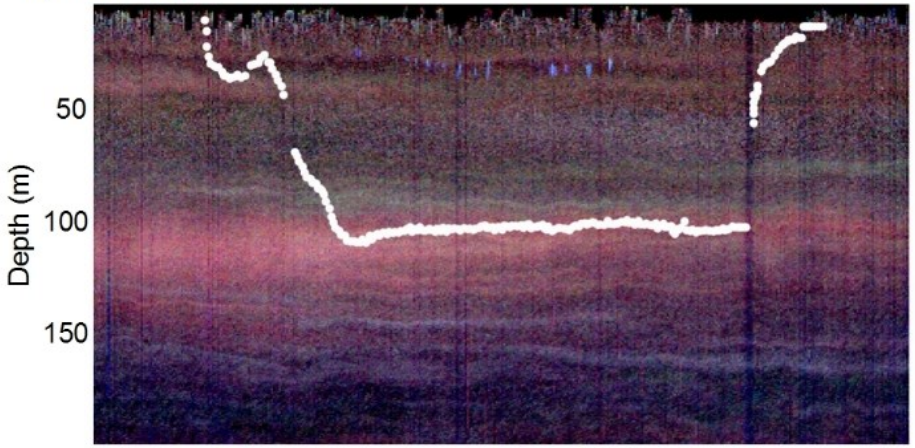

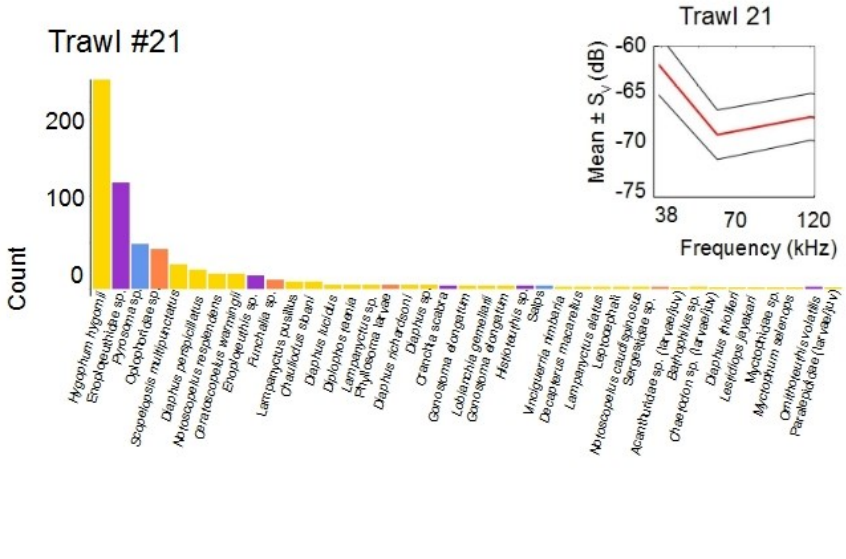

Figure 4.10(a-d) RGB composites of Sv values (dB re 1 m^{-}1) of trawls 14 and 15 (flank), 16 (summit) and 21 (southern Mozambique Channel) during MAD-Ridge. White dotted lines represent the trawl path as determined from Scanmar depth sensor. The seamount summit is denoted by the black polygon and labelled accordingly. The 38, 70 and 120 kHz frequencies were given red, green and blue colour codes respectively. Corresponding frequency diagrams of the species count for trawls #14, 15, 16 and 21 and mean ± standard deviation of the frequency responses (in dB) during the "horizontal trawl fishing period" are given. Broad categories are coloured orange (crustaceans), yellow (fishes), blue (gelatinous organisms), and violet (cephalopods).

4.4 Discussion

4.4.1 Sampling biases and constraints

Pelagic trawls like the IYGPT have coarse meshes at the front through which an unknown fraction of mesopelagic organisms may escape (Kaartvedt et al., 2012). Highly mobile micronekton such as cephalopods and fishes may show avoidance reactions to nets, which may lead to discrepancies between net-based and acoustic estimates (Reid, 1991; Kaartvedt et al., 2012). Organisms with fragile bodies, such as gelatinous plankton, may break apart, biasing final abundance/biomass estimates (Domokos et al., 2010; Rogers et al., 2017; Proud et al., 2018). La Pérouse acoustic data at sampling stations were incomplete and hence a thorough comparison in mean backscatter between La Pérouse and MAD-Ridge could not be carried out. Owing to bad quality acoustic data beyond 750 m, echo-integrations were limited to that depth. Biases in acoustic density estimates may arise from variations in fish swimbladder volume (that depends on the depth range and subsequent swimbladder compression), the swimbladder size distribution and aspect (Benoit-Bird & Lawson, 2016; Cascão et al., 2017; Proud et al., 2018). Some organisms also have low acoustic target strengths and hence low acoustic backscatter even if found in dense aggregations on seamounts (McClatchie & Combs, 2005). The RGB visualisation technique is colour-vision dependent but however, provides information on the mean backscatter at all three frequencies on a single plot and at high resolution compared to a single frequency echogram. Studies have demonstrated a seasonal effect in the variability of micronekon acoustic densities (Wilson & Boehlert, 2004; Cascão et al. 2017) owing to the life strategies and behaviour of the seamount-associated fauna. This study therefore, only provided a snapshot in time of the composition of micronekton at La Pérouse and MAD-Ridge during a declining phase of oceanic productivity.

4.4.2 Oceanography and biological response

This thesis highlighted contrasting environmental patterns at La Pérouse and MAD-Ridge. While MAD-Ridge was under the influence of strong cyclonic and anticyclonic eddies

originating from the South East Madagascar current (Vianello et al., 2020), La Pérouse was under the influence of moderate mesoscale activities. As topographic obstacles, seamounts may either bifurcate, trap, split or destroy eddies (Schouten et al., 2000; Herbette et al., 2003; Adduce & Cenedese, 2004; Sutyrin, 2006; Lavelle & Mohn, 2010). Trapping duration of eddies may last for several months, with important estimated effects on biological production and plankton retention (Bograd et al., 1997). Eddies are well known in influencing local water properties, such as the trapping of anomalous water masses (Swart et al., 2010; Pollard & Read, 2015), or the advection of coastal waters with high phytoplankton biomass from the coast to open waters (Quartly & Srokosz, 2004; Tew-Kai & Marsac, 2009; Kolasinski et al., 2012). Coastally upwelled waters of high biological productivity over the southern Madagascar shelf (Ramanantsoa et al., 2018) may be trapped by mesoscale features that propagate over MAD-Ridge.

Local productivity at MAD-Ridge did not result from a Taylor column (see Chapter 3) since the latter may form transiently, under specific conditions of summit depth, water column stratification and current speeds (Owens & Hogg, 1980, Freeland, 1994, Mohn et al., 2009, Wagawa et al., 2012; Bashmachnikov et al., 2013). Read & Pollard (2017) concluded that while, Taylor columns may theoretically be formed over several seamounts of the Madagascar Ridge, the relatively strong currents associated with mesoscale eddies may prevent their formation or sweep away any incipient Taylor cap before settlement. The complex crescent shape of La Pérouse seamount, shallow summit depth and relatively high current speeds were not favourable for Taylor column formation (see Chapter 3). The high yearly biological productivity at MAD-Ridge and connectivity with neighbouring seamounts of the Madagascar Ridge (Letessier et al., 2017) and with the Madagascar shelf might be one of the reasons accounting for the greater micronekton species richness and denser SSL and DSL at MAD-Ridge compared to La Pérouse. Higher mean acoustic responses were also recorded along Petal V during MAD-Ridge, which may be an aggregating effect on organisms of the strong local gradient of sea level anomalies at the anticyclonic eddy periphery (Sabarros et al., 2009).

4.4.3 Effect of seamounts on the DVM of micronekton

As evidenced in this study, the majority of micronekton taxa including various myctophids performed daily DVM whereas the deep-dwelling *Pasiphaea* spp., *A. aculeatus*, *A. hemigymnus* and *Cyclothone* sp. did not migrate to surface layers at dusk. Diel vertical migration did not occur as a single event, but as a series of events from the mid-water migrants which migrated from the intermediate layer to the DSL or deeper before sunrise. The surface

migrants migrated from the SSL to the DSL or deeper during sunrise. Various cues such as light penetration and intensity, productivity, oxygen minima, temperature, food, clear oligotrophic waters and chemoreception of kairomones (chemical cues) released by fish, are commonly thought to influence the vertical migration of organisms and the onset of DVM (Youngbluth, 1975; Andersen et al., 1998; Cohen & Forward, 2009; Ekau et al., 2010; Bernal et al., 2015; Olivar et al., 2012, 2017). Some of the vertically migrating organisms may be concentrated on the flanks of the pinnacle. The "topographic blockage" mechanism/sound-scattering layer interception hypothesis has been previously described (Isaacs & Schwartzlose, 1965; Genin, 2004; Porteiro & Sutton, 2007; Hirch & Christiansen, 2010), whereby the pre-dawn migratory descent of some mesopelagic organisms was found to be temporarily halted by the seamount topography and presence of predators using the seamount as a barrier to concentrate prey (Johnston et al., 2008). This mechanism was hardly observed in the acoustic transects throughout La Pérouse and MAD-Ridge cruises.

4.4.4 Micronekton scattering layers and assemblages at La Pérouse and MAD-Ridge

At both La Pérouse and MAD-Ridge seamounts, the night SSL was shown to consist of gelatinous organisms (pyrosomes) and a range of common open-water swim-bladdered mesopelagic fishes that undergo DVM and are strong acoustic targets at the 38 kHz frequency. The day SSL, on the other hand, consisted of non-migrant gelatinous organisms, phyllosoma larvae, leptocephali (La Pérouse and MAD-Ridge) and few cephalopods (MAD-Ridge). While gelatinous organisms are strong targets at 38 khz, phyllosoma larvae, leptocephali and cephalopods are relatively weak targets at this frequency. Scattering layers being strong targets at the 70/120 kHz frequencies were observed at various distances from MAD-Ridge summit. These biological scatterers were not sampled by the IYGPT net but were shown to be associated with the depth of the maximum fluorescence (see Chapter 3). These organisms may be phytoplankton-eaters, siphonophores with pneumatophores smaller than those having a high response to the 38 kHz frequency (Arthur Blanluet, pers. comm.), or larger crustaceans that have a response to the 70 kHz frequency but have escaped the trawls. The day and night SSL may also have consisted of organisms that were horizontally advected in addition to species showing vertical migration (see Chapter 3).

A DSL was present both during the day and night at La Pérouse and MAD-Ridge seamounts. The DSL is a ubiquitous acoustic signature and is commonly formed by mesopelagic fishes and invertebrates (Aksnes et al., 2017; Proud et al., 2017). DSLs were shown to be dominated

by non-migrant swimbladdered sternoptychids and gonostomatids in the Atlantic (Fennell & Rose, 2015; Ariza et al., 2016), Pacific (Romero-Romero et al., 2019) and Indian Oceans, south of Mauritius Island and in the Mozambique Channel (Annasawmy et al., 2018). However, the DSL depth is not uniform across ocean basins. The lower limit of the DSL was deeper in the SWIO at La Pérouse (500-650m), MAD-Ridge (400-700 m), south of Mauritius and Réunion Islands and over the Madagascar Ridge (400-800 m) (Boersch-Supan et al., 2017), compared to the Chagos Archipelago in the central Indian Ocean, where it extended from 300 to 600 m (Letessier et al., 2015). Micronekton taxa showing delayed vertical migration or no DVM contributed to the backscatter intensities within the night DSL. Delayed vertical migration of organisms at night is commonly employed by organisms to reduce competition during feeding (Watanabe et al., 2002). Some of these organisms were bathypelagic species possibly still ascending from depths deeper than 1000 m at the time that the acoustic transects were conducted.

The most common squids sampled at La Pérouse and MAD-Ridge can be divided into the following main groups (as defined by Nesis, 1993): nerito-oceanic species that occur over seamounts as paralarvae, juveniles or sub-adults (eg. Onychoteuthidae and Histioteuthidae) and diel vertically migrating species that are advected over seamounts at night and descend to deeper depths at dawn (*Abraliopsis* sp.-Enoploteuthidae, Histioteuthidae and Octopoteuthidae). *Abraliopsis* sp. may descend deeper than 1000 m during daytime, hence the low numbers caught in the day deep trawls. Of the 77 cephalopod taxa reported from the region of the Madagascar Ridge (Laptikhovsky et al., 2017), this study sampled only 17 taxa at both La Pérouse and MAD-Ridge seamounts, largely under sampling this broad category. Squids are also relatively weak acoustic targets at 38 kHz (Simmonds & MacLennan, 2005) and studies commonly used a combination of frequencies to locate squid schools (Starr & Thorne, 1998). A total of 32 species of decapods and lophogastrids were reported from the Madagascar Ridge (Letessier et al., 2017). Due to low sampling effort and identification, only 13 and 10 crustacean taxa were correctly identified at La Pérouse and MAD-Ridge respectively. Studies have found elevated abundances of crustacean taxa in the vicinity of seamounts of the South West Indian Ridge and have concluded that some taxa may resist advective lost from seamounts by active migration (Letessier et al., 2017). These taxa were reported to support rich communities of benthopelagic fishes living close to the bottom of the ridge (Vereshchaka, 1995).

The mesopelagic fishes *N. macrolepidotus* and *B. fibulatum* are diel vertical migrants, that are associated with the summit and flanks of seamounts but can also be found in the open ocean. The non-migrant benthopelagic fish species *C. japonicus* and larvae from the Priacanthidae family, on the other hand, were exclusively caught over the summit of MAD-Ridge and were hence truly resident at the seamount. Large populations of *D. suborbitalis* have previously been found to be associated with the Equator seamount (close to the shallow peak called Travin Bank) in the Indian Ocean (Parin & Prut'ko, 1985; Porteiro & Sutton, 2007). These fishes were reported to be located on the slopes at 500-600 m depth during daylight hours and to ascend in dense schools to 80-150 m depth at night for feeding on oceanic plankton, mainly copepods (Gorelova & Prut'ko, 1985), while at the same time being preyed upon by several top predators such as tunas and swordfish (Parin & Prut'ko, 1985). The fish *B. fibulatum* was found to be associated with the Hawaiian Cross seamount summit (330 m below the sea surface) in the Pacific (De Forest & Drazen, 2009), but abundance estimates at the seamount depended largely on lunar illumination (Drazen et al., 2011).

4.4.5 Do seamounts have higher abundances/biomasses/densities over the summit?

The physical obstruction created by a seamount has been hypothesized to reduce the density of animals over the flanks and summits, particularly at night (eg. Genin et al., 1988; Diekmann et al., 2006; De Forest & Drazen, 2009). The lower abundance/biomass estimates of micronekton recorded over the summits of La Pérouse and MAD-Ridge compared to the immediate vicinity seem to support this hypothesis. However, gas-bearing seamount-associated/resident fauna including *D. suborbitalis*, *N. macrolepidotus*, *B. fibulatum*, *C. japonicus* (MAD-Ridge) and *D. suborbitalis* (La Pérouse), might have formed dense aggregations below the SSL, in close proximity to the summits and flanks (hence the "white patches" seen on RGB composites). The densities and/or target strengths of these organisms are high. These high acoustic detections might also have been caused by deep-water fish aggregations (more commonly described as "plumes") (Bull et al., 2001; O'Driscoll et al., 2012) that were not sampled by the IYGPT net. Fish species such as orange roughy which are commercially fished at Walters Shoal along the Madagascar Ridge (Collette & Parin, 1991), are poor acoustic targets due to their wax ester swimbladders and are known to avoid mesopelagic trawls (Kloser et al., 2002). These plumes may represent aggregations of seamount-resident fishes that avoided advective loss from the seamounts and formed dense aggregations over the summits and flanks. In the open ocean such as the southern Mozambique Channel, micronekton were more dispersed in the water column since no dense aggregations ("white patches") were observed.

Various hypotheses may be put forward to explain the preferential association of organisms with seamounts. Organisms may associate with La Pérouse and MAD-Ridge: (1) to increase feeding efficiency (Vereshchaka, 1995; Wilson & Boehlert, 2004), (2) to take advantage of a broader range of habitat diversity created by the topography (Wilson & Boehlert, 2004; Porteiro & Sutton, 2007) such as shelter regions for spawning, and (3) to decrease energy loss by using this habitat as a shelter during non-feeding intervals whereby in the open ocean organisms may have to swim constantly. Benthopelagic animals (such as *C. japonicus*) were reported to prefer rocky seabeds and may take advantage of strong currents over seamounts for advection of their main prey items while avoiding being swept from the summit by using rocky canyons within the seamount topography as shelter regions (Vereshchaka, 1995).

The reasons for the observed variability in mean backscatter at MAD-Ridge summit compared to the immediate vicinity and the reasons for the observed decrease in trawl abundance/biomass estimates at the summit are further discussed with respect to the sampling strategy and IYGPT net used. Although trawl surveys are necessary to determine the taxonomic composition of micronekton present in the water column in space and time, the composition and biomass obtained largely depend on the type of trawl used (Kwong et al., 2018), their catchability towards various taxonomic groups of nekton and the depth range sampled. Trawl sampling is difficult on shallow topographies because of the high risk of damaging the sampling gear (Christiansen et al., 2009). Hence, the time spent surveying the summit is generally limited. The trawls #14, 15 and 16 over the summit and flanks of MAD-Ridge were directed to specifically sample dense aggregations observed by acoustics and hence the trawl had failed to capture the full suite of organisms present at the study sites. While trawl surveys are useful in terms of the determination of the species composition and assemblages of micronekton, they are also generally expensive, time-consuming and allow a relatively limited collection of samples at any given area. Trawl catches provide only a snapshot of the communities dwelling at seamounts which depends strongly on the time of day and the sampling depths.

Active acoustics, on the other hand, while not being able to correctly resolve the taxonomic composition of the micronekton fauna yet, provide continuous measurements of the mesopelagic layer and can be used to determine organisms' abundances/densities, movements and migrations at various spatial and temporal scales. The combination of active acoustics with trawl and Scanmar data in the form of RGB composites provide invaluable insights into the distributions, the depths of the different scattering layers, the scattering properties of organisms and can be used to speculate about organisms' aggregating behaviour. Kloser et al. (2002) used

a similar approach, but the composite image was produced by assigning a separate colour palette to each frequency (12, 38 and 120 kHz) and dynamically optimising the frequencies to highlight the amplitude differences in the echogram. The RGB composite approach has the added advantage of further highlighting the presence of structures under-sampled by trawls due to their patchy distribution ("blue patches" with a high frequency response to the 120 kHz; Fig. 4.10d, Trawl #21 at ~30 m) and that could be further investigated using multi-frequency classification.

4.5 Concluding remarks

A combination of datasets (active acoustics and mesopelagic trawls) was used to investigate the dynamics of micronekton at two shallow seamounts. The higher year-round oceanic productivity, eddy dynamics, advection of productivity from the Madagascar landmass and connectivity with neighbouring seamounts and landmasses may result in greater micronekton species richness at MAD-Ridge compared to La Pérouse which is located in an oligotrophic environment. The night SSL (between 10 and 200 m) over the summit and flanks concentrated common open-water species of gelatinous (salps and pyrosomes), crustaceans (Euphausiacea, *Funchalia* sp. and phyllosoma larvae), squids (Enoploteuthidae, *C. scabra* and *Abraliopsis* sp.), and fishes (leptocephali, *H. hygomii* and various species of *Diaphus* spp.). In addition to the vertically migrant organisms forming the SSL, this study provided evidence that La Pérouse and MAD-Ridge seamounts support an important community of seamount-associated/resident fishes (La Pérouse and MAD-Ridge: *D. suborbitalis*; MAD-Ridge: *B. fibulatum* and *C. japonicus*) that occur in dense aggregations over the summits and flanks. Despite several shortcomings in this work, notably during La Pérouse and MAD-Ridge cruise sampling, this study fills an important knowledge gap. The combined use of satellite, mesopelagic trawl and acoustic data at the time of the cruises, provides an integrative and accurate picture as to the mechanisms involved in micronekton vertical/horizontal distributions and assemblages at shallow topographies. More importantly, this study helps contribute to our growing understanding of seamount ecosystems in the south-western Indian Ocean. Improving our knowledge of the ecosystems associated to shallow seamounts is a key issue towards the promotion of specific sustainable use and conservation measures dedicated to protecting such critical environments.

Acknowledgements

The authors acknowledge the work carried by the non-scientific staff on board the RV *Antea* and the scientific staff who participated in the data acquisition and data processing, including Delphine Thibault (MIO, Marseille, France), P. Alexander Hulley (South Africa) for confirming the taxonomy of the micronekton taxa and Hervé Demarcq (IRD, Sète, France) for providing the SSC data. This study was mainly supported by the Flotte Océanographique Française (French Oceanographic Fleet) and IRD in relation to the logistics of the RV *Antea*. Additional funding was received from Région Réunion (Réunion Regional Council) for La Pérouse cruise, and from the Fonds Français pour l'Environnement Mondial (FFEM) as part of the FFEM-SWIO project on Areas Beyond National Jurisdiction (ABNJ) of the South West Indian Ocean for MAD-Ridge cruise. Pavanee Annasawmy was the beneficiary of a doctoral bursary granted by the Institut de Recherche pour le Développement (IRD, France) and the ICEMASA French-South African International Laboratory.

Inter-chapter II

As shown in Chapter 4, the large-scale oceanic productivity in the vicinity of the MAD-Ridge seamount is twice that found at La Pérouse all year round. Both the La Pérouse and MAD-Ridge cruises took place during a decreasing trend of oceanic productivity in September and November-December, respectively. The breeding and foraging patterns of top predators including seabirds of the SWIO suggest that austral winter (June-October) is characterised by enhanced prey biomasses. The densities of micronekton may hence be several degrees of magnitude higher a few weeks after the observed peak in productivity in July than that recorded in this study.

Chapter 4 also showed that the physical obstacles that represent the La Pérouse and MAD-Ridge seamounts did not perturb the distribution and diel migration of common oceanic micronekton taxa. Diel vertical migration of several micronekton taxa started at sunset towards the surface layer and at sunrise towards the deep layer such that all migrants reached the DSL before daylight, even in presence of the seamounts. Several micronekton taxa, however, are non-migrants, i.e. they stayed in the DSL at night-time, while other scatterers stayed in the SSL during daylight. Other micronekton communities showed delayed migration strategies to the surface at dusk or mid-water migration to the lower limit of the SSL within the intermediate layer at night. Micronekton is a broad group consisting of crustaceans, squids and mesopelagic fishes, all having specific foraging, migration and behavioural patterns. As shown in Chapter 2, marine mammals are able to adapt their foraging strategies to utilize the different micronekton resources in the epipelagic zone at night (as in the case of *Stenella* spp. and *Tursiops* spp.) or deeper in the water column (as in the case of sperm and beaked whales). Swordfish that is physiologically adapted to dive deeper, may also preferentially associate with seamounts as seen in Chapter 2 and utilize the resources found at these topographic features.

Within the micronekton, some species are commonly oceanic and avoid seamounts, some preferentially associate with areas of high oceanic productivity, some taxa aggregate at topographic features, whereas others would use a combination of the above strategies. The SSL over La Pérouse and MAD-Ridge seamounts did not show enhanced densities relative to the immediate vicinity. However, dense aggregations of scatterers were observed during day and night at the summits of both seamounts. These aggregations were shown to consist of seamount-associated mesopelagic fishes. At MAD-Ridge, benthopelagic fishes further

aggregated over the seamount summit. La Pérouse and MAD-Ridge may hence represent favourable habitats for these organisms not only in their adult stages, but also in their larval forms. As seen in Chapter 2, higher larval fish densities (with the most common family being Myctophidae and Gonostomatidae), were recorded at the summits of La Pérouse and MAD-Ridge which suggest local spawning at both seamounts.

While acoustics and trawl surveys provide important information on densities, biomasses, abundances and taxonomic diversity at different sites and at different depths, these techniques provide little information about the link between micronekton and the other components of the foodweb. Chapter 5 hence aims at understanding the trophic relationships of the sampled micronekton with respect to POM and zooplankton. Tissues of micronekton organisms were analysed for stable isotopes of ^{13}C and ^{15}N to determine the sources of primary production and the trophic position of individuals respectively. The factors influencing the $\delta^{15}N$ and $\delta^{13}C$ values of consumer tissues were determined. A "seamount effect" in either depletion or enhancement of $\delta^{15}N$ and $\delta^{13}C$ values of micronekton were further investigated by investigating the values of omnivorous/carnivorous fishes collected over the flank, summit and vicinity of La Pérouse and MAD-Ridge relative to an off-seamount location in the southern Mozambique Channel.

Chapter 5: Stable isotope patterns of mesopelagic communities over two shallow seamounts of the south-western Indian Ocean

Chauliodus sloani

Model made by: www.10tons.dk

Model Sculptors: Peter Rask Møller and Jørgen G. Nielsen (Statens Naturhistoriske Museum, Copenhagen, Denmark)

Photo title: Chauliodus sloani

Techniques: Sculpted by hand from chemical clays and foam board. Molded in silicone and cast from layers of crystal clear and coloured polyurethane-resins.

Stable isotope patterns of mesopelagic communities over two shallow seamounts of the south-western Indian Ocean

Pavanee Annasawmy[1,2], Yves Cherel[3], Evgeny V. Romanov[4], François Le Loc'h[5], Frédéric Ménard[6], Jean-François Ternon[1], Francis Marsac[1,2]

[1] *MARBEC, IRD, Univ Montpellier, CNRS, Ifremer, Sète, France*

[2] *Department of Biological Sciences and Marine Research Institute/ICEMASA, University of Cape Town, Cape Town, South Africa*

[3] *Centre d'Etudes Biologiques de Chizé (CEBC), UMR7372 du CNRS- La Rochelle Université, Villiers-en-Bois, France*

[4] *Centre technique d'appui à la pêche réunionnaise (CAP RUN - CITEB), Île de la Réunion, France*

[5] *IRD, Univ Brest, CNRS, Ifremer, LEMAR, IUEM, F-29280 Plouzane, France*

[6] *Aix Marseille Univ, Université de Toulon, CNRS, IRD, MIO, UM110, Marseille, France*

* Corresponding author: angelee-pavanee.annasawmy@ird.fr

Abstract

The stable carbon ($\delta^{13}C$) and nitrogen ($\delta^{15}N$) isotope values of soft tissues of micronekton (crustaceans, squids, mesopelagic fishes) and zooplankton were measured from organisms collected on the RV *Antea* at two seamounts located in the south-western Indian Ocean: La Pérouse (summit depth ~60 m) and "MAD-Ridge" (thus named in this study; summit depth ~240 m). Surface particulate organic matter (POM-Surf) showed higher $\delta^{13}C$ at MAD-Ridge than at La Pérouse. Particulate organic matter and zooplankton were depleted in ^{15}N at the oligotrophic La Pérouse pinnacle compared with the more productive MAD-Ridge seamount. Gelatinous organisms and crustaceans occupied the lowest and intermediate trophic levels (TL ~2 and 3 respectively) at both seamounts. Mesopelagic fishes and smaller-sized squids sampled at both seamounts occupied TL ~3 to 4, whereas the large nektonic squids *Ommastrephes bartramii*, collected at MAD-Ridge only, exhibited a TL of ~5. The $\delta^{15}N$ values of common open-water mesopelagic taxa were strongly influenced by specimen size and feeding habits at both seamounts, with an increase in $\delta^{15}N$ values with increasing size. Carnivorous fish species sampled exclusively over the seamounts' flanks and summits exhibited TL values of ~4, irrespective of their wide size ranges. This work could not demonstrate any differences in $\delta^{15}N$ values of mesopelagic fishes between the seamounts and the surrounding oceanic areas. This study segregated cluster of mesopelagic organisms according to their $\delta^{13}C$ and $\delta^{15}N$ values, with variations in stable isotope values reflecting a complex range of processes possibly linked to productivity as well as biological and ecological traits of the species (size and feeding mode).

Keywords: micronekton, crustaceans, fish, $\delta^{13}C$, $\delta^{15}N$, trophic level

5.1 Introduction

Micronekton are a broad group of organisms mostly dwelling in the mesopelagic zone (<1000 m). They consist of crustaceans (adult euphausiids, hyperiid amphiphods, pelagic decapods and mysids), cephalopods (small species and juvenile stages of large oceanic species) and fishes (mainly mesopelagic species and juveniles of pelagic fish) (Brodeur & Yamamura, 2005; De Forest & Drazen, 2009; Ménard et al., 2014). They range in size from 2-20 cm and represent a substantial biomass in oceanic waters (Brodeur & Yamamura, 2005). Many species exhibit extensive DVM, thus playing an important role in the biological pump by transporting carbon and nutrients from the epipelagic to the mesopelagic zone (Hidaka et al., 2001; Brodeur & Yamamura, 2005; Catul et al., 2011; Bianchi et al., 2013). Micronekton also form a key trophic link between zooplankton and top predators because they are preyed upon by several species of seabird, tuna and billfish (Guinet et al., 1996; Bertrand et al., 2002; Brodeur & Yamamura, 2005; Potier et al., 2007; Karakulak et al., 2009; Cherel et al., 2010; Danckwerts et al., 2014; Jaquemet et al., 2014; Duffy et al., 2017; Watanuki & Thiebot, 2018). Various studies have investigated the trophic interactions of micronekton to better understand their role in foodwebs across numerous ocean basins (Fanelli et al., 2011b; Colaço et al., 2013; Fanelli et al., 2013; Ménard et al., 2014; Valls et al.., 2014a, b; Annasawmy et al., 2018). For instance, mesopelagic organisms were shown to transfer energy between primary consumers and deeper benthic and benthopelagic animals at Condor seamount in the Atlantic (Colaço et al., 2013).

Tuna, billfish, pelagic armorheads, alfonsinos and orange roughy are common predators fished extensively at seamounts in the Atlantic (Fonteneau, 1991; Morato et al., 2008; Dubroca et al., 2013), Pacific (Rogers, 1994; Koslow, 1997; Holland et al., 1999; Musyl et al., 2003; Paya et al., 2006; Morato et al., 2010) and Indian oceans (Romanov, 2003; Clark et al., 2007; Marsac et al., 2014). Although, La Pérouse does not represent an outstanding fishing spot, tuna (*Thunnus* spp.) and swordfish (*Xiphias gladius*) are present in the vicinity of the seamount throughout the year (Marsac et al., 2020). Albacore (*Thunnus alalunga*), bigeye (*T. obesus*), yellowfin (*T. albacares*) tuna and swordfish commonly occur along the Madagascar Ridge and MAD-Ridge pinnacle (IOTC, www.iotc.org/data-and-statistics). The Madagascar Ridge has also been targeted for orange roughy in 1999/2000 before the catch dropped significantly in subsequent years (Ingole & Koslow, 2005; Lack et al., 2003). Due to the increased pressure on marine organisms, characterizing the overall trophic pathways within pelagic ecosystems (Young et al., 2015) contributes to making better informed fisheries and ecosystem-based management decisions.

Two seamounts of the SWIO, La Pérouse and and an unnamed pinnacle, thereafter named "MAD-Ridge", were studied in an effort to understand how seamounts may affect DVM and aggregations of micronekton. While micronekton acoustic densities were not significantly different between the summit and immediate vicinity of the pinnacles, dense aggregations of scatterers, referred to as seamount-associated species, were recorded over the summit of both seamounts during day and night. La Pérouse is situated in the ISSG province (Longhurst, 2007; Reygondeau et al., 2013) with low mesoscale activities and primary productivity, whereas MAD-Ridge is located within an "eddy corridor" to the south of Madagascar, in a region with high occurrence of cyclonic and anticyclonic eddies and relatively high sea surface chlorophyll concentrations all year round relative to La Pérouse (see Chapter 4; Halo et al., 2014; Vianello et al., 2020). The enhanced productivity on the Madagascar shelf and its offshore entrainment by mesoscale eddy interactions (Quartly et al., 2006), were one possible reasons leading to greater micronekton acoustic densities at MAD-Ridge relative to La Pérouse. Trapped, enclosed circulations known as Taylor columns may also develop over seamounts and contribute to the retention of productivity (Genin & Boehlert, 1985; Dower et al., 1992; Mouriño et al., 2001; Mohn & White, 2007). No Taylor columns were observed at La Pérouse and MAD-Ridge seamounts, however, during the cruises most likely because of the high current speeds observed over the summits and the seamount structure not being favourable for the development and retention of such features.

Foodwebs are shaped by a complex set of interactions controlled by the availability of organic (C-based nutrients) and inorganic (nitrate, nitrite, phosphate and silicate) nutrients, the efficiency of energy transfer to higher trophic levels and the control of species biomass by predators (Pomeroy, 2001). Carbon ($\delta^{13}C$) and nitrogen ($\delta^{15}N$) stable isotope analyses are a valuable tool for foodweb investigations in deep-sea ecosystems (Michener & Kaufman, 2007) and are based on time-integrated assimilated food (Martínez del Rio et al., 2009). Trophodynamic studies commonly employ $\delta^{13}C$ to investigate the source of organic matter and $\delta^{15}N$ to determine trophic level and trophic interactions (Michener & Kaufman, 2007). The heavier isotopes (^{13}C and ^{15}N) are preferentially retained in tissues of consumers relative to their prey, while lighter ^{12}C and ^{14}N isotopes are preferentially excreted (Fry, 2006). Overall, there is a small isotopic enrichment of 0.5-1‰ in the heavier ^{13}C isotope of an organism's tissue relative to its diet (Fry, 2006). Differences in $\delta^{13}C$ values can thus indicate different sources of primary production such as inshore vs offshore, or pelagic vs benthic contributions to food intake (Hobson et al., 1994; Rubenstein & Hobson, 2004). In contrast, $\delta^{15}N$ values

increase stepwise by 2-4‰ in a consumer's tissue relative to its diet (Vanderklift & Ponsard, 2003; Michener & Kaufman, 2007; Martínez del Rio et al., 2009), thus allowing the discrimination of trophic levels.

Identification of the trophic position of various biotic components of the pelagic ecosystem is essential for our understanding of ecosystem functioning and trophic interactions. Food chain length (i.e. number of TLs) is a descriptor of community structure and ecosystem functioning (Post et al., 2000). Measuring the length of a food chain integrates the assimilation of energy flow through all trophic pathways leading to top predators. The understanding of this is essential from an ecosystem-based management perspective, and may provide important insights on ecosystem responses to fisheries pressure and/or climate-induced changes. Knowledge of micronekton trophic interactions at seamount ecosystems of the SWIO are scarce and fragmentary. In order to investigate the trophic pathways at La Pérouse and MAD-Ridge, $\delta^{13}C$ and $\delta^{15}N$ values of POM, zooplankton and micronekton were measured and trophic levels were estimated using additive isotopic models (as in Post, 2002, and Caut et al., 2009). The main goals of this thesis were to investigate at La Pérouse and MAD-Ridge seamounts, (1) the trophic interactions of sampled mesopelagic organisms, (2) the influence of trophic groups, specimen size and time of sampling (MAD-Ridge only) on $\delta^{13}C$ and $\delta^{15}N$ values of micronekton, (3) the $\delta^{13}C$ and $\delta^{15}N$ values of omnivorous/carnivorous fishes collected over the flank relative to the vicinity of La Pérouse; and summit, flanks and vicinity of MAD-Ridge compared with an off-seamount location in the southern Mozambique Channel.

5.2 Material and methods

5.2.1 Study sites

5.2.1.1 La Pérouse seamount

La Pérouse is located on the outskirts of the oligotrophic ISSG province (Longhurst, 1998, 2007; Reygondeau et al., 2013), 160 km northwest of Réunion Island at latitude 19°43'S and longitude 54°10'E (Fig. 5.1a, b). The seamount summit reaches the euphotic zone, being ~60 m below the sea surface. The summit is 10 km long with narrow and steep flanks and rises from a depth of 5000 m from the ocean floor. This pinnacle was sampled on board the RV *Antea* from 15 to 29 September 2016 (DOI: 10.17600/16004500).

5.2.1.2 MAD-Ridge seamount

This topographic feature, located ~240 km to the south of Madagascar, along the Madagascar Ridge at latitude 27°29'S and longitude 46°16'E has been named "MAD-Ridge" in this study (Fig. 5.1a, c). The seamount rises from a depth of 1600 m from the ocean floor to ~240 m below the sea surface. The summit is 33 km long (north to south) and 22 km wide (east to west). MAD-Ridge is surrounded by four smaller pinnacles, reaching depths of 600 m, 900 m, 800 m and 1200 m below the sea surface, between latitudes 27°S-28°S and longitudes 46°E-46°45'E. The MAD-Ridge pinnacle was sampled on board the RV *Antea* (DOI: 10.17600/16004800 and 10.17600/16004900) from 26 November to 14 December 2016.

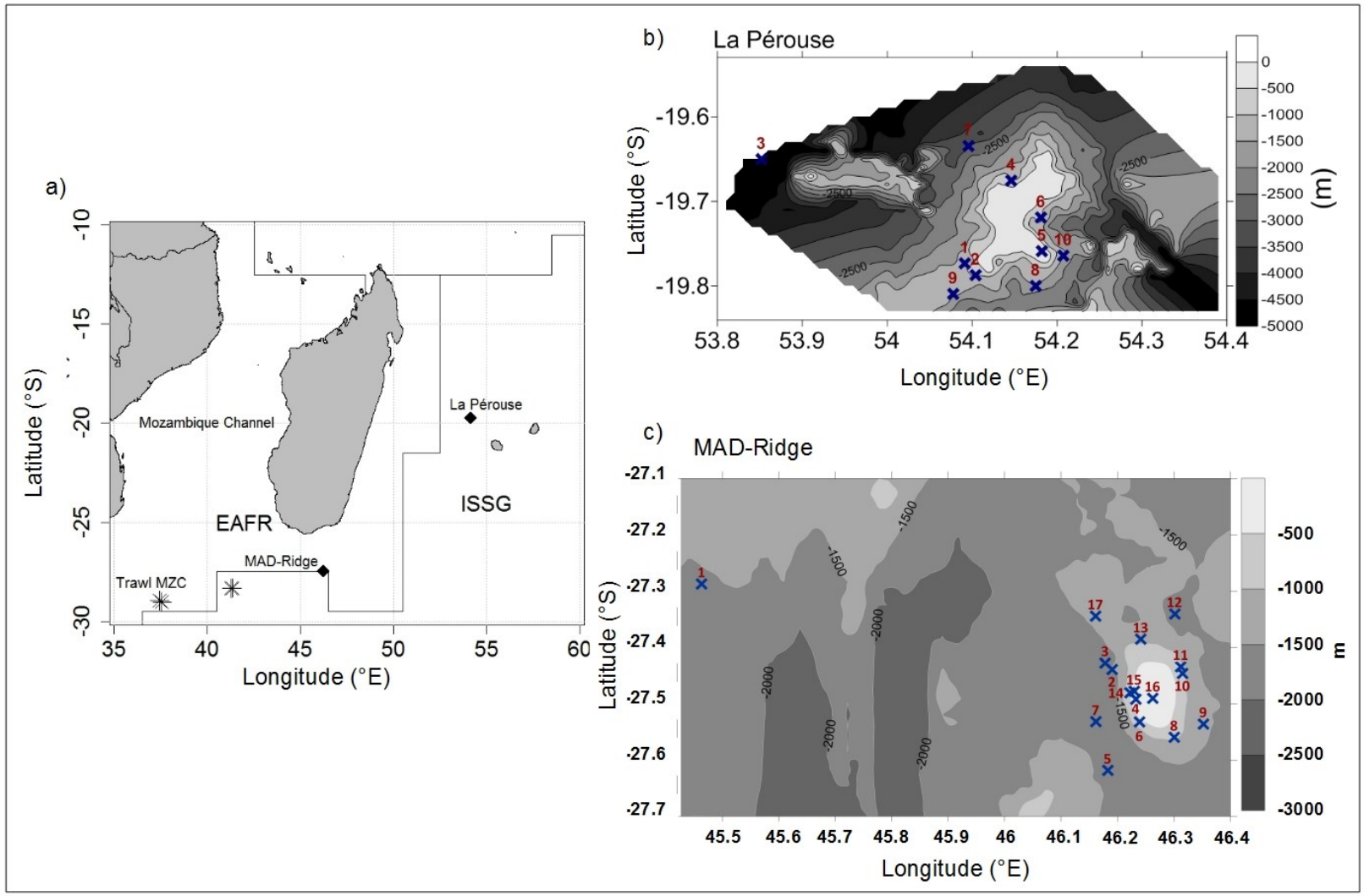

Figure 5.1(a) Location of the MAD-Ridge and La Pérouse seamounts (black diamond symbols) in the East African Coastal (EAFR) and Indian South Subtropical Gyre (ISSG) provinces, respectively. Longhurst's (1998) biogeochemical provinces are delimited by black solid lines. Landmasses are shown in grey. Trawls #18-21 in the southern Mozambique Channel are shown by black stars and labelled "Trawl MZC". Map of (b) La Pérouse trawl stations numbered 1 to 10, (c) MAD-Ridge trawl stations numbered 1 to 17 plotted on the bathymetry (m). The colour bar indicates depth below the sea surface (m).

5.2.2 Satellite observations

Sea surface chlorophyll data were downloaded from the MODIS dataset (http://oceancolor.gsfc.nasa.gov) at a daily and 4.5 km resolution. Five-day averages were calculated to obtain a proxy of phytoplankton abundance in the surface layer. To investigate the annual variability in surface chlorophyll *a* concentrations, monthly mean concentrations were averaged from January to December 2016 for the defined regions (La Pérouse: 18.5-20°S/53-33°E; MAD-Ridge: 27-28°S/44-48°E) (Fig. 5.2a).

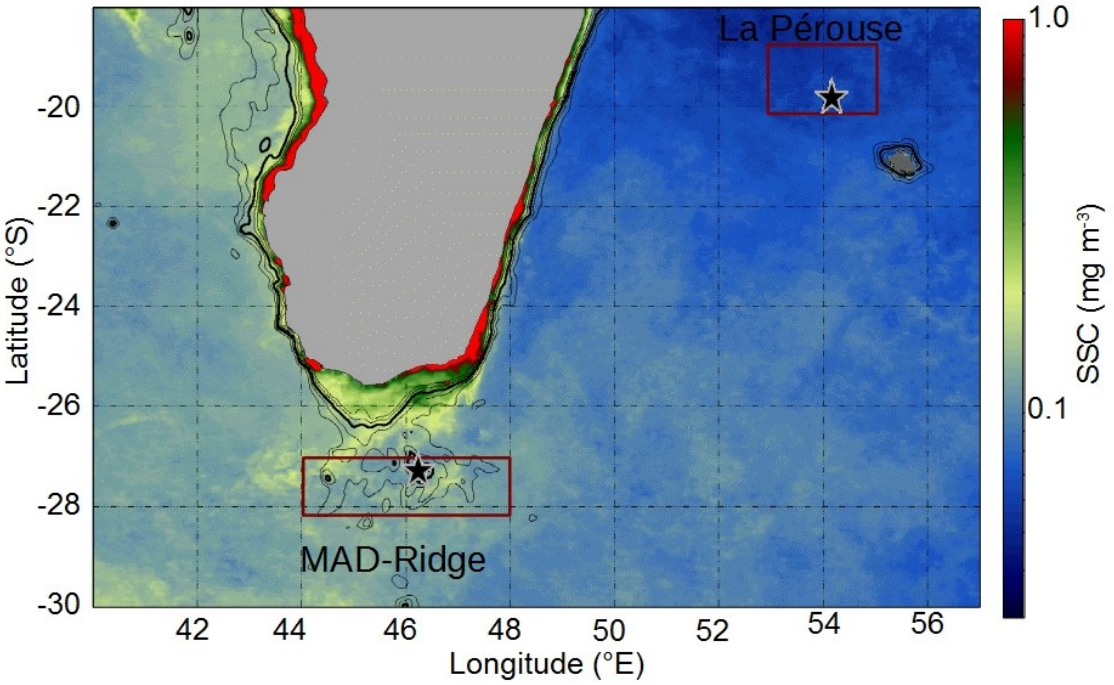

Figure 5.2(a) Averaged satellite image of surface chlrophyll a concentrations from 18/09/2016 to 07/12/2016 at La Pérouse and MAD-Ridge (represented by black star symbols). The colour bar indicates the mean concentrations in mg m^{-3}.

5.2.3 Sampling and sample processing

5.2.3.1 Particulate organic matter (POM)

During both cruises, water samples for stable isotope analyses of POM were collected using Niskin bottles mounted on a Sea-Bird 911 + CTD rosette system at approximately 5 m depth (referred to as POM-Surf) and at the depth of maximum fluorescence (referred to as POM-Fmax) between ~60 and 125 m at La Pérouse and ~80 and 150 m at MAD-Ridge. Between 4 and 8 l (depending on the load of each sample) of seawater were filtered on precombusted 25 or 47 mm glassfibre of 0.7 µm pore size. The filters were oven-dried at 50°C for 24 h and saved at room temperature in aluminium foil until further analyses.

5.2.3.2 Zooplankton sampling

Zooplankton samples were collected during daylight only with a Bongo net (300 µm mesh to a maximum depth of 500 m and 200 µm mesh to a maximum depth of ~200 m) towed obliquely at La Pérouse (10 stations). At MAD-Ridge, zooplankton samples were also collected during daylight with a Bongo net (300 µm mesh to a maximum depth of 500 m towed obliquely and 63 µm mesh to the depth of the maximum fluorescence towed vertically) at 19 stations. The nets were fitted with a flowmeter and were towed at a vessel speed of 1.5-2 knots for 15-20 min (0.28 m^2 mouth area). Zooplankton samples from the 200 and 300 µm meshes at La Pérouse and, from the 63 and 300 µm meshes at MAD-Ridge were combined at each station. The combined samples at each station were sieved on a stack of seven sieves of decreasing mesh size and divided into six fractions: >4000 µm, 4000-2000 µm, 2000-1000 µm, 1000-500 µm, 500-250 µm, 250-125 µm during La Pérouse and MAD-Ridge and a 7^{th} fraction (125-63 µm) during MAD-Ridge only. Each fraction was oven-dried at 50°C for 24 h and frozen on board at -20°C before being analysed for stable isotope analyses (section 5.2.4). Zooplankton abundances, biomasses and taxa composition at the seamounts and off-seamount locations are investigated in Noyon et al. 2020.

5.2.3.3 Trawl sampling

During both cruises, a 40-m long International Young Gadoid Pelagic Trawl (IYGPT) net (codend with 0.5 cm knotless nylon delta mesh; front tapering end with 8 cm mesh; ~96 m^2 mouth opening) was towed at a vessel speed of 2-3 knots for 60 min during La Pérouse and for 30 min during MAD-Ridge to sample mesopelagic organisms. Trawls were carried out in the shallow (0-200 m), intermediate (200-400 m) and deep (below 400 m) layers during both cruises (Table 5.1). Trawl stations at La Pérouse and MAD-Ridge (Fig. 5.1b, c) were further classified into the categories summit, flank and vicinity, according to whether they occurred on the summit plateaus of the seamounts, along the flanks (seafloor depth of 300-1300 m) or in the immediate vicinity (depth >1300 m). Four other mesopelagic trawls (#18-21) were conducted in the southern Mozambique Channel (depth >4000 m) during the MAD-Ridge cruise as reference stations for non-seamount locations within the EAFR province (Fig. 5.1a).

Table 5.1 Summary of trawl stations during La Pérouse and MAD-Ridge cruises

Cruise	Trawl #	Latitude Beginning (°S)	Longitude Beginning(°E)	Maximum Trawl Depth (m)	Seabed Depth (m)	Trawl Position	Day/Night
La Pérouse	1	19.77	54.09	590	2300	Vicinity	Night
	2	19.79	54.10	400	1240	Flank	Night
	3	19.65	53.85	90	4300	Vicinity	Night
	4	19.68	54.15	110	860	Flank	Night
	5	19.76	54.18	35	65	Summit	Day
	6	19.72	54.18	60	800	Flank	Night
	7	19.63	54.10	500	3100	Vicinity	Night
	8	19.80	54.17	430	1220	Flank	Night
	9	19.81	54.08	240	1750	Vicinity	Night
	10	19.76	54.21	250	1500	Vicinity	Night
MAD-Ridge	1	27.41	45.67	500	1560	Vicinity (northwest)	Day
	2	27.65	46.43	542	1515	Vicinity (northwest)	Night
	3	27.44	46.23	43	1560	Vicinity (northwest)	Night
	4	27.67	46.44	100	310	Flank (west)	Day
	5	27.75	46.28	324	1610	Vicinity (southwest)	Night
	6	27.69	46.46	45	605	Flank (southwest)	Night
	7	27.64	46.37	437	1680	Vicinity (southwest)	Day
	8	27.78	46.35	38	940	Flank (south)	Night
	9	27.70	46.45	76	1420	Vicinity (southeast)	Night
	10	27.60	46.53	470	950	Flank (northeast)	Day
	11	27.69	46.53	90	940	Flank (northeast)	Night
	12	27.41	46.38	550	1520	Vicinity (north)	Night
	13	27.65	46.31	460	1190	Flank (north)	Day
	14	27.68	46.27	210	575	Flank (west)	Night
	15	27.67	46.22	150	330	Flank (west)	Night
	16	27.59	46.32	205	240	Summit	Night
	17	27.51	46.32	550	1340	Vicinity (northwest)	Day

Cruise	Trawl #	Latitude Beginning (°S)	Longitude Beginning(°E)	Maximum Trawl Depth (m)	Seabed Depth (m)	Trawl Position	Day/Night
MAD-Ridge	18	28.25	41.26	550	4620	south Mozambique Channel	Night
	19	28.24	41.21	83	4630	south Mozambique Channel	Night
	20	28.82	37.39	450	4420	south Mozambique Channel	Night
	21	28.80	37.35	104	4420	south Mozambique Channel	Night

All organisms collected with the trawl were sorted on board, divided into four broad categories (gelatinous, crustaceans, cephalopods and fishes), counted and identified to the lowest possible taxon. Individuals from these four broad categories were randomly selected according to their occurrence and abundance and measured (total length for selected gelatinous organisms, abdomen and carapace length for selected crustaceans, dorsal mantle length for cephalopods and standard length for fishes). Approximately 2-5 mg of soft tissues of these selected individuals (muscle tissue for leptocephali, muscle abdomen for crustaceans, mantles for squids, dorsal muscle for fishes) and whole salps and pyrosomes, were sampled on board in 2 ml Eppendorf tubes and stored at -20°C, before being processed in the laboratory to determine $\delta^{13}C$ and $\delta^{15}N$ values (section 5.2.4). A full list of selected gelatinous and micronekton taxa used in stable isotope analyses is given in the Appendix (Table C).

5.2.4 Stable isotope analysis

Micronekton and zooplankton samples were freeze-dried using Christ Alpha 1-4 LSC freeze-dryers for 48 h and ground to a fine homogeneous powder using an automatic ball mill RETSCH MM200. As variations in lipid composition may influence $\delta^{13}C$ and $\delta^{15}N$ values (Bodin et al., 2009; Ryan et al., 2012), lipids were removed from zooplankton and micronekton samples with dichloromethane on an accelerated solvent extraction system (ASE®, Dionex; Bodin et al., 2009). Prior to $\delta^{13}C$ analyses, POM filters and zooplankton samples were reacted with 1 N HCl to remove carbonates (Cresson et al., 2012). Untreated subsamples of POM and zooplankton were used to measure $\delta^{15}N$ because acid treatment may lead to the loss of nitrogenous compounds (Kolasinski et al., 2008). POM filters were cut, folded and put into tin capsules. Approximately 400-600 µg of each zooplankton and micronekton sample were weighed and placed in tin capsules. These samples were run through continuous flow on a Thermo Scientific Flash EA 2000 elemental analyser coupled to a Delta V Plus mass spectrometer at the Pôle de Spectrométrie Océan (Plouzané, France). The samples were combusted in the elemental analyser to separate CO_2 and N_2. A reference gas set was used to determine isotopic ratios by comparison. The isotopic ratios are expressed in the conventional δ notations as parts per thousand (‰) deviations from the international standards:

$$\delta^{13}C \text{ or } \delta^{15}N \text{ (‰)} = [(R_{sample}/R_{standard}) - 1] \times 1000$$

where R is the ratio of $^{13}C/^{12}C$ or $^{15}N/^{14}N$.

5.2.5 Data analyses

5.2.5.1 Overall $\delta^{13}C$ and $\delta^{15}N$ signatures

Shapiro-Wilk and Bartlett tests were computed to test for the assumptions of normality and homogeneity of variances. Links between $\delta^{13}C$ and $\delta^{15}N$ values and the foodweb components (POM-Surf, POM-Fmax, zooplankton, gelatinous organisms, crustaceans, squids and fishes), were investigated using Kruskal-Wallis (KW) tests and pairwise comparisons in R (version 3.3.1) because the data did not follow normal distributions. Kruskal-Wallis tests and pairwise comparisons were also computed to investigate whether there was a significant difference in $\delta^{13}C$ and $\delta^{15}N$ values for each the foodweb component between La Pérouse and MAD-Ridge. To assess the association between $\delta^{13}C$ and $\delta^{15}N$ values, Spearman rank correlation coefficients were calculated with all foodweb components at each seamount. Wilcoxon rank sum tests investigated the effect of time (day or night) on $\delta^{13}C$ and $\delta^{15}N$ values of gelatinous plankton and micronekton at MAD-Ridge only (because a single daylight trawl was conducted at La Pérouse and too few species were caught). To test for the effect of trawl position with respect to the seamounts on $\delta^{13}C$ and $\delta^{15}N$ values of omnivorous/carnivorous fishes, Wilcoxon Rank sum tests and KW tests were performed on the La Pérouse and MAD-Ridge datasets, respectively.

5.2.5.2 Layman community-wide metrics

The Layman community-wide metrics SEA_c and the $\delta^{13}C$ and $\delta^{15}N$ ranges (Layman et al., 2007) were calculated using the SIBER package (version 2.1.4, Jackson et al., 2011). The SEA_c (sample-size-corrected standard ellipse area) describes the overall extent of the isotopic niches. The SEA_c is robust for sample sizes >10 (Daly et al., 2013), which is the case for all the broad categories within this study. The SEA_c of each foodweb component was described in terms of the space occupied by the group on a $\delta^{15}N$-$\delta^{13}C$ plot based on all the individuals sampled within the group. The $\delta^{13}C$ and $\delta^{15}N$ ranges were used to describe and compare the overall extents of the foodwebs at the La Pérouse and MAD-Ridge sites. Increased $\delta^{13}C$ range would be expected in foodwebs with multiple basal sources with varying $\delta^{13}C$ values suggesting niche diversification at the base of the foodweb, whereas the $\delta^{15}N$ range describes the sampled food chain lengths (Portail et al., 2016).

5.2.5.3 Trophic level estimations

Different models have been applied across several studies to estimate the trophic level of organisms: additive model with a fixed enrichment factor, additive enrichment model with a variable isotopic enrichment or scaled model with decreasing isotopic enrichment factors

(Minagawa & Wada, 1984; Post, 2002; Caut et al., 2009; Hussey et al., 2014). Ménard et al. (2014) and Annasawmy et al. (2018) used a fixed enrichment factor of 3.2‰ to estimate trophic levels of foodweb components POM, zooplankton, gelatinous plankton and micronekton collected in the SWIO. In this study, two alternative trophic enrichment assumptions were compared to estimate the trophic level of all the measured individuals within the groups (zooplankton, gelatinous organisms, crustaceans, squids and fishes) at La Pérouse and MAD-Ridge.

The TPA model (additive model with constant isotopic enrichment) was proposed by Minagawa & Wada (1984) and Post (2002) with the reference level set at a trophic level of 2 for the primary consumer and a fixed and additive enrichment factor of 3.2‰:

$$\text{Trophic level, TPA} = 2.0 + \frac{\delta^{15}N_i - \delta^{15}N_{\text{primary consumer}}}{3.2} \quad \text{Eq. 1}$$

where, $\delta^{15}N_i$ is the nitrogen isotopic composition of any given micronekton taxon i, $\delta^{15}N_{\text{primary consumer}}$ is the $\delta^{15}N$ reference baseline value at trophic level 2, and 3.2‰ is an estimate of the trophic enrichment factor between consumers and their primary prey (Michener & Kaufman, 2007; Vanderklift & Ponsard, 2003). The $\delta^{15}N$ values of POM, primary consumers and zooplankton have been used in trophic level calculations as isotopic baseline (e.g. Lorrain et al., 2015). Primary consumers are generally used as baseline to reduce errors in estimations (Martínez del Rio et al., 2009). Salps are known filter-feeders that have been used as baseline in previous studies in the region (Ménard et al., 2014). At La Pérouse, the mean $\delta^{15}N$ values of six pyrosomes and one salp specimen was estimated at 5.31 ± 0.31‰ and was used as $\delta^{15}N_{\text{primary consumer}}$ to estimate the trophic position of all upper trophic level individuals that were collected. At MAD-Ridge, the mean $\delta^{15}N$ values of six salps was 4.22 ± 1.01‰ and was used as $\delta^{15}N_{\text{primary consumer}}$ to estimate the trophic position of all individuals sampled.

The second model, TPC, is an additive trophic enrichment model with variable isotopic enrichment, estimated from a meta-analysis study on fish muscle (Caut et al. 2009):

$\text{TEF} = -0.281\ \delta^{15}N_{\text{primary consumer}} + 5.879$, where TEF is the trophic enrichment factor

$$\text{TPC} = 2.0 + [(\delta^{15}N_i - \delta^{15}N_{\text{primary consumer}})/\text{TEF}] \quad \text{Eq. 2}$$

5.2.5.4 Micronekton habitat ranges and feeding mode

Information on habitat ranges of selected micronekton individuals was obtained from the literature (Clarke & Lu, 1975; Pearcy et al., 1977; Smith & Heemstra, 1986; van der Spoel &

Bleeker, 1991; Brodeur & Yamamura, 2005; Davison et al., 2015; Romero-Romero et al., 2019). Organisms were classified as being epipelagic (<200 m), mesopelagic (from 200 to 1000 m), bathypelagic (below 1000 m to ~100 m from the seafloor) and benthopelagic (living near the bottom) according to definitions of the vertical zonation of the pelagic ocean from Del Giorgio & Duarte (2002) and Sutton (2013). The feeding modes of gelatinous plankton and selected micronekton were obtained from the literature and are summarised in the Appendix section (Table C). Organisms were classified into the four trophic groups filter-feeders (salps and pyrosomes), detritivores (leptocephali), omnivores (mainly crustaceans and the fish species *Ceratoscopelus warmingii*) and carnivores (most mesopelagic fishes and squids). Crustaceans were classified as omnivores because they prey on zooplankton, such as euphausiids and copepods and are also known for occasional herbivory (Hopkins et al., 1994; Birkley & Gulliksen, 2003; Mauchline, 1959; Foxton & Roe, 1974). Most mesopelagic fishes were classified as carnivores since they were reported to be zooplankton feeders, preying on copepods, amphipods, euphausiids and ostracods (Dalpadado & Gjøsaeter, 1988; Pakhomov et al., 1996; Tanaka et al., 2007; Hudson et al., 2014; Bernal et al., 2015; Carmo et al., 2015; Young et al., 2015), with no herbivorous feeding strategy except *C. warmingii*, that has developed an adaptive response to competition in low-productive environments (Robison, 1984). For species with unknown diets, the feeding mode was determined based on the feeding habit identified from species within the same genus.

In order to give an overview of the foodwebs at the La Pérouse and MAD-Ridge seamounts, hierarchical cluster analyses (average grouping methods) were carried out on resemblance matrices (calculated using Euclidean distances) of normalised $\delta^{13}C$ and $\delta^{15}N$ values per gelatinous plankton and micronekton species at each seamount and for all sampled stations in PRIMER v6 software according to Clarke & Warwick (2001). Further cluster analyses were performed on log-transformed $\delta^{13}C$ values and normalised $\delta^{13}C$ and $\delta^{15}N$ values of micronekton (excluding the outliers salps, pyrosomes, *Funchalia* sp. and leptocephali) for each seamount.

5.2.5.5 Effect of size on $\delta^{15}N$ values of micronekton

The size distributions of all gelatinous and micronekton organisms captured during the La Pérouse and MAD-Ridge cruises were heavily left-skewed with most organisms being <100 mm in length due to net catchability and selectivity. To test for the effect of size on $\delta^{15}N$ values, gelatinous and micronekton organisms <100 mm were considered and linear regressions were computed. Linear models were developed to investigate the effect of body lengths on $\delta^{13}C$ and

$\delta^{15}N$ values of gelatinous and micronekton individuals and to investigate the difference in $\delta^{15}N$ values with respect to size between La Pérouse and MAD-Ridge. Additionally, eight micronekton specimens were selected according to their common occurrence at both seamounts, relatively large sample sizes and wide body length ranges, and their $\delta^{15}N$ values were compared between the two seamounts. Information on the migration patterns of these eight taxa was obtained from the literature (Utrecht et al., 1987; Butler et al., 2001; Feunteun et al., 2015; Romero-Romero et al., 2019).. Linear regressions were fitted to $\delta^{15}N$ values of these eight taxa according to their body lengths and the seamount factor (whether $\delta^{15}N$ values were significantly different between La Pérouse and MAD-Ridge). To investigate if the seamount has an effect on the size and related diet of fish, $\delta^{15}N$ values of selected omnivorous/ carnivorous fish species collected on the summits, flanks, vicinity of the seamounts and the southern Mozambique Channel, were examined using linear models.

5.3 Results

5.3.1 Prevailing environmental conditions at La Pérouse and MAD-Ridge seamounts

Sea surface chlorophyll concentrations followed the same seasonal pattern in both regions of La Pérouse and MAD-Ridge seamounts, although concentrations were twice as high at MAD-Ridge (0.10-0.22 mg m^{-3}) relative to La Pérouse (0.04-0.13 mg m^{-3}) all year round (Fig. 5.2b). A peak in productivity was observed in July in both the ISSG and EAFR provinces because of intense mixing caused by austral trade winds. Both La Pérouse and MAD-Ridge cruises took place during a declining phase of oceanic productivity in the region.

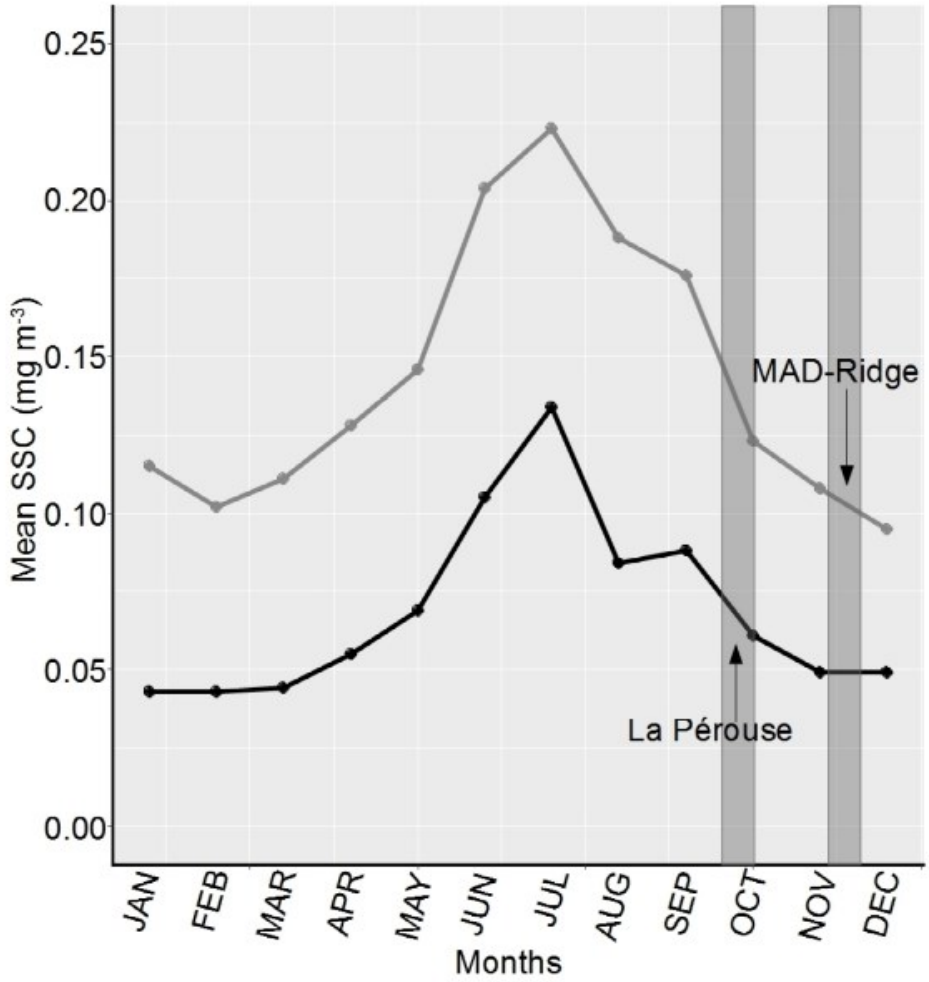

Figure 5.2(b) Monthly mean sea surface chlorophyll a concentrations (mg m^{-3}) from January to December 2016 for the regions defined by the red squares in Figure 5.2(a). The dates of the La Pérouse and MAD-Ridge cruises are marked by grey bars.

5.3.2 General foodweb structure

The description of the foodweb structure included POM collected at the surface (POM-Surf) and at the depth of maximum fluorescence (POM-Fmax), zooplankton at both seamounts, two taxonomic groups of gelatinous organisms (salps and pyrosomes), and 42 and 49 taxonomic groups of micronekton, representing 145 and 180 individuals at La Pérouse and MAD-Ridge, respectively. At both La Pérouse and MAD-Ridge, the foodweb components were segregated in their $\delta^{13}C$ (La Pérouse: KW, $H=170.5$, $p < 0.05$; MAD-Ridge: KW, $H=268.1$, $p < 0.05$) and $\delta^{15}N$ values (La Pérouse: KW, $H=153.1$, $p < 0.05$; MAD-Ridge: KW, $H=127.4$, $p < 0.05$) (Fig. 5.3). POM-Surf and POM-Fmax did not differ significantly in their $\delta^{13}C$ and $\delta^{15}N$ values at both seamounts ($p > 0.05$). At La Pérouse, gelatinous organisms exhibited higher $\delta^{13}C$ values compared with POM-Surf and POM-Fmax ($p < 0.05$), and they exhibited lower $\delta^{13}C$ and $\delta^{15}N$

values than crustaceans, fishes and squids at both seamounts ($p < 0.05$). Crustaceans, fishes and squids did not differ significantly in their $\delta^{15}N$ values ($p > 0.05$), but they differed in their $\delta^{13}C$ values at La Pérouse ($p < 0.05$). Crustaceans did not differ significantly from squids in their $\delta^{13}C$ values ($p > 0.05$), whereas all other categories differed in their $\delta^{13}C$ values at MAD-Ridge ($p < 0.05$). Squids did not differ significantly from crustaceans and fishes in their $\delta^{15}N$ values ($p > 0.05$) but ^{15}N was more depleted in crustaceans relative to fishes at MAD-Ridge ($p < 0.05$). At La Pérouse (all depths combined), POM, zooplankton and micronekton covered a large $\delta^{13}C$ range of ~11‰ (-17.2 to -28.0‰), with POM-Fmax and the unidentified caridean crustacean representing the lowest and highest values, respectively. The $\delta^{15}N$ values of all micronekton individuals ranged from 2.5‰ (fish: leptocephali) to 13.3‰ (fish: *Coccorella atrata*). At MAD-Ridge (all depths combined), POM, zooplankton and micronekton also covered a large $\delta^{13}C$ range of ~10‰ (-17.1 to -27.2‰), with POM-Surf and the fish species *Chauliodus sloani* representing the lowest and highest values, respectively. The $\delta^{15}N$ values of sampled micronekton individuals ranged from 2.3‰ (fish: leptocephali) to 13.5‰ (fish: *Argyropelecus aculeatus*).

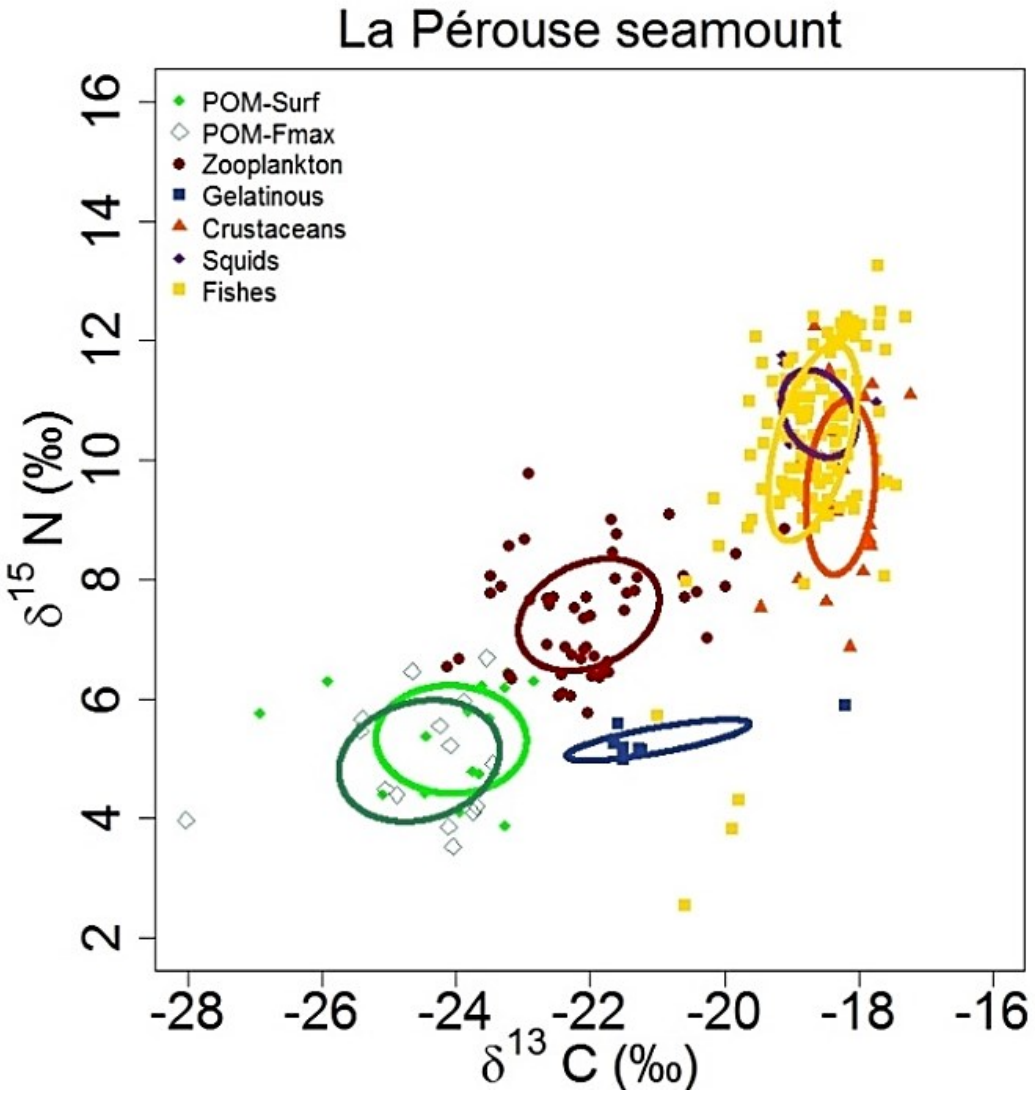

Figure 5.3(a) Bivariate plot of $\delta^{15}N$ and $\delta^{13}C$ values (‰) for particulate organic matter at the surface (POM-Surf) and the maximum fluorescence (POM-Fmax), zooplankton, gelatinous organisms, crustaceans, squids and mesopelagic fishes sampled at La Pérouse seamount. Standard ellipse areas (coloured solid lines), calculated using SIBER, provide estimates of the size of the isotopic niche for each of these categories.

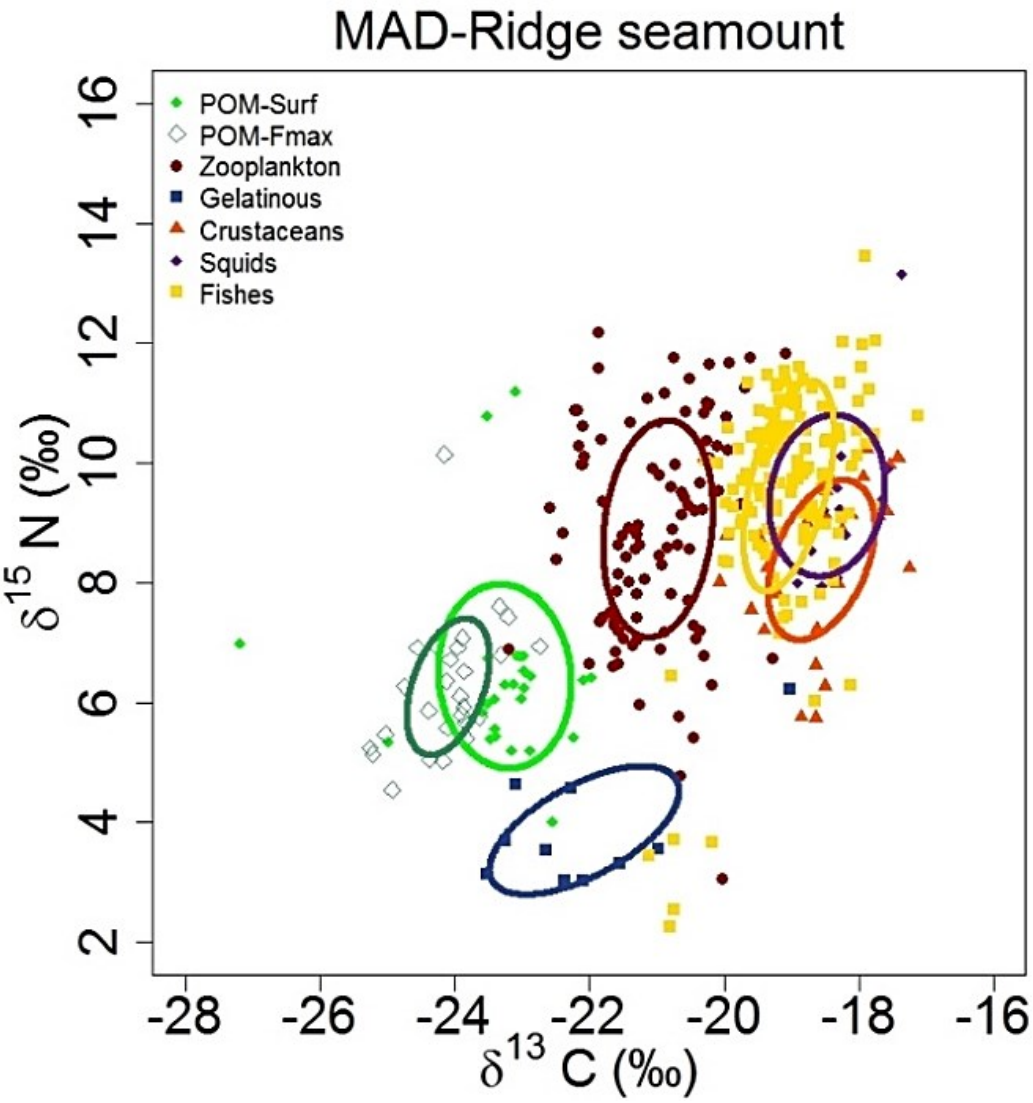

Figure 5.3(b) Bivariate plot of $\delta^{15}N$ and $\delta^{13}C$ values (‰) for particulate organic matter at the surface (POM-Surf) and the maximum fluorescence (POM-Fmax), zooplankton, gelatinous organisms, crustaceans, squids and mesopelagic fishes sampled at MAD-Ridge seamount. Standard ellipse areas (coloured solid lines), calculated using SIBER, provide estimates of the size of the isotopic niche for each of these categories.

Standard ellipse corrected areas (SEA_c) refer to the trophic niche widths of the broad categories at La Pérouse and MAD-Ridge. At La Pérouse, POM-Surf and POM-Fmax showed overlapping standard ellipses with the largest SEA_c (3.2 and 3.8‰^{2}, respectively) among all components of the foodweb (Fig. 5.3a). Gelatinous organisms showed the smallest SEA_c of 0.92‰^{2}. Crustaceans, squids and fishes had overlapping standard ellipses with SEA_c values of 2.3, 1.2 and 2.9‰^{2}, respectively (Fig. 5.3a). At MAD-Ridge, POM-Surf and POM-Fmax also exhibited overlapping standard ellipses (SEAc= 4.8 and 2.0‰^{2}, respectively), but with greater

variability in POM-Surf $\delta^{15}N$ values. Crustaceans, squids and fishes had overlapping standard ellipses with SEA_c of 3.0, 3.6 and 3.2‰^{2}, respectively (Fig. 5.3b).

The $\delta^{13}C$ and $\delta^{15}N$ values of the foodweb components POM-Surf, POM-Fmax, zooplankton, gelatinous organisms, crustaceans, squids and fishes were significantly different between La Pérouse and MAD-Ridge ($\delta^{13}C$: KW, H=474.4, df=13, $p < 0.05$; $\delta^{15}N$: KW, H=311.3, df=13, $p < 0.05$, Fig. 5.4). Pairwise comparisons showed $\delta^{13}C$ values of POM-Surf, zooplankton and fishes to differ significantly between La Pérouse and MAD-Ridge ($p < 0.05$ each) (Fig. 5.4). The median $\delta^{13}C$ and $\delta^{15}N$ values of lower trophic level foodweb components: POM-Surf, POM-Fmax and zooplankton were greater at MAD-Ridge ($\delta^{13}C$: -23.1, -24.1, -20.9‰; $\delta^{15}N$: 6.3, 6.1 and 8.9‰, respectively) than at La Pérouse ($\delta^{13}C$: -23.7, -24.1, -22.1‰; $\delta^{15}N$: 5.5, 4.9 and 7.5‰, respectively) (Fig. 5.4). Gelatinous organisms, crustaceans and fishes displayed higher median $\delta^{13}C$ values at La Pérouse (-21.5, -18.4 and -18.7‰, respectively) than at MAD-Ridge (-22.4, -18.6 and -19.1‰, respectively) (Fig. 5.4). Gelatinous organisms, crustaceans, squids and fishes also exhibited higher median $\delta^{15}N$ values at La Pérouse (5.2, 9.8, 10.7 and 10.4‰, respectively) than at MAD-Ridge (3.7, 8.8, 9.5 and 10.0‰, respectively) (Fig. 5.4) but differences were not statistically significant ($p > 0.05$ each). The $\delta^{13}C$ values of crustaceans, squids and mesopelagic fishes encompassed the same narrow range at La Pérouse and MAD-Ridge (-17.2 to -21.0‰ and -17.1 to -21.1‰, respectively). Gelatinous salps and pyrosomes exhibited $\delta^{13}C$ values of -18.2 to -21.7‰ at La Pérouse and -19.0 to -23.5‰ at MAD-Ridge.

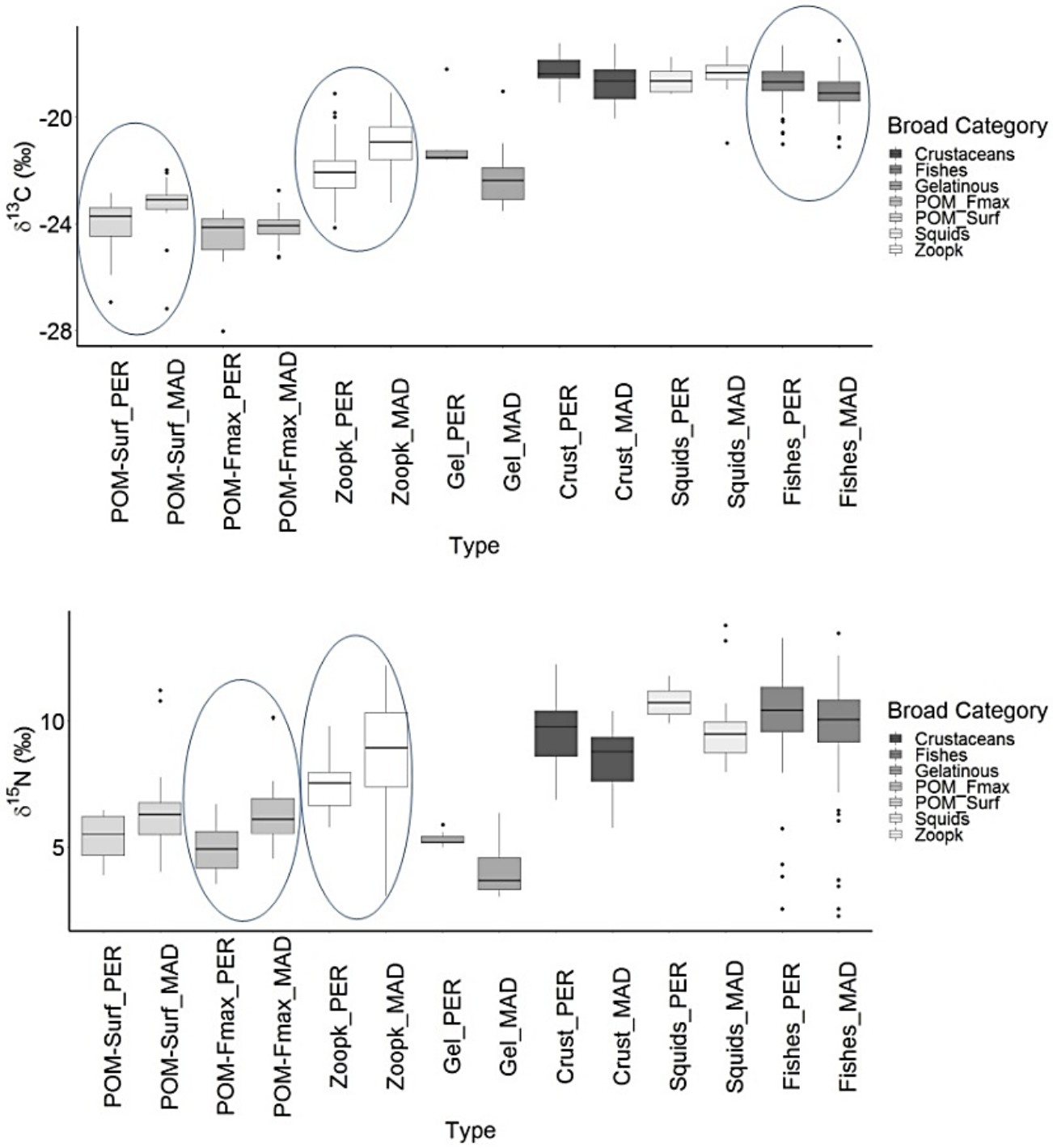

Figure 5.4 Boxplots of $\delta^{13}C$ and $\delta^{15}N$ values (‰) of the foodweb components POM-Surf, POM-Fmax, zooplankton (Zoopk), gelatinous organisms (Gel), crustaceans (Crust), squids and mesopelagic fishes at La Pérouse (PER) and MAD-Ridge (MAD). Groups having significantly different $\delta^{13}C$ and $\delta^{15}N$ values (‰) are shown by solid blue lines.

5.3.3 Relationships between $\delta^{13}C$ and $\delta^{15}N$ values

Ascending the foodweb, from POM-Surf to mesopelagic fishes at La Pérouse and MAD-Ridge seamounts, there was a general increase in $\delta^{13}C$ and $\delta^{15}N$ values (Figs. 5.3 and 5.4). There was a significantly positive correlation between $\delta^{13}C$ and $\delta^{15}N$ values of all sampled components of the foodweb at La Pérouse and MAD-Ridge seamount stations ($p < 0.05$), with Spearman correlation coefficients of $r= 0.74$ and $r= 0.51$, respectively.

5.3.4 Trophic levels at La Pérouse and MAD-Ridge seamounts

Albeit small differences in trophic positions between the two methods, they both identified the same organisms at the lowest (leptocephali and gelatinous organisms) and highest (mesopelagic fishes excluding leptocephali, and squids) trophic positions. For comparison with other studies published in the region (Ménard et al., 2014; Annasawmy et al., 2018), the additive trophic enrichment model with fixed enrichment factor, TPA, (Eq. 1), is explored in further details.

Leptocephali showed estimated TL values (from Eq. 1) of 1.9 and 1.8 at both La Pérouse and MAD-Ridge, respectively (Fig. 5.5a, b). TL values of crustaceans fell between 2.7 (La Pérouse and MAD-Ridge: *Funchalia* sp.) and 3.7 (La Pérouse: Sergestidae; MAD-Ridge: Oplophoridae). Squids had TL values of 3.6 (*Abraliopsis* sp.) and 4.0 (*Histioteuthis* spp.) at La Pérouse. At MAD-Ridge seamount, smaller-sized nektonic squids (26-111 mm DML) displayed TL values of 3.2 (Enoploteuthidae) and 3.6 (*Abraliopsis* sp.), and larger-sized nektonic squids (365-367 mm DML) had TL values of 4.0 (*Histioteuthis* spp.) and 4.8 (*O. bartramii*). TL values of fishes (excluding leptocephali) fell between 3.2 (*C. warmingii*) and 4.5 (*C. atrata*) at La Pérouse and between 2.6 (*Decapterus macarellus*) and 4.4 (*Stomias longibarbatus*) at MAD-Ridge (Fig. 5.5a, b). Overall, the TL values of the micronekton broad categories displayed the same range of TL values at both seamounts.

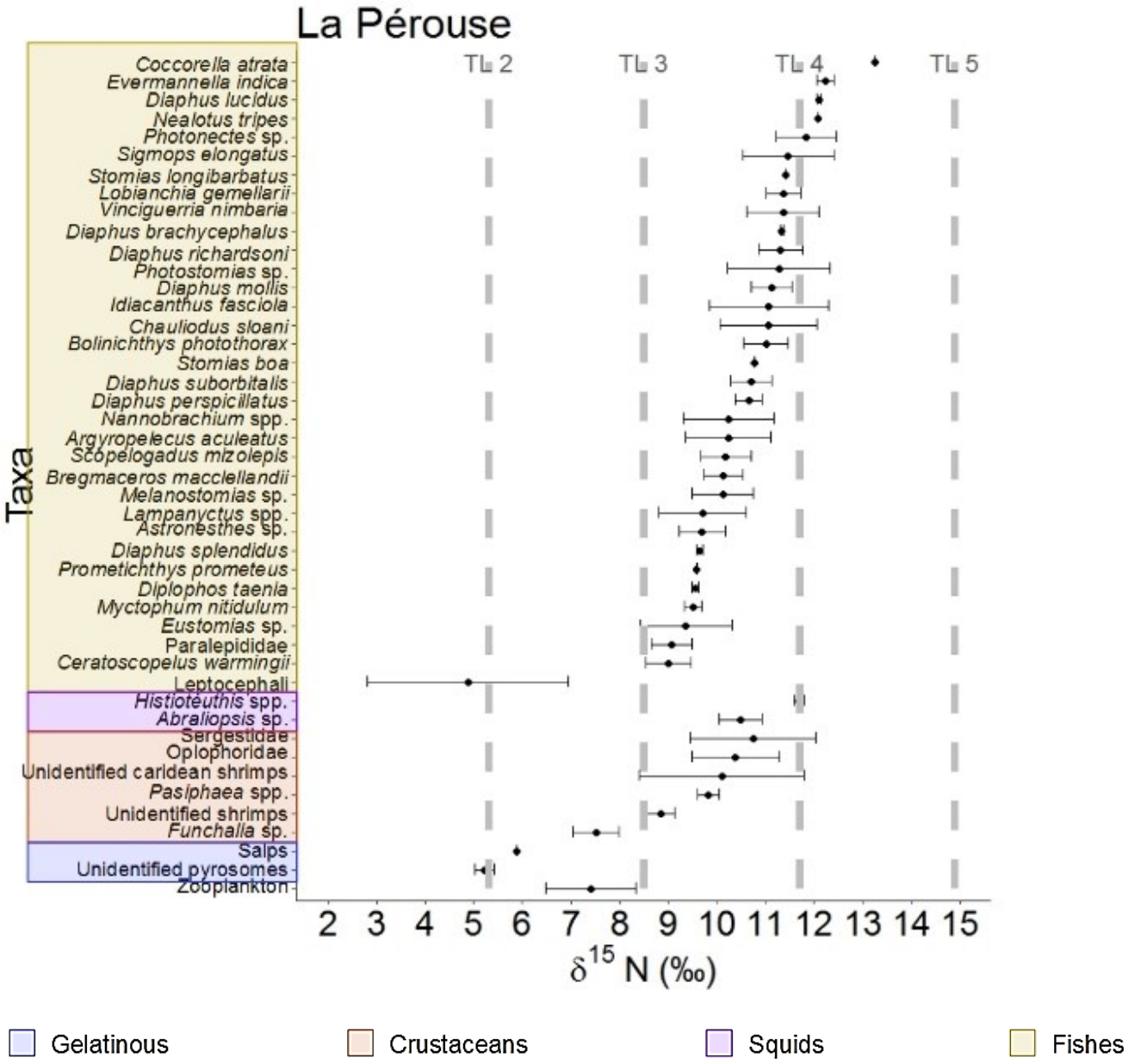

Figure 5.5(a) $\delta^{15}N$ (mean ± S.D.) values (‰) and estimated trophic level (TL as estimated from the TPA method) of POM-Surf, POM-Fmax, zooplankton, gelatinous and sampled micronekton species at the La Pérouse seamount. Taxa are placed in their broad categories and $\delta^{15}N$ compositions are sorted in ascending order of their values.

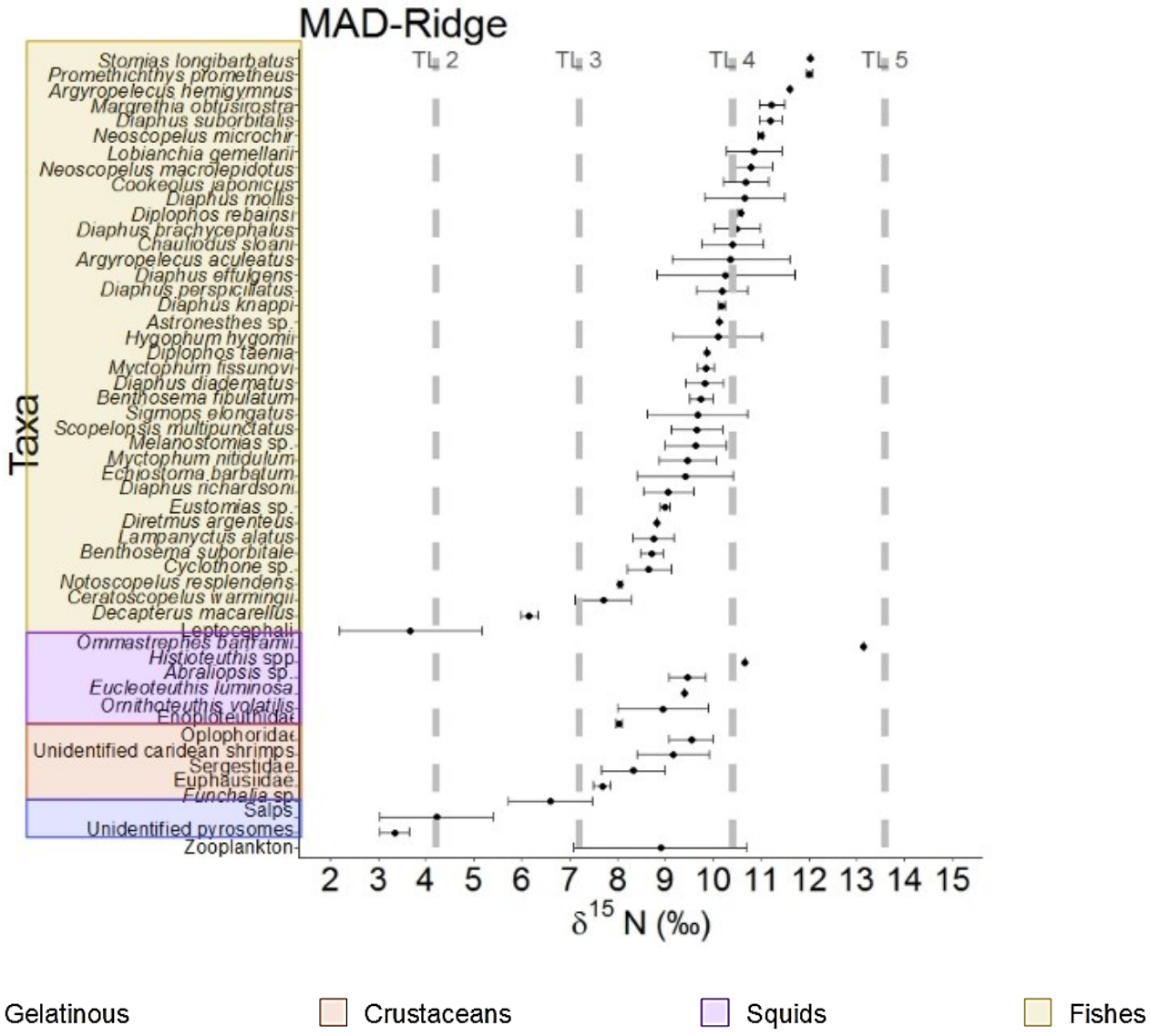

Figure 5.5(b) $\delta^{15}N$ (mean ± S.D.) values (‰) and estimated trophic level (TL as estimated from the TPA method) of POM-Surf, POM-Fmax, zooplankton, gelatinous and sampled micronekton species at the MAD-Ridge seamount. Taxa are placed in their broad categories and $\delta^{15}N$ compositions are sorted in ascending order of their values.

5.3.5 Effect of feeding mode of gelatinous plankton and micronekton on stable isotope values

The trophic groups identified by cluster analyses are in general agreement with the postulated feeding habits of the group members at both La Pérouse and MAD-Ridge seamounts, although significant differences exist when individual species are considered. The cluster analyses based on $\delta^{13}C$ and $\delta^{15}N$ values identified two main groups, designated I and II, and two subgroups within group I and group II at La Pérouse and MAD-Ridge (Fig. 5.6a). At La Pérouse, Group I included the filter-feeding pyrosomes (IA) and the detritivorous leptocephali (IB) that showed

similar $\delta^{13}C$ values (-21.5 ± 0.2 and -20.4 ± 0.5‰, respectively) and $\delta^{15}N$ values (5.2 ± 0.2 and 4.9 ± 2.1‰, respectively). Group IIa compared a single salp specimen ($\delta^{13}C$: -18.2‰ and $\delta^{15}N$: 5.9‰) and an omnivorous crustacean *Funchalia* sp. with similar $\delta^{13}C$ and $\delta^{15}N$ values (-18.7 ± 0.6 and 7.5 ± 0.5‰, respectively). All other crustaceans having an omnivorous feeding mode displayed greater $\delta^{15}N$ values (10.0 ± 1.1‰) and were thus segregated within subgroup IIB along with carnivorous mesopelagic fishes and squids (Fig. 5.6a). All values are given in mean ± S.D.

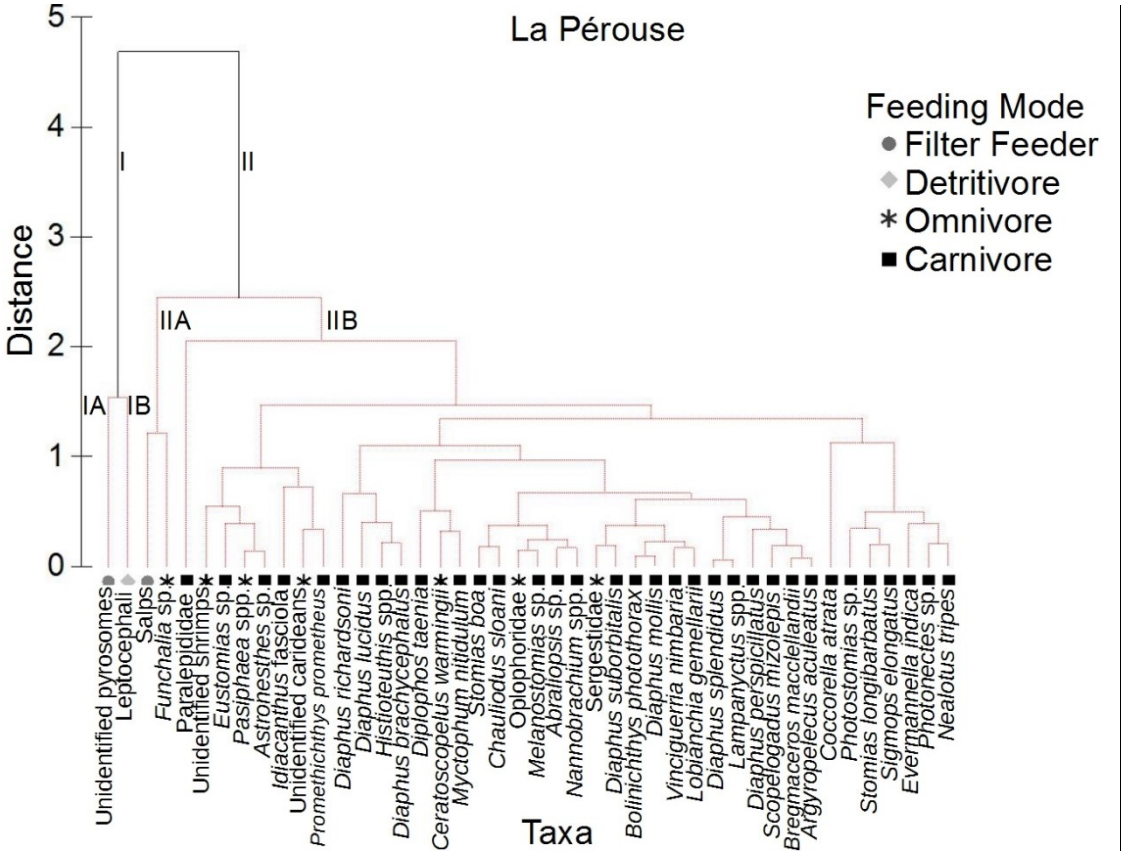

Figure 5.6(a) Hierarchical clustering (Euclidean distance of normalised data subjected to averaged grouping) of $\delta^{13}C$ and $\delta^{15}N$ values (‰) of sampled gelatinous organisms, crustaceans, squids and mesopelagic fishes at La Pérouse seamount. Roman numerals at the tree branches identify groups of species belonging to the different trophic guilds: group I– filter-feeders and detritivores; group II- omnivores and carnivores; subgroup IA- filter-feeders; subgroup IB- detritivores; subgroup IIA- filter-feeders and omnivorous crustaceans; subgroup IIB- omnivorous and carnivorous micronekton.

At MAD-Ridge, Group I included filter feeding pyrosomes (IA) and salps, and detritivorous leptocephali (IB) that exhibited the most depleted $\delta^{13}C$ and $\delta^{15}N$ values relative to omnivorous and carnivorous micronekton (Fig. 5.6b). Group II was subdivided into Group IIA and included the squid *O. bartramii*, the fishes *Promethichthys prometheus* and *S. longibarbatus*, all three having carnivorous feeding modes with similar $\delta^{13}C$ values and the highest $\delta^{15}N$ values for the

greatest sizes. The single large squid *Histioteuthis* spp. (DML: 367 mm) showed a high $\delta^{15}N$ value of 10.7‰ and a more depleted $\delta^{13}C$ value of -21.0‰ compared with *O. bartramii*, *P. prometheus* and *S. longibarbatus*. This squid was hence segregated from subgroup IIA. All other omnivorous and carnivorous organisms exhibited lower $\delta^{15}N$ values (Fig. 5.6b) and were thus included within subgroup IIB. Cluster analyses run on $\delta^{13}C$ and $\delta^{15}N$ values of micronekton and excluding the outliers salps, pyrosomes, *Funchalia* sp. and leptocephali, also segregated individuals according to their feeding mode at MAD-Ridge ($p < 0.05$).

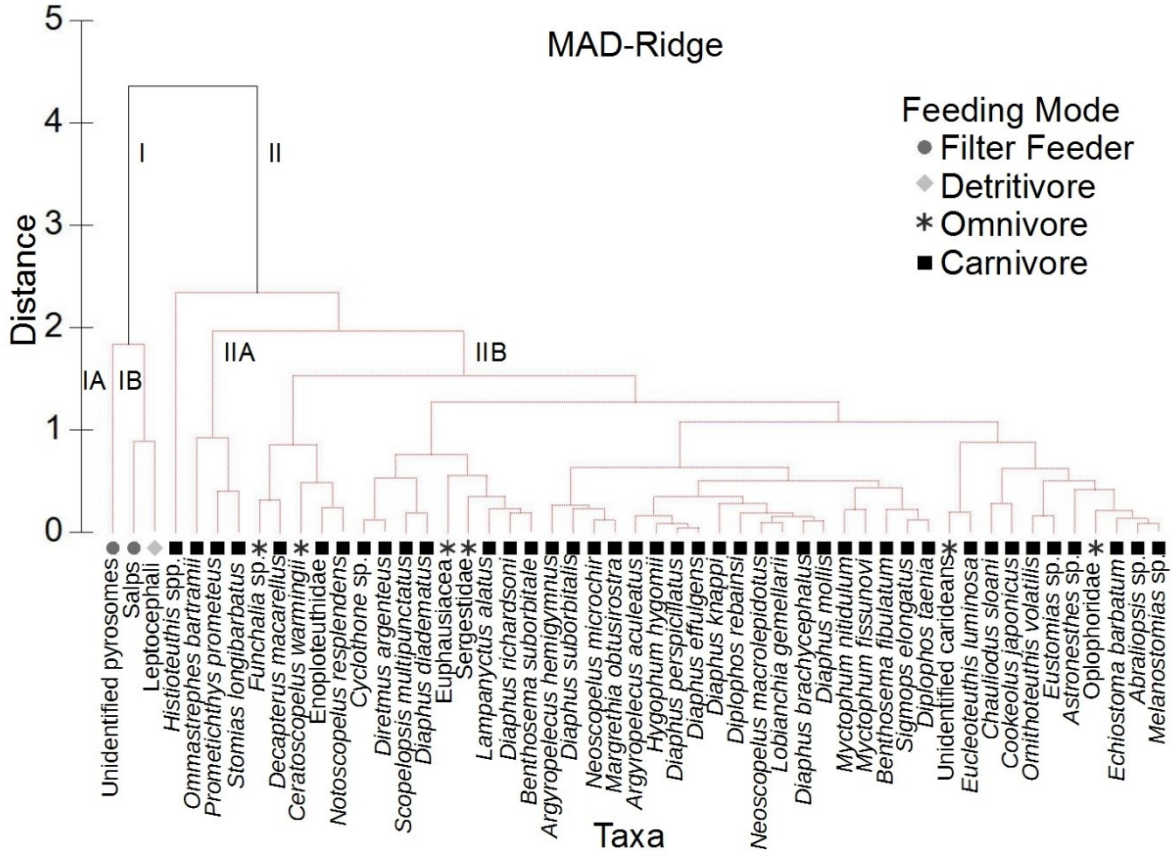

Figure 5.6(b) Hierarchical clustering (Euclidean distance of normalised data subjected to averaged grouping) of $\delta^{13}C$ and $\delta^{15}N$ values (‰) of sampled gelatinous organisms, crustaceans, squids and mesopelagic fishes at MAD-Ridge. Roman numerals at the tree branches identify groups of species belonging to the different trophic guilds: group I– filter-feeders and detritivores; group II- omnivores and carnivores; subgroup IA- filter-feeders; subgroup IB- detritivores; subgroup IIA- highest trophic level mesopelagic fishes at MAD-Ridge; subgroup IIB- omnivorous and carnivorous micronekton.

5.3.6 Effect of size of micronekton on $\delta^{15}N$ values

The $\delta^{15}N$ values of individuals were significantly influenced by their sizes at both La Pérouse ($F_{1,113}=6.695$, $p < 0.05$) and MAD-Ridge ($F_{1, 160}= 23.33$, $p < 0.05$), with increasing $\delta^{15}N$ values as the size of the organisms increased (La Pérouse: $\delta^{15}N_{\text{gelatinous and micronekton <100 mm}} = 8.83 + 0.02$ x Size; MAD-Ridge: $\delta^{15}N_{\text{gelatinous and micronekton <100 mm}} = 7.33 + 0.03$ x Size). Eight micronekton

species were further selected according to sample size, their common occurrence at both seamounts, their wide body length ranges, differing feeding modes and vertical migration patterns. The $\delta^{15}N$ values of the selected species *Sigmops elongatus* (carnivore; diel vertical migrator) and *C. warmingii* (omnivore; diel vertical migrator) were significantly influenced by their lengths (Fig. 5.7a, 5.7b, Table 5.2), with higher $\delta^{15}N$ values at La Pérouse than at MAD-Ridge. The $\delta^{15}N$ values of the fish *A. aculeatus* (carnivore, mid-water migrant) and of the crustacean *Funchalia* sp. (omnivore, diel vertical migrator) were significantly influenced by their lengths but were not significantly different between La Pérouse and MAD-Ridge (Fig. 5.7c, 6.7d, Table 5.2). The mesopelagic fish *D. suborbitalis* and the squid *Abraliopsis* sp. (both carnivores and diel vertical migrators) exhibited the same range of $\delta^{15}N$ values irrespective of size at La Pérouse and MAD-Ridge (Fig. 5.7e, 5.7f, Table 5.2). For the same body length, *Abraliopsis* sp. showed higher $\delta^{15}N$ values at La Pérouse relative to MAD-Ridge (Fig. 5.7f). Models fitted to *C. sloani* (carnivore, diel vertical migrator) and leptocephali (detritivore, migrant or non-migrant depending on species) were not significant (Fig. 5.7g, 5.7h, Table 5.2). The detritivorous leptocephali had varied $\delta^{15}N$ values irrespective of size and irrespective of the sampling location.

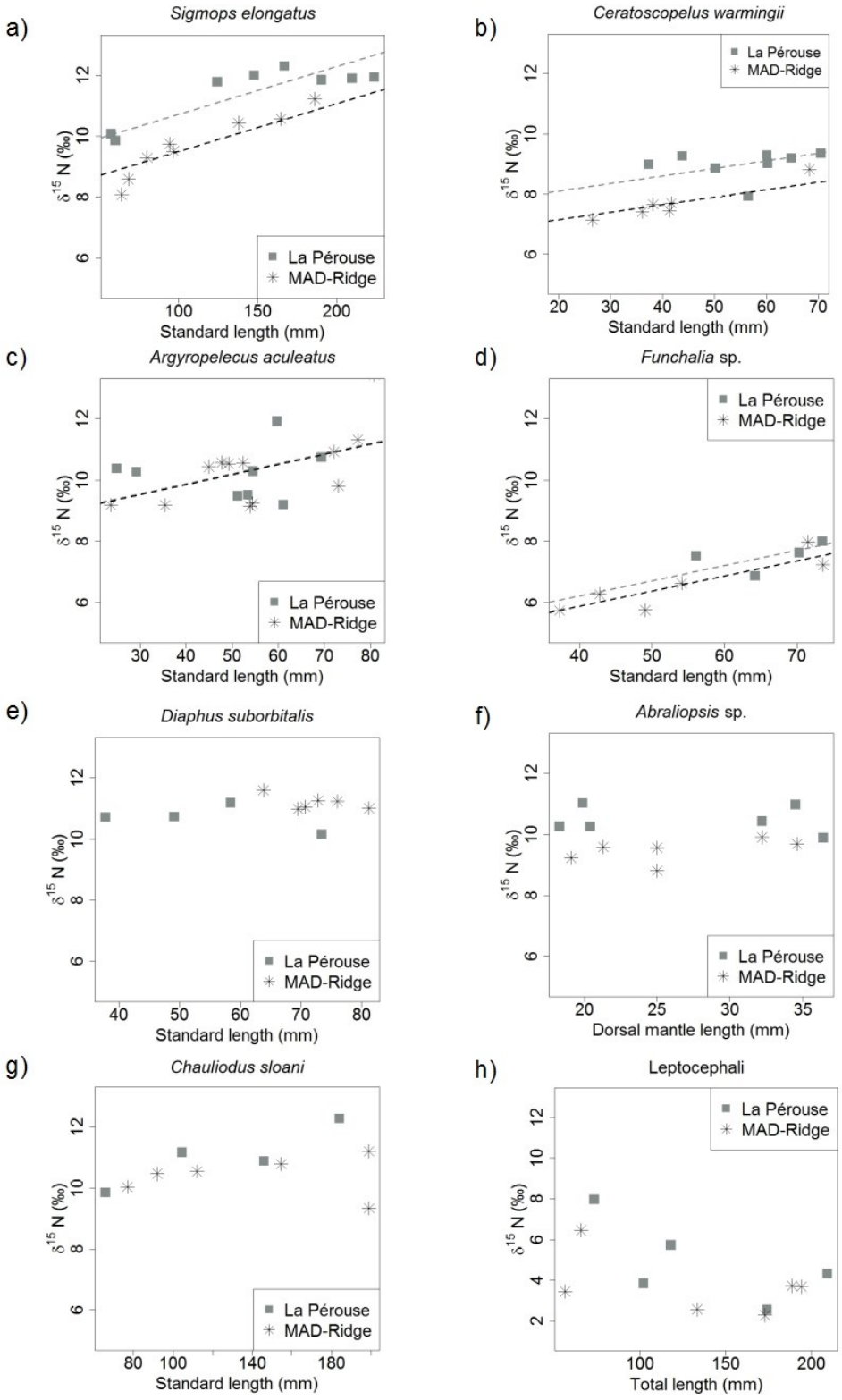

Figure 5.7 $\delta^{15}N$ values (‰) of (a) fish: Sigmops elongatus, (b) fish: Ceratoscopelus warmingii, (c) fish: Argyropelecus aculeatus, (d) crustacean: Funchalia sp., (e) fish: Diaphus suborbitalis, (f) squid: Abraliopsis sp., (g) fish: Chauliodus sloani, (h) fish: leptocephali, plotted against size in mm [standard length for (a)-(c), (e), (g)-(h); abdomen and carapace length for (d); dorsal mantle length for (f)], at La Pérouse (squares) and MAD-Ridge (stars). Simple linear regressions for $\delta^{15}N$ values versus size are plotted for (a)-(d).

Table 5.2 Linear regression models fitted to $\delta^{15}N$ values (‰) with respect to body length in mm (SL, standard length for fishes; TL, total length for leptocephali larvae; ACL, abdomen and carapace length for the crustacean; DML, dorsal mantle length for the squid specimen) and the seamount variable (whether values were significantly different between La Pérouse and MAD-Ridge) of 8 micronekton taxa- Sigmops elongatus (fish), Ceratoscopelus warmingii (fish), Argyropelecus aculeatus (fish), Funchalia sp. (crustacean), Diaphus suborbitalis (fish), Abraliopsis sp. (squid), Chauliodus sloani (fish), and leptocephali (fish).

Taxon	**Regression equation**	**Adjusted r^2 (%)**	**F-statistic**	**Degrees of freedom**	**P-value**
Sigmops elongatus	$\delta^{15}N = 9.15 + 0.0157 \times SL - 1.2210 \times$ seamount La Pérouse: $\delta^{15}N = 9.15 + 0.0157 \times SL$ MAD-Ridge: $\delta^{15}N = 7.93 + 0.0157 \times SL$	85.2	46.0	13	**< 0.05** for size and seamount
Ceratoscopelus warmingii	$\delta^{15}N = 7.61 + 0.0249 \times SL - 0.9521 \times$ seamount La Pérouse: $\delta^{15}N = 7.61 + 0.0249 \times SL$ MAD-Ridge: $\delta^{15}N = 6.66 + 0.0249 \times SL$	72.4	18.0	11	**< 0.05** for size and seamount
Argyropelecus aculeatus	$\delta^{15}N = 8.57 + 0.0331 \times SL - 0.0272 \times$ seamount	16.5	2.87	17	**< 0.05** for size; > 0.05 for seamount
Funchalia sp.	$\delta^{15}N = 4.23 + 0.0496 \times ACL - 0.3460 \times$ seamount	72.7	13.0	7	**< 0.05** for size; > 0.05 for seamount
Diaphus suborbitalis	$\delta^{15}N = 11.5 - 0.0151 \times SL + 0.7594 \times$ seamount	43.8	4.51	7	> 0.05 for size; **< 0.05** for seamount
Abraliopsis sp.	$\delta^{15}N = 10.3 + 0.0069 \times DML - 1.006 \times$ seamount	56.2	8.06	9	> 0.05 for size; **< 0.05** for seamount
Chauliodus sloani	$\delta^{15}N = 10.2 - 0.0065 \times SL + 0.7431 \times$ seamount	12.5	1.64	7	> 0.05 for size and seamount
Leptocephali larvae	$\delta^{15}N = 7.18 - 0.0170 \times TL - 1.1971 \times$ seamount	25.3	2.69	8	> 0.05 for size and seamount

The $\delta^{15}N$ values of omnivorous/ carnivorous fishes collected in the vicinity of the La Pérouse and MAD-Ridge seamounts and in the southern Mozambique Channel were significantly influenced by individual body size ($F_{3,171}$ = 10.3, Adjusted R^2=13.8, $p < 0.05$) (Fig. 5.8a). However, there were no significant influence of body size on the $\delta^{15}N$ values of seamount flank- and summit-associated fish species *D. suborbitalis* (La Pérouse and MAD-Ridge), *B. fibulatum*, *D. knappi* and *C. japonicus* ($F_{1,10}$= 0.07, $p > 0.05$) at MAD-Ridge. These seamount flank- and summit-associated fish species (Cherel et al., 2020) exhibited minimum and maximum $\delta^{15}N$ values of 9.8‰ (*B. fibulatum*) and 11.2‰ (*D. suborbitalis*) for individuals ranging in size from 38 mm (*D. suborbitalis*) to 328 mm (*C. japonicus*) (Fig. 5.8b). Despite the differing sizes of these seamount flank- and summit-associated fish species, they exhibited an estimated TL value (TPA model) of ~4 at both La Pérouse and MAD-Ridge pinnacles.

a)

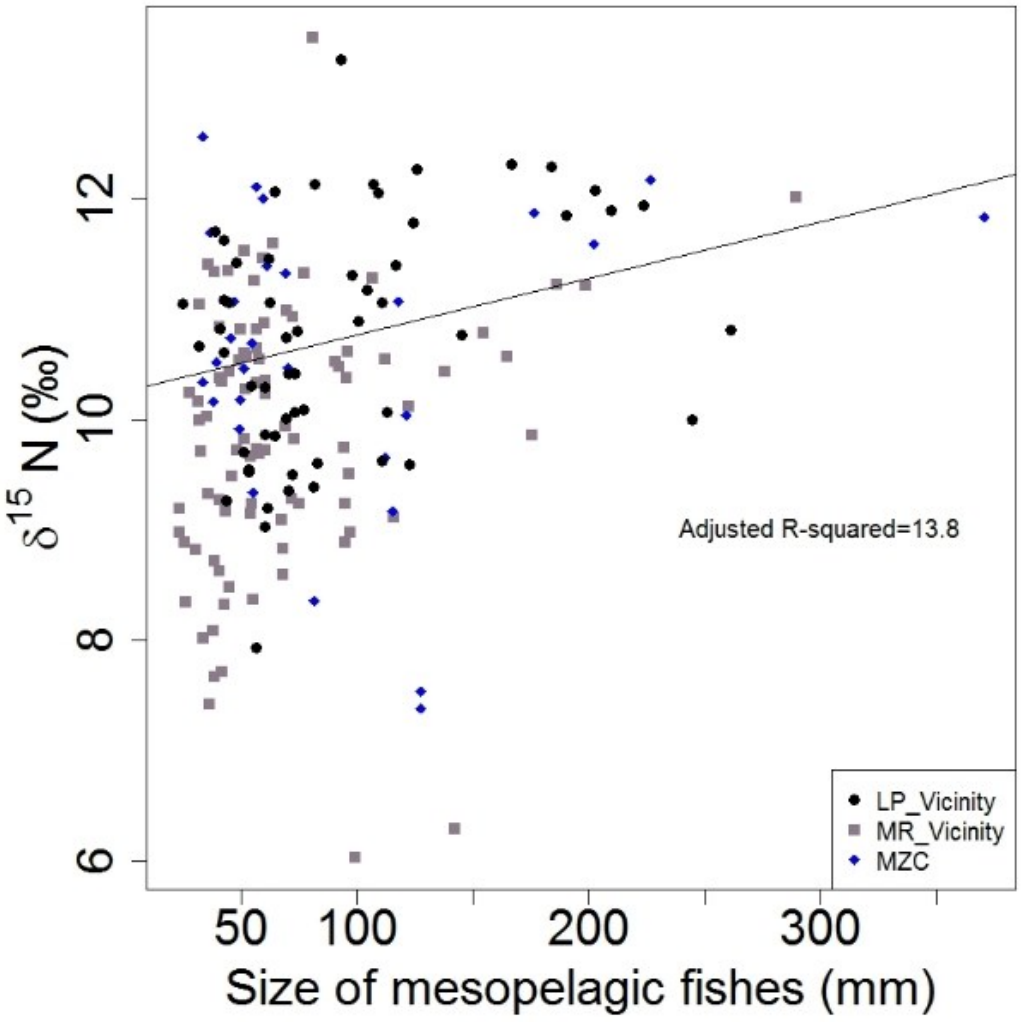

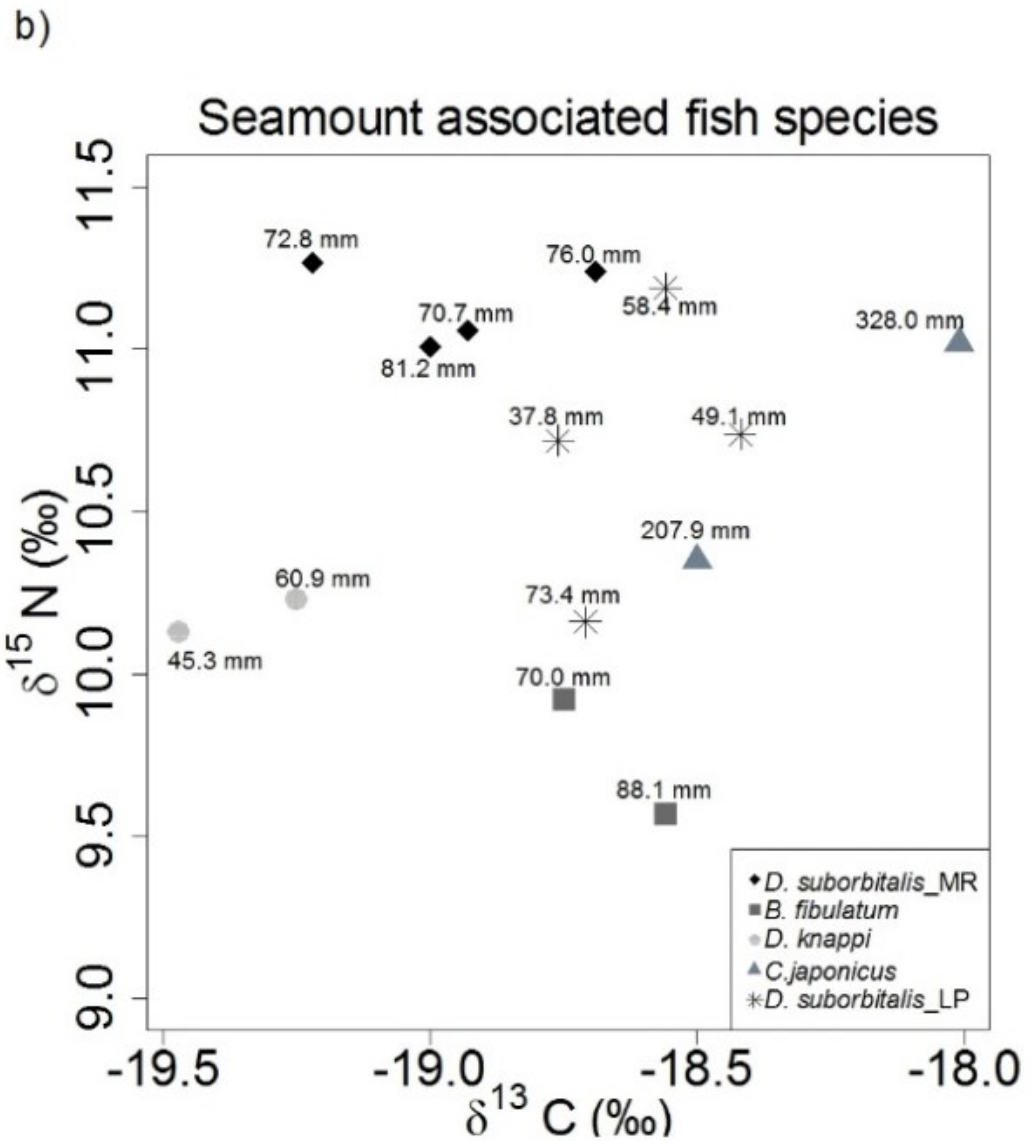

Figure 5.8(a) $\delta^{15}N$ values (‰) of mesopelagic fishes from La Pérouse and MAD-Ridge seamount vicinities (LP_Vicinity and MR_Vicinity respectively) and from the Mozambique Channel, plotted against their standard lengths (mm). Simple linear regressions are plotted. (b) Bivariate plots of $\delta^{15}N$ and $\delta^{13}C$ values (‰) for selected seamount flank- and summit-associated fish species D. suborbitalis at La Pérouse (LP) and B. fibulatum, D. knappi, C. japonicus and D. suborbitalis at MAD-Ridge (MR) seamounts. Standard lengths are given in mm.

5.3.7 Effect of time of day on $\delta^{13}C$ and $\delta^{15}N$ values at MAD-Ridge seamount

Gelatinous and micronekton organisms sampled at MAD-Ridge exhibited similar $\delta^{13}C$ values (-19.6 and -19.4‰ respectively) during day and night ($W= 3055.5$, $p > 0.05$). However, individuals collected during daylight showed higher median $\delta^{15}N$ values (9.22‰) than those collected at night (8.12‰) ($W= 4757.5$, $p < 0.05$).

5.3.8 Seamount effect on $\delta^{13}C$ and $\delta^{15}N$ values of omnivorous/carnivorous fishes

The $\delta^{13}C$ and $\delta^{15}N$ values of omnivorous/carnivorous fishes had overlapping ranges at La Pérouse flank and vicinity stations; as well as overlapping ranges at MAD-Ridge flank, summit and vicinity and Mozambique Channel stations (Fig. 5.9). There were no significant differences in $\delta^{13}C$ ($W= 1619$, $p > 0.05$) of omnivorous/carnivorous fishes collected between flank stations and the vicinity of La Pérouse seamount, whereas a significant difference was observed for $\delta^{15}N$ values between flank (median: 10.1‰) and vicinity (median: 10.8‰) stations ($W= 1876$, $p < 0.05$). There was also no significant differences in $\delta^{13}C$ values (KW, $H= 1.0$, $df= 2$, $p > 0.05$) of omnivorous/carnivorous fishes collected in the southern Mozambique Channel, the vicinity, flank and summit of MAD-Ridge. However, there was a significant difference in $\delta^{15}N$ values (KW, $H= 8.5$, $df= 3$, $p > 0.05$) of omnivorous/carnivorous fishes collected from the southern Mozambique Channel (median: 10.6‰) and in the vicinity of MAD-Ridge (median: 10.0‰).

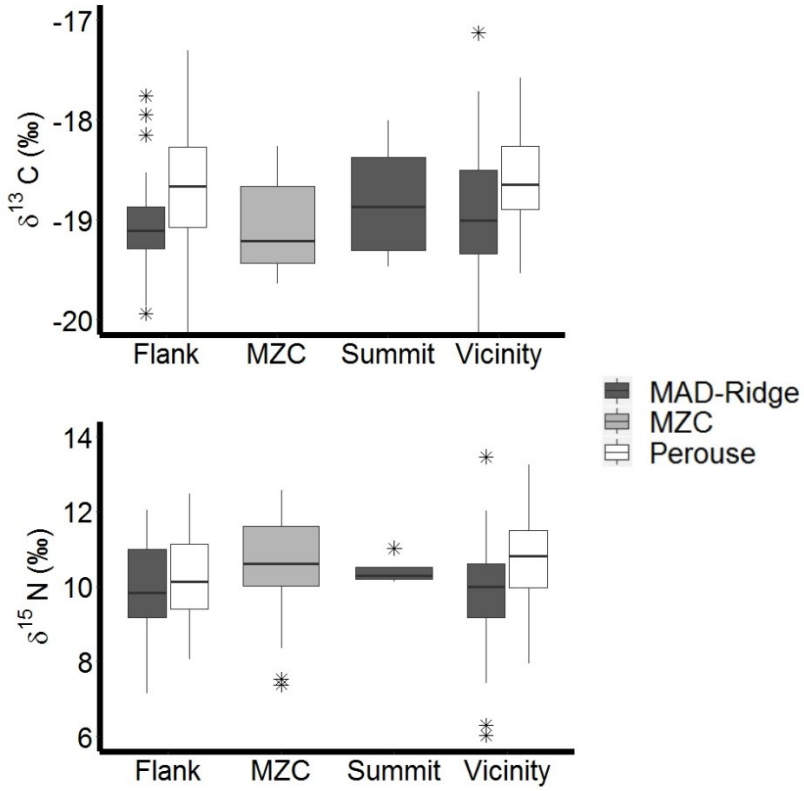

Figure 5.9 Boxplots of $\delta^{13}C$ and $\delta^{15}N$ values (‰) of omnivorous/carnivorous mesopelagic fishes at La Pérouse flank (n = 50 samples) and vicinity (n = 60 samples) stations and, MAD-Ridge vicinity (n =91 samples), flank (n = 38 samples) and summit (n = 4 samples), and stations from the southern Mozambique Channel (n = 28 samples). Outliers are shown as star symbols.

5.4 Discussion

To our knowledge, this thesis is the first to investigate trophic interactions of mesopelagic communities at La Pérouse and MAD-Ridge seamounts using $\delta^{13}C$ and $\delta^{15}N$ stable isotopes. The foodweb components POM-Surf, POM-Fmax, zooplankton, gelatinous organisms and 42 and 49 taxonomic groups of micronekton were identified at La Pérouse and MAD-Ridge, respectively. Despite the low sample sizes for some species, the datasets used in this study provide a first overview of the trophic relationships of micronekton at both seamounts.

5.4.1 Sampling bias and constraints

The full suite of foodweb components could not be sampled at both seamounts because of trawl gear catchability, selectivity and net avoidance of some species of squids and larger fishes. Stable isotopes have numerous limitations in the extent to which they can be used to elucidate complex foodweb dynamics. Isotopic baselines vary seasonally and spatially (Ménard et al., 2014), and organisms or tissues within a single individual may incorporate the isotopic signal of their diets at varying rates, thereby influencing the stable isotope values of individuals (Martínez del Rio et al., 2009). The use of pelagic tunicates as isotopic baseline in TL calculations can also be problematic because pelagic tunicates may be members of an alternate microbial foodweb (Pakhomov et al., 2019). There have been concerns in previous studies of the inappropriate use of fixed discrimination factors for trophic position estimations (Caut et al., 2009; Hussey et al., 2014). However, as shown in Olivar et al. (2019) for myctophid species, and in this study for zooplankton and micronekton, the methods for trophic position estimates maintained the essential differences among all species. Furthermore, the $\delta^{15}N$ values of gelatinous plankton and micronekton were significantly different between day and night samples at MAD-Ridge. This was probably due to the sampling depth, because night-time samples were collected in the shallow, intermediate and deep layers, whereas daylight samples were collected mostly in the deep layer (apart from two leptocephali collected in the shallow depth category). Previous studies found higher $\delta^{15}N$ and $\delta^{13}C$ values with depth, which have been linked to the increase of $\delta^{15}N$ in POM with depth (Kolasinski et al., 2012; Fanelli et al., 2013). However, as the IYGPT net had no closing device, the effect of sampling depth on $\delta^{13}C$ and $\delta^{15}N$ values of individuals could not be investigated further.

Recent studies have cautioned against the use of a fixed additive nitrogen enrichment factor of ~3.2-3.4‰ that is commonly used to estimate the trophic position of an organism relative to its diet. Caut et al. (2009) showed that the consumer taxonomic group and consumer tissue significantly affect the discrimination factor used in trophic level calculations, and Hussey et

al. (2014) stressed that the enrichment between consumers and their primary prey items becomes narrower in the upper parts of a food chain. Bastos et al. (2017) developed a novel method using food-specific trophic discrimination factors to estimate trophic positions of omnivorous fishes given that plant-based and animal-based materials in diets are not assimilated in the same manner. Olivar et al. (2019) observed small variations in trophic level calculations of mesopelagic fishes when using alternative models to estimate trophic positions. However, those authors also concluded that the important differences among species are retained by all trophic models, similarly to the findings of this study.

5.4.2 Trophic interactions at La Pérouse and MAD-Ridge seamounts

Particulate organic matter collected at the surface generally consists of phytoplankton, bacteria, faecal pellets and detritus (Riley, 1971; Saino & Hattori, 1987; Fabiano et al., 1993; Dong et al., 2010; Liénart et al., 2017). The $\delta^{13}C$ values of POM (collected at the surface and at the Fmax depth) were different at the La Pérouse and MAD-Ridge seamounts. $\delta^{13}C$ baselines can be affected by various processes such as latitude, nutrient source, depth, ocean mixing and primary productivity (Fry, 2006). Research has found that chlorophyll *a* concentrations explained the variability in POM $\delta^{13}C$ values within the EAFR province but not in the ISSG (Annasawmy et al., 2018). Surface chlorophyll *a* concentrations at MAD-Ridge (within the EAFR province) was greater than at La Pérouse (within the ISSG) all year round (see Chapter 4), likely a result of terrestrial input of nutrients from the Madagascar landmass, upwelling events on the shelf to the south of Madagascar (Ramanantsoa et al., 2018), offshore advection of this shelf productivity through cross-shelf transport (Noyon et al., 2018) and vertical mixing in the mesoscale eddy system over MAD-Ridge (De Ruijter et al., 2004; Vianello et al., 2020). High levels of photosynthetic rate (currently occurring at the south Madagascar upwelling and being transported south), would induce higher $\delta^{13}C$ POM values at MAD-Ridge compared with the oligotrophic La Pérouse (Fry, 1996; Savoye et al., 2003). Surface POM at MAD-Ridge might have possibly been both of marine and terrestrial origin, yielding higher $\delta^{13}C$ values relative to surface POM at La Pérouse, which might have consisted of phytoplankton with no terrestrial POM input.

The $\delta^{13}C$-$\delta^{15}N$ correlations of all foodweb components were not relatively strong at the La Pérouse and MAD-Ridge seamounts ($r = 0.74$ and 0.51 respectively) at the times of the cruises. A strong correlation during periods of high productivity would have supported the hypothesis of a unique and isotopically homogeneous pelagic food source (Fanelli et al., 2013; Papiol et al., 2013; Preciado et al., 2017), i.e. a single source of carbon for plankton (Fanelli et al., 2009).

The relatively weaker correlation observed in this study suggests a wide array of sources of production sustaining the different assemblages once the main input from surface production has decreased (Fanelli et al., 2011a, b; Papiol et al., 2013), or exploitation of organic matter at different stages of degradation from fresh phytodetritus to highly recycled (Fanelli et al., 2009), or refractory materials such as chitin from copepod exoskeleton becoming abundant in sinking marine snow or inorganic carbonates (Polunin et al., 2001). This would be the case in low productive environments such as the ISSG, where production at La Pérouse would be reduced in September and thus zooplankton would have to expand their food spectrum, as demonstrated by the larger span of their niche widths over the $\delta^{13}C$ range. Alternatively, the $\delta^{13}C$-$\delta^{15}N$ correlations could reflect temporal variations in the baseline isotope values coupled with varying rates of isotopic incorporation (Fanelli et al., 2009, 2011b, 2013). Higher trophic level organisms such as large crustaceans and fishes reportedly do not show seasonal patterns in their isotope values owing to their much slower tissue turnover rates (Polunin et al., 2001). Additional seasonal studies are required to investigate POM and resulting zooplankton $\delta^{13}C$ and $\delta^{15}N$ signatures in July when surface oceanic phytoplankton production is enhanced within the ISSG and EAFR provinces.

Among the mesopelagic organisms sampled, gelatinous plankton exhibited the lowest trophic level (~2), crustaceans showed an intermediate trophic level (~3), and smaller squids and mesopelagic fishes exhibited TL values between 3 and 4, as estimated from the TPA method. Assuming a fixed and additive trophic fractionation of 3.2‰ (for comparison with other SWIO studies), the overall range of $\delta^{15}N$ values implied a two-step (3 trophic levels) and three-step (four trophic levels) pelagic food chain at La Pérouse and MAD-Ridge seamounts, respectively. Unfortunately, no top predators were sampled during these cruises to provide information on higher trophic level organisms. Earlier studies within the EAFR province, showed swordfish *Xiphias gladius* collected off the coast of Madagascar to have a TL of ~4.7 ($\delta^{15}N$: 14.0 ± 0.59‰). Specimens collected within the ISSG province had a TL of ~5.2 ($\delta^{15}N$: 15.1 ± 0.36‰) (Annasawmy et al., 2018). Several authors described the number of trophic levels averaging between four and six in marine ecosystems, from primary consumers to top predators, and appearing higher in coastal environments, reefs and shelves and lower in oceanic upwelling systems (Arreguín-Sánchez et al., 1993; Browder, 1993; Christensen & Pauly, 1993; Bulman et al,, 2002). Similar to those studies, it seems that both La Pérouse and MAD-Ridge seamounts exhibit trophic levels typical of oceanic systems, although small variations may

exist in the $\delta^{13}C$ and $\delta^{15}N$ values of an organism's tissues according to various environmental, behavioural and physiological factors (Ménard et al., 2014; Annasawmy et al., 2018).

5.4.3 Influence of feeding mode and size on $\delta^{13}C$ and $\delta^{15}N$ values

The trophic guilds established at La Pérouse and MAD-Ridge seamounts were segregated in terms of $\delta^{13}C$ and $\delta^{15}N$ values, from depleted (detritivores and filter-feeders) to enriched (omnivores and carnivores) isotope values, highlighting the fact that these trophic guilds consist of species that exploit distinct classes of resources (Bulman et al., 2002; Papiol et al., 2013; Choy et al., 2016). The large range of $\delta^{13}C$ values (~-17 to - 23‰) when gelatinous organisms are considered together with crustaceans, squids and mesopelagic fishes suggests that these organisms exploit different sources of production, thus giving rise to different trophic pathways (Ménard et al., 2014). Gelatinous filter-feeders such as salps and pyrosomes ingest a variety of suspended particles (Harbou, 2009; Conley, 2017) and leptocephali include a wide range of species feeding on detrital material (Otake et al., 1993) such as larvacean houses and faecal pellets (Lecomte-Finiger et al., 2004; Feunteun et al., 2015) and hence exhibited depleted $\delta^{13}C$ values relative to other micronekton broad categories. Species depleted in ^{13}C reportedly feed near the base of the chain and are closely associated with plankton relative to fishes with higher $\delta^{13}C$ values (Polunin et al., 2001).

Crustacean taxa were at intermediate trophic levels at both seamounts, below that of strict carnivores and above that of detritivores or filter-feeding organisms. Some species of crustaceans would prey on chaetognaths (Heffernan & Hopkins, 1981), molluscs, olive-green debris containing phytoplankton and protists (Hopkins et al., 1994) and they would share common food sources with mesopelagic fishes by foraging on copepods, decapods and euphausiids (Fanelli et al., 2009). Similar to previous studies conducted in the SWIO (Ménard et al., 2014; Annasawmy et al., 2018), crustaceans exhibited overlapping isotopic niches with carnivorous mesopelagic fishes and squids at both seamounts. The narrow range of $\delta^{13}C$ values and the greater overlap of isotopic niches between crustaceans and carnivorous squids and mesopelagic fishes at both seamounts might suggest some degree of similarity in the diet components with low level of resource partitioning and a high level of competition among these broad categories (Fanelli et al., 2009) or alternatively, different diets but with prey items having similar isotopic compositions.

Whereas lower trophic level components, POM-Fmax and zooplankton showed significantly different and higher $\delta^{15}N$ values at MAD-Ridge relative to La Pérouse (most likely because of

differing productivity and fast turnover rate of these organisms), higher trophic level components such as crustaceans, squids and fishes showed no significant differences in their $\delta^{15}N$ values between the two seamounts. There are several hypotheses for similar isotopic signatures of higher trophic levels when baseline levels differ. Firstly, the sampled organisms might not have had time to incorporate the isotopic composition of their most recent diets, especially if transient productivity bouts had impacted the density or composition of their diet. Whereas some studies reported tissue turnover rates of ~0.1-0.2% per day in deep-sea fishes (Hesslein et al., 1993), other studies showed a lack of tissue turnover information in more specific mesopelagic families including Myctophidae and Stomiidae (Choy et al., 2012). Second, the difference in the $\delta^{15}N$ values of POM and zooplankton observed at La Pérouse and MAD-Ridge, although significant, may have been too negligible to be reflected in the $\delta^{15}N$ values of higher trophic levels. Third, the number of squid and crustacean specimens analysed for stable isotopes might not be large enough to reflect the full diversity in the isotopic signatures, and hence the apparent lack of variations in $\delta^{15}N$ values for these individuals between the two seamounts. Finally, as a result of movements, zooplankton grazers and subsequent trophic levels might have fed on prey components that are not those sampled in the water column, leading to a mismatch in isotopic signatures between lower and higher trophic levels.

In this study, $\delta^{15}N$ values of micronekton were correlated to body size. This phenomenon was observed in various organisms such as phytoplankton, zooplankton, decapods and fishes and across numerous studies (Sholto-Douglas et al., 1991; France et al., 1998; Waite et al., 2007; Ventura & Catalan, 2008; Hirch & Christiansen, 2010; Choy et al., 2012, 2015; Papiol et al., 2013) and is probably attributable to size-related predation. As organisms grow in size, they can feed further up the foodweb on larger prey with greater $\delta^{15}N$ values (Parry, 2008; Ménard et al., 2014). For those species whose $\delta^{15}N$ values (*S. elongatus*, *C. warmingii* and *Abraliopsis* sp.) were significantly influenced by size, their $\delta^{15}N$ values were greater (around 1‰ difference) at La Pérouse than at MAD-Ridge for the same body lengths. As suggested in Parry (2008), if the $\delta^{15}N$ values, and hence the TL of an organism, are influenced by size, then the $\delta^{15}N$ signal will also depend on baseline values and the variables that affect an organism's size such as feeding mode, growth rate, body condition and available prey items. As $\delta^{15}N$ values of POM and zooplankton were higher at MAD-Ridge than at La Pérouse, we hypothesize that those intermediate TLs at the oligotrophic La Pérouse seamount had a different trophic

functioning, with the diet of those species being based on a larger proportion of higher TL prey than at MAD-Ridge.

Body size did not have an effect on $\delta^{15}N$ values of leptocephali that encompass a wide range of species having a detritivorous and opportunistic feeding mode at both seamounts. Such lack of effect was also observed for *C. sloani* individuals ranging in size from 66 to 184 mm at La Pérouse and from 77 to 199 mm at MAD-Ridge. These individuals are semi-migrants, caught in deep and intermediate trawls during both day and night. Individuals 45-178 mm long feed on myctophids and other fish species (Utrecht et al., 1987; Butler et al., 2001) with prey items being more than 63% of their own length (Clarke, 1982). Smaller individuals were reported to feed on euphausiids (Butler et al., 2001). The trawls in this study failed to capture smaller *C. sloani* individuals that may have had a different diet and possibly different $\delta^{15}N$ values relative to larger individuals. There might also be a trophic plateau whereby subsequent increases in trophic position with size are not possible due to physical constraints on the organism or lack of appropriate prey of higher trophic levels, as was observed with *O. bartramii* specimens from the central north Pacific (Parry, 2008).

5.4.4 Seamount effect on $\delta^{13}C$ and $\delta^{15}N$ values of fish species

Omnivorous/carnivorous fishes sampled in the southern Mozambique Channel exhibited slightly enriched $\delta^{15}N$ values relative to those sampled in the vicinity of the MAD-Ridge seamount. Productivity in the southern Mozambique Channel may be both entrained from the African landmass and locally generated within mesoscale eddies, hence leading to enhanced chlorophyll *a* concentration, micronekton abundances and enriched $\delta^{15}N$ values within tissues of micronekton (Tew-Kai & Marsac, 2009; Annasawmy et al., 2018). For an increase in phytoplankton biomass to take place at the seamounts, physical processes leading to retention (e.g. Taylor columns trapping a body of water), enrichment (e.g. localised upwelling and uplift of nutrients) and concentration of productivity must co-occur (Bakun, 2006). However, as seen at La Pérouse and MAD-Ridge seamounts, the current speeds were too strong during the cruises, and the seamount structures unfavourable for Taylor column formation and for significant retention and assimilation of productivity. This would have inhibited any subsequent energy transfer to higher trophic levels, potentially explaining the lack of differences in $\delta^{15}N$ values between the seamount and the area not influenced by the seamount.

Seamount-associated fish species *D. suborbitalis*, *B. fibulatum* and *C. japonicus* (Cherel et al., 2020), sampled at the summit and on the flanks of MAD-Ridge showed similar $\delta^{13}C$, $\delta^{15}N$ and

TL values irrespective of their size, similarly to *D. suborbitalis* sampled at La Pérouse. This most likely reflects similar food sources at the summit and flanks of both pinnacles or ingestion of different prey items having similar isotopic composition. These fishes may associate with the La Pérouse and MAD-Ridge summits and flanks owing to enhanced availability of prey and/or the quiescent shelters offered by the topography. All seamount-associated fish individuals collected on the summit and flanks of La Pérouse and MAD-Ridge with the IYGPT net were adults, previously reported to prey on copepods (Go, 1986; Olivar et al., 2019; Vipin et al., 2018) and chaetognaths (Appelbaum, 1982), organisms present in similar proportions on and away from both seamounts (Noyon et al., 2020).

Although $\delta^{13}C$ and $\delta^{15}N$ values may depend on a range of factors, there were few differences between $\delta^{13}C$ and $\delta^{15}N$ values of mesopelagic fishes sampled at La Pérouse and MAD-Ridge and those collected in the Indian Ocean, within the oligotrophic ISSG province (*A. aculeatus* $\delta^{13}C$ and $\delta^{15}N$ values: -18.6 and 9.5‰, *C. sloani*: -18.1 and 9.5‰, and *L. gemellarii*: -18.5 and 9.9‰; Annasawmy et al., 2018) and the western Mozambique Channel (*A. aculeatus*: -18.4 and 10.0‰ and *L. gemellarii*: -18.4 and 11.1‰; Annasawmy et al., 2018). Even though mesopelagic fishes exhibit small variations in their $\delta^{13}C$ and $\delta^{15}N$ values across different studies in various oceanic environments, they generally occupy trophic positions between 2 and 4, irrespective of the approach used to estimate trophic positions (Fanelli et al., 2011b; Choy et al., 2012, 2015, 2016; Colaço et al., 2013; Ménard et al., 2014; Valls et al., 2014a,b; Denda et al., 2017b; Annasawmy et al., 2018; Olivar et al., 2019). Despite the possible bias induced by the different time-scales in sampling (Mill et al., 2008), within a stable isotope approach, the trophic positions of mesopelagic fishes across numerous studies confirmed similar dietary patterns and food sources with similar isotopic compositions. Hence, these mesopelagic fish species by their opportunistic feeding mode may play a similar trophic role across different environments (Olivar et al., 2019).

5.5 Concluding Remarks

This study has shown that despite the different productivity at the two shallow seamounts and the significant differences in lower trophic level $\delta^{13}C$ and $\delta^{15}N$ values, crustaceans, smaller-sized squids and mesopelagic fishes, because of their varied feeding modes, occupy trophic positions between 3 and 4. Specimen size had an influence on the $\delta^{15}N$ values of most individuals, although that also depended on the life strategy and feeding mode of the species considered. The $\delta^{13}C$ and $\delta^{15}N$ values of mesopelagic organisms sampled during both cruises reflected those of typical oceanic systems and the seamounts did not seem to have any impact

on the overall isotopic signatures of the mesopelagic taxa sampled. However, the few seamount-associated/resident fishes sampled showed similar $\delta^{15}N$ values and trophic levels irrespective of their size at the summits and flanks of the pinnacles. La Pérouse and MAD-Ridge seamounts may hence be important foraging grounds for the few taxa that preferentially associate with their slopes and summits, and thus benefit from the varied habitat types that the seamounts offer relative to the open ocean environment.

Acknowledgements

The authors would like to acknowledge the work carried out by the scientific/non-scientific staff on board the RV *Antea* for collection of samples at La Pérouse and MAD-Ridge seamounts. The authors would also like to thank colleagues at the Plateau Chimie / Pole Technique MARBEC (Sète, France) and the Pôle de Spectrométrie Océan (Plouzané, France) for providing support with the stable isotope analyses. This study was mainly supported by the Flotte Océanographique Française (French Oceanographic Fleet) and IRD in relation to the logistics of the RV *Antea*. Additional funding was also received from Région Réunion (Réunion Regional Council) for the La Pérouse cruise, and from the Fonds Français pour l'Environnement Mondial (FFEM) as part of the FFEM-SWIO project on Areas Beyond National Jurisdiction (ABNJ) of the South West Indian Ocean for the MAD-Ridge cruise. Pavanee Annasawmy was the beneficiary of a doctoral bursary granted by the Institut de Recherche pour le Développement (IRD, France) and the ICEMASA French-South African International Laboratory.

Chapter 6: General Discussion and Conclusion

Walters Shoal summit, Indian Ocean

MD 208 Cruise, RV Marion Dufresne

April-May 2017

Photo Credit: IUCN

6.1 Introduction

This research project was motivated by the fact that SWIO seamounts are currently subject to anthropogenic pressures resulting from fishing and pollution and are potentially at risk of future mining and dredging activities while still being poorly explored scientifically. Two research cruises were conducted in 2016 at the La Pérouse and MAD-Ridge seamounts with the aims of studying the current-topography interactions and the resulting biological responses of phytoplankton, mesozooplankton, ichthyoplankton and micronekton communities.

6.2 Review of the thesis aims and objectives

The overarching aim of this thesis was to investigate the patterns among micronekton communities at the La Pérouse and MAD-Ridge seamounts in the SWIO. A combination of satellite, *in situ* environmental, mesopelagic trawl, acoustic and stable isotope data were used to address the thesis objectives. Satellite and *in situ* environmental data were employed to describe the prevailing environmental patterns at both seamounts. Mesopelagic trawl and acoustic data were used to investigate the assemblages and vertical and horizontal distributions of micronekton as influenced by the pinnacles and the physical oceanographic processes. Stable isotope data were used to study the trophic relationships of micronekton with respect to zooplankton and POM at both seamounts.

It was first necessary to provide an overview of all the physical processes that might result from current-topography interactions and the resulting biological responses recorded from phytoplankton, zooplankton, micronekton communities and associated/ resident fishes at seamounts that have been extensively studied in the Atlantic and Pacific basins (Chapter 1).

Since the geographic focus of this study is the SWIO, Chapter 2 provided an overview of the ridge systems in the region, along with the physical oceanographic processes that likely have an impact on all trophic levels. Special focus has been paid to top predators of micronekton, which are fished in the region. Chapter 2 also outlined the previous seamount cruises in the region and the main results on the assemblages of lower trophic level compartments-phytoplankton, mesozooplankton and ichthyoplankton communities at La Pérouse and MAD-Ridge.

The horizontal and vertical patterns in micronekton's distributions as influenced by physical oceanographic processes and topographic features were investigated in Chapter 3. Theoretical calculations were implemented to determine the likelihood of Taylor column formation at La Pérouse and MAD-Ridge. Micronekton's DVM patterns were revisited in light of the acoustic and environmental data collected.

Chapter 4 aimed at investigating the year-round sea surface productivity at La Pérouse and MAD-Ridge using satellite data. The assemblages of the micronekton communities at the summits, flanks and vicinities of the seamounts were studied, along with the scattering intensities in the SSL and DSL. A combination of mesopelagic trawl data and multi-frequency acoustic visualisation technique have been used to investigate the composition of the SSL and the dense aggregations observed over the summit of MAD-Ridge. Micronekton's vertical and horizontal distributions and the different migration strategies of various species are analysed in more detail.

Chapter 5 investigated the trophic position of several micronekton taxa with respect to other components of the foodweb such as zooplankton and POM at both La Pérouse and MAD-Ridge. The various factors possibly influencing the isotopic composition of a consumer's tissue are also discussed.

6.3 La Pérouse and MAD-Ridge seamount ecosystems

Both the La Pérouse seamount, located to the northwest of Réunion Island and MAD-Ridge, located to the south of Madagascar, represent elevated topographies in an otherwise deep ocean that extends to 2000 and 5000 m in some places (see Fig. 2.15). The La Pérouse seamount which has been created by a volcanic hotspot, is not part of a ridge system unlike MAD-Ridge that is bounded by several other topographic features along the Madagascar Ridge. Both seamounts have shallow summits that extend into the euphotic zone, with the summit of La Pérouse being well above the mean depth of the maximum fluorescence. The shape of the summits of both pinnacles also differ, with La Pérouse being crescent-shaped and MAD-Ridge being circular.

Both seamounts are located in two different oceanographic regimes and biogeochemical provinces, characterised by different mesoscale activities and primary productivity. Indeed, annual sea surface chlorophyll *a* concentrations at MAD-Ridge were twice greater than at La Pérouse all year-round, despite the same seasonal patterns in both regions. A peak in productivity occurs throughout the region in austral winter (July) as a result of intense mixing caused by the austral winter trade winds, as opposed to lower wind stress recorded at the time of the La Pérouse and MAD-Ridge cruises (spring and summer). Furthermore, being located in the ISSG province, the La Pérouse seamount is under the influence of the oligotrophic conditions of this gyre. The large-scale anticyclonic rotation of the gyre causes downwelling and limited supply of nutrients or biogenic pigments to the sunlit zone, hence decreasing productivity all year-round (Jena et al., 2013). The MAD-Ridge seamount, being found in the

EAFR province and within an "eddy-corridor" to the south of Madagascar, experiences higher productivity and mesoscale activities all year round.

As seen in Chapters 1 and 3, seamounts may bifurcate, trap, split, rebound or destroy eddies. La Pérouse was located at the edge of a cyclonic eddy with an average speed of 12 km per day during the first part of the cruise (Marsac et al., 2020), and did not seem to have any substantial effects on the eddy dynamics. MAD-Ridge seamount was frequently crossed by mesoscale eddies with 38.5%, 25.4% and 30% dipoles, cyclones or anticyclones occurrences, respectively within a 90 km radius from the summit, between 1993 to 2016 (Vianello et al., 2020). During MAD-Ridge cruise Legs 1 and 2, a cyclonic-anticyclonic eddy dipole was located near the seamount, with the anticyclone positioned on the pinnacle. Altimetry data tracked both eddies back to the 12th of November with the dipole being fully formed but still remaining attached to the EMC (Vianello et al., 2020). The dipole was subsequently detached from the Madagascar coast and travelled south-westward within the MAD-Ridge seamount area where it remained trapped for two weeks. The anticyclonic part was subsequently split into two cores on the 7th of December before dissipation. Another similar dipole was then shown to interact with MAD-Ridge seamount (Vianello et al., 2020).

Eddies formed off the Madagascan coast trap water masses from the EMC and possibly larvae from the surroundings, which are then advected to the MAD-Ridge region (Crochelet et al., 2020). These vortices maybe trapped on the seamount for several weeks. Eddy trapping or splitting depend on a combination of factors related to the potential vorticity anomaly associated with the pinnacle, the steepness of the seamount, the distance between the vortex and the seamount, the vortex radii, among other factors (Herbette et al., 2003). The fact that eddies have to travel through uneven and hilly dynamic topography along the Madagascar Ridge may reduce their potential vorticity by dissipation of the energy whenever the vortices encounter a steep bottom, eventually leading to their splitting and/or decay. The MAD-Ridge seamount is sufficiently close to the site of eddy formation off the Madagascan coast to allow the eddies-entrained water masses and biological productivity to reach the pinnacle before eventually splitting and/or decaying. Due to the high occurrences of eddies in the region; this process seems to be a common phenomenon for the resident fauna at MAD-Ridge.

As seen in Chapter 1, current-topography interactions may also lead to the formation of isopycnal doming, Taylor columns, tidal amplifications, internal waves and enhanced vertical mixing. These processes may trigger a biological response from phytoplankton communities. No isopycnal doming was observed from temperature, salinity and density fields over the

summit of MAD-Ridge possibly due to the anticyclone. Doming is generated when the fluid is forced to rise over the topographic feature. Due to the anticyclonic rotation of the eddy at MAD-Ridge, fluid was depressed instead. As for the La Pérouse seamount, the available datasets from the cruise do not allow the accurate determination of whether an isopycnal doming occurred over the pinnacle. Based on theoretical calculations, Taylor columns are not likely to be formed over the La Pérouse and MAD-Ridge seamounts most likely because of a combination of factors related to the seamounts' shapes/sizes, depth of summit (as in the case of La Pérouse that is shallow) and the prevailing current speeds.

As shown in Chapter 1, tides may also interact with topographic features resulting in the formation of closed circulation cells, internal waves, flow rectification and trapped waves. Weak tidal amplitudes were recorded near La Pérouse, but authors also reported disturbances in the distribution of flow in the vertical plane when the flow encountered the flanks of the pinnacle (Marsac et al., 2020). MAD-Ridge and some of the other deeper surrounding seamounts having summit depths between 500 and 1500 m, were reported to be sites of strong vertical mixing due to internal tides. Internal tides occur when strong tidal currents encounter a steep topography in a stratified ocean. These internal tides allow nutrients to enter the euphotic layer, thus promoting productivity. At MAD-Ridge, mixing mostly occurred on the edge of the seamount above the 700 m contour and none occurred above the summit (Koch-Larrouy et al., in review). Modelling studies have further shown that non-linear processes such as lee waves could occur on the side of each seamount within the complex seamount group around the MAD-Ridge pinnacle, along with high likelihood of strong propagative internal tides (Koch-Larrouy et al., in review). These physical processes were shown to influence the biological productivity, with an intensification of chlorophyll in the region of internal tides' generation on the side of the MAD-Ridge seamount (Koch-Larrouy et al., in review).

La Pérouse seamount is thus located in an oligotrophic environment with no observed significant increase in primary production brought about by interactions between the pinnacle and the local flow. On the other hand, various physical processes may bring about an increase in productivity at MAD-Ridge, (1) advection of productivity from the Madagascan coast by mesoscale eddies in the vicinity of the pinnacle, (2) local enrichment processes within mesoscale eddies, (3) internal tide generation leading to enhanced vertical mixing and productivity. Authors however have reported no observed enrichment/depletion in zooplankton biovolumes and abundances over the summits of both La Pérouse and MAD-Ridge relative to off-seamount locations (Noyon et al., 2020). No gap formation as described in Chapter 1 were

observed either. As seen in Chapter 1, several mechanisms are likely to promote aggregation of zooplankton over seamounts:

(1) the topographic blockage mechanism whereby the predawn descent of some mesopelagic taxa is blocked by the topography was not observed over both pinnacles.

(2) depth retention

The observed increase of weakly migrating zooplankton communities over a greater depth range at MAD-Ridge station 18 would suggest that some organisms were able to maintain their depths in the water column possibly to benefit from enhanced foraging opportunities. Authors also observed spatial differences in zooplankton abundances with higher productivity on the leeward flank of La Pérouse due to small circulation cells being created along the seamount slopes. These processes likely enhanced nutrient and chlorophyll availability for zooplankton communities that maintained their dwelling depth at this site (Marsac et al., 2020).

(3) trophic focusing

This mechanism occurs when prey from the flowing water over the summit become trapped and hence support higher trophic levels. The currents speed might have been too strong and the likely presence of predators over both seamounts might not have allowed permanent retention of zooplankton over the summit.

Furthermore, as seen in Chapter 4, due to the high risk associated with damaging the sampling gears, the summits of both La Pérouse and MAD-Ridge were poorly sampled and hence have not captured the full spectrum of mesozooplankton and micronekton communities present at these sites, likely biasing net-based estimates.

Studies have argued against bottom-up transfer of energy from locally generated phytoplankton above seamounts since phytoplankton entrapment of the order of weeks/months are thought necessary to have a significant effect on zooplankton and micronekton (Genin & Dower, 2007). However, MAD-Ridge station 19 close to the seamount slopes exhibited enhanced picoplankton biomass. Station 18 showed enhanced records of small weakly migrating zooplankton communities over a greater depth range and enhanced fish larval densities and micronekton acoustic estimates. Enhanced turbidity on the slopes may have resulted in an increase in primary production and currents may have entrained this productivity towards station 18. The physical process leading to the biological responses described at station 18 may be a quasi-permanent feature at that location or secondary and tertiary trophic levels are able to rapidly adapt and preferentially stay at depths with enhanced foraging opportunities.

Higher epipelagic and mesopelagic larval densities of different developmental stages were recorded over the summits of both pinnacles relative to off-seamount locations (excluding station 18) (Harris et al., 2020). As shown in Chapter 1, larvae released over a seamount may settle into the benthos (if the larvae are benthic), be swept off by currents or retained by local physical processes. The fact that MAD-Ridge summit showed higher larval densities relative to off-seamount locations, mostly of the Myctophidae, Bregmacerotidae, Gonostomatidae and Molidae families, would suggest local spawning (Harris et al., 2020). Additionally, although the summits of the pinnacles recorded relatively high current speeds, the foraging opportunities or specific habitat structure with possibility of shelter sites offered by the topography and by stony and soft corals may favour the retention of these taxa over the summit.

Higher species richness and micronekton acoustic densities were also recorded at MAD-Ridge relative to La Pérouse and are most likely attributed to a combination of the local physical processes discussed previously: (1) productivity and larvae driven from the shelf by eddies, (2) productivity associated with mesoscale eddies, (3) internal tides generation and enhanced mixing. The enhanced primary productivity at MAD-Ridge may attract zooplankton and hence provide greater prey availability for micronekton at MAD-Ridge. Lagrangian models have further shown that larval dispersions can be very far between seamounts in the region and their coastal systems, with larval distances increasing with pelagic larval duration (Crochelet et al., 2020). The greater proportion of neritic larvae at MAD-Ridge seamount relative to La Pérouse (Harris et al., 2020) seem to support the hypothesis of connectivity between MAD-Ridge and the Madagascar shelf. Authors have further noted decreased probability of larvae generated from the seamounts reaching their coastal systems (Crochelet et al., 2020). This would suggest a dominant "one-way" transport of larvae from the shelf to the seamounts of the Madagascar ridge, most likely owing to the prevailing structure of the current circulation system in this region as seen in Chapter 2.

Additionally, as seen in Chapter 4, the SSL consisted of common diel vertically migrating organisms at night above the summits of both La Pérouse and MAD-Ridge and also at off-seamount locations. However, dense aggregations of scatterers were recorded only over the summits and flanks of both seamounts during day and night, relative to the open ocean. A combination of acoustic and trawl surveys have revealed these dense aggregations to consist of taxa known to preferentially associate with seamounts and rocky bottoms such as *D. suborbitalis* (La Pérouse and MAD-Ridge), *B. fibulatum*, *N. macrolepidotus* and *C. japonicus* (MAD-Ridge only). Dense aggregations over seamount summits have been previously observed from acoustic transects over seamounts of the SWIR, the Equator (Indian Ocean),

Southeast Hancock (Pacific) seamounts and the Graveyard seamount complex (New Zealand) and may have consisted of a range of mesopelagic and benthopelagic taxa (Parin & Prut'ko, 1985; Boehlert, 1988; O'Driscoll et al., 2012; Letessier et al., 2017).

Gonostomatids of adult forms were not sampled over the summits and poorly sampled over the flanks of both seamounts relative to myctophids (adult and larval forms) sampled over the summit and/or flanks of MAD-Ridge and La Pérouse. This might suggest that, compared to myctophids, larval forms of Gonostomatidae would associate with the summit and move to surrounding waters in their adult forms. Myctophidae consists of a wider diversity of species compared to Gonostomatidae (Davis et al., 2014), that have probably evolved to adapt to a wider range of habitat types apart from the open-water oceanic habitat. Unfortunately, trawl records of both adult and larval forms of both species are insufficient to accurately test this hypothesis. The only notable observation is the high association of large populations of some myctophids (*D. suborbitalis* and *B. fibulatum*) with seamounts in the Indian and Pacific Oceans (Parin & Prut'ko, 1985; Drazen et al., 2011).

As mentioned in Chapter 1, the interactions of fishes with seamounts may be divided into different groups: (1) Diurnal vertically migrating taxa to the surface layer at dusk and that are advected to the seamount summit by surface currents, (2) weakly migrant/non-migrant fishes that are not able to counter the currents and are advected over the benthopelagic zone around seamounts, (3) adults of meso- and bathypelagic species that live in the benthopelagic zone to increase feeding efficiency, and (4) "pseudooceanic" or "neritopelagic" species that preferentially associate with seamounts and resist advection off the pinnacles. A combination of all these interactions are likely to occur at La Pérouse and MAD-Ridge. A strong SSL was recorded at night-time over the La Pérouse and MAD-Ridge seamounts. These organisms may have been advected to the summit by surface currents, although it might be argued that these organisms may benefit from the seamount slopes having the more favourable currents to ascend to the surface layer at dusk.

Large populations of *D. suborbitalis* have been reported off the slopes of the Equator seamount in the Indian Ocean and to ascend in dense schools over the pinnacle at dusk (Parin & Prutko, 1985). As seen in Chapter 4, *D. suborbitalis* also seem to preferentially associate with the La Pérouse and MAD-Ridge slopes and to ascend to the summit at night. As seen in Chapter 1, to prevent advective loss from the summit, these organisms would have to use their active locomotory capacities to decrease nearest-neighbour distances and orient themselves in the direction of other con-specifics. Some taxa may have shown the "feed-rest" hypothesis, i.e.

fishes would rest in the quiescent shelter offered by the topography and sense the environment above the pinnacle to take advantage of flow-advected prey. Members of the Priacanthidae family, *C. japonicus*, most likely exhibited this strategy. As shown in Chapter 5, seamount-associated fishes displayed similar trophic levels irrespective of their body sizes compared to some of the other fish species, indicating foraging on the same prey items or on prey having similar trophic levels on the summits of the seamounts. The summits of both seamounts may be important feeding grounds for some mesopelagic/benthopelagic taxa that are able to resist advective loss by strong currents. However, some communities may also have actively avoided the seamount due to greater presence of predators. The high densities of various marine organisms including seabirds, swordfish and whales being able to predate on a wide range of micronekton taxa and at various depths (as seen in Chapter 2), in the vicinities of La Pérouse and MAD-Ridge do not exclude the latter hypothesis.

While fishes have been extensively studied in this (and previous) research work, little attention has been paid to cephalopods and crustaceans in the vicinity of seamounts. The scarcity of data related to cephalopod ecology at seamounts partly arise due to the inability to efficiently capture these organisms in the nets. Unlike fish that tend to be herded by nets, squids are able to turn and rapidly escape through the meshes (Clarke, 2007). Top predators are believed to be more accurate "samplers" of cephalopods because cephalopod beaks may be identified from the stomach contents of their predators (Clarke, 2007). Stomach content of swordfish specimens collected close to MAD-Ridge seamount during a 2009 - 2010 survey (https://wwz.ifremer.fr/lareunion/Projets/Grands-pelagiques/IOSSS-ESPADON), recorded the cephalopods *Chiroteuthis* spp., *O. bartramii* and *S. oualaniensis* and other crustaceans and fishes to a lesser extent (unpublished data). However, the problem with this approach is that the beaks of cephalopods may persist in the guts of top predators for extended periods. Given that many of these top predators are highly mobile, the presence of beaks in their guts may not reflect the importance of seamounts as habitats for cephalopods.

The trawls in this study collected two *O. bartramii* specimens at MAD-Ridge and a greater number of lower trophic level cephalopod taxa. As shown in Chapter 4, *Abraliopsis* sp. were caught in larger numbers relative to all other cephalopod species at the La Pérouse and MAD-Ridge seamounts' flanks and in the open ocean. While *Abraliopsis* sp. were caught at various depth categories, they were mostly found in the shallow layer at night, reflecting their diel migration strategies. These organisms were also abundantly recorded at the northern portion of the SWIR (Laptikhovsky et al., 2017) and were among the dominating species at the Great Meteor seamount in the north Atlantic (Diekmann et al., 2006; Diekmann & Piatkowski, 2004).

Other families caught at La Pérouse and MAD-Ridge included specimens of the Onychoteuthidae, Histioteuthidae, Enoploteuthidae, Cranchiidae, Sepiolidae, Ommastrephidae, Chtenopterygidae and Spirulidae families. During the 2009 cruise on the RV Dr *Fridtjof Nansen*, all the above named families were collected at the station closest to MAD-Ridge seamount (see Laptikhovsky et al., 2017). However, maximum cephalopod diversity were associated with the subtropical convergence zone along the SWIR (Laptikhovsky et al., 2017).

Nesis (1993) has described several ecological groups of cephalopods that associate with seamounts: diel vertically migrating species (such as *Abraliopsis* sp.-Enoploteuthidae, and some Histioteuthidae) that are advected over seamounts at night and descend to deeper depths at dawn; nerito-oceanic species (including Enoploteuthidae, Onychoteuthidae and Histioteuthidae) that occur over seamounts as paralarvae, juveniles or sub-adults; benthopelagic species (such as Sepiolidae- typically benthic or neritic; FAO, 2005) that spawn on the bottom but rise into midwater above the seamount; non-migrating species (including some Cranchiidae and Octopoteuthidae) advected over the tops or slopes of seamounts by currents; pelagic species (including Ommastrephidae) that may be advected over seamounts as larvae but avoid areas over the summits of shallow seamounts as juveniles and adults. However, as mentioned by Clarke (2007), all the species found associated with seamounts, also have circumpolar and ocean wide distributions as shown by the diets of top predators. Only very few benthic cephalopod species without pelagic life stages can be considered permanently associated with seamounts but even these were reported to have wide distributions and were poorly sampled in this and other studies (Clarke, 2007). Some cephalopods are believed to use seamounts largely as spawning grounds and as foraging grounds to a lesser extent (Clarke, 2007). However, due to the paucity of data, this hypothesis remains to be verified.

Crustaceans also represent an important group within the micronekton that have been poorly sampled and identified in this study. The La Pérouse and MAD-Ridge cruises recorded the following order and/or families of crustaceans at both seamounts (Oplophoridae, Sergestidae, Caridea, Euphausiacea, Penaeidae, Pasiphaeidae, Gnathophausiidae, Phronimidae and Cystisomatidae), at La Pérouse only (Hyperridea, Phrosinidae, Scinidae) and Oxycephalidae at MAD-Ridge only. Some of these taxa are similar to those sampled along the SWIR during the 2009 RV Dr *Fridtjof Nansen* cruise (see Letessier et al., 2017). Increased numerical abundance and species richness of several crustacean taxa were reported over seamounts of the SWIR and Walters Shoal relative to off-seamount locations (Letessier et al., 2017). The authors

attributed such observations to the topographic blockage mechanism, to organisms being able to actively resist advection from the pinnacles and that make use of the different pelagic and benthic habitat types that seamounts offer. The mesopelagic trawl datasets in this study did not allow this hypothesis to be tested further. Moreover, as seen in Chapters 2 and 4, gelatinous taxa seem to have a ubiquitous distribution irrespective of the presence of topographic features. Despite the high breakability of species in nets, the sheer numbers and biomasses of whole individuals usually dominate the trawl catches or are secondly dominant after the mesopelagic fishes.

The different components of the micronekton have different spatial patterns with respect to topographic features such as seamounts. While some species do not seem to be influenced by seamounts (such as gelatinous organisms), others may preferentially associate with seamounts and prevent advection from the pinnacles or avoid such features (such as few mesopelagic fishes and crustaceans). Other species may have oceanic lifestyles but associate with elevated topographic features at specific time periods during their life cycle (eg. some fishes and squids when they spawn). Micronekton communities also show varied patterns in their horizontal and vertical distributions as shown in Chapters 3 and 4 and in their trophic relationships (as shown in Chapter 5) and these will be further discussed below.

6.4 Horizontal and vertical distributions of micronekton

As shown in Chapters 3 and 4, some micronekton communities migrate horizontally, towards sites with enhanced foraging opportunities. The different locomotory capacities of these organisms may allow them to respond to enhanced prey availability by swimming to advantageous foraging grounds. As shown previously, the different micronekton components have different interactions with the La Pérouse and MAD-Ridge seamounts and hence will not be discussed further.

Diel vertical migration of the mesopelagic community represents one of the Earth's largest daily animal migration when taken as a whole. The stimulus for triggering this vertical movement is believed to be a change in light intensity (Frank & Widder, 2002). The main biological reason is thought to be the enhanced foraging opportunities at the surface and decreased predation rate than in daytime. A number of zooplankton taxa which are important prey items of micronekton undertake nocturnal migrations (Lampert, 1989). One of the main hypothesis put forward to explain the migration of the zooplankton is the presence of larger and nutritionally richer algal cells at dusk in the euphotic zone and/ or decreased risk of being

detected by a predator by day (Lampert, 1989). Migrant micronekton may hence be following the movements of their main prey to the surface at dusk.

The horizontal and vertical distributions of micronekton may also depend largely on their swimming speeds. The sustained swimming speeds of myctophids were estimated at 75 cm s^{-1}, with larger individuals having higher rates than smaller ones (Benoit-Bird & Au, 2006). Shrimps were reported to have sustained swimming speeds of 6 cm s^{-1}, with the rates increasing with larger individuals (Benoit-Bird & Au, 2006). However, macroplankton crustaceans, micronekton fishes and squids may exhibit different swimming speeds for migrational, foraging and escape swimming (Ignatyev, 1996). Organisms having overall body lengths of 1-5 cm were observed to adapt their swimming speeds with fastest swimming during escape (20-50 cm s^{-1} for crustaceans and fishes, and 20-70 cm s^{-1} for squids), intermediate swimming during foraging (2-10 cm s^{-1} for crustaceans, 2.5-30 cm s^{-1} for fishes and 30 cm s^{-1} for squids) and lower swimming speeds during migration (0.5–3 cm s^{-1} for crustaceans, 1.5–10 cm s^{-1} for fishes and 1–3 cm s^{-1} for squids) (Ignatyev, 1996).

Notwithstanding the varied swimming speeds of the broad micronekton groups, while micronekton are thought to be evenly distributed in the bathypelagic zone, high variability in their distributions exist in upper layers of the water column (Lambert et al., 2014). Some organisms may hence be too weak to overcome some of the strong physical currents they are subjected to in the upper layers and may hence be concentrated or dispersed at specific sites. Mesoscale eddies for example, provide mechanisms that dissipate or aggregate micronekton communities (as seen in Chapter 3). Enhanced predation pressures also exist in upper layers, probably leading to enhanced local variability, while only few organisms (mostly Globicephalinae, sperm and beaked whales) are able to dive to 1000 m to forage on deeper fauna as seen in Chapter 2. However, these marine mammals probably prey on larger-sized squids (Clarke, 2007) that already have patchy distributions in the open ocean.

The vertical migration patterns of the different micronekton taxa are also not uniform as seen in Chapters 3 and 4. While some taxa are active migrants to the surface at dusk and to deeper layers at dawn (such as various myctophids), others are non-migrants (eg. Cyclothone) and weakly/non-migrants (e.g. some sternoptychids). Still other taxa, as shown in Chapter 4, undertake mid-water migration to the lower limit of the SSL at night-time and back to the DSL before daytime. Upward and downward migrations seem to occur in a series of events. Differential migration strategies used by smaller and larger fishes have been reported, with smaller fishes (swimming at slower speed) leaving their location first (Benoit-Bird & Au,

2006). Differential use of habitat at different times of the night by organisms in order to reduce competition between individuals in dense aggregations have also been reported (Benoit-Bird & Au, 2006). Migrating organisms possibly have to compromise between the need to feed and to avoid predators. Different individuals within the micronekton communities likely have different preferred habitats in order to strike a balance between the selective pressures of optimising foraging while avoiding competition and predators.

Furthermore, the permanent distribution of some taxa at deeper depths during both day and night (eg. Cyclothone) may be linked to these organisms having developed distinct evolutionary traits such as small and simple, larval-like body structure which would allow them to survive in food-poor environments at greater depths (Miya & Nishida, 1996). Deep-dwelling Cyclothone individuals exhibited lower $\delta^{15}N$ values relative to relatively larger, diel migratory deep sea fishes which forage at the surface at dusk (Chapter 5). Diel migratory fishes have higher energetic needs due to the energy spent in vertically migrating hundreds of metres up and down the water column daily. Such energetic costs have to be met by higher probability for these organisms to forage on greater abundances of prey and/or on prey of greater energetic content. Some mesopelagic fish and squid taxa have developed bioluminescent organs, enabling them to forage, attract a mate, recognize con-specifics or camouflage themselves against predators in deep-sea environments (Young et al., 1979; Young, 1983; Mensinger & Case, 1990; Catul et al., 2011; Davis et al., 2014). While it is difficult to disentangle all the factors that may have led to the horizontal and vertical migration strategies of individual species, organisms clearly have morphological adaptations enabling them to exploit a wide range of vertical and horizontal habitat types.

6.5 Trophic relationships and importance of micronekton in foodwebs

The stable isotope values of carbon, which may help differentiate sources of primary production, were significantly different between the POM at the surface of the La Pérouse and MAD-Ridge seamounts, with higher median values at MAD-Ridge (Chapter 5). Primary production at MAD-Ridge may result from a wide range of sources as seen previously in this Chapter relative to La Pérouse that is located in a less dynamic and oligotrophic system. Due to the anticyclonic conditions during the MAD-Ridge cruise, the depth of the maximum fluorescence was within the same range as that measured in a weak cyclonic eddy at La Pérouse. The higher median $\delta^{15}N$ values of the POM at the maximum fluorescence, collected within the anticyclonic eddy at MAD-Ridge possibly reflect the more active physical dynamics influencing productivity at MAD-Ridge relative to La Pérouse.

Stable isotope values of all micronekton communities, however, did not reveal major differences between the La Pérouse and MAD-Ridge seamounts (Chapter 5). At both seamounts, gelatinous salps and pyrosomes occupied the lowest trophic level (TL 2). This is linked to the filter feeding strategy of these organisms that ingest a variety of suspended particles in their different environments (Harbou, 2009; Conley, 2017). The sampled crustaceans occupied an intermediate trophic level (TL ~3). This group comprises different species having feeding modes relative to that of organisms that prey on zooplankton, euphausiids, and copepods, and are known for occasional herbivory. Mesopelagic fishes and smaller-sized squids occupied TL between 3 and 4 at both seamounts. Some carnivorous/omnivorous diel vertical migrators (fishes *S. elongatus*, *C. warmingii* and squid *Abraliopsis* sp.), however exhibited slightly greater $\delta^{15}N$ values at La Pérouse relative to MAD-Ridge with respect to body size compared to other organisms that showed no significant differences. While small variability may exist within species, overall patterns reveal stable isotope values linked to size since, as individuals grow bigger, they generally feed on larger prey.

Seamount-associated fishes, however, displayed similar trophic levels irrespective of their wide body sizes (Chapter 5). As seen previously, this suggest foraging on similar organisms or organisms having similar trophic levels. This seem to confirm the importance of La Pérouse and MAD-Ridge summits and flanks as feeding grounds for some mesopelagic/benthopelagic taxa foraging on populations of calanoids and chaetognaths. The complex diversity of organisms within the micronekton reflect a complex set of embedded processes linked to feeding mode, size and possibly productivity, foraging patterns, tissue turnover rate of individuals, time of day and depth. The different crustacean, smaller-sized fishes and squids species studied may channel the same amount of energy to top predators. Larger nekton *O. bartramii* are at a higher trophic level than micronekton and may provide more energy to predators. They are the preferred prey of deeper diving swordfish, especially in oligotrophic systems like the ISSG (Ménard et al., 2013; Annasawmy et al., 2018). Top predators capable of foraging at deeper depths and on larger nekton can take advantage of this additional resource in oligotrophic environments of the ISSG where prey resources are limited. The sheer biomass of all the different micronekton species in more eutrophic environments, on the other hand, may provide a wider range of food sources for the various top predators.

6.6 Ecosystem functioning at seamounts

This study has shed new light on the ecosystem functioning at two poorly studied topographic features of the SWIO. When placed in a broader context in the region (Fig. 6.1a), total micronekton acoustic densities at the La Pérouse seamount is typical of the ISSG province, whereas acoustic responses at the MAD-Ridge seamount is typical of the EAFR province (Fig. 6.1b). Micronekton acoustic densities were greater within the EAFR and at the MAD-Ridge seamount relative to the ISSG and the La Pérouse seamount, probably due to the effect of mesoscale eddies and enhanced productivity in the EAFR (Fig. 6.1b). No clear enhancement of micronekton was observed at the seamounts relative to the surrounding ocean in the biogeochemical provinces. However, high backscatter intensities were observed in the surface layer during the day at both seamounts probably due to the presence of dense scatterers aggregating over the seamounts' summits and flanks.

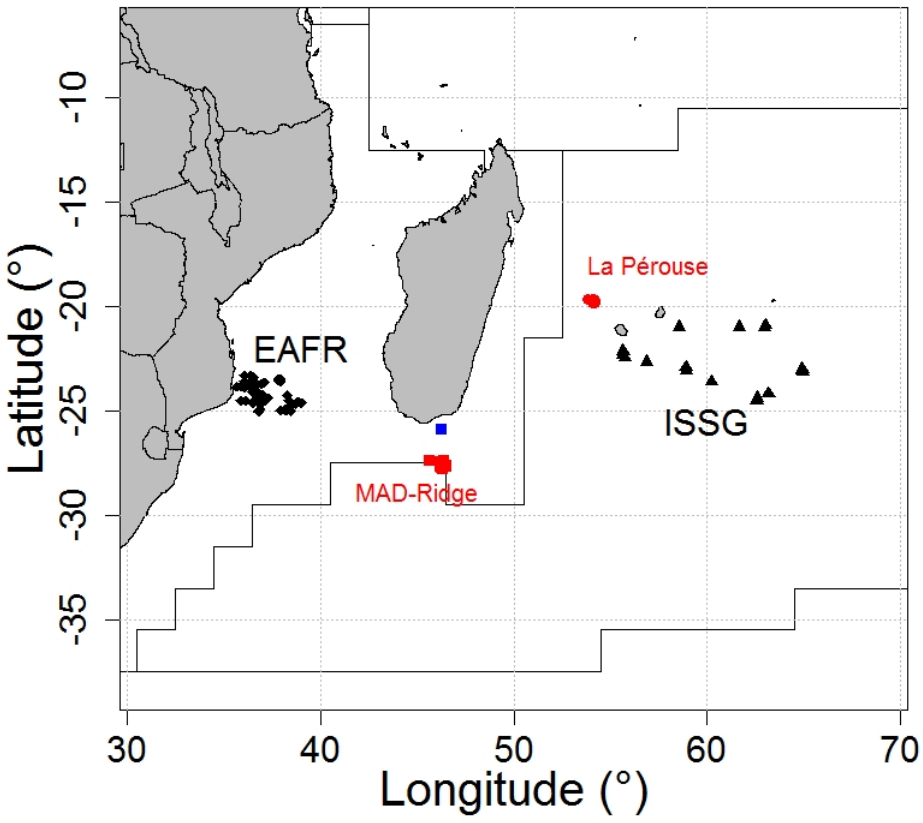

Figure 6.1(a) Map of the MICROTON stations (black triangles) and La Pérouse seamount (red dot) in the ISSG province, of the MESOP 2009 stations (diamond symbols) (Annasawmy et al., 2018), Madagascar shelf station (blue square) and MAD-Ridge stations (red squares) in the EAFR province. Longhurst's (2007) biogeochemical provinces (ISSG and EAFR) are delimited by black solid lines.

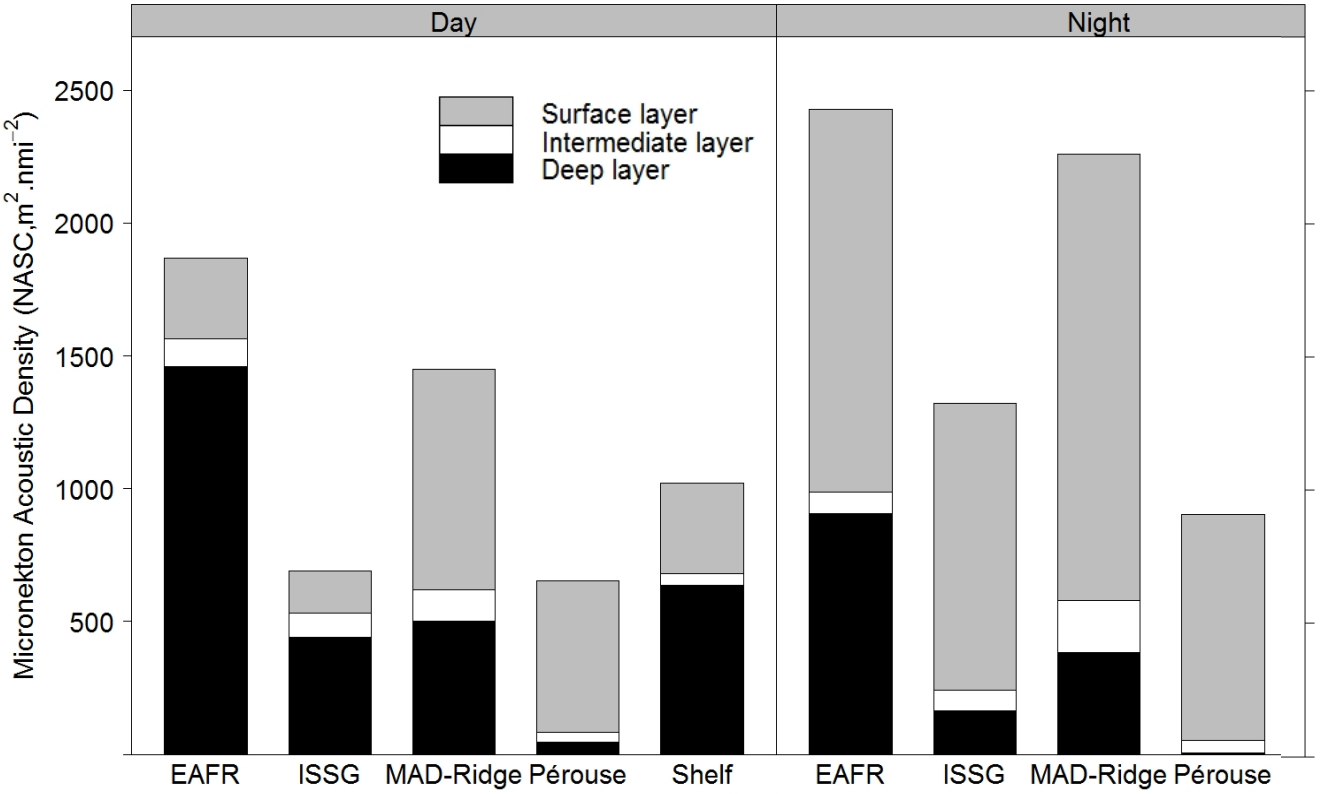

Figure 6.1(b) Mean s_A during MESOP 2009 cruise in the EAFR, MICROTON cruise in the ISSG provinces (Annasawmy et al., 2018), at MAD-Ridge and La Pérouse seamounts and over the Madagascar shelf for day and night sections: grey for the surface layer (10-200 m), white for the intermediate layer (200-400 m), and black for the deep layer (400-740 m).

As seen in Table 6.1, the ecosystem functioning at both the La Pérouse and MAD-Ridge seamounts are complex. Local physical processes such as Taylor columns and isopycnal domings leading to significant phytoplankton enhancement were not observed during the La Pérouse and MAD-Ridge cruises. No major zooplankton enrichment were observed at MAD-Ridge and at La Pérouse, except on the leeward side of the seamount (Marsac et al., 2020). Ichthyoplankton enhancements were recorded on MAD-Ridge summit, suggesting spawning sites (Harris et al., 2020). No ichthyoplankton enhancements were observed on the La Pérouse summit relative to off-seamount locations, possibly owing to small sample sizes. While, micronekton acoustic densities were lower at the seamounts relative to the surrounding ISSG

and EAFR biogeochemical provinces, both seamounts hosted resident fishes over the summits and flanks. These seamount-associated species exhibited the same trophic levels at both pinnacles despite their different size ranges. Despite the differing productivity and eddy dynamics at both pinnacles, the micronekton sampled exhibited the same range of trophic levels. Micronekton would thus channel similar amount of energy to higher trophic levels such as humpback whales and marine birds foraging in the vicinity of the seamounts.

Table 6.1 Summary of the ecosystem functioning at the La Pérouse and MAD-Ridge seamounts. Crosses indicate that the corresponding attribute was not observed while tick marks indicate that the corresponding attribute has been observed and recorded.

Attribute	La Pérouse	MAD-Ridge	Additional comments
Local physical enrichment from Taylor column/ doming of isopycnals	✗	✗	Internal tide generation at MAD-Ridge (Koch-Larrouy et al., in review)
Phytoplankton enhancement relative to off-seamount locations	✗	✗	Only moderate picoplankton biomass over the summit of MAD-Ridge
Zooplankton enhancement relative to off-seamount locations	✓	✗	No major enrichment observed. except on the leeward side of La Pérouse
Ichthyoplankton enhancement relative to off-seamount locations	✗	✓	La Pérouse and MAD-Ridge may serve as spawning sites
Greater micronekton acoustic response relative to off-seamount locations	✗	✗	Greater at MAD-Ridge relative to La Pérouse
Seamount-associated species	Presence of *D. suborbitalis*	Presence of *D. suborbitalis*, *C. japonicus*, *B. fibulatum*	Presence at seamounts' summits and flanks during day and night
Presence of micronekton predators	Humpback whales	Marine birds	Marine birds and humpback whales use both seamounts during their breeding season

Trophic levels (TL) of gelatinous organisms and micronekton	Gelatinous: ~2 Crustaceans: ~3 Smaller-sized squids: ~3 to 4 Fishes: 3 to 4	Gelatinous: ~2 Crustaceans: ~3 Smaller-sized squids: ~3 to 4 Larger-sized squids: ~5 Fishes: 3 to 4	Seamount-associated species *D. suborbitalis*, *C. japonicus*, *B. fibulatum* exhibited a TL of 4 despite their different size ranges

Despite being ubiquitous topographic features in the world's oceans, seamounts and their ecosystems are still poorly known. Only 0.4-4% of the world's seamount population have been directly sampled for scientific research (Kvile et al., 2014). Data sharing and accessibility represent further important obstacles in seamount research. This study therefore adds to the current knowledge pool of the ecosystem functioning at seamounts. An important finding in this study is the presence of dense aggregations over the summits and flanks of La Pérouse and MAD-Ridge during day and night. This finding is similar to previous other studies, whereby fish were found in close association with seamounts in over 150 cases (Kvile et al., 2014). Despite their complex topographies or local physical processes, seamounts were shown to confer selective advantages to aggregating fishes that utilize these features for feeding, spawning or resting (Porteiro & Sutton, 2007). Feeding the observations from this study in global databases such as the SEEF (Seamount Ecosystem Evaluation Framework) (Kvile et al., 2014) may help identify knowledge gaps, characterize peculiarities of individual seamounts and further test potential seamount effects to understand which factors are driving the dynamics of the different types of seamounts.

6.7 Growing interest in commercialising micronekton communities

Cephalopod fisheries already exist targeting a wide range of species (Roper et al., 1984). Due to their sheer numbers and ubiquitous nature, interests in exploiting mesopelagic fishes is rapidly growing (Dalpadado & Gjøsæter, 1988). Vertically migrating myctophids are reported to contain triglycerides, potassium, sodium and calcium and to lack harmful bacteria (Gopakumar et al., 1983), making their commercialisation attractive to many interested parties. In the Arabian Sea, the mesopelagic myctophid stock has been estimated at 20-100 million tons with a potential yield of ~200 000 tons per year (Gjøsæter & Kawaguchi, 1980; Catul et al., 2011). In order to meet the ever-increasing demand for more fish for domestic use and export and in the face of a growing human population, other viable options to increase fish production

and hence to ensure the human food security are being explored. Commercial exploitation of mesopelagic organisms may be used for human consumption, as fishmeal in aquaculture farms and for providing nutraceuticals. Previous studies have estimated that ~2.7% of the most recent global estimate of mesopelagic fish would be needed for a global aquaculture production of 67 million tons (FAO, 2014). It was further estimated that 5 billion tons of mesopelagic biomass could result in 1.25 billion tons of food for human consumption (St John et al., 2016), and that lanternfishes are highly attractive sources of raw materials in the production of nutraceutical products (Koizumi et al., 2014).

However, commercial fishing of mesopelagic taxa will lead to a number of issues if not sustainably managed. As seen with the Antarctic krill, predator foraging grounds overlap with fisheries (Hinke et al., 2017), putting an additional pressure on the predators. Moreover, mesopelagic taxa are increasingly being impacted by microplastic pollution through ingestion (Wieczorek et al., 2018) and through plastic contaminants (Rochman et al., 2014). This may put a negative pressure on the stocks of mesopelagic organisms but also on their predators. Even when foraging prey are abundant, tunas were found to show a decline in condition due to variabilities in the size structure and nutritional composition of their prey (Golet et al., 2015). Climate change is another pressure to which organisms will have to adapt. Additionally, as seen in Chapter 2, some sites such as seamounts are already under fishing pressures and all the related pollution impacts linked to fishing. Mesopelagic fishing can further enhance fishing gear pollution, by-catch rates of top predators, and depletion of the resource (if not appropriately managed) at these already vulnerable ecosystems. In any case, trial catch in the Oman Sea were too low to support fishing costs (Valinassab et al., 2007) and to date, the correct fishing methods, gears and vessel size still need to be identified for a viable fishery.

6.8 Conservation measures and issues

As seen previously, the La Pérouse and MAD-Ridge seamounts host important benthic habitats, seamount-resident/associated fauna, are important sites for several top predator species (some of which being of commercial interests), and probably contain mineral resources such as manganese and other polymetallic nodules. Both seamounts are of significant interests for fishing and deep-sea mining and nowadays, they both potentially suffer the adverse effects of fishing and pollution. Deep-sea bottom trawling may remove coral habitats with negative impacts on benthic biodiversity, foraging and spawning grounds of several species in the foodweb. As seen in Chapters 1 and 2, the effective implementation of conservation measures is challenging, especially on the high seas, where illegal, unreported and unregulated fishing occur due to the inability to control and monitor activities owing to the remoteness of locations

and the associated costs. Hence, conservation measures that are set-up should ensure appropriate monitoring and control plans to prevent illegal activities on the high seas.

Management actions will also require a balance between exploitation (to satisty fisher's needs, guarantee jobs and food security) and conservation (to protect vulnerable resources and ensure sustainability of fish stocks). Conservation measures are seldom effective if enforced without concerting all the relevant parties such as scientists, government officials, fishery managers, fishers, and the local population. Scientific research on seamount ecosystems are of paramount importance to improve the knowledge base on seamount-associated communities and to facilitate discussion between managing bodies. As seen previously, countries in the SWIO often lack scientific, technical, human-resource and management capacities that will enable effective conservation plans and implementation. In addition to the current managing bodies that are sometimes blocked in their managing capacities, a special regional task-force providing scientific, technical, human-resource and management capacities (not only for key species such as tunas) but also all fauna and the benthic environment, should be set-up. There is an urgent need to recognize that ecosystems function as a whole and the different components or species do not function independently of each other.

Furthermore, as seen in Chapters 1 and 2, several potential management actions could be implemented such as site-specific regulations or activity-specific regulations, single MPAs or whole MPA networks. The La Pérouse seamount is not part of a ridge system and does not seem to support a large diversity of species relative to MAD-Ridge. Regulations banning possible future bottom trawling to protect the seamount habitat and temporary fishing closures during the breeding season of humpback whales are some measures that could be promoted. MPA networks are often deemed more successful than other management actions since significant spill-over effects may occur if the networks are appropriately located. To have a significant impact, we have further seen in Chapter 2, that the MPAs will need to have at least four or five of the following features: older (>10 years), larger (>100 km^2), isolated by deep water or sand, non-extractive and effectively enforced (Edgar et al., 2014).

The set-up of MPA networks for at least 10 years along the Madagascar Ridge, covering at least 100 km^2 around each pinnacle having an elevation of more than 1500 m and reaching into the euphotic zone (such as the MAD-Ridge and Walters Shoal seamounts) are among possible conservation measures. They may prove beneficial for benthic habitats, mesopelagic organisms having specific life patterns at these seamounts and for top predators using the pinnacles as foraging grounds, during their migration routes and breeding seasons. Bottom, mid-water

trawling and mining activities would have to be banned at these seamounts to protect the integrity of the associated ecosystems. Moreover, since seamounts from the Madagascan shelf to MAD-Ridge are located within the EEZ of Madagascar, conservation measures and actions could only be implemented by Madagascar. Scientific and financial support, as well as, assistance for enforcement, could be sought from other nations. The other seamounts along the Madagascar Ridge, since they are located in areas beyond national jurisdiction, could only be preserved by promoting cooperation with member states at the regional and international level. While MPA networks may prove highly beneficial if appropriately set-up and enforced, they may be faced with significant oppositions from states in the region, fisheries operators or managers, governing bodies and mining lobbyists. Presently, the prospect of high economic yields do not encourage efforts to preserve the resources even if conservation actions can sustainably support, in the medium term, not only fish stocks of commercial value, but also whole ecosystems which are under various anthropogenic pressures.

6.9 Future Perspectives

6.9.1 Multi-frequency acoustic classification

While this thesis work has allowed to address the knowledge deficit as to the horizontal and vertical distributions, the assemblages and trophic relationships of micronekton communities with respect to environmental conditions at the La Pérouse and MAD-Ridge seamounts, significant knowledge gaps still remain. One significant gap identified stems from the low number of mid-water trawls that have been conducted owing to the multi-disciplinary nature of the cruises. As seen in Chapter 4, the trawl sampling failed to capture the full range of organisms present due to avoidance reactions and escape from the nets, damage done to soft-bodied individuals and inadequate sampling over the summits. The net used was further selective in the size range of organisms that have been captured. Crustaceans and squids were poorly represented in net-based estimates.

The multi-frequency acoustic visualisation technique employed in this study is useful in identifying scattering layers with similar frequency responses at their respective depths and identifying dense aggregations of scatterers. However to be able to classify the overall acoustic backscatter into a number of acoustic groups corresponding to biological samples, an algorithm tool that discriminates groups of scatterers in the first 200 m of the water column has to be developed and calibrated for each dataset. Such multi-frequency classification techniques have already been explored (Anderson et al., 2007; Soto, 2010; Woillez et al., 2012; Kloser et al., 2016; Béhagle et al., 2017) and typically uses a combination of frequencies to discriminate several acoustic classes.

Different organisms have different frequency responses. While the backscatter of fluid-like and elastic-shelled organisms increases with the size/frequency between 38 and 120 kHz; that of larvae and adult-swimbladdered fish remains relatively constant or decreases between 38 and 120 kHz frequencies (Korneliussen & Ona, 2003). The combination of RGB composites and trawl surveys (as seen in Chapter 4) can be used to identify and create acoustic classes from the different groups of scatterers. This would apply to cases such as: (i) the dense aggregations over the summits of La Pérouse and MAD-Ridge pinnacles; (ii) the aggregations dominating RGB composites within the depth of the maximum fluorescence; (iii) the night-time SSL over the summits of the seamounts; and (iv) under-represented groups such as the “blue patches” observed on RGB composite of trawl #21 during MAD-Ridge. Pairwise frequency differences (Δ Sv 70-38, Δ Sv 120-38) and the sums Δ Sv 38 + 120 + 70 can be used as discriminatory variables for the classification of the different acoustic classes. Each class will form libraries of acoustic groups. Thresholds will have to be determined to obtain the best comprise in

separating the different acoustic groups. The thresholds can be calculated from the mean and standard deviation of the libraries. A confidence interval index will also have to be determined based on the percentages of acoustic backscatter well classified and that classified in another acoustic class. The libraries of acoustic groups can further be investigated statistically using a K-means clustering.

Once the acoustic classes have been confidently determined, these criteria can be used to classify the acoustic backscatter from the whole cruise transects into the identified groups. Trawl surveys can be used to complement acoustic surveys in validating the groups. However, since acoustic data were not recorded during six out of ten trawl surveys during the La Pérouse cruise, applying multi-frequency acoustic techniques to this dataset will be more risky. Furthermore, due to the nature of the system, trawl surveys were not mono-specific, and hence, confidently attributing acoustic groups to distinct biological samples is more risky. However, a combination of RGB composites with trawl transects (Chapter 4), and RGB plots with Scanfish transects can be used. The Scanfish recorded the temperature and fluorescence profiles horizontally and vertically in the first 100 m of the water column during MAD-Ridge cruise (Herbette, unpublished data). Using a combination of trawl and environmental data sets, combined with RGB composites and multi-frequency classification algorithms may allow a more accurate classification of the different groups: dense swim-bladdered fish aggregations, gelatinous organisms and plankton-like organisms associating with the maximum fluorescence.

6.9.2 Trace metal analyses

Micronekton may concentrate trace elements such as Mercury, Cadmium, Zinc, Copper, Selenium, Lead, Iron and Chromium. While zinc, copper, chromium, iron and selenium are essential elements, mercury, cadmium and lead can be potentially toxic (Bodin et al., 2017). Essential elements are those which are important for the normal functioning of the cell, such as enzyme cofactors (e.g. zinc is a cofactor to over 300 enzymes, Chasapis et al., 2012) and antioxidants (e.g. selenium, Tingii, 2008). Mercury, on the other hand, is known to be methylated by microorganisms, to bioaccumulate in marine biota and to biomagnify along the food chain, with predators showing higher tissue concentrations than their main prey items (Bustamante et al., 2006). In the marine environment, methyl mercury is the most stable, but also the most toxic form to organisms (Cossa et al., 1990). The bioaccumulation and biomagnification of toxic trace elements can thus be harmful to micronekton and top predators if a significant transfer occurs.

Ultimately, high concentrations of hazardous trace elements in tissues of top marine predators such as tunas and swordfish can lead to food insecurity if the trace element concentrations exceed the guideline values established by the Ministry of Agriculture, Fisheries and Food (MAFF, 2000). Recommended guideline values have been established at 0.3 µg/g wet weight (ww) for mercury, 0.2 µg/g ww for cadmium, 50 µg/g ww for zinc, 20 µg/g ww for copper and 2 µg/g ww for lead (Asante et al., 2010). Concentrations of essential minerals in tissues of micronekton, on the other hand, will provide knowledge on the nutritional composition of the species that support top marine predators in pelagic ecosystems. While trace element concentrations in tissues of top pelagic predators of the Indian Ocean have been previously described (Bodin et al., 2017), knowledge of trace mineral concentration in tissues of micronekton is scarce and fragmentary in other ocean basins (Asante et al., 2008, 2010), and non-existent in the south-western Indian Ocean.

The combined actions of terrigenous inputs and washouts of trace minerals and nutrients into coastal Malagasy waters from land and advection of these nutrients and minerals by mesoscale cyclonic and anticyclonic eddies to MAD-Ridge may lead to greater trace mineral concentrations in tissues of micronekton at MAD-Ridge relative to La Pérouse. Highly migratory top predators consuming micronekton at the MAD-Ridge seamount may have higher or similar trace element concentrations. As shown in Asante et al. (2008), higher trophic animals may retain higher concentrations of trace elements than lower trophic organisms. The micronekton species from La Pérouse and MAD-Ridge cruises, previously selected for stable isotope analyses, will be used to investigate trace mineral dynamics as part of a post-doctoral project starting January 2020 at the SFA (Seychelles Fishing Authority) and GET (Géosciences Environnement Toulouse), and funded by the WIOMSA (Western Indian Ocean Marine Science Association) MARG I grant. The concentrations of trace minerals in tissues of migrant vs. non-migrant micronekton taxa will be investigated to determine the horizontal distribution of trace minerals in the water column. These minerals will also be studied with respect to body size and feeding habits of the different micronekton taxa. The relationship between concentrations of trace minerals and stable isotope ($\delta^{13}C$ and $\delta^{15}N$) values in tissues of sampled micronekton will be determined.

6.10 Conclusion

The SWIO is a contrasted region with elevated bathymetric features, circulation patterns in the form of currents and mesoscale eddies, and water masses navigating through its ridge systems. This region hosts a wide range of marine organisms including seabirds, turtles, cetaceans, whales, sharks, tunas, billfishes and demersal fishes. Tunas, billfishes, demersal fishes and a few shark species are targeted by industrial fisheries. Interactions also occur between fisheries activities and other components of the megafauna. As shown in this thesis, the La Pérouse and MAD-Ridge seamounts represent elevated topographies in the SWIO, offering varied habitat types in an otherwise deep and open ocean environment. Various organisms in the region are associated with the La Pérouse or MAD-Ridge seamounts during their breeding season, foraging or migration patterns. These two seamounts possibly host coral communities thus attracting a wide range of benthopelagic organisms. Acoustic detections during this study have suggested permanent residency of biological scatterers over the seamounts during day and night. The shelter-like character and possibly enhanced foraging opportunities for these organisms may explain this observation.

The La Pérouse and MAD-Ridge seamounts did not show elevated concentrations of zooplankton and micronekton communities relative to off-seamount locations. Elevated concentrations of ichthyoplankton were observed on MAD-Ridge summit relative to off-seamount habitats. The physical and biological environment at both seamounts may not be attractive enough for adult forms of some mesopelagic taxa relative to other regions of the EAFR province including the more productive Madagascar shelf and Mozambique Channel. Some taxa possibly avoid the seamounts due to higher predation risk. This thesis has demonstrated that micronekton is a diverse group of organisms exhibiting different migrating, foraging, spawning patterns and trophic levels. A combination of trawl and acoustic surveys have shown that some organisms perform their daily DVM irrespective of the presence of the seamounts. Other organisms, such as few lanternfishes, reside at the seamounts' flanks during the day and vertically migrate to the seamount summits at dusk. The different migrants may vary their speed, direction and timing of their daily migration to take advantage of prey items at different spatial and temporal scales. This may allow prey and space partitioning to avoid competition. DVM may also depend on the physiological limit of the species and the differing life stages within the same species. For some organisms, including the widely distributed *Cyclothone* sp., it is more advantageous to stay at deeper depths. Some organisms in the mesopelagic realm depend mostly on sinking particles through degradation of organic matter, part of which comes from the faecal matter of migrants that forage in the euphotic zone. Despite

their varied migration and foraging strategies, micronekton (crustaceans, mesopelagic fishes and smaller-sized squids) occupy trophic levels between three and four at both seamounts, thus potentially channeling similar amounts of energy to top predators present at these sites.

Mesopelagic organisms (from gelatinous plankton to nekton) support a wide variety of predators in the region, which are able to physiologically forage at various depths and cover a wide spatial range to reach most productive sites. Although the La Pérouse and MAD-Ridge seamounts did not show enhanced diversity and biomass of organisms relative to the surrounding ocean, both pinnacles are important sites for specific communities that would suffer from various anthropogenic pressures if appropriate conservation measures were not implemented. This thesis underlined the need to conduct more multi-disciplinary scientific research work in the SWIO in order to identify and fill important knowledge gaps, allowing the detection of vulnerable marine ecosystems, and proposing an Ecosystem Approach to Fisheries (EAF) management and marine spatial planning strategies.

References

Adduce, C., Cenedese, C., 2004. An experimental study of a mesoscale vortex colliding with topography of varying geometry in a rotating fluid. J. Mar. Res. 62, 611-638. https://doi.org/10.1357/0022240042387583

Ahamada, S., Bijoux, J., Bigot, L., Cauvin, B., Maharavo, J., Meunier, S., Moine-Picard, M., Quod, J.-P., Pierre-Louis, R., 2004. Status of the coral reefs of the south west Indian Ocean island states. Status of coral reefs of the world. 1: 189-212.

Aksnes, D. L., Røstad, A., Kaartvedt, S., Martinez, U., Duarte, C.M., Irigoien, X., 2017. Light penetration structures the deep acoustic scattering layers in the global ocean. Sci. Adv. 3: e1602468

Altabet, M.A., Francois, R., 1994. Sedimentary nitrogen isotopic ratio as a recorder for surface ocean nitrate utilization. Glob. Biogeochem. Cycles 8: 103–116. https://doi.org/10.1029/93GB03396

Alverson, F.G., 1961. Daylight Surface Occurrence of Myctophid Fishes Off the Coast of Central America. Pac Sci. 15(3): 483. http://hdl.handle.net/10125/9088

Amandè, M-J., Chassot, E., Chavance, P., Pianet, R., 2008. Silky shark (*Carcharhinus falciformis*) bycatch in the French tuna purse-seine fishery of the Indian Ocean. IOTC WPEB.

Amorim, P., Figueiredo, M., Machete, M., Morato, T., Martins, A., Santos, R.S., 2008. Spatial variability of seabird distribution associated with environmental factors: a case study of marine important bird areas in the Azores. ICES J. Mar. Sci. 66(1): 29-40.

Andersen, V., Sardou, J., 1994. *Pyrosoma atlanticum* (Tunicata, Thaliacea): diel migration and vertical distribution as a function of colony size. J. Plankton Res. 16: 337–349. https://doi.org/10.1093/plankt/16.4.337

Andersen, V., François, F., Sardou, J., Picheral, M., Scotto, M., Nival, P., 1998. Vertical distributions of macroplankton and micronekton in the Ligurian and Tyrrhenian Seas (northwestern Mediterranean). Oceanologica Acta 21(5): 655-676.

Anderson, C.I.H., Horne, J.K., Boyle, J., 2007. Classifying multi-frequency fisheries acoustic data using a robust probabilistic classification technique. J. Acoust. Soc. Am. 121: EL230. https://doi.org/10.1121/1.2731016

Annasawmy, P., Ternon, J.F., Marsac, F., Cherel, Y., Béhagle, N., Roudaut, G., Lebourges-Dhaussy, A., Demarcq, H., Moloney, C.L., Jaquemet, S., Ménard, F., 2018. Micronekton diel migration, community composition and trophic position within two biogeochemical provinces of the South West Indian Ocean: Insight from acoustics and stable isotopes. Deep Sea Res. Part Oceanogr. Res. Pap. 138: 85–97. https://doi.org/10.1016/j.dsr.2018.07.002

Annasawmy, P., Ternon, J-F., Cotel, P., Demarcq, H., Cherel, Y, Romanov, E., Roudaut, G., Lebourges-Dhaussy, A., Ménard, F., Marsac, F., 2019. Micronekton distribution and assemblages at two shallow seamounts in the south-western Indian Ocean: Insights from acoustics and mesopelagic trawl data. Prog. Oceanogr. 178. https://doi.org/10.1016/j.pocean.2019.102161

Appelbaum, S., 1982. Studies on food organisms of pelagic fishes as revealed by the 1979 North Atlantic Eel Expedition. Helgoländer Meeresuntersuchungen. 35, 357–367. https://doi.org/10.1007/BF02006143

Ariza, A., Landeira, J.M., Escánez, A., Wienerroither, R., Aguilar de Soto, N., Røstad, A., Kaartvedt, S., Hernández-León, S., 2016. Vertical distribution, composition and migratory patterns of acoustic scattering layers in the Canary Islands. J. Mar. Syst. 157, 82–91. https://doi.org/10.1016/j.jmarsys.2016.01.004

Arreguín-Sánchez, F., Valero-Pacheco, E., Chávez, E.A., 1993. A Trophic Box Model of the Coastal Fish Communities of the Southwestern Gulf of Mexico. In: Christensen, V., Pauly, D. (Eds), Trophic Models of Aquatic Ecosystems. ICLARM Conference Proceedings, 26: 390.

Asante, K.A., Agusa, T., Mochizuki, H., Ramu, K., Inoue, S., Kubodera, T., Takahashi, S., Subramanian, A., Tanabe, S., 2008. Trace elements and stable isotopes ($\delta^{13}C$ and $\delta^{15}N$) in shallow and deep-water organisms from the East China Sea. Environ. Pollut. 156: 862–873. https://doi.org/10.1016/j.envpol.2008.05.020

Asante, K.A., Agusa, T., Kubota, R., Mochizuki, H., Ramu, K., Nishida, S., Ohta, S., Yeh, H., Subramanian, A., Tanabe, S., 2010. Trace elements and stable isotope ratios ($\delta^{13}C$ and $\delta^{15}N$) in fish from deep-waters of the Sulu Sea and the Celebes Sea. Mar. Pollut. Bull. 60: 1560–1570. https://doi.org/10.1016/j.marpolbul.2010.04.011

Atkinson, A., Siegel, V., Pakhomov, E.A., Jessopp, M.J., Loeb, V., 2009. A re-appraisal of the total biomass and annual production of Antarctic krill. Deep Sea Res. Part Oceanogr. Res. Pap. 56: 727–740. https://doi.org/10.1016/j.dsr.2008.12.007

Attwood, C.G., Harris, J.M., Williams, A.J., 1997. International experience of marine protected areas and their relevance to South Africa. South Afr. J. Mar. Sci. 18: 311–332. https://doi.org/10.2989/025776197784161162

Bailey, R.S., 1968. The Pelagic Distribution of Sea-birds in the Western Indian Ocean. Ibis. 110(4): 493–519. https://doi.org/10.1111/j.1474-919X.1968.tb00060.x

Bakun, A. 1996. Patterns in the ocean: ocean processes and marine population dynamics. California Sea Grant, in cooperation with Centro de Investigaciones Biologicas del Noroeste, La Paz, Mexico.

Bakun, A., 2006. Fronts and eddies as key structures in the habitat of marine fish larvae: opportunity, adaptive response and competitive advantage. Sci. Mar. 70, 105–122. https://doi.org/10.3989/scimar.2006.70s2105

Baliño, B.M, Aksnes, D.L., 1993. Winter distribution and migration of the sound scattering layers, zooplankton and micronekton in Masfjorden, western Norway. Mar. Ecol. Prog. Ser. 102: 35-50. https://www.int-res.com/articles/meps/102/m102p035.pdf

Ballorain, K., Bourjea, J., Ciccione, S., Kato, A., Hanuise, N., Enstipp, M., Fossette, S., Georges, J., 2013. Seasonal diving behaviour and feeding rhythms of green turtles at Mayotte Island. Mar. Ecol. Prog. Ser. 483: 289–302. https://doi.org/10.3354/meps10301

Barcelos, L., Porteiro, F.M., Melo, O., Clarke, M., Menezes, G., 2005. Feeding Ecology of orange roughy, *Hoplostethus atlanticus* Colett, 1889, in the Azores Archipelago. In: 40th European Marine Biology Symposium. pp 61-62.

Barlow, R., Kyewalyanga, M., Sessions, H., van den Berg, M., Morris, T., 2008. Phytoplankton pigments, functional types, and absorption properties in the Delagoa and Natal Bights of the Agulhas ecosystem. Estuar. Coast. Shelf Sci. 80: 201–211. https://doi.org/10.1016/j.ecss.2008.07.022

Barlow, R., Lamont, T., Morris, T., Sessions, H., van den Berg, M., 2014. Adaptation of phytoplankton communities to mesoscale eddies in the Mozambique Channel. Deep Sea Res. Part II Top. Stud. Oceanogr. 100: 106–118. https://doi.org/10.1016/j.dsr2.2013.10.020

Barnett, A., Abrantes, K.G., Seymour, J., Fitzpatrick, R., 2012. Residency and Spatial Use by Reef Sharks of an Isolated Seamount and Its Implications for Conservation. PLoS ONE, 7: e36574. https://doi.org/10.1371/journal.pone.0036574

Bashmachnikov, I., Mohn, C., Pelegrí, J.L., Martins, A., Jose, F., Machín, F., White, M., 2009. Interaction of Mediterranean water eddies with Sedlo and Seine Seamounts, Subtropical Northeast Atlantic. Deep Sea Res. Part II Top. Stud. Oceanogr. 56: 2593–2605. https://doi.org/10.1016/j.dsr2.2008.12.036

Bashmachnikov, I., Loureiro, C.M., Martins, A., 2013. Topographically induced circulation patterns and mixing over Condor seamount. Deep Sea Res. Part II Top. Stud. Oceanogr. 98: 38–51. https://doi.org/10.1016/j.dsr2.2013.09.014

Bastos, R.F., Corrêa, F., Winemiller, K.O., Garcia, A.M., 2017. Are you what you eat? Effects of trophic discrimination factors on estimates of food assimilation and trophic position with a new estimation method. Ecol. Indic. 75: 234-241. http://dx.doi.org/10.1016/j.ecolind.2016.12.007

Beal, L. M., De Ruijter, W. P. M., Biastoch, A., Zahn, R., 2011. On the role of the Agulhas system in ocean circulation and climate. Nature 472(7344): 429–436. doi:10.1038/nature09983

Beckmann, A., Timmermann, R., Pereira, A.F., Mohn, C., 2001. The effect of flow at Maud Rise on the sea-ice cover - numerical experiments. Ocean Dynamics. 52: 11-25.

Béhagle, N., du Buisson, L., Josse, E., Lebourges-Dhaussy, A., Roudaut, G., Ménard, F., 2014. Mesoscale features and micronekton in the Mozambique Channel: An acoustic approach. Deep Sea Res. Part II Top. Stud. Oceanogr. 100: 164–173. https://doi.org/10.1016/j.dsr2.2013.10.024

Béhagle, N., Cotté, C., Ryan, T.E., Gauthier, O., Roudaut, G., Brehmer, P., Josse, E., Cherel, Y., 2016. Acoustic micronektonic distribution is structured by macroscale oceanographic processes across 20–50°S latitudes in the South-Western Indian Ocean. Deep Sea Res. Part Oceanogr. Res. Pap. 110: 20–32. https://doi.org/10.1016/j.dsr.2015.12.007

Béhagle, N., Cotté, C., Lebourges-Dhaussy, A., Roudaut, G., Duhamel, G., Brehmer, P., Josse, E., Cherel, Y., 2017. Acoustic distribution of discriminated micronektonic organisms from a bi-frequency processing: The case study of eastern Kerguelen oceanic waters. Prog. Oceanogr. 156: 276–289. https://doi.org/10.1016/j.pocean.2017.06.004

Benitez-Nelson, C.R., McGillicuddy, D. J., 2008. Mesoscale Physical-Biological-Biogeochemical Linkages in the Open Ocean: An Introduction to the results of the E-Flux and EDDIES Programs. Deep Sea Res. Part II Top. Stud. Oceanogr. 55(10-13): 1133–38. https://doi.org/10.1016/j.dsr2.2008.03.001

Benoit-Bird, K.J., Au, W.W.L., 2003. Prey dynamics affect foraging by a pelagic predator (*Stenella longirostris*) over a range of spatial and temporal scales. Behav. Ecol. Sociobiol. 53: 364-373. DOI 10.1007/s00265-003-0585-4

Benoit-Bird, K.J., Au, W.W.L, 2004. Diel migration dynamics of an island-associated sound-scattering layer. Deep-Sea Res. I. 51: 707-719. doi:10.1016/j.dsr.2004.01.004

Benoit-Bird, K., Au, W., 2006. Extreme diel horizontal migrations by a tropical nearshore resident micronekton community. Mar. Ecol. Prog. Ser. 319: 1–14. https://doi.org/10.3354/meps319001

Benoit-Bird, K. J., Lawson, G. L., 2016. Ecological Insights from Pelagic Habitats Acquired Using Active Acoustic Techniques. Annu. Rev. Mar. Sci. 8, 21.1–21.28. https://doi.org/10.1146/annurev-marine-122414-034001

Bensch, A., Gianni, M., Gréboval, D., Sanders, J., Hjort, A., 2009. Worldwide review of bottom fisheries in the high seas. FAO Fisheries and Aquaculture Technical Paper. 522(1). Rome. 145p.

Berger, W. H., 1974. Deep-sea sedimentation. In: The geology of continental margins. Springer, Berlin, Heidelberg. pp. 213-241.

Bernal, A., Olivar, M.P., Maynou, F., Fernández de Puelles, M.L., 2015. Diet and feeding strategies of mesopelagic fishes in the western Mediterranean. Progr. Oceanogr. 135: 1–17. https://doi.org/10.1016/j.pocean.2015.03.005.

Bertrand, A., Le Borgne, R., Josse, E., 1999. Acoustic characterisation of micronekton distribution in French Polynesia. Mar. Ecol. Prog. Ser. 191: 127-140. doi:10.3354/meps191127

Bertrand, A., Bard, F.-X., Josse, E., 2002. Tuna food habits related to the micronekton distribution in French Polynesia. Mar. Biol. 140: 1023–1037. https://doi.org/10.1007/s00227-001-0776-3

Best, P.B., Findlay, K.P., Sekiguchi, K., Peddemors, V.M., Rakotonirina, B., Rossouw, A., Gove, D., 1998. Winter distribution and possible migration routes of humpback whales *Megaptera novaeangliae* in the southwest Indian Ocean. Mar. Ecol. Prog. Ser. 162: 287-299.

Bhattacharya, G. C., Chaubey, A. K., 2001. Western Indian Ocean—a glimpse of the tectonic scenario. The Indian ocean–a perspective, 691-729.

Bianchi, D., Stock, C., Galbraith, E.D., Sarmiento, J.L., 2013. Diel vertical migration: Ecological controls and impacts on the biological pump in a one-dimensional ocean model. Glob. Biogeochem. Cycles. 27: 478–491. https://doi.org/10.1002/gbc.20031

Bianchi, D., Mislan, K.A.S., 2016. Global patterns of diel vertical migration times and velocities from acoustic data. Limnol. Oceanogr. 61: 353-364. doi: 10.1002/lno.10219

Birkley, S.-R., Gulliksen, B., 2003. Feeding Ecology in Five Shrimp Species (Decapoda, Caridea) from an Arctic Fjord (Isfjorden, Svalbard), with Emphasis on *Sclerocrangon boreas* (Phipps, 1774). Crustaceana. 76(6): 699-715. https://doi.org/10.1163/156854003322381513

Bodin, N., Budzinski, H., Le Ménach, K., Tapie, N., 2009. ASE extraction method for simultaneous carbon and nitrogen stable isotope analysis in soft tissues of aquatic organisms. Analytica Chimica Acta 643: 54-60. DOI: 10.1016/j.aca.2009.03.048

Bodin, N., Lesperance, D., Albert, R., Hollanda, S., Michaud, P., Degroote, M., Churlaud, C., Bustamante, P., 2017. Trace elements in oceanic pelagic communities in the western Indian Ocean. Chemosphere 174: 354–362. https://doi.org/10.1016/j.chemosphere.2017.01.099

Boehlert, G. W., Seki, M. P. 1984. Enhanced micronekton abundance over mid-Pacific seamounts. EOS, Transactions of the American Geophysical Union. 65: 928.

Boehlert, G.W., Genin, A., 1987. A review of the effects of seamounts on biological processes. In: Keating, B.H., Fryer, P., Batiza, R. and Boehlert, G.W. (Eds), Seamounts, Islands and Atolls. p. 319–34. Geophysics Monographic Series 43. American Geophysical Union. Washington, DC.

Boehlert, G.W., 1988. Current-Topography Interactions at Mid-Ocean Seamounts and the Impact on Pelagic Ecosystems. GeoJournal, 16.1: 45-52.

Boehlert, G.W., Wilson, C.D., Mizuno, K., 1994. Populations of the Sternoptychid Fish *Maurolicus muelleri* on Seamounts in the Central North Pacific. Pac. Sci. 48(1): 57-69.

Boersch-Supan, P.H., Rogers, A.D., Brierley, A.S., 2017. The distribution of pelagic sound scattering layers across the southwest Indian Ocean. Deep Sea Res. Part II Top. Stud. Oceanogr. 136: 108–121. https://doi.org/10.1016/j.dsr2.2015.06.023

Bograd, S.J., Rabinovich, A.B., LeBlond, P.H., Shore, J.A., 1997. Observations of seamount-attached eddies in the North Pacific. J. Geophys. Res. Oceans. 102: 12441–12456. https://doi.org/10.1029/97JC00585

Bonneville, A., Von Herzen, R.P., Lucazeau, F., 1997. Heat flow over Reunion hot spot track: Additional evidence for thermal rejuvenation of oceanic lithosphere. J. Geophys. Res. Solid Earth. 102: 22731–22747. https://doi.org/10.1029/97JB00952

Bourjea, J., Nel, R., Jiddawi, N.S., Koonjul, M.S., Bianchi, G., 2008. Sea Turtle Bycatch in the West Indian Ocean: Review, Recommendations and Research Priorities. Western Indian Ocean J. Mar. Sci. 7(2): 137-150.

Bouveroux, T., Melly, B., McGregor, G., Plön, S., 2018. Another dolphin in peril? Photo-identification, occurrence, and distribution of the endangered Indian Ocean humpback dolphin (*Sousa plumbea*) in Algoa Bay. Aquat. Conserv. Mar. Freshw. Ecosyst. 28: 723–732. https://doi.org/10.1002/aqc.2877

Bower, A.S., Armi, L., Ambar, I., 1995. Direct evidence of meddy formation off the southwestern coast of Portugal. Deep Sea Res. Part Oceanogr. Res. Pap. 42: 1621–1630. https://doi.org/10.1016/0967-0637(95)00045-8

Bradbury, I.R., Snelgrove, P.V.R., 2001. Contrasting larval transport in demersal fish and benthic invertebrates: the roles of behaviour and advective processes in determining spatial pattern. Can. J. Fish. Aquat. Sci. 58: 811–823. https://doi.org/10.1139/cjfas-58-4-811

Brainard, R.E., 1986. Fisheries Aspects of Seamounts and Taylor Columns. Naval Postgraduate School. PhD Thesis. Pp 21,

Branch, T.A., Stafford, K.M., Palacios, D.M., Allison, C., Bannister, J.L., Burton, C.L.K., Cabrera, E., Carlson, C.A., Galletti Vernazzani, B., Gill, P.C., Hucke-Gaete, R., Jenner, K.C.S., Jenner, M.-N.M., Matsuoka, K., Mikhalev, Y.A., Miyashita, T., Morrice, M.G., Nishiwaki, S., Sturrock, V.J., Tormosov, D., Anderson, R.C., Baker, A.N., Best, P.B., Borsa, P., Brownell Jr, R.L., Childerhouse, S., Findlay, K.P., Gerrodette, T.,

Ilangakoon, A.D., Joergensen, M., Kahn, B., Ljungblad, D.K., Maughan, B., Mccauley, R.D., Mckay, S., Norris, T.F., Rankin, S., Samaran, F., Thiele, D., Van Waerebeek, K., Warneke, R.M., 2007. Past and present distribution, densities and movements of blue whales *Balaenoptera musculus* in the Southern Hemisphere and northern Indian Ocean. Mammal Rev. 37: 116–175. https://doi.org/10.1111/j.1365-2907.2007.00106.x

Braulik, G.T., Findlay, K., Cerchio, S., Baldwin, R., 2015. Assessment of the Conservation Status of the Indian Ocean Humpback Dolphin (*Sousa plumbea*) Using the IUCN Red List Criteria. In: Advances in Marine Biology. Elsevier, pp. 119–141. https://doi.org/10.1016/bs.amb.2015.08.004

Brechner Owens, W., Hogg, N.G., 1980. Oceanic observations of stratified Taylor columns near a bump. Deep Sea Res. Part Oceanogr. Res. Pap. 27: 1029–1045. https://doi.org/10.1016/0198-0149(80)90063-1

Brierley, A.S., 2014. Diel vertical migration. Current Biology. 24(22): R1074-R1076. https://doi.org/10.1016/j.cub.2014.08.054

Brink, K.H., 1989. The effect of stratification on seamount-trapped waves. Deep Sea Res. Part Oceanogr. Res. Pap. 36: 825–844. https://doi.org/10.1016/0198-0149(89)90031-9

Brink, K.H., 1995. Tidal and lower frequency currents above Fieberling Guyot. J. Geophys. Res. 100: 10817. https://doi.org/10.1029/95JC00998

Brodeur, R.D., Seki, M.P., Pakhomov, E.A., Suntsov, A.V., 2005. Micronekton-What are they and why are they important? PICES Press 14: 7–11.

Brodeur, R., Yamamura, O., 2005. PICES Scientific Report No. 30 Micronekton of the North Pacific. PICES Scientific Report, Sidney, B.C., Canada, pp. 1–115.

Browder, J.A., 1993. A pilot model of the Gulf of Mexico continental shelf. In: Christensen, V., Pauly, D. (Eds), Trophic Models of Aquatic Ecosystems. ICLARM Conference Proceedings. 26: 390.

Bruland, K.W., Silver, M.W., 1981. Sinking rates of fecal pellets from gelatinous zooplankton (Salps, Pteropods, Doliolids). Mar. Biol. 63: 295–300. https://doi.org/10.1007/BF00395999

Brunnschweiler, J.M., Baensch, H., Pierce, S.J., Sims, D.W., 2009. Deep-diving behaviour of a whale shark *Rhincodon typus* during long-distance movement in the western Indian Ocean. J. Fish Biol. 74: 706–714. https://doi.org/10.1111/j.1095-8649.2008.02155.x

Bull, B., Doonan, I., Tracey, D., Hart, A., 2001. Diel variation in spawning orange roughy (*Hoplostethus atlanticus*, Trachichthyidae) abundance over a seamount feature on the north-west Chatham Rise. New Zeal. J. Mar. Fresh.. 35(3): 435-444. DOI: 10.1080/00288330.2001.9517013

Bulman, C.M., He, X., Koslow, J.A., 2002. Trophic ecology of the mid-slope demersal fish community off southern Tasmania, Australia. Mar. Freshwater Res. 53: 59-72. DOI: 10.1071/MF01057

Bustamante, P., Lahaye, V., Durnez, C., Churlaud, C., Caurant, F., 2006. Total and organic Hg concentrations in cephalopods from the North Eastern Atlantic waters: Influence of geographical origin and feeding ecology. Sci. Total Environ. 368: 585–596. https://doi.org/10.1016/j.scitotenv.2006.01.038

Butler, M., Bollens, S.M., Burkhalter, B., Madin, L.P., Horgan, E., 2001. Mesopelagic fishes of the Arabian Sea: distribution, abundance and diet of *Chauliodus pammelas*,

Chauliodus sloani, *Stomias aznis*, and *Stomias nebulosus*. Deep Sea Res. Part II Top. Stud. Oceanogr. 48: 1369-1383.

Cardona, L., Álvarez de Quevedo, I., Borrell, A., Aguilar, A., 2012. Massive Consumption of Gelatinous Plankton by Mediterranean Apex Predators. PLoS ONE 7: e31329. https://doi.org/10.1371/journal.pone.0031329

Carmo, V., Santos, M., Menezes, G.M., Loureiro, C.M., Lambardi, P., Martins, A., 2013. Variability of zooplankton communities at Condor seamount and surrounding areas, Azores (NE Atlantic). Deep Sea Res. Part II Top. Stud. Oceanogr. 98: 63–74. https://doi.org/10.1016/j.dsr2.2013.08.007

Carmo, V., Sutton, T., Menezes, G., Falkenhaug, T., Bergstad, O.A., 2015. Feeding ecology of the Stomiiformes (Pisces) of the northern Mid-Atlantic Ridge. 1. The Sternoptychidae and Phosichthyidae. Prog. Oceanogr. 130: 172-187. https://doi.org/10.1016/j.pocean.2014.11.003

Caron, D.A., Madin, L.P., Cole, J.J., 1989. Composition and degradation of salp fecal pellets: Implications for vertical flux in oceanic environments. J. Mar. Res. 47: 829–850. https://doi.org/10.1357/002224089785076118

Cascão, I., Domokos, R., Lammers, M.O., Marques, V., Domínguez, R., Santos, R.S., Silva, M.A., 2017. Persistent Enhancement of Micronekton Backscatter at the Summits of Seamounts in the Azores. Front. Mar. Sci. 4: 25. https://doi.org/10.3389/fmars.2017.00025

Catry, T., Ramos, J., Le Corre, M., Phillips, R., 2009. Movements, at-sea distribution and behaviour of a tropical pelagic seabird: the wedge-tailed shearwater in the western Indian Ocean. Mar. Ecol. Prog. Ser. 391: 231–242. https://doi.org/10.3354/meps07717

Catul, V., Gauns, M., Karuppasamy, P.K., 2011. A review of mesopelagic fishes belonging to family Mcytophidae. Rev. Fish Biol. Fisheries. 21: 339-354. doi: 10.1007/s11160-010-9176-4

Caut, S., Angulo, E., Courchamp, F., 2009. Variation in discrimination factors ($\Delta^{15}N$ and $\Delta^{13}C$): the effect of diet isotopic values and applications for diet reconstruction. J Appl. Ecol. 46: 443-453. DOI: 10.1111/j.1365-2664.2009.01620.x

Cavicchioli, R., Ostrowski, M., Fegatella, F., Goodchild, A., Guixa-Boixereu, N., 2003. Life under nutrient limitation in oligotrophic marine environments: an eco/physiological perspective of *Sphingopyxis alaskensis* (formerly *Sphingomonas alaskensis*). Microb. Ecol. 45(3): 203-217. https://doi.org/10.1007/s00248-002-3008-6

Cerchio, S., Trudelle, L., Zerbini, A., Geyer, Y., Mayer, F.X., Charrassin, J-B., Jung, J-L., Adam, O., Rosenbaum, H., 2013. Satellite tagging of humpback whales off Madagascar reveals long range movements of individuals in the South West Indian Ocean during the breeding season. Document IWC: SC/65a/SH22.

Chapman, D.C., Haidvogel, D.B., 1992. Formation of Taylor caps over a tall isolated seamount in a stratified ocean. Geophys. Astrophys. Fluid Dyn. 64: 31–65. https://doi.org/10.1080/03091929208228084

Chasapis, T.C., Loutsidou, A.C., Spiliopoulou, C.A., Stefanidou, M.E., 2012. Zinc and human health: an update. Arch. Toxicol. 86: 521-534. DOI: 10.1007/s00204-011-0775-1

Chelton, D.B., Schlax, M.G., Samelson, R.M., 2011. Global observations of nonlinear mesoscale eddies. Prog. Oceanogr. 91: 167-216. https://doi.org/10.1016/j.pocean.2011.01.002

Cherel, Y., Corre, M., Jaquemet, S., Ménard, F., Richard, P., Weimerskirch, H., 2008. Resource partitioning within a tropical seabird community: new information from stable isotopes. Mar. Ecol. Prog. Ser. 366: 281–291. https://doi.org/10.3354/meps07587

Cherel, Y., Fontaine, C., Richard, P., Labat, J.-P., 2010. Isotopic niches and trophic levels of myctophid fishes and their predators in the Southern Ocean. Limnol. Oceanogr. 55: 324–332. https://doi.org/10.4319/lo.2010.55.1.0324

Cherel, Y., Romanov, E.V., Annasawmy, P., Thibault, D., Ménard, F., 2020. Micronektonic fish species over three seamounts in the southwestern Indian Ocean. Deep-Sea Res. II. https://doi.org/10.1016/j.dsr2.2020.104777

Choy, C.A., Davison, P.C., Drazen, J.C., Flynn, A., Gier, E.J., Hoffman, J.C., McClain-Counts, J.P., Miller, T.W., Popp, B.N., Ross, S.W., Sutton, T.T., 2012. Global trophic position comparison of two dominant mesopelagic fish families (Myctophidae, Stomiidae) using amino acid nitrogen isotopic analyses. PLoS One. 7(11): e50133. DOI: 10.1371/journal.pone.0050133

Choy, C.A., Popp, B.N., Hannides, C.C.S., Drazen, J.C., 2015. Trophic structure and food resources of epipelagic and mesopelagic fishes in the North Pacific Subtropical Gyre ecosystem inferred from nitrogen isotopic compositions. Limnol. Oceanogr. 60: 1156-1171.

Choy, C.A., Wabnitz, C.C.C., Weijerman, M., Woodworth-Jefcoats, P.A., Polovina, J.J., 2016. Finding the way to the top: how the composition of oceanic mid-trophic micronekton groups determines apex predator biomass in the central North Pacific. Mar. Ecol. Prog. Ser. 549: 9-25. DOI: 10.3354/meps11680

Christensen, V., Pauly, D., 1993. Flow Characteristics of Aquatic Ecosystems. In: Christensen, V., Pauly, D. (Eds), Trophic Models of Aquatic Ecosystems. ICLARM Conference Proceedings. 26: 390.

Christiansen, B., Martin, B., Hirch, S., 2009. The benthopelagic fish fauna on the summit of Seine Seamount, NE Atlantic: Composition, population structure and diets. Deep Sea Res. Part II Top. Stud. Oceanogr. 56: 2705–2712. https://doi.org/10.1016/j.dsr2.2008.12.032

Christiansen, B., Vieira, R.P., Christiansen, S., Denda, A., Oliveira, F., Gonçalves, J.M.S., 2015. The fish fauna of Ampère Seamount (NE Atlantic) and the adjacent abyssal plain. Helgol. Mar. Res. 69: 13–23. https://doi.org/10.1007/s10152-014-0413-4

Clark, M., 1999. Fisheries for orange roughy (*Hoplostethus atlanticus*) on searnounts in New Zealand. 22(6): 593-602.

Clark, M., 2001. Are deepwater fisheries sustainable? - the example of orange roughy (*Hoplostethus atlanticus*) in New Zealand. Fish. Res. 51: 123-135.

Clark, M.R., Koslow, J.A., 2007. Impacts of fisheries on seamounts. In: Pitcher, T.J., Morato, T., Hart, P.J.B., Clark, M.R., Haggan, N., Santos, R.S. (Eds), Seamounts: Ecology, Fisheries & Conservation. Blackwell Publishing Ltd, Oxford, UK, pp. 413-441.

Clark, M.R., Vinnichenko, V.I., Gordon, J.D.M., Beck-Bulat, G.Z., Kukhavev, N.N., Kakora, A.F., 2007. Large-scale distant-water trawl fisheries on seamounts. In: Pitcher, T.J.,

Morato, T., Hart, P.J.B., Clark, M.R., Haggan, N., Santos, R.S. (Eds), Seamounts: Ecology, Fisheries & Conservation. Blackwell Publishing Ltd, Oxford, UK, pp. 361-399.

Clark, M.R., 2009. Deep-sea seamount fisheries: a review of global status and future prospects. Lat. Am. J. Aquat. Res. 37(3): 501-512. DOI: 10.3856/vol37-issue3-fulltext-17

Clark, M.R., Althaus, F., Williams, A., Niklitschek, E., Menezes, G.M., Hareide, N.-R., Sutton, P., O'Donnell, C., 2010a. Are deep-sea demersal fish assemblages globally homogenous? Insights from seamounts. Mar. Ecol. 31: 39–51. https://doi.org/10.1111/j.1439-0485.2010.00384.x

Clark, M.R., Rowden, A.A., Schlacher, T., Williams, A., Consalvey, M., Stocks, K.I., Rogers, A.D., O'Hara, T.D., White, M., Shank, T.M., Hall-Spencer, J.M., 2010b. The Ecology of Seamounts: Structure, Function, and Human Impacts. Annu. Rev. Mar. Sci. 2: 253–278. https://doi.org/10.1146/annurev-marine-120308-081109

Clark, M.R., Dunn, M.R., 2012. Spatial management of deep-sea seamount fisheries: balancing sustainable exploitation and habitat conservation. Environ. Conserv. 39(3): 204-214. DOI:10.1017/S0376892912000021

Clark, M.R., Schlacher, T.A., Rowden, A.A., Stocks, K.I., Consalvey, M., 2012. Science Priorities for Seamounts: Research Links to Conservation and Management. PLoS ONE. 7: e29232. https://doi.org/10.1371/journal.pone.0029232

Clarke, M.R., Lu, C.C., 1975. Vertical distribution of cephalopods at 18°N 25°W in the North Atlantic. J. mar. biol. Ass. 55: 165-182. https://doi.org/10.1017/S0025315400015812

Clarke, T.A., 1982. Feeding habits of stomiatoid fishes from Hawaiian waters. Fish. Bull. 80(2): 287-304.

Clarke, K., Warwick, R., 2001. Change in Marine Communities: An Approach to Statistical Analysis and Interpretation. PRIMER-E Ltd: Plymouth, United Kingdom.

Clarke, M., 2007. Seamounts and Cephalopods. In: Pitcher, T.J., Morato, T., Hart, P.J.B., Clark, M.R., Haggan, N., Santos, R.S. (Eds), Seamounts: Ecology, Fisheries & Conservation. Blackwell Publishing Ltd, Oxford, UK, pp. 207-229.

Cliff, G., Dudley, S.F.J., Davis, B., 1988. Sharks caught in the protective gill nets off Natal, South Africa. 1. The sandbar shark *Carcharhinus plumbeus* (Nardo). South Afr. J. Mar. Sci. 7: 255–265. https://doi.org/10.2989/025776188784379035

Codiga, D.L., Eriksen, C.C., 1997. Observations of low-frequency circulation and amplified subinertial tidal currents at Cobb Seamount. J. Geophys. Res. Oceans. 102: 22993–23007. https://doi.org/10.1029/97JC01451

Cohen, J.H., Forward, R.B., 2009. Zooplankton diel vertical migration- a review of proximate control. Oceanogr. Mar. Biol. 47: 77-109. DOI: 10.1201/9781420094220.ch2

Colaço, A., Giacomello, E., Porteiro, F., Menezes, G.M., 2013. Trophodynamic studies on the Condor seamount (Azores, Portugal, North Atlantic). Deep Sea Res. Part II Top. Stud. Oceanogr. 98: 178–189. https://doi.org/10.1016/j.dsr2.2013.01.010

Collette, B.B., Parin, N.V., 1991. Shallow-Water Fishes of Walters Shoals, Madagascar Ridge. Bull. Mar. Sci. 48(1): 1-22.

Comeau, L.A., Vézina, A.F., Bourgeois, M., Juniper, S.K., 1995. Relationship between phytoplankton production and the physical structure of the water column near Cobb Seamount, northeast Pacific. Deep Sea Res. Part Oceanogr. Res. Pap. 42: 993–1005. https://doi.org/10.1016/0967-0637(95)00050-G

Conley, K.P., 2017. Mechanics and Selectivity of filtration by tunicates. PhD Thesis, University of Oregon, USA. Pp 4, 84.

Conway, D.V.P., 2005. Island-coastal and oceanic epipelagic zooplankton biodiversity in the southwestern Indian Ocean. Indian J. Mar. Sci. 34(1): 50-56.

Cossa, D., Thibaud, Y., Roméo, M., Gnassia-Barelli, M., 1990. Le mercure en milieu marin. Biogéochimie et écotoxicologie. Rapport scientifiques et techniques de l'IFREMER, No. 19, Brest.

Costello, M.J., Cheung, A., De Hauwere, N., 2010. Surface Area and the Seabed Area, Volume, Depth, Slope, and Topographic Variation for the World's Seas, Oceans and Countries. Environ. Sci. Technol. 44(8821-8828).

Cowen, R.K., 2006. Scaling of Connectivity in Marine Populations. Science 311: 522–527. https://doi.org/10.1126/science.1122039

Craig, C.H., Sandwell, D.T., 1988. Global distribution of seamounts from Seasat profiles. J. Geophys. Res. Solid Earth 93: 10408–10420. https://doi.org/10.1029/JB093iB09p10408

Cresson, P., Ruitton, S., Fontaine, M-F., Harmelin-Vivien, M., 2012. Spatio-temporal variation of suspended and sedimentary organic matter quality in the Bay of Marseilles (NW Mediterranean) assessed by biochemical and isotopic analyses. Mar. Pollut. Bull. 1112-1121. http://dx.doi.org/10.1016/j.marpolbul.2012.04.003

Crochelet, E., Barrier, N., Andrello, M., Marsac, F., Spadone, A., Lett, C., 2020. Connectivity between seamounts and coastal ecosystems in the South West Indian Ocean. Deep Sea Res. II. https://doi.org/10.1016/j.dsr2.2020.104774

Dalpadado, P., Gjøsæter, J., 1988. Feeding ecology of the lanternfish *Benthosema pterotum* from the Indian Ocean. Mar. Biol. 99: 555–567. https://doi.org/10.1007/BF00392563

Daly, R., Froneman, P.W., Smale, M.J., 2013. Comparative Feeding Ecology of Bull Sharks (*Carcharhinus leucas*) in the Coastal Waters of the Southwest Indian Ocean Inferred from Stable Isotope Analysis. PLoS ONE 8(10): e78229. doi:10.1371/journal.pone.0078229

Danckwerts, D.K., McQuaid, C.D., Jaeger, A., McGregor, G.K., Dwight, R., Le Corre, M., Jaquemet, S., 2014. Biomass consumption by breeding seabirds in the western Indian Ocean: indirect interactions with fisheries and implications for management. ICES J. Mar. Sci. 71: 2589–2598. https://doi.org/10.1093/icesjms/fsu093

Davies, A.J., Guinotte, J.M., 2011. Global Habitat Suitability for Framework-Forming Cold-Water Corals. PLoS ONE 6: e18483. https://doi.org/10.1371/journal.pone.0018483

Davis, M.P., Holcroft, N.I., Wiley, E.O., Sparks, J.S., Leo Smith, W., 2014. Species-specific bioluminescence facilitates speciation in the deep sea. Mar. Biol. 161: 1139–1148. https://doi.org/10.1007/s00227-014-2406-x

Davison, P. C., Koslow, J. A., Kloser, R. J., 2015. Acoustic biomass estimation of mesopelagic fish: backscattering from individuals, populations, and communities. ICES Jour. Mar. Sci. 72(5): 1413-1424. https://doi.org/10.1093/icesjms/fsv023

De Bruyn, P., Dudley, S., Cliff, G., Smale, M., 2005. Sharks caught in the protective gill nets off KwaZulu-Natal, South Africa. 11. The scalloped hammerhead shark *Sphyrna lewini* (Griffith and Smith). Afr. J. Mar. Sci. 27: 517–528. https://doi.org/10.2989/18142320509504112

De Forest, L., Drazen, J., 2009. The influence of a Hawaiian seamount on mesopelagic micronekton. Deep Sea Res. Part Oceanogr. Res. Pap. 56: 232–250. https://doi.org/10.1016/j.dsr.2008.09.007

De Forges, B.R., Koslow, J.A., Poore, G.C.B., 2000. Diversity and endemism of the benthic seamount fauna in the southwest Pacific. Nature 405: 944–947. https://doi.org/10.1038/35016066

De Robertis, A., Higginbottom, I., 2007. A post-processing technique to estimate the signal-to-noise ratio and remove echosounder background noise. ICES J. Mar. Sci. 64: 1282-1291. https://doi.org/10.1093/icesjms/fsm112

De Ruijter, W.P.M., Ridderinkhof, H., Lutjeharms, J.R.E., Schouten, M.W., Veth, C., 2002. Observations of the flow in the Mozambique Channel. Geophys. Res. Lett. 29(10): 140-1.

De Ruijter, W.P.M., Aken, H.M. van, Beier, E.J., Lutjeharms, J.R.E., Matano, R.P., Schouten, M.W., 2004. Eddies and dipoles around South Madagascar: formation, pathways and large-scale impact. Deep Sea Res. Part Oceanogr. Res. Pap. 51: 383–400. https://doi.org/10.1016/j.dsr.2003.10.011

Décima, M., Stukel, M.R., López-López, L., Landry, M.R., 2018. The unique ecological role of pyrosomes in the Eastern Tropical Pacific. Limnol. Oceanogr. 64: 728-743. https://doi.org/10.1002/lno.11071

Del Giorgio A., P., Duarte M., C., 2002. Respiration in the open ocean. Nature. 420: 379–384.

Demopoulos, A.W.J., Smith, C.R., Tyler, P.A., 2003. The Deep Indian Ocean Floor. Ecosystems of the world. Pp 219-238.

Denda, A., Christiansen, B., 2014. Zooplankton distribution patterns at two seamounts in the subtropical and tropical NE Atlantic. Mar. Ecol. 35: 159–179. https://doi.org/10.1111/maec.12065

Denda, A., Mohn, C., Wehrmann, H., Christiansen, B., 2017a. Microzooplankton and meroplanktonic larvae at two seamounts in the subtropical and tropical NE Atlantic. J. Mar. Biol. Assoc. U. K. 97: 1–27. https://doi.org/10.1017/S0025315415002192

Denda, A., Stefanowitsch, B., Christiansen, B., 2017b. From the epipelagic zone to the abyss: Trophic structure at two seamounts in the subtropical and tropical Eastern Atlantic - Part I zooplankton and micronekton. Deep Sea Res. Part Oceanogr. Res. Pap. 130: 63–77. https://doi.org/10.1016/j.dsr.2017.10.010

Denda, A., Stefanowitsch, B., Christiansen, B., 2017c. From the epipelagic zone to the abyss: Trophic structure at two seamounts in the subtropical and tropical Eastern Atlantic - Part II Benthopelagic fishes. Deep Sea Res. Part Oceanogr. Res. Pap. 130: 78-92. http://dx.doi.org/10.1016/j.dsr.2017.08.005

Diekmann, R., Piatkowski, U., 2004. Species composition and distribution patterns of early life stages of cephalopods at Great Meteor Seamount (subtropical North-east Atlantic). Arch. Fish. Mar. Res. 51: 115–131.

Diekmann, R., Nellen, W., Piatkowski, U., 2006. A multivariate analysis of larval fish and paralarval cephalopod assemblages at Great Meteor Seamount. Deep-Sea Res. I. 53: 1635-1657. doi:10.1016/j.dsr.2006.08.008

Domokos, R., Pakhomov, E.A., Suntsov, A.V., Seki, M.P., Polovina, J.J., 2010. PICES Scientific Report. No. 38. Acoustic characterization of the mesopelagic community off the leeward coast of Oahu Island, Hawaii. E. A. Pakhomov, O. Yamamura (Eds), Report of the Advisory Panel on Micronekton Sampling Intercalibration Experiment.pp 19-26.

Dong, H-P., Wang, D-Z., Dai, M., Hong, H-S., 2010. Characterization of particulate organic matter in the water column of the South China Sea using a shotgun proteomic approach. Limnol. Oceanogr. 55(4): 1565-1578. DOI: 10.4319/lo.2010.55.4.1565

Dower, J., Freeland, H., Juniper, K., 1992. A strong biological response to oceanic flow past Cobb Seamount. Deep Sea Res. Part Oceanogr. Res. Pap. 39: 1139–1145. https://doi.org/10.1016/0198-0149(92)90061-W

Dower, J.F., Mackas, D.L., 1996. "Seamount effects" in the zooplankton community near Cobb Seamount. Deep Sea Res. Part Oceanogr. Res. Pap. 43: 837–858. https://doi.org/10.1016/0967-0637(96)00040-4

Dower, J., Yelland, D., Crawford, W., 2004. Physical and Biological Interactions Between Haida Eddies and Seamounts in the NE Pacific. University of Victoria, BC. Poster.

Drazen, J. F., De Forest, L. G., Domokos, R., 2011. Micronekton abundance and biomass in Hawaiian waters as influenced by seamounts, eddies and the moon. Deep Sea Res Part I. 58, 557-566. http/doi.org/10.1016/j.dsr.2011.03.002

Druon, J.-N., Chassot, E., Murua, H., Lopez, J., 2017. Skipjack Tuna Availability for Purse Seine Fisheries Is Driven by Suitable Feeding Habitat Dynamics in the Atlantic and Indian Oceans. Front. Mar. Sci. 4: 315. https://doi.org/10.3389/fmars.2017.00315

Du Preez, M., Nel, R., Bouwman, H., 2018. First report of metallic elements in loggerhead and leatherback turtle eggs from the Indian Ocean. Chemosphere. 197: 716-728. https://doi.org/10.1016/j.chemosphere.2018.01.106

Dubroca, L., Chassot, E., Floch, L., Demarcq, H., Assan, C., Delgado de Molina, A., 2013. Seamounts and tuna fisheries: Tuna hotspots or fishermen habits? Collect. Vol. Sci. Pap. ICCAT. 69(5): 2087-2102.

Dudley, S.F.J., Cliff, G., 1993. Sharks caught in the protective gill nets off Natal, South Africa. 7. The blacktip shark *Carcharhinus limbatus* (Valenciennes). South Afr. J. Mar. Sci. 13: 237–254. https://doi.org/10.2989/025776193784287356

Dudley, S., Cliff, G., Zungu, M., Smale, M., 2005. Sharks caught in the protective gill nets off KwaZulu-Natal, South Africa. 10. The dusky shark *Carcharhinus obscurus* (Lesueur 1818). Afr. J. Mar. Sci. 27: 107–127. https://doi.org/10.2989/18142320509504072

Duffy, L.M., Kuhnert, P.M., Pethybridge, H.R., Young, J.W., Olson, R.J., Logan, J.M., Goñi, N., Romanov, E., Allain, V., Staudinger, M.D., Abecassis, M., Choy, C.A., Hobday, A.J., Simier, M., Galván-Magaña, F., Potier, M., Ménard, F., 2017. Global trophic ecology of yellowfin, bigeye, and albacore tunas: Understanding predation on

micronekton communities at ocean-basin scales. Deep Sea Res. Part II Top. Stud. Oceanogr. 40: 55-73. http://dx.doi.org/10.1016/j.dsr2.2017.03.003

Dufois, F., Hardman-Mountford, N.J., Greenwood, J., Richardson, A.J., Feng, M., Herbette, S., Matear, R., 2014. Impact of eddies on surface chlorophyll in the South Indian Ocean. J. Geophys. Res. Oceans. 119: 8061–8077. https://doi.org/10.1002/2014JC010164

Dulau, V., Pinet, P., Geyer, Y., Fayan, J., Mongin, P., Cottarel, G., Zerbini, A., Cerchio, S., 2017. Continuous movement behavior of humpback whales during the breeding season in the southwest Indian Ocean: on the road again! Mov. Ecol. 5:11. https://doi.org/10.1186/s40462-017-0101-5

Dulau-Drouot, V., Fayan, J., Mouysset, L., Boucaud, V., 2012. Occurence and residency patterns of humpback whales off Réunion Island during 2004–10. J. Cetacean Res. Manage. 12(2): 255-263.

Dupuy, C., Pagano, M., Got, P., Domaizon, I., Chappuis, A., Marchessaux, G., Bouvy, M., 2016. Trophic relationships between metazooplankton communities and their plankton food sources in the Iles Eparses (Western Indian Ocean). Mar. Environ. Res. 116: 18–31. https://doi.org/10.1016/j.marenvres.2016.02.011

Ebert, D.A., Clerkin, P.J., 2015. A new species of deep-sea catshark (Scyliorhinidae: *Bythaelurus*) from the southwestern Indian Ocean. J Ocean Sci. Foundation. 15: 53-63.

Edgar, G.J., Stuart-Smith, R.D., Willis, T.J., Kininmonth, S., Baker, S.C., Banks, S., Barrett, N.S., Becerro, M.A., Bernard, A.T.F., Berkhout, J., Buxton, C.D., Campbell, S.J., Cooper, A.T., Davey, M., Edgar, S.C., Försterra, G., Galván, D.E., Irigoyen, A.J., Kushner, D.J., Moura, R., Parnell, P.E., Shears, N.T., Soler, G., Strain, E.M.A., Thomson, R.J., 2014. Global conservation outcomes depend on marine protected areas with five key features. Nature 506: 216–220. https://doi.org/10.1038/nature13022

Ekau, W., Auel, H., Pörtner, H.-O., Gilbert, D., 2010. Impacts of hypoxia on the structure and processes in pelagic communities (zooplankton, macro-invertebrates and fish). Biogeosciences 7: 1669–1699. https://doi.org/10.5194/bg-7-1669-2010.

Eriksen, C.C., 1991. Observations of amplified flows atop a large seamount. J. Geophys. Res. 96: 15227. https://doi.org/10.1029/91JC01176

Eriksen, C.C., 1995. Waves, mean flows, and mixing at a seamount. In: Topographic Effects in the Ocean, Proceedings 9th Huliko'a Hawaiian Winter Workshop, edited by P. Muller and D. Henderson. 1995. p. 1-13.

Eriksen, C.C., 1998. Internal wave reflection and mixing at Fieberling Guyot. J. Geophys. Res. Oceans. 103: 2977–2994. https://doi.org/10.1029/97JC03205

Ersts, P.J., Pomilla, C., Kiszka, J., Cerchio, S., Rosenbaum, H.C., Vély, M., Razafindrakoto, Y., Loo, J.A., Leslie, M.S., Avolio, M., 2011. Observations of individual humpback whales utilising multiple migratory destinations in the south-western Indian Ocean. Afr. J. Mar. Sci. 33: 333–338. https://doi.org/10.2989/1814232X.2011.600436

Etnoyer, P.J., Wood, J., Shirley, T.C., 2010. BOX 12 | How Large Is the Seamount Biome? Oceanography. 23(1): 206-209.

Everett, B., Groeneveld, J.C., Fennessy, S., Porter, S., Munga, C.N., Dias, N., Filipe, O., Zacarias, L., Igulu, M., Kuguru, B., Rabarison, G., Razafindrakoto, H., 2015. Demersal trawl surveys show ecological gradients in Southwest Indian Ocean slope fauna. 14(1/2): 73-92.

Ewart, C.S., Meyers, M.K., Wallner, E.R., McGillicuddy, D.J., Carlson, C.A., 2008. Microbial dynamics in cyclonic and anticyclonic mode-water eddies in the northwestern Sargasso Sea. Deep Sea Res. Part II Top. Stud. Oceanogr. 55: 1334–1347. https://doi.org/10.1016/j.dsr2.2008.02.013

Fabiano, M., Povero, P., Danovaro, R., 1993. Distribution and composition of particulate organic matter in the Ross Sea (Antarctica). Polar Biol. 13: 525-533.

Falkowski, P.G., Ziemann, D., Kolber, Z., Bienfang, P.K., 1991. Role of eddy pumping in enhancing primary production in the ocean. Nature 352: 55–58. https://doi.org/10.1038/352055a0

Fanelli, E., Cartes, J.E., Rumolo, P., Sprovieri, M., 2009. Food-web structure and trophodynamics of mesopelagic-suprabenthic bathyal macrofauna of the Algerian Basin based on stable isotopes of carbon and nitrogen. Deep-Sea Res. I. 56: 1504-1520. DOI: 10.1016/j.dsr.2009.04.004

Fanelli, E., Papiol, V., Cartes, J.E., Rumolo, P., Brunet, C., Sprovieri, M., 2011a. Food web structure of the epibenthic and infaunal invertebrates on the Catalan slope (NW Mediterranean): Evidence from $\delta^{13}C$ and $\delta^{15}N$ analysis. Deep-Sea Res. I: Oceanographic Research Papers. 58: 98–109. https://doi.org/10.1016/j.dsr.2010.12.005

Fanelli, E., Cartes, J.E., Papiol, V., 2011b. Food web structure of deep-sea macrozooplankton and micronekton off the Catalan slope: Insight from stable isotopes. J Mar. Syst. 87: 79-89. DOI: 10.1016/j.jmarsys.2011.03.003

Fanelli, E., Papiol, V., Cartes, J.E., Rumolo, P., López-Pérez, C., 2013. Trophic webs of deep-sea megafauna on mainland and insular slopes of the NW Mediterranean: a comparison by stable isotope analysis. Mar. Ecol. Prog. Ser. 490: 199-221. DOI: 10.3354/meps10430

FAO, 2005. Cephalopods of the world: An annotated and illustrated catalogue of cephalopod species known to date. In: Jereb, P., Roper, C.F.E. (Eds), 4(1).

FAO, 2014. State of World Fisheries and Aquaculture. Food and Agriculture Organization. Rome. http://fao.org/2/sofia14e

FAO, 2016. Fisheries and aquaculture software. FishStatJ - Software for Fishery and Aquaculture Statistical Time Series. In: FAO Fisheries and Aquaculture Department [Online]. Rome. Updated 21 July 2016.

Fennell, S., Rose, G., 2015. Oceanographic influences on Deep Scattering Layers across the North Atlantic. Deep-Sea Res I. 105: 132-141. http://dx.doi.org/10.1016/j.dsr.2015.09.002

Fennessy, S.T., 1994. Incidental capture of elasmobranchs by commercial prawn trawlers on the Tugela Bank, Natal, South Africa. South Afr. J. Mar. Sci. 14: 287–296. https://doi.org/10.2989/025776194784287094

Fennessy, S.T., Groeneveld, J.C., 1997. A review of the offshore trawl fishery for crustaceans on the east coast of South Africa. Fish. Manag. Ecol. 4: 135–147. https://doi.org/10.1046/j.1365-2400.1997.00104.x

Feunteun, E., Miller, M.J., Carpentier, A., Aoyama, J., Dupuy, C., Kuroki, M., Pagano, M., Réveillac, E., Sellos, D., Watanabe, S., Tsukamoto, K., Otake, T., 2015. Stable isotopic composition of anguiliform leptocephali and other food web components from west of

the Mascarene Plateau. Prog. Oceanogr. 137: 69-83. http://dx.doi.org/10.1016/j.pocean.2015.05.024

Fiori, C., Paoli, C., Alessi, J., Mandich, A., Vassallo, P., 2016. Seamount attractiveness to top predators in the southern Tyrrhenian Sea (central Mediterranean). J. Mar. Biol. Assoc. U. K. 96(3): 769–775.

Fonteneau, A., 1991. Monts sous-marins et thons dans l'Atlantique tropical est. Aquat. Living Resour. 4: 13–25. https://doi.org/10.1051/alr:1991001

Fonteneau A., Pallares, P. Pianet R., 2000. A worldwide review of purse seine fisheries on FADs. In: Le Gall, J.-Y., Cayré, P., Taquet, M. (Eds), Pêche thonière et dispositifs de concentration de poissons. Ifremer, Actes Colloq. 28: 15-35.

Fonteneau, A., Lucas, V., Tew-Kai, E., Delgado, A., Demarcq, H., 2008. Mesoscale exploitation of a major tuna concentration in the Indian Ocean. Aquat. Living Resour. 21: 109–121. https://doi.org/10.1051/alr:2008028

Fonteneau, A., 2010. Atlas of Indian Ocean tuna fisheries. IRD Editions, Marseille. 189 p.

Fontes, J., Schmiing, M., Afonso, P., 2014. Permanent aggregations of a pelagic predator at shallow seamounts. Mar. Biol. 161: 1349–1360. https://doi.org/10.1007/s00227-014-2423-9

Foote, K. G., Knudsen, H. P., Vestnes, G., MacLennan, D. N., Simmonds, E. J., 1987. Calibration of acoustic instruments for fish density estimation: a practical guide. ICES Coop. Res. Rep. 144, 1-69.

Fossette, S., Heide-Jørgensen, M.-P., Jensen, M.V., Kiszka, J., Bérubé, M., Bertrand, N., Vély, M., 2014. Humpback whale (*Megaptera novaeangliae*) post breeding dispersal and southward migration in the western Indian Ocean. J. Exp. Mar. Biol. Ecol. 450: 6–14. https://doi.org/10.1016/j.jembe.2013.10.014

Foxton, P., Roe, H.S.J., 1974. Observations on the Nocturnal Feeding of some Mesopelagic Decapod Crustacea. Mar. Biol. 28: 37-49.

France, R., Chandler, M., Peters, R., 1998. Mapping trophic continua of benthic foodwebs: body size-δ^{15}N relationships. Mar. Ecol. Prog. Ser. 174: 301-306.

Frank, T.M., Widder, E.A., 2002. Effects of a decrease in downwelling irradiance on the daytime vertical distribution patterns of zooplankton and micronekton. Mar. Biol. 140: 1181-1193.

Freeland, H., 1994. Ocean circulation at and near Cobb Seamount. Deep Sea Res. Part Oceanogr. Res. Pap. 41: 1715–1732. https://doi.org/10.1016/0967-0637(94)90069-8

Fréon, P., Dagorn, L., 2000. Review of fish associative behaviour: Toward a generalisation of the meeting point hypothesis. Rev. Fish Biol. Fisher. 10: 183-207. DOI: 10.1023/A:1016666108540

Fry, B. 2006. Stable Isotope Ecology. Springer, New York. 308pp.

Furusawa, M., Miyanohana, Y., Ariji, M., Sawada, Y., 1994. Prediction of krill target strength by liquid prolate spheroid model. Fisheries Sci. 60(3): 261-265.

Furuya, K., Odate, T., Taguchi, K., 1995. Effects of a seamount on phytoplankton production in the western Pacific Ocean. Biogeochemical Processes and Ocean Flux in the Western Pacific. 255-273.

Gallienne, C.P., Conway, D.V.P., Robinson, J., Naya, N., William, J.S., Lynch, T., Meunier, S., 2004. Epipelagic mesozooplankton distribution and abundance over the Mascarene Plateau and Basin, south-western Indian Ocean. J. Mar. Biol. Assoc. UK 84: 1–8. https://doi.org/10.1017/S0025315404008835h

García-Cortés, B., Mejuto, J., 2002. Size-weight relationships of the swordfish (*Xiphias gladius*) and several pelagic shark species caught in the Spanish surface longline fishery in the Atlantic, Indian and pacific oceans. Collect. Vol. Sci. Pap. ICCAT, 54(4), 1132-1149.

Garrigue, C., Clapham, P.J., Geyer, Y., Kennedy, A.S., Zerbini, A.N., 2015. Satellite tracking reveals novel migratory patterns and the importance of seamounts for endangered South Pacific humpback whales. R. Soc. Open Sci. 2: 150489. https://doi.org/10.1098/rsos.150489

Gaube, P., McGillicuddy, D.J., Chelton, D.B., Behrenfeld, M.J., Strutton, P.G., 2014. Regional variations in the influence of mesoscale eddies on near-surface chlorophyll. J. Geophys. Res. Oceans 119: 8195–8220. https://doi.org/10.1002/2014JC010111

Genin, A., Boehlert, G.W., 1985. Dynamics of temperature and chlorophyll structures above a seamount: An oceanic experiment. J. Mar. Res. 43: 907–924. https://doi.org/10.1357/002224085788453868

Genin, A., Haury, L., Greenblatt, P., 1988. Interactions of migrating zooplankton with shallow topography: predation by rockfishes and intensification of patchiness. Deep Sea Res. Part Oceanogr. Res. Pap. 35: 151–175. https://doi.org/10.1016/0198-0149(88)90034-9

Genin, A., Greene, C., Haury, L., Wiebe, P., Gal, G., Kaartvedt, S., Meir, E., Fey, C., Dawson, J., 1994. Zooplankton patch dynamics: daily gap formation over abrupt topography. Deep Sea Res. Part Oceanogr. Res. Pap. 41: 941–951. https://doi.org/10.1016/0967-0637(94)90085-X

Genin, A., 2004. Bio-physical coupling in the formation of zooplankton and fish aggregations over abrupt topographies. J. Mar. Syst. 50: 3–20. https://doi.org/10.1016/j.jmarsys.2003.10.008

Genin, A., 2005. Swimming Against the Flow: A Mechanism of Zooplankton Aggregation. Science 308: 860–862. https://doi.org/10.1126/science.1107834

Genin, A., Dower, J.F., 2007. Seamount Plankton Dynamics. In: Pitcher, T.J., Morato, T., Hart, P.J.B., Clark, M.R., Haggan, N., Santos, R.S. (Eds), Seamounts: Ecology, Fisheries & Conservation. Blackwell Publishing Ltd, Oxford, UK, pp. 85-100.

Giorli, G., Au, W.W.L., Ou, H., Jarvis, S., Morrissey, R., Moretti, D., 2015. Acoustic detection of biosonar activity of deep diving odontocetes at Josephine Seamount High Seas Marine Protected Area. J. Acoust. Soc. Am. 137(5): 2495-2501.

Gjerde, K.M., Currie, D., Wowk, K., Sack, K., 2013. Ocean in peril: Reforming the management of global ocean living resources in areas beyond national jurisdiction. Mar. Pollut. Bull. 74: 540–551. https://doi.org/10.1016/j.marpolbul.2013.07.037

Gjøsæter, J., 1978. Aspects of the distribution and ecology of the Myctophidae from the Western and Northern Arabian Sea. Development Report Indian Ocean Programme, 43: 62–108.

Gjøsæter, J., Kawaguchi, K., 1980. A review of the world resources of mesopelagic fish. FAO Fisheries Technical paper No. 193: 1-149.

Gjøsæter, J., 1984. Mesopelagic fish, a large potential resource in the Arabian Sea. Deep-Sea Res. Part A. 31:1019–1035.

Go, Y.B., 1986. Diet and feeding chronology of mesopelagic micronektonic fish, *Diaphus suborbitalis*, in Suruga Bay, Japan. In: 1. Asian Fisheries Forum, Manila (Philippines), 26-31 May 1986.

Godø, O.R., Patel, R., Pedersen, G., 2009. Diel migration and swimbladder resonance of small fish: some implications for analyses of multifrequency echo data. ICES J. Mar. Sci. 66: 1143–1148. https://doi.org/10.1093/icesjms/fsp098

Godø, O.R., Samuelsen, A., Macaulay, G.J., Patel, R., Hjøllo, S.S., Horne, J., Kaartvedt, S., Johannessen, J.A., 2012. Mesoscale Eddies Are Oases for Higher Trophic Marine Life. PLoS ONE. 7(1): e30161. https://doi.org/10.1371/journal.pone.0030161

Golet, W.J., Record, N.R., Lehuta, S., Lutcavage, M., Galuardi, B., Cooper, A.B., Pershing, A.J., 2015. The paradox of the pelagics: why bluefin tuna can go hungry in a sea of plenty. Mar. Ecol. Prog. Ser. 527: 181-192. DOI: 10.3354/meps11260

González-Pola, C., Díaz del Río, G., Ruiz-Villarreal, M., Sánchez, R.F., Mohn, C., 2012. Circulation patterns at Le Danois Bank, an elongated shelf-adjacent seamount in the Bay of Biscay. Deep Sea Res. Part Oceanogr. Res. Pap. 60: 7–21. https://doi.org/10.1016/j.dsr.2011.10.001

Gopakumar, K., Nair, K.G.R., Nair, P.G.V., Nair, A.L., Radhakrishnan, A.G., Nair, P.R., 1983. Studies on Lantern Fish (*Benthosema plerotum*) I. Biochemical and Microbiological Investigations. 20: 17-19.

Gordon, A.L., Lutjeharms, J.R.E., Gründlingh, M.L., 1987. Stratification and circulation at the Agulhas Retroflection. Deep-Sea Res. 34(4): 565-599.

Gorelova, T. A., and Prutʹko, V. G., 1985. Feeding of *Diaphus suborbitalis* (Myctophidae, Pisces) in the Equatorial Indian Ocean. Okeanologiya, Academy of Sciences of the USSR, (25): 523-529

Gorsky, G., Ohman, M.D., Picheral, M., Gasparini, S., Stemmann, L., Romagnan, J-B., Gawood, A., Pesant, S., García-Lomas, C., Prejger, F., 2010. Digital zooplankton image analysis using the ZooScan integrated system. J. Plankton Res. 32(3): 285-303. doi:10.1093/plankt/fbp124

Goslin, J., Segoufin, J., Schlich, R., Fisher, R.L., 1980. Submarine topography and shallow structure of the Madagascar Ridge, western Indian Ocean. Geol. Soc. Am. Bull. 91: 741-753. https://doi.org/10.1130/0016-7606(1980)91<741:STASSO>2.0.CO;2

Grantham, H., Petersen, S., Possingham, H., 2008. Reducing bycatch in the South African pelagic longline fishery: the utility of different approaches to fisheries closures. Endanger. Species Res. 5: 291–299. https://doi.org/10.3354/esr00159

Groeneveld, J., Van Dalsen, A., Griffiths, C., 2006. A new species of spiny lobster, *Palinurus Barbarae* (Decapoda, Palinuridae) from Walters Shoals on the Madagascar Ridge. Crustaceana. 79: 821–833. https://doi.org/10.1163/156854006778008177

Groeneveld, J.C., Cliff, G., Dudley, S.F.J., Foulis, A.J., Santos, J., Wintner, S.P., 2014. Population structure and biology of shortfin mako, *Isurus oxyrinchus*, in the south-west Indian Ocean. Mar. Freshw. Res. 65: 1045. https://doi.org/10.1071/MF13341

Groeneveld, J., Koranteng, K.A., 2017. The RV Dr Fridtjof Nansen in the Western Indian Ocean: voyages of marine research and capacity development. [1975-2016]. Food and Agriculture Organization of the United Nations (FAO).

Grubbs, R.D., Holland, K.N., Itano, D.G., 2001. Food habits and trophic dynamics of structure-associated aggregations of yellowfin and bigeye tuna (*Thunnus albacares* and *Thunnus obesus*) in the Hawaiian Islands: Project description, rationale and preliminary results. Yellowfin Research Group–SCTB, 2001, vol. 14.

Gubbay, S., 2005. Toward the Conservation and Management of the Sedlo Seamount. Hamburg (Institut f. Hydrobiologie und Fischereiwissenschaft) OASIS report.

Guduff, S., Rochette, J., Simard, F., Spadone, A., Wright, G., 2018. Laying the foundations for management of a seamount beyond national jurisdiction. IUCN Report. pp 1-40.

Guinet, C., Cherel, Y., Ridoux, V., Jouventin, P., 1996. Consumption of marine resources by seabirds and seals in Crozet and Kerguelen waters: changes in relation to consumer biomass 1962–85. Antarct. Sci. 8(1): 23-30. https://doi.org/10.1017/S0954102096000053

Hall, I.R., Hemming, S.R., LeVay, L.J., Barker, S., Berke, M.A., Brentegani, L., Caley, T., Cartagena-Sierra, A., Charles, C.D., Coenen, J.J., Crespin, J.G., Franzese, A.M., Gruetzner, J., Han, X., Hines, S.K.V., Jimenez Espejo, F.J., Just, J., Koutsodendris, A., Kubota, K., Lathika, N., Norris, R.D., Periera dos Santos, T., Robinson, R., Rolinson, J.M., Simon, M.H., Tangunan, D., van der Lubbe, J.J.L., Yamane, M., Zhang, H., 2017. Expedition 361 summary. In: Proceedings of the International Ocean Discovery Program. 361. doi:10.14379/iodp.proc.361.101.2017

Hall-Spencer, J., Rogers, A., Davies, J., Foggo, A., 2007. Deep-sea coral distribution on seamounts, oceanic islands, and continental slopes in the Northeast Atlantic. Bull. Mar. Sci. 81(3): 135-146.

Halo, I., Backeberg, B., Penven, P., Ansorge, I., Reason, C., Ullgren, J.E., 2014. Eddy properties in the Mozambique Channel: A comparison between observations and two numerical ocean circulation models. Deep Sea Res. Part II Top. Stud. Oceanogr. 100: 38-53. http://dx.doi.org/10.1016/j.dsr2.2013.10.015

Haney, J.C., Haury, L.R., Mullineaux, L.S., Fey, C.L., 1995. Seabird aggregation at a deep North Pacific seamount. Mar. Biol. 123: 1-9.

Harbou, L.V., 2009. Trophodynamics of salps in the Atlantic Southern Ocean. PhD thesis, Universität Bremen, Germany. Pp 17

Harris, S.A., Noyon, M., Roberts, M., Marsac, F., 2020. Ichthyoplankton assemblages at three shallow seamounts in the South West Indian Ocean. Deep Sea Res. II.

Hart, P., Pearson, E., 2011. An application of the theory of island biogeography to fish speciation on seamounts. Mar. Ecol. Prog. Ser. 430: 281–288. https://doi.org/10.3354/meps08948

Haury, L., Fey, C., Gal, G., Hobday, A., Genin, A., 1995. Copepod carcasses in the ocean. I. Over seamounts. Mar. Ecol. Prog. Ser. 123: 57–63. https://doi.org/10.3354/meps123057

Haury, L., Fey, C., Newland, C., Genin, A., 2000. Zooplankton distribution around four eastern North Pacific seamounts. Prog. Oceanogr. 45: 69–105. https://doi.org/10.1016/S0079-6611(99)00051-8

Hazen, E., Johnston, D.W., 2010. Meridional patterns in the deep scattering layers and top predator distribution in the central equatorial Pacific. Fish. Oceanogr. 19(6): 427-433. doi:10.1111/j.1365-2419.2010.00561.x

Hazin, F.H.V., Zagaglia, J.R., Broadhurst, M.K., Travassos, P.E.P., Bezerra, T.R.Q., 1998. Review of a small-scale pelagic longline fishery off Northeastern Brazil. Mar. Fish. Rev. 60(3): 1-8.

Heffernan, J.T., Hopkins, T.L., 1981. Vertical Distribution and Feeding of the Shrimp Genera *Gennadas* and *Bentheogennema* (Decapoda: Penaeida) in the Eastern Gulf of Mexico. J Crustacean Biol. 1(4): 461-473.

Heimlich-Boran, J.R., 1988. Behavioral ecology of killer whales (*Orcinus orca*) in the Pacific Northwest. Can. J. Zool. 66: 565–578. https://doi.org/10.1139/z88-084

Henry, L-A., Chaniotis, P., Roberts, J.M., 2012. An offshore resource of biological diversity, ecosystem processes and services: Scottish Seamounts. 2nd Annual Science Meeting of the Marine Alliance for Science and Technology, Scotland. [Available online: https://www.slideshare.net/CMBB_HW/scottish-seamounts-masts].

Henschke, N., Everett, J.D., Richardson, A.J., Suthers, I.M., 2016. Rethinking the Role of Salps in the Ocean. Trends Ecol. Evol. 31: 720–733. https://doi.org/10.1016/j.tree.2016.06.007

Herbette, S., Morel, Y., Arhan, M., 2003. Erosion of a surface vortex by a seamount. J. Phys. Oceanogr. 33(1): 664-679. https://doi.org/10.1175/2382.1

Hesslein, R.H., Hallard, K.A., Ramlal, P., 1993. Replacement of Sulfur, Carbon, and Nitrogen in Tissue of Growing Broad Whitefish (Coregonus nasus) in Response to a Change in Diet Traced by δ34S, δ13C, and δ15N. Can. J. Fish. Aquat. Sci. 50: 2071-2076.

Hestetun, J.T., Rapp, H.T., Xavier, J., 2017. Carnivorous sponges (Porifera, Cladorhizidae) from the Southwest Indian Ocean Ridge seamounts. Deep Sea Res. Part II Top. Stud. Oceanogr. 137: 166–189. https://doi.org/10.1016/j.dsr2.2016.03.004

Heywood, K.J., 1996. Diel vertical migration of zooplankton in the Northeast Atlantic. J Plankton Res. 18(2): 163-184.

Hidaka, K., Kawaguchi, K., Murakami, M., Takahashi, M., 2001. Downward transport of organic carbon by diel migratory micronekton in the western equatorial Pacific: its quantitative and qualitative importance. Deep-Sea Res. I. 48: 1923-1939.

Hillier, J.K., Watts, A.B., 2007. Global distribution of seamounts from ship-track bathymetry data. Geophys. Res. Lett. 34: L13304. https://doi.org/10.1029/2007GL029874

Hinke, J.T., Cossio, A.M., Goebel, M.E., Reiss, C.S., Trivelpiece, W.Z., Watters, G.M., 2017. Identifying Risk: Concurrent Overlap of the Antarctic Krill Fishery with Krill-Dependent Predators in the Scotia Sea. PLOS ONE 12: e0170132. https://doi.org/10.1371/journal.pone.0170132

Hirch, S., Martin, B., Christiansen, B., 2009. Zooplankton metabolism and carbon demand at two seamounts in the NE Atlantic. Deep Sea Res. Part II Top. Stud. Oceanogr. 56: 2656–2670. https://doi.org/10.1016/j.dsr2.2008.12.033

Hirch, S., Christiansen, B., 2010. The trophic blockage hypothesis is not supported by the diets of fishes on Seine seamount. Mar. Ecol. 31(Suppl. 1): 107-120. DOI:10.1111/j.1439-0485.2010.00366.x

Ho, C-R., Zheng, Q., Kuo, N-J., 2004. SeaWifs observations of upwelling south of Madagascar: long-term variability and ineraction with East Madagascar Current. Deep Sea Res. Part II Top. Stud. Oceanogr. 51: 59-67. doi:10.1016/j.dsr2.2003.05.001

Hobson, K.A., Piatt, J.F., Pitocchelli, J., 1994. Using stable isotopes to determine seabird trophic relationships. J Anim. Ecol. 63: 786-798.

Holland, K.N., Kleiber, P., Kajiura, S.M., 1999. Different residence times of yellowfin tuna, *Thunnus albacares*, and bigeye tuna, *T. obesus*, found in mixed aggregations over a seamount. Fish. Bull. 97: 392–395.

Holland, K., Grubbs, D., Graham, B., Itano, D., Dagorn, L., 2003. The biology of FAD-associated tuna: temporal dynamics of association and feeding ecology. WP YFT-7, Mooloolaba, Australia, 9-16.

Holland, K.N., Grubbs, R.D., 2007. Fish visitors to seamounts: Tunas and billfish at seamounts. In: Pitcher, T.J., Morato, T., Hart, P.J.B., Clark, M.R., Haggan, N., Santos, R.S. (Eds), Seamounts: Ecology, Fisheries & Conservation. Blackwell Publishing Ltd, Oxford, UK, pp. 189-201.

Hood, R.R., Beckley, L.E., Wiggert, J.D., 2017. Biogeochemical and ecological impacts of boundary currents in the Indian Ocean. Prog. Oceanogr. 156: 290–325. https://doi.org/10.1016/j.pocean.2017.04.011

Hopkins, T.L., Flock, M.E., Gartner, J.V. Jr., Torres, J.J., 1994. Structure and trophic ecology of a low latitude midwater decapod and mysid assemblage. Mar. Ecol. Prog. Ser. 109: 143-156.

Hubbs, 1959. Initial discoveries of fish faunas on seamounts and offshore banks in the Eastern Pacific. Pacific Science 13: 311-316.

Hudson, J.M., Steinberg, D.K., Sutton, T.T., Graves, J.E., Latour, R.J., 2014. Myctophid feeding ecology and carbon transport along the northern Mid-Atlantic Ridge. Deep-Sea Res. I. 93:104-116. https://doi.org/10.1016/j.dsr.2014.07.002

Huggett, J.A., 2014. Mesoscale distribution and community composition of zooplankton in the Mozambique Channel. Deep Sea Res. Part II Top. Stud. Oceanogr. 100: 119–135. https://doi.org/10.1016/j.dsr2.2013.10.021

Hunkins, K., 1986. Anomalous diurnal tidal currents on the Yermak Plateau. J. Mar. Res. 44: 51–69. https://doi.org/10.1357/002224086788460139

Huppert, H.E., 1975. Some remarks on the initiation of inertial Taylor columns. J. Fluid Mech. 67: 397. https://doi.org/10.1017/S0022112075000377

Huppert, H.E., Bryan, K., 1976. Topographically generated eddies. Deep-Sea. Res. 23: 655-679.

Hussey, N.E., MacNeil, M.A., McMeans, B.C., Olin, J.A., Dudley, S.F.J., Cliff, G., Wintner, S.P., Fennessy, S.T., Fisk, A.T., 2014. Rescaling the trophic structure of marine food webs. Ecol. Lett. 17: 239-250. DOI: 10.1111/ele.12226

Huthnance, J.M., 1974. On the diurnal tidal currents over Rockall Bank. Deep Sea Res. Oceanogr. 21: 23–35. https://doi.org/10.1016/0011-7471(74)90016-3

Ignatyev, S.M., 1996. Pelagic fishes and their macroplankton prey: Swimming speeds. In: Forage Fishes in Marine Ecosystems. pp 31-39.

IHO, 2008. Standardization of undersea feature names: Guidelines proposal form terminology, 4th edition. International Hydrographic Organization and International Oceanographic Commission, International Hydrographic Bureau, Monaco. Pp 32

Ingole, B., Koslow, J.A., 2005. Deep-sea ecosystems of the Indian Ocean. Indian J. Mar. Sci. 34(1): 27-34.

IOTC, 2018. Report of the 21st Session of the IOTC Scientific Committee. Seychelles, 3 – 7 December 2018. IOTC–2018–SC21–R[E]: 249 pp.

Irigoien, X., Klevjer, T.A., Røstad, A., Martinez, U., Boyra, G., Acuña, J.L., Bode, A., Echevarria, F., Gonzalez-Gordillo, J.I., Hernandez-Leon, S., Agusti, S., Aksnes, D.L., Duarte, C.M., Kaartvedt, S., 2014. Large mesopelagic fishes biomass and trophic efficiency in the open ocean. Nat. Commun. 5: 3271. https://doi.org/10.1038/ncomms4271

Isaacs, J. D., Schwartzlose, R. A., 1965. Migrant sound scatterers: Interaction with the sea floor. Science 150(3705): 1810-1813. https://doi.org/10.1126/science.150.3705.1810

Iseki, K. 1981. Particulate Organic Matter Transport to the Deep Sea by Salp Fecal Pellets. Mar. Ecol. Prog. Ser. 5: 55-60.

Isern-Fontanet, J., Font, J., García-Ladona, E., Emelianov, M., Millot, C., Taupier-Letage, I., 2004. Spatial structure of anticyclonic eddies in the Algerian basin (Mediterranean Sea) analyzed using the Okubo-Weiss parameter. Deep Sea Res. Part II Top. Stud. Oceanogr. 51: 3009-3028. doi:10.1016/j.dsr2.2004.09.013

IUCN, 2018. Progress in the Southern Indian Ocean towards better protection of biodiversity in the high seas. [Online] https://www.iucn.org/news/marine-and-polar/201807/progress-southern-indian-ocean-towards-better-protection-biodiversity-high-seas. Accessed on 02/08/2019.

Ivanov, B.G., Krylov, V.V., 1980. Length-Weight Relationship in Some Common Prawns and Lobsters (Macrura, Natantia and Reptantia) From the Western Indian Ocean. Crustaceana. 38: 279–289. https://doi.org/10.1163/156854080X00193

Iversen, M.H., Pakhomov, E.A., Hunt, B.P.V., van der Jagt, H., Wolf-Gladrow, D., Klaas, C., 2017. Sinkers or floaters? Contribution from salp pellets to the export flux during a large bloom event in the Southern Ocean. Deep Sea Res. Part II Top. Stud. Oceanogr. 138: 116–125. https://doi.org/10.1016/j.dsr2.2016.12.004

Iyer, S.D., Mehta, C.M., Das, P., Kalangutkar, N.G., 2012. Seamounts – characteristics, formation, mineral deposits and biodiversity. Geol. Acta 10(3): 295-308. https://doi.org/10.1344/105.000001758

Jackson, A.L., Inger, R., Parnell, A.C., Bearhop, S., 2011. Comparing isotopic niche widths among and within communities: SIBER – Stable Isotope Bayesian Ellipses in R. Journal of Animal Ecology. 80: 595-602. DOI: 10.1111/j.1365-2656.2011.01806.x

Jaquemet, S., Le Corre, M., Quartly, G.D., 2007. Ocean control of the breeding regime of the sooty tern in the southwest Indian Ocean. Deep Sea Res. Part Oceanogr. Res. Pap. 54: 130–142. https://doi.org/10.1016/j.dsr.2006.10.003

Jaquemet, S., Ternon, J.F., Kaehler, S., Thiebot, J.B., Dyer, B., Bemanaja, E., Marteau, C., Le Corre, M., 2014. Contrasted structuring effects of mesoscale features on the seabird community in the Mozambique Channel. Deep Sea Res. Part II Top. Stud. Oceanogr. 100: 200–211. https://doi.org/10.1016/j.dsr2.2013.10.027

Jasmine, P., Muraleedharan, K., Madhu, N., Asha Devi, C., Alagarsamy, R., Achuthankutty, C., Jayan, Z., Sanjeevan, V., Sahayak, S., 2009. Hydrographic and productivity characteristics along 45°E longitude in the southwestern Indian Ocean and Southern Ocean during austral summer 2004. Mar. Ecol. Prog. Ser. 389: 97–116. https://doi.org/10.3354/meps08126

Jean, C., Ciccione, S., Ballorain, K., Georges, J.-Y., Bourjea, J., 2010. Ultralight aircraft surveys reveal marine turtle population increases along the west coast of Reunion Island. Oryx. 44: 223–229. https://doi.org/10.1017/S003060530999072X

Jefferson, T.A., Weir, C.R., Anderson, R.C., Ballance, L.T., Kenney, R.D., Kiszka, J.J., 2014. Global distribution of Risso's dolphin *Grampus griseus*: a review and critical evaluation. Mammal Rev. 44: 56–68. https://doi.org/10.1111/mam.12008

Jena, B., Swain, D., Avinash, K., 2012. Investigation of the biophysical processes over the oligotrophic waters of South Indian Ocean subtropical gyre, triggered by cyclone Edzani. International Journal of Applied Earth Observation and Geoinformation 18: 49-56. doi:10.1016/j.jag.2012.01.006

Jena, B., Sahu, S., Avinash, K., Swain, D., 2013. Observation of oligotrophic gyre variability in the south Indian Ocean: Environmental forcing and biological response. Deep Sea Res. Part Oceanogr. Res. Pap. 80: 1–10. https://doi.org/10.1016/j.dsr.2013.06.002

Johnston, D. W., McDonald, M., Polovina, J., Domokos, R., Wiggins, S., Hildebrand, J., 2008. Temporal patterns in the acoustic signals of beaked whales at Cross Seamount. Biol. Lett. 4: 208–211. https://doi.org/10.1098/rsbl.2007.0614

José, Y.S., Aumont, O., Machu, E., Penven, P., Moloney, C.L., Maury, O., 2014. Influence of mesoscale eddies biological production in the Mozambique Channel: Several contrasted examples from a coupled ocean-biogeochemistry model. Deep Sea Res. Part II Top. Stud. Oceanogr. 100: 79-93. http://dx.doi.org/10.1016/j.dsr2.2013.10.018

Judkins, D.C., Haedrich, R.L., 2018. The deep scattering layer micronektonic fish faunas of the Atlantic mesopelagic ecoregions with comparison of the corresponding decapod shrimp faunas. Deep-Sea Res. I. 136: 1-30. https://doi.org/10.1016/j.dsr.2018.04.008

Junior, T.V., Vooren, C.M., Lessa, R.P., 2009. Feeding strategy of the night shark (*Carcharhinus signatus*) and scalloped hammerhead shark (*Sphyrna lewini*) near seamounts off North Eastern Brazil. Brazilian J. of Ocean. 57(2): 97-104.

Kaartvedt, S., Røstad, A., Klevjer, T., Staby, A., 2009. Use of bottom-mounted echo sounders in exploring behavior of mesopelagic fishes. Mar. Ecol. Prog. Ser. 395: 109–118. https://doi.org/10.3354/meps08174

Kaartvedt, S., Klevjer, T.A., Aksnes, D.L., 2012. Internal wave-mediated shading causes frequent vertical migrations in fishes. Mar. Ecol. Prog. Ser. 452: 1-10. DOI: 10.3354/meps09688

Kamen-Kaye, M., Meyerhoff, A.A., 1980. Petroleum Geology of the Mascarene Ridge, Western Indian Ocean. J. Petrol. Geo. 3(2): 123-138.

Karakulak, F.S., Salman, A., Oray, I.K., 2009. Diet composition of bluefin tuna (*Thunnus thynnus* L. 1758) in the Eastern Mediterranean Sea, Turkey. J. Appl. Ichthyol. 25: 757-761. DOI: 10.1111/j.1439-0426.2009.01298.x

Kaschner, K., 2007. Air-breathing visitors to seamounts: Section A, Marine mammals. In: Pitcher, T.J., Morato, T., Hart, P.J.B., Clark, M.R., Haggan, N., Santos, R.S. (Eds),

Seamounts: Ecology, Fisheries & Conservation. Blackwell Publishing Ltd, Oxford, UK, pp. 230-238.

Kensley, B.F., 1975. Five species of *Jaeropsis* from the southern Indian Ocean [Crustacea, Isopoda, Asellota]. Ann. S. Afr. Mus. 67(10): pp. 367- 380.

Kensley, B.F., 1981. On the zoogeography of southern African decapod Crustacea, with a distributional checklist of the species. Smithsonian Contributions to Zoology. 338, pp. 1-64.

Kimani, E.N., Okemwa, G.M., Kazungu, J.M., 2009. Fisheries in the Southwest Indian Ocean. trends and governance challenges. In: Laipson, E., Pandya, A. (Eds), The Indian Ocean: Resource and Governance Challenges. The Henry L. Stimson Center Washington DC. pp 3-17.

Kiriakoulakis, K., Vilas, J.C., Blackbird, S.J., Arístegui, J., Wolff, G.A., 2009. Seamounts and organic matter—Is there an effect? The case of Sedlo and Seine seamounts, Part 2. Composition of suspended particulate organic matter. Deep Sea Res. Part II Top. Stud. Oceanogr. 56: 2631–2645. https://doi.org/10.1016/j.dsr2.2008.12.024

Kiszka, J., Ersts, P.J., Ridoux, V. 2007. Cetacean diversity around the Mozambique Channel island of Mayotte (Comoros archipelago). J. Cetacean Res. Manage. 9(2): 105-109.

Kitchingman, A., Lai, S., 2004. Inferences of potential seamount locations from mid-resolution bathymetric data. In: Morato, T., Pauly, D. (Eds), Seamounts: Biodiversity and Fisheries. pp 7-12.

Kitchingman, A., Lai, S., Morato, T., Pauly, D., 2007. How many seamounts are there and where are they located? In: Pitcher, T.J., Morato, T., Hart, P.J.B., Clark, M.R., Haggan, N., Santos, R.S. (Eds), Seamounts: Ecology, Fisheries & Conservation. Blackwell Publishing Ltd, Oxford, UK, pp. 26-40.

Klein, P., Lapeyre, G., 2009. The Oceanic Vertical Pump Induced by Mesoscale and Submesoscale Turbulence. Annu. Rev. Mar. Sci. 1: 351–375. https://doi.org/10.1146/annurev.marine.010908.163704

Klimley, A.P., Nelson, D.R., 1984. Diel movement patterns of the scalloped hammerhead shark (*Sphyrna lewini*) in relation to El Bajo Espiritu Santo: a refuging central-position social system. Behav. Ecol. Sociobiol. 15: 45-54.

Klimley, A.P., Butler, S.B., Nelson, D.R., Stull, A.T., 1988. Diel movements of scalloped hammerhead sharks, *Sphyrna lewini* Griffith and Smith, to and from a seamount in the Gulf of California. J. Fish. Biol. 33: 751-761.

Klimley, A.P., 1993. Highly directional swimming by scalloped hammerhead sharks, *Sphyrna lewini*, and subsurface irradiance, temperature, bathymetry, and geomagnetic field. Mar. Biol. 117: 1–22. https://doi.org/10.1007/BF00346421

Klimley, A.P., Jorgensen, S.J., Muhlia-Melo, A., Beavers, S.C., 2003. The occurrence of yellowfin tuna (T*hunnus albacares*) at Espiritu Santo Seamount in the Gulf of California. Fish. Bull. 101: 684-692.

Kloppmann, M., Mohn, C., Bartsch, J., 2001. The distribution of blue whiting eggs and larvae on Porcupine Bank in relation to hydrography and currents. Fish. Res. 50: 89–109. https://doi.org/10.1016/S0165-7836(00)00244-7

Kloser, R. J., Ryan, T., Sakov, P., Williams, A., Koslow, J. A., 2002. Species identification in deep water using multiple acoustic frequencies. Can. J. Fish. Aquat. Sci. 59: 1065–1077. https://doi.org/10.1139/f02-076

Kloser, R.J., Ryan, T.E., Young, J.W., Lewis, M.E., 2009. Acoustic observations of micronekton fish on the scale of an ocean basin: potential and challenges. ICES J. Mar. Sci. 66(6): 998–1006. https://doi.org/10.1093/icesjms/fsp077

Kloser, R.J., Ryan, T.E., Keith, G., Gershwin, L., 2016. Deep-scattering layer, gas-bladder density, and size estimates using a two-frequency acoustic and optical probe. ICES J Mar Sci. 73(8): 2037-2048. DOI:10.1093/icesjms/fsv257

Koch-Larrouy, A., Ternon, J-F., Roberts, M., Herbette, S., Arbic, B.K., Chanut, J., Lyard, F., Bourdalle-Badié, R., Ansong, J.K., Tchilibou, M., Buijsman, M.C., Vianello, P., Allain, D., Demarcq, H., Shriver, J-F., Ferron, B., Mixing above a group of seamounts on the northern Madagascar Ridge with impacts on algal blooms. Deep Sea Res. II, in review.

Koizumi, K., Hiratsuka, S., Saito, H., 2014. Lipid and Fatty Acids of Three Edible Myctophids, *Diaphus watasei*, *Diaphus suborbitalis*, and *Benthosema pterotum*: High Levels of Icosapentaenoic and Docosahexaenoic Acids. J. Oleo Sci. 63: 461–470. https://doi.org/10.5650/jos.ess13224

Kojadinovic, J., Corre, M.L., Cosson, R.P., Bustamante, P., 2007. Trace Elements in Three Marine Birds Breeding on Reunion Island (Western Indian Ocean): Part 1—Factors Influencing Their Bioaccumulation. Arch. Environ. Contam. Toxicol. 52: 418–430. https://doi.org/10.1007/s00244-005-0225-2

Kolasinski, J., Rogers, K., Frouin, P., 2008. Effects of acidification on carbon and nitrogen stable isotopes of benthic macrofauna from a tropical coral reef. Rapid Commun Mass Spectrom. 22: 2955−2960. DOI: 10.1002/rcm.3694

Kolasinski, J., Kaehler, S., Jaquemet, S., 2012. Distribution and sources of particulate organic matter in a mesoscale eddy dipole in the Mozambique Channel (south-western Indian Ocean): Insight from C and N stable isotopes. J. Mar. Syst. 96-97: 122-131. https://doi.org/10.1016/j.jmarsys.2012.02.015

Kolla, V., Eittreim, S., Sullivan, L., Kostecki, J.A., Burckle, L.H., 1980. Current-controlled, abyssal microtopography and sedimentation in Mozambique Basin, southwest Indian Ocean. Mar. Geol. 34: 171–206. https://doi.org/10.1016/0025-3227(80)90071-7

Korneliussen, R. J., Ona, E., 2003. Synthetic echograms generated from the relative frequency response. ICES J. Mar. Sci. 60: 636-640. https://doi.org/10.1016/S1054-3139(03)00035-3

Koslow, J.A., 1996. Energetic and life-history patterns of deep-sea benthic, benthopelagic and seamount-associated fish. J. Fish Biol. 49: 54–74. https://doi.org/10.1111/j.1095-8649.1996.tb06067.x

Koslow, J.A., 1997. Seamounts and the Ecology of Deep-Sea Fisheries: The firm-bodied fishes that feed around seamounts are biologically distinct from their deepwater neighbors-and may be especially vulnerable to overfishing. Am. Sci. 85(2): 168-176.

Koslow, T. 2007. The Silent Deep: The Discovery, Ecology and Conservation of the Deep Sea. University of New South Wales Press, Sydney, Australia.

Kremer, P., 2002. Towards an understanding of salp swarm dynamics. ICES publication CM2002. Vol 12.

Kunze, E., Sanford, T.B., 1996. Abyssal Mixing: Where It Is Not. J. Phys. Oceanogr. 26: 2286-2296.

Kunze, E., Toole, J.M., 1997. Fine- and Microstructure Observations of Trapped Diurnal Oscillations Atop Fieberling seamount. In: Topographic effects in the ocean. Proceedings of Aha Huliko, a Hawaiian Winter Workshop. School of Ocean and Earth Science and Technology, University of Hawaii, Honolulu. 1995. p. 15-42.

Kunze, E., Llewellyn Smith, S., 2004. The Role of Small-Scale Topography in Turbulent Mixing of the Global Ocean. Oceanography. 17: 55–64. https://doi.org/10.5670/oceanog.2004.67

Kvile, K.Ø., Taranto, G.H., Pitcher, T.J., Morato, T. 2014. A global assessment of seamount ecosystems knowledge using an ecosystem evaluation framework. Biol. Conserv. 173: 108-120. http://dx.doi.org/10.1016/j.biocon.2013.10.002

Kwong, L.E., Pakhomov, E.A., Suntsov, A.V., Seki, M.P., Brodeur, R.D., Pakhomova, L.G., Domokos, R., 2018. An intercomparison of the taxonomic and size composition of tropical macrozooplankton and micronekton collected using three sampling gears. Deep Sea Res. Part I. https://doi.org/10.1016/j.dsr.2018.03.013

Lack, M., Short, K., Willock, A., 2003. Managing risk and uncertainty in deep-sea fisheries: lessons from Orange Roughy. Traffic Oceania and WWF Endangered Seas Programme, Australia.

Lambardi, P., Lutjeharms, J., Mencacci, R., Hays, G., Luschi, P., 2008. Influence of ocean currents on long-distance movement of leatherback sea turtles in the Southwest Indian Ocean. Mar. Ecol. Prog. Ser. 353: 289–301. https://doi.org/10.3354/meps07118

Lambert, C., Mannocci, L., Lehodey, P., Ridoux, V., 2014. Predicting Cetacean Habitats from Their Energetic Needs and the Distribution of Their Prey in Two Contrasted Tropical Regions. PLoS ONE. 9: e105958. https://doi.org/10.1371/journal.pone.0105958

Lamont, T., Barlow, R.G., Morris, T., van den Berg, M.A., 2014. Characterisation of mesoscale features and phytoplankton variability in the Mozambique Channel. Deep Sea Res. Part II Top. Stud. Oceanogr. 100: 94–105. https://doi.org/10.1016/j.dsr2.2013.10.019

Lampert, W., 1989. The Adaptive Significance of Diel Vertical Migration of Zooplankton. Funct. Ecol. 3(1): 21-27. DOI:10.2307/2389671

Laptikhovsky, V., Boersch-Supan, P., Bolstad, K., Kemp, K., Letessier, T., Rogers, A.D., 2017. Cephalopods of the Southwest Indian OceanRidge: A hotspot of biological diversity and absence of endemism. Deep Sea Res. Part II Top. Stud. Oceanogr. 136: 98–107. https://doi.org/10.1016/j.dsr2.2015.07.002

Laran, S., Authier, M., Van Canneyt, O., Dorémus, G., Watremez, P., Ridoux, V., 2017. A Comprehensive Survey of Pelagic Megafauna: Their Distribution, Densities, and Taxonomic Richness in the Tropical Southwest Indian Ocean. Front. Mar. Sci. 4: 139. https://doi.org/10.3389/fmars.2017.00139

Lavelle, J.W., Lozovatsky, I.D., Smith, D.C., 2004. Tidally induced turbulent mixing at Irving Seamount-Modeling and measurements. Geophys. Res. Lett. 31:L10308. https://doi.org/10.1029/2004GL019706

Lavelle, J. W., Mohn, C., 2010. Motion, commotion, and biophysical connections at deep ocean seamounts. Oceanography. 23(1): 90-103. https://doi.org/10.5670/oceanog.2010.64

Layman, C.A., Arrington, D.A., Montaña, C.G., Post, D.M., 2007. Can stable isotope ratios provide for community-wide measures of trophic structure? Ecology. 88: 42–48.

Le Corre, M., 2001. Breeding seasons of seabirds at Europa Island (southern Mozambique Channel) in relation to seasonal changes in the marine environment. J. Zool. 254: 239–249. https://doi.org/10.1017/S0952836901000759

Le Corre, M., Jaeger, A., Pinet, P., Kappes, M.A., Weimerskirch, H., Catry, T., Ramos, J.A., Russell, J.C., Shah, N., Jaquemet, S., 2012. Tracking seabirds to identify potential Marine Protected Areas in the tropical western Indian Ocean. Biol. Conserv. 156: 83–93. https://doi.org/10.1016/j.biocon.2011.11.015

Le Pichon, X., 1960. The deep water circulation in the southwest Indian Ocean. J. Geophys. Res. 65: 4061–4074. https://doi.org/10.1029/JZ065i012p04061

Lebourges-Dhaussy, A., Marchal, E., Menkès, C., Champalbert, G., Biessy, B., 2000. *Vinciguerria nimbaria* (micronekton), environment and tuna: their relationships in the Eastern Tropical Atlantic. Oceanol. Acta 23: 515–528. https://doi.org/10.1016/S0399-1784(00)00137-7

Lecomte-Finiger, R., Maunier, C., Khafif, M., 2004. Leptocephali, these unappreciated larvae. Cybium. 28(2): 83-95.

Legand, M., 1967. Seasonal variations in the Indian Ocean along 110°E, VI. Macroplankton and micronekton biomass. Aust. J. Mar. Freshwater. Res. 20(1): 85-104

Lehodey, P., Murtugudde, R., Senina, I., 2010. Bridging the gap from ocean models to population dynamics of large marine predators: A model of mid-trophic functional groups. Prog. Oceanogr. 84: 69-84. DOI:10.1016/j.pocean.2009.09.008

Letessier, T.B., Cox, M.J., Meeuwig, J.J., Boersch-Supan, P.H., Brierley, A.S., 2015. Enhanced pelagic biomass around coral atolls. Mar. Ecol. Prog. Ser. 546: 271-276. DOI: 10.3354/meps11675

Letessier, T.B., De Grave, S., Boersch-Supan, P.H., Kemp, K.M., Brierley, A.S., Rogers, A.D., 2017. Seamount influences on mid-water shrimps (Decapoda) and gnathophausiids (Lophogastridea) of the South-West Indian Ridge. Deep Sea Res. Part II Top. Stud. Oceanogr. 136: 85–97. https://doi.org/10.1016/j.dsr2.2015.05.009

Lévy, M., Klein, P., Treguier, A-M., 2001. Impact of sub-mesoscale physics on production and subduction of phytoplankton in an oligotrophic regime. J. Mar. Res. 59: 535-565.

Lévy, M., Franks, P.J.S., Smith, K.F. 2018. The role of submesoscale currents in structuring marine ecosystems. Nature Communications. 9(4758). DOI: 10.1038/s41467-018-07059-3

Liénart, C., Savoye, N., Bozec, Y., Breton, E., Conan, P., David, V., Feunteun, E., Grangeré, K., Kerhervé, P., Lebreton, B., Lefebvre, S., L'Helguen, S., Mousseau, L., Raimbault, P., Richard, P., Riera, P., Sauriau, P.-G., Schaal, G., Aubert, F., Aubin, S., Bichon, S., Boinet, C., Bourasseau, L., Bréret, M., Caparros, J., Cariou, T., Charlier, K., Claquin, P., Cornille, V., Corre, A.-M., Costes, L., Crispi, O., Crouvoisier, M., Czamanski, M., Del Amo, Y., Derriennic, H., Dindinaud, F., Durozier, M., Hanquiez, V., Nowaczyk, A., Devesa, J., Ferreira, S., Fornier, M., Garcia, F., Garcia, N., Geslin, S., Grossteffan,

E., Gueux, A., Guillaudeau, J., Guillou, G., Joly, O., Lachaussée, N., Lafont, M., Lamoureux, J., Lecuyer, E., Lehodey, J.-P., Lemeille, D., Leroux, C., Macé, E., Maria, E., Pineau, P., Petit, F., Pujo-Pay, M., Rimelin-Maury, P., Sultan, E., 2017. Dynamics of particulate organic matter composition in coastal systems: A spatio-temporal study at multi-systems scale. Prog. Oceanogr. 156: 221–239. https://doi.org/10.1016/j.pocean.2017.03.001

Litvinov, F., 2007. Fish visitors to seamounts: Aggregations of large pelagic sharks above seamounts. In: Pitcher, T.J., Morato, T., Hart, P.J.B., Clark, M.R., Haggan, N., Santos, R.S. (Eds), Seamounts: Ecology, Fisheries & Conservation. Blackwell Publishing Ltd, Oxford, UK, pp. 202-206.

Longhurst, A., 1998. Ecological Geography of the Sea. Academic Press, San Diego. 398p.

Longhurst, A., 2007. The Indian Ocean-Indian South Subtropical Gyre Province (ISSG). In: Academic Press (Ed.), Ecological Geography of the Sea, 2nd ed. Elsevier, USA, pp 285.

Lorrain, A., Graham, B.S., Popp, B.N., Allain, V., Olson, R.J., Hunt, B.P.V., Potier, M., Fry, B., Galván-Magaña, F., Menkes, C.E.R., Kaehler, S., Ménard, F., 2015. Nitrogen isotopic baselines and implications for estimating foraging habitat and trophic position of yellowfin tuna in the Indian and Pacific Oceans. Deep Sea Res. Part II Top. Stud. Oceanogr. 113: 188-198. https://doi.org/10.1016/j.dsr2.2014.02.003

Lueck, R.G., Mudge, T.D., 1997. Topographically Induced Mixing Around a Shallow Seamount. Science 276: 1831–1833. https://doi.org/10.1126/science.276.5320.1831

Lutjeharms, J.R.E., Bang, N.D., Duncan, C.P., 1981. Characteristics of the currents east and south of Madagascar. Deep Sea Res. Part Oceanogr. Res. Pap. 28: 879–899. https://doi.org/10.1016/0198-0149(81)90008-X

Lutjeharms, J.R.E., Biastoch, A., van derWerf, P.A., Ridderhinkhof, H., De Ruijter,W.P.M., 2012. On the discontinuous nature of the Mozambique Current. S. Afr. J. Sci. 108(1/2). http://dx.doi.org/10.4102/sajs.v108i1/2.428

Machu, E., Lutjeharms, J.R.E., Webb, A.M., Van Aken, H.M. 2002. First hydrographic evidence of the southeast Madagascar upwelling cell. Geophys. Res. Lett. 29(21). https://doi.org/10.1029/2002GL015381

MacKinnon, J.A., Johnston, T.M.S., Pinkel, R., 2008. Strong transport and mixing of deep water through the Southwest Indian Ridge. Nat. Geosci. 1: 755–758. https://doi.org/10.1038/ngeo340

MacLennan, D.V., Fernandes, P.G., Dalen, J. 2002. A consistent approach to definitions and symbols in fisheries acoustics. ICES J. Mar. Sci. 59: 365-369. doi:10.1006/jmsc.2001.1158

Madhupratap, M., 1983. Zooplankton standing stock and diversity along an oceanic tract in the Western Indian Ocean. Mahasagar-Bulletin of the National Institute of Oceanography. 16(4): 463-467.

Madin, L.P., Kremer, P., Hacker, S., 1996. Distribution and vertical migration of salps (Tunicata, Thaliacea) near Bermuda. J. Plankton Res. 18: 747–755. https://doi.org/10.1093/plankt/18.5.747

Madin, L.P., Kremer, P., Wiebe, P.H., Purcell, J.E., Horgan, E.H., Nemazie, D.A., 2006. Periodic swarms of the salp *Salpa aspera* in the Slope Water off the NE United States:

Biovolume, vertical migration, grazing, and vertical flux. Deep Sea Res. Part Oceanogr. Res. Pap. 53: 804–819. https://doi.org/10.1016/j.dsr.2005.12.018

MAFF (Ministry of Agriculture, Fisheries and Food), 2000. Monitoring and surveillance of non-radioactive contaminants in the aquatic environment and activities regulating the disposal of wastes at sea. In: Aquatic Environment Monitoring Report, No. 52. Center for Environment, Fisheries and Aquaculture Science, Lowestoft, UK.

Mann, K.H., Lazier, J.R., 2006. Dynamics of marine ecosystems: biological-physical interactions in the oceans. 3rd edition. John Wiley and Sons.

Mannocci, L., Laran, S., Monestiez, P., Dorémus, G., Van Canneyt, O., Watremez, P., Ridoux, V., 2014. Predicting top predator habitats in the Southwest Indian Ocean. Ecography. 37: 261–278. https://doi.org/10.1111/j.1600-0587.2013.00317.x

Marchal, E., Lebourges-Dhaussy, A., 1996. Acoustic evidence for unusual diel behaviour of a mesopelagic fish (*Vinciguerria nimbaria*) exploited by tuna. ICES J. Mar. Sci. 53: 443–447. https://doi.org/10.1006/jmsc.1996.0062

Marsac, F., Fonteneau, A., Michaud, P., 2014. Le « Coco de Mer », une montagne sous la mer. In: L'or bleu des Seychelles: Histoire de la pêche industrielle au thon dans l'océan Indien. IRD Editions, pp 151- 163.

Marsac, F., Annasawmy, P., Noyon, M., Demarcq, H., Soria, M., Rabearisoa, N., Bach, P., Cherel, Y., Grelet, J., Romanov, E., 2020. Seamount effect on circulation and distribution of ocean taxa at and near La Pérouse, a shallow seamount in the southwestern Indian Ocean. Deep-Sea II.

Martin, A.P., Richards, K.J., Law, C.S., Liddicoat, M., 2001. Horizontal dispersion within an anticyclonic mesoscale eddy. Deep Sea Res. Part II Top. Stud. Oceanogr. 48: 739–755. https://doi.org/10.1016/S0967-0645(00)00095-3

Martin, B., Christiansen, B., 2009. Distribution of zooplankton biomass at three seamounts in the NE Atlantic. Deep Sea Res. Part II Top. Stud. Oceanogr. 56: 2671–2682. https://doi.org/10.1016/j.dsr2.2008.12.026

Martínez del Rio, C., Wolf, N., Carleton, S.A., Gannes, L.Z., 2009. Isotopic ecology ten years after a call for more laboratory experiments. Biol. Rev. 84: 91-111. DOI: 10.1111/j.1469-185X.2008.00064.x

Mauchline, J., 1959. The Biology of the Euphausiid Crustacean, *Meganyctiphanes norvegica* (M. Sars). Proceedings of the Royal Society of Edinburgh, Section B: Biological Sciences 67(2): 141-179

McCave, I.N., Kiefer, T., Thornalley, D.J.R., Elderfield, H., 2005. Deep flow in the Madagascar–Mascarene Basin over the last 150000 years. Philos. Trans. R. Soc. Math. Phys. Eng. Sci. 363: 81–99. https://doi.org/10.1098/rsta.2004.1480

McClain, C.R., 2007. Seamounts: identity crisis or split personality? J. Biogeogr. 34: 2001–2008. https://doi.org/10.1111/j.1365-2699.2007.01783.x

McClatchie, S., Coombs, R.F., 2005. Low target strength fish in mixed species assemblages: the case of orange roughy. Fish. Res. 72: 185-192. DOI:10.1016/j.fishres.2004.11.008

McDonald, M.A., Hildebrand, J.A., Wiggins, S.M., Johnston, D.W., Polovina, J.J., 2009. An acoustic survey of beaked whales at Cross Seamount near Hawaii. J. Acoust. Soc. Am. 125: 624-627. DOI: 10.1121/1.3050317

McGillicuddy, D.J., Robinson, A.R., 1997. Eddy-induced nutrient supply and new production in Sargasso Sea. Deep-Sea Res. I. 44(8): 1427-1450.

McGillicuddy, D.J., Robinson, A.R., Siegel, D.A., Jannasch, H.W., Johnson, R., Dickey, T.D., McNeil, J., Michaels, A.F., Knap, A.H., 1998. Influence of mesoscale eddies on new production in the Sargasso Sea. Nature 394: 263–266. https://doi.org/10.1038/28367

McGillicuddy, D.J., 2016. Mechanisms of Physical-Biological-Biogeochemical Interaction at the Oceanic Mesoscale. Annu. Rev. Mar. Sci. 8: 125-59. doi: 10.1146/annurev-marine-010814-015606

Ménard, F., Lorrain, A., Potier, M., Marsac, F., 2007. Isotopic evidence of distinct feeding ecologies and movement patterns in two migratory predators (yellowfin tuna and swordfish) of the western Indian Ocean. Mar. Biol. 153: 141–152. https://doi.org/10.1007/s00227-007-0789-7

Ménard, F., Potier, M., Jaquemet, S., Romanov, E., Sabatié, R., Cherel, Y., 2013. Pelagic cephalopods in the western Indian Ocean: New information from diets of top predators. Deep Sea Res. Part II Top. Stud. Oceanogr. 95: 83–92. https://doi.org/10.1016/j.dsr2.2012.08.022

Ménard, F., Benivary, H.D., Bodin, N., Coffineau, N., Le Loc'h, F., Mison, T., Richard, P., Potier, M., 2014. Stable isotope patterns in micronekton from the Mozambique Channel. Deep Sea Res. Part II Top. Stud. Oceanogr. 100: 153–163. https://doi.org/10.1016/j.dsr2.2013.10.023

Mencacci, R., De Bernardi, E., Sale, A., Lutjeharms, J.R.E., Luschi, P., 2010. Influence of oceanic factors on long-distance movements of loggerhead sea turtles displaced in the southwest Indian Ocean. Mar. Biol. 157: 339–349. https://doi.org/10.1007/s00227-009-1321-z

Mendel, V., Sauter, D., 1997. Seamount volcanism at the super slow-spreading Southwest Indian Ridge between 57°E and 70°E. Geology 25(2): 99-102.

Menkes, C.E., Allain, V., Rodier, M., Gallois, F., Lebourges-Dhaussy, A., Hunt, B.P.V., Smeti, H., Pagano, M., Josse, E., Daroux, A., Lehodey, P., Senina, I., Kestenare, E., Lorrain, A., Nicol, S., 2015. Seasonal oceanography from physics to micronekton in the south-west Pacific. Deep Sea Res. Part II Top. Stud. Oceanogr. 113: 125-144. http://dx.doi.org/10.1016/j.dsr2.2014.10.026

Mensinger, A.F., Case, J.F., 1990. Luminescent properties of deep sea fish. J. Exp. Mar. Biol. Ecol. 144: 1–15. https://doi.org/10.1016/0022-0981(90)90015-5

Meyer, C.G., Holland, K.N., Papastamatiou, Y.P., 2005. Sharks can detect changes in the geomagnetic field. J. R. Soc. Interface 2: 129–130. https://doi.org/10.1098/rsif.2004.0021

Meyer, C.G., Papastamatiou, Y.P., Holland, K.N., 2010. A multiple instrument approach to quantifying the movement patterns and habitat use of tiger (*Galeocerdo cuvier*) and Galapagos sharks (*Carcharhinus galapagensis*) at French Frigate Shoals, Hawaii. Mar. Biol. 157: 1857-1868.

Michener, R.H., Kaufman, L., 2007. Stable isotope ratios as tracers in marine food webs: an update. In: Michener, R.H., Lajtha, K. (Eds), Stable Isotopes in Ecology and Environmental Science (2nd ed.). Blackwell, Malden, MA. pp. 238-282.

Mill, A.C., Sweeting, C.J., Barnes, C., Al-Habsi, S.H., MacNeil, M.A., 2008. Mass-spectrometer bias in stable isotope ecology. Limnol. Oceanogr: Methods 6(1): 34-39.

Miller, K.A., 2007. Climate variability and tropical tuna: Management challenges for highly migratory fish stocks. Mar. Policy. 31: 56–70. https://doi.org/10.1016/j.marpol.2006.05.006

Minagawa, M., Wada, E., 1984. Stepwise enrichment of ^{15}N along food chains: further evidence and the relation between $\delta^{15}N$ and animal age. Geochim. Cosmochim. Acta 48: 1135-1140.

Miya, M., Nishida, M., 1996. Molecular phylogenetic perspective on the evolution of the deep-sea fish genus Cyclothone (Stomiiformes: Gonostomatidae). Ichthyol. Res. 43: 375–398. https://doi.org/10.1007/BF02347637

Mohn, C., 2002. Observations of the mass and flow field at Porcupine Bank. ICES J. Mar. Sci. 59: 380–392. https://doi.org/10.1006/jmsc.2001.1174

Mohn, C., Beckmann, A., 2002. The upper ocean circulation at Great Meteor Seamount. Ocean Dyn. 52: 179–193. https://doi.org/10.1007/s10236-002-0017-4

Mohn, C., White, M., 2007. Remote sensing and modelling of bio-physical distribution patterns at Porcupine and Rockall Bank, Northeast Atlantic. Cont. Shelf Res. 27: 1875-1892. DOI:10.1016/j.csr.2007.03.006

Mohn, C., White, M., Bashmachnikov, I., Jose, F., Pelegrí, J.L., 2009. Dynamics at an elongated, intermediate depth seamount in the North Atlantic (Sedlo Seamount, 40°20′N, 26°40′W). Deep Sea Res. Part II Top. Stud. Oceanogr. 56: 2582–2592. https://doi.org/10.1016/j.dsr2.2008.12.037

Mohn, C., White, M., 2010. Seamounts in a restless ocean: Response of passive tracers to sub-tidal flow variability. Geophys. Res. Lett. 37: L15606. https://doi.org/10.1029/2010GL043871

Monticelli, D., Ramos, J., Quartly, G., 2007. Effects of annual changes in primary productivity and ocean indices on breeding performance of tropical roseate terns in the western Indian Ocean. Mar. Ecol. Prog. Ser. 351: 273–286. https://doi.org/10.3354/meps07119

Morato, T., Cheung, W.W.L., Pitcher, T.J., 2006. Vulnerability of seamount fish to fishing: fuzzy analysis of life-history attributes. J. Fish Biol. 68: 209–221. https://doi.org/10.1111/j.0022-1112.2006.00894.x

Morato, T., Varkey, D., Damaso, C., Machete, M., Santos, M., Prieto, R., Pitcher, T., Santos, R., 2008. Evidence of a seamount effect on aggregating visitors. Mar. Ecol. Prog. Ser. 357: 23–32. https://doi.org/10.3354/meps07269

Morato, T., Bulman, C., Pitcher, T.J., 2009. Modelled effects of primary and secondary production enhancement by seamounts on local fish stocks. Deep Sea Res. Part II Top. Stud. Oceanogr. 56: 2713–2719. https://doi.org/10.1016/j.dsr2.2008.12.029

Morato, T., Hoyle, S.D., Allain, V., Nicol, S.J., 2010a. Seamounts are hotspots of pelagic biodiversity in the open ocean. Proc. Natl. Acad. Sci. 107: 9707–9711. https://doi.org/10.1073/pnas.0910290107

Morato, Telmo, Hoyle, S.D., Allain, V., Nicol, S.J., 2010b. Tuna Longline Fishing around West and Central Pacific Seamounts. PLoS ONE 5: e14453. https://doi.org/10.1371/journal.pone.0014453

Morato, T., Miller, P.I., Dunn, D.C., Nicol, S.J., Bowcott, J., Halpin, P.N., 2016. A perspective on the importance of oceanic fronts in promoting aggregation of visitors to seamounts. Fish Fish. 17: 1227–1233. https://doi.org/10.1111/faf.12126

Morris, R.J., Bone, Q., Head, R., Braconnot, J.C., Nival, P., 1988. Role of salps in the flux of organic matter to the bottom of the Ligurian Sea. Mar. Biol. 97: 237–241. https://doi.org/10.1007/BF00391308

Mouriño, B., Fernández, E., Serret, P., Harbour, D., Sinha, B., Pingree, R., 2001. Variability and seasonality of physical and biological fields at the Great Meteor Tablemount (subtropical NE Atlantic). Oceanol. Acta 24: 167–185. https://doi.org/10.1016/S0399-1784(00)01138-5

Muller, M.R., Minshull, T.A., White, R.S., 2000. Crustal structure of the Southwest Indian Ridge at the Atlantis II Fracture Zone. J. Geophys. Res. Solid Earth 105: 25809–25828. https://doi.org/10.1029/2000JB900262

Mullineau, L.S., Mills, S.W., 1997. A test of the larval retention hypothesis in seamount-generated flows. Deep Sea Res. Part Oceanogr. Res. Pap. 44: 745–770. https://doi.org/10.1016/S0967-0637(96)00130-6

Munschy, C., Bodin, N., Potier, M., Héas-Moisan, K., Pollono, C., Degroote, M., West, W., Hollanda, S.J., Puech, A., Bourjea, J., Nikolic, N., 2016. Persistent Organic Pollutants in albacore tuna (*Thunnus alalunga*) from Reunion Island (Southwest Indian Ocean) and South Africa in relation to biological and trophic characteristics. Environ. Res. 148: 196–206. https://doi.org/10.1016/j.envres.2016.03.042

Musyl, M.K., Brill, R.W., Boggs, C.H., Curran, D.S., Kazama, T.K., Seki, M.P., 2003. Vertical movements of bigeye tuna (*Thunnus obesus*) associated with islands, buoys, and seamounts near the main Hawaiian Islands from archival tagging data. Fish. Oceanogr. 12: 152–169. https://doi.org/10.1046/j.1365-2419.2003.00229.x

Narayanaswamy, B.E., Rea, T., Serpetti, N., Lamont, P.A., 2017. What lies within; Annelid polychaetes found in micro-habitats of coral/carbonate material from SW Indian Ocean seamounts. Deep Sea Res. Part II Top. Stud. Oceanogr. 137: 157–165. https://doi.org/10.1016/j.dsr2.2016.06.018

Nesis, K., 1993. Cephalopods of seamounts and submarine ridges. In: Okutani, T., O'Dor, R.K., Kubodera, T. (Eds), Recent Advances in Cephalopod Fisheries Biology. Tokai University Press, Tokyo, Japan, pp. 365–374.

New, A.L., Stansfield, K., Smythe-Wright, D., Smeed, D.A., Evans, A.J., Alderson, S.G., 2005. Physical and Biochemical Aspects of the Flow across the Mascarene Plateau in the Indian Ocean. Philos. Trans. Math. Phys. Eng. Sci. 363: 151–168.

New, A.L., Alderson, S.G., Smeed, D.A., Stansfield, K.L., 2007. On the circulation of water masses across the Mascarene Plateau in the South Indian Ocean. Deep Sea Res. Part Oceanogr. Res. Pap. 54: 42–74. https://doi.org/10.1016/j.dsr.2006.08.016

Newton, K.M., DeVogelaere, A., 2013. Marine mammal and seabird abundance and distribution around the Davidson Seamount, July 2010. Monterey Bay National Marine Sanctuary Technical Report, 28 pp.

Nishikawa, J., Naganobu, M., Ichii, T., Ishii, H., Terazaki, M., Kawaguchi, K., 1995. Distribution of salps near the South Shetland Islands during austral summer, 1990-1991 with special reference to krill distribution. Polar Biol. 15: 31-39. https://doi.org/10.1007/BF00236121

Nishino, S., Itoh, M., Kawaguchi, Y., Kikuchi, T., Aoyama, M., 2011. Impact of an unusually large warm-core eddy on distributions of nutrients and phytoplankton in the southwestern Canada Basin during late summer/early fall 2010. Geophys. Res. Lett. 38: L16602. doi:10.1029/2011GL047885, 2011

Noble, M., Mullineaux, L.S., 1989. Internal tidal currents over the summit of cross seamount. Deep Sea Res. Part Oceanogr. Res. Pap. 36: 1791–1802. https://doi.org/10.1016/0198-0149(89)90112-X

Noyon, M., Morris, T., Walker, D., Huggett, J., 2018. Plankton distribution within a young cyclonic eddy off south-western Madagascar. Deep Sea Res. Part II Top. Stud. Oceanogr. In Press. https://doi.org/10.1016/j.dsr2.2018.11.001

Noyon, M., Rasoloarijao, Z., Huggett, J., Ternon, J-F., Roberts, M., 2020. Comparison of mesozooplankton communities at three shallow seamounts in the South West Indian Ocean. Deep Sea Res. II https://doi.org/10.1016/j.dsr2.2020.104759.

Nye, V., 2013. New species of hippolytid shrimps (Crustacea: Decapoda: Caridea: Hippolytidae) from a southwest Indian Ocean seamount. Zootaxa 3637(2): 101-112. https://doi.org/10.11646/zootaxa.3637.2.1

Obura, D., 2012. The Diversity and Biogeography of Western Indian Ocean Reef-Building Corals. PLoS ONE 7: e45013. https://doi.org/10.1371/journal.pone.0045013

Ockhuis, S., Huggett, J. A., Gouws, G., & Sparks, C., 2017. The 'suitcase hypothesis': Can entrainment of meroplankton by eddies provide a pathway for gene flow between Madagascar and KwaZulu-Natal, South Africa?. African J Mar. Sci. 39(4): 435-451. https://doi.org/10.2989/1814232X.2017.1399292

O'Driscoll, R., De Joux, P., Nelson, R., Macaulay, G.J., Dunford, A.J., Marriott, P.M., Stewart, C., Miller, B.S., 2012. Species identification in seamount fish aggregations using moored underwater video. ICES J Mar. Sci. 69(4): 648-659. DOI:10.1093/icesjms/fss010

Ohman, M.D., Frost, B.W., Cohen, E.B., 1983. Reverse Diel Vertical Migration: An Escape from Invertebrate Predators. Science 220(4604): 1404-1407. DOI: 10.1126/science.220.4604.1404

Oksanen, J., Blanchet, F. G., Friendly, M., Kindt, R., Legendre, P., McGlinn, D., Minchin, P. R., O'Hara, R. B., Simpson, G. L., Solymos, P., Stevens, M. H. H., Szoecs, E., Wagner, H., 2018. Package 'vegan': Community Ecology Package, R package version 2.5-1. https://CRAN.R-project.org/package=vegan

Okubo, A., 1970. Horizontal dispersion of floatable particles in the vicinity of velocity singularities such as convergences. Deep Sea Res. 17: 445–454.

Olivar, M.P., Bernal, A., Molí, B., Peña, M., Balbín, R., Castellón, A., Miquel, J., Massutí, E., 2012. Vertical distribution, diversity and assemblages of mesopelagic fishes in the western Mediterranean. Deep Sea Res. Part I 62: 53–69.

Olivar, M.P., Hulley, P.A., Castellón, A., Emelianov, M., López, C., Tuset, V.M., Contreras, T., Molí, B., 2017. Mesopelagic fishes across the tropical and equatorial Atlantic: biogeographical and vertical patterns. Progr. Oceanogr. 151: 116–137.

Olivar, M.P., Bode, A., López-Pérez, C., Hulley, P.A., Hernández-León, S., 2019. Trophic position of lanternfishes (Pisces: Myctophidae) of the tropical and equatorial Atlantic estimated using stable isotopes. ICES J Mar. Sci. DOI: 10.1093/icesjms/fsx243.

Oliver, S.P., Hussey, N.E., Turner, J.R., Beckett, A.J., 2011. Oceanic Sharks Clean at Coastal Seamount. PLoS ONE. 6: e14755. https://doi.org/10.1371/journal.pone.0014755

O'Loughlin, P.M., Mackenzie, M., VandenSpiegel, D., 2013. New sea cucumber species from the seamounts on the Southwest Indian Ocean Ridge (Echinodermata: Holothuroidea: Aspidochirotida, Elasipodida, Dendrochirotida). Mem. Mus. Vic. 70: 37–50. https://doi.org/10.24199/j.mmv.2013.70.04

Olson, R.J., Young, J.W., Ménard, F., Potier, M., Allain, V., Goñi, N., Logan, J.M., Galván-Magaña, F., 2016. Bioenergetics, Trophic Ecology and Niche Separation of Tunas. In: Advances in marine biology. Academic Press. 74: 199-344.

Oschlies, A., Garçon, V., 1998. Eddy-induced enhancement of primary production in a model of the North Atlantic Ocean. Nature 394: 266–269.

O'Shea, O.R., Kingsford, M.J., Seymour, J., 2010. Tide-related periodicity of manta rays and sharks to cleaning stations on a coral reef. Mar. Freshw. Res. 61: 65-73. https://doi.org/10.1071/MF08301

OSPAR Commission, 2004. Summary Record OSPAR 2004 (OSPAR 04/23/1 E), Annex 5: Initial OSPAR List of Threatened and/or Declining Species and Habitats (Reference Number: 2004-06). OSPAR Convention for the Protection of the Marine Environment of the North East Atlantic, p. 4.

Otake, T., Nogami, K., Maruyama, K., 1993. Dissolved and particulate organic matter as possible food sources for eel leptocephali. Mar. Ecol. Prog. Ser. 92: 27-34.

Owen, R.W., 1980. Eddies of the California Current System: Physical and ecological characteristics, in The California Islands: Proceedings of a Multidisciplinary Symposium, [Ed] D. Power, 237–263. Santa Barbara Mus. of Nat. Hist., Santa Barbara, California.

Owens, W.B., Hogg, N.G., 1980. Oceanic observations of stratified Taylor columns near a bump. Deep Sea Res. (27a): 1029-1045.

Owen, R.W., 1981. Fronts and eddies in the sea: mechanisms, interactions, and biological effects.197-233 in Longhurst, A. R., [Ed]. Analysis of marine ecosystems. Academic Press, New York.

Packmor, J., Müller, F., George, K.H., 2015. Oceanic islands and seamounts as staging posts for Copepoda Harpacticoida (Crustacea) – Shallow-water Paramesochridae Lang, 1944 from the North-East Atlantic Ocean, including the (re-)description of three species and one subspecies from the Madeiran Archipelago. Prog. Oceanogr. 131: 59–81. https://doi.org/10.1016/j.pocean.2014.11.012

Paiva, V.H., Geraldes, P., Ramírez, I., Meirinho, A., Garthe, S., Ramos, J.A., 2010. Oceanographic characteristics of areas used by Cory's shearwaters during short and long foraging trips in the North Atlantic. Mar. Biol. 157: 1385-1399. DOI: 10.1007/s00227-010-1417-5

Pakhomov, E. A., Perissinotto, R., McQuaid, C. D., 1996. Prey composition and daily rations of myctophid fishes in the Southern Ocean. Mar. Ecol. Prog. Ser. 134: 1-14.

Pakhomov, E.A., Henschke, N., Hunt, B.P.V., Stowasser, G., Cherel, Y., 2019. Utility of salps as a baseline proxy for food web studies. J. Plankton Res. 1-9. DOI: 10.1093/plankt/fby051

Pante, E., France, S.C., Gey, D., Cruaud, C., Samadi, S., 2015. An inter-ocean comparison of coral endemism on seamounts: the case of *Chrysogorgia*. J. Biogeogr. 42: 1907–1918. https://doi.org/10.1111/jbi.12564

Papiol, V., Cartes, J.E., Fanelli, E., Rumolo, P., 2013. Food web structure and seasonality of slope megafauna in the NW Mediterranean elucidated by stable isotopes: Relationship with available food sources. J Sea Res. 77: 53-69. http://dx.doi.org/10.1016/j.seares.2012.10.002

Parin, N. V., Prut'ko, V. G., 1985. Thalassal mesobenthopelagic ichthyocoenosis above the Equator Seamount in the western tropical Indian Ocean. Okeanologiya, Academy of Sciences of the USSR, 25(6): 1017-1020.

Parin, N.V., Timokhin, I.G., Novikov, N.P., Shcherbachev, Y.N., 2008. On the composition of talassobathyal ichthyofauna and commercial productivity of Mozambique Seamount (the Indian Ocean). J Ichthyol. 48(5): 361-366. https://doi.org/10.1134/S0032945208050019

Parker, T., Tunnicliffe, V., 1994. Dispersal Strategies of the Biota on an Oceanic Seamount: Implications for Ecology and Biogeography. Biol. Bull. 187: 336–345. https://doi.org/10.2307/1542290

Parry, M., 2008. Trophic variation with length in two ommastrephid squids, *Ommastrephes bartramii* and *Sthenoteuthis oualaniensis*. Mar. Biol. 153: 249-256. DOI: 10.1007/s00227-007-0800-3

Paya, I., Montecinos, M., Ojeda, V., Cid, L., 2006. An overview of the orange roughy (*Hoplostethus* sp.) fishery off Chile. In: Shotton, R. (Ed.) Deep Sea 2003: Conference on the Governance and Management of Deep-sea fisheries. Part 2: Conference poster papers and workshop papers. Queenstown, New Zealand, 1-5 December 2003 and Dunedin, New Zealand 27-29 November 2003. FAO Fisheries Proceedings No. 3/2, Rome, FAO. 487 pp.

Payne, R.P., 2015. Taxonomy and diversity of the sponge fauna from Walters Shoal, a shallow seamount in the Western Indian Ocean region. Masters Thesis. University of Western Cape. South Africa. Pp 28

Pearcy, W.G., Krygier, E.E., Mesecar, R., Ramsey, F., 1977. Vertical distribution and migration of oceanic micronekton off Oregon. Deep-Sea Res. 24: 223-245.

Pentz, B., Klenk, N., 2017. The 'responsiveness gap' in RFMOs: The critical role of decision-making policies in the fisheries management response to climate change. Ocean Coast. Manag. 145: 44–51. https://doi.org/10.1016/j.ocecoaman.2017.05.007

Pentz, B., Klenk, N., Ogle, S., Fisher, J.A.D., 2018. Can regional fisheries management organizations (RFMOs) manage resources effectively during climate change? Mar. Policy. 92: 13–20. https://doi.org/10.1016/j.marpol.2018.01.011

Perissinotto, R., A. Pakhomov, E., 1998. The trophic role of the tunicate *Salpa thompsoni* in the Antarctic marine ecosystem. J. Mar. Syst. 17: 361–374. https://doi.org/10.1016/S0924-7963(98)00049-9

Perrot, Y., Brehmer, Y., Habasque, J., Roudaut, G., Béhagle, N., Sarré, A., Lebourges-Dhaussy, A., 2018. Matecho: An open-source tool for processing fisheries acoustics data. Acoust Aust. https://doi.org/10.1007/s40857-018-0135-x

Phillips, B., Kremer, P., Madin, L.P., 2009. Defecation by *Salpa thompsoni* and its contribution to vertical flux in the Southern Ocean. Mar. Biol. 156: 455–467. https://doi.org/10.1007/s00227-008-1099-4

Pinet, P., Jaquemet, S., Phillips, R.A., Le Corre, M., 2012. Sex-specific foraging strategies throughout the breeding season in a tropical, sexually monomorphic small petrel. Anim. Behav. 83: 979–989. https://doi.org/10.1016/j.anbehav.2012.01.019

Piontkovski, S.A., Williams, R., 1995. Multiscale variability of tropical ocean zooplankton biomass. ICES J. Mar. Sci. 52: 643-656.

Pitcher, T.J., Morato, T., Hart, P.J.B., Clark, M.R., Haggan, N., Santos, R.S., 2007. Seamounts: Ecology, Fisheries & Conservation. Blackwell Publishing, UK. Pp xviii

Pitcher, T. J., Clark, M. R., Morato, T., Watson, R. 2010. Seamount fisheries: do they have a future? Oceanography 23(1): 134-144.

Poisson, F., Filmalter, J.D., Vernet, A.-L., Dagorn, L., 2014. Mortality rate of silky sharks (*Carcharhinus falciformis*) caught in the tropical tuna purse seine fishery in the Indian Ocean. Can. J. Fish. Aquat. Sci. 71: 795–798. https://doi.org/10.1139/cjfas-2013-0561

Pollard, R., Read, J., 2015. Circulation, stratification and seamounts in the Southwest Indian Ocean. Deep Sea Res Part II Top. Stud. Oceanogr. 136: 36-43. https://doi.org/10.1016/j.dsr2.2015.02.018

Pollard, R., Read, J., 2017. Circulation, stratification and seamounts in the Southwest Indian Ocean. Deep Sea Res. Part II Top. Stud. Oceanogr. 136: 36-43. https://doi.org/10.1016/j.dsr2.2015.02.018

Pollock, D.E., Cockcroft, A.C., Groeneveld, J.C., Schoeman, D.S., 2000. The Commercial Fisheries for *Jasus* and *Palinurus* Species in the South-east Atlantic and South-west Indian Oceans. In: Phillips, B., Kittaka, J. (Eds), Spiny lobsters: fisheries and culture. John Wiley & Sons, pp. 105-120.

Polunin, N.V.C., Morales-Nin, B., Pawsey, W.E., Cartes, J.E., Pinnegar, J.K., Moranta, J., 2001. Feeding relationships in Mediterranean bathyal assemblages elucidated by stable nitrogen and carbon isotope data. Mar. Ecol. Prog. Ser. 220: 13-23.

Pomeroy, L.R., 2001. Caught in the food web: complexity made simple? Sci. Mar. 65 (Suppl. 2): 31-40.

Popova, E., Vousden, D., Sauer, W.H.H., Mohammed, E.Y., Allain, V., Downey-Breedt, N., Fletcher, R., Gjerde, K.M., Halpin, P.N., Kelly, S., Obura, D., Pecl, G., Roberts, M., Raitsos, D.E., Rogers, A., Samoilys, M., Sumaila, U.R., Tracey, S., Yool, A., 2019. Ecological connectivity between the areas beyond national jurisdiction and coastal waters: Safeguarding interests of coastal communities in developing countries. Mar. Policy 104: 90–102. https://doi.org/10.1016/j.marpol.2019.02.050

Portail, M., Olu, K., Dubois, S.F., Escobar-Briones, E., Gelinas, Y., Menot, L, Sarrazin, J., 2016. Food-Web Complexity in Guaymas Basin Hydrothermal Vents and Cold Seeps. PLoS ONE. 11(9): e0162263. DOI: 10.1371/journal.pone.0162263

Porteiro, F.M., and Sutton, T., 2007. Midwater Fish Assemblages and Seamounts. In: Pitcher, T.J., Morato, T., Hart, P.J.B., Clark, M.R., Haggan, N., Santos, R.S. (Eds), Seamounts: Ecology, Fisheries & Conservation. Blackwell Publishing Ltd, Oxford, UK, pp. 101–116. https://doi.org/10.1002/9780470691953.ch6

Post, D.M., Pace, M.L., Hairston, N.G.J., 2000. Ecosystem size determines food chain length in lakes. Nature. 405: 1047-1049.

Post, D.M., 2002. Using stable isotopes to estimate trophic position: models, methods, and assumptions. Ecology 83(3): 703-718.

Potier, M., Marsac, F., Lucas, V., Sabatié, R., Hallier, J-P., Menard, F., 2004. Feeding partitioning among tuna taken in surface and mid-water layers: The Case of Yellowfin (*Thunnus albacares*) and Bigeye (*T. obesus*) in the western tropical Indian Ocean. Western Indian Ocean J. Mar. Sci. 3(1): 51-62.

Potier, M., Marsac, F., Cherel, Y., Lucas, V., Sabatié, R., Maury, O., Ménard, F., 2007. Forage fauna in the diet of three large pelagic fishes (lancetfish, swordfish and yellowfin tuna) in the western equatorial Indian Ocean. Fish. Res. 83: 60–72. https://doi.org/10.1016/j.fishres.2006.08.020

Potier, M., Romanov, E., Cherel, Y., Sabatié, R., Zamorov, V., Ménard, F., 2008. Spatial distribution of *Cubiceps pauciradiatus* (Perciformes: Nomeidae) in the tropical Indian Ocean and its importance in the diet of large pelagic fishes. Aquat. Living Resour. 21: 123–134. https://doi.org/10.1051/alr:2008026

Potier, M., Bach, P., Ménard, F., Marsac, F., 2014. Influence of mesoscale features on micronekton and large pelagic fish communities in the Mozambique Channel. Deep Sea Res. Part II Top. Stud. Oceanogr. 100: 184–199. https://doi.org/10.1016/j.dsr2.2013.10.026

Poulet, S.A., 1983. Factors controlling utilization of non-algal diets by particle-grazing copepods. A review. Oceanol. Acta 6(3): 221-234.

Pous, S., Lazure, P., André, G., Dumas, F., Halo, I., Penven, P., 2014. Circulation around La Réunion and Mauritius islands in the south-western Indian Ocean: A modeling perspective. J. Geophys. Res. Oceans 119: 1957–1976. https://doi.org/10.1002/2013JC009704

Pratt, N., Chen, T., Li, T., Wilson, D.J., van de Flierdt, T., Little, S.H., Taylor, M.L., Robinson, L.F., Rogers, A.D., Santodomingo, N., 2019. Temporal distribution and diversity of cold-water corals in the southwest Indian Ocean over the past 25,000 years. Deep Sea Res. Part Oceanogr. Res. Pap. 149: 103049. https://doi.org/10.1016/j.dsr.2019.05.009

Preciado, I., Cartes, J.E., Punzón, A., Frutos, I., López-López, L., Serrano, A., 2017. Food web functioning of the benthopelagic community in a deep-sea seamount based on diet and stable isotope analyses. Deep Sea Res. Part II Top. Stud. Oceanogr. 137: 56–68. https://doi.org/10.1016/j.dsr2.2016.07.013

Pripp, T., Gammelsrød, T., Krakstad, J.O., 2014. Physical influence on biological production along the western shelf of Madagascar. Deep Sea Res. Part II Top. Stud. Oceanogr. 100: 174-183. http://dx.doi.org/10.1016/j.dsr2.2013.10.025

Probert, P.K., 1999. Seamounts, sanctuaries and sustainability: moving towards deep-sea conservation. Aquat. Conserv. Mar. Freshw. Ecosyst. 9: 601–605.

Probert, P.K., Christiansen, S., Gjerde, K.M., Gubbay, S., Santos, R.S., 2007. Management and conservation of seamounts. In: Pitcher, T.J., Morato, T., Hart, P.J.B., Clark, M.R., Haggan, N., Santos, R.S. (Eds), Seamounts: Ecology, Fisheries & Conservation. Blackwell Publishing Ltd, Oxford, UK, pp. 442-475.

Proud, R., Cox, M. J., Brierley, A. S., 2017. Biogeography of the global ocean's mesopelagic zone. Current Biology. 27: 113-119. http://dx.doi.org/10.1016/j.cub.2016.11.003

Proud, R., Handegard, N. O., Kloser, R. J., Cox, M. J., Brierley, A. S., 2018. From siphonophores to deep scattering layers: uncertainty ranges for the estimation of global mesopelagic fish biomass. ICES J. Mar. Sci. fsy037. https://doi.org/10.1093/icesjms/fsy037

Pusch, C., Beckmann, A., Porteiro, F.M., 2004. The influence of seamounts on mesopelagic fish communities*). Arch. Fish. Mar. Res. 51(1-3): 165-186.

Quartly, G.D., Srokosz, M.A., 2004. Eddies in the southern Mozambique Channel. Deep Sea Res. Part II Top. Stud. Oceanogr. 51: 69–83. https://doi.org/10.1016/j.dsr2.2003.03.001

Quartly, G.D., Buck, J.J.H., Srokosz, M.A., 2005. Eddy variability east of Madagascar. Philos. Trans. R. Soc. Math. Phys. Eng. Sci. 363: 77–79. https://doi.org/10.1098/rsta.2004.1479

Quartly, G.D., Buck, J.J.H., Srokosz, M.A., Coward, A.C., 2006. Eddies around Madagascar-The retroflection re-considered. J. Mar. Sys. 63: 115-129. DOI:10.1016/j.jmarsys.2006.06.001

Rabehagasoa, N., Lorrain, A., Bach, P., Potier, M., Jaquemet, S., Richard, P., Ménard, F., 2012. Isotopic niches of the blue shark *Prionace glauca* and the silky shark *Carcharhinus falciformis* in the southwestern Indian Ocean. Endanger. Species Res. 17: 83–92. https://doi.org/10.3354/esr00418

Raj, R.P., Peter, B.N., Pushpadas, D., 2010. Oceanic and atmospheric influences on the variability of phytoplankton bloom in the Southwestern Indian Ocean. J. Mar. Syst. 82: 217–229. https://doi.org/10.1016/j.jmarsys.2010.05.009

Ramanantsoa, J. D., Krug, M., Penven, P., Rouault, M., Gula, J., 2018. Coastal upwelling south of Madagascar: Temporal and spatial variability. J. Mar. Syst. 178: 29-37. http://dx.doi.org/10.1016/j.jmarsys.2017.10.005

Rao, T.S.S., 1973. Zooplankton Studies in the Indian Ocean. In: Zeitzschel, B., Gerlach S.A., (Eds), The Biology of the Indian Ocean. Ecological Studies (Analysis and Synthesis). vol 3. Springer, Berlin, Heidelberg. https://doi.org/10.1007/978-3-642-65468-8_19

Read, J., Pollard, R., 2017. An introduction to the physical oceanography of six seamounts in the southwest Indian Ocean. Deep Sea Res. Part II Top. Stud. Oceanogr. 136: 44–58. https://doi.org/10.1016/j.dsr2.2015.06.022

Reid, S.B., Hirota, J., Young, R.E., Hallacher, L.E., 1991. Mesopelagic-boundary community in Hawaii: micronekton at the interface between neritic and oceanic ecosystems. Mar. Biol. 109: 427-440.

Ressurreição, A., Giacomello, E., 2013. Quantifying the direct use value of Condor seamount. Deep Sea Res. Part II Top. Stud. Oceanogr. 98: 209–217. https://doi.org/10.1016/j.dsr2.2013.08.005

Reygondeau, G., Maury, O., Beaugrand, G., Fromentin, J.M., Fonteneau, A., Cury, P., 2012. Biogeography of tuna and billfish communities. J. Biogeogr. 39: 114–129. https://doi.org/10.1111/j.1365-2699.2011.02582.x

Reygondeau, G., Longhurst, A., Martinez, E., Beaugrand, G., Antoine, D., and Maury, O., 2013. Dynamic biogeochemical provinces in the global ocean. Global Biogeochem. Cy. 27(4): 1046-1058. http://doi.org/10.1002/gbc.20089

Richardson, P. L., D. Walsh, L. Armi, M. Schroder, and J. F. Price, 1989: Tracking three meddies with SOFAR floats. J. Phys. Oceanogr. 19: 371-383.

Richardson, P.L., Bower, A.S., Zenk, W., 2000. A census of Meddies tracked by floats. Prog. Oceanogr. 45: 209-250.

Richert, J.E., Jorgensen, S.J., Ketchum, J.T., Mohajerani, L., Klimley, P.A., 2017. The importance of pinnacles and seamounts to pelagic fishes and fisheries off the Southern Baja California Peninsula. Oceanography & Fisheries. 4(2). DOI: 10.19080/OFOAJ.2017.04.555634

Riley, G.A., 1971. Particulate organic matter in sea water. Ad. Mar. Biol. 8: 1-118. https://doi.org/10.1016/S0065-2881(08)60491-5

Roberts, K.E., Valkan, R.S., Cook, C.N., 2018. Measuring progress in marine protection: A new set of metrics to evaluate the strength of marine protected area networks. Biol. Conserv. 219: 20–27. https://doi.org/10.1016/j.biocon.2018.01.004

Robison, B.H., 1984. Herbivory by the myctophid fish *Ceratoscopelus warmingii*. Mar. Biol. 84: 119-123.

Rochman, C.M., Lewison, R.L., Eriksen, M., Allen, H., Cook, A-M., Teh, S.J., 2014. Polybrominated diphenyl ethers (PBDEs) in fish tissue may be an indicator of plastic contamination in marine habitats. Sci Total Environ. 476-477: 622-633. http://dx.doi.org/10.1016/j.scitotenv.2014.01.058

Rocke, E., Noyon, M., Ternon, J-F., Roberts, M., 2020. Pico- and nanoplankton composition on a seamount, south of Madagascar, using flow cytometry. Deep-Sea Res. II. https://doi.org/10.1016/j.dsr2.2020.104744

Roger, C., 1994. The plankton of the tropical western Indian ocean as a biomass indirectly supporting surface tunas (yellowfin, *Thunnus albacares* and skipjack, *Katsuwonus pelamis*). Environ. Biol. Fishes 39: 161–172. https://doi.org/10.1007/BF00004934

Rogers, A.D., 1994. The Biology of Seamounts, In: Advances in Marine Biology. Elsevier, pp. 305–350. https://doi.org/10.1016/S0065-2881(08)60065-6

Rogers, E.A.D., Taylor, M.L., 2011. Benthic biodiversity of seamounts in the southwest Indian Ocean. Cruise Report- R/V James Cook 066. Southwest Indian Ocean Seamounts expedition.

Rogers, A.D., Bemanaja, O.A.E., Benivary, D., Boersch-Supan, P., Bornman, T.G., Cedras, R., Du Plessis, N., Gotheil, S., Høines, A., Kemp, K., Kristiansen, J., Letessier, T., Mangar, V., Mazungula, N., Mørk, T., Pinet, P, Pollard, R., Read, J., Sonnekus, T., 2017. Pelagic communities of the South West Indian Ocean seamounts: R/V Dr *Fridtjof* Nansen Cruise 2009-410. Deep Sea Res. Part II Top. Stud. Oceanogr. 136: 5-35. https://doi.org/10.1016/j.dsr2.2016.12.010

Romanov, E.V., 2003. Summary and review of Soviet and Ukrainian scientific and commercial fishing operations on the deepwater ridges of the southern Indian Ocean. FAO Fisheries Circular. No. 991. Rome, FAO. 84p.

Romero-Romero, S., Choy, C.A., Hannides, C.C.S., Popp, B.N., Drazen, J.C., 2019. Differences in the trophic ecology of micronekton driven by diel vertical migration. Limnol. Oceanogr. 64: 1473-1483. DOI: 10.1002/lno.11128

Roper, C.F.E., Sweeney, M.J., Nauen, C.E., 1984. FAO Species Catalogue: Cephalopods of the world, An annotated and illustrated catalogue of species of interest to fisheries. 3: 1-277.

Rowden, A.A., Dower, J.F., Schlacher, T.A., Consalvey, M., Clark, M.R., 2010a. Paradigms in seamount ecology: fact, fiction and future. Mar. Ecol. 31: 226–241. https://doi.org/10.1111/j.1439-0485.2010.00400.x

Rowden, A.A., Schlacher, T.A., Williams, A., Clark, M.R., Stewart, R., Althaus, F., Bowden, D.A., Consalvey, M., Robinson, W., Dowdney, J., 2010b. A test of the seamount oasis hypothesis: seamounts support higher epibenthic megafaunal biomass than adjacent slopes. Mar. Ecol. 31: 95–106. https://doi.org/10.1111/j.1439-0485.2010.00369.x

Royer, T.C., 1978. Ocean Eddies Generated by Seamounts in the North Pacific. Science 199: 1063–1064. https://doi.org/10.1126/science.199.4333.1063-a

Rubenstein, D.R., Hobson, K.A., 2004. From birds to butterflies: animal movement patterns and stable isotopes. Trends in Ecology and Evolution 19(5): 256-263.

Ryan, C., McHugh, B., Trueman, C.N., Harrod, C., Berrow, S., O'Connor, I., 2012. Accounting for the effects of lipids in stable isotope ($\delta^{13}C$ and $\delta^{15}N$ values) analysis of skin and blubber of balaenopterid whales. Rapid Commun. Mass Spectrom. 26: 2745-2754. DOI: 10.1002/rcm.6394

Ryan, T.E., Downie, R.A., Kloser, R.J., Keith, G., 2015. Reducing bias due to noise and attenuation in open-ocean echo integration data. ICES J. Mar. Sci. 72(8): 2482-2493. doi:10.1093/icesjms/fsv121

Sabarros, P.S., Ménard, F., Lévénez, J-J., Tew-Kai, E., Ternon, J-F., 2009. Mesoscale eddies influence distribution and aggregation patterns of micronekton in the Mozambique Channel. Mar. Ecol. Prog. Ser. 395: 101-107. DOI: 10.3354/meps08087

Sabarros, P.S., Romanov, E., Dagorne, D., Foulgoc, L.L., Ternon, J.-F., Bach, P., 2014. Environmental drivers of swordfish local abundance in the south-west Indian Ocean. IOTC-2014-WPB12-15.

Saino, T., Hattori, A., 1987. Geographical variation of the water column distribution of suspended particulate organic nitrogen and its ^{15}N natural abundance in the Pacific and its marginal seas. Deep-Sea Res. 34(5/6): 807-827.

Salm, R.V., 1983. Coral Reefs of the Western Indian Ocean: A Threatened Heritage. Ambio. 12(6): 349-353.

Saltzman, J., Wishner, K.F., 1997. Zooplankton ecology in the eastern tropical Pacific oxygen minimum zone above a seamount: 1. General trends. Deep Sea Res. Part Oceanogr. Res. Pap. 44: 907–930. https://doi.org/10.1016/S0967-0637(97)00007-1

Samadi, S., Bottan, L., Macpherson, E., De Forges, B.R., Boisselier, M.-C., 2006. Seamount endemism questioned by the geographic distribution and population genetic structure of marine invertebrates. Mar. Biol. 149: 1463–1475. https://doi.org/10.1007/s00227-006-0306-4

Santos, M.A., Bolten, A.B., Martins, H.R., Riewald, B., Bjorndal, K.A., 2007. Air-breathing visitors to seamounts: Section B, Sea turtles. In: Pitcher, T.J., Morato, T., Hart, P.J.B., Clark, M.R., Haggan, N., Santos, R.S. (Eds), Seamounts: Ecology, Fisheries & Conservation. Blackwell Publishing Ltd, Oxford, UK, pp. 239-244.

Santos, R.S., Christiansen, S., Christiansen, B., Gubbay, S., 2009. Toward the conservation and management of Sedlo Seamount: A case study. Deep Sea Res. Part II Top. Stud. Oceanogr. 56: 2720-2730. DOI:10.1016/j.dsr2.2008.12.031

Sardenne, F., Bodin, N., Chassot, E., Amiel, A., Fouché, E., Degroote, M., Hollanda, S., Pethybridge, H., Lebreton, B., Guillou, G., Ménard, F., 2016. Trophic niches of sympatric tropical tuna in the Western Indian Ocean inferred by stable isotopes and neutral fatty acids. Prog. Oceanogr. 146: 75–88. https://doi.org/10.1016/j.pocean.2016.06.001

Sautya, S., Ingole, B., Ray, D., Stöhr, S., Samudrala, K., Raju, K.A.K., Mudholkar, A., 2011. Megafaunal Community Structure of Andaman Seamounts Including the Back-Arc Basin – A Quantitative Exploration from the Indian Ocean. PLoS ONE 6: e16162. https://doi.org/10.1371/journal.pone.0016162

Schlich, R., 1974. Initial Reports of the Deep Sea Drilling Project, 25. U.S. Government Printing Office. https://doi.org/10.2973/dsdp.proc.25.1974

Schlitzer, R., 2013. Ocean Data View, http://odv.awi.de

Schouten, M.W., De Ruijter, W.P.M., van Leeuwen, P.J., Lutjeharms, J.R.E., 2000. Translation, decay and splitting of Agulhas rings in the southeastern Atlantic Ocean. J. Geophys. Res. Oceans 105: 21913–21925. https://doi.org/10.1029/1999JC000046

Schouten, M.W., De Ruijter, W.P.M., Van Leeuwen, P.J., Ridderinkhof, H., 2003. Eddies and variability in the Mozambique Channel. Deep Sea Res. Part II Top. Stud. Oceanogr. 50(12-13):1987–2003. https://doi.org/10.1016/S0967-0645(03)00042-0

Schultz-Tokos, K.L., Hinrichsen, H-H., Zenk, W., 1994. Merging and Migration of two Meddies. J. Phys. Oceanogr. 24: 2129-2141.

Sedberry, G., Loefer, J., 2001. Satellite telemetry tracking of swordfish, *Xiphias gladius*, off the eastern United States. Mar. Biol. 139: 355–360. https://doi.org/10.1007/s002270100593

Seki, M.P., Somerton, D.A., 1994. Feeding ecology and daily ration of the pelagic armorhead, *Pseudopentaceros wheeleri*, at Southeast Hancock Seamount. Environ. Biol. Fishes 39: 73–84. https://doi.org/10.1007/BF00004758

Sequeira, A., Mellin, C., Rowat, D., Meekan, M.G., Bradshaw, C.J.A., 2012. Ocean-scale prediction of whale shark distribution. Divers. Distrib. 18: 504–518. https://doi.org/10.1111/j.1472-4642.2011.00853.x

Shapiro, G.I., Meschanov, S.L., Emelianov, M.V., 1995. Mediterranean lens "Irving" after its collision with seamounts. Oceanol. Acta 18(3): 309-318.

Sholto-Douglas, A.D., Field, J.G., James, A.G., van der Merwe, N.J., 1991. $^{13}C/^{12}C$ and $^{15}N/^{14}N$ isotope ratios in the Southern Benguela Ecosystem: indicators of food web relationships among different size-classes of plankton and pelagic fish; differences between fish muscle and bone collagen tissues. Mar. Ecol. Prog. Ser. 78: 23-31.

Shotton, R., 2006. Managment of Demersal Fisheries Resources of the Southern Indian Ocean. FAO Fisheries Circular No. 1020. FAO, Rome, Italy, 90.

Sibert, J., Holland, K., Itano, D., 2000. Exchange rates of yellowfin and bigeye tunas and fishery interaction between Cross seamount and near-shore FADs in Hawaii. Aquat. Living Resour. 13:225-232.

Simmonds, J., MacLennan, D., 2005. Fisheries Acoustics: theory and practice. 2nd Edition. Blackwell Science, Oxford, UK. 437 pp.

Singh, A., Gandhi, N., Ramesh, R., Prakash, S., 2015. Role of cyclonic eddy in enhancing primary and new production in the Bay of Bengal. J. Sea Res. 97: 5–13. https://doi.org/10.1016/j.seares.2014.12.002

Sinha, M.C., Louden, K.E., Parsons, B., 1981. The crustal structure of the Madagascar Ridge. Geophys. J. Int. 66: 351–377. https://doi.org/10.1111/j.1365-246X.1981.tb05960.x

Smale, M.J., Cliff, G., 1998. Cephalopods in the diets of four shark species (*Galeocerdo cuvier*, *Sphyrna lewini*, *S. zygaena* and *S. mokarran*) from KwaZulu-Natal, South Africa. South Afr. J. Mar. Sci. 20: 241–253. https://doi.org/10.2989/025776198784126610

Smith, M.M., Heemstra, P.C., 1986. Smith's Sea Fishes. J.L.B. Smith Institute of Ichthyology, Grahamstown, South Africa. 1047 p.

Sobrinho-Gonçalves, L., Cardigos, F., 2006. Fish Larvae Around A Seamount With Shallow Hydrothermal Vents From The Azores. Thalassas–An International Journal of Marine Sciences 22(1): 19-28.

Sonnekus, M.J., Bornman, T.G., Campbell, E.E., 2017. Phytoplankton and nutrient dynamics of six South West Indian Ocean seamounts. Deep Sea Res. Part II Top. Stud. Oceanogr. 136: 59–72. https://doi.org/10.1016/j.dsr2.2016.12.008

Soto, R.M.B., 2010. Acoustic study of macrozooplankton off Peru: biomass estimation, spatial patterns, impact of physical forcing and effect on forage fish distribution. PhD Thesis, Université Montpellier II, France.

Stéquert, B., Marsac, F., 1989. Tropical tuna: surface fisheries in the Indian Ocean. FAO Fisheries Technical Paper, No. 282. Rome, FAO. 238p.

St John, M.A., Borja, A., Chust, G., Heath, M., Grigorov, I., Martin, A.P., Santos, S., Mariani, P., 2016. A dark hole in our understanding of marine ecosystems and their services: Perspectives from the mesopelagic community. Front. Mar. Sci. 3:31. DOI:10.3389/fmars.2016.00031

Stahl, J-C., Bartle, J.A., 1991. Distribution, abundance and aspects of the pelagic ecology of Barau's petrel (*Pterodroma baraui*) in the south-west Indian Ocean. Notornis. 38: 211-225.

Starr, R.M., Throne, R.E., 1998. Acoustic assessment of squid stocks. FAO Fisheries Technical Paper, 181-198.

Stillwell, C., Kohler, N., 1985. Food and feeding ecology of the swordfish *Xiphias gladius* in the western North Atlantic Ocean with estimates of daily ration. Mar. Ecol. Prog. Ser. 22: 239–247. https://doi.org/10.3354/meps022239

Stocks, K.I., Hart, P.J.B., 2007. Synoptic views of seamounts: Biogeography and biodiversity of seamounts. In: Pitcher, T.J., Morato, T., Hart, P.J.B., Clark, M.R., Haggan, N., Santos, R.S. (Eds), Seamounts: Ecology, Fisheries & Conservation. Blackwell Publishing Ltd, Oxford, UK, pp. 255-281.

Sutton, T.T., Porteiro, F.M., Horne, J.K., Anderson, C.I.H., 2010. Meso- and bathypelagic fish interactions with seamounts and mid-ocean ridges. Proceedings of an International Symposium: Into the Unknown, Researching Mysterious Deep-sea Animals. Japan

Sutton T., T., 2013. Vertical ecology of the pelagic ocean: classical patterns and new perspectives. J. Fish. Biol. 83, 1508–1527. https://doi.org/10.1111/jfb.12263.

Sutyrin, G. G., 2006. Critical effects of a tall seamount on a drifting vortex. J. Mar. Res. 64(2): 297-317. https://doi.org/10.1357/002224006777606489

Swart, N. C., Lutjeharms, J. R. E., Ridderinkhof, H., De Ruijter, W. P. M., 2010. Observed characteristics of Mozambique Channel eddies. J. Geophys. Res. 115: C09006/1-C09006/14. https://doi.org/10.1029/2009JC005875

Tanaka, H., Ohshimo, S., Sassa, C., Aoki, I., 2007. Feeding habits of mesopelagic fishes off the coast of western Kyushu, Japan. PICES 16th: Bio, p-4200. 1st November.

Taquet, C., Taquet, M., Dempster, T., Soria, M., Ciccione, S., Roos, D., Dagorn, L., 2006. Foraging of the green sea turtle *Chelonia mydas* on seagrass beds at Mayotte Island (Indian Ocean), determined by acoustic transmitters. Mar. Ecol. Prog. Ser. 306: 295–302. https://doi.org/10.3354/meps306295

Taranto, G.H., Kvile, K.Ø., Pitcher, T.J., Morato, T., 2012. An Ecosystem Evaluation Framework for Global Seamount Conservation and Management. PLoS ONE 7: e42950. https://doi.org/10.1371/journal.pone.0042950

Tew-Kai, E., Marsac, F., 2009. Patterns of variability of sea surface chlorophyll in the Mozambique Channel: a quantitative approach. J. Mar. Syst. 77 (1-2): 77-88. DOI: 10.1016/j.jmarsys.2008.11.007

Tew-Kai, E., Marsac, F., 2010. Influence of mesoscale eddies on spatial structuring of top predators' communities in the Mozambique Channel. Prog. Oceanogr. 86: 214-223. doi:10.1016/j.pocean.2010.04.010

Thomalla, S.J., Waldron, H.N., Lucas, M.I., Read, J.F., Ansorge, I.J., Pakhomov, E., 2011. Phytoplankton distribution and nitrogen dynamics in the southwest Indian subtropical gyre and Southern Ocean waters. Ocean Sci. 7: 113–127. https://doi.org/10.5194/os-7-113-2011

Thompson, P.A., Pesant, S., Waite, A.M., 2007. Contrasting the vertical differences in the phytoplankton biology of a dipole pair of eddies in the south-eastern Indian Ocean. Deep Sea Res. Part II Top. Stud. Oceanogr. 54: 1003–1028. https://doi.org/10.1016/j.dsr2.2006.12.009

Tingii, U., 2008. Selenium: its role as antioxidant in human health. Environ. Health Prev. Med. 13: 102-108. DOI: 10.1007/s12199-007-0019-4

Tittensor, D.P., Baco, A.R., Brewin, P.E., Clark, M.R., Consalvey, M., Hall-Spencer, J., Rowden, A.A., Schlacher, T., Stocks, K.I., Rogers, A.D., 2009. Predicting global habitat suitability for stony corals on seamounts. J. Biogeogr. 36: 1111–1128. https://doi.org/10.1111/j.1365-2699.2008.02062.x

Tittensor, D.P., Baco, A.R., Hall-Spencer, J.M., Orr, J.C., Rogers, A.D., 2010. Seamounts as refugia from ocean acidification for cold-water stony corals. Mar. Ecol. 31: 212–225. https://doi.org/10.1111/j.1439-0485.2010.00393.x

Tomczak, M., Godfrey, J.S., 2001. Water mass formation, subduction, and the oceanic heat budget. In: Regional Oceanography: an introduction. Elsevier. pp 51-61.

Toole, J.M., Schmitt, R.W., Polzin, K.L., Kunze, E., 1997. Near-boundary mixing above the flanks of a midlatitude seamount. J. Geophys. Res. Oceans 102: 947–959. https://doi.org/10.1029/96JC03160

Torgersen, T., Kaartvedt, S., 2001. *In situ* swimming behaviour of individual mesopelagic fish studied by split-beam echo target tracking. ICES J. Mar. Sci. 58: 346-354. doi:10.1006/jmsc.2000.1016

Torres, C.R., Mascarenhas, A.S., Castillo, J.E., 2004. Three-dimensional stratified flow over Alarcón Seamount, Gulf of California entrance. Deep Sea Res. Part II Top. Stud. Oceanogr. 51: 647–657. https://doi.org/10.1016/j.dsr2.2004.05.012

Tracey, D. M., Clark, M. R., Anderson, O. F., Kim, S. W., 2012. Deep-sea fish distribution varies between seamounts: Results from a seamount complex off New Zealand. PLOS One 7(6). https://doi.org/10.1371/journal.pone.0036897

Tree, A.J., 2005. The known history and movements of the Roseate tern *Sterna dougallii* in South Africa and the western Indian Ocean. Marine Ornithology 33: 41-47.

Trenkel, V.M., Berger, L., Bourguignon, S., Doray, M., Fablet, R., Massé, J., Mazauric, V., Poncelet, C., Quemener, G., Scalabrin, C., Villalobos, H., 2009. Overview of recent progress in fisheries acoustics made by Ifremer with examples from the Bay of Biscay. Aquat. Living Resour. 22: 433-445. DOI: 10.1051/alr/2009027

Trudelle, L., 2019. Baleines à bosse de l'Hemisphere sud on fait le point! Etudier les déplacements des baleines à bosse dans leurs zones de reproduction. [Online] https://baleinesabosseenenzonedereproduction.blogspot.com/2019/03/baleines-bosse-de-lhemisphere-sud on.html?fbclid=IwAR0bkVWhdOH0wlEd81uZQzqNsPYwsEncaA8ujPOq3jdO9m1BbKgxpPO7bik. Accessed on 02/08/2019.

Turner, J., Klaus, R., 2005. Coral reefs of the Mascarenes, Western Indian Ocean. Philos. Trans. R. Soc. Math. Phys. Eng. Sci. 363: 229–250. https://doi.org/10.1098/rsta.2004.1489

Turnewitsch, R., Reyss, J.-L., Chapman, D.C., Thomson, J., Lampitt, R.S., 2004. Evidence for a sedimentary fingerprint of an asymmetric flow field surrounding a short seamount. Earth Planet. Sci. Lett. 222: 1023–1036. https://doi.org/10.1016/j.epsl.2004.03.042

Turnewitsch, R., Dumont, M., Kiriakoulakis, K., Legg, S., Mohn, C., Peine, F., Wolff, G., 2016. Tidal influence on particulate organic carbon export fluxes around a tall seamount. Prog. Oceanogr. 149: 189–213. https://doi.org/10.1016/j.pocean.2016.10.009

UNEP, 2006. Seamounts, deep-sea corals and fisheries: vulnerability of deep-sea corals to fishing on seamounts beyond areas of national jurisdiction World Conservation Monitoring Centre, & Census of Marine Life on Seamounts (Programme). Data Analysis Working Group. (No. 183). UNEP/Earthprint.

Utrecht, W.L., van Utrecht-Cock, C.N., De Graaf, A.M.J., 1987. Growth and seasonal variations in distribution of *Chauliodus sloani* and *C. danae* (pisces) from the mid north atlantic. Bijdragen tot de Dierkunde. 57(2): 164-182.

Valinassab, T., Pierce, G.J., Johannesson, K., 2007. Lantern fish (*Benthosema pterotum*) resources as a target for commercial exploitation in the Oman Sea. J. Appl. Ichthyol. 23: 573–577. https://doi.org/10.1111/j.1439-0426.2007.01034.x

Valls, M., Sweeting, C.J., Olivar, M.P., Fernández de Puelles, M.L., Pasqual, C., Polunin, N.V.C., Quetglas, A., 2014a. Structure and dynamics of food webs in the water column on shelf and slope grounds of the western Mediterranean. J Mar. Syst. 138: 171: 181. http://dx.doi.org/10.1016/j.jmarsys.2014.04.002

Valls, M., Olivar, M.P., Fernández de Puelles, M.L., Molí, B., Bernal, A., Sweeting, C.J., 2014b. Trophic structure of mesopelagic fishes in the western Mediterranean based on stable isotopes of carbon and nitrogen. J Mar. Syst. 138: 160-170. http://dx.doi.org/10.1016/j.jmarsys.2014.04.007

van der Elst, R.P., Groeneveld, J.C., Baloi, A.P., Marsac, F., Katonda, K.I., Ruwa, R.K., Lane, W.L., 2009. Nine nations, one ocean: A benchmark appraisal of the South Western Indian Ocean Fisheries Project (2008–2012). Ocean Coast. Manag. 52: 258–267. https://doi.org/10.1016/j.ocecoaman.2009.02.003

van der Elst, R.P., Everett, B.I., 2015. (Eds), Offshore Fisheries of the SouthWest Indian Ocean: their status and the impact on vulnerable species. Oceanographic Research Institute, Special Publication, 10: 448pp.

van der Spoel, S., Bleeker, J., 1991. Distribution of Myctophidae (Pisces, Myctophiformes) during the four seasons in the mid North Atlantic. Contributions to Zoology 61(2): 89-106.

van Geffen, J.H.G.M., Davies, P.A., 1999. Interaction of a monopolar vortex with a topographic ridge. Geophys. Astrophys. Fluid Dynamics. 90:1-41.

van Geffen, J.H.G.M., Davies, P.A., 2000a. A monopolar vortex encounters an isolated topographic feature on a β-plane. Dynam. Atmos. Ocean. 32: 1-26.

van Geffen, J.H.G.M., Davies, P.A., 2000b. A monopolar vortex encounters a north–south ridge or trough. Fluid Dyn. Res. 26: 157–179. https://doi.org/10.1016/S0169-5983(99)00022-2

Vanderklift, M.A., Ponsard, S., 2003. Sources of variation in consumer-diet $\delta^{15}N$ enrichment: a meta-analysis. Oecologia 136(2): 169-182.

Vassallo, P., Paoli, C., Alessi, J., Mandich, A., Würtz, M., Fiori, C., 2018. Seamounts as hotspots of large pelagic aggregations. Mediterranean Marine Science 19(3): 444-458. DOI: http://dx.doi.org/10.12681/mms.15546

Ventura, M., Catalan, J., 2008. Incorporating life histories and diet quality in stable isotope interpretations of crustacean zooplankton. Freshwater Biol. 53: 1453-1469. DOI: 10.1111/j.1365-2427.2008.01976.x

Vereshchaka, A.L., 1995. Macroplankton in the near-bottom layer of continental slopes and seamounts. Deep Sea Res. Part Oceanogr. Res. Pap. 42: 1639–1668. https://doi.org/10.1016/0967-0637(95)00065-E

Vianello, P., Herbette, S., Ternon, J-F., Demarcq, H., Roberts, M., 2020. Circulation and hydrography in the vicinity of a shallow seamount on the northern Madagascar Ridge. Deep Sea Res. II.

Vilas, J.C., Arístegui, J., Kiriakoulakis, K., Wolff, G.A., Espino, M., Polo, I., Montero, M.F., Mendonça, A., 2009. Seamounts and organic matter—Is there an effect? The case of Sedlo and Seine Seamounts: Part 1. Distributions of dissolved and particulate organic matter. Deep Sea Res. Part II Top. Stud. Oceanogr. 56: 2618–2630. https://doi.org/10.1016/j.dsr2.2008.12.023

Villani, N., Alessi, J., Roccatagliata, N., Fiori, C., 2014. Tyrrhenian seamounts influence on pelagic visitors: cetaceans, seabirds, sea turtles and pelagic fishes. 28th Annual Conference of the European Cetacean Society, Belgium. 5-9 April 2014.

Vipin, P.M., Harikrishnan, M., Renju, R., Boopendranath, M.R., Remesan, M.P., 2018. Population Dynamics of Spinycheek Lanternfish *Benthosema fibulatum* (Gilbert and Cramer 1897), Caught off the South- west Coast of India. Asian Fisheries Science 31: 161-171.

Viricel, A., Simon-Bouhet, B., Ceyrac, L., Dulau-Drouot, V., Berggren, P., Amir, O.A., Jiddawi, N.S., Mongin, P., Kiszka, J.J., 2016. Habitat availability and geographic isolation as potential drivers of population structure in an oceanic dolphin in the Southwest Indian Ocean. Mar. Biol. 163:219. https://doi.org/10.1007/s00227-016-2999-3

Vousden, D., Scott, L.E.P., Sauer, W., Bornman, T.G., Ngoile, M., Stapley, J., Lutjeharms, J.R.E., 2008. Establishing a basis for ecosystem management in the western Indian Ocean. South Afr. J. Sci. 104: 417-420.

Wagawa, T., Yoshikawa, Y., Isoda, Y., Oka, E., Uehara, K., Nakano, T., Kuma, K., Takagi, S., 2012. Flow fields around the Emperor Seamounts detected from current data. J. Geophys. Res. Oceans 117: C06006. https://doi.org/10.1029/2011JC007530

Waite, A.M., Muhling, B.A., Holl, C.M., Beckley, L.E., Montoya, J.P., Strzelecki, J., Thompson, P.A., Pesant, S., 2007. Food web structure in two counter-rotating eddies based on $\delta^{15}N$ and $\delta^{13}C$ isotopic analyses. Deep Sea Res. Part II Top. Stud. Oceanogr. 54: 1055-1075. DOI: 10.1016/j.dsr2.2006.12.010

Walker, M.M., 1984. Learned magnetic field discrimination in yellowfin tuna,*Thunnus albacares*. J. Comp. Physiol. A. 155: 673–679. https://doi.org/10.1007/BF00610853

Watanabe, H., Kawaguchi, K., Hayashi, A., 2002. Feeding habits of juvenile surface migratory myctophid fishes (family Myctophidae) in the Kuroshio region of the western North Pacific. Mar. Ecol. Prog. Ser. 236: 263–272. https://doi.org/10.3354/meps236263

Watanuki, Y., Thiebot, J-B., 2018. Factors affecting the importance of myctophids in the diet of the world's seabirds. Mar. Biol. 165: 79. https://doi.org/10.1007/s00227-018-3334-y

Watson, R., Morato, T., 2004. Exploitation patterns in seamount fisheries: a preliminary analysis. In: Seamounts: Biodiversity and Fisheries (eds. Morato, T. and Pauly, D.), pp. 25–32. Fisheries Centre Research Reports, 12(5): 61–5.

Watson, R., Kitchingman, A., Cheung, W.W., 2007. Catches from world seamount fisheries. In: Pitcher, T.J., Morato, T., Hart, P.J.B., Clark, M.R., Haggan, N., Santos, R.S. (Eds), Seamounts: Ecology, Fisheries & Conservation. Blackwell Publishing Ltd, Oxford, UK, pp. 398-412.

Weigmann, S., Ebert, D.A., Clerkin, P.J., Stehmann, M.F.W., Naylor, G.J.P., 2016. *Bythaelurus bachi* n. sp., a new deep-water catshark (Carcharhiniformes, Scyliorhinidae) from the southwestern Indian Ocean, with a review of *Bythaelurus* species and a key to their identification. Zootaxa 4208(5): 401-432. https://doi.org/10.11646/zootaxa.4208.5.1

Weigmann, S., Kaschner, C.J., Thiel, R., 2018. A new microendemic species of the deep-water catshark genus *Bythaelurus* (Carcharhiniformes, Pentanchidae) from the northwestern Indian Ocean, with investigations of its feeding ecology, generic review and identification key. PLOS ONE 13: e0207887. https://doi.org/10.1371/journal.pone.0207887

Weimerskirch, H., 2007. Are seabirds foraging for unpredictable resources? Deep Sea Res. Part II Top. Stud. Oceanogr. 54: 211–223. https://doi.org/10.1016/j.dsr2.2006.11.013

Weimerskirch, H., Corre, M.L., Kai, E.T., Marsac, F., 2010. Foraging movements of great frigatebirds from Aldabra Island: Relationship with environmental variables and interactions with fisheries. Prog. Oceanogr. 86: 204–213. https://doi.org/10.1016/j.pocean.2010.04.003

Weiss, J., 1991. The dynamics of enstrophy transfer in two-dimensional hydrodynamics. Physica D: Nonlinear Phenomena 48: 273–294.

Wessel, P., 2001. Global distribution of seamounts inferred from gridded Geosat/ERS-1 altimetry. J. Geophys. Res. Solid Earth 106: 19431–19441. https://doi.org/10.1029/2000JB000083

Wessel, P., 2007. Seamount characteristics. In: Pitcher, T.J., Morato, T., Hart, P.J.B., Clark, M.R., Haggan, N., Santos, R.S. (Eds), Seamounts: Ecology, Fisheries & Conservation. Blackwell Publishing Ltd, Oxford, UK, pp. 3-25.

Wessel, P., Sandwell, D., Kim, S.-S., 2010. The Global Seamount Census. Oceanography 23: 24–33. https://doi.org/10.5670/oceanog.2010.60

White, M., Mohn, C., 2004. Seamounts: a review of physical processes and their influence on the seamount ecosystem. OASIS Report contract. 38.

White, M., Bashmachnikov, I., Arstegui, J., Martins, A., 2007. Physical Processes and Seamount Productivity. In: Pitcher, T.J., Morato, T., Hart, P.J.B., Clark, M.R., Haggan, N., Santos, R.S. (Eds), Seamounts: Ecology, Fisheries & Conservation. Blackwell Publishing Ltd, Oxford, UK, pp. 62–84. https://doi.org/10.1002/9780470691953.ch4

Wiebe, P.H., Madin, L.P., Haury, L.R., Harbison, G.R., Philbin, L.M., 1979. Diel vertical migration by *Salpa aspera* and its potential for large-scale particulate organic matter transport to the deep-sea. Mar. Biol. 53: 249–255. https://doi.org/10.1007/BF00952433

Wieczorek, A.M., Morrison, L., Croot, P.L., Allcock, A.L., MacLoughlin, E., Savard, O., Brownlow, H., Doyle, T.K., 2018. Frequency of Microplastics in Mesopelagic Fishes from the Northwest Atlantic. Front. Mar. Sci. 5(39): 1-9. https://doi.org/10.3389/fmars.2018.00039

Wilson, R.R., Kaufmann, R.S., 1987. Seamount Biota and Biogeography. In: Seamounts, islands, and atolls. 43: 355-377.

Wilson, C. D., Boehlert, G. W., 1990. Acoustic measurement of micronekton distribution over Southeast Hancock Seamount, central Pacific Ocean. In: Acoustic remote sensing. Proceedings of the 5th International Symposium on Acoustic Remote Sensing of the Atmosphere and Oceans. Tata-McGraw Hill Publications, New Dehli pp. 222-229.

Wilson, C.D., Firing, E., 1992. Sunrise swimmers bias acoustic Doppler current profiles. Deep Sea Res. Part Oceanogr. Res. Pap. 39: 885–892. https://doi.org/10.1016/0198-0149(92)90127-F

Wilson, C.D., Boehlert, G.W., 2004. Interaction of ocean currents and resident micronekton at a seamount in the central North Pacific. J. Mar. Syst. 50: 39–60. https://doi.org/10.1016/j.jmarsys.2003.09.013

Woillez, M., Ressler, P.H., Wilson, C.D., Horne, J.K., 2012. Multifrequency species classification of acoustic-trawl survey data using semi-supervised learning with class discovery. J. Acoust. Soc. Am. 131: EL184–EL190. https://doi.org/10.1121/1.3678685

Wong, S.N.P., Whitehead, H., 2014. Seasonal occurrence of sperm whales (*Physeter macrocephalus*) around Kelvin Seamount in the Sargasso Sea in relation to oceanographic processes. Deep-Sea Res. I. 91:10-16

Woodall, L.C., Robinson, L.F., Rogers, A.D., Narayanaswamy, B.E., Paterson, G.L.J., 2015. Deep-sea litter: a comparison of seamounts, banks and a ridge in the Atlantic and Indian Oceans reveals both environmental and anthropogenic factors impact accumulation and composition. Front. Mar. Sci. 2(3). https://doi.org/10.3389/fmars.2015.00003

Worm, B., Lotze, H.K., Myers, R.A., 2003. Predator diversity hotspots in the blue ocean. Proc. Natl. Acad. Sci. 100: 9884–9888. https://doi.org/10.1073/pnas.1333941100

Yesson, C., Clark, M.R., Taylor, M.L., Rogers, A.D., 2011. The global distribution of seamounts based on 30 arc seconds bathymetry data. Deep Sea Res. Part Oceanogr. Res. Pap. 58: 442–453. https://doi.org/10.1016/j.dsr.2011.02.004

Yesson, C., Taylor, M.L., Tittensor, D.P., Davies, A.J., Guinotte, J., Baco, A., Black, J., Hall-Spencer, J.M., Rogers, A.D., 2012. Global habitat suitability of cold-water octocorals. J. Biogeogr. 39: 1278-1292. doi:10.1111/j.1365-2699.2011.02681.x

Young, R.E., Roper, C.F.E., Mangold, K., Leisman, G., Hochberg, F.G., 1979. Luminescence from non-bioluminescent tissues in oceanic cephalopods. Mar. Biol. 53: 69–77. https://doi.org/10.1007/BF00386530

Young, R.E., 1983. Oceanic bioluminescence: An overview of general functions. B. Mar. Sci. 33(4): 829-845.

Young, J.W., Hunt, B.P.V., Cook, T.R., Llopiz, J.K., Hazen, E.L., Pethybridge, H.R., Ceccareli, D., Lorrain, A., Olson, R.J., Allain, V., Menkes, C., Patterson, T., Nicol, S., Lehodey, P., Kloser, R.J., Arrizabalaga, H., Choy, C.A., 2015. The trophodynamics of marine top predators: Current knowledge, recent advances and challenges. Deep Sea Res. Part II Top. Stud. Oceanogr. 113: 170-187. http://dx.doi.org/10.1016/j.dsr2.2014.05.015

Youngbluth, M.J., 1975. The vertical distribution and diel migration of euphausiids in the central waters of the eastern South Pacific. Deep-Sea Res. 22: 519–536. https://doi.org/10.1016/0011-7471(75)90033-9.

Zeldis, J., Davis, C., James, M., Ballara, S., Booth, W., Chang, F., 1995. Salp grazing:effects on phytoplankton abundance, vertical distribution and taxonomic composition in a coastal habitat. Mar. Ecol. Prog. Ser. 126: 267–283. https://doi.org/10.3354/meps126267

Zhang, T., Lin, J., Gao, J., 2011. Interactions between hotspots and the Southwest Indian Ridge during the last 90 Ma: Implications on the formation of oceanic plateaus and intra-plate seamounts. Sci. China Earth Sci. 54: 1177–1188. https://doi.org/10.1007/s11430-011-4219-9

Zucchi, S., Ternon, J-F., Demarcq, H., Ménard, F., Guduff, S. and Spadone, A. 2018. State of knowledge on seamount and hydrothermal vent ecosystems – FFEM-SWIO Project Bibliography study. Gland, Switzerland: IUCN. 45pp.

Zudaire, I., Murua, H., Grande, M., Goñi, N., Potier, M., Ménard, F., Chassot, E., Bodin, N., 2015. Variations in the diet and stable isotope ratios during the ovarian development of female yellowfin tuna (*Thunnus albacares*) in the Western Indian Ocean. Mar. Biol. 162: 2363–2377. https://doi.org/10.1007/s00227-015-2763-0

APPENDIX

Table A. Physical oceanographic processes observed at few seamounts of the Atlantic and Pacific Oceans.

Seamount Attributes **Oceanographic Factors**	**Observations**	**References**
Isopycnal doming	Alarcón seamount (Entrance to the Gulf of California) East Pacific Rise	Torres et al., 2004
	Minami-kasuga seamount (NW Pacific)	Lavelle et al., 2010
	Great Meteor seamount	Genin and Boehlert, 1985
	Over a 400-m high feature in the Gulf Stream system	Mohn & Beckmann, 2002 Owens & Hogg, 1980
Taylor column	Corner Rise seamount (NW Atlantic)	Owens & Hogg, 1980
	Sedlo seamount (N Atlantic)	Mohn et al., 2009
	Cobb seamount (Pacific)	Freeland, 1994
	Emperor seamounts (N Pacific)	Wagawa et al., 2012
	Minami-kasuga seamount (NW Pacific)	Genin & Boehlert, 1985
	Condor seamount	Bashmachnikov et al., 2013
	Madagascar Ridge; Any Taylor column formed may be swept away by mesoscale eddies	Read & Pollard, 2017
	Cobb seamount	Codiga & Eriksen, 1997

Tidal amplification and rectification	Fieberling Guyot	Eriksen, 1991, 1995; Brink, 1995; Kunze & Toole, 1997
	Rockall Bank (Atlantic)	Huthnance, 1974
	Yermak Plateau (Arctic)	Hunkins, 1986
	Cross seamount (Pacific)	Noble & Mullineaux, 1989
	Great Meteor seamount	Mohn & Beckmann, 2002
	Porcupine Bank (W of Ireland)	Mohn, 2002
Internal waves and turbulent mixing	Fieberling Guyot	Toole et al., 1997
	Irving Seamount	Lavelle et al., 2004
	Middle of What seamount (Indian Ocean)	Read & Pollard, 2017
	Sapmer seamount (Indian Ocean)	Read & Pollard, 2017

Table B. Physical oceanographic processes and associated biological responses observed at few seamounts of the Atlantic and Pacific Oceans.

Ecological Factors	**Observations**	**Physical processes**	**Biological responses**	**References**
Phytoplankton enhancement	Rockall Bank (NE Atlantic)	Taylor cap, Tidal rectification, generation of dome of cold, dense water	30% increase in annual chlorophyll *a* levels over the summit	Mohn & White, 2007
	Great Meteor seamount		Different phytoplankton species and greater chlorophyll *a* concentrations relative to surrounding environment	Mouriño et al., 2001
	Minami-Kasuga seamount	Taylor column, dome-like structures	Enhanced chlorophyll *a* concentrations with residence time of several days	Genin & Boehlert, 1985
	Senghor seamount	Tidal dynamics	Particulate organic carbon (POC) export, pulses of primary production into the euphotic zone	Turnewitsch et al., 2016
	Seine seamount		Higher suspended POC concentrations	Kiriakoulakis et al., 2009; Vilas et al., 2009
	Komahashi No. 2 seamount (W Pacific)	Topographic-current interactions, upward transport of nutrients in the euphotic zone	Occasional increase in chlorophyll *a* concentrations	Furuya et al., 1995
	Cobb seamount		2-5 times increase in chlorophyll *a* that lasted for 2-3 weeks	Dower et al., 1992; Comeau et al., 1995
Zooplankton enhancement	Minami-kasuga seamount	Within and above a dome of cold dense water	Increase in zooplankton densities	Genin & Boehlert, 1985

Seamount-associated species	Seine seamount	Suitable environment for benthopelagic fish species such as *Macroramphosus* sp., *Capros ager*, *Anthias anthias*, *Callanthias ruber* and *Centracanthus cirrus*	Christiansen et al., 2009
Seamount-associated species	Equator seamount (Indian Ocean)	*Diaphus suborbitalis* resides at ~500-600 m seamount slope during the day (to avoid predation) and ascends in dense schools to ~80-150 m at night while feeding on copepods and *Cyclothone* species	Parin & Prut'ko, 1985
	south Atlantic and north Pacific seamounts	Presence of mesopelagic sternoptychid fish *Maurolicus muelleri*	Boehlert & Genin, 1987; Boehlert et al., 1994
	Southeast Hancock seamount (central N Pacific)	Dense aggregations of *M. muelleri* and *Gnathophausia longispina* remain on the seamount's flanks at ~400 m during the day and migrate to ~50 m above the summit every night. Shallow scattering layer is displaced ~2-7 km in the direction consistent with the current direction above the summit every night	Boehlert & Seki, 1984; Boehlert & Genin, 1987; Boehlert, 1988; Wilson & Boehlert, 1990; Wilson & Boehlert, 2004
		Spawning site for individuals of *M. muelleri*	Boehlert et al., 1994; Brodeur & Yamamura, 2005
	Dom João de Castro seamount	Spawining site for *Ceratoscopelus maderensis*	Sobrinho-Concalves & Cardigos, 2006

Table C. Mean body length (mm) of gelatinous organisms (total length from mouth to anus); squids (dorsal mantle length); crustaceans (abdomen and carapace length); fishes (standard length), total number of specimens (n), habitat range, feeding mode, $\delta^{15}N$ and $\delta^{13}C$ (‰), and mean estimated trophic level (Mean TL from TPA model) for the species or taxa on which stable isotope analyses were performed at La Pérouse (ISSG) and MAD-Ridge (EAFR) seamounts. Values are mean ± standard deviation.

Broad Class	Order/ Suborder/Infraorder	Family/ Species	Habitat Range	Feeding Mode	Seamount cruises	Trawl No.	n	Mean Size (mm)	Mean $\delta^{15}N$ (‰)	Mean $\delta^{13}C$ (‰)	Mean TL (TPA model)
Gelatinous	Pyrosomatida	Pyrosomatidae	Mesopelagic	Filter Feeder	La Pérouse	3, 6, 7	6	20.1 ± 4.8	5.2 ± 0.20	-21.5 ± 0.17	2.0 ± 0.06
		Unidentified pyrosomes			MAD-Ridge	2, 6	4	23.8 ± 9.0	3.3 ± 0.31	-22.9 ± 0.64	1.7 ± 0.10
					MZC	18	2	22.3 ± 10.5	3.8 ± 0.13	-22.4 ± 0.73	1.9 ± 0.04
	Salpida	Salpidae	Mesopelagic	Filter Feeder	La Pérouse	6	1	NA	5.9	-18.2	2.2
		Salpa sp.			MAD-Ridge	5, 6, 11	6	29.5 ± 14.2	4.2 ± 1.19	-21.5 ± 1.44	2.0 ± 0.37
					MZC	18	1	28.5	6.4	-23.2	2.7
Crustaceans	Euphausiacea	Euphausiidae	Mesopelagic	Omnivore	MAD-Ridge	6	2	23.7 ± 1.20	7.7 ± 0.18	-19.4 ± 0.27	3.1 ± 0.06
	Decapoda	Unidentified shrimps	Mesopelagic	Omnivore	La Pérouse	4, 7	4	36.0 ± 3.91	8.8 ± 0.29	-18.0 ± 0.27	3.1 ± 0.09
	Decapoda	Oplophoridae	Mesopelagic-Bathypelagic	Omnivore	La Pérouse	1, 2, 7	6	49.0 ± 9.65	10.4 ± 0.89	-18.3 ± 0.26	3.6 ± 0.28
	…..Pleocyemata				MAD-Ridge	1, 2, 5	8	47.2 ± 11.8	9.5 ± 0.47	-18.1 ± 0.33	3.7 ± 0.15
	…….Caridea	Pasiphaeidae	Mesopelagic-Bathypelagic	Omnivore	La Pérouse	9	2	70.4 ± 20.5	9.8 ± 0.23	-18.0 ± 0.53	3.4 ± 0.07
		Pasiphaea spp.									
	…….Caridea	Unidentified caridean shrimps	Mesopelagic	Omnivore	La Pérouse	2, 8	3	48.6 ± 7.41	10.1 ± 1.69	-17.7 ± 0.40	3.5 ± 0.53
					MAD-Ridge	2, 5	4	55.2 ± 8.89	9.2 ± 0.75	-17.5 ± 0.19	3.5 ± 0.23
	Decapoda	Penaeidae	Mesopelagic-Bathypelagic	Omnivore	La Pérouse	3, 8	4	66.0 ± 7.66	7.5 ± 0.47	-18.7 ± 0.57	2.7 ± 0.15
	…..Dendrobranchiata				MAD-Ridge	5, 6, 8	6	54.7 ± 14.9	6.6 ± 0.88	-18.6 ± 0.18	2.7 ± 0.28
		Funchalia sp.			MZC	18	2	68.6 ± 7.42	7.2 ± 0.68	-19.1 ± 0.44	2.9 ± 0.21
	Decapoda	Sergestidae	Mesopelagic	Omnivore	La Pérouse	1, 2	3	71.7 ± 5.83	10.7 ± 1.30	-18.8 ± 0.15	3.7 ± 0.40
	…..Dendrobranchiata				MAD-Ridge	2	6	47.2 ± 16.6	8.3 ± 0.67	-19.5 ± 0.47	3.3 ± 0.21
					MZC	18	4	65.3 ± 13.8	9.5 ± 0.71	-19.3 ± 0.27	3.7 ± 0.22

Broad Class	Order/ Suborder/Infraorder	Family/ Species	Habitat Range	Feeding Mode	Seamount cruises	Trawl No.	n	Mean Size (mm)	Mean $\delta^{15}N$ (‰)	Mean $\delta^{13}C$ (‰)	Mean TL (TPA model)
Squids	Oegopsida	Enoploteuthidae	Mesopelagic-Bathypelagic	Carnivore	MAD-Ridge	11	2	34.1 ± 16.8	8.0 ± 0.06	-18.6 ± 0.42	3.2 ± 0.02
		Enoploteuthidae	Mesopelagic-Bathypelagic	Carnivore	La Pérouse	3, 4, 6	6	27.0 ± 8.26	10.5 ± 0.45	-18.4 ± 0.48	3.6 ± 0.14
		Abraliopsis sp.			MAD-Ridge	2, 9, 10	6	26.2 ± 6.06	9.5 ± 0.39	-18.3 ± 0.45	3.6 ± 0.12
		Histioteuthidae	Mesopelagic	Carnivore	La Pérouse	9	2	29.2 ± 0.35	11.7 ± 0.10	-19.1 ± 0.01	4.0 ± 0.03
		Histioteuthis spp.			MAD-Ridge	10	1	367.0	10.7	-21.0	4.0
		Ommastrephidae	Mesopelagic	Carnivore	MAD-Ridge	12, 14, 16	4	90.1 ± 52.2	9.0 ± 0.93	-18.5 ± 0.18	3.5 ± 0.29
		Ornithoteuthis volatilis									
		Ommastrephidae	Mesopelagic	Carnivore	MAD-Ridge	1	1	364.8	13.2	-17.4	4.8
		Ommastrephes bartramii			MZC	20	1	NA	13.8	-17.3	5.0
		Ommastrephidae	Mesopelagic	Carnivore	MAD-Ridge	2	1	111.3	9.4	-17.7	3.6
		Eucleoteuthis luminosa									

Broad Class	Order/ Suborder/Infraorder	Family/ Species	Habitat Range	Feeding Mode	Cruises	Trawl No.	n	Mean Size (mm)	Mean $\delta^{15}N$ (‰)	Mean $\delta^{13}C$ (‰)	Mean TL
Fishes	Anguiliformes	Leptocephali	Epipelagic	Detritivore	La Pérouse MAD-Ridge	2, 3, 4 3, 4, 6	5 6	135.3 ± 55.3 135.1 ± 61.3	4.9 ± 2.07 3.7 ± 1.48	-20.4 ± 0.52 -20.7 ± 0.30	1.9 ± 0.65 1.8 ± 0.46
	Aulopiformes	Evermannellidae *Coccorella atrata*	Mesopelagic	Carnivore	La Pérouse	9	1	92.8	13.3	-17.7	4.5
		Evermannellidae *Evermannella indica*	Mesopelagic	Carnivore	La Pérouse	1, 2	4	109.9 ± 9.19	12.2 ± 0.19	-17.9 ± 0.19	4.2 ± 0.06
		Paralepididae	Epipelagic-Bathypelagic	Carnivore	La Pérouse	4, 8	4	64.4 ± 18.9	9.1 ± 0.42	-19.7 ± 0.50	3.2 ± 0.13
	Beryciformes	Diretmidae *Diretmus argenteus*	Mesopelagic	Carnivore	MAD-Ridge	7	1	30.3	8.8	-19.9	3.4
	Gadiformes	Bregmacerotidae *Bregmaceros maclellandi*	Mesopelagic	Carnivore	La Pérouse	9	2	67.5 ± 4.0	10.1 ± 0.40	-18.8 ± 0.23	3.5 ± 0.13
	Myctophiformes	Neoscopelidae *Neoscopelus macrolepidotus*	Mesopelagic-Benthopelagic over slope regions	Carnivore	MAD-Ridge	10	2	80.9 ± 49.3	10.8 ± 0.44	-19.2 ± 0.37	4.1 ± 0.14
		Neoscopelidae *Neoscopelus microchir*	Mesopelagic-Benthopelagic over slope regions	Carnivore	MAD-Ridge	10	2	59.8 ± 19.3	11.0 ± 0.05	-19.0 ±0.10	4.1 ± 0.02
		Myctophidae *Benthosema fibulatum*	Mesopelagic	Carnivore	MAD-Ridge	14	2	79.1 ± 12.8	9.7 ± 0.25	-18.7 ± 0.13	3.7 ± 0.08
		Myctophidae *Benthosema suborbitale*	Mesopelagic	Carnivore	MAD-Ridge	3, 6	3	26.4 ± 2.71	8.7 ± 0.24	-19.4 ± 0.14	3.4 ± 0.07
Fishes	Myctophiformes	Myctophidae *Bolinichthys photothorax*	Mesopelagic	Carnivore	La Pérouse	9, 10	4	67.5 ± 7.78	11.0 ± 0.46	-18.8 ± 0.15	3.8 ± 0.14

		Myctophidae *Ceratoscopelus warmingii*	Mesopelagic	Omnivore	La Pérouse MAD-Ridge	1, 4, 8, 9 2, 3, 6	8 6	55.4 ± 11.0 42.0 ± 14.0	9.0 ± 0.46 7.7 ± 0.59	-18.9 ± 0.40 -18.9 ± 0.33	3.2 ± 0.14 3.1 ± 0.18
		Myctophidae *Diaphus brachycephalus*	Mesopelagic	Carnivore	La Pérouse MAD-Ridge	8 5	2 2	32.0 ± 2.12 35.9 ± 6.43	11.3 ± 0.04 10.5 ± 0.48	-19.2 ± 0.13 -19.3 ± 0.09	3.9 ± 0.01 4.0 ± 0.15
		Myctophidae *Diaphus diadematus*	Mesopelagic	Carnivore	MAD-Ridge	5, 7	4	32.0 ± 3.41	9.8 ± 0.39	-19.9 ± 0.18	3.7 ± 0.12
		Myctophidae *Diaphus effulgens*	Mesopelagic	Carnivore	MAD-Ridge	5	2	90.7 ± 22.5	10.3 ± 1.44	-19.1 ± 0.21	3.9 ± 0.45
		Myctophidae *Diaphus knappi*	Mesopelagic-Epibenthic	Carnivore	MAD-Ridge	16	2	53.1 ± 11.0	10.2 ± 0.07	-19.4 ± 0.16	3.9 ± 0.02
		Myctophidae *Diaphus lucidus*	Mesopelagic	Carnivore	La Pérouse MZC	10 20	2 2	73.1 ± 12.1 62.0 ± 10.3	12.1 ± 0.05 11.0 ± 0.45	-19.0 ± 0.76 -19.2 ± 0.04	4.1 ± 0.02 4.1 ± 0.14
		Myctophidae *Diaphus metoclampus*	Mesopelagic	Carnivore	MZC	20	2	58.1 ± 1.12	12.1 ± 0.07	-19.6 ± 0.06	4.4 ± 0.02
		Myctophidae *Diaphus mollis*	Mesopelagic	Carnivore	La Pérouse MAD-Ridge	10 5, 7	2 4	44.4 ± 5.09 55.5 ± 6.48	11.1 ± 0.42 10.7 ± 0.84	-18.8 ± 0.04 -19.4 ± 0.07	3.8 ± 0.13 4.0 ± 0.26
		Myctophidae *Diaphus perspicillatus*	Mesopelagic	Carnivore	La Pérouse MAD-Ridge	4, 10 2, 5, 7, 9, 12	4 10	53.4 ± 8.26 56.0 ± 4.59	10.7 ± 0.28 10.2 ± 0.53	-19.0 ± 0.42 -19.1 ± 0.24	3.7 ± 0.09 3.9 ± 0.17
		Myctophidae *Diaphus richardsoni*	Mesopelagic	Carnivore	La Pérouse MAD-Ridge	8 15	2 2	40.7 ± 3.54 36.9 ± 10.1	11.3 ± 0.45 9.1 ± 0.53	-19.5 ± 0.13 -19.3 ± 0.15	3.9 ± 0.14 3.5 ± 0.17
Fishes	Myctophiformes	Myctophidae *Diaphus splendidus*	Mesopelagic	Carnivore	La Pérouse	8	2	51.4 ± 6.36	9.6 ± 0.06	-18.7 ± 0.35	3.4 ± 0.02
		Myctophidae *Diaphus suborbitalis*	Mesopelagic-over slope regions	Carnivore	La Pérouse MAD-Ridge	2, 4 10, 14, 17	4 6	54.7 ± 15.1 72.3 ± 5.93	10.7 ± 0.42 11.2 ± 0.23	-18.6 ± 0.15 -18.8 ± 0.44	3.7 ± 0.13 4.2 ± 0.07

	Myctophidae *Hygophum hygomii*	Mesopelagic	Carnivore	MAD-Ridge	2, 3, 6, 12, 17	12	53.4 ± 4.73	10.1 ± 0.93	-19.0 ± 0.68	3.8 ± 0.29
	Myctophidae *Lampanyctus* spp.	Mesopelagic	Carnivore	La Pérouse	8	2	45.0 ± 6.51	9.7 ± 0.89	-18.7 ± 0.30	3.4 ± 0.28
	Myctophidae *Lampanyctus alatus*	Mesopelagic	Carnivore	MAD-Ridge	3, 5, 10	6	41.0 ± 2.69	8.8 ± 0.43	-19.2 ± 0.54	3.4 ± 0.13
	Myctophidae *Lobianchia dofleini*	Mesopelagic	Carnivore	MZC	20	2	35.1 ± 2.12	12.1 ± 0.62	-18.9 ± 0.42	4.5 ± 0.19
	Myctophidae *Lobianchia gemellarii*	Mesopelagic	Carnivore	La Pérouse MAD-Ridge	9, 10 5, 7	4 4	42.0 ± 2.50 41.1 ± 2.50	11.4 ± 0.35 10.9 ± 0.57	-18.9 ± 0.14 -19.3 ± 0.27	3.9 ± 0.11 4.1 + 0.18
	Myctophidae *Myctophum fissunovi*	Mesopelagic	Carnivore	MAD-Ridge	6, 14	3	62.7 ± 2.70	9.8 ± 0.17	-19.2 ± 0.25	3.8 ± 0.05
	Myctophidae *Myctophum nitidulum*	Mesopelagic	Carnivore	La Pérouse MAD-Ridge	4 6, 14	2 2	56.3 ± 14.2 67.4 ± 4.88	9.5 ± 0.17 9.5 ± 0.59	-19.0 ± 0.23 -19.3 ± 0.66	3.3 ± 0.05 3.6 ± 0.19
	Myctophidae *Nannobrachium* spp.	Mesopelagic-Bathypelagic	Carnivore	La Pérouse	10	2	111.5 ± 15.6	10.2 ± 0.92	-18.5 ± 0.10	3.5 ± 0.29
	Myctophidae *Notoscopelus resplendens*	Mesopelagic-Bathypelagic	Carnivore	MAD-Ridge	3	2	35.6 ± 3.04	8.1 ± 0.04	-18.4 ± 0.01	3.2 ± 0.01
	Myctophidae *Scopelopsis multipunctatus*	Mesopelagic	Carnivore	MAD-Ridge	5	2	37.9 ± 3.61	9.7 ± 0.54	-20.1 ± 0.29	3.7 ± 0.17
Perciformes	Carangidae *Decapterus macarellus*	Mesopelagic	Carnivore	MAD-Ridge	7	2	121.0	6.2 ± 0.18	-18.4 ± 0.37	2.6 ± 0.06
	Gempylidae *…..Nealotus tripes*	Mesopelagic	Carnivore	La Pérouse	9	1	202.8	12.1	-18.3	4.1

	Gempylidae *Promethichthys prometheus*	Mesopelagic-Benthopelagic	Carnivore	La Pérouse MAD-Ridge	4 14	2 2	219.3 ± 6.01 300.1 ± 91.5	9.6 ± 0.01 12.0 ± 0.06	-17.6 ± 0.18 -17.9 ± 0.13	3.3 4.4 ± 0.02
	Priacanthidae *Cookeolus japonicus*	Mesopelagic-Benthopelagic	Carnivore	MAD-Ridge	16	2	268.0 ± 84.9	10.7 ± 0.47	-18.3 ± 0.35	4.0 ± 0.15
Stephanoberyciformes	Melamphaidae *Scopelogadus mizolepis*	Mesopelagic	Carnivore	La Pérouse	9, 10	4	66.3 ± 11.2	10.2 ± 0.52	-18.9 ± 0.10	3.5 ± 0.16
Stomiiformes	Gonostomatidae *Cyclothone* sp.	Mesopelagic-Bathypelagic	Carnivore	MAD-Ridge	7	2	24.7 ± 1.98	8.7 ± 0.45	-19.8 ± 0.14	3.4 ± 0.14
	Gonostomatidae *Sigmops elongatus*	Mesopelagic-Bathypelagic	Carnivore	La Pérouse MAD-Ridge MZC	1, 7, 8, 10 2, 5, 10, 12 20	8 8 2	147.6 ± 63.5 111.5 ± 45.9 201.8 ± 35.6	11.5 ± 0.94 9.7 ± 1.05 12.0 ± 0.21	-18.4 ± 0.64 -18.8 ± 0.60 -18.3 ± 0.05	3.9 ± 0.30 3.7 ± 0.33 4.4 ± 0.07
	Gonostomatidae *Margrethia obtusirostra*	Mesopelagic	Carnivore	MAD-Ridge	12	2	33.8 ± 2.69	11.2 ± 0.26	-19.0 ± 0.25	4.2 ± 0.08
	Phosichthyidae *Vinciguerria nimbaria*	Mesopelagic	Carnivore	La Pérouse	8, 10	4	38.7 ± 13.6	11.4 ± 0.74	-18.8 ± 0.10	3.9 ± 0.23
	Sternoptychidae *Argyropelecus aculeatus*	Mesopelagic	Carnivore	La Pérouse MAD-Ridge	1, 2, 7, 8 1, 2, 5, 7, 10, 12	8 12	50.4 ± 15.5 55.4 ± 17.5	10.2 ± 0.87 10.4 ± 1.23	-18.8 ± 0.38 -19.0 ± 0.56	3.5 ± 0.27 3.9 ± 0.39
	Sternoptychidae *Argyropelecus hemigymnus*	Mesopelagic	Carnivore	MAD-Ridge	13	1	27.4	11.6	-18.9	4.3
	Stomiidae *Astronesthes* sp.	Mesopelagic	Carnivore	La Pérouse MAD-Ridge	2, 3, 8, 9, 10 5	5 1	88.2 ± 24.4 122.3	9.7 ± 0.48 10.1	-18.1 ± 0.36 -18.0	3.4 ± 0.15 3.8

		Stomiidae *Chauliodus sloani*	Mesopelagic-Bathypelagic	Carnivore	La Pérouse MAD-Ridge	8, 9 1, 5, 10	4 6	125.1 ± 51.1 138.9 ± 53.3	11.1 ± 1.0 10.4 ± 0.65	-18.5 ± 0.31 -18.5 ± 0.84	3.8 ± 0.31 3.9 ± 0.20
	Stomiiformes	Stomiidae *Diplophos rebainsi*	Mesopelagic-Bathypelagic	Carnivore	MAD-Ridge	1	2	93.3 ± 3.54	10.6 ± 0.06	-19.2	4.0 ± 0.02
		Stomiidae *Diplophos taenia*	Mesopelagic	Carnivore	La Pérouse MAD-Ridge	9 5	2 1	77.3 ± 7.64 175.5	9.6 ± 0.07 9.9	-19.3 ± 0.22 -18.9	3.3 ± 0.02 3.8
		Stomiidae *Echiostoma barbatum*	Mesopelagic-Bathypelagic	Carnivore	MAD-Ridge	9, 10, 11	6	71.2 ± 5.39	9.4 ± 1.0	-18.4 ± 0.30	3.6 ± 0.31
		Stomiidae *Eustomias* sp.	Mesopelagic-Bathypelagic	Carnivore	La Pérouse MAD-Ridge	4, 8, 9, 10 2, 12	4 3	96.4 ± 19.8 102.7 ± 11.6	9.4 ± 0.94 9.0 ± 0.11	-18.3 ± 0.48 -18.7 ± 0.16	3.3 ± 0.29 3.5 ± 0.03
		Stomiidae *Idiacanthus fasciola*	Mesopelagic-Bathypelagic	Carnivore	La Pérouse	4, 7, 10	3	249.6 ± 10.3	11.1 ± 1.22	-17.6 ± 0.24	3.8 ± 0.38
		Stomiidae *Melanostomias* sp.	Mesopelagic	Carnivore	La Pérouse MAD-Ridge	4, 7, 8, 9 5, 9, 12	7 3	71.4 ± 14.1 87.4 ± 13.4	10.1 ± 0.64 9.6 ± 0.65	-18.3 ± 0.25 -18.3 ± 0.51	3.5 ± 0.20 3.7 ± 0.20
		Stomiidae *Photonectes* sp.	Mesopelagic	Carnivore	La Pérouse	9, 10	2	121.1 ± 6.43	11.8 ± 0.62	-18.1 ± 0.62	4.0 ± 0.19
		Stomiidae *Photostomias* sp.	Mesopelagic-Bathypelagic	Carnivore	La Pérouse	4, 9	3	85.9 ± 22.9	11.3 ± 1.04	-18.1 ± 0.30	3.9 ± 0.33
		Stomiidae *Stomias boa*	Mesopelagic	Carnivore	La Pérouse	10	1	145.0	10.8	-18.4	3.7
		Stomiidae *Stomias longibarbatus*	Mesopelagic-Bathypelagic	Carnivore	La Pérouse MAD-Ridge	8 2	1 1	248.9 289.9	11.4 12.0	-18.3 -18.3	3.9 4.4

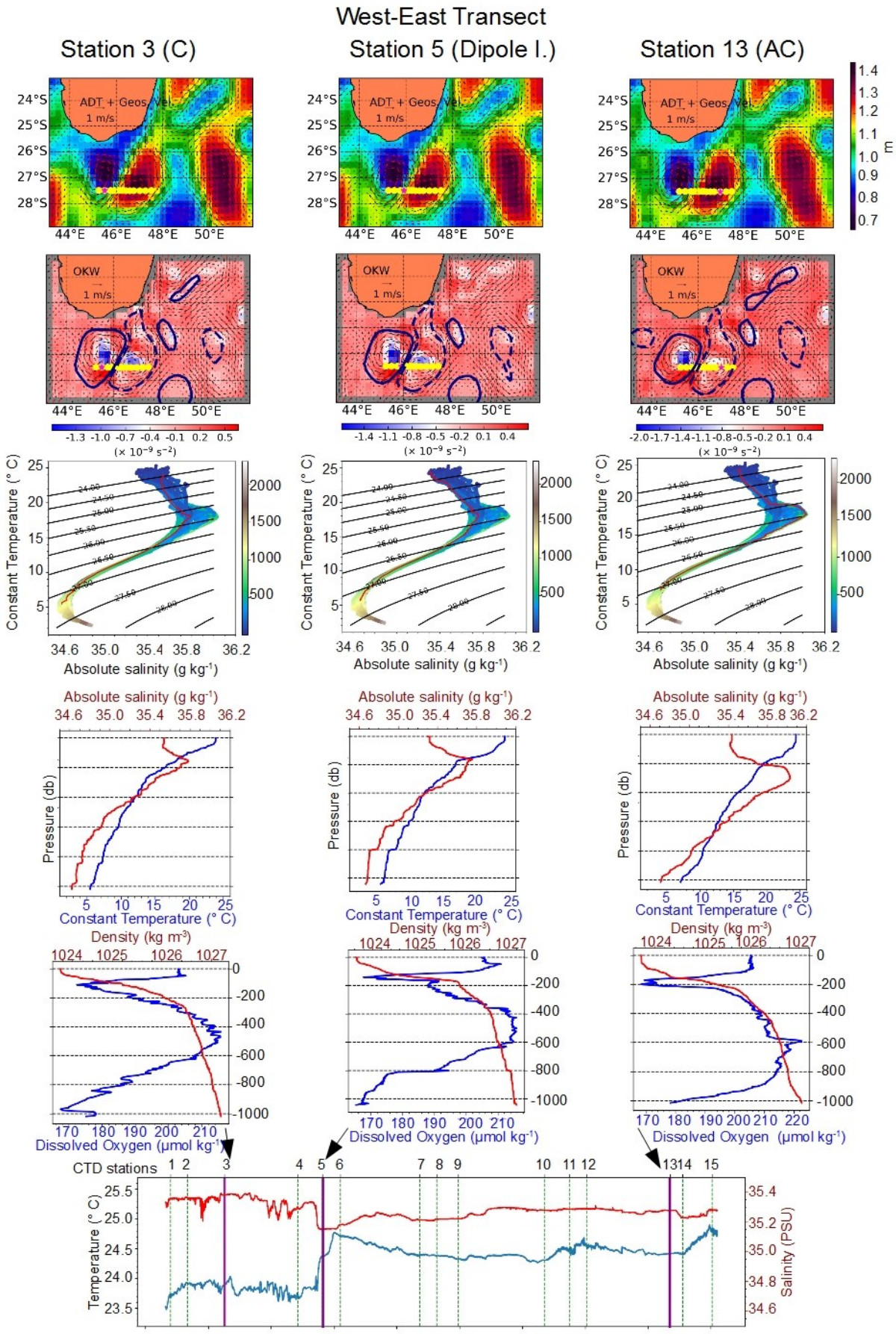
West-East Transect
Station 3 (C)
Station 5 (Dipole I.)
Station 13 (AC)
ADT + Geos. Vel.
1 m/s
OKW
Constant Temperature (° C)
Absolute salinity (g kg-1)
Pressure (db)
Density (kg m-3)
Dissolved Oxygen (µmol kg-1)
CTD stations
Temperature (° C)
Salinity (PSU)

Figure A. Example of classification of CTD stations (#3, 5 and 13) of the MAD-Ridge cruise. The absolute dynamic topography (line 1) together with the Okubo-Weiss parameters (line 2) give an indication of how the stations are located according to the dipole observed during MAD-Ridge. The contours of the anticyclone (dashed blue) and the cyclone (plain blue) are superimposed with the vectors of the surface geostrophic currents (black arrows). However, due to its spatial and temporal resolution, altimetry is not accurate enough to classify stations located less than 30 km from each other. Conservative Temperature (CT) vs. Absolute Salinity (SA) diagrams (line 3) provide a more accurate information: waters trapped within the anticyclone have a salinity maximum on the sigma=26 kg m^{-3} density layer. This is confirmed by the vertical profiles of CT in °C and SA in g kg^{-1} (line 4). Vertical profiles of oxygen in µmol kg^{-1} (line 5) also show that the layer with maximum oxygen concentrations is thicker in the anticyclone. Finally, the sea surface temperature (SST) in °C and sea surface salinity (SSS) in PSU recorded along the ship track (line 6) clearly identify a density front at the interface of the cyclone and anticyclone. All the other CTD stations during Leg 1 of MAD-Ridge cruise were classified the same way.